Chemistry and speciation of potentially toxic and radioactive elements during mine water treatment

Godfrey Madzivire

MSc Chemistry (UWC, 2010); BSc (Hons) Chemistry (UZ, 2003)

A thesis submitted in fulfillment of the requirements of Doctor of Philosophy in Chemistry

Chemistry Department of the University of the Western Cape

Supervisor: Prof. L.F. Petrik
Co-supervisors: Drs. W.M. Gitari and Viswanath R.K.Vadapalli

CHEMISTRY AND SPECIATION OF POTENTIALLY TOXIC AND RADIOACTIVE ELEMENTS DURING MINE WATER TREATMENT

Godfrey Madzivire

Key words

Fly ash

Mine water

Ettringite

Potential toxic elements

Geochemist's workbench

Jet loop reactor

Aluminium hydroxide

Aluminium chlorohydrate

Hydrodynamic cavitation

Impingement

Naturally occurring radioactive materials

ABSTRACT

Mine water poses a serious environmental challenge and contains elements such as Fe, Al, and Mn in potentially toxic concentrations. The major anion in mine water is sulphate. The complexity and diversity of mine water composition makes its treatment very expensive, and there is no "one-fits-all" treatment option available for mine water. Active treatment of mine water produces water with good quality but the processes are not sustainable because of the costs. Previous studies have shown that acid mine drainage can be treated with coal FA to produce better quality water. The use of coal FA, a waste material from coal fired power station and mine water would go a long way in achievement of sustainable treatment of mine water as per previous studies. In this study mine water and coal FA were characterized to determine their physiochemical properties. This study linked the modelling results obtained by using the Geochemist's workbench (GWB) software to the results obtained during the actual treatment of Matla mine water and Rand Uranium mine water using coal FA and lime. The chemistry involved when Matla mine water and Rand Uranium mine water were treated with flocculants was also investigated. Lastly the chemistry and kinetics involved was investigated when mine water was treated with various ameliorants such as Matla coal FA, lime and/or $Al(OH)_3$ using jet loop mixing or overhead stirring.

Mine water from Matla coal mine had a pH of 8 and therefore was classified as neutral mine drainage (NMD). Rand Uranium mine water had a pH of less than 3 and therefore was classified as acid mine drainage (AMD). The concentration of sulphate, Na, Ca, Mg, B, Hg, Se and Cd ions in Matla mine water was 1475, 956, 70, 40, 15, 2.43, 1.12 and 0.005 mg/L respectively. The concentration of sulphate, Fe, Ca, Mn, Mg, Al, B, Cr, Pb, U, Cd, Se and As ions in Rand Uranium mine water was 4126, 896, 376, 282, 155, 27, 5.43, 3.15, 0.51, 0.29, 0.007, 0.06 and 0.006 mg/L respectively . These concentrations were above the target water quality range (TWQR) for potable water set by the Department of Water Affairs (DWA) and World Health Organization (WHO). The gross alpha radioactivity was 6.01 Bq/L and gross beta radioactivity was 6.05 Bq/L in Rand Uranium mine water. This was 12 and 6 times more

than the required limit for potable water respectively. Radioisotopes analysis of Rand Uranium mine water showed that ^{234}U was 4.71 Bq/L which was above the TWQR for potable water of 0-1 Bq/L. Species distribution was calculated by SpecE8 program of the Geochemist's workbench (GWB) software. It was found by the SpecE8 program that major ions such as Mg, Mn, Na, K and sulphate mainly existed as free ions in both Rand Uranium and Matla mine waters. This means these elements would be highly mobile in the environment, which increases their bioavailability and toxicity. Aqueous speciation of Fe and Al were found to occur in association with hydroxyl ions. Therefore, these species were less mobile hence Fe and Al had reduced bioavailability and toxicity.

Matla coal FA that was used to treat the mine water was made up of mullite, quartz, lime, hematite and gypsum minerals. Gross alpha radioactivity was 3440 mg/L and beta radioactivity was 1200 Bq/L in Matla coal FA. The radioactive isotopes detected in Matla coal FA were 186 Bq/L of ^{238}U, 5.58 Bq/L of ^{235}U, 188 Bq/L of ^{234}U, 156 Bq/L of ^{232}Th, 184 Bq/L of ^{228}Th, 182 Bq/L of ^{228}Ra, 182 Bq/L of ^{226}Ra, 320 Bq/L of ^{210}Pb and 330 Bq/L of ^{40}K. The analysis showed that the radioactivity of Matla coal FA was in the range of most of the coal FA worldwide, but was much higher than that of normal soil. This indicated that any process using Matla coal FA would need to be evaluated for the ultimate fate of radioactive elements. Analysis of Matla coal FA indicated that it contained various rare earth elements (REEs). The REEs that were detected in Matla coal FA were, Ce (189.78 mg/kg), La (81.66 mg/kg), Nd (63.50 mg/kg), Y (52.30 mg/kg), Sc (24.94 mg/kg), Pr (18.35 mg/kg), Sm (11.95 mg/kg), Gd (10.40 mg/kg), Dy (9.50 mg/kg), Er (5.38 mg/kg), Yb (5.27 mg/kg), Ho (1.97 mg/kg), Tb (1.60 mg/kg), Tm (0.77mg/kg), and Lu (0.72 mg/kg). Rare earth elements have wide applications in catalysis, magnetic resonance imaging and other applications in industry. Since the concentration of REEs in Matla coal FA was much higher than that in soil, it is worthwhile to find cheap technologies to recover these elements from coal FA. This would minimize the release of these elements into the environment in addition of finding a cheap source of these valuable minerals.

It was predicted by the Act2 program of the GWB software that mine water could be treated with Matla coal FA to remove Mg, Al, Mn, U and Th by almost 100 % by increasing

the pH of the mine water to greater than 10. Also the Act2 program predicted that sulphate, Na and K ions would not be removed from Matla mine water if it was to be treated with coal FA. The Act2 program predicted that sulphate ions could be removed as alunite or gypsum when Rand Uranium mine water was to be treated with coal FA, but Na and K would remain in solution.

The modelling results were then experimentally verified in terms of the removal of major contaminants (Fe, Al, Mn, Mg and sulphate ions). Treatment of Matla mine water with coal FA resulted in the removal of Mg to within TWQR for potable water. This was noticed when the pH was increased to greater than 10. However, it was observed that sulphate, K and Na could not be removed during this treatment. Treatment of Rand Uranium mine water with coal FA resulted in the removal of major ions such as Fe, Al, Mn, Mg and sulphate ions from mine water. Iron, Al, Mn and Mg were removed to within the TWQR for potable water, while the sulphate ions were reduced from 2562 mg/L to about 1500 mg/L, which was still above the TWQR for potable water. These results agreed well with the modelling results obtained using Act2 program of the GWB software. When both Rand Uranium mine water or Matla mine water was treated with coal FA it was found that most of the potentially toxic elements (Zn, Ni, Cu, As, Pb, Be, Cr, V and Cd) and naturally radioactive elements (NORMs) (U and Th) were removed to below the required limit for potable water. These results were obtained by mixing mine water with various amounts of Matla coal FA and/or lime using an overhead stirrer or a jet loop reactor. The experimental results obtained when Rand Uranium mine water and Matla mine water were treated with Matla coal FA confirmed the results obtained by the Act2 program of the GWB software. This meant that GWB software is a powerful tool that can be used to predict what can be expected when treating mine water. This would help water scientists to plan the best treatment protocol because they could predict what to expect.

The product water after treatment of Matla mine water or Rand Uranium mine water with coal FA and/or lime contained a high concentration of sulphate and Ca ions (and Na ions in case of Matla mine water). It was found that the sulphate concentration could be removed to within the TWQR for potable water by using aluminium chlorohydrate (ACH) or $Al(OH)_3$. When Rand mine water or Matla mine water was treated with ACH using an overhead

stirrer it was found that sulphate ions could be removed to below 500 mg/L at pH 4 and Al:SO_4^{2-} molar ratio of 4:1. The main disadvantages of using ACH to remove sulphate ions from mine water was the amount of Cl^- ions that were added into the mine water from ACH and the high viscosity of the mixture. The high viscosity of the mixture of mine water with ACH made the recovery of product almost impossible. The product water from ACH treatment contained more than 1000 mg/L of Cl ions when the sulphate concentration was less than 500 mg/L. Treatment of Rand Uranium mine water or Matla mine water with $Al(OH)_3$ could not remove the sulphate ions to the acceptable level at pH less than 10. When mine water was treated with coal FA, lime and $Al(OH)_3$ for 120 min in jet loop reactor, the sulphate concentration was reduced to less than 500 mg/L at pH greater than 11. According to the XRD results, the sulphate ions were removed through the precipitation of ettringite and gypsum.

It was evident from the studies that the kinetics of sulphate removal from mine water was improved by hydrodynamic mixing of mine water and coal FA in a jet loop reactor. The treatment of mine water with Matla coal FA, lime and $Al(OH)_3$ in a jet loop reactor was carried out at 80 L capacity. This means that the process can be up scaled.

This research has proved that mine water of different qualities can be treated successfully with coal FA, lime and $Al(OH)_3$ to obtain product water that meet TWQR guidelines for most of the elements. However, the product water may require polishing to regulate the pH and remove the remaining potentially toxic elements such as Na, Ca, As, Mo and Cr. This means that coal FA treatment of mine water can substitute the lime and limestone mine water treatment which could reduce the costs associated with treatment of mine water significantly. Moreover, coal FA is a waste material that occurs close to the source of contaminated mine water and therefore transport costs can be minimized. The use a jet loop reactor enhanced the kinetics of the treatment of mine water with coal FA, lime and $Al(OH)_3$. The residues from the treatment of mine water with coal FA, lime and $Al(OH)_3$ are suitable for mine backfill to seal mine voids and prevent mine water formation based on previous studies. Therefore this process does not produce any waste material that would require disposal problems and offers an AMD prevention option.

DECLARATION

I declare that "***Chemistry and speciation of potentially toxic and radioactive elements during mine water treatment***" is my own work and it has not been submitted for any degree or examination in any university. All the resources I have used or quoted have been indicated and acknowledged by complete references.

Godfrey Madzivire November 2012

Signed……

ACKNOWLEDGEMENT

My sincere gratitude goes to my supervisor Prof. L.F Petrik for the guidance and a lot of knowledge that she imparted to me during this study and the opportunities of attending national and international conferences and workshops. This gave a platform to share and gain knowledge in the field of water treatment and waste management.

I also want to thank Dr. W.M. Gitari, Dr. V.R.K Vadapalli and Prof. T.V. Ojumu for the advice on the project. I am most grateful to Dr P.P. Maleka, Research Scientist in the Environmental Radioactivity Laboratory at iThemba Labs and Prof R. Lindsay in the Physics Department, University of the Western Cape for the vast knowledge that you shared with me in terms of radioactivity analysis. Thank you to A. Abbott and all my colleagues in ENS group for making the computer lab and the ENS laboratory such an enjoyable place. I also want to thank Natasha Misheer (for the provision of the material used for this study), ESKOM, Water Research Commission and National Research Foundation for funding this project. My sincere gratitude goes to Org Nieuwoudt of Biofuelson for designing the jet loop reactor used in this research.

Special thanks to my family for the support and encouragement that they accorded me the past five years through my MSc and PhD studies. My wife Memory I really appreciate the support that you have given me throughout this study. You are really a pillar of strength. My brothers and sisters, thank you for the moral support. To my daughter Ruzivo for always making smile when came back home stressed with experiments in the laboratory, playing with you always make me to reboot my mind.

DEDICATION

This piece of work is dedicated to my mother, the late **Mrs C. Madzivire**. I know you would have been proud to see this achievement as you always encouraged me to work extra hard in whatever I do.

TABLE OF CONTENTS

TABLE OF CONTENTS

TABLE OF CONTENTS

LIST OF FIGURES

LIST OF FIGURES

LIST OF FIGURES

LIST OF TABLES

LIST OF ABBREVIATIONS

ABC = alkali-barium-calcium

ACH = aluminium chlorohydrate

ALD = anoxic limestone drains

AMD = acid mine drainage

DWA = Department of Water Affairs

EARTH = Environmental and Remedial Technology Holdings

EC = electrical conductivity

ED = electro dialysis

EDR = electro dialysis reversal

FA = fly ash

GWB = Geochemist's workbench

HDS = high density sludge

IC = ion chromatography

ICP-MS = inductively coupled plasma-mass spectrometry

ICP-OES = inductively coupled plasma-optical emission spectrometry

LA-ICP-MS = laser ablation-inductively coupled plasma-mass spectrometry

MBA = magnesium-barium-alkali

NAA = neutron activation analysis

NMD = neutral mine drainage

NORMs = naturally occurring radionuclides

OLD = open limestone drains

REEs = rare earth elements

RSD = relative standard deviation

SAPS = successive alkali producing systems

SPARRO = slurry precipitation and recycling reverse osmosis

SRB = sulphate reducing bacteria

TDS = total dissolved solids

TWQR = target water quality range

WHO = World Health Organization

XRD = X-ray diffraction

XRF = X-ray fluorescence

ACADEMIC OUTPUT FROM THIS RESEARCH

1. Madzivire G, Gitari W.M, Vadapalli V.R.K, Ojumu T.V, Petrik L.F. (2011), "Fate of sulphate removed during the treatment of circumneutral mine water and acid mine drainage with coal fly ash: Modelling and experimental approach", *Minerals Engineering*, 24(13), pp 1467–1477.

2. Madzivire. G.; Gitari, W.M.; Vadapalli, V.R.K.; Petrik, L.F. (2012), "Jet loop reactor application for mine water treatment using fly ash, lime and $Al(OH)_3$"; *International Journal of Environmental Science and Technology* (submitted in August 2012).

3. Madzivire. G.; Gitari W.M.; Vadapalli, V.R.K and Petrik, L.F. (2012), Application of a jet loop reactor to enhance removal of sulphates from mine water using coal fly ash, lime and aluminium hydroxide; *International Mine Water Conference*, 30 September-4 October 2012, Burnbury, Australia.

CHAPTER 1: INTRODUCTION

1.1. BACKGROUND

Mine water and coal fly ash (FA) are waste materials produced by mines and coal power stations respectively. Mine water can be acidic, neutral or alkaline depending on the geological location of the mine (Lottermoser, 2007). Acid mine water, often termed acid mine drainage (AMD) is produced when the rock that was disturbed during mining contains more acid producing minerals such as pyrite (FeS_2) than acid neutralizing minerals such as dolomite ($CaMg(CO_3)_2$) or calcite ($CaCO_3$). Mining exposes the FeS_2 to oxidation by oxygen in the presence of water according to Equation 1.1, resulting in the formation of sulphuric acid and Fe^{3+}. The reaction is catalysed by bacteria called *Acidobacillus sp*.

$$FeS_2 + \frac{7}{2}O_2 + H_2O \xrightarrow{bacteria} Fe^{3+} + 2H^+ + 2SO_4^{2-} \quad \text{.....1.1}$$

Sulphuric acid generated from the above reaction causes chemical weathering of the surrounding rocks, thereby causing the leaching of potentially toxic metals and radioactive elements into the water. Mine water from gold and uranium mines is usually acidic and may contain radioactive elements such as U (Winde, 2010).

Neutral mine drainage (NMD) is produced when the rock disturbed during mining contains stoichiometrically equal proportion of acid producing minerals and acid neutralizing minerals such as dolomite. Therefore the acidity produced from the oxidation of FeS_2 is neutralized by the acid neutralizing minerals as shown in Equation 1.2.

$$FeS_2 + CaMg(CO_3)_2 + \frac{15}{4}O_2 + \frac{3}{2}H_2O \rightarrow Fe(OH)_3 + Ca^{2+} + Mg^{2+} + 2SO_4^{2-} + 2CO_2 \quad \text{.....1.2}$$

Acid mine drainage is mainly composed of Fe, Al and Mn cations and sulphate ions. Neutral mine drainage contains Na, Ca, Mg, sulphate and carbonate ions.

In South Africa mining has been taking place for over 100 years. It has left empty spaces underground called mine voids. The mine voids in the Witwatersrand Gold Fields are filling up at a rate of 0.59 m/day. As at November 2010 the level of AMD was 510 m below the surface. At this rate, if decant prevention and management is not put into place, the water will reach the surface in March 2013 resulting in AMD flowing in the streets of Johannesburg central business district and the popular tourist attraction Gold Reef City (Coetzee et al., 2010). The problem of mine water in South Africa is not only confined to Witwatersrand Gold Field. It is also a huge problem in Mpumalanga Coal Fields. Mine water containing high concentrations of Fe, Al, Mn and sulphate ions, from the Mpumalanga coal fields is threatening the freshwater resources of the Vaal and Olifants River ecosystems. Due to the aforementioned problems, mine water in South Africa needs proper management. Some of the mine water management schemes proposed by the Acid Mine Drainage Inter-Ministerial Committee under the Coordination of the Council for Geoscience of South Africa includes (Coetzee et al., 2010):

- Decant prevention and management
- Controlling ingress of clean water (rainfall) into mine voids
- Water quality management

Decant prevention can be achieved by pumping the water out of the mine voids. Pumped water needs to be treated to remove potential toxic elements and sulphate ions before the water can be discharged into the freshwater resources. Many treatment options are available to treat the contaminated mine water to the required standards for potable, industrial and agricultural purposes, but are too costly and unsustainable. Cheap treatment technologies are continually being investigated.

1.2. PROBLEM STATEMENT

Mine water is an environmental liability produced during mining activities. Mine water usually results from pumping underground water in order for miners to access the minerals, or leaches from mine tailings. The composition of mine water differs from mine

to mine depending on the exploited geology. Types of mine water are classified according to their chemical composition. Mine water composition depends on the mined ore and the chemical additives used in the mineral processing and hydrometallurgical processing. This means that there is no typical composition of mine waters and as a result, the classification of mine water based on its composition is very complex. A number of classification schemes of mine water have been proposed using one or several water parameters (Lottermoser, 2007; Morin and Hutt, 1997). These include the classification:

- based on the major cations and anions;
- or the classification based on pH;
- or the classification based on alkalinity vs acidity.

1.2.1. TECHNIQUES FOR MINE WATER TREATMENT

Mine water is mainly composed of Fe, Al, and Mn (for AMD) or Ca and Mg (for NMD) cations together with other potential toxic elements depending on the geology that is mined. Sulphate is the major anion found in mine water and ranges from around 1 000 to 30 000 mg/L. Due to vast differences in the chemistry of mine waters and the variety of physical, chemical and biological methods to separate metals from mine water, there is a wide range of treatment technologies for mine water treatment. Treatment of mine drainage can be achieved through passive or active processes (Neculita et al., 2007).

Passive treatment schemes take advantage of naturally occurring geochemical and biological processes in order to improve the quality of the influent waters with minimal operation and maintenance requirements. Passive treatment can be broadly classified as chemical or biological systems depending on the processes that are occurring to ameliorate the mine water (Neculita et al., 2007). Although passive treatment of mine water is cheaper, it is limited by the unavailability of enough space to set up the proper facility. Also the quality of the product water is not guaranteed.

Active treatment technologies improve the water quality by processes which require continuous input of artificial energy, biochemical or chemical reagents. Active treatment

methods are recognized by the presence of a water treatment plant that is being monitored regularly by a skilled workforce to operate and maintain the equipment. Active treatment technologies are broadly classified as biological, chemical and membrane methods. Biological methods involve the use of sulphate reducing bacteria (Johnson, 2000). Chemical treatment include the precipitation of contaminants from the mine water using chemicals such as lime/limestone, $BaCO_3$, BaS, $Ba(OH)_2$, $Mg(OH)_2$, $MgCO_3$ and $Al(OH)_3$ (Geldenhuys et al., 2001; Bosman, 1983, Smit, 1999; Adelm, 1997; Bosman et al., 1990). Membrane methods for the treatment of mine water are nano filtration, reverse osmosis and electro dialysis (Kentish and Stevens, 2001; Del Pino and Durham, 1999; Matsuura, 2001; Valerdi-Perez et al., 2001; Schoeman and Steyn, 2001). Mine water treatment can also be done using ion exchange (Kitchener, 1957).

The major advantage of active treatment is the capability to handle any changes in mine water quality and quantity. This is because of the precise process control in response to these changes. Also active treatment is a preferred technique to passive treatment if the land availability is a limiting factor. The major disadvantage of the active treatment method is the brines and sludge that are produced as wastes, which are more expensive to handle and dispose than the water purification process itself. Also the continuous input of energy, reagents and the need of manpower to run and maintain the treatment plant makes the technique expensive.

The choice of a suitable treatment technology depends on; the mine water quality, the mine water quantity, the treated water quality, the storage options for any sludge produced and the cost of the treatment technique. In reality, there is no technical limit to the quality of the water which can be achieved using current existing techniques, but the cost is the limiting factor. Therefore the selection of treatment technique comes down to economic and environment benefit analysis. New methods to remove contaminants from mine water, which are cheaper, are constantly sought. One of those methods is the use of coal fly ash (FA) from coal power stations (Gitari et al., 2008). The advantage of that method is that FA is a waste material from coal combustion found close to coal mines. This means that the use of FA treatment of mine water can be sustainable since coal FA is a waste material. South

African electricity produces about 80 % of its electricity from coal and generates large amounts of coal FA. Disposing FA has proved to be an environmental concern, and therefore recycling of coal FA for mine drainage treatment is important to achieve zero effluent discharge.

1.2.2. COAL FLY ASH

Coal FA is the mineral matter that remains after coal has been thermally altered through the combustion process to produce electricity and is collected from flue gas using electrostatic precipitators or filter bags (Adriano, 1980). The major constituents of coal are C, O, H, N and S, which are thermally oxidized during coal combustion to produce electricity. Coal also contains inorganic components such as As, Hg, B, Pb, Ni, Se, Sr, V and Zn in association with different types of inorganic minerals such as aluminosilicates (clay minerals), carbonates (calcite and dolomite), sulphides (pyrites), and silica (quartz). The inorganic minerals make up 5 to 40 % of coal. South African power stations burn low quality coal with very high inorganic content containing up to 40 % inorganic material (Pinetown et al., 2007).

It is these incombustible materials that form the ash that remains after combustion of coal. The chemical composition of coal FA is made up of Si, Ca, Al, Fe, Mg and S oxides along with unburnt C and various trace elements. The silica in the form of mineral quartz passes through the combustion process and remains as quartz in the coal FA. The clay minerals transform into crystalline and non-crystalline (amorphous) aluminosilicates materials. Elements such as Fe, Ca, and Mg are oxidized to form oxide minerals such as magnetite (Fe_3O_4), hematite (Fe_2O_3), lime (CaO) and periclase (MgO) (Mattigod et al., 1990). The constituents and mineralogy of FA mainly depend on the chemical composition of the coal burnt and the combustion technology employed (Roy et. al., 1985). The amount of crystalline material and glass phase material depends largely on the combustion and gasification (cooling of the ash) process used at a particular power plant.

Coal fly ash contains elevated amounts of radioactive elements and rare earth elements compared to the coal burnt during the combustion process (Senior et al., 2000; Depoi et

al., 2008; Zielinski and Budahn, 1998). This is because these minerals are concentrated as the carbon component of coal is burnt off during the combustion process to produce electricity. Therefore products from reuse of coal FA need to be evaluated for radioactivity before they can be channelled to the market.

1.3. MOTIVATION OF THE STUDY

Treatment of AMD and NMD with coal FA was found to remove Fe, Al and Mn at pH 9. Sulphate ions were found to be removed to between 2000-3000 mg/L when AMD was treated with coal FA to pH 9 (Gitari et al., 2008, Surender, 2009). On the other hand treatment of NMD with FA was found to remove an insignificant amount sulphate when the pH was raised to 9. When the pH of NMD was raised to greater than 11, about 100 % of Mg^{2+} as $Mg(OH)_2$ was found to be removed and significant amounts of sulphate ions were found to precipitate out as gypsum (Madzivire, 2010). Addition of amorphous $Al(OH)_3$ to the mixture of FA and NMD at pH greater than 11 resulted in sulphate concentration decreasing from 1500-2000 mg/L to 400-500 mg/L through ettringite precipitation (Madzivire et al., 2010).

Upscale of the treatment of mine water with coal FA is hindered by the fact that large amounts of FA are required (2:1 and 3:1 using an overhead stirrer). Also the time required to take up the pH of 200 L of mine water to greater than 11 using about 67 kg of coal FA in tabulator aerator was about 44 hours (Surender, 2009). This makes the treatment process industrially not feasible as;

1. Large silos would be required to store the coal FA.
2. Long stirring times are required to neutralize the mine water.

The possible ways that can reduce the mixing time and the amount of coal FA that can be used to treat mine water are:

1. The use of superior mixing of the mine water and coal FA to enhance the dissolution of lime from FA and speed up the reactions responsible for the removal of the impurities from the mine water.
2. The use of flocculants in conjunction with the coal FA treatment process to precipitate out the sulphate from mine water.

1.4. TREATMENT OF MINE WATER USING FLOCCULANTS

Recently, Al and Fe coagulants have received considerable attention in water treatment. These coagulants include; polyaluminium chloride (PACl), aluminium chlorohydrate (ACH) and alum or $Al_2(SO_4)_3$, $Fe_2(SO_4)_3$, $AlCl_3$, $FeCl_3$, polyaluminium sulphate (PAS). These coagulants are mainly used to remove colloids (Duan and Gregory, 2003; Yang et al., 2010; Liu and Chin, 2009). Colloids are usually negatively charged and are stabilized in solution due to the repulsive force of like charges and hence will stay as separate entities in solution. The removal of these colloids by coagulants involves charge destabilization or incorporation of the impurities in an amorphous hydroxide precipitate (sweep flocculation). Charge destabilization occurs through charge neutralization when negatively charged colloids interact with positively charged hydrolysis products from Fe and Al coagulants. Addition of Al^{3+} and Fe^{3+} salts in water results in the formation of different kinds of Al and Fe hydrolysis products depending on the pH and ionic potential of the water as depicted in the scheme below (Duan and Gregory, 2003; Bratby, 2006).

$$X(H_2O)_6^{3+} \xleftrightarrow{-H^+} X(H_2O)_5OH^{2+} \xleftrightarrow{-H^+} X(H_2O)_4(OH)_2^{+} \xleftrightarrow{H^+} X(H_2O)_3(OH)_3 \xleftrightarrow{-H^+} X(H_2O)_2(OH)_4^{-}$$

The use of coagulants mainly focuses on the removal of anionic colloidal particles and does not focus on the removal of inorganic anions such as sulphate ions. Recently the removal of sulphate ions was explored using $AlCl_3$ and polyaluminium chloride (PACl) from mine water. It was discovered that the PACl and $AlCl_3$ were capable of removing sulphate ions below 200 mg/L (Silva et al., 2010). Also the use of $Al(OH)_3$ at pH greater than 10 has proved to reduce the sulphate ions to less than 400 mg/L through the precipitation of

ettringite (Madzivire et al., 2010). The chemistry of the removal of sulphate ions using $Al(OH)_3$ at pH below 10 has not been evaluated previously.

1.5. RESEARCH FOCUS

This research focuses on the following areas;

1. Studying the effect of treatment of mine water with FA and flocculants at pH less than 10. The two flocculants that are investigated are aluminium chlorohydrate (ACH) and $Al(OH)_3$. This part of research aims to understand the chemistry of the removal of sulphate ions from mine water using ACH or $Al(OH)_3$ at pH less than 10.
2. Application of the jet loop reactor for the treatment of mine water. The aim of this research was to reduce the amount of FA that is required to treat mine water using the fly ash/ettringite treatment method.
3. Studying the effect of the treatment of mine water using FA, lime and $Al(OH)_3$ on the removal of potentially toxic and radioactive elements from mine water.
4. Modelling as a predictive tool for mine water treatment options.

1.6. AIMS AND OBJECTIVES

The aims of this research are to:

1. Understand the physiochemical and radioactivity properties of mine water and coal FA.
2. Understand the form in which different ions exist in the mine water using Geochemist's workbench (GWB) geochemical modelling software.
3. Prediction of the probable stable mineral phases that form at various pH end points during treatment of mine water with coal FA using GWB geochemical modelling.
4. To understand the chemistry during treatment of mine water using the combination of coal FA and ACH or $Al(OH)_3$ to remove both the toxic metals and sulphate ions from mine water.

5. To understand the chemistry during treatment of mine water with a jet loop reactor using a combination of coal FA, lime and $Al(OH)_3$.
6. Determine the radioactivity of the water produced during treatment of mine water with coal FA.

1.7. RESEARCH QUESTIONS

1. What are the physiochemical properties of mine water, fly ash, ACH, $Al(OH)_3$ and lime used in this research?
2. Are $Al(OH)_3$ or ACH flocculants capable of removing sulphate ions from mine water?
3. What is the radioactivity of FA used in this research?
4. What is the radioactivity of mine water?
5. What are the kinetics of the removal of sulphate ions from mine water using an overhead stirrer versus using a jet loop reactor?
6. What is the radioactivity of the solid residues after the treatment of mine water using FA, lime and $Al(OH)_3$?
7. What is the radioactivity of the product water from the treatment of mine water with FA, lime and $Al(OH)_3$?

1.8. HYPOTHESES

This study has three hypotheses:

1. Flocculants are capable of removing sulphate ions from mine water.
2. Jet loop mixing enhance the kinetics of removal of sulphate ions compared to overhead mixing.
3. Potentially toxic and radioactive elements are removed from mine water during treatment of mine water with coal FA, lime and aluminium hydroxide.

1.9. DELIMITATION OF THE STUDY

The radioactivity of the Rand Uranium mine water after the treatment of the mine water was not determined because of the cost of the analysis. Otherwise the analysis was only done for the total concentration of the natural occurring radioactive materials (NORM) that were determined in the mine water and FA using ICP-OES, which are Th and U. The alpha and beta radioactivity of the treated water needs to be evaluated before the water can be reused.

1.10. THESIS OUTLINE

The outline of the thesis is composed of the following chapters apart from the Chapter 1: Introduction;

Chapter 2: Literature Review

This chapter covers the background literature related to this study. The literature reviewed includes the mine water formation and composition; different mine water treatment technologies, fly ash formation and composition, different uses of FA, disposal methods of fly ash and the radioactivity of mine water and fly ash.

Chapter 3: Methodology

Chapter 3 describes how the sampling of mine water and FA was conducted. It also details how the different experimental methods were conducted to obtain the data used to answer the research questions. It also describes the various analytical techniques employed in this research.

Chapter 4: Characterization of the mine water and fly ash

In this section the results from the characterization of the FA, lime, $Al(OH)_3$, aluminium chlorohydrate (ACH) and mine waters used in this study are presented. Characterization of the mine water included the physiochemical properties and also the distribution of the major elements in the aqueous media. The radioactivity of the FA and Rand Uranium mine

water is also discussed in this section. The distribution of the potentially toxic elements in Matla and Rand Uranium mine water was elucidated using the SpecE8 program of the Geochemist's workbench (GWB) software.

Chapter 5: Prediction of the stable mineral phases

In this chapter the results from the characterization were used to predict the possible stable mineral phases that form when the mine water sampled was treated with FA to various pH end points. The prediction was conducted using Act2 program of the GWB software.

Chapter 6: Treatment of mine water with flocculants

Chapter 6 involves the understanding of the chemistry of the removal of sulphate ions and other major contaminants when mine water was treated with FA and polished using $Al(OH)_3$ or ACH.

Chapter 7: Application of the jet loop reactor

The effect of the jet loop on the kinetics of the removal of potentially toxic elements was evaluated in this section. This was also compared to the kinetics of the removal of the same contaminants using an overhead stirrer. In this section the treatment of mine water using FA, lime and $Al(OH)_3$ in a jet loop reactor was optimized. Different combinations of FA, lime and $Al(OH)_3$ was evaluated for the treatment of mine water in a jet loop reactor.

Chapter 8: Conclusions and Recommendations

This Chapter presents the conclusions obtained in this research, which are deduced based on the results obtained in Chapter 3, 4, 5, 6 and 7. This presents the answers to the research questions that were initially highlighted in Chapter 1. Chapter 8 also presents the recommendations and future work that can emanate from the findings undertaken in this study.

References

This section lists all the periodicals, books, newspapers, websites and any form of literature that was used and cited in this research document.

CHAPTER 2: LITERATURE REVIEW

This chapter provides a literature review that covers the formation of mine water and composition of mine water. It also explains the different methods for treatment of mine water. The advantages and disadvantages of each mine water treatment technology will be highlighted in this chapter.

2.1. MINE WATER

Mine water has become a major hydrological and geochemical problem arising from human exploitation of the geosphere. Mine water composition depends on the mined ore and the chemical additives used in the mineral and hydrometallurgical processing. This means that there is no typical composition of mine waters and as a result, the classification of mine water based on its composition is difficult to achieve. A number of classification schemes of mine water have been proposed using one or several water parameters such as major cations and anions, pH and alkalinity/acidity of the mine water (Lottermoser, 2007).

Major cations and anions

The classification of mine waters in terms of their major cations and anions involves plotting the major cation (Ca^{2+}, Mg^{2+}, Na^{+}, K^{+}) and anions (Cl^{-}, SO_4^{2-}, CO_3^{2-}, HCO_3^{-}) on Piper or trilinear diagrams. The plots are then applied in classifying the waters according to their cation and anion abundances.

pH

Another way of classification is by the pH of the water which classifies mine water based based on pH as acidic, alkaline or circumneutral (Morin and Hutt, 1997).

Alkalinity vs acidity

A further method to classify mine water is to distinguish mine waters according to their ability to be treated using either anaerobic or aerobic passive treatment. Acidic mine drainage (AMD) requires anaerobic treatment while alkaline mine water require aerobic treatment (Younger et al., 2002). Acidic mine drainage is characterized by low pH (usually

less than 3), being heavy-metal-laden and containing high sulphate ions. Neutral mine drainage is characterized by neutral pH, transition metal-poor with moderate concentration of ions.

2.1.1. ACID MINE DRAINAGE

Mining exposes geology that is being mined to oxygen and water, therefore allowing the oxidation of minerals that are in the reduced state. The oxidation can occur either underground or on the surface. The most common types of these minerals are the metal sulphides (Table 2.1.1).

Table 2.1.1: Important metal sulphides that occur in mining regions (Lottermoser, 2007).

Name of compound	Chemical formula
Pyrite	FeS_2
Marcosite	FeS_2
Pyrrhotite	Fe_xS_x
Chalcocite	Cu_2S
Covellite	CuS
Chalcopyrite	$CuFeS_2$
Molybdenite	MoS_2
Millerite	NiS
Galena	PbS
Sphalerite	ZnS
Arsenopyrite	FeAsS

Pyrite and marcosite are the most common metal sulphides found in coal deposits and other mineral deposits. The oxidation of pyrite in the presence of water produces sulphuric acid that in turn causes chemical weathering of the bedrock. This leads to the leaching and dissolution of the toxic metals into the water. The sulphuric acid acidifies the water, introducing sulphate ions and heavy metals into the water, thereby creating AMD which in turn pollutes groundwater and surface water.

Figure 2.1.1: Mine water released into the environment in the West Rand basin of the Witwatersrand Goldfields.

Upon exposure of sulphide bearing minerals such FeS_2, to O_2 and water during mining operations, the minerals are oxidized to form AMD according to the following set of reactions (Stumm and Morgan, 1996):

$$2FeS_2 + 7O_2 + 2H_2O \rightarrow 2Fe^{2+} + 4SO_4^{2-} + 4H^+ \quad \text{.....2.1}$$

$$4Fe^{2+} + O_2 + 4H^+ \rightarrow 4Fe^{3+} + 2H_2O \quad \text{.....2.2}$$

$$4Fe^{3+} + 12H_2O \leftrightarrow 4Fe(OH)_3 + 12H^+ \quad \text{.....2.3}$$

$$FeS_2 + 14Fe^{3+} + 8H_2O \rightarrow 15Fe^{2+} + 2SO_4^{2-} + 16H^+ \quad \text{.....2.4}$$

In the initial step, FeS_2 reacts with O_2 and water to produce Fe^{2+}, SO_4^{2-} and acidity (Equation 2.1). The conversion of Fe^{2+} to Fe^{3+} in Equation 2.2 has been termed the rate

determining step for the overall sequence, because at pH values below 5 under abiotic conditions the rate of this reaction is very slow (Stumm and Morgan, 1996). However, Fe-oxidizing bacteria, principally *Acidothiobacillus sp*, accelerate the reaction rate by orders of magnitude, so the activities of the bacteria enhance the generation of AMD (Johnson and Hallberg, 2003). The third step involves the hydrolysis of Fe^{3+} to form the $Fe(OH)_3$ precipitates and releases additional acidity (Equation 2.3). This third reaction is pH dependent. Under very acid conditions (pH < 3.5), the solid hydroxide does not form and Fe^{3+} remains in solution, and at high pH values, $Fe(OH)_3$ precipitate forms. The fourth step involves the autocatalysis oxidation of additional FeS_2 by Fe^{3+} (Equation 2.4). More of Fe^{3+} is generated by the initial oxidation reactions in steps one and two. This cyclic propagation of acid generation takes place rapidly and continues until the supply of Fe^{3+} or FeS_2 is exhausted. Oxygen is not required for the fourth reaction to occur. The overall pyrite reaction series is among the most acid-producing of all weathering processes in nature. AMD is produced if acid producing minerals are far more abundant than acid neutralizing minerals. Acid base accounting (ABA) for acid producing minerals and acid neutralizing minerals can be used as an initial step to predict if a certain geology can produce AMD, neutral or alkaline mine water during and after mining (Skousen et al., 1990).

The oxidation of sulphide minerals produces acidity and this enhances the leaching of heavy metals (Fe, Cu, Pb, Zn, Cd, Co, Cr, Ni, and Hg), metalloids (As and Sb), other elements (Al, Mn, Si, Ca, Na, K, Mg and Ba) and SO_4^{2-} from other minerals associated with the FeS_2 containing rock. Acid mine drainage is characterized by low pH, high concentration of Fe and Al (greater than 100 mg/L), elevated amounts of Cu, Cr, Ni, Pb, and Zn (greater than 10 mg/L) and SO_4^{2-} (greater than 1000 mg/L) (Lottermoser, 2007).

The products of AMD formation, acidity and Fe, can devastate water resources by lowering the pH and coating stream bottoms with $Fe(OH)_3$, forming the orange coloured "yellow boy" common in areas with abandoned mines. As acidity increases, very few living things can tolerate the harsh conditions. The corrosive acid water also attacks culverts and bridge abutments, resulting in a shorter than normal life span for exposed infrastructure.

Small amounts of AMD can harm the life in streams because the metals, SO_4^{2-} and/or other suspended solids precipitate out of the water and coat the rocks and gravel on the stream bottom. When this happens, the flora and fauna that live on and under the rocks literally are smothered because they cannot get oxygen out of the water. High levels of Na make the water unsuitable for irrigation while hardness influences the toxicity of heavy metals such as Zn (Lottermoser, 2007).

2.1.2. NEUTRAL MINE DRAINAGE

A low pH is not a universal characteristic of all the mine waters. In AMD, SO_4^{2-} is the principal anion and Fe, Mn and Al are major cations. In contrast NMD, SO_4^{2-} and HCO_3^- are principal anions and the concentrations of Ca, Mg and Na are generally elevated compared to Fe and Al (Cravotta et al., 1990). Depending on the geology that is being exploited by mining the resultant water that comes from the mine water or from the mine tailings can be acidic, neutral or alkaline. Naturally occurring carbonates and silicates are capable of neutralizing the acidity that is produced during sulphide mineral oxidation. Carbonate minerals include calcite ($CaCO_3$), dolomite ($CaMg(CO_3)_2$), magnesite ($MgCO_3$) and ankerite ($Ca_2MgFe(CO_3)_4$) deposits, which neutralize acidity (Equation 2.5) that is produced during pyrite oxidation.

$$FeS_2 + 2CO_3^{2-} + \tfrac{15}{4}O_2 + \tfrac{3}{2}H_2O \rightarrow Fe(OH)_3 + 2SO_4^{2-} + 2CO_2 \quad \text{.....2.5}$$

The most common and fast reacting carbonate is $CaCO_3$ and its solubility depends on the proton concentration as shown in the following equation.

$$CaCO_3 + H^+ \leftrightarrow Ca^{2+} + HCO_3^- \quad \text{.....2.6}$$

This reaction will buffer pH at near neutral (6.5-7), while in more acidic environments the carbonate is completely neutralized to CO_2 and H_2O.

$$CaCO_3 + 2H^+ \leftrightarrow Ca^{2+} + CO_2 + H_2O \quad \text{.....2.7}$$

Silicate minerals also consume H^+ protons and leach base cations (Ca, Mg, and Fe), alkali elements (Na, K) and dissolved Si and Al into the tailing water (Blowes and Ptacek, 1994). The dissolution of aluminosilicate minerals is slower than that of metal hydroxides and much slower than that of carbonates. Feldspar ($KAlSiO_3O_8$) weathering is mainly controlled by pH, silica, Na, K, and Ca concentrations. The reaction path is feldspar to kaolinite ($Al_2Si_2O_5(OH)_4$) and then gibbsite ($Al(OH)_3$) as shown in Equations 2.8 and 2.9.

$$2KAlSiO_3O_8 + H_2O + 16H^+ \leftrightarrow Al_2Si_2O_5(OH)_4 + 2K^+ + 14OH^- \quad \text{.....2.8}$$

$$Al_2Si_2O_5(OH)_4 + 5H_2O \leftrightarrow 2Al(OH)_3 + 2H_4SiO_4 \quad \text{.....2.9}$$

The formation of kaolinite from feldspar consumes acidity and generates alkalinity (Equation 2.8). Hydrolysis of kaolinite to gibbsite does not consume or produce alkalinity (Equation 2.9).

Neutral mine drainage is produced when the acid producing capacity and the neutralizing capacity of the geology to be exploited during mining is almost equal. The NMD is characterised by pH 6-7, moderate amounts of SO_4^{2-} and low concentration of metals, especially Fe and Al. This is due to the precipitation of the metals as hydroxides and SO_4^{2-} as gypsum due to the neutralization by the carbonates that are found associated with the FeS_2. Although the generic term AMD (or acid rock drainage) is used frequently to describe mine water discharges, the pH of these waters may be above 6, particularly at the point of discharge (where dissolved O_2 concentrations are frequently very low). In the case of Fe and Mn, these metals are generally present in their reduced (Fe^{2+} and Mn^{2+}) ionic states in anoxic AMD, and these forms of the metals are much more stable at higher pH than the fully oxidized (Fe^{3+} and Mn^{4+}) ions.

Some AMD streams remain neutral-to-alkaline, although others show a marked decline in pH as they oxygenate. This is because the total (or net) acidity derived both from proton acidity (H^+ concentration) and mineral acidity (the combined concentration of soluble metals, notably Fe, Al, and Mn, which produce protons when they are hydrolysed) is greater than acid neutralizing capacity (Lottermoser, 2007). The net acidity in AMD needs to be offset against any alkalinity present; this is chiefly in the form of bicarbonate (HCO_3^-)

deriving from the dissolution of basic minerals (calcium carbonate), although biological processes may also generate alkalinity in AMD streams (Johnson and Hallberg, 2005).

2.1.3. PREDICTION OF MINE WATER TYPE

Knowing the type of mine water that can be produced from a particular geology to be exploited during mining is vital in order to decide on the strategies for treating the effluent. In predicting the type of mine water that can be produced the following information is required:

- The amount of acid producing minerals
- The amount of acid neutralizing minerals
- The kinetics of acid producing processes
- The kinetics of acid neutralizing processes

Determining the amount of acid producing and acid neutralizing minerals is the first step in predicting the type of mine water to be produced. The amount of acid producing minerals gives the value of acid producing potential (APP) and the amount of acid neutralizing minerals give the acid neutralizing potential (ANP). This is achieved by acid base accounting (ABA) technique, which involves the determination of APP and ANP values (Skousen et al., 1990). The difference between ANP and APP gives the net neutralizing potential (NNP):

$$ANP - APP = NNP$$

Acid producing potential values are obtained based on the following stoichiometric equations (Cravotta et al., 1990):

$$FeS_2 + 2CaCO_3 + \tfrac{15}{4}O_2 + \tfrac{3}{2}H_2O \rightarrow 2SO_4^{2-} + Fe(OH)_3 + 2Ca^{2+} + 2CO_2 \quad \text{.....2.10}$$

$$FeS_2 + 4CaCO_3 + \tfrac{15}{4}O_2 + \tfrac{7}{2}H_2O \rightarrow 2SO_4^{2-} + Fe(OH)_3 + 4Ca^{2+} + 4HCO_3^- \quad \text{.....2.11}$$

In an open system (under oxic conditions), FeS_2 oxidation and neutralization allows CO_2 gas produced to escape into the atmosphere as shown in Equation 2.10. Under anoxic

conditions (in a closed system), HCO_3^- is produced in the system (Equation 2.11). This is because the CO_2 produced reacts with H_2O in situ thereby producing HCO_3^-.

Acid producing potential is the potential of the sample containing reduced minerals such as sulphide minerals to produce acidity after oxidation. Sulphide minerals include iron minerals pyrite (FeS_2) and pyrrhotite ($Fe_{1-X}S_X$), and metallic sulphides such as chalcopyrite ($CuFeS_2$), sphalerite (ZnS), galena (PbS), etc. The sulphide sulphur can be determined stoichiometrically from Equations 2.10 and 2.11 depending on the system, hence acid generation potential in % w/w $CaCO_3$ can be determined. However some SO_4^{2-} containing minerals such as $FeSO_4.7H_2O$, brochantite ($Cu_4(SO_4)(OH)_6$), jarosite ($KFe_3(SO_4)_2(OH)_6$), and alunite ($KAl_3(SO_4)_2(OH)_6$) produce acidity on hydrolysis. If these minerals occur in substantial amounts there is a need to include their contribution (Sobek et al., 1978); otherwise sulphide S may be assumed as the acid producing parameter for calculation of the APP value.

Translating mineralogical data into ANP values proved to be a complex process that is prone to errors; chemical procedures have therefore been developed as a substitute for mineralogical procedures (Lawrence and Wang, 1997). However, to maximise the information obtained from chemical procedures in mine water prediction, mineralogical data should be complemented with chemical data for ANP determination.

A number of chemical procedures for the determination of ANP exist (Lapakko, 1994; Lawrence and Wang, 1997; Skousen et al., 1997). These are:

- Lapakko Neutralisation Potential Test
- BC Research Inc. Initial Test
- Modified Acid Base Accounting Procedure for Neutralization Potential
- Peroxide Siderite Correction for Sobek Method

These methods all involve the following steps in the determination of ANP:

- reaction of a sample with a mineral acid of measured quantity
- determination of the base equivalency of the acid consumed
- conversion of the measured values to % w/w $CaCO_3$

2.1.4. RADIOACTIVITY OF MINE WATER

The geology that contains pyrite (FeS_2) together with radioactive containing elements such as U and Th, could form mine drainage with radioactive materials. This is because when FeS_2 is oxidized in the presence of H_2O and O_2, it forms acidic water that in turn dissolves the radioactive containing minerals. Gold ores in the Witwatersrand basin contains about 3 % FeS_2, U, Th, Ra and Pb (Scott, 1995; Durand, 2012). Mining of Au in the Witwatersrand basin leaves FeS_2 exposed to H_2O and O_2 in mine tailing and mine voids. Therefore the mine water from the mine voids and mine tailings in the basin is acidic and contains elevated concentration of radioactive elements such as U, Th, Ra and Pb in addition to heavy metals such as Fe, Al, Mn, Ca and Mg.

Radioactivity is the disintegration of the nucleus of an unstable atom by emitting particles containing ionization energy. Three type of radiation particles are alpha, beta and gamma.

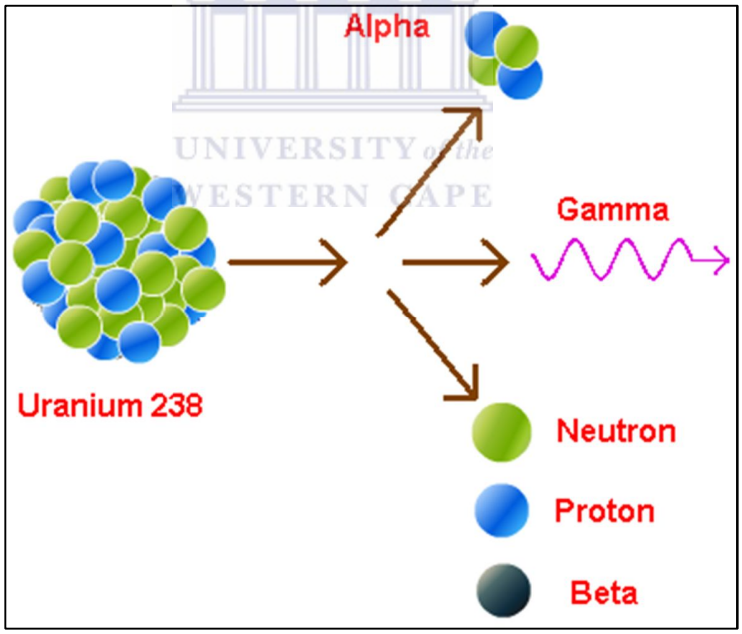

Figure 2.1.2: Schematic representation of different types of radioactive decay of an unstable atom (http://chemistry.tutorvista.com/nuclear-chemistry/radioactivity.htmL).

Alpha particles are produced when the nucleus of an unstable atom loses two protons and two neutrons (He-nucleus), while beta radiation occurs when a nucleus of an unstable atom loses either a positron or an electron. Gamma radiation is produced when the nucleus that was left in an excited state after alpha or beta decay loses excess energy to attain a stable state. An alpha particle is positively charged, the beta particle is neutral while the gamma particle can be negative (electron) or positive (positron). Different radioactive particle have different penetrating potential. An alpha particle can be stopped by a sheet of paper, while a beta particle can penetrate a sheet of paper but cannot pass through an aluminium foil. The gamma particle can pass through an aluminium foil but can be reduced significantly by a thick block of lead.

Mine water from Au and U mines is usually contaminated with radioactive elements such as U and its decay products such as Ra and Th. Naturally, the most abundant isotope is ^{238}U (99.27 %) with a half-life of 4.5×10^{9} years. Other isotopes that exist in nature are ^{235}U (0.72 %) and ^{234}U (0.006 %). The half-life of ^{235}U and ^{234}U are 7.04×10^{8} and 2.46×10^{5} years respectively (Bonotto et al., 2009). Uranium exists in various oxidation states of +2, +3, +4, +5 or +6). The most stable oxidation states are +4 and +6. The uranium (IV) state mainly exists as species which are highly insoluble in the natural environment and therefore are generally far less mobile than U(VI). In nature Th exists mainly as ^{232}Th with half-lives of 1.4×10^{10} years (Paschoa and Steinhäusler, 2010). The radioactive decay series of U and Th form various nuclides and the end product is a stable ^{206}Pb isotope as shown in Figure 2.1.3.

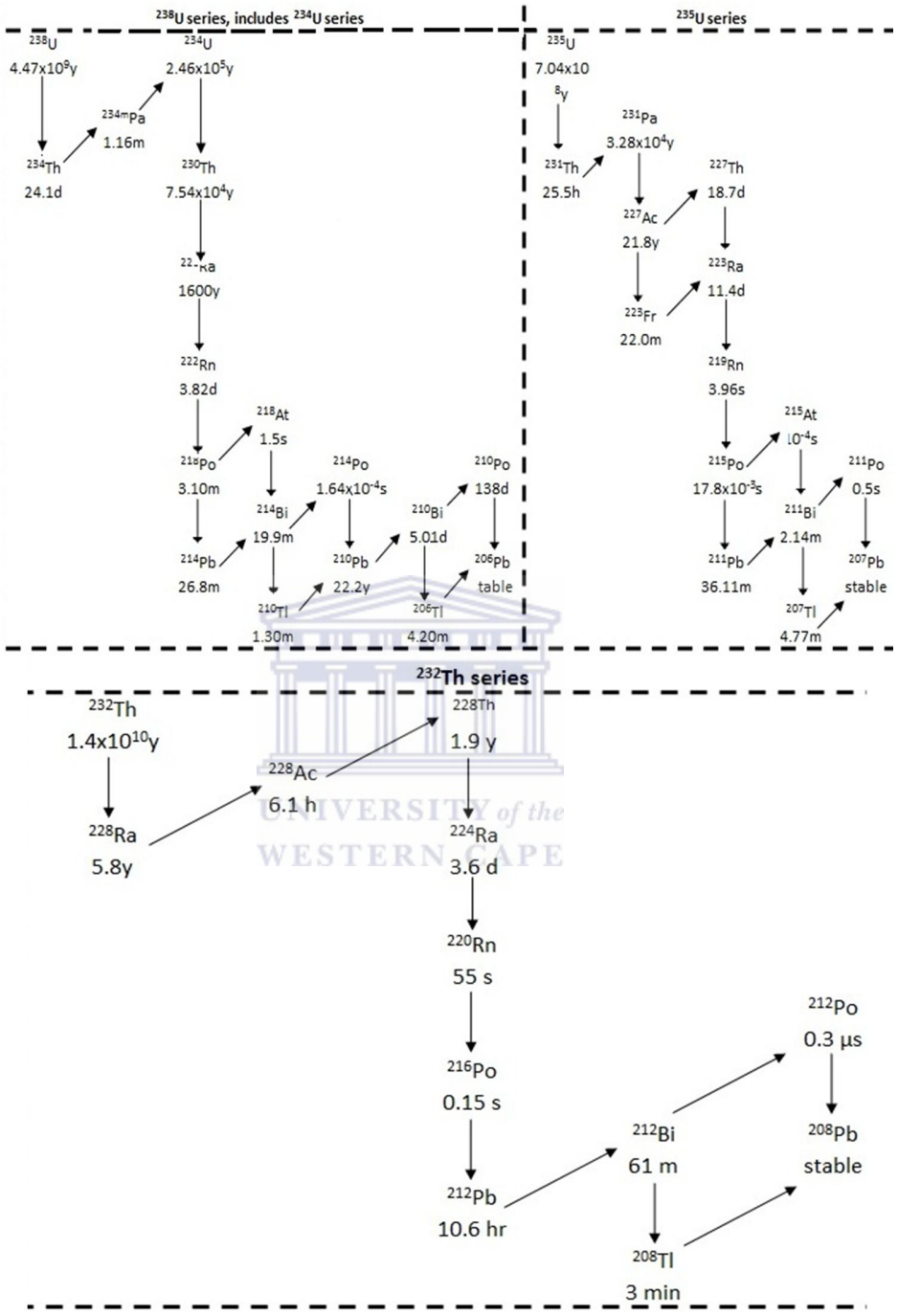

Figure 2.1.3: The radioactive decay series of ^{238}U, ^{235}U and ^{232}Th (*Arrows pointing downwards represent an alpha decay and the arrows pointing upwards represent beta decay*) (http://www.world-nuclear.org/info/inf30.htmL).

The varied decay intermediates have different geochemical properties and therefore are fractionated into different geological environments. In acidic aqueous media, the chemistry of U and Th generally exist as free cations. Each isotope in the ^{238}U, ^{235}U and ^{232}Th decay series has a unique fingerprint of alpha and gamma decay energies that can be used to identify and quantify each radioisotope as shown in Table 2.1.2 and Table 2.1.3.

Table 2.1.2: Alpha energy particle (MeV) in the ^{238}U, ^{235}U and ^{232}Th with absolute intensity greater than 5 % (Bonotto et al., 2009).

^{238}U decay series			**^{235}U decay series**		
nuclide	energy	intensity	nuclide	energy	intensity
^{238}U	4.15	20.9	^{235}U	4.21	5.7
	4.2	79		4.37	17
^{234}U	4.72	28.4		4.4	55
	4.77	71.4		4.41	2.1
^{230}Th	4.62	23.4	^{231}Pa	4.74	8.4
	4.69	76.3		4.95	22.8
^{226}Ra	4.6	5.6		5.01	25.4
	4.78	94.4		5.03	20
^{222}Rn	5.49	99.9		5.06	11
^{218}Po	6	100	^{227}Th	5.76	20.4
^{214}Po	7.69	100		5.98	23.5
^{210}Po	5.3	100		6.04	24.2
^{232}Th decay series			^{223}Ra	5.61	25.7
nuclide	energy	intensity		5.72	52.6
^{232}Th	3.95	21.7		5.75	9.2
	4.01	78.2	^{219}Rn	6.42	7.5
^{228}Th	5.34	27.2		6.55	12.9
	5.42	72.2		6.82	79.4
^{224}Ra	5.45	5.1	^{215}Po	7.39	100
	5.68	94.9	^{211}Bi	6.28	16.2
^{220}Rn	6.29	99.9		6.62	83.8
^{216}Po	6.78	100			
^{212}Bi	6.01	7.5			
	6.05	69.9			
	6.09	27.1			
	6.3	38.8			
	6.34	52.2			
^{212}Po	8.78	100			

Table 2.1.3: Gamma emissions (MeV) related to negative beta emitting radioisotopes in the ^{238}U, ^{235}U and ^{232}Th decay series with absolute intensity greater than 1 % (Bonotto et al., 2009).

^{238}U decay series			**^{232}Th decay series**			**^{235}U decay series**		
nuclide	energy	intensity	nuclide	energy	intensity	nuclide	energy	Intensity
^{234}Th	0.063	4.8	^{228}Ra	0.014	1.6	^{231}Th	0.026	14.5
	0.092	2.8	^{228}Ac	0.099	1.3		0.084	6.6
	0.093	2.8		0.129	2.4	^{211}Pb	0.405	3.8
^{214}Pb	0.053	1.2		0.209	3.9		0.427	1.8
	0.242	7.4		0.27	3.5		0.837	3.5
	0.295	19.3		0.328	3			
	0.352	37.6		0.338	11.3			
	0.786	1.1		0.409	1.9			
^{214}Bi	0.609	46.1		0.463	4.4			
	0.665	1.5		0.772	1.5			
	0.768	4.9		0.794	4.2			
	0.806	1.2		0.836	1.6			
	0.934	3		0.911	25.8			
	1.12	15.1		0.965	5			
	1.155	1.6		0.969	15.8			
	1.238	5.8		1.588	3.2			
	1.281	1.4		1.631	1.5			
	1.378	4	^{212}Pb	0.239	43.3			
	1.402	1.3		0.3	3.3			
	1.408	2.2	^{212}Bi	0.04	1.1			
	1.509	2.1		0.727	6.6			
	1.661	1.2		0.785	1.1			
	1.73	2.9		1.62	1.5			
	1.764	15.4	^{208}Tl	0.277	6.3			
	1.847	2.1		0.511	22.6			
	2.118	1.1		0.583	84.5			
	2.204	5.1		0.763	1.8			
	2.448	1.6		0.86	12.4			
^{210}Pb	0.046	4.2		2.614	99			

The energies shown in Table 2.1.2 and Table 2.1.3 can be used to identify the respective radionuclides using alpha or gamma spectrometry respectively. The height of a peak with particular energy can be used to quantify the radionuclides in the samples based on the calibration with known concentration of specific radionuclides.

2.1.4.1. Guidance levels for radioactive nuclides in drinking water

Radioactivity species identification in drinking water is a very expensive and sophisticated process. The screening steps used to identify if the water is suitable for drinking purposes in terms of radioactivity is as shown in Figure 2.1.4 below.

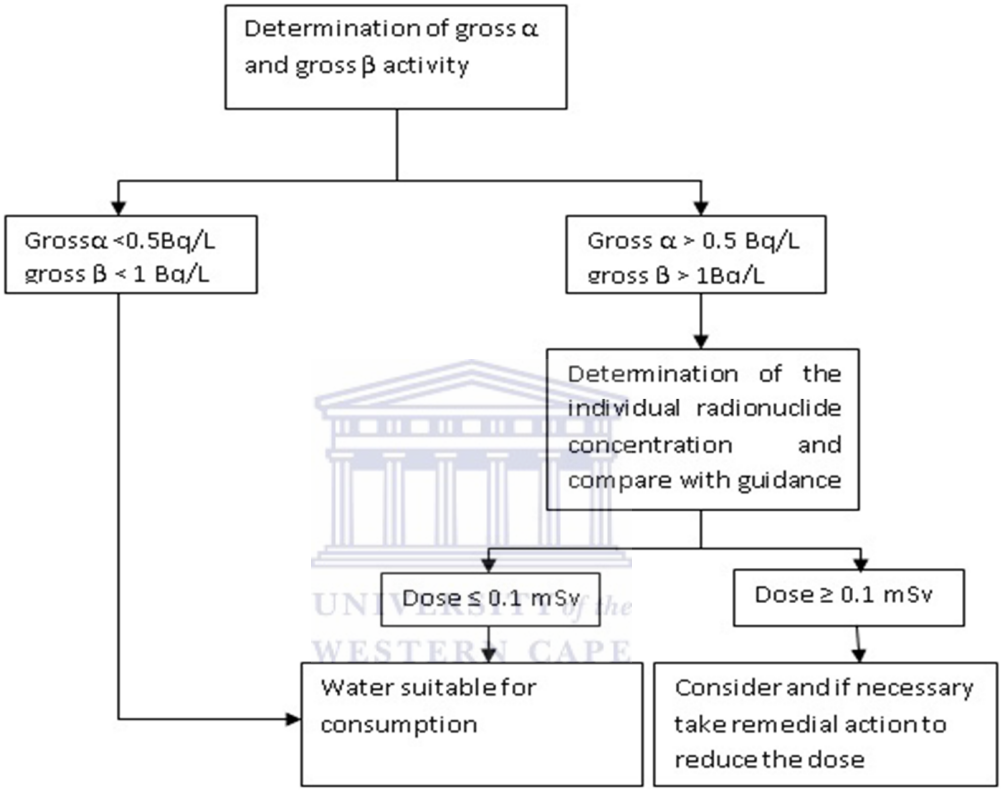

Figure 2.1.4: The outline of the screening process for the suitability of drinking water in terms of radioactivity (WHO, 2011).

The first step before determining the concentration of individual radionuclides in water is to determine the gross alpha and gross beta activity of the water. If the gross alpha and beta are less than 0.5 Bq/L and 1 Bq/L respectively, the water will be suitable for drinking in terms of radioactivity (WHO, 2011). On the other hand if the gross alpha and beta activities are greater than 0.5 and 1 Bq/L respectively then the concentration of the individual radionuclide should be measured and compared to the World Health Organization (WHO) guidelines. If the dose is at most 0.1 mSv, the water is suitable for drinking. If the dose is

greater than 0.1 mSv then remedial action should be undertaken. A dose of at most 0.1 mSv is achieved if the following formula is satisfied:

$$\sum_i \frac{C_i}{GL_i} \leq 1$$

Where, C_i= measured activity of radionuclide *i*, and GL_i is the guideline concentration of radionuclide at an intake of 2 litres per day for one year. This will result in an effective dose of 0.1 mSv per year (WHO, 2011).

2.2. TREATMENT OF MINE WATER

Mine water treatment is complex and very expensive. The complexity of mine water treatment is because of the diversity of mine water composition. High costs associated with mine water treatment are due to the complexity and diversity of mine water composition, which means there is no "one-fits-all" treatment option for mine water treatment. Mine water treatment options can be broadly classified as passive or active methods. Active treatment of mine water requires frequent monitoring of the system, while passive mine water treatment does not require continuous monitoring of the treatment systems.

2.2.1. PASSIVE MINE WATER TREATMENT

Passive mine water amelioration is the use of natural occurring resources to promote chemical and biological processes to remove contaminants from mine water in systems designed in such a way that they require infrequent monitoring. Passive mine water treatment can be broadly classified as biological and chemical methods (Younger et al., 2002).

(a) (b)

Figure 2.2.1: Typical passive biological (a) and chemical (b) treatment of mine water systems (INAP, 2012).

Biological passive treatment involves directing contaminated mine water through an environment containing sulphate reducing bacteria or plants (Hedin et al., 1994; Wieder and Lang, 1982; Neculita et al., 2007; Steed et al., 2000). The wetlands remediate mine water through adsorption, reduction and oxidation of the pollutants. Passive chemical methods involve passing contaminated mine water through drains filled with limestone gravel where mine water is neutralized and contaminants are removed mainly through precipitation. The other two types of passive mine water treatment systems can be classified as chemical, biological or both, depending on the inputs for the systems. These systems are successive alkalinity producing systems and reactive barriers.

The advantages of passive treatment methods for mine water are:

- Inexpensive
- Does not require frequent monitoring
- More pleasant in appearance than active treatment systems
- No use of chemicals that produce sludge that can be a liability.
- Can be integrated into the surrounding ecosystem.

The disadvantages of passive treatment of mine water are:

- Recovery of treated water is very minimum

- Require extensive land area to accommodate high flow and/or highly contaminated discharges of mine water
- The quality of process water is not guaranteed since the process is not monitored frequently.

2.2.1.1. Wetlands

Wetlands are a complex ecosystem where wastewater is channelled, and remediation occurs through physical, chemical and biological processes (Wieder and Lang, 1982). Wetlands are usually applied to coal mine drainage. This is because coal mine water contains relatively low concentration of metals and is mildly acidic or alkaline compared to AMD from metal mines (Younger et al., 2002). Constructed wetlands fall into two categories; aerobic and anaerobic wetlands. Aerobic wetlands are suitable for treatment of net alkaline mine waters. Anaerobic wetlands are suited for passive remediation of net acidic mine waters (Johnson and Hallberg, 2004).

Aerobic wetlands

Aerobic wetlands are designed to allow metal oxidation and precipitation and are normally shallow, vegetated and have surface flow predominating (Robb and Robinson, 1995; Mayes et al., 2009).

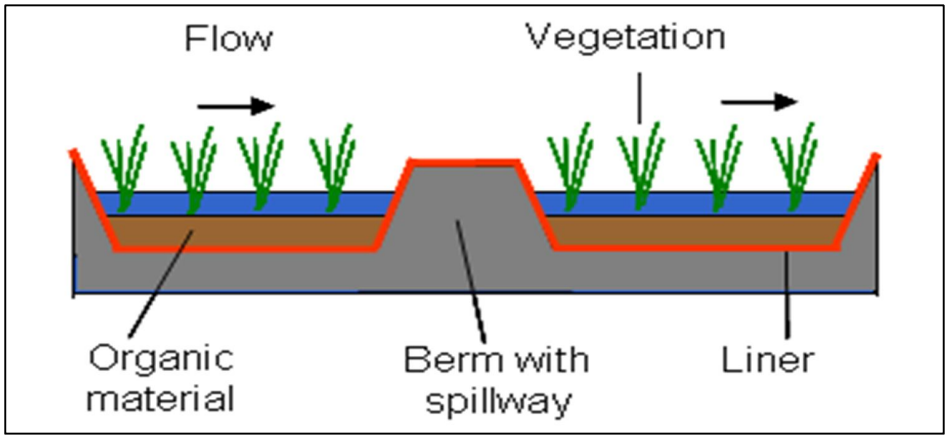

Figure 2.2.2: Schematic representation showing the movement of mine water through an aerobic wetland (http://wiki.biomine.skelleftea.se/biomine/srb/index_08.htm).

Oxidation and hydrolysis reactions commonly cause concentrations of Fe^{2+}, Fe^{3+}, Mn^{2+}, and Al^{3+} to decrease when mine water flows through an aerobic environment. Whether these reactions occur quickly enough to lower metal concentrations to an acceptable level depends on the availability of oxygen for oxidation reactions, the pH of the water, the activity of microbial and/or other catalysts and inhibitors, and the retention time of water in the treatment system (Neculita et al., 2007; Gazea et al., 1996).

The pH is an especially important parameter because it influences both the solubility of metal hydroxide precipitates and the kinetics of the oxidation and hydrolysis processes. The relationship between pH and metal-removal processes in passive treatment systems is complex because it differs among metals and also between abiotic and biotic processes. The stoichiometries of the major metal removing reactions in passive treatment systems are:

$$Fe^{3+} + 3H_2O \leftrightarrow Fe(OH)_3 + 3H^+ \quad \text{.....2.12}$$

$$Al^{3+} + 3H_2O \leftrightarrow Al(OH)_3 + 3H^+ \quad \text{.....2.13}$$

$$Fe^{2+} + \tfrac{1}{4}O_2 + \tfrac{5}{2}H_2O \rightarrow Fe(OH)_3 + 2H^+ \quad \text{.....2.14}$$

$$Mn^{2+} + \tfrac{1}{4}O_2 + \tfrac{3}{2}H_2O \rightarrow MnOOH + 2H^+ \quad \text{.....2.15}$$

The first two Equations (2.12 and 2.13) are simple hydrolysis reactions. They require only the presence of water and enough alkalinity to neutralize the H^+ produced. The neutralization of acidity produced in Equations 2.12 and 2.13 shifts the equilibrium reactions to the right by removing the H^+ protons from the product side and adding more H_2O to the reactants side by Le Chatelier's principle. Equations 2.14 and 2.15 require the presence of O_2 to oxidize the metal prior to hydrolysis. All of the reactions produce acidity. The goal of passive treatment systems is to drive these reactions to completion and collect the resulting solids before the water enters a receiving stream and hence the prerequisite that the input water should be net alkaline for aerobic wetlands to be effective (Hedin et al., 1994).

Anaerobic wetlands

In anaerobic wetlands the mine water flows through an organic layer containing sulphate reducing bacteria (SRB).

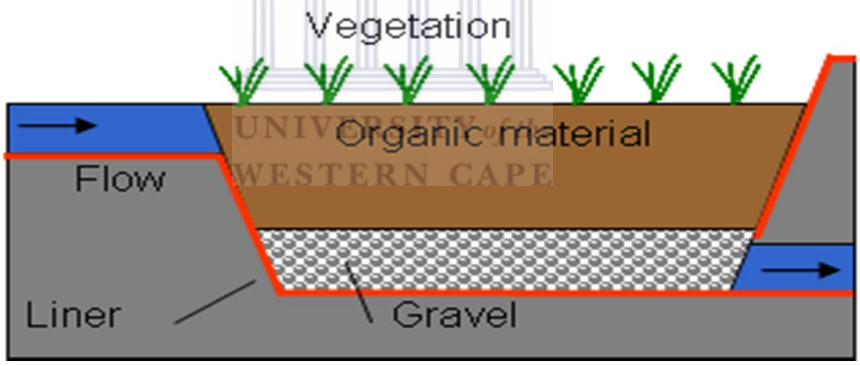

Figure 2.2.3: Schematic diagram showing movement of mine water through an anaerobic wetland (http://wiki.biomine.skelleftea.se/biomine/srb/index_08.htm)

The organic layer traps the O_2 from the mine water. The water chemistry is affected by bacterial sulphate reduction. Bacteria oxidize organic compounds using SO_4^{2-} as the terminal electron acceptor and release H_2S and HCO_3^{2-}.

$$2CH_2O + SO_4^{2-} \rightarrow H_2S + 2HCO_3^{2-} \quad \text{.....2.16}$$

CH_2O represents organic matter (Postgate, 1984). Bacterial sulphate reduction not only improves water quality by the addition of bicarbonate alkalinity, it can also lower the concentrations of dissolved metals, M^{2+} (Fe^{2+}, Mn^{2+}, Zn^{2+}, Ni^{2+}, Cu^{2+}, Cd^{2+}, Pb^{2+}) by precipitating them as metal sulphide (MS) solids:

$$M^{2+} + H_2S + 2HCO_3^- \rightarrow MS + 2H_2O + 2CO_2 \quad \text{.....2.17}$$

This means that the toxic H_2S gas should in theory not be released into the environment as it is converted to MS (Equation 2.17). In the case of Fe, the formation of FeS and even pyrite (FeS_2) is possible.

$$Fe^{2+} + H_2S + S \rightarrow FeS_2 + 2H^+ \quad \text{.....2.18}$$

The removal of dissolved metals as sulphide compounds depends on pH, the solubility product of the specific metal sulphide, and the concentrations of the reactants (Hammack et al., 1993). The first metal sulphide that forms is CuS, followed by PbS, ZnS, and CdS. FeS is one of the last metal sulphides to form. MnS is the most soluble metal sulphide known, and is not expected to form. Due to the low solubility of some of these metal sulphides relative to their solubilities as oxides or hydroxides, SO_4^{2-} reduction can be an important process in lowering some metal concentrations to acceptable levels, particularly heavily metal laden AMD (Gazea et al., 1996; Neculita et al., 2007).

Sulphate reducing bacteria require the presence of sulphate ions, suitable concentrations of low molecular weight carbon compounds as an energy source, and the absence of oxidizing agents, such as O_2, Fe^{3+} and Mn^{4+}. These conditions are commonly satisfied in treatment systems that receive AMD and are constructed with an organic substrate, such as a compost material. High concentrations of sulphate ions are characteristic of contaminated AMD. The O_2 demand of organic substrates causes the development of anoxic conditions and an absence of oxidized forms of Fe or Mn. The low molecular-weight compounds that SRB utilise (lactate, acetate) are common end-products of microbial fermentation processes in

anoxic environments. These sulphate reducing and fermentative bacteria are more active above pH 5. However, they can be very active in drainages with lower pH levels, due to the presence of near-neutral pH microenvironments. These microenvironments allow the SRB to become established, and because they generate alkalinity, these microenvironments are increased.

2.2.1.2. Open limestone drains

Limestone drains are one of the passive chemical methods to remediate mine water. To make up open limestone drains (OLD), open ditches are filled with crushed limestone. Mine water flows over the limestone resulting in the dissolution of calcite ($CaCO_3$), which is the major mineral in limestone. The dissolution of $CaCO_3$ produces alkalinity thereby neutralizing the pH. This results in the increase in pH, HCO_3^-, OH^- and Ca^{2+} according to the following reactions (Stumm and Morgan, 1996; Cravotta and Trahan, 1999):

$$CaCO_3 + H^+ \leftrightarrow Ca^{2+} + CO_2 + H_2O \quad \text{.....2.19}$$

$$CaCO_3 + H_2O + CO_2 \leftrightarrow Ca^{2+} + 2HCO_3^- \quad \text{.....2.20}$$

$$CaCO_3 + H_2O \leftrightarrow Ca^{2+} + HCO_3^- + OH^- \quad \text{.....2.21}$$

Increase in pH of the mine water results in the removal of soluble Al, Fe and Mn due to precipitation as hydroxides. Sulphate ions react with Ca^{2+} that dissolves from limestone to form gypsum (Mukhopadhyay et al., 2007; Ziemkiewicz et al., 1997; Nairn et al., 1991).

$$Fe^{3+}(aq) + 3HCO_3^-(aq) \rightarrow Fe(OH)_3(s) + 3CO_2(g) \quad \text{.....2.22}$$

$$Al^{3+}(aq) + 3HCO_3^-(aq) \rightarrow Al(OH)_3(s) + 3CO_2(g) \quad \text{.....2.23}$$

$$Ca^{2+}(aq) + SO_4^{2-}(aq) \leftrightarrow CaSO_4.2H_2O(s) \quad \text{.....2.24}$$

Open limestone systems work effectively when mine water flows over a long distance before exiting the treatment system. This is because as Fe and Al precipitate from the AMD,

the limestone gets coated or armoured by the metal hydroxides and thereby the solubility of limestone is reduced and the system becomes ineffective over time and needs replacement.

2.2.1.3. Anoxic limestone drains

Anoxic limestone drains (ALD) are made up of limestone that is buried in trenches using clay soil or plastic to prevent oxygen from coming in contact with the mine water. As the AMD flows through, the limestone dissolves and alkalinity is added to the mine water resulting in pH being increased (Equations 2.19, 2.20 and 2.21). To prevent the limestone from becoming coated or armoured with precipitated metal hydroxides, the AMD must not come into contact with oxygen throughout the ALD channel (Cravotta and Trahan, 1999; Hedin et al., 1994).

Deep mine discharges often have no oxygen, so the water can be channelled directly into the drain, which is covered with clay and/or plastic liners to avoid oxygen ingression. If the AMD is already oxygenated, the water must be put through an anaerobic wetland in which organic material removes the oxygen, after which the water is channelled into the ALD. A major source of HCO_3^- in many anoxic environments is the dissolution of carbonate minerals, such as $CaCO_3$. Sulphate ions are removed during ALD treatment of mine water through the precipitation of gypsum (Equation 2.24). After the net alkaline waters pass through the ALD, then the water is exposed to atmospheric conditions and Fe^{3+} is produced by the oxidation of Fe^{2+}. Hydroxide mineral of Fe^{3+} is then produced as shown in Equation 2.22 (Nairn et al., 1991).

Higher concentrations of HCO_3^- occur in anoxic mine water environments than oxic environments. This is because of the absence of precipitated $Fe(OH)_3$ in most anoxic environments that may armour carbonate surfaces and inhibit further $CaCO_3$ dissolution in oxic environments. The solubility of carbonate compounds are directly affected by the partial pressure of dissolved CO_2 as shown in Equation 2.23 (Cravotta and Trahan, 1999; Stumm and Morgan, 1996). Anoxic mine water environments commonly contain high CO_2 partial pressures due to the decomposition of organic matter and the neutralization of

proton acidity. This results in the dissolution of more $CaCO_3$, thereby producing more alkalinity and Ca^{2+} ions, therefore enhancing the removal of heavy metal as hydroxides and sulphate ions as gypsum.

Although ALD produce alkalinity at a lower cost than constructed compost wetlands, they are not suitable for treating all AMD waters. In situations where the AMD contains significant concentrations of Fe^{3+} or Al^{3+}, the short-term performance of ALDs may be good, but the build-up of hydroxide precipitates gradually decreases drain permeability, which may cause failure of the drain within six months of construction (Johnson and Hallberg, 2005). This means that ALD systems are more efficient in handling mine water with Fe^{2+}.

2.2.1.4. Successive alkalinity producing systems

Successive alkalinity producing systems (SAPS) are composed of a compost layer above a bed of limestone layer.

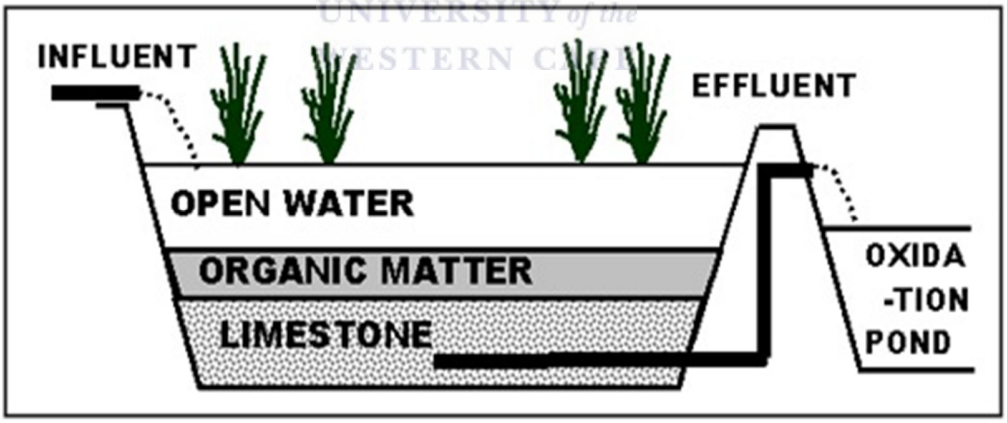

Figure 2.2.4: The schematic representation of a typical SAPS for mine water treatment (Jagea et al., 2001).

Mine water drains past through the compost layer where dissolved O_2 is removed from the water. This creates a suitable environment for sulphate reducing bacteria (SRB) in the

middle of the compost layer. The SRB reduces sulphate according to Equation 2.16 producing bicarbonate alkalinity and H_2S. The alkalinity neutralizes the acidity in the mine water and the H_2S reacts with metal contaminants to produce metal sulphide precipitates. The anoxic conditions created by the compost layer cause the reduction of Fe^{3+} to Fe^{2+} thereby reducing the armouring potential of the water (Keplar and McCleary, 1994; Nairn and Mercer, 2000). When the water enters the limestone layer more alkalinity is produced through limestone dissolution.

After the water has passed through two successive alkaline producing systems (organic and limestone layers) the water drains into a settling tank where it is oxygenated and the metals precipitate out. Enough residence time is required in the settling tank to allow the precipitation of the metals. The alkalinity produced by SRB or limestone dissolution should be enough to buffer the acidity that is produced in the aerobic ponds in order to produce effluent water with a suitable pH that can be discharged into the environment (Nairn and Mercer, 2000).

2.2.1.5. Reactive barriers

Permeable reactive barriers (PRBs) can be classified as chemical or biological passive treatment depending on the reactive material used. Construction of PRBs involves digging of a trench in the flow path of contaminated groundwater. The void is filled with reactive materials (a mixture of organic solids or limestone gravel or zero valent iron) that are sufficiently permeable to allow unimpeded flow of the groundwater, and landscaping of the disturbed surface as shown in Figure 2.2.5.

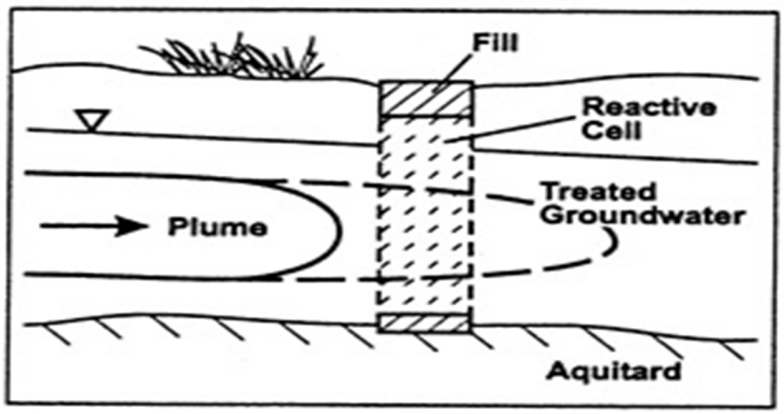

Figure 2.2.5: The schematic diagram of permeable reactive barrier (Gavaskar, 1999)

Alkalinity is generated due to dissolution of limestone (Equations 2.19, 2.20 and 2.21) or microbiological processes (Equation 2.16) or the oxidation of zero valent iron (Equations 2.25 and 2.26) within the PRB. Metals are removed as sulphides, hydroxides, and carbonates (Younger et al., 2002; Gavaskar, 1999).

$$2Fe + O_2 + 2H_2O \rightarrow 2Fe^{2+} + 4OH^- \quad \text{.....2.25}$$

$$Fe + 2H_2O \rightarrow Fe^{2+} + H_2 + 2OH^- \quad \text{.....2.26}$$

2.2.1.6. Selection of a passive mine water treatment system

Choosing the best passive mine water system depends on the flow rate and the chemical composition of the mine water. The following steps in Figure 2.4.6 are used to select the most ideal passive treatment method.

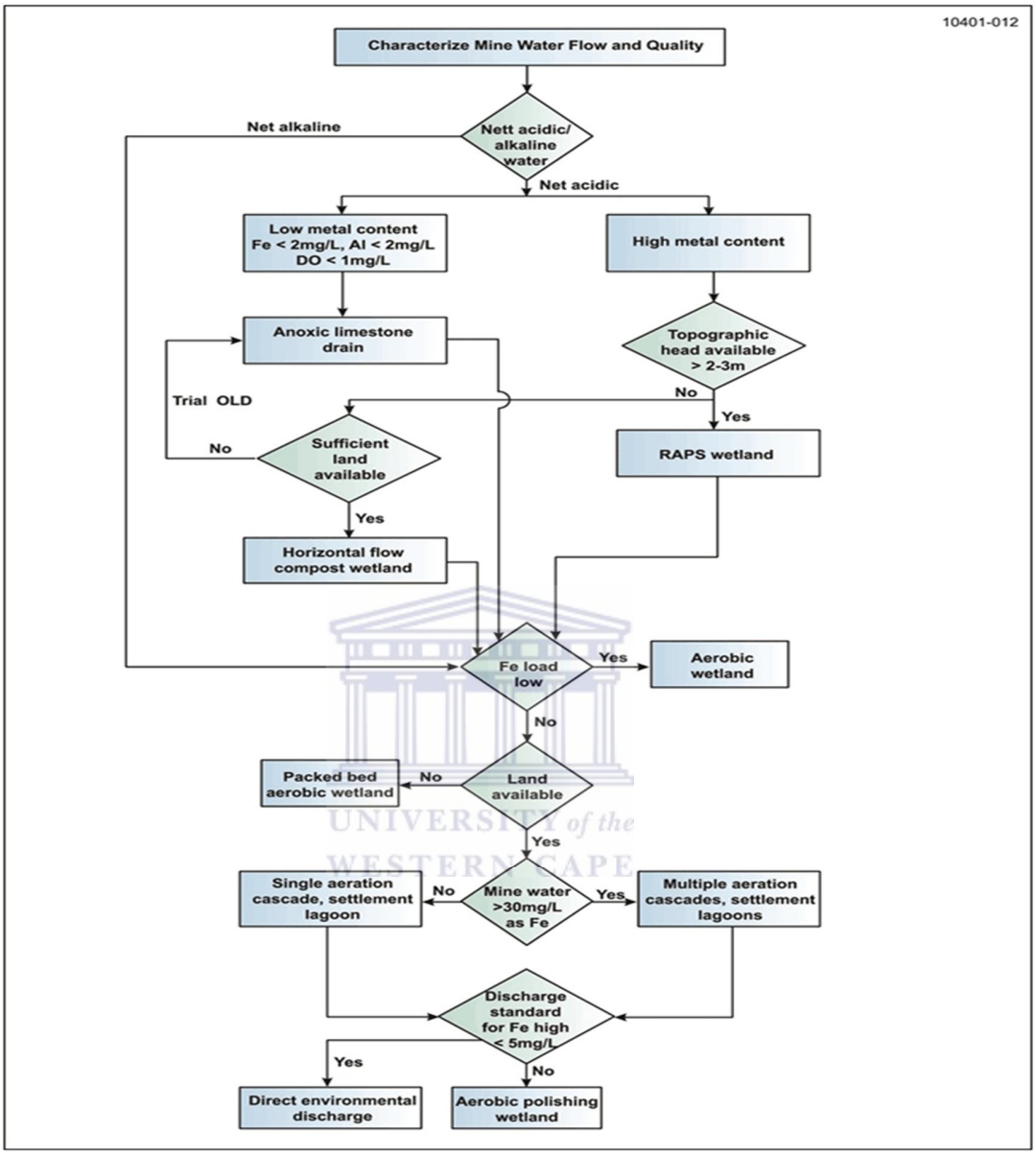

Figure 2.2.6: The flow diagram for selecting the most ideal passive mine water treatment system based on the water chemistry and flow (Hedin et al., 1994; INAP, 2012).

As highlighted earlier, passive systems cannot properly remediate high flow rates of highly contaminated mine water. Also if there is no enough space to set up a passive treatment

facility, active mine water treatment plant should be set up to produce a particular quality of product water.

2.2.2. ACTIVE TREATMENT OF MINE WATER

Active treatments of mine water are technologies that improve the water quality of mine water through processes that require continuous inputs of artificial energy, biochemical or chemical reagents (Young et al., 2002). Active treatment methods are recognized by the presence of a water treatment plant that is monitored regularly by a skilled workforce. The major advantage of active treatment is the capability to handle any changes in mine water quality and quantity, because of the precise process control in response to these changes. Active treatment is also a preferred technique to passive treatment if the land availability is a limiting factor. The major disadvantage of active treatment method is that the brines and sludge that are produced as wastes are expensive to handle and dispose. The continuous input of energy, reagents and the need of skilled manpower to run and maintain the treatment plant makes these techniques expensive. Due to vast differences in the chemistry of mine waters and the variety of physical, chemical and biological methods for separating metals from mine water, there is a wide range of treatment technologies that can be applied for active mine water treatment. The choice of a suitable treatment technology depends on:

- The mine water quality
- The mine water quantity
- The treated water quality required
- Cost of the treatment technique

In reality, there is no technical limit to the quality of the water which can be achieved using current existing techniques, but the cost is the limiting factor. Therefore the selection of a treatment technique comes down to economic and environment cost benefit analysis.

2.2.2.1. Sulphate reducing bioreactors

Bioreactors represent an active treatment approach for remediating AMD (Johnson, 2000). These engineered systems have potential advantages over passive biological remediation in that their performance is more predictable and readily controlled. The concentrations of sulphate and heavy metals in processed waters may be significantly lowered to potable standards depending on the process control of the system. On the negative side, the construction and operational costs of these systems are considerable.

Bioreactors utilize the biogenic production of H_2S (Equation 2.16) to generate alkalinity and to remove metals as insoluble sulphides (Equation 2.17 and 2.18). The SRB used in the bioreactors are sensitive to even moderate acidity. Therefore the treatment systems should be engineered such that the microorganisms are not exposed to the inflowing AMD (Rowley et al., 1997; Johnson and Hallberg, 2005). This is done by mixing AMD with H_2S generated in the biological sulphate reduction so that the metals are precipitated out as metal sulphide. If the process is controlled carefully in terms of pH and H_2S, selective separation of metal sulphide can be achieved.

The water that has been treated using H_2S is then subjected to biological reduction where sulphate ions are reduced to H_2S. The energy sources for SRB include alcohols, sugars, sewage sludge, H_2, etc. If the total acidity is greater than the alkalinity produced by SRB, additional alkali will be added chemically. The use of H_2 as an energy source is advantageous because it is more economical to use for high sulphate ions loadings and results in lesser production of bacterial biomass. Hydrogen may conveniently be formed by cracking CH_3OH or from natural gas. In both cases, CO_2 is also produced, and some SRB are able to fix this as their source of carbon (Johnson and Hallberg, 2005).

2.2.2.2. Membrane technologies of mine water treatment

Membrane systems remove contaminants by selectively allowing only certain ions to pass through the pores of the membranes by size exclusion (reverse osmosis, nano-filtration, ultrafiltration and microfiltration). Membrane systems that use a combination of size exclusion and electric charge to remove contaminants from water are called electro dialysis.

Membrane treatment can be classified as secondary processes for treatment of mine water. This is because these systems require pre-treatment of mine water to remove suspended solids to reduce fouling of membranes.

Microfiltration

Microfiltration is the purification of water by passing it through membranes with pore size ≥0.1 µm and < 0.45 µm. Removal of bacteria is achieved but viruses, colloids, colour and solutes remain in the water.

Ultrafiltration

Ultrafiltration involves passing contaminated water through membranes with pore sizes between 0.01 µm and 0.1 µm. The treated water is free from colloids and microorganisms, but still contains solutes. Ultrafiltration and microfiltration can be used as pre-treatment options for nano-filtration and reverse osmosis (RO) treatment of mine water to produce drinking water.

Nano-filtration

Nano filtration uses a pressure gradient to separate ions through a porous membrane. The pores on nano-filtration membranes are greater than 0.001 µm and less than 0.01 µm. Nano-filtration is capable of separating bigger divalent anions, such as sulphate and organic molecules, from water and monovalent small cations (Kentish and Stevens, 2001).

Reverse osmosis

Reverse osmosis is a pressure driven membrane process in which the solution is transferred through a semi-permeable membrane (pore size < 0.001 µm). During this process a substantially high pressure difference across the membrane is necessary to overcome the osmotic pressure difference between the salt free permeate and the saline reject solution (brine). The smaller water molecules are literally pushed through the semi-permeable membrane, while the larger solute species are retained. This process is the “reverse” of

natural osmosis, which involves water diffusion from a dilute to concentrated region through a semipermeable membrane.

The principle by which these membranes choose or reject ions, are based on size and electrical charge (Kentish and Stevens, 2001; Matsuura, 2001). Although RO and UF are perceived as an economically feasible desalination process for specialized applications, these techniques are yet to overcome certain drawbacks which include the following (Del Pino and Durham, 1999):

- Extremely high operating pressures are required to overcome osmotic pressure gradients leading to substantial increase in energy consumption, and the fact that such plant installations and operation are relatively costly, makes this an exceedingly expensive treatment option.
- Another major problem is the membrane susceptibility to fouling by suspended solids, colloidal material, or certain dissolved ions such as Fe^{3+}, Al^{3+}, Mn^{2+}, Ca^{2+} and sulphate ions in the feed water. The implications of fouling are irreversible membrane damage, reduced flux rates and increased capital and operating costs.
- One critical issue for the successful application of RO is pre-treatment. Pre-treatment has to ensure that the quality of the effluent fed to the RO membranes is consistent to avoid variability in the feed water quality. Pre-treatment on its own has high costs attached to it.
- The basic principle on which RO operates is size exclusion, therefore selectivity for specific metal ions is restricted and as such limits the scope of the process.

Nano filtration operating costs are lower compared to RO. This is because of increased permeability of nano-filtration membrane due to bigger pore size than RO membranes.

One of the technologies that have been tested for RO technology is the slurry precipitation and recycling reverse osmosis (SPARRO). This technology is applied after the mine water has been pre-treated by neutralization using an alkali, followed by clarification to remove colloids and suspended solids. The pre-treated water is then fed to tubular RO membranes

where the pure water is separated from dissolved salts called reject, as shown in Figure 2.2.7 (Pulles et al., 1992; Juby et al., 1996).

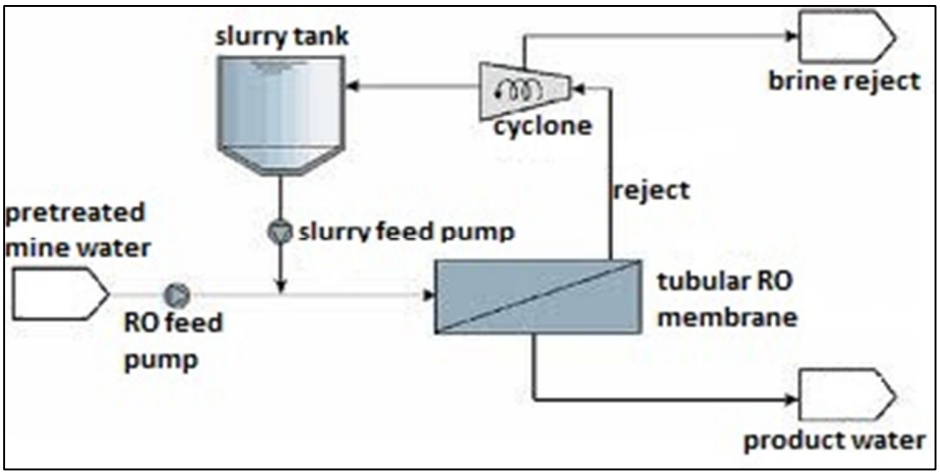

Figure 2.2.7: Flow diagram of the SPARRO water treatment technology (Pulles et al., 1992).

The pre-treated water is mixed with slurry containing gypsum crystals from the cyclone before reaching the RO membrane. This initiates gypsum precipitation from the water which is saturated with respect to gypsum. The precipitated gypsum crystals are removed from the water through blow downs before the water is passed through tubular RO membranes. The cyclone receives the reject from RO membrane, where gypsum crystals are separated from the brine. The advantages of the SPARRO over the normal RO include (Juby et al., 1996):

- reduced power consumption
- reduced pump wear and scaling problems

Electro dialysis

Electro dialysis (ED) is an electrochemical separation process which involves the selective movement of aqueous ions through ion selective membranes as a result of an applied electrical potential difference (Valerdi-Perez et al., 2001). An ED system consists of two oppositely charged electrodes, a cathode and anode, with a number of compartments in-

between. These compartments are separated by alternative cation and anion exchange membranes, filled with polluted water as shown Figure 2.2.8.

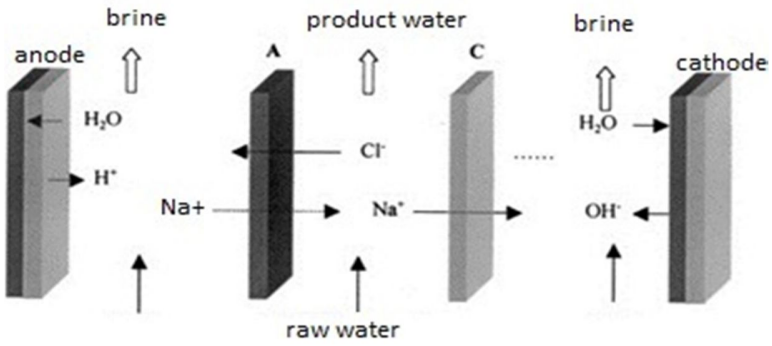

Figure 2.2.8: Schematic diagram of the electro dialysis cell (A-anion resin and C-cation resin) (Tongwen, 2002).

When the electrical potential difference is introduced in an ED cell (Figure 2.2.8), electrochemical reactions such as the reduction of water at the cathode and oxidation at the anode propel the ions through the selective membranes (Valerdi-Perez et al., 2001, Tran et al., 2012). The rate and direction of movement of ions depend on:

- its charge,
- solution conductivity,
- relative concentrations and
- applied voltage.

The anions migrate through the anion exchange membrane into the adjacent compartment toward the anode. Cations move through a cation resin towards the cathode. Two main streams flow in parallel. One stream is progressively desalted and is referred to as the product water. The other stream is dewatered and is referred to as the salt rich stream or brine.

Electro dialysis systems are prone to fouling. To reduce membrane fouling in ED systems, the polarity reversal process was developed. This process involves periodic charge reversal

(anode is changed to cathode and vice-versa) and is referred to as electro dialysis reversal (EDR). This results in the reversal of the direction of ion movement within the membrane configuration. The dilute stream then becomes the concentrate stream and vice versa. Reversing the polarity of electrodes will flush out scale and other deposits on the membrane walls. This increases the life span of the membrane (Del Pino and Durham, 1999). Consequently the EDR treatment system has reduced sensitivity to scaling and fouling compared to normal ED treatment systems.

The ED/EDR plant operation efficiency increases with an increase in feed water temperature and consequently at a typical plant, a preheating stage, which raises the temperature of the feed water to approximately 35°C immediately prior to the ED/EDR is included (Schoeman and Steyn, 2001). The increased energy input arising from the heating process evidently adds to the capital and process costs (Schoeman and Steyn, 2001).

The presence of contaminants including suspended solids, high molecular weight dissolved solids, organic compounds and colloids in the feed water may give rise to membrane fouling resulting in irreversible membrane damage. Therefore feed water pre-treatment also exerts a pivotal role in ED/EDR process treatment performance, by trying to ensure that the water fed to the ED/EDR membranes is of a consistently quality. In order to maintain optimum performance of ED/EDR systems, membrane stacks need to be cleaned intermittently to remove scale and other surface foulants (Del Pino and Durham, 1999). Normal cleaning is usually done by a cleaning-in-place (CIP) system, which utilizes special cleaning solutions that are circulated through the membrane stack; however, the membrane stack needs to be periodically disassembled, cleaned and reassembled at regular intervals for effective removal of scalants and other potential surface foulants (Schoeman and Steyn, 2001).

The major disadvantage of ED/EDR systems, as is the case in all other membrane systems, is that membranes have a limited lifetime before fouling or failure of adhesive bonds necessitates replacement. The costs of periodic replacement are an expensive expedient and need to be included in any analysis of their economic viability (Kentish and Stevens, 2001). The water to the ED/EDR needs to adhere to specific guidelines pertaining to pH, organic constituents, turbidity and other characteristics. The system is equipped with

pH adjustment chemicals (normally acid, e.g. H_2SO_4), as well as imbedded cartridge filters to alleviate source water contamination and as such, adds to the operating costs.

2.2.2.3. Ion exchange

The process of ion exchange can be defined as the reversible interchange of a charged ion (cation or anion) for a similarly charged ion, between a solid material (the ion exchanger) and the surrounding liquid, in which there is no permanent change in the structure of the solid (Kitchener, 1957). Ion exchange resembles sorption, in that in both cases, a dissolved species is taken up by a solid; however, the characteristic difference between the two phenomena is that ion exchange, unlike sorption, is a stoichiometric process where every ion which is removed from the solution is replaced by an equivalent amount of another species of the same sign as shown in Figure 2.2.9. In sorption, on the other hand, a solute is taken up without being replaced by another species.

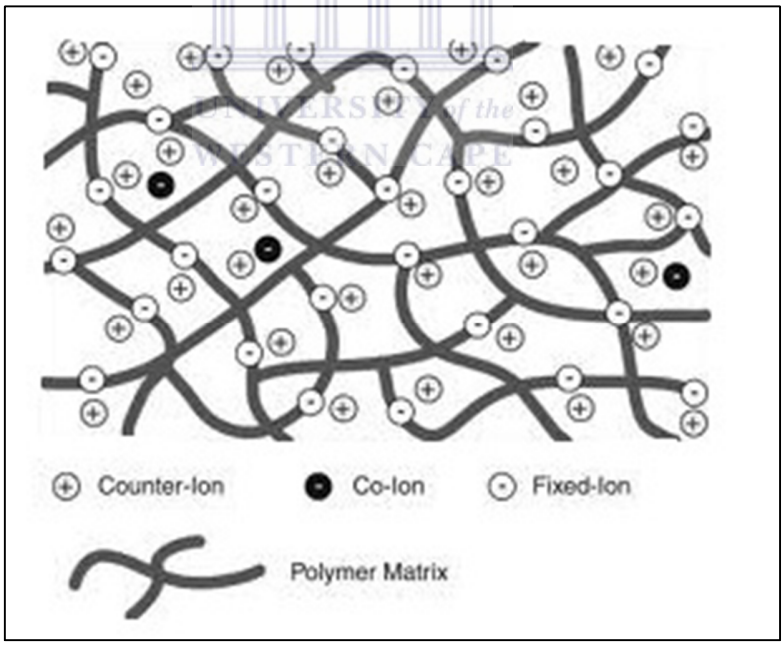

Figure 2.2.9: The diagram depicting an ion exchange phenomenon (Strathmann, 2010).

The characteristic properties of ion exchangers can be attributed to a distinctive feature in their structure. They consist of a framework, held together by chemical bonds or lattice energy and the framework carries a positive or negative electric surplus charge, which is compensated by ions of opposite sign, also referred to as counter-ions (Kitchener, 1957). The counter-ions are mobile thus able to move within the framework and can be replaced by other ions of the same sign (counter ions). However, electro-neutrality must be preserved, i.e., the electric surplus charge of the ion exchanger must be compensated at any time by a stoichiometrically equivalent number of counter-ions within the pores. A counter ion can subsequently leave the framework, only when, simultaneously, another ion enters and takes over the task of contributing its share to the compensation of the framework charge (Kitchener, 1957).

Ion exchange technologies are usually used as the polishing of the pre-treated water. Examples of the ion exchange technologies developed to polish and produce good quality water together with valuable products that can be used in industry are the GYPCIX and Environmental and Remedial Technology Holdings (EARTH) technologies.

a. GYPCIX process

This process involves the polishing of the treated water in two stages to produce water of potable standards as shown in Figure 2.2.10. Acid mine drainage is pre-treated by neutralization with alkalis, thereby removing the metals such as Fe, Al and Mn.

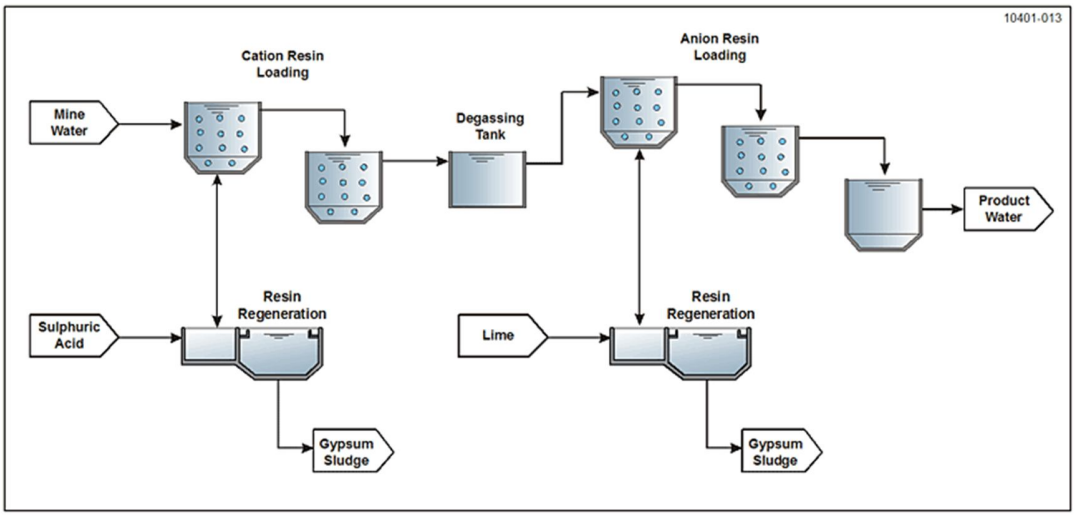

Figure 2.2.10: Process flow diagram of the GYPCIX process.

Pre-treated water is then passed through a cation resin to remove cations such as Ca, Na and K by exchanging with H^+ protons in the resin.

$$R-H+X^{n+} \rightarrow R_n \bullet X + nH^+ \quad \text{.....2.27}$$

The recovered water from the cation resin still contains an elevated concentration of sulphate ions and low pH. The water is then passed through an anion resin where the sulphate ions are exchanged with OH^- ion, thereby correcting the pH. The final product water is suitable for domestic use.

$$R-OH+SO_4^{2-} \rightarrow R_2 \bullet SO_4 + 2OH^- \quad \text{.....2.28}$$

After the ion exchange active sites have been exhausted, they are regenerated. Anions resin are regenerated using lime solution (Equation 2.29) and the cation resins are generated adding sulphuric acid (Equations 2.30 and 2.31) to produce good quality gypsum that can be used in construction.

$$R_2 \bullet SO_4 + Ca(OH)_2 + 2H_2O \leftrightarrow 2R-OH + CaSO_4.2H_2O \quad \text{.....2.29}$$

$$R_2 \bullet Ca + H_2SO_4 + 2H_2O \leftrightarrow 2R-H + CaSO_4.2H_2O \quad \text{.....2.30}$$

$$2R \bullet Na + H_2SO_4 \leftrightarrow 2R - H + 2Na^+ + SO_4^{2-} \quad \text{.....2.31}$$

2.2.2.4. Chemical treatment of mine water

Chemical treatment of mine waters involves the use of alkalis such as lime, limestone, ammonia and sodium hydroxide to neutralize acid mine water. Alkali treatment plants prefer to use limestone because it is cheaper than the other chemicals. The alkali raises the pH of the water with subsequent precipitation of metals as hydroxides. Different metal hydroxides precipitate at different pH values. Fe^{3+}, Al^{3+}, Mn^{2+} and Mg^{2+} precipitate at pH values 3, 6, 9 and 11 respectively. Barium salts such as $Ba(OH)_2$, BaS and $BaCO_3$ are also used to treat mine water specifically for sulphate precipitation.

Barium salts

Barite ($BaSO_4$) is a highly insoluble mineral (Ksp ≈ 1 x 10^{-10}). Introducing sufficient amounts of Ba^{2+} into SO_4^{2-} rich waters will result in removal of SO_4^{2-} to below 200 mg/L. The common sources of Ba^{2+} are $BaCO_3$, $Ba(OH)_2$ and BaS. Sulphates are removed according to equations (Bosman et al., 1990; Hlabela et al., 2007, Bologo et al., 2012):

$$BaCO_3(s) + 2H^+(aq) + SO_4^{2-}(aq) \rightarrow BaSO_4(s) + H_2CO_3(aq) \quad \text{.....2.32}$$

$$Ba(OH)_2(s) + 2H^+(aq) + SO_4^{2-}(aq) \rightarrow BaSO_4(s) + 2H_2O \quad \text{.....2.33}$$

$$BaS(s) + 2H^+(aq) + SO_4^{2-}(aq) \rightarrow BaSO_4(s) + H_2S(g) \quad \text{.....2.34}$$

$BaCO_3$ treatment will not remove SO_4^{2-} that are associated with Mg^{2+} in aqueous solution. This means Mg^{2+} ions should be removed from the water before Ba^{2+} can be added. This is achieved by addition of an alkali to increase the pH to 11 for $Mg(OH)_2$ precipitation before Ba^{2+} treatment. Addition of BaS results in neutralization of acidity and generation of H_2S as shown in Equation 2.34. The H_2S will react with heavy metals that might be in the mine water to metal sulphide precipitate (Equation 2.17). This means that the mine water should

have enough heavy metals to react with H_2S that is produced by the addition of BaS; otherwise the product water will contain toxic H_2S.

The presence of Ca^{2+} increases the dissolution of $BaCO_3$ (Equation 2.35) by precipitation of $CaCO_3$ according to Equation 2.36 (Hlabela et al., 2007).

$$BaCO_3(s) \leftrightarrow Ba^{2+}(aq) + CO_3^{2-}(aq) \quad \text{.....2.35}$$

$$Ca^{2+} + CO_3^{2-} \rightarrow CaCO_3(s) \quad \text{.....2.36}$$

This means that presence of Ca^{2+} will enhance SO_4^{2-} removal since more Ba^{2+} will come into solution. The dissolution of $BaCO_3$ is negatively affected by carbonate alkalinity thereby reducing the efficiency of using $BaCO_3$ to remove SO_4^{2-} (Hlabela et al., 2007). This is because the addition of CO_3^{2-} when alkalinity is increased will cause the dissolution reaction to shift to the left according to the Le-Chatelier's principle.

BaS and $Ba(OH)_2$ treatment is capable of increasing the pH to above 11, since the treatment generates alkalinity according to Equations 2.33 and 2.34 thereby precipitating $Mg(OH)_2$. Treatment of mine water using BaS and $Ba(OH)_2$ does not require alkali treatment prior to addition of Ba salts. Metals in the mine water will react with H_2S produced in reaction 2.34 to produce metal sulphides precipitates. (Adlem, 1997; Maree et al., 1989). If the metal cations present in the raw water are not stoichiometrically equivalent to the H_2S produced, then the H_2S needs to be removed before discharging the water (Hlabela et al., 2007) to avoid H_2S release into atmosphere since it is poisonous.

The major disadvantage of Ba^{2+} treatment of mine water is the cost of the salts. In addition H_2S produced by BaS is a toxic gas that needs to be removed and any failure to remove all of the gas will be fatal. The product water should have Ba concentration of less than 0.7 mg/L because Ba is a toxic element (WHO, 2011). While the chemical treatment works well to raise pH and to precipitate the metals, the treatment plants are very expensive to operate and maintain. Also the disposal of the toxic metal-laden sludge is a very big environmental problem.

Some of the major technologies that use Ba salts have been developed by Council of Scientific and Industrial Research (CSIR) of South Africa and Tswane University of Technology. These include Alkali-Barium-Calcium (ABC) and Magnesium-Barium-Alkali (MBA) technologies (Bologo et al., 2012, Beer et al., 2010).

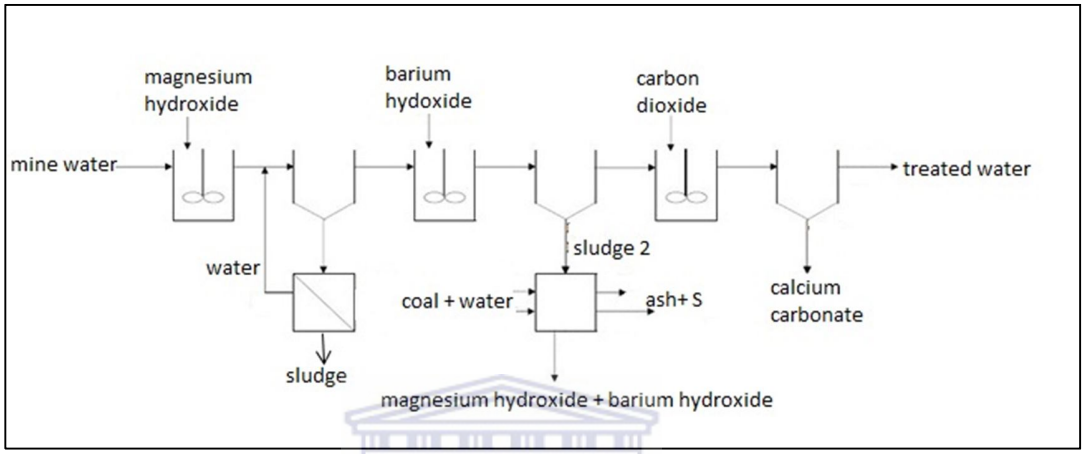

Figure 2.2.11: Process flow diagram for the MBA technology for mine water treatment (Bologo et al., 2012).

Magnesium-Barium-Alkali process involves mixing mine water with $Mg(OH)_2$. This will result in the neutralization of the mine water (Equation 2.37) and the precipitation of Fe, Al and Mn as their respective hydroxides.

$$Mg(OH)_2 + 2H^+ \rightarrow Mg^{2+} + 2H_2O \quad \text{.....2.37}$$

The sludge 1 is then separated from the water and then the water is mixed with $Ba(OH)_2$ to precipitate out sulphate and Mg ions according to Equation 2.33 and Equation 2.38 respectively. According to Madzivire et al (2011), $Mg(OH)_2$ forms at pH greater than 11.

$$Mg^{2+} + 2OH^- \rightarrow Mg(OH)_2 \quad \text{.....2.38}$$

The mixture is then separated to produce water with pH which greater than 11 and sludge 2. Sludge 2 is composed of $BaSO_4$ and $Mg(OH)_2$. The pH of the water is adjusted by bubbling CO_2 and the sludge is mixed with coal and then subjected to heat to produce ash,

S, $Ba(OH)_2$ and $Mg(OH)_2$. The $Ba(OH)_2$ and $Mg(OH)_2$ are recycled, while S can be sold to offset the costs of the treatment process.

Lime/limestone

Treatment of mine water using limestone removes acidity of the mine water by the alkalinity generated by the dissolution of limestone (Equation 2.19, 2.20 and 2.21). The sulphate concentration in mine water is decreased due to the reaction with Ca^{2+} ions from lime or limestone to form gypsum (Equation 2.24) and due to co precipitation with or adsorption on metal hydroxides.

All the metals are removed to below the allowed effluent limit (Equation 2.22 and 2.23) but sulphate concentration usually remains above the required WHO and DWA limit for potable water of less than 400 mg/L because gypsum is partially soluble in water. Solubility of gypsum ranges from 1500 mg/L to 2000 mg/L depending on the composition and ionic strength of the solution. Gypsum precipitation is reduced in the presence of Mg^{2+}, Na^{+} and K^{+} ions.

An integrated limestone/lime process was developed for reducing sulphate concentration to less than 1200 mg/L (Geldenhuys et al., 2001). This process involves the addition of limestone to pH 9. The pH is then taken up to greater than 11 using lime to precipitate out $Mg(OH)_2$ thereby enhancing the formation of gypsum. Integrated lime/limestone is cheaper than the use of only limestone to treat mine water.

The process reduces the concentration of potentially toxic elements such Fe, Al and Mn to below the effluent limit and sulphate concentration to below the saturation point of gypsum, therefore reducing the scaling potential of the water. This process is most suitable as pre-treatment for further purification using costly processes such as membrane methods.

This process produces a voluminous sludge (95 % water content) that is left after the treatment. The sludge is laden with metals that were in the mine water making it extremely expensive to handle. If the low density sludge is recycled and mixed with incoming raw AMD, high density sludge is produced with 80 % water content (Bosman, 1983). Recycled

low density sludge provides nuclei for metal hydroxide precipitation and growth as shown in Figure 2.2.12.

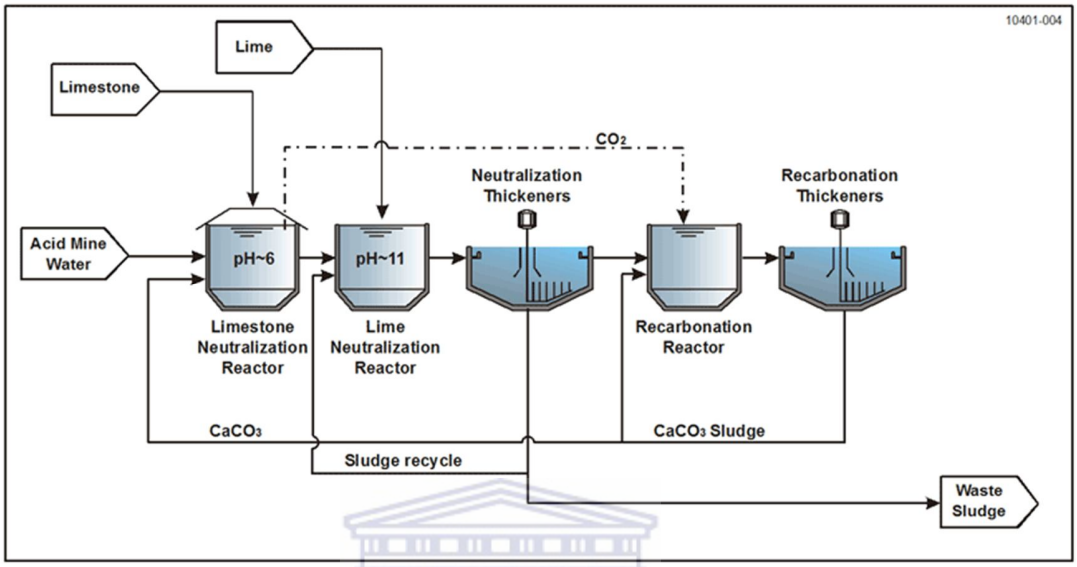

Figure 2.2.12: Flow diagram of the high density sludge treatment technology (INAP, 2012).

Lime treatment of mine water is the current emergency option that is being employed to treat decanting water in the West Rand Basin of the Witwatersrand Goldfields, South Africa. High density sludge pre-treatment of 25 ML per day of AMD from four coal mines in Mpumalanga is being carried out at Emahlahleni water treatment plant. The three mines involved are Navigation, Greenside and Kleinkopje owned by Anglo Coal and one mine owned by BHP Billiton. Water from the HDS is then treated to potable standards using High Pressure Reverse Osmosis (HiPRO).

Although the potable water is sold to the Witbank municipality to offset some of the costs of the treatment process, the income generated is not enough to make this plant sustainable. Also the process produces brine that is accumulating and very expensive to store or dispose. Research has advanced to recover valuable products such as sulphur and lime from gypsum by the process called GypSLim process (Gunter and Naidu, 2008).

SAVMIN process

The SAVMIN process involves a number of precipitation stages to remove the contaminants in AMD to produce treated water as shown in Figure 2.2.13. This process was developed by Smit (Smit, 1999; Smit and Sibilski, 2003). Mine water is mixed with lime to take up the pH to greater than 11 and in the process precipitating most metals including Mg. The metal hydroxide precipitates are separated from the water. Gypsum seeds are added to the water which is supersaturated with respect to gypsum. This further precipitates gypsum from mine water thereby further removing sulphate ions. The water, which is under saturated with respect to gypsum is then mixed with amorphous $Al(OH)_3$ where sulphate ions are further precipitated out in the form of ettringite (Equation 2.39).

$$6Ca^{2+} + 3SO_4^{2-} + 2Al(OH)_3 + 31H_2O \rightarrow 3CaO.3CaSO_4.Al_2O_3.31H_2O + 6H_2O \quad \text{.....2.39}$$

After precipitating out the sulphate as ettringite to within the potable limit of WHO and DWA, the pH of the water is still greater than 11. The pH of the water is then adjusted to 6-9 by bubbling CO_2 to form $CaCO_3$ producing water of potable standard.

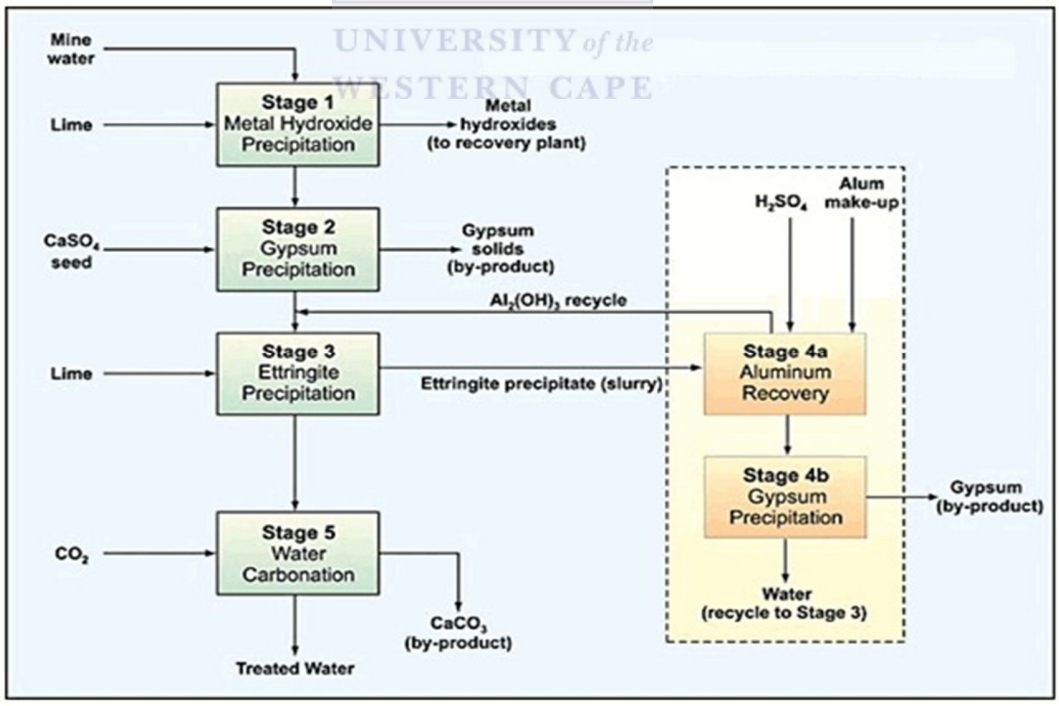

Figure 2.2.13: Flow diagram of the SAVMIN process (INAP, 2012).

Ettringite is decomposed to form $Al(OH)_3$ by adding H_2SO_4 to the ettringite containing slurry to pH between 6 and 9. The $Al(OH)_3$ recovered from the ettringite slurry is then recycled to precipitate more sulphate ions. The water obtained from the decomposition of ettringite during the recovery of $Al(OH)_3$ is supersaturated with respect to gypsum. This water is seeded with gypsum crystals to initiate precipitation of gypsum. The gypsum is separated and the water is then returned to the ettringite stage for further clean up.

Treatment of mine water has proved to be very costly. The Inter-ministerial Committee on acid mine drainage of South Africa has summarized the current and possible treatment methods that can be used as a solution for active remediation of mine water. The summary in Table 2.2.1 showed that all the treatment methods are not sustainable except the MBA technology that is still at pilot scale. This is because the difference of the running costs and the income that can be generated from the products from the treatment process is negative as shown in Table 2.2.1.

Table 2.2.1: The running costs and possible income that can be generated from the products of the various technology proposed by the Inter-ministerial Committee on acid mine drainage (Coetzee et al., 2010).

Technology	Running costs ($R.m^{-3}$)	Income ($R.m^{-3}$)	Difference ($R.m^{-3}$)
Alkali Barium Calcium	4.04	3.56	-0.49
HDS HiPRO	9.12	3.35	-5.78
SPARRO	12.79	4.29	-8.51
SAVMIN	11.30	3.84	-7.46
EARTH ion exchange	12.95	10.70	-2.25
Paques Thiopaq	8.73	5.70	-3.03
CSIRosure	8.73	6.12	-2.61
BioSURE	3.80	0.00	-3.80
MBA	2.22	5.58	3.36
Lime treatment	5.50	0.70	-4.80

Since most of the methods are not sustainable to treat mine water, research is still on going to come up with a sustainable treatment technology. Sustainability in mine water treatment can be achieved if:

1. Suitable waste materials can be used as part of the treatment of mine water or,
2. Valuable materials can be recovered from the waste materials from the treatment process.

Use of waste materials will reduce the cost of the treatment process as well as the disposal of the waste material used.

2.2.3. TREATMENT OF MINE WATER WITH COAL FLY ASH

One of the waste materials that can be used for mine water treatment is coal FA. Coal FA is found close to the most coal mines in South Africa. This will reduce the transportation costs of the FA to the treatment facility. Coal FA is an aluminosilicate waste trapped from the flue gas of the coal fired power stations to avoid atmospheric contamination. Fly ash is alkaline, containing mainly residual inorganic species that survived the combustion process to generate steam. The lime in the FA is the species that is mainly exploited for the neutralization and treatment of mine water.

Treatment of acid mine drainage (AMD) and neutral mine drainage (NMD) with coal FA was found to remove Fe and Al at pH values 4-6 and Mn was found to be removed at pH 9. Sulphate ions were found to be removed from high levels of about 18000 mg/L to between 2000 and 2500 mg/L when AMD was treated with coal FA to pH 9 (Gitari et al., 2008; Gitari et al., 2006; Surender, 2009). Treatment of NMD with FA was found to remove an insignificant amount of sulphate ions when pH was raised to 9. When pH of NMD was raised to greater than 11, about 100 % of Mg^{2+} was found to be removed and a significant amount of sulphate was found to precipitate out as gypsum (Madzivire, 2010). Addition of amorphous $Al(OH)_3$ to the mixture of FA and NMD at pH greater than 11 resulted in sulphate concentration decreasing from 4500 mg/L to approximately 400 mg/L through ettringite precipitation (Madzivire et al., 2010).

The benefits of using coal FA treatment of mine water over using lime include; the costs, produce high slurry and the solid residue have shown suitable properties for backfilling of mine voids with capacity to continuously remediate mine water (Vadapalli et al., 2008; Gitari et al., 2008, Surender, 2009). Treatment of mine water with coal FA is cheaper compared to limestone because FA is found close to the coal mines since most coal power station are built close to the coal mines. This means low transport costs of FA to the treatment facility. Since coal FA is a waste material; using FA for water treatment will go a long way to achieve zero effluent discharge in coal mines and coal fired power stations.

Upscale of the treatment of mine water with coal FA is hindered by the fact that large amounts of coal FA (2:1 and 3:1 of liquid to solid ratio) were used. This makes the treatment process industrially problematic. The amount of coal FA to treat mine water could be reduced if superior mixing techniques can be employed such as a cavitation mixing. Also if another processes could be developed and used in conjunction with coal FA treatment such as using flocculants to polish the water from coal FA treatment. Previous studies on coal FA treatment of mine water did not consider the chemistry of the radionuclides in the coal FA and/or in the mine water during treatment of mine water with coal FA.

2.2.4. RADIOACTIVITY IN COAL FLY ASH

The growing population coupled with the exponential depletion of natural resources has resulted in most research and development focusing on recycling to promote sustainability of the industrial processes. The use of coal FA in construction, agriculture and acid mine drainage treatment is some of the opportunities for the recycling of waste materials (Kovler, 2012, Madzivire et al., 2010; Gitari et al., 2008).

Fly ash is known to accumulate the incombustible constituents of coal in the combustion cycle during production of electricity. About 550 MT per year of FA is produced by coal fired powered stations worldwide. After China, USA and India, South Africa is the fourth largest producer of FA. The radioactivity of most FA all over the world was found to be orders of magnitude higher as compared to the parent coal. The concentration of U and Th in coal in American FA ranges between 1-4 mg/L (USGS, 1997; Turhan et al., 2010; Papasternou, 2010;

Baykala and Saygılı, 2011; Peppas et al., 2010). As such, there is a great need to evaluate the radioactivity of South African FA and products produced from use of coal FA.

During coal combustion to produce electricity in power stations, most of the U, Th and their decay products are released from the coal and are partitioned between the gas phase and solid phase of the combustion products. The partitioning between the gas and solid phase is controlled by the volatility and chemistry of the individual elements. Virtually 100 % of the radon gas present in the feed coal is transferred to the gas phase and is lost in stack emissions. In contrast, less volatile elements such as Th, U, and the majority of their decay products are almost entirely retained in the solid combustion wastes (USGS, 1997). The concentration of most radioactive elements in solid combustion wastes is approximately 10 times the concentration in the original coal (USGS, 1997).

The reuse of FA from South African coal power stations for water treatment or construction depends on its radioactivity. The leachability of radionuclides in FA needs to be evaluated to find out if the radioactivity will not be transferred into the product water. Also the use of FA in construction needs to be managed in such a way that the final structure is not a radioactive emitting entity.

2.2.5. FLOCCULANTS FOR TREATMENT OF MINE WATER

Wastewater impurities occur as suspended and dissolved particles. Dissolved particles are approximately 0.1 nm, while colloids are suspended particles which are greater than 0.1 nm but smaller than 1 nm (Bratby, 2006). Treatment of waste water using Al and Fe salts has been widely used to remove colloidal particles. Colloids are usually negatively charged particles which are uniformly dispersed in an aqueous media. Colloids remain as separate entities in solution because they repel each other (like charges). Removal of colloids from waste water occurs through charge neutralization and encapsulation of the impurities when hydroxide precipitates forms (sweep flocculation).

Flocculants when added into wastewater occur either as cationic or anionic forms depending on the pH of the solution. Salts of Fe and Al when added into solution dissociate

forming octahedrally bonded cations to water ligands. Depending on the properties, such as pH and ionic potential, Fe and Al ions exist as products of the following reactions;

$$X(H_2O)_6^{3+} \xleftrightarrow{-H^+} X(H_2O)_5OH^{2+} \xleftrightarrow{-H^+} X(H_2O)_4(OH)_2^{+} \xleftrightarrow{H^+} X(H_2O)_3(OH)_3 \xleftrightarrow{-H^+} X(H_2O)_2(OH)_4^{-}$$

Polynuclear products such as; $Al_2(OH)_2^{4+}$, $Al_3(OH)_4^{5+}$, $Al_8(OH)_{20}^{4+}$ and $Al_{13}O_4(OH)_{24}(H_2O)_{12}^{7+}$ exists through the interaction of the mononuclear species as depicted in the scheme 2 below (Bratby, 2006). The waste water pH therefore has to be adjusted in order to improve the performance of the flocculants. Most flocculants have been used in the removal of colloidal particles. Recently polyaluminium chloride and $AlCl_3$ have been studied for the removal of sulphate ions from mine water (Silva et al., 2010). That study has proved that sulphate ions could be removed from mine water but the chemistry of other anions such as chlorides were not investigated. The removal of sulphate ions from mine water was found to depend on pH and the amount of polyaluminium chloride or $AlCl_3$ added. The optimum pH for sulphate removal was found to be 4.5.

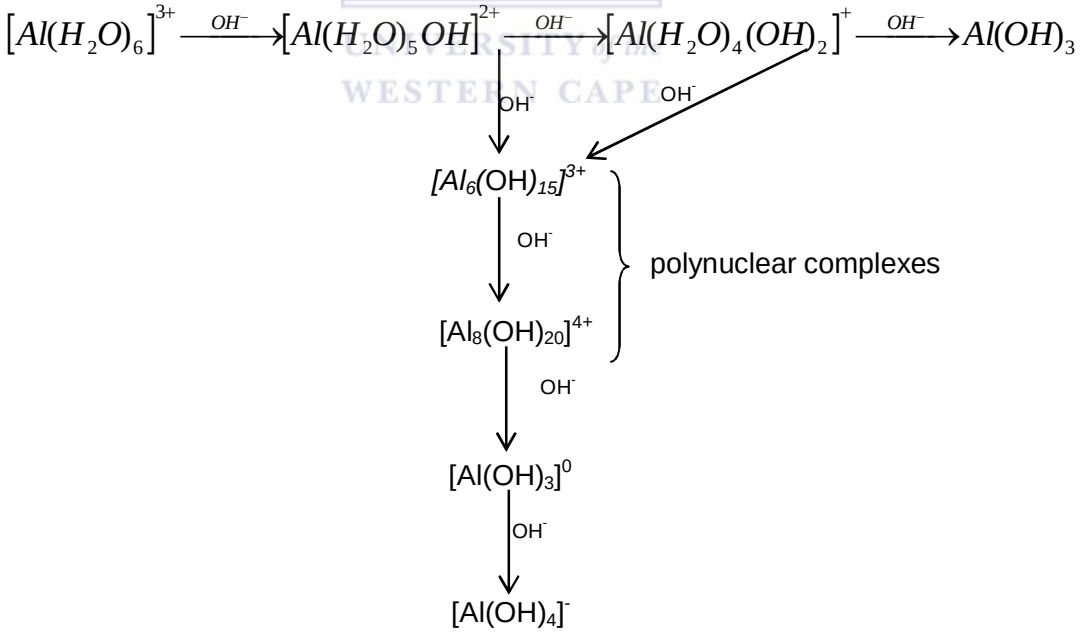

Scheme 2: The schematic diagram of the hydrolysis reaction of Al^{3+} ions in water (Bratby, 2006).

Also the removal of phosphates from water using $Al(OH)_3$ and alum was studied at different pH end points (Figure 2.2.14) and various aluminium to phosphate ratio (Georgantas and Grigoropoulou, 2007). They concluded that alum was more efficient in the removal of phosphates compared to $Al(OH)_3$ and the best removal was observed at pH 4-6 as shown in Figure 2.2.14 below. Alum is a chemical with the general formula $AB(SO_4)_2{\cdot}12H_2O$. An example of alum is hydrated potassium aluminium sulphate ($KAl(SO_4)_2{\cdot}12H_2O$).

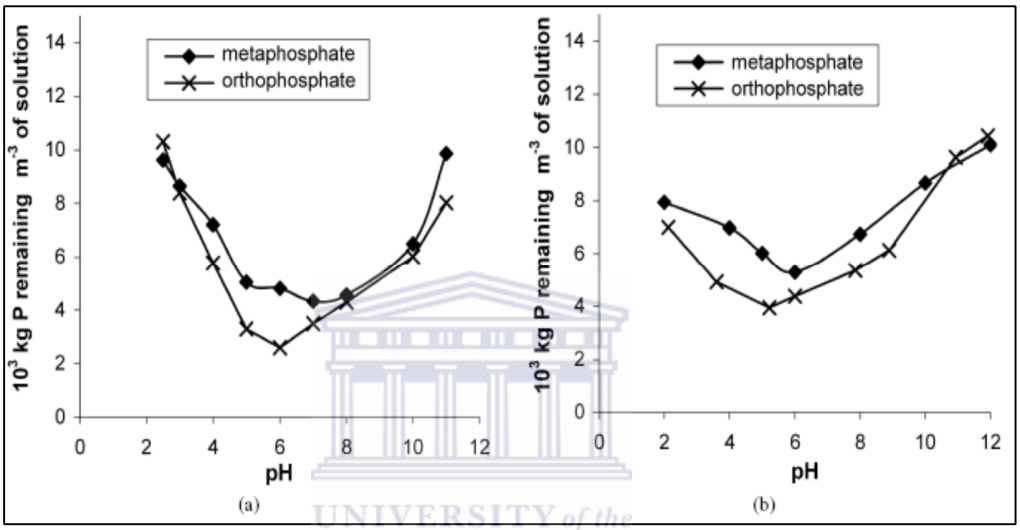

Figure 2.2.14: Comparison between metaphosphate and orthophosphate in the case of alum (a) and aluminium hydroxide (b) regarding their efficiency to remove phosphates from water at various pH end points at 25 ^oC (Georgantas and Grigoropoulou, 2007).

The removal was of phosphates was found to correspond to the pH when the positively polynuclear aluminium species are predominant ($Al_2(OH)_2^{4+}$, $Al_3(OH)_4^{5+}$, and $Al_{13}O_4(OH)_{24}^{7+}$) as shown in Figure 2.2.15.

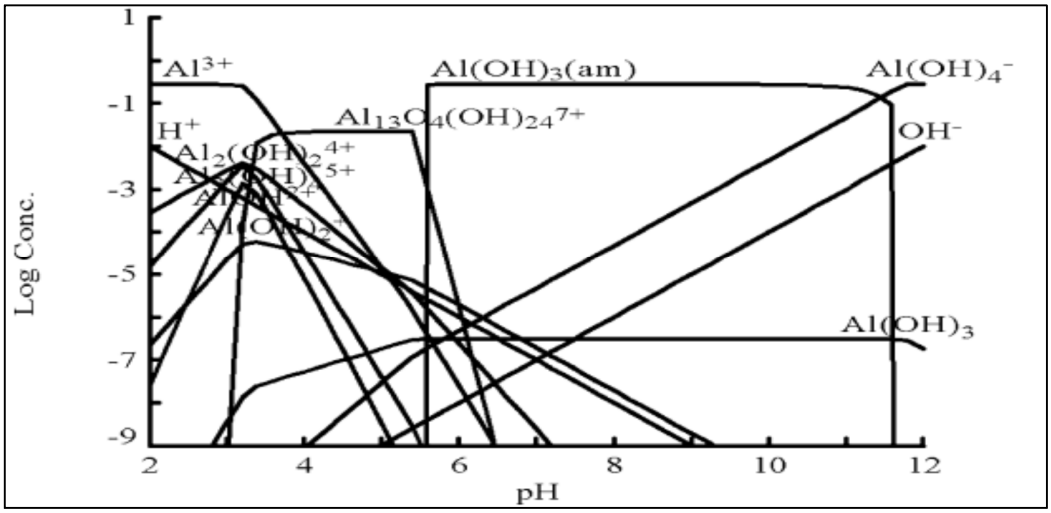

Figure 2.2.15: Al species distribution vs pH at 25 °C (Georgantas and Grigoropoulou, 2007).

These high molecular weight positively charged aluminium species interact with negatively charged phosphates to form flocs that can easily settle and be removed from the solution. When pH exceeds 5 solid amorphous aluminium hydroxide is produced. After the pH value of 11 the solid aluminium hydroxide is dissolved and the predominant species are $Al(OH)_4^-$ ions.

2.3. MIXING TECHNIQUES THAT COULD ENHANCE FLY ASH TREATMENT OF MINE WATER

Treatment of mine water with coal requires large amount of coal FA. This makes the process industrially problematic. Cavitation mixing of coal FA and mine water could enhance this treatment process. Cavitation is the generation, growth and collapse of cavities creating energy densities of 1-1018 kW/m^3. There are two main types of cavitation, acoustic and hydrodynamic cavitation.

2.3.1. ACOUSTIC CAVITATION

Acoustic cavitation is produced in a reactor by the use of sound waves with frequency of 16-100 MHz. Passing sound waves through a solution causes molecular motion by a series of

compression and relaxation as shown in Figure 2.3.1. The succeeding compression cycles continue to make the bubbles grow in size until they become unstable and collapse violently. At the point when the bubbles collapse, extreme temperatures and pressures are generated. The temperature and pressure generated depends on the frequency exerted in the solution (Cobley and Mason, 2010).

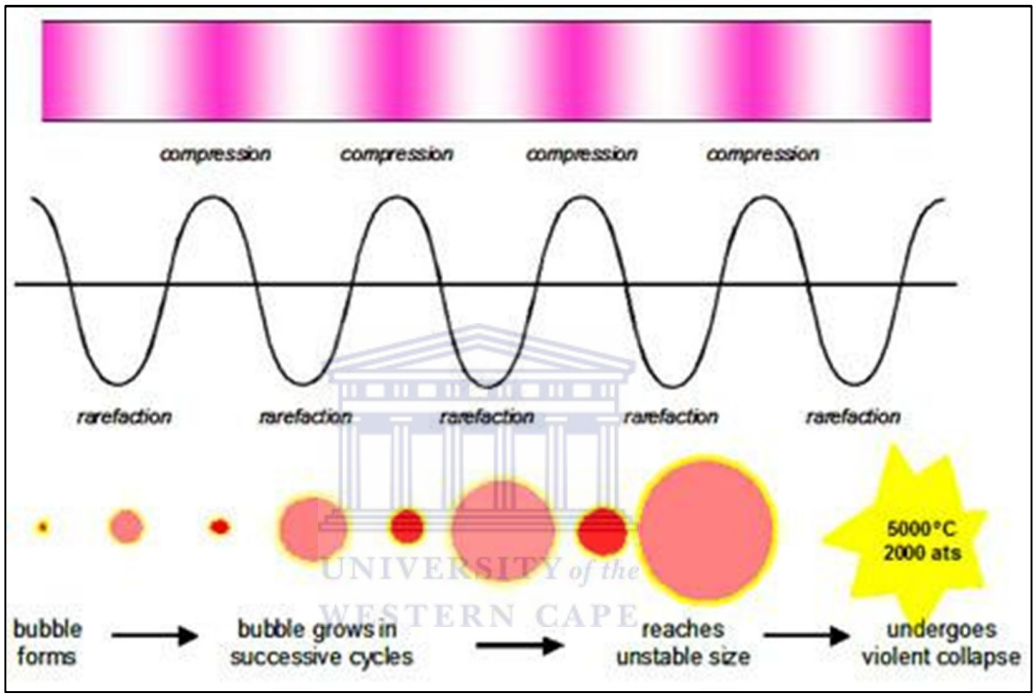

Figure 2.3.1: The process of acoustic cavitation (Cobley and Mason, 2010).

The sound waves are usually produced using an ultrasound machine. Sonochemistry is the term used to define the chemical changes that occur due to cavitation produced by the passage of sound waves into the reaction mixture.

2.3.2. HYDRODYNAMIC CAVITATION

Hydrodynamic cavitation is produced by pressure variations. The pressure variations are obtained due to the changes in the geometry of the system in which the solution is flowing. When the geometry of the system is changed, the pressure and kinetic energy also changes.

The turbulence produces an area of greatly reduced fluid pressure. The fluid vaporizes due to the low pressure, forming a cavity. This can happen when a solution is forced to flow through an orifice, venture, etc (Jyoti and Pandit, 2001; Mason, 2007).

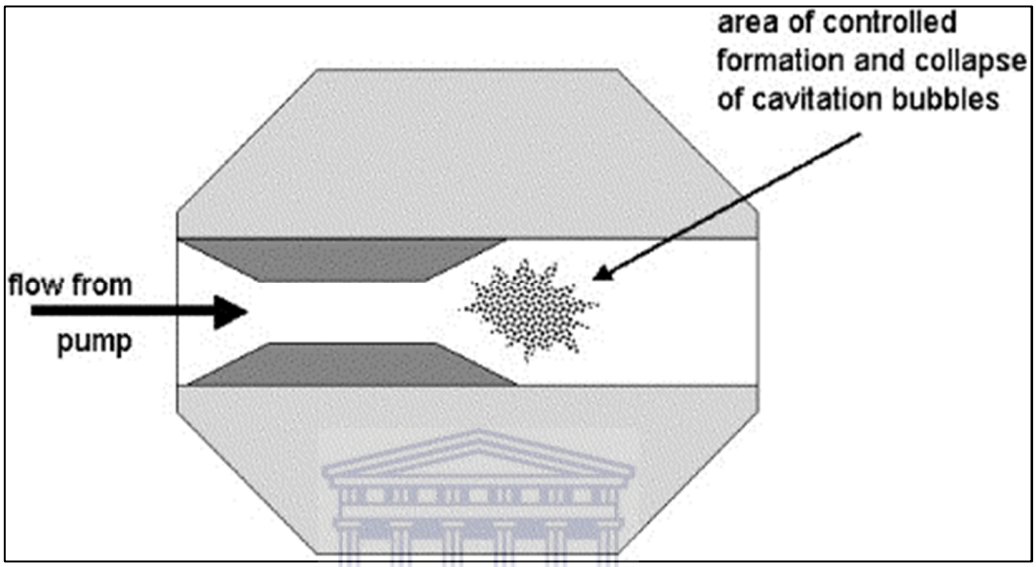

Figure 2.3.2: Schematic representation of hydrodynamic cavitation (Mason, 2007).

Hydrodynamic cavitation can be controlled easily by only adjusting the process parameters such as the flow rate, pressure and orifice size. The high Reynolds flow conditions allow for intense micro mixing of the reactants, which can be an advantage in the synthesis of metastable support phases. A very important aspect of this type of processing is that it can be scaled up easily to allow commercial processing.

Cavitation is an enormously powerful process. The collapsing cavity can reach 5000 °C and 1000 atm. The implosion takes place during the cavitation process in milliseconds, releasing tremendous energy in the form of shockwaves. The power of these waves generated by the cavitation process disrupts anything in their path.

2.3.3. APPLICATION OF CAVITATION

Cavitation has found wide application in the field of medicine and science. One of the applications of cavitation is in water treatment (Mason, 2007; Entezari et al., 2006; Jyoti and

Pandit, 2001) also discovered that hydrodynamic cavitation was an economical physical technique for water disinfection, while ultrasound cavitation was more efficient in killing the microorganisms.

Bacteria usually occur as clusters or entrapped inside flocs of clays minerals in wastewater. Application of biocides will only kill the bacteria on the surface leaving the core of bacteria intact. Therefore application of cavitation was found to disrupt colonies of bacteria, deactivate bacteria or enhance the susceptibility of bacteria to biocides.

The use of a combination of sonication and horse radish peroxidase enzyme was found to enhance the removal of 2-chlorophenol from wastewater compared to the use horse radish peroxidase or sonication separately (Entezari et al. 2006). The kinetics of the removal of 2-chlorophenol wastewater improved when the wastewater was sonicated but the addition of horse radish enzyme was found to remove more 2-chlorophenol over a prolonged time. The combination of sonication and enzyme achieved 100 % removal of the contaminant from wastewater. This was due to; enhancement of the diffusion process, structural changes of the enzyme and hydroxyl radical production through cavitation. Enhancement of the diffusion process improved action of the enzymatic action on 2-chorophenol. Structural changes of the enzyme made the enzyme active centre more available to the substrate and hydroxyl, while radicals produced through cavitation further degraded the intermediates from enzymatic action.

Hydrodynamic and acoustic cavitation has also proved to enhance the kinetics of many reactions in aqueous media (Senthil et al., 2000; Wei et al., 2007). Senthil et al., (2000) have shown that the dissolution of KI in aqueous media is enhanced by hydrodynamic cavitation. At the same power output hydrodynamic cavitation was found to be three times more efficient than acoustic cavitation in the liberation of I_2 from KI. In another case, Wei et al., (2007) proved that the jet loop anaerobic fluidized bed reactor was more efficient in the treatment of the high sulphate wastewater than the normal fluidized bed anaerobic reactor.

Cavitation enhanced the production of I_2 and the removal of sulphate from the aqueous media. This is because high temperature and pressure causes the formation of OH^- radicals as a result of the cleavage of the water. These radicals oxidises I^- ions to I_2. In the case of

removal of sulphate from wastewater, the OH^- radicals reduce the accumulation of S^{2-} and H_2S in water. The presence of S^{2-} and H_2S inhibit the efficiency of the sulphate reducing bacteria.

Based on these findings by other researchers, cavitation could enhance the performance of the coal FA treatment process of mine water. This could reduce the amount of coal FA needed and time of the treatment, therefore making the treatment process industrially feasible.

2.4. CONCLUSION

Previous research has shown that coal FA could be used to treat mine water to produce good quality water. The problem of this treatment process is that; it requires a lot of coal FA making the up scaling of the treatment not feasible. Literature has also shown that sulphate ions could be removed from water by the use of flocculants such as polyaluminium chlorohydrate or $AlCl_3$ salt. Flocculants could be used to polish the mine water from the coal FA system to remove the residual sulphate ions in the product water. In addition coal from other countries such as Turkey, Greece and America has been reported to contain radioactive nuclides. The radioactivity of coal FA in South Africa is not extensively studied. On the other hand the fate of radioactive nuclides in coal FA and mine water is not known during treatment of mine water with coal FA.

Based on these gaps in the literature, this thesis describes the experimental investigations and modelling approaches used as well as presenting findings and conclusions of the current work. This study used hydrodynamic cavitation to enhance the performance of the coal FA treatment of mine water. Hydrodynamic cavitation was used in order to reduce the amount of coal FA and to enhance the performance of the treatment process such that the process could be up scaled. The fate of radionuclides in coal FA and mine water during treatment of mine water with coal FA was also studied. The chemistry of the removal of sulphate ion from mine water or product water from the coal FA treatment process using aluminium chlorohydrate or $Al(OH)_3$ was also investigated. This was done in order to find out if ACH or $Al(OH)_3$ could produce water that is fit for reuse.

CHAPTER 3: METHODOLOGY

South Africa produces different types of mine water depending on the geological environment being disturbed during mining. The different conditions that are required to treat mine waters of varying composition using a combination of coal FA and $Al(OH)_3$ or aluminium chlorohydrate (ACH) flocculant were investigated in this study.

3.1. STUDY AREA

The water used for this study was collected from Matla coal mine in Mpumalanga province and Rand Uranium gold mine in the Western basin of Witwatersrand Goldfields in Krugersdorp (Figure 3.1.1).

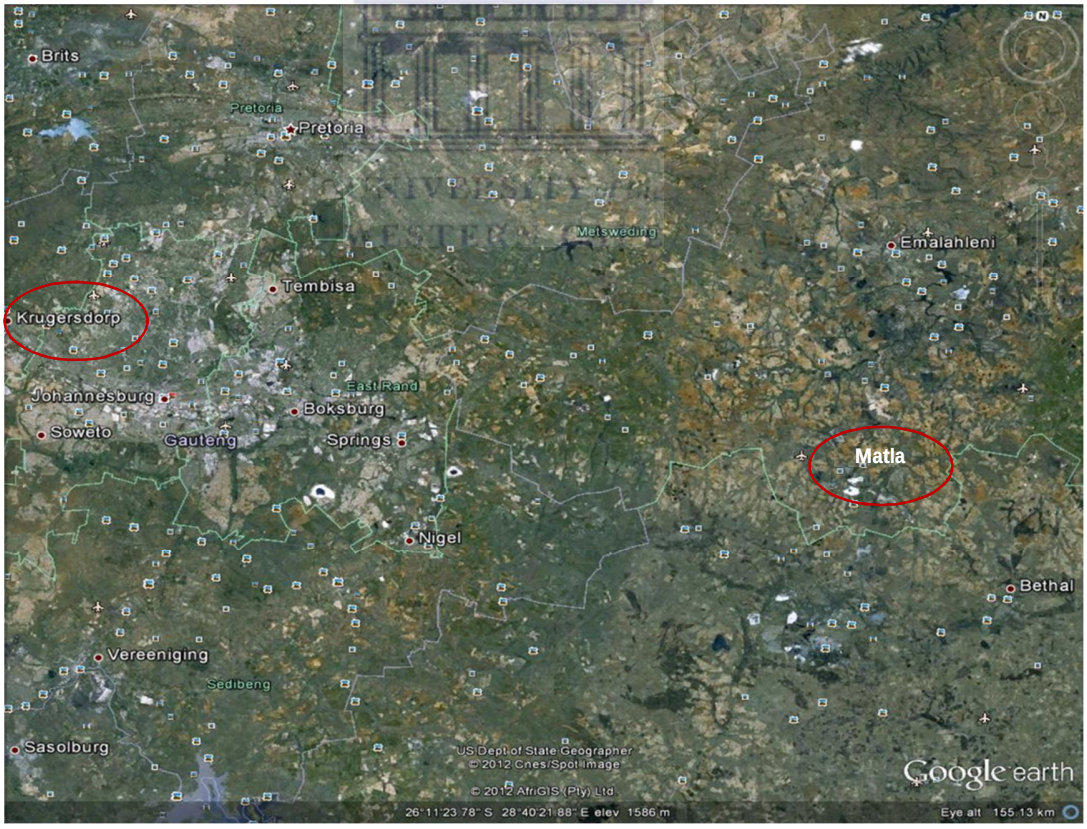

Figure 3.1.1: Map showing the mine water and FA sampling sites.

The Matla coal mine where the water was sampled is still active. Rand Uranium mine is semi abandoned since there is no longer any underground mining taking place and only mining of tailings is still on going. There is no active pumping of underground mine water and the water has started decanting since 2002, threatening the Cradle of Humankind and the Hippopotamus dam in the vicinity.

3.2. SAMPLING AND CHARACTERIZATION OF FLY ASH

Fresh FA was collected directly from the hoppers of Matla coal power station. Samples of FA were sealed in plastic bags devoid of air to avoid the reaction of CaO in the FA with atmospheric CO_2 which would cause the formation of calcite therefore reducing the CaO content. The FA samples were analysed using x-ray diffraction (XRD) spectroscopy and x-ray fluorescence (XRF) spectroscopy for mineralogy and elemental composition respectively. Trace elements was analysed with XRF and Laser Ablation ICP-MS. Scanning electron microscopy was used to understand the morphology of FA. Gross alpha and gamma radioactivity of FA was determined to estimate the total radioactivity. Neutron activation analysis (NAA) was used to determine the ^{238}U and ^{232}Th radioisotopes. Low energy gamma spectrometry was used to measure the activity of ^{210}Pb, ^{235}U, and other products in the ^{232}Th and ^{235}U decay series. High energy gamma spectrometry was used to measure the activity of ^{228}Ra, ^{226}Ra, ^{228}Th and ^{40}K. Radium-226 was determined by measuring its decay products of which a three week waiting period was allowed for the equilibrium between Ra and its decay products.

3.2.1. SCANNING ELECTRON MICROSCOPE

Matla FA was analysed using a HITACHI X-650 Scanning Electron Microanalyzer. The samples were prepared by fixing the samples on aluminium stubs using carbon adhesive. The carbon adhesive was attached to the top part of an aluminium stub and then the sample was sprinkled on the carbon adhesive with great precaution to avoid forming a thick layer that would absorb the incident light. Since the samples that were analysed were poor

electromagnetic conductors, they were gold coated using argon gas on Sputter Coater S150B. The gold coating was done under vacuum.

3.2.2. X-RAY DIFFRACTION SPECTROSCOPY

Qualitative XRD was performed to evaluate any mineralogical changes between the fresh coal FA and the solid residues recovered after mixing FA with mine water. This was performed using a Philips X-ray diffractometer and Cu-K_α radiation with a PW3011 (Miniprop) detector. The instrument settings are as shown in Table 3.2.1.

Table 3.2.1: The XRD settings during analysis of coal FA and the solid residues.

Radiation source	Cu-K_α
Radiation wavelength (λ)	1.541
Voltage	40 kV
Current	25 mA
2ϑ	$4^o<2\theta<65^o$
Step size	0.02
Anti-scatter slit	1^o

The mineral phases were identified by search and match technique with the powder diffraction file data. This identification was complemented with Joint Committee of Powder Diffraction Standards (JCPDS) files for inorganic compounds.

3.2.3. X-RAY FLUORESCENCE SPECTROSCOPY

Matla FA samples were crushed into a fine powder (particle size < 100 µm) with a jaw crusher and milled in a tungsten zib mill (to prevent from trace and REE contamination) prior to the preparation of a fused disc for major element and trace analysis. The jaw crusher and mill are cleaned with uncontaminated quartz after analysing each sample to avoid cross contamination. Pressed powder pellets were prepared for XRF analysis using 8 g of the sample and few drops of MOVIOL was added for binding.

The composition was then determined by XRF spectrometry on a Philips 1404 Wavelength Dispersive spectrometer. The spectrometer was fitted with an Rh tube and with the following analysing crystals: LIF200, LIF220, LIF420, PE, TLAP and PX1. The instrument is fitted with a gas-flow proportional counter and a scintillation detector. The gas-flow proportional counter uses 90 % argon and 10 % methane gas mixture. Trace elements were analysed on a pressed powder pellet at various kV and mA tube operating conditions, depending on the analysed element. Matrix effects in the samples were corrected for by applying theoretical alpha factors and measured line overlap factors to the raw intensities measured with the SuperQ Philips software. Control standards that were used in the calibration procedures were NIM-G (Granite from the Council for Mineral Technology, South Africa) and BHVO-1 (Basalt from the United States Geological Survey, Reston).

3.2.4. LASER ABLATION INDUCTIVELY COUPLED PLASMA-MASS SPECTROMETRY

The instrument was set by connecting a 213 nm laser ablation system connected to an Agilent 7500ce ICP-MS. The FA sample was coarsely crushed and fusion disks were made by an automatic Claisse M4 Gas Fusion instrument and ultrapure Claisse Flux. A chip of sample was mounted in a 2.4cm round resin disk. The mounted sample was then polished for analysis. The sample was ablated using He gas and then mixed with Ar after coming out of the ablation cell. The sample was then passed through a mixing chamber before being introduced into the ICP-MS.

Trace elements were quantified using NIST 612 for calibration method and 29Si as internal standard. Three replicate measurements were made on each sample. The calibration standard was run after every 12 samples. A quality control standard was run in the beginning of the sequence as well as with the calibration standards throughout. Both basaltic glass, BCR-2 or BHVO 2G were certified reference standards produced by USGS (Dr Steve Wilson, Denver, CO 80225) that were used for this purpose. A fusion control standard from certified basaltic reference material (BCR-2, also from USGS) was also analysed in the beginning of a sequence to verify ablation on fused material. Data was processed using Glitter software.

3.2.5. RADIOACTIVE ANALYSIS OF MATLA FLY ASH

Matla fly ash samples were dried overnight in an oven at 105 ^{o}C. The samples were then milled to obtain a homogeneous powder so that representative portions could be sampled for the various analyses. The homogenized sample (500 g) was placed in Marinelli beakers and analysed for gross alpha and beta to obtain a first order estimate of the total activity of the sample. After determination of the gross alpha and beta the samples were analysed for various radioisotopes using low energy gamma analysis and high energy gamma analysis according to a method used by Newman et al. (2008) and Radium-226 was determined by measuring its decay products. A three week waiting period was allowed to establish radioactive equilibrium between radium and its decay products.

3.2.5.1. Radioactive analysis of fly ash using gamma spectrometry

Two high-resolution ERL gamma ray spectrometers with p-type coaxial hyper-pure germanium (HPGe) detectors were used for the determination of ^{210}Pb, ^{238}U, ^{235}U, ^{234}U, ^{228}Ra, ^{226}Ra, ^{232}Th, ^{228}Th, ^{40}K and other products in the thorium-232 and uranium-235 decay series in Matla fly ash. One of the HPGe detectors has a relative efficiency of 45 % and an energy resolution of 2 keV at 1.33 MeV. The other detector has a relative efficiency of 110 % and an energy resolution of 2.1 keV. To avoid background radiation both detectors were shielded from background radiation. Gamma reference materials were used to determine the absolute efficiency of the gamma spectrometers. Measurement of the sample was done at the same conditions with background measurements and subtracted from the sample measurement. Several gamma ray peaks at various energies obtained in Table 2.1.3 were averaged assuming secular equilibrium in ^{238}U and ^{232}Th decay series as follows:

- Uranium-238 activity concentration was determined by using the gamma-ray peaks of the 351.9 keV from ^{214}Pb and the 609.3 keV from ^{214}Bi.
- Radium-226 was determined using the gamma ray with energy of 186 keV.
- To determine the activity concentration of ^{232}Th, the gamma-ray peaks of the 911.2 keV from ^{228}Ac and the 583.2 keV from ^{208}Tl were used.

- Activity concentration of ^{40}K was determined from its own gamma-ray peak at 1460.8 keV.

3.3. CHARACTERIZATION OF ALUMINIUM CHLOROHYDRATE

Aluminium chlorohydrate (ACH) was obtained from Veolia Chemicals in South Africa with a purity of 23 %. It was gel like in appearance. Aluminium chlorohydrate was diluted 25000 times with ultra-pure water. The diluted sample was than analysed using inductively coupled plasma-optical emission spectroscopy (ICP-OES) and ion chromatography (IC).

3.3.1. ION CHROMATOGRAPHY

Ion chromatography (IC) was used to determine the concentration of anions in mine water. The samples were filtered through 0.45 µm nucleopore membrane filter paper and preserved at 4 ^{o}C until analysis was conducted. A Dionex DX-120 Ion Chromatograph with an AS40 automated sampler, ASRS- 300 suppresser, AS14 analytical column, AG14 guard column and a conductivity detector was used for the analysis. The eluent used was a mixture of 3.5 mM $NaHCO_3$ and 1.0 mM Na_2CO_3.

A Dionex SEVEN ANION certified standard was used to check the efficiency of the IC machine. The SEVEN ANION was made up of the composition as shown in Table 3.3.1 below.

Table 3.3.1: Composition of the Dionex SEVEN ANION certified standard.

anion	Concentration (mg/L)
F^-	20
Cl^-	30
NO_2^-	100
Br^-	100
NO_3^-	100
PO_4^{3-}	150
SO_4^{2-}	150

3.3.2. INDUCTIVELY-COUPLED PLASMA-OPTICAL EMISSION SPECTROSCOPY

The cation concentration was analysed using Varian 710-ES ICP Optical Emission Spectrometry to follow the changes in the composition of mine water during treatment. The sample was introduced through a high sensitivity glass, single-pass cyclone spray chamber and conical nebulizer using argon gas. It was then passed through axially oriented plasma. The wavelength released by different analytes was detected with a CCD detector and auto integrated using ICP Expert II software. The ICP-OES instrument was calibrated before analysis. The accuracy of the instrument was checked using certified standards. Three replicates were run for each sample in order to check the reproducibility of the analysis.

3.4. CHARACTERIZATION OF ALUMINIUM HYDROXIDE AND LIME

The aluminium hydroxide and lime used in this research were obtained from KIMIX chemicals in South Africa. Aluminium hydroxide had a purity of 96 % and lime was 95 % pure. Lime and aluminium hydroxide were characterized using SEM (as outlined in section 3.2.1), XRD (as outlined in 3.2.2) and XRF (as outline in 3.2.3) to determine the morphology, mineralogy and its chemical composition.

3.5. SAMPLING AND CHARACTERIZATION OF MINE WATER

The mine water used in this study was collected from the Matla coal mine in Mpumalanga province and the Rand Uranium Gold mine in the West Rand Basin in Gauteng Province. The water was filtered through a 0.45 µm pore membrane filter paper using manual pumping device. The filtered samples were divided into two portions of 100 mL each for cation and anion analysis. The cation samples were preserved with 2-3 drops of concentrated HNO_3 for approximately 100 mL of sample. Both cation and anion samples were preserved at 4 ^{o}C until analysis for anions using IC (as outlined in section 3.2.1) and cations use ICP-OES (as outlined in section 3.3.2). The mine water was also filtered through a 0.45 µm filter paper and the acidity or the alkalinity was determined using Metrohm Autotitrator. Mine water

samples that were supposed to be analysed for radioactivity were first filtered through 8 µm and 0.45 µm to remove coarse materials and suspended solids. The samples were then acidified to ensure radionuclides are not adsorbed on the container walls.

3.5.1. DETERMINATION OF ACIDITY OR ALKANINITY

The alkalinity of mine water used in the experiments was determined to gain an understanding of the acid neutralising potential. This parameter is very important for cation/anion balance in Geochemist's workbench geochemical modelling. The alkalinity was determined by titrating mine water (20 mL) with 0.1 M HCl to an end point of pH 4 (Eaton et al., 1995). The alkalinity was calculated as follows:

$$mg \cdot L^{-1}(HCO_3^-) = \frac{1000 \times 61.02 \times V(acid) \times [HCl]}{V(sample)}$$; where V = mL and [ ] = mol/L.

Acidity was determined by titrating AMD (20 mL) sample with 0.1 M NaOH to an end point of 8.3. The acidity was calculated as follows:

$$mg \cdot L^{-1}(CaCO_3) = \frac{V(NaOH) \times [NaOH] \times 1000}{V(sample)}$$; where V = mL and [ ] = mol/L.

3.5.2. RADIOACTIVITY ANALYSIS OF RAND URANIUM MINE WATER

Rand Uranium mine water samples were filtered, acidified and then stored at 4 °C before analysis. Before the samples were analysed using alpha spectrometry, they were first pre-treated and prepared specifically for analysis of a specific element. The following steps cover how the samples were prepared and analysed using alpha spectrometry.

Sample preparation for uranium determination by alpha spectrometry

The method was based on solid phase extraction of uranium from water samples, with detection of the uranium isotopes by alpha spectrometry. An aliquot (200 mL) of the sample was measured into a beaker and uranium-232 internal tracer was added for

recovery determination. The sample was evaporated to a volume of 10 mL, and acidified using 2 drops of 2 M HNO_3. The sample was loaded on a TruSpec (Eichrom resins) column to absorb uranium. A mixture of HCl and HF acid was added to the column to elute uranium. The separated uranium was loaded on a cation exchange column to further purify uranium. Uranium was eluted with concentrated 2 M HCl and collected on a filter paper by lanthanum fluoride micro co-precipitation.

Sample preparation for thorium determination by alpha spectrometry

The method was based on solid phase extraction of thorium from water samples with detection of the different thorium isotopes by alpha spectrometry. Thorium-229 was added as an internal tracer to a 200 mL aliquot of the sample. Sample volume was reduced to a volume of 10 mL by evaporation and acidified using 2 M HNO_3. The sample was loaded on a TruSpec column (Eichrom resins) to absorb thorium and other nuclides. Thorium is eluted with a mixture of HCl and HF. The collected eluent was loaded on a cation column for further purification. Thorium was finally eluted with 2 M H_2SO_4 solution and collected on a filter paper by lanthanum fluoride micro co-precipitation.

Sample preparation for radium determination by alpha spectrometry

Barium-131 was added as an internal tracer to the sample. Radium was separated from the bulk of the sample material by adding Pb and Ba carriers to the sample followed by precipitating these elements and radium present as sulphates. The precipitate is purified from other ions by washing, and then dissolved again by adding a complexing agent. Barium (and radium) was again precipitated and filtered as sulphate while Pb was kept in solution by careful adjustment of the pH. Barium-131 in the separated fraction is measured for on a radiation detector for yield determination.

Sample preparation for lead and polonium determination by alpha spectrometry

Polonium-209 was added as internal tracer for recovery determination. The sample was acidified with 2 M HCl and heated to a temperature of 90 ^{o}C. A silver disk was added to the sample and the solution was stirred for several hours to induce spontaneous deposition of polonium-210. A reducing agent was added at the start of the process to prevent iron from

plating on the silver disk. The disk was removed, washed and air-dried to prepare it for measurement on the alpha spectrometer.

Alpha spectrometry analysis of the prepared samples

Prepared samples were counted on Canberra Alpha Analyst or Alpha Apex systems. These systems consists of 12 vacuum chambers hosting each an alpha PIPS detector. Samples were counted for a period of 24 hours to reach the required detection limits. The acquired spectra were analysed for counts collected in the respective alpha peak positions shown in Table 3.5.1.

Table 3.5.1: Peaks position used for identification of nuclides using alpha spectrometry.

Nuclide	Peaks position energy (MeV)
^{238}U	4.72
^{235}U	4.40
^{234}U	4.77
^{232}Th	4.01
^{230}Th	4.69
^{227}Th	5.76, 5.93 and 6.04
^{228}Th	5.42
^{226}Ra	4.78
^{224}Ra	5.68
^{210}Po	5.30

The peaks positions were chosen based on the highest intensities of the alpha energy of the respective decay of the nuclide (Bonotto et al., 2009). These counts were entered into data reduction programs to calculate nuclide activities, associated uncertainties and minimum detectable activity concentrations. A control sample containing known amounts of the analyte nuclides were used to calibrate the machine for each batch of samples. Measured activities must lie within prescribed limits for the results of the batch to be accepted. The yield for a sample must also be within a range. Background, energy, peak-width and efficiency checks were performed on a weekly basis to ensure correct operation of detectors.

3.6. GEOCHEMIST'S WORKBENCH MODELLING

The Geochemist's Workbench (GWB) is a software that is comprised of different programs to manipulate chemical reactions, calculate stability diagrams and the equilibrium states of natural waters, trace reaction processes, model reactive transport, plot the results of these calculations, and store the related data (Bethke and Yeakel, 2010). The software is constantly upgraded. In this study SpecE8 and Act2 programs of the GWB 8.0 essential software were used.

SpecE8 is capable of calculating the species distributions in aqueous solutions, mineral saturation indices and gas fugacities. SpecE8 can also account for sorption of species onto mineral surfaces according to a variety of methods, including surface complexation and ion exchange. Act2 program calculates and plots activity-activity diagrams. These diagrams show the stability of minerals and predominance of aqueous species in chemical systems. Variables of the axes of the stability diagrams include; species activity, gas fugacity, activity or fugacity ratio, pH, or redox potential (Bethke and Yeakel, 2010).

3.6.1. SPECIES DISTRIBUTION

The Act2 program of the GWB software was used to calculate the species distribution and the saturation indices of the different minerals in Rand Uranium mine water and Matla mine water. This was done using the pH, electrical conductivity (EC), alkalinity and acidity of the mine waters and the concentration of individual ions. The pH and electrical conductivity (EC) of the mine water was measured in the field. Alkalinity was determined using a Metrohm Autotitrator. The elemental composition of Rand Uranium and Matla mine water was obtained using ICP-OES and IC.

3.6.2. PREDICTION OF THE MINERAL PHASES

During treatment of mine water with alkaline chemical, potentially toxic constituents are mainly removed through precipitation. The Act2 program of the GWB software was used to

predict the stable mineral phases of potentially toxic elements/ions from Rand Uranium and Matla mine water. The prediction was done using the analytical and physical results measured using the IC, ICP-OES, pH/EC/TDS meter and the autotitrator. The independent variable was chosen as $\log_a Ca^{2+}$ and the dependent variable was the pH. These values were chosen based on the fact that treatment of mine water with coal is based on the neutralization of pH due to the dissolution of the lime fraction in coal FA.

3.7. TREATMENT OF MINE WATER WITH A COMBINATION OF COAL FA AND FLOCCULANTS

Before the flocculants were used for the treatment of mine water the aluminium chlorohydrate (ACH) and $Al(OH)_3$ were characterized using IC and ICP-OES analytical techniques and the Geochemist's workbench software. The composition of ACH was studied using ICP-OES and IC as explained in Section 3.3.1 and 3.3.2 to determine the concentration of Al and Cl ions that make up the ACH. The ACH was first diluted 2500 times using deionized water before being analysed for elemental composition. Using the results from IC and ICP-OES, the species that make up ACH were elucidated using the Geochemist's workbench SPEC 8 to determine the species distribution in ACH as explained in section 3.6. The mineral composition of $Al(OH)_3$ was elucidated using XRD as explained in Section 3.2.2, while the morphology was studied using SEM as explained in section 3.2.1

3.7.1. TREATMENT OF MATLA MINE WATER WITH FLOCCULANTS

The chemistry of the treatment of Matla mine water with $Al(OH)_3$ or ACH was done to understand;

1. The effect of pH on the removal of sulphate ions from Matla mine water and
2. The effect of the $Al:SO_4^{2-}$ mol ratio on the removal of sulphate ions from Matla mine water.

3.7.1.1. Effect of pH on the removal of sulphate ions

A. Matla mine water was treated with $Al(OH)_3$ at different pH end points between 2 to 8. The initial pH of Matla mine water was 8. The pH was adjusted to an acidic pH using 1 M HCl. After the pH of Matla mine water had been taken to the required end point, 500 mL of the water was mixed with 2.3942 g of $Al(OH)_3$. This amount of $Al(OH)_3$ added represented a mol ratio of 4:1 of the Al ions to the sulphate ions in Matla mine water. The mixture was stirred using a magnetic stirrer at 250 rpm for 20 min. After 20 min the mixture was allowed to settle for 30 min and then filtered through a 0.45 µm filter paper and analysed using an IC as explained in section 3.3.1. The conditions 4:1 mol ratio and 20 min stirring time were selected as optimum in accordance to the study by Silva et al., (2010) on sulphate removal from mine water using $AlCl_3$.

B. Matla mine water was treated with ACH at different pH end points between 2 to 8. The pH of Matla mine water was 8. The pH of the mixture was maintained at the required pH using 0.1 M of NaOH or 0.1 M HCl. Matla mine water (50 mL) was mixed with 0.61 mL of ACH. This volume represented a ratio of 4:1 of the Al ions to the sulphate ions in Matla mine water. The mixture was stirred using a magnetic stirrer at 250 rpm for 20 min. After 20 min the mixture was allowed to settle for 30 min and then filtered through a 0.45 µm filter paper and analysed using an IC as explained in section 3.3.1.

3.7.1.2. Effect of the Al:SO_4^{2-} mol ratio on the removal of sulphate ions

A. Matla mine water pH was first adjusted to the optimum pH obtained in experimental section 3.7.1.1a above using 1 M HCl. After the pH of Matla mine water was adjusted to the optimum pH it was mixed with different proportions of $Al(OH)_3$ as shown in Table 3.7.1. The mixture was stirred using a magnetic stirrer for 20 min at 250 rpm maintaining the pH of the mixture between 4-6 using 0.1 M HCl. The mixture was then allowed to settle for 30 min and then filtered through a 0.45 µm filter paper and analysed using IC and ICP-OES as outlined in section 3.2.1 and 3.2.2.

Table 3.7.1: The amount of $Al(OH)_3$ added for different molar ratios.

Mol ratio (Al^{3+}:SO_4^{2-})	Matla mine water (mL)	$Al(OH)_3$(g)
1:1	50	0.0624
2:1	50	0.1247
3:1	50	0.1871
4:1	50	0.2494
5:1	50	0.3118
6:1	50	0.3742
7:1	50	0.4366
8:1	50	0.4990

B. After the optimum pH of the removal of sulphate ions from Matla mine water was determined as explained in section 3.7.1b, Matla mine water was mixed with different proportions of ACH as shown in Table 3.7.2.

Table 3.7.2: The amount of ACH added for different molar ratios.

Mol ratio (Al^{3+}:SO_4^{2-})	Matla mine water (mL)	ACH (mL)
1:1	50	0.16
2:1	50	0.31
3:1	50	0.47
4:1	50	0.61
5:1	50	0.78
6:1	50	0.91
7:1	50	1.09
8:1	50	1.25

After addition of the required proportion of ACH the mixture was stirred using a magnetic stirrer for 20 min at 250 rpm maintaining the pH of the mixture at the optimum pH value obtained in section 3.7.1b using 0.1 M NaOH. The mixture was then allowed to settle for 30 min and then filtered through a 0.45 µm filter paper and analysed using IC as explained in section 3.3.1 and 3.3.2.

3.7.2. TREATMENT OF THE RAND URANIUM MINE WATER WITH FLOCCULANTS

Rand Uranium mine water was reacted with coal FA to different final pH end points using a solid to liquid ratio of 6:1. The water was filtered through a 0.45 µm filter paper and analysed using IC and ICP-OES. After the amount of sulphate ions was determined using IC in the recovered water from FA treatment was further treated using different amounts of aluminium chlorohydrate (ACH) or $Al(OH)_3$ as explained in section 3.7.1.2. Different amounts of $Al(OH)_3$ or ACH added during the polishing of the water from FA treatment are as shown in Table 3.7.3.

Table 3.7.3: The proportions of $Al(OH)_3$ or ACH added during further treatment of the product water from FA treatment of Rand Uranium mine water.

mol ratio	recovered water (mL)	$Al(OH)_3$ added (g)	ACH added (mL)
1:2	50	-	0.15
1:1	50	0.1404	0.34
2:1	50	0.2808	0.70
3:1	50	0.4212	1.00
4:1	50	0.5412	1.30
5:1	50	0.6102	
6:1	50	0.7816	
7:1	50	0.9156	
8:1	50	1.0156	
9:1	50	1.157	
10:1	50	1.2597	

3.8. APPLICATION OF A JET LOOP REACTOR

Matla mine water collected from Mpumalanga province in South Africa was treated in an 80 L pilot plant as shown in Figure 3.8.1. The pilot plant was composed of an 80 L tank, a centrifugal pump, a motor and a jet loop reactor. The pilot plant was designed by Org Nieuwoudt of Biofuelson.

Figure 3.8.1: The setup of the 80 L pilot plant.

The water was pumped into the reactor and distributed into two sets of jets as shown in Figure 3.8.2. In each jet the water was forced through small adjustable orifices, which had diameters ranging from 6 to 12 mm. The jet sizes can be replaced by unscrewing off one set of adjustable orifice and replacing it with one of the required size.

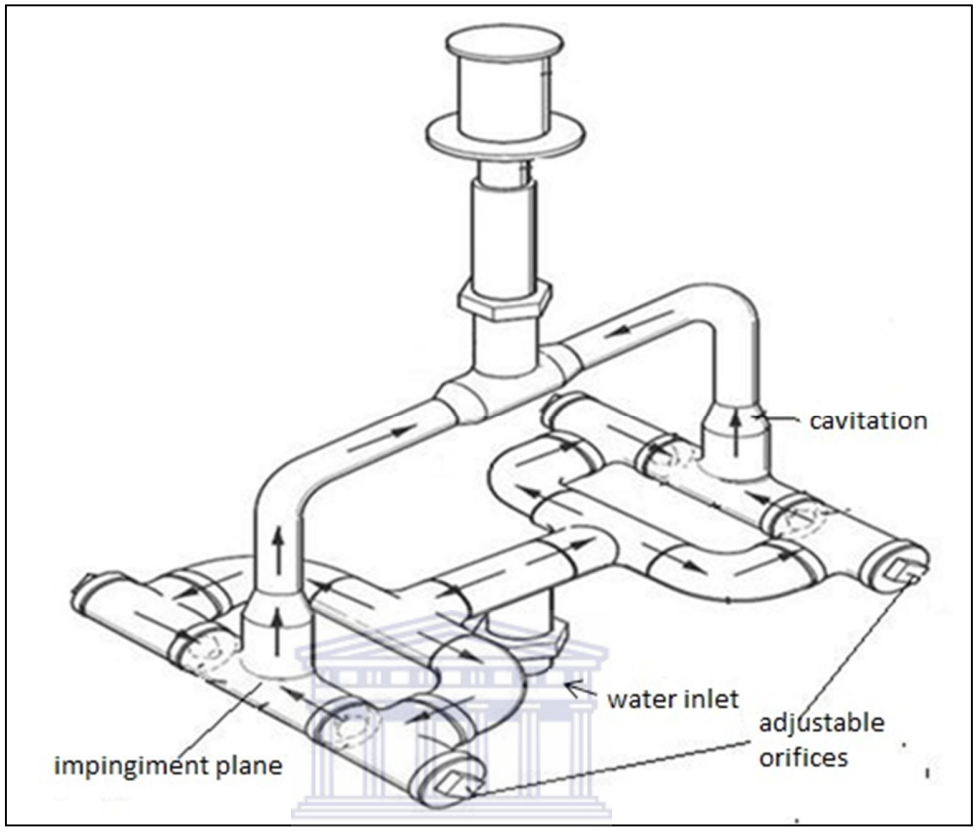

Figure 3.8.2: Schematic representation of the movement of the water in the jet loop reactor.

By forcing the water through small orifices the kinetic energy of the mixture of mine water and FA decreased. When the mixture comes out of the small orifice the pressure decreased and the kinetic energy increased. This caused hydrodynamic cavitation in the mixture of FA and mine water as the low pressure caused the bubble to form, grow and collapse as shown in Figure 3.8.3.

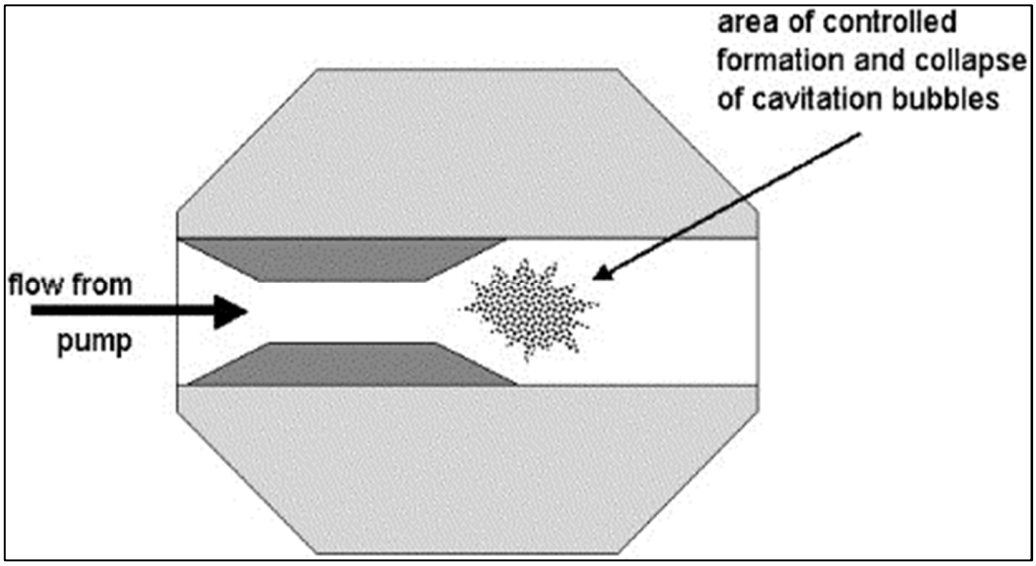

Figure 3.8.3: Schematic representation of hydrodynamic cavitation (Mason, 2007).

The water from two orifices in opposite direction, with high kinetic energy collided with each other inside the jet loop reactor as shown in Figure 3.8.4. The collision of two water streams with high kinetic energy is called impingement.

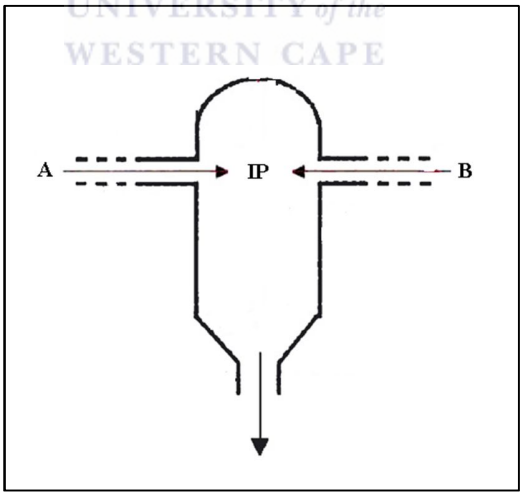

Figure 3.8.4: The schematic representation of impingement phenomenon inside a jet loop reactor (Gavi et al., 2007; Chung and Luo, 2002).

3.8.1. TREATMENT OF MATLA MINE WATER WITH FLY ASH

A number of experiments were carried out using Matla mine water at 80 L capacity. The experiments can be broadly classified as; the optimization of the amount of Matla FA and lime required and the optimization of the jet loop reactor settings.

3.8.1.1. Optimization of the amount fly ash and lime required

The following experiments were conducted in order to find the optimum conditions (jet sizes, amount of FA and minimum amount of lime) required to increase the pH of the mine water to pH greater than 11 in order to precipitate sulphate in the form of ettringite.

A. Matla mine water (80 L) and Matla coal FA (13 kg) were mixed together using a jet loop reactor with jet nozzle sizes set at 8 mm. The mine water and coal FA were mixed by a combination of impingement and cavitation in the reactor. Temperature, pH and EC were measured after every 15 min and samples were collected after every 30 min. The samples were filtered using a 0.45 µm and analysed using ICP-OES and IC.

B. Matla mine water (80 L) was mixed with 16 kg of Matla coal FA using a jet loop reactor with jet nozzle sizes set at 8 mm. The mixture was mixed by a combination of impingement and cavitation in the jet loop reactor. Temperature, pH and EC were measured after every 15 min. Aliquot samples were collected after 30 min, filtered using a 0.45 µm and analysed using ICP-OES and IC.

C. The jet nozzle sizes were changed from 8 mm to 6 mm by unscrewing one jet and replacing it with the right orifice diameter. Then Matla mine water (80 L) and 16 kg Matla coal FA were mixed by a combination of impingement and cavitation in a jet loop reactor; measuring pH and EC after every 15 min. Aliquot samples were collected for analysis using ICP-OES and IC after every 30 min.

D. Matla mine water (500 mL) was mixed with Matla coal FA (83 g) using an overhead stirrer. This volume of mine water and mass of Matla coal FA was chosen to represent a liquid to solid ratio of 6:1 which was the same as 80 L of mine water and 13 kg of Matla coal FA used in the pilot plant. Various amounts of lime (0.125 g, 0.250 g, 0.375 g or 0.620 g) were together with 13 kg of Matla coal FA. For each mixture, 0.52 g of $Al(OH)_3$ was added after 30 min. The reaction was carried on after adding $Al(OH)_3$ measuring pH and EC after 15 min and collecting samples after every 30 min for 150 min. The samples were filtered through 0.45 µm micro pores and analysed using ICP-OES and IC.

3.8.1.2. Optimizing the settings of jet loop reactor

Experiments were further carried out to treat Matla mine water using a combination of Matla coal FA and 0.25 % of lime (w/v) at liquid to solid ratio of 6:1 in a jet loop reactor. The first set of three experiments was done to investigate the effect of jet size on sulphate removal from Matla mine water. The jet nozzle sizes were varied from 8, 10 and 12 mm. Matla mine water (80 L) was reacted with Matla coal FA (13 kg) and 0.25 % lime (w/v %). After 15 min 83.2 g of $Al(OH)_3$ was added. The reaction was allowed to proceed for 150 min measuring pH and EC after every 15 min. Samples were collected after every 30 min, filtered through a 0.45 µm and analysed using ICP-OES and IC. The solids residues after 150 min were dried and analysed using XRD and XRF as outlined in section 3.2.2 and 3.2.3 respectively. The results were compared to the XRD and XRF analysis obtained on the Matla coal FA, lime and $Al(OH)_3$.

The last set of experiments was conducted in order to compare the effect of cavitation only to that of cavitation and impingement. The jet nozzle sizes were maintained at 12 mm and mine water (80 L) was mixed with coal FA (13 kg) and one pair of jets on one side was closed. This meant that there is one jet flowing such that it would not collide with another jet, thereby avoiding impingement mixing. So the mixing of mine water and FA was due to cavitation only as shown in Figure 3.8.5.

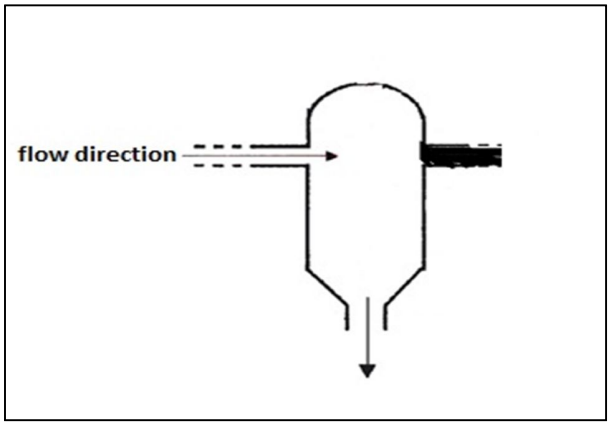

Figure 3.8.5: Schematic diagram showing one orifice closed so that impingement cannot take place.

After 15 min 83.2 g of $Al(OH)_3$ was added. The temperature, pH and EC were measured after every 15 min. Aliquot samples were collected after every 30 min, filtered through a 0.45 µm filter paper and analysed using ICP-OES and IC.

3.8.1.3. Effect of temperature on the removal of sulphate ions

Matla mine water (500 mL) was mixed with Matla coal FA (83 g) and lime (1.25 g) using a magnetic stirrer at 20 ^{o}C. This volume of mine water and mass of FA was chosen to represent a liquid to solid ratio of 6:1 which was the same as 80 L of mine water and 13 kg of FA used in the pilot plant. The amount of lime added represented 0.25 % lime (w/v) which was the same as used in one of the pilot plant experiments. After 30 min of mixing, 0.52 g of $Al(OH)_3$ was added. The reaction was carried on after adding $Al(OH)_3$ measuring pH and EC after 15 min. The reaction was stopped after 150 min maintaining the temperature at 20 ^{o}C by conducting the reaction in a water bath in order to regulate the temperature. The temperature was maintained at 20 ^{o}C by adding ice cold water when the temperature went up. The samples were filtered through 0.45 µm and analysed using ICP-OES and IC. The above reaction was repeated at 30, 40, 50, 60, 70 and 80 ^{o}C using a temperature regulated heating mantle attached to a magnetic stirring mechanism.

3.8.2. TREATMENT OF RAND URANIUM MINE WATER USING JET LOOP REACTOR

Rand Uranium mine water was treated in an 80 L pilot plant (Figure 3.8.1) using the optimum reactor settings obtained during treatment of Matla mine water as explained in section 3.8.1.2. Different combinations of Matla coal FA, lime and/or $Al(OH)_3$ were used to understand the optimum conditions required to remove the sulphate ions and potentially toxic elements from Rand Uranium mine water to the required limit for potable water.

3.8.2.1. Effect of $Al(OH)_3$

Rand Uranium mine water (80 L) was mixed with 86.58 g of $Al(OH)_3$ in a jet loop reactor with jet sizes set at 12 mm. The pH, EC and temperature were measured after 15 min and aliquot samples were collected after every 30 min. The samples were filtered through a 0.45 µm filter paper and analysed using IC and ICP-OES.

3.8.2.2. Effect of different amounts of fly ash

Rand Uranium mine water (80 L) was mixed with either 8 or 13 kg of Matla coal FA in a jet loop reactor with jet sizes set at 12 mm. The pH, EC and temperature were measured after 15 min and aliquot samples were collected after every 30 min. The samples were filtered through a 0.45 µm filter paper and analysed using IC and ICP-OES.

3.8.2.3. Effect of the amount of fly ash and $Al(OH)_3$

Rand Uranium mine water was mixed with either 8 kg or 13 kg Matla coal FA in a jet loop reactor with jet sizes set at 12mm. After 30 min, 86.58 g of $Al(OH)_3$ was added to the mixture. The pH, EC and temperature were measured after 15 min and aliquot samples were collected after every 30 min. The samples were filtered through a 0.45 µm filter paper and analysed using IC and ICP OES.

3.8.2.4. Effect of different amounts of lime and $Al(OH)_3$

Rand Uranium mine water (80 L) was mixed with different amounts of lime (100, 150 and 100 g) in a jet loop reactor with jet sizes set at 12 mm. To each mixture 86.58 g of $Al(OH)_3$ was added after 30 min. The pH, EC and temperature were measured after every 15 min and aliquot samples were collected after every 30 min. The samples were filtered through a 0.45 µm filter paper and analysed using IC and ICP-OES.

3.8.2.5. Effect of different amounts of fly ash, lime and $Al(OH)_3$

Rand Uranium mine water (80 L) was mixed with 200 g of lime and different amounts of Matla coal FA (8 and 13 kg) in a jet loop reactor with jet sizes set at 12 mm. To each mixture 86.58 g of $Al(OH)_3$ was added after 30 min. The pH, EC and temperature were measured after 15 min and aliquot samples were collected after every 30 min. The samples were filtered through a 0.45 µm filter paper and analysed using IC and ICP-OES.

3.8.2.6. Effect of jet reactor mixing followed by overhead stirring

Rand Uranium mine water (80 L) was mixed with 100 g of lime and 13 kg of Matla coal FA in a jet loop reactor with jet sizes set at 12 mm. After 30 min, 86.58 g $Al(OH)_3$ was added to the mixture of Rand Uranium mine water and Matla coal FA. About 1 L of the mixture was collected and mixed with using an overhead stirrer. The pH, EC and temperature were measured after 15 min and aliquot samples were collected after every 30 min. The samples were filtered through a 0.45 µm filter paper and analysed using IC and ICP-OES.

CHAPTER 4: CHARACTERIZATION

In this chapter the physical and chemical characteristics of the raw materials; fly ash (FA), $Al(OH)_3$ and aluminium chlorohydrate (ACH) and mine water are presented and explained based on the data obtained from the analytical protocols explained in Chapter 3.

4.1. CHARACTERIZATION OF MATLA COAL FLY ASH

The FA used in this study was collected from Matla coal fired power station in Mpumalanga province of South Africa. Morphological characteristics of FA were visualized on a scanning electron microscope (SEM) as outlined in section 3.2.1. The results in Figure 4.1.1a show that FA is made up of mainly smooth spherical particles of less than 40 µm. Energy dispersive spectroscopy (EDS) showed that FA particles were composed of mainly Si and Al. Other elements such as O, Ca, K, Fe and Cu were present in small proportions as shown in Figure 4.1.1b.

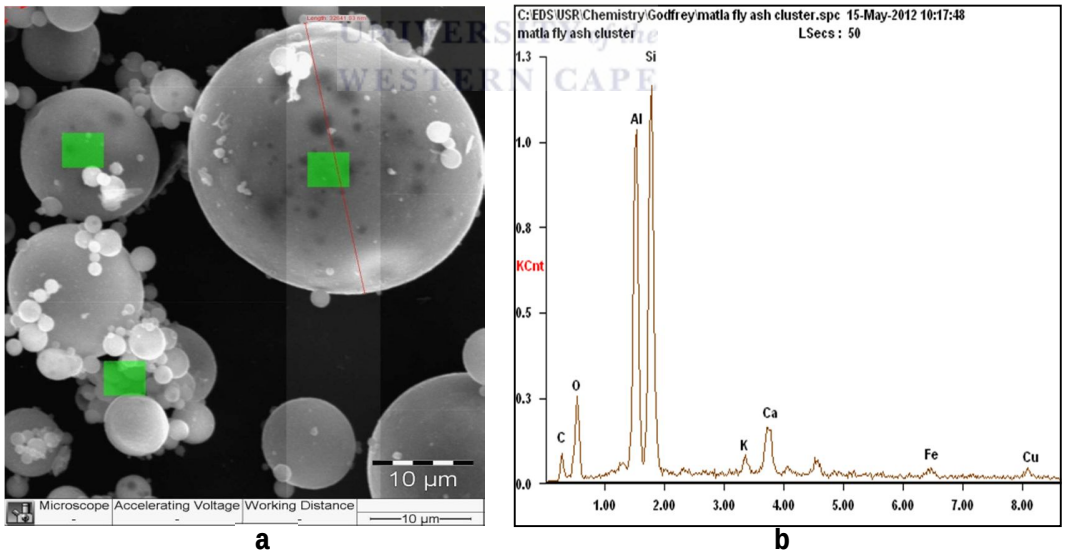

a b

Figure 4.1.1: The morphology of Matla FA using scanning electron microscopy at magnification x1000 (a) and the EDS spot analysis on the areas marked in green (b).

Matla FA was further characterized using XRD for the mineralogical composition as explained in section 3.2.2 and the results are as shown in Figure 4.1.2 below.

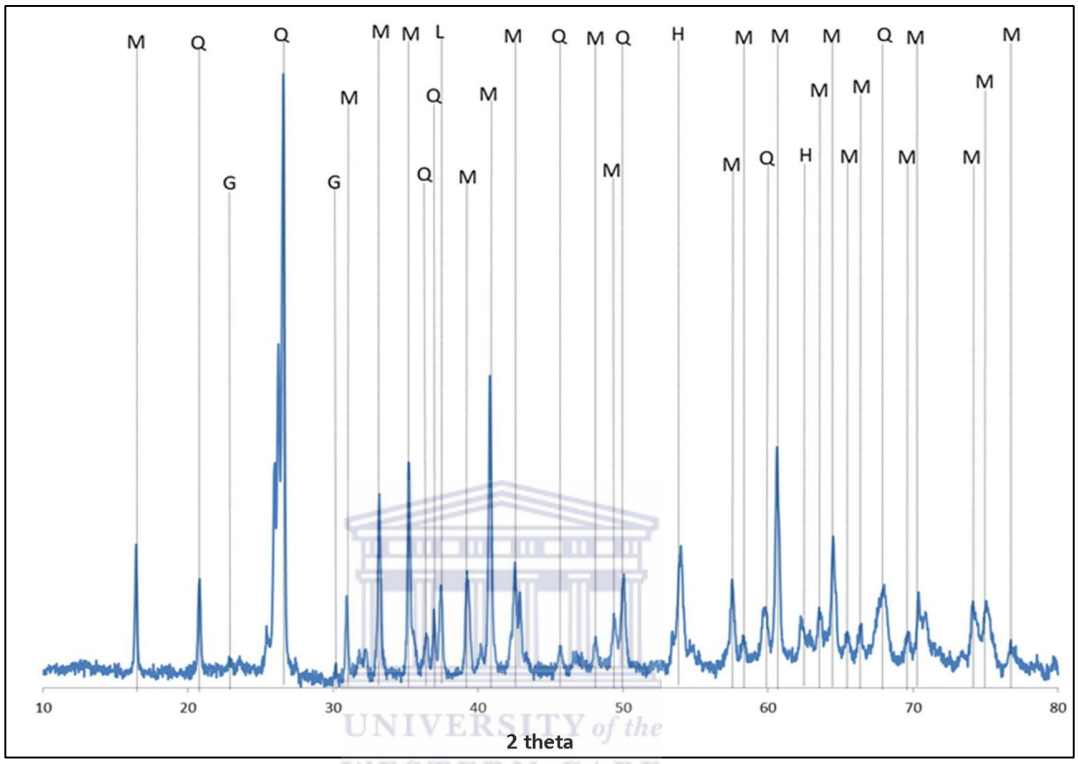

Figure 4.1.2: The XRD spectrum showing the mineralogical composition of Matla coal FA (M-mullite; Q-quartz; G-gypsum; L-lime; H-hematite).

From the XRD spectrum above the crystalline phases that make up Matla coal FA are mullite ($Al_2Si_2O_{13}$), quartz (SiO_2), hematite (Fe_2O_3), gypsum ($CaSO_4.2H_2O$) and lime (CaO). The XRD results correlated well with the EDS results.

Matla coal FA was also analysed using quantitative XRD to determine the percentage composition of the minerals determined by qualitative XRD in Figure 4.1.2. The percentage quantitative XRD results obtained are shown in Figure 4.1.3.

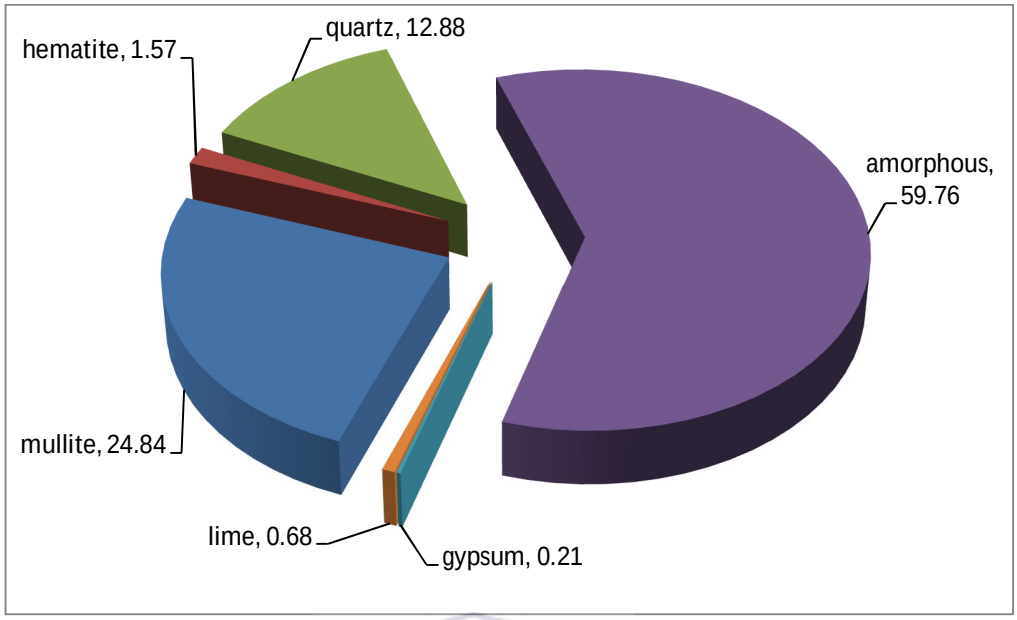

Figure 4.1.3: Quantitative XRD of fresh Matla coal FA.

The results of quantitative XRD for Matla coal FA show that, it was mainly composed of the amorphous phase which made up about 60 % of the Matla coal FA. Mullite, quartz, hematite, lime and gypsum constituted about 25 %, 13 %, 2 %, 1 % and 0.2 % respectively of Matla coal FA.

The quantitative elemental composition was analysed using XRF as outlined in section 3.2.3 and the results are as shown in the Table 4.1.1 below. The composition of FA shows that it was Class F since the sum of SiO_2, Fe_2O_3 and Al_2O_3 was greater than 70 % (ASTM, 1994; McCarthy, 1988). Class F is produced from the burning of bituminous coal and anthracites. Also Class F FA has pozzolanic properties, that is it hardens when reacted with $Ca(OH)_2$ and water (Vassilev and Vassileva, 2007). Matla FA was found to contain CaO (6.71 %). The lime imparts alkalinity to FA. It is this alkaline property that was exploited during the treatment of mine water with FA in this study. Loss on ignition is the carbon content that passed through the combustion process of the feed coal.

Table 4.1.1: The elemental composition of Matla coal fly ash obtained using XRF.

Majors			Minors		
oxide	% RSD	% w/w	element	% RSD	(mg/kg)
SiO_2	0.09	48.27 ± 0.044	Sr	-65	3495.55 ± 5.63
Al_2O_3	-0.52	30.89 ± 0.22	Ba	-11.67	2079.31 ± 12.80
CaO	-0.32	6.71 ± 0.08	Zr	9.00	787.73 ± 3.35
Fe_2O_3	-1.61	2.81 ± 0.03	Ce	1.79	226.02 ± 30.00
MgO	25	2.12 ± 0.04	Cu	-112.5	117.26 ± 3.38
TiO_2	-2.78	1.26 ± 0.02	La	2.75	111.45 ± 6.51
P_2O_5	0.53	0.89 ± 0.01	Y	2.80	103.71 ± 1.46
K_2O	0.15	0.84 ± 0.01	Nd	39.62	100.32 ± 2.45
Na_2O	-4.32	0.55 ± 0.01	Pb	2.50	100.25 ± 4.02
SO_3	NC	0.19 ± 0.002	Cr	NC	89.36 ± 2.29
MnO	12.50	0.02 ± 0.0004	Ni	18.5	88.97 ± 6.41
Loss on ignition	NC	5.24 ± 0	Rb	0.63	72.48 ± 0.89
Sum		**99.79 ± 0.07**	V	-75	64.91 ± 6.24
			Zn	-14	64.61 ± 4.41
			U	43.33	63.28 ± 2.43
			Ga	1.85	61.87 ± 1.89
			Nb	31.94	51.50 ± 1.80
			Th	3.92	46.60 ± 3.33
			As	26.67	20.07 ± 2.68
			Co	-100	16.08 ± 6.89
			Mo	NC	2.28 ± 0.02

NC and % RSD stand for not calculated and % relative standard deviation respectively.

Matla FA was found to contain potentially toxic elements such as Cr, Pb, Ba, Cu, Zn, V, etc and radioactive elements such as U and Th that could leach into surface or ground water if the FA is subjected to conditions that may mobilize these elements. Mobilization of these potentially toxic elements would enhance the bioavailability of these elements, thereby posing a health risk to the surrounding ecosystem. The trace elements detected in Matla coal FA were limited to the standards that were available. Elements that are not shown in Table 4.1.1 do not necessarily mean that they are not available in coal FA.

The minor and trace elements in Matla FA were also analysed using Laser Ablation Inductively coupled plasma-mass spectrometry (LA ICP-MS) as outlined in section 3.2.4. The results obtained are as depicted in Table 4.1.2 below. The results obtained using LA ICP-MS correlates well with the values obtained using XRF (for the minor elements analysed),

although the values are not the same. The highest minor elements in Matla FA were found to be Ba and Sr which were in g/kg values as shown in Table 4.1.1 and 4.1.2. Concentration of other elements determined by LA ICP-MS did not agree with XRF results, but generally the abundances of these elements seemed to correlate well.

Table 4.1.2: Concentration of trace elements in Matla FA obtained using LA ICP-MS.

element	% RSD	mg/kg	element	% RSD	mg/kg
Ba	8.25	2372.11 ± 32.01	Pr	6.32	18.35 ± 0.60
Sr	5.29	2137.02 ± 81.70	Co	2.35	17.30 ± 0.49
Zr	1.30	313.94 ± 19.57	Cs	1.55	13.64 ± 0.11
Ce	4.76	189.78 ± 4.13	U	7.64	13.38 ± 0.38
Cr	4.48	183.01 ± 2.41	Sm	8.95	11.95 ± 0.56
V	1.41	154.31 ± 3.49	Mo	8.26	10.45 ± 0.33
La	9.46	81.66 ± 4.31	Gd	6.36	10.40 ± 0.82
Pb	5.68	69.00 ± 1.78	Dy	5.42	9.50 ± 0.56
Nd	8.21	63.50 ± 1.78	Hf	7.03	8.63 ± 0.57
Cu	0.25	61.84 ± 0.96	Er	3.12	5.38 ± 0.28
Rb	3.87	55.46 ± 2.20	Yb	8.83	5.27 ± 0.47
Y	3.72	52.30 ± 3.47	Ta	4.34	2.69 ± 0.11
Ni	3.86	49.54 ± 1.80	Eu	9.48	2.35 ± 0.13
Zn	8.57	45.25 ± 2.67	Ho	4.81	1.97 ± 0.19
Nb	4.69	42.97 ± 1.35	Tb	7.23	1.60 ± 0.12
Th	10.56	35.44 ± 1.53	Tm	1.51	0.77 ± 0.06
Sc	1.71	24.94 ± 1.46	Lu	2.22	0.72 ± 0.04

% RSD stands for percentage relative standard deviation.

Minor and trace element analysis of Matla FA has shown that it contained about 34 elements. These elements included 16 (Ce, La, Nd, Y, Sc, Pr, Sm, Gd, Dy, Er, Eu, Ho, Tb, Tm and Lu) of the rare earth elements (REE) excluding promethium (Pm). The concentration of REE was found to be much higher than the normal concentration in the soil (Long et al., 2010). Rare earth elements have found wide applications in catalysis, magnetic resonance imaging and other applications in industry. It is worthwhile to study cheap technologies to recover these elements from FA. This would minimize the release of these elements into the environment in addition to finding a readily available source of these valuable minerals.

Radioactivity of Matla FA was undertaken using gamma spectrometric analysis as explained in Chapter 3, section 3.2.5 and the results are as shown in Table 4.1.3. There were no anthropogenic (man-made) radionuclides found in Matla coal FA. Only naturally occurring radionuclides materials (NORM) were detected, which were U, Th, Ra, Pb and K. The activities ($Bq.kg^{-1}$) were converted to mg/L using the relationship (Debertin, 1996):

$$1Bq = \frac{m}{Ar} \times N \times \frac{\ln 2}{t_{\frac{1}{2}}}$$

$$where\ m = mass\ in\ g, Ar = atomic\ mass\ in\ g.mol^{-1},$$

$$N = Avogadro's\ number\ and\ t_{\frac{1}{2}} = half\ life\ in\ sec$$

Table 4.1.3: Gross alpha and beta radioactivity and the activity of the different radioisotope in Matla coal FA.

Nuclide	Activity ($Bq.kg^{-1}$)	Concentration (mg/kg)
^{238}U	186 ± 2	14.95 ± 0.0002
^{234}U	188 ± 2	$8.14 \times 10^{-4} \pm 8.68 \times 10^{-9}$
^{235}U	8.58 ± 0.009	$0.11 \pm 1.12 \times 10^{-7}$
^{232}Th	156 ± 3	$1.13 \times 10^{-6} \pm 1.07 \times 10^{-10}$
^{228}Th	184 ± 10	$38.42 \pm 7.4 \times 10^{-4}$
^{228}Ra	182 ± 13	$1.82 \times 10^{-8} \pm 2.46 \times 10^{-12}$
^{226}Ra	161 ± 9	$4.4 \times 10^{-6} \pm 1.3 \times 10^{-10}$
^{210}Pb	320 ± 32	$1.07 \times 10^{-6} \pm 1.07 \times 10^{-10}$
^{40}K	330 ± 39	$1.24 \pm 1.47 \times 10^{-4}$
Gross alpha	3440 ± 210	
Gross beta	1200 ± 20	

The results in Table 4.1.3 showed that Matla coal FA was much more radioactive than average radioactivity in the soil. The radioactivity was found to be attributed to mainly ^{238}U, ^{234}U, ^{235}U, ^{232}Th, ^{228T}h, ^{228}Ra, ^{226}Ra, ^{210}Pb, and ^{40}K. The Th concentration in Matla coal FA was almost ten times greater than the concentration of ^{232}Th in soil samples collected from a gold mine dump in Witwatersrand Goldfields, South Africa. The ^{238}U and ^{40}K concentration was comparable to the same soil sample collected from a gold mine dump (Newman et al., 2008). The ^{232}Th activity of Matla coal FA was slightly greater than the average activity concentration of ^{232}Th in Greece. The activity concentration of ^{238}U and ^{40}K

in Matla FA was within the range of the activity concentration found in Greece FA (Papastefanou, 2010; Baykal and Saygili, 2011; Turhan et al., 2010; USGS, 1997). Exposing of the FA to aqueous conditions such as in the remediation of the AMD might cause the mobilization of these radioisotopes thereby contaminating the treated water. So it is necessary to find out if these radioisotopes are mobilized when Matla coal FA is mixed with AMD.

The total concentrations of Th obtained using XRF, LA ICP-MS and NAA and gamma analysis were close to each other. Thorium concentration obtained using LA ICP-MS (35.44 mg/kg) was closer to that obtained using gamma spectrometry analysis (38.42 mg/kg) than that obtained using XRF (46.60 mg/kg). Scheid et al (2009) have found that gamma spectrometry analysis and LA ICP-MS gave Th results that were in agreement to each other when the brick clay was analysed using the two techniques. On the other hand it was not possible to detect Th in brick clay of concentration less than 14 mg/kg of Th.

Uranium concentration obtained using XRF (63 mg/kg) was well above the values obtained using LA ICP-MS (13.38 mg/kg) and that of gamma spectrometry (14.95 mg/L). This shows that XRF analysis of the radioactive elements such as U and Th was not that accurate. Thus XRF produced values that were higher than the more sensitive techniques such as gamma spectrometry and LA ICP-MS. The accuracy of XRF analysis of U and other trace elements was not reliable because of the higher percentage relative standard deviation of most trace elements as shown in Table 4.1.1. Percentage relative standard deviation was calculated as follows:

$$\frac{Expected\ value - Analytical\ Value}{Expected\ value} \times 100$$

$$where\ expected\ value\ is\ the\ value\ on\ the\ certified\ standard\ and$$
$$analytical\ value\ is\ the\ value\ obtained\ when\ the\ certified\ was\ analysed$$

The total concentration of Pb in Matla coal FA obtained using XRF and LA ICP-MS was 100 mg/kg and 69 mg/kg respectively. Gamma spectrometry analysis of Pb showed that

1.07 x 10^{-6} mg/kg was the radioactive ^{210}Pb. Also the gamma spectrometry analysis showed that 1.24 mg/kg of K was ^{40}K out of 6973 mg/L detected by XRF in Matla FA.

4.2. CHARACTERIZATION OF ALUMINIUM CHLOROHYDRATE

The composition of aluminium chlorohydrate gel (ACH) was determined using ICP-OES and IC as outlined in section 3.4. The results are as shown in Table 4.2.1 below. From Table 4.2.1, ACH gel was acidic and comprised of Al and Cl ions in its structure.

Table 4.2.1: The composition of aluminium chlorohydrate gel.

Element	Concentration (mg/L)
pH	3.38
Al	135769
Cl	170578

The speciation of ACH gel was elucidated using Geochemist's workbench (GWB) software, to determine how the Al and Cl are associated in the ACH gel. It was shown that Al existed as Al^{3+}, $Al_{13}O_4(OH)_{24}^{7+}$, $Al_3(OH)_4^{5+}$, $Al_2(OH)_2^{4+}$, $AlOH^{2+}$, $Al(OH)_2^{+}$, $Al(OH)_3$ and $Al(OH)_4^{-}$ as shown in Figure 4.2.1 below.

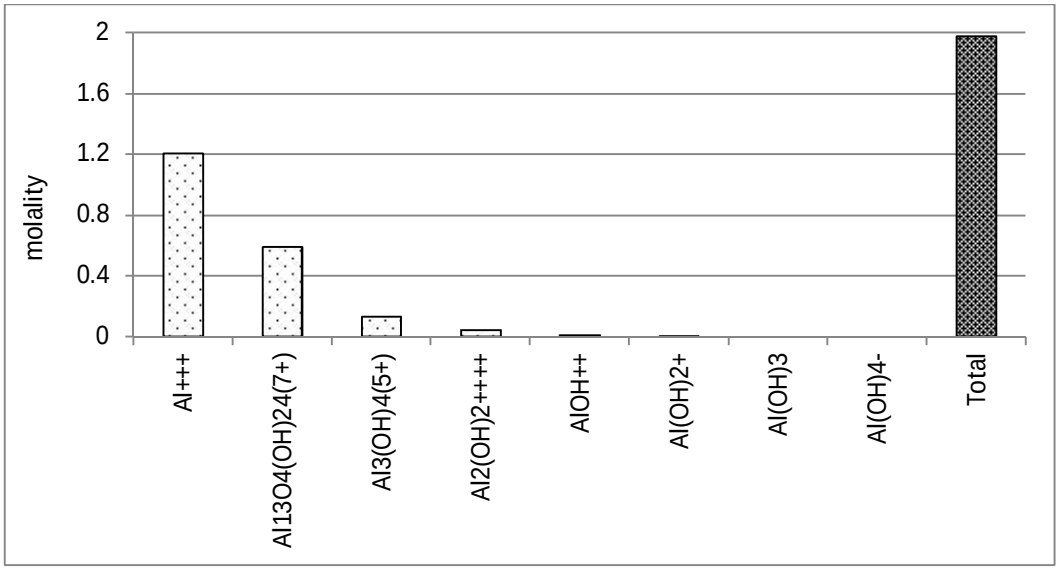

Figure 4.2.1: The Al species in aluminium chlorohydrate gel.

Free Al^{3+} ions make up about 61 % of the total Al concentration in ACH. Oligomeric Al species such as $Al_{13}O_4(OH)_{24}^{7+}$, $Al_3(OH)_4^{5+}$and $Al_2(OH)_2^{4+}$ make up about 30, 6 and 2 % of the total Al concentration in ACH. Mononuclear species such as $AlOH^{2+}$, $Al(OH)_2^{+}$, $Al(OH)_3$ and $Al(OH)_4^{-}$ were in very low abundances in ACH. The results obtained using GWB software agreed with those obtained by other researchers who used sophisticated analytical protocols such Al-Ferron kinetics method and ^{27}Al-nuclear magnetic resonance spectrometry (^{27}Al-NMR). They found that most Al based flocculants are made of mainly hydrated Al^{3+} and $Al_{13}O_4(OH)_{24}^{7+}$ species (Zhou et al., 2006; Chen et al., 2009).

The Cl species in ACH gel was determined using the Geochemist's workbench and are as shown in Figure 4.2.2 below. It was found that the Cl mainly existed as free Cl^- ions, with very low amounts of HCl species in ACH gel.

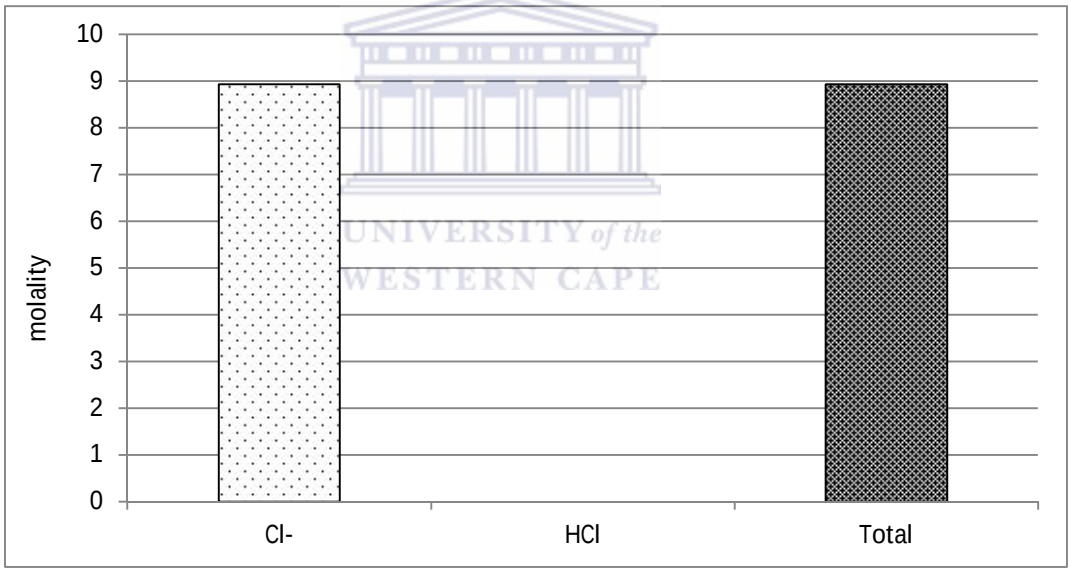

Figure 4.2.2: The Cl species in aluminium chlorohydrate gel.

4.3. CHARACTERIZATION OF ALUMINIUM HYDROXIDE

Aluminium hydroxide was analysed using SEM to establish the morphological make up. It was established that $Al(OH)_3$ was made up of spherical particles with rough surfaces. The energy dispersive X-ray spectroscopy (EDS) spot analysis on selected areas in the microgram

revealed that $Al(OH)_3$ was made up of mainly Al and O. The C element that was present in the spectrum was due to the C-coating of the sample before analysis.

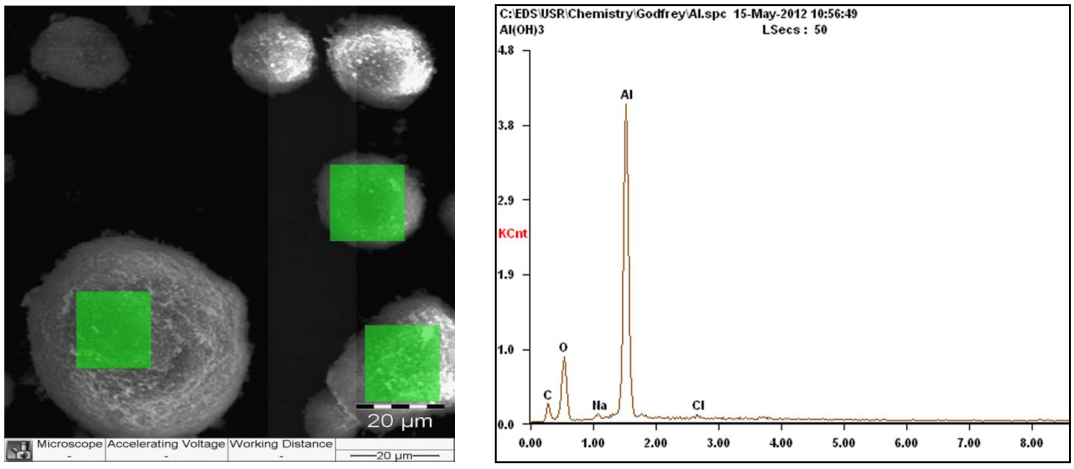

a **b**

Figure 4.3.1: The SEM micrograph (a) and the EDS spot analysis (b) of $Al(OH)_3$ (*green squares indicate the spots were EDS analysis was carried out on the micrograph*).

The mineral phases of $Al(OH_3$ were determined using XRD and the spectrum is as shown in Figure 4.3.2 below.

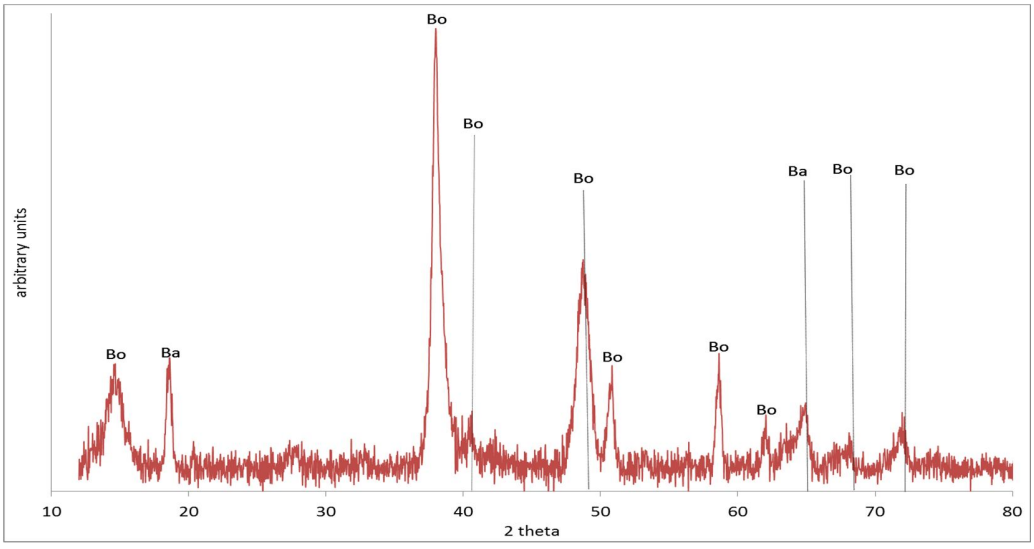

Figure 4.3.2: XRD spectrum of $Al(OH)_3$ (Bo stands for boehmite and Ba stand for bayerite). $Al(OH)_3$ was made of bayerite ($Al_2O_3.3H_2O$) and boehmite (AlOOH) mineral phases.

These results correlated well with the EDS results obtained, which showed that $Al(OH)_3$ was made of almost exclusively Al and O (Figure 4.3.1b).

The aluminium hydroxide was analysed using XRF to determine the elemental composition and the results obtained are shown in Table 4.3.1.

Table 4.3.1: Elemental composition of aluminium hydroxide.

Oxide	% composition ± standard deviation
Al_2O_3	65.13 ± 0.86
Fe_2O_3	11.67 ± 0.54
SO_3	4.24 ± 0.45
SiO_2	1.75 ± 0.24
CaO	0.48 ± 0.05
Na_2O	0.38 ± 0.004
K_2O	0.05 ± 0.01
Loss on ignition	16.25 ± 0.13
Sum	99.93 ± 0.29

From the XRF results obtained aluminium hydroxide was made up of mainly Al with contaminants of Fe, S, Si, Ca and Na. The loss of ignition of about 16.25 % was determined. This can be attributed to the moisture that was in the aluminium hydroxide.

4.4. CHARACTERIZATION OF LIME

Lime was analysed using SEM to determine its structure as shown in Figure 4.4.1a. Figure 4.4.1b show the EDS spot analysis results of lime. It was observed that lime was made of agglomerated irregular particles which were made up of mainly Ca and O.

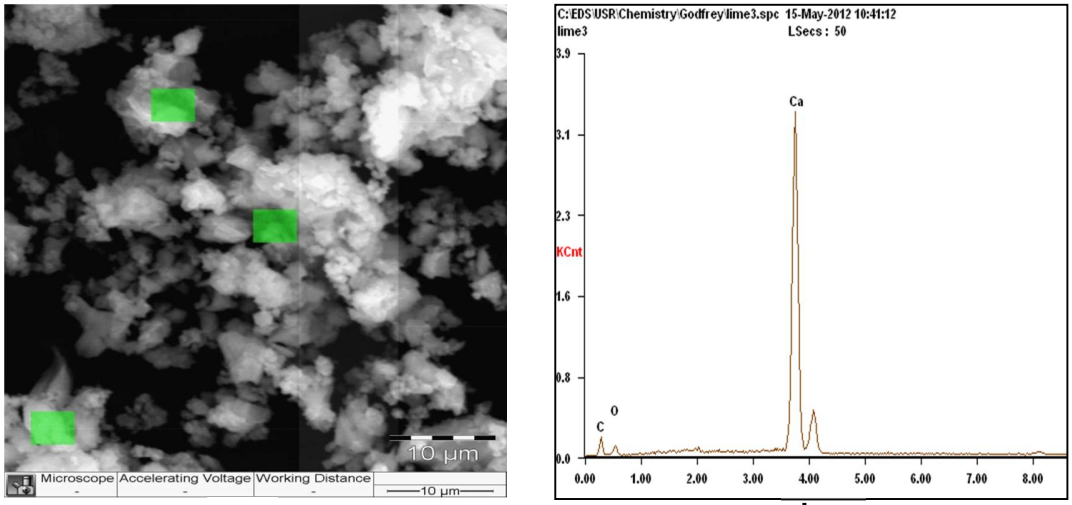

a **b**

Figure 4.4.1: The SEM (a) and the EDS (b) analysis of lime *(green squares indicate the spots were EDS analysis was carried out on the microgram*).

Characterization of lime obtained from KIMIX chemicals was conducted using XRD and XRF. According to the XRF results the lime was found to be composed of mainly CaO which made up about 72 % of the lime as shown in Table 4.4.1. The other major composition of the lime was loss on ignition (LOI), which made up of about 27 %. The LOI in this case can be attributed to moisture content. This correlates well with the EDS results.

Table 4.4.1: Elemental composition of lime.

oxide	**% (w/w) composition ± standard deviation**
CaO	72.19 ± 1.27
MgO	0.72 ± 0.24
Na_2O	0.23 ± 0.05
SiO_2	0.12 ± 0.02
Al_2O_3	0.09 ± 0.04
Fe_2O_3	0.06 ± 0.01
K_2O	0.02 ± 0.003
MnO	0.02 ± 0.001
P_2O_5	0.01 ± 0.002
TiO2	0.01 ± 0.001
Loss on ignition	26.65 ± 1.34
total	**100.12** ± 0.98

Mineralogy analysis of lime using XRD showed that it was indeed made of mainly lime (CaO) and calcite ($CaCO_3$) minerals as shown in Figure 4.4.2. Calcite could have resulted from the interaction of CaO with CO_2 from the atmosphere.

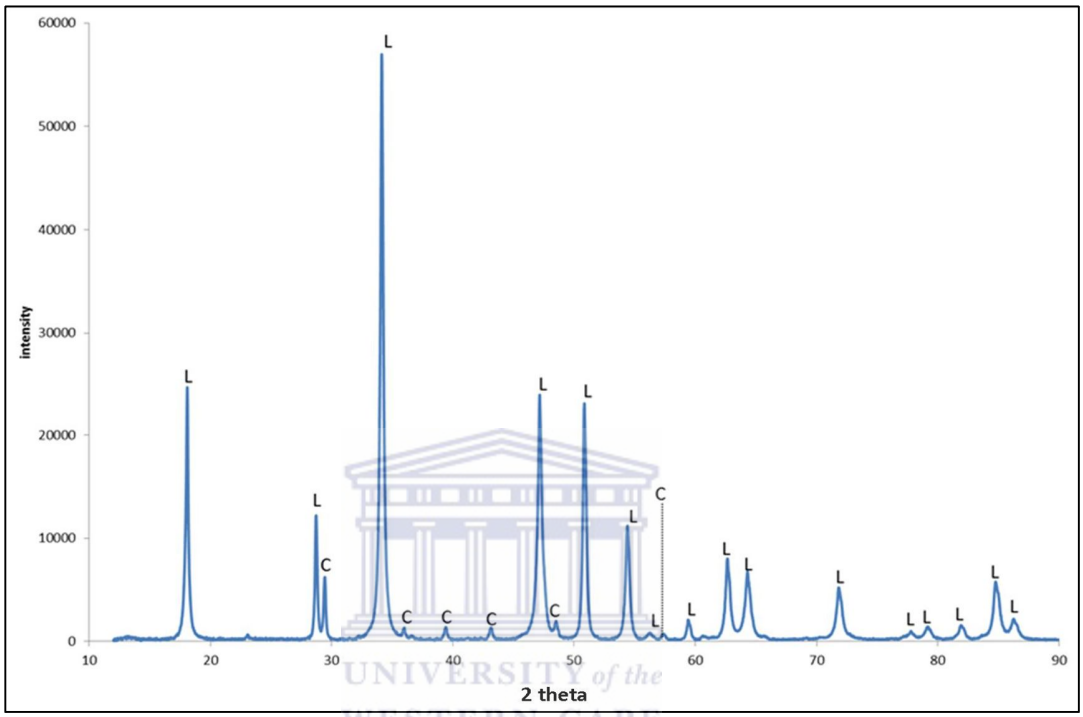

Figure 4.4.2: XRD spectrum of lime (L-lime and C-calcite).

4.5. CHARACTERIZATION OF MATLA MINE WATER

Matla mine water was collected from a coal mine in Mpumalanga province. The composition and alkalinity of mine water was determined using the inductively coupled plasma-optical emission spectroscopy (ICP-OES), ion chromatography (IC) and Metrohm Autotitrator as explained in section 3.5. The results obtained are as shown in Table 4.5.1. From Table 4.5.1 the pH of Matla mine water was 8. This means that Matla mine water was neutral mine drainage (NMD) because the pH was between 6 and 8 (Morin and Hutt, 1997; Younger et al., 2002).

Table 4.5.1: The physicochemical parameters of Matla mine water.

Parameter	units	value	TWQR for potable water
pH	-	8.00 ± 1.07	6-9
Electrical conductivity	µS/cm	**3371 ± 24**	0-700
Alkalinity	mg/L of $CaCO_3$	561.6 0± 7.16	NA
TDS	mg/L	**1955 ± 14.28**	0-600 (450)
Hardness	mg/L of $CaCO_3$	**333.33 ± 9.76**	0-200 (100)
Sulphate	mg/L	**1475 ± 2**	200-500
Na	mg/L	**956.05 ± 19.26**	0-200 (100)
Ca	mg/L	**70.35 ± 3.05**	(0-32)
Mg	mg/L	**39.54 ± 1.12**	(0-30)
Cl	mg/L	24.00 ± 1.84	0-250 (100)
B	mg/L	**14.93 ± 1.07**	0-2.4
K	mg/L	10.08 ± 0.92	(0-50)
Hg	mg/L	**2.43 ± 0.13**	0-0.006 (0.001)
Sr	mg/L	2.05 ± 0.06	NA
Se	mg/L	**1.12 ± 0.09**	0-0.04 (0.02)
Zn	mg/L	0.41 ± 0.012	0-0.5 (3)
Ba	mg/L	0.2 ± 0.0009	0-0.7
Cu	mg/L	0.19 ± 0.0073	0-2 (1)
Fe	mg/L	0.06 ± 0.0017	0-0.3 (0.1)
Al	mg/L	0.056 ± 0.0013	0-0.2 (0.15)
Ni	mg/L	0.023 ± 0.0012	0-0.07
Be	mg/L	**0.017 ± 0.0035**	0-0.012
Mn	mg/L	0.0094 ± 1.12 x 10^{-4}	0-0.1 (0.05)
V	mg/L	0.0081 ± 1.98 x 10^{-4}	0-0.01
Cd	mg/L	**0.005 ± 1.79 x 10^{-5}**	0-0.003 (0-0.005)
As	mg/L	0.0027 ± 2.01 x 10^{-5}	0-0.01
Cr	mg/L	nd	0-0.05
Pb	mg/L	nd	0-0.01
Mo	mg/L	nd	NA
Co	mg/L	nd	NA
Th	mg/L	nd	NA
U	mg/L	nd	0-0.03 (0.07)

Note: values in brackets obtained from Department of Water Affairs of South Africa if the values are different from those indicated by World Health Organization (WHO, 2011; DWAF, 1996). NA and nd stand for "not applicable" and "not detected" respectively. TWQR stands for target water quality target.

Matla mine water was formed from the oxidation of pyrite followed by in situ neutralization by acid neutralizing minerals such as Na_2CO_3 as shown in Equation 4.1. This resulted in water

with pH of 8, which was near neutral and contained elevated concentration of Na and sulphate ions.

$$4FeS_2+8Na_2CO_3+6H_2O+15O_2\rightarrow 4Fe(OH)_3+16Na^{+}+8CO_2+8SO^{2-}_4 \quad \text{.....4.1}$$

The water contained low concentration of Fe, Al and Mn. This was because at pH greater than 6, Fe and Al precipitate out as hydroxides, while Mn is known to precipitate out at pH greater than 9 (Gitari et al., 2008, Madzivire, 2010). Elevated concentration of sulphate ions causes water to have a taste. Taste varies with the cation associated with the sulphate ion. For water containing sulphate ions associated with Na ions such as Matla mine water the taste threshold is 250 mg/L. If the sulphate ions are associated with Ca the taste threshold is about 1000 mg/L (WHO, 2011). On the hand water containing sulphate concentration of greater than 1000 mg/L can cause laxative effects to individual who have not adapted to the water (WHO, 2011). This means that Matla mine water can have noticeable taste and can also cause laxative effects to individuals who are not used to the water.

Other than Na and sulphate ions, Matla mine water contained elevated concentration of potentially toxic elements such as B, Hg and Se. These elements were above the TWQR for potable water set by World Health Organization (WHO, 2011) and Department of Water Affairs (DWA, 1996). The concentration of Mg and Ca ions was also above the TWQR for potable water. These elements contributed to the high total hardness of Matla water since hardness is proportional to the concentration of Ca and Mg as shown by the following equation (DWA, 1996).

$$total\ hardness = 2.497[Ca] + 4.118[Mg], where\ [X] is\ the\ concentration\ in\ mg/L$$

4.6. CHARACTERIZATION OF RAND URANIUM MINE WATER

Rand Uranium mine water was collected from the Western Rand basin in Witwatersrand Goldfields, South Africa. The mine is a semi abandoned mine since the mine tailings are being reworked and no underground mining is taking place anymore. The pH, EC and total dissolved solids (TDS) were measured onsite. The chemical composition of the samples were

analysed using IC and ICP-OES as outlined in Chapter 3, section 3.5. The results obtained are shown in Table 4.6.1.

Table 4.6.1: The physicochemical parameters of Rand Uranium mine water.

Parameter	mine water 1	mine water 2	Potable water limit
pH	3.48 ± 0.58	2.65 ± 0.81	6-9
EC	3292 ± 36	2000 ± 27	0-700
acidity	752 ± 3	266 ± 7	NA
TDS	1685 ± 52	1076 ± 34	0-600 (0-450)
hardness	1549 ± 33	1529 ± 28	0-200 (0-100)
Sulphate	4126 ± 44	2562 ± 5	0-500
Fe	895.62 ± 0.45	201.10 ± 0.55	0-0.3 (0-0.1)
Ca	376.33 ± 0.78	360.10 ± 4.25	0-32
Mn	282.21 ± 38	60.16 ± 0.17	0-0.1 (0-0.05)
Mg	155.46 ± 0.34	153.00 ± 0.70	0-30
Na	81.08 ± 0.55	89.44 ± 0.085	0-200 (0-100)
Cl	10.24 ± 1.04	26.89 ±0.67	250 (0-100)
B	5.43 ± 0.22	0.231 ± 0.004	0-2.4
Al	4.06 ± 0.89	26.63 ± 0.29	0-0.2 (0-0.15)
Cr	$3.15 \pm 4.16 \times 10^{-3}$	$0.023 \pm 2.9 \times 10^{-4}$	0-0.05
Sr	0.56 ± 0.15	$0.45 \pm 3.39 \times 10^{-3}$	NA
Pb	0.51 ± 0.013	$7.5 \times 10^{-3} \pm 1.7 \times 10^{-5}$	0-0.01
K	0.46 ± 0.02	6.47 ± 0.013	0-50
Cu	0.21 ± 0.052	$0.28 \pm 3.26 \times 10^{-3}$	0-2 (0-0-1)
U	0.29 ± 0.083	$0.27 \pm 1.01 \times 10^{-3}$	0.07 (0-0.03)
Zn	0.25 ± 0.19	1.93 ± 0.013	0-3 (0-0.5)
Th	0.013 ± 0.18	$0.018 \pm 3.06 \times 10^{-5}$	NA
P	$0.11 \pm 1.72 \times 10^{-3}$	$0.024 \pm 1.14 \times 10^{-5}$	NA
Se	0.058 ± 0.42	$0.061 \pm 2.30 \times 10^{-3}$	0-0.02 (0-0.04)
Ba	$0.06 \pm 6.46 \times 10^{-3}$	$0.026 \pm 4.31 \times 10^{-4}$	0-0.7
Li	0.003 ± 0.01	$0.069 \pm 4.18 \times 10^{-5}$	NA
Be	$5.7 \times 10^{-3} \pm 8.6 \times 10^{-4}$	$3.9 \times 10^{-3} \pm 4.2 \times 10^{-5}$	0-0.012
Cd	$7.1 \times 10^{-3} \pm 1.27 \times 10^{-3}$	$6.8 \times 10^{-3} \pm 1.2 \times 10^{-5}$	0-0.003 (0-0.005)
As	$4.1 \times 10^{-3} \pm 3.46 \times 10^{-3}$	$5.8 \times 10^{-3} \pm 2.5 \times 10^{-5}$	0-0.001
V	$1.7 \times 10^{-3} \pm 1.41 \times 10^{-3}$	$1.2 \times 10^{-3} \pm 7.7 \times 10^{-6}$	(0-0.01)
Ni	$7.1 \times 10^{-4} \pm 7.25 \times 10^{-6}$	$5.3 \times 10^{-4} \pm 4.3 \times 10^{-3}$	NA
Mo	$4.81 \times 10^{-4} \pm 2.08 \times 10^{-4}$	$5.3 \times 10^{-5} \pm 2.4 \times 10^{-5}$	0-0.07
Hg	$1.2 \times 10^{-6} \pm 4.3 \times 10^{-7}$	$3.9 \times 10^{-6} \pm 1.2 \times 10^{-6}$	0-0.006 (0-0.001)

Note: values in brackets obtained from Department of Water Affairs of South Africa 1996 if the values are different from those indicated by World Health Organization (WHO, 2011; DWAF, 1996). NA stands for not applicable. TWQR stands for target water quality range. The units for parameters are mg/L except pH which is unitless, EC (mS/cm) and TDS and hardness (mg/L of $CaCO_3$)

In Table 4.6.1, there are two different analyses of Rand Uranium mine water given because the waters were sampled during different seasons. Rand Uranium mine water 1 (RU1) was sampled in May 2011, which was the beginning of winter in Johannesburg, South Africa. Rand Uranium mine water 2 (RU2) was sampled in January 2012, which was mid-summer season. RU2 looks like a diluted sample of RU1 because the concentration of most of the elements was less than that of RU1.

The pH of the two Rand Uranium mine waters were 3.48 and 2.68 which was not within the target water quality range (TWQR) as shown in Table 4.61. According to Morin and Hutt (1997), Rand Uranium mine water can be classified as acid mine drainage (AMD) because the pH was below 6. Rand Uranium mine water has a high concentration of Fe and Al. Typically AMD contains more of the combined concentration of Fe, Al and Mn than the combined concentration of Ca, Mg and Na (Cravotta et al., 1990; Lottermosser, 2007 and Younger et al., 2002).

In the Western Rand basin Au occurs in association with pyrite (FeS_2). Pyrite makes up about 3 % of the Au bearing minerals (Durand, 2012). Rand Uranium mine water was formed by oxidation of the acid producing mineral FeS_2 by exposure to O_2 and H_2O as shown in Equation 4.2.

$$FeS_2 + \tfrac{7}{2}O_2 + H_2O \rightarrow Fe^{2+} + 2H^+ + 2SO_4^{2-} \quad \text{.....4.2}$$

The other associated minerals such as dolomite and limestone occurred in insufficient proportions to neutralize the acidity generated by the oxidation of acid producing minerals resulting in acidic water. The acidity generated from FeS_2 caused the chemical weathering of surrounding rocks, therefore leaching potentially toxic elements into the water such as Ca, Mg, Na, Cl, Al, Mn, B, Cr, Pb, Th, Ba, Hg, As and Se. Out of these elements, Rand Uranium mine water contained elevated concentration of Fe, Ca, Mn, Mg, B, Al, Cr, Pb, U and sulphate above the TQWR for domestic use as shown in Table 4.6.1 (DWAF, 1996; WHO, 2011). The pH of Rand Uranium mine water makes it unsuitable for domestic, agricultural and industrial use (DWAF 1996; WHO, 2011).

4.6.1. RADIOACTIVITY CHARACTERIZATION OF RAND URANIUM MINE WATER

The geology of the West Rand basin is made of more U minerals than Au bearing minerals (Cole, 1998). Analysis of the Rand Uranium mine water 2 for radioactivity was carried out using alpha and gamma spectrometry as outlined in section 3.5.2. The results obtained indicated that the gross alpha and beta radioactivity of the mine water was 12 and 6 times more than the required limit for potable water respectively, as shown in Table 4.6.2. The maximum gross alpha and beta radioactivity for potable water are 0.5 $Bq.L^{-1}$ and 1 $Bq.L^{-1}$ respectively (WHO, 2011).

Table 4.6.2: Alpha, beta and isotope activities of Rand Uranium mine water 2.

isotope	activity ($Bq.L^{-1}$)	Concentration (µg/L)	WHO, 2011 ($Bq.L^{-1}$)
^{238}U	3.16 ± 0.04	253.99 ± 3.22	10
^{234}U	**4.71 ± 0.05**	0.020 ± 2.17 x 10^{-4}	1
^{230}Th	0.69 ± 0.11	9.59 x 10^{-4} ± 1.47 x 10^{-4}	1
^{226}Ra	0.36 ± 0.01	9.87 x 10^{-6} ± 2.74 x 10^{-7}	1
^{210}Po	0.02 ± 0.0037	4.47 x10^{-8} ± 8.10 x 10^{-9}	0.1
^{235}U	**0.145 ± 0.002**	1.81 ± 0.025	1
^{227}Th	0.202 ± 0.016	1.77 x 10^{-10} ± 1.41 x 10^{-11}	10
^{229}Ra	0.101 ± 0.01	1.33 x 10^{-14} ± 1.32 x 10^{-15}	-
^{232}Th	0.0619 ± 0.071	15.24 ± 1.75	1
^{228}Th	**0.124 ± 0.01**	4.23 x 10^{-9} ± 3.41 x 10^{-10}	1
^{224}Ra	0.0306 ± 0.045	5.11 x 10^{-12} ± 7.51 x 10^{-13}	1
gross alpha	**6.01 ± 0.93**		0.5
gross beta	**6.05 ± 0.41**		1

Radioisotopes that contributed to the radioactivity of Rand Uranium mine water were; ^{238}U, ^{234}U, ^{230}Th, ^{226}Ra, ^{235}U, ^{227}Th, ^{229}Ra, ^{232}Th, ^{228}Th, and ^{224}Ra. The activities of radioisotopes that were greater than the allowed limit for potable water were ^{234}U, ^{235}U and ^{228}Th as shown in Table 4.6.2. If U is allowed to accumulate in the kidneys it causes kidney failure (WHO, 2011). Total U concentration that was determined for U in Rand Uranium mine water was about 256 µg/L. This was well above the allowed limit for total U concentration set by WHO in 2011, which is 30 µg/L. Analysis of Rand Uranium mine water with ICP-OES showed that the water contained 290 µg/L of U and 18 µg/L of Th as shown in Table 4.6.1. These results were close to those obtained using alpha and gamma spectrometry which found that the

concentration of U and Th were about 256 µg/L and 15 µg/L respectively. This showed that ICP-OES can be used to analyse radioactive elements such as Th and U (in aqueous solutions) instead of the sophisticated, rigorous and expensive analytical techniques such as alpha and gamma spectrometry. There were no radioactive isotopes for K and Pb detected in Rand Uranium mine water using alpha and gamma spectrometry.

The radioactivity detected in the mine water is attributed to the fact that U is mined in addition to Au mining at Rand Uranium mine. The exposure of FeS_2 to oxidizing conditions results in formation of AMD. The low acidity of the water enhances the dissolution of the associated U containing minerals, resulting in AMD which is radioactive. Since the radioactive of Rand Uranium mine water was much greater than the required limit for potable water, the treated water should be evaluated for radioactivity as well.

4.7. CHEMICAL SPECIATION MODELLING OF THE MINE WATER

Speciation as defined here is the chemical form in which ions exist in aqueous or natural waters. Speciation is very important because the bioavailability of an ion or element as a required nutrient or toxicant depends on its chemical form. The toxicology of some elements is very complex because some elements can be toxic in one form and also be an essential nutrient if they exist in another form (Jain and Ali 2000; Florence et al., 1992; Allen et al., 1980). Mostly hydrated metal ions are considered to be toxic, while complexed species are usually deemed less toxic (Russeva 1995). Different analytical protocols and models have been used to elucidate the different forms of ions in natural water. In this study Geochemist's workbench (GWB) software was used to speciate the ions that were detected in Matla mine water and Rand Uranium mine water using ICP-OES and IC as explained in section 3.6.

4.7.1. AQUEOUS DISTRIBUTION OF MAJOR ELEMENTS IN MATLA MINE WATER

Matla mine water was speciated using the SpecE8 sub program of the GWB software as explained in section 3.6. Matla mine water was found to be a Na-SO_4 type of water. This

means that the main cation for Matla mine water was Na and the water contained sulphate ions as the main anion.

The predicted distribution of the Mg species in Matla mine water obtained using SpecE8 sub program of the GWB software is shown in Figure 4.7.1 below. From Figure 4.7.1, the Mg species in Matla mine water were found to be mainly free Mg^{2+} ions and $MgSO_4$ which made up 65 % and 31 % respectively of the total Mg content in Matla mine water. $MgHCO_3^-$ species contributed about 4 % of the total Mg content in Matla mine water.

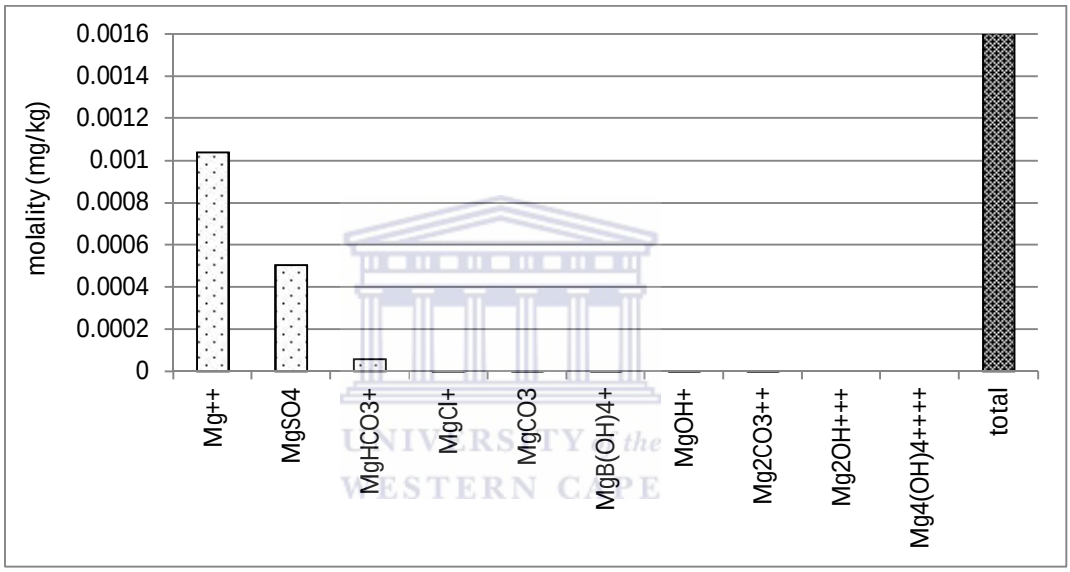

Figure 4.7.1: Magnesium aqueous species distribution in Matla mine water.

Other species such as $MgCl^+$, $MgCO_3$, $MgB(OH)_4^+$, $MgOH^+$, $Mg_2CO_3^{2+}$, Mg_2OH^{3+} and $Mg_4(OH)_4^{4+}$ contributed less than 0.05 % of the total Mg content in Matla mine water.

Sulphate species in Matla mine water that were predicted using SpecE8 program of the GWB software are depicted in Figure 4.7.2. The program predicted that sulphate existed mainly as free SO_4^{2-} ions in Matla mine water and constituted about 86 %. About 7 %, 4 % and 3 % of the sulphate ions in Matla mine water comprised of $NaSO_4^-$, $CaSO_4$ and $MgSO_4$ species. Less than 0.1 % of the sulphate content in Matla mine water was comprised of KSO_4^-, $SrSO_4$, $ZnSO_4$, $BaSO_4$, HSO_4^-, $MnSO_4$, $AlSO_4^+$, $Al(SO_4)_2^-$, $CuSO_4$, $Al_{13}O_4(OH)_{24}^{7+}$, $FeSO_4^+$, $Fe(SO_4)_2^-$, H_2SO_4 and $FeHSO_4^{2+}$.

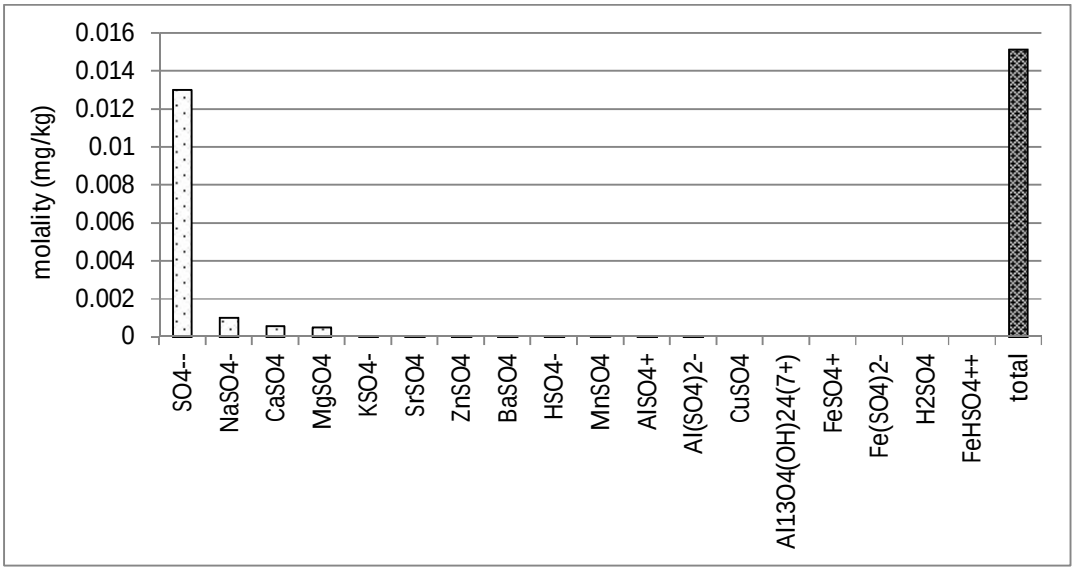

Figure 4.7.2: Sulphate aqueous species distribution in Matla mine water.

There was an appreciable amount of sulphate predicted to be associated with Na in Matla mine water (7 %). This was because the Na concentration in Matla mine water was very high. The amount of Mg and Ca associated with sulphate in Matla mine water were similar to each other because the molar concentration of Ca and Mg in Matla mine water were almost identical. The sulphate species associated with Fe was insignificant in Matla mine water. This was because the Fe concentration in Matla mine water was very low.

The speciation of aluminium in Matla mine water is shown in Figure 4.7.3. Most of the Al species in Matla mine water (Figure 4.7.3) were mainly associated with hydroxyl ions, which make up about 99 % of the total Al concentration. These hydroxyl Al species were $Al(OH)_4^-$, $Al(OH)_3$, $Al(OH)_2^+$ and $AlOH^{2+}$. The Al species that were associated with sulphate ions; $AlSO_4^+$ and $Al(SO_4)_2^-$ made up less than 1 % of the total Al content in Matla mine water. Free Al^{3+} in Matla mine water was less than 0.5 %. The oligomeric species of Al; $Al_{13}O_4(OH)_{24}^{7+}$, $Al_2(OH)_2^{4+}$ and $Al_3(OH)_4^{5+}$ in Matla mine water were negligible.

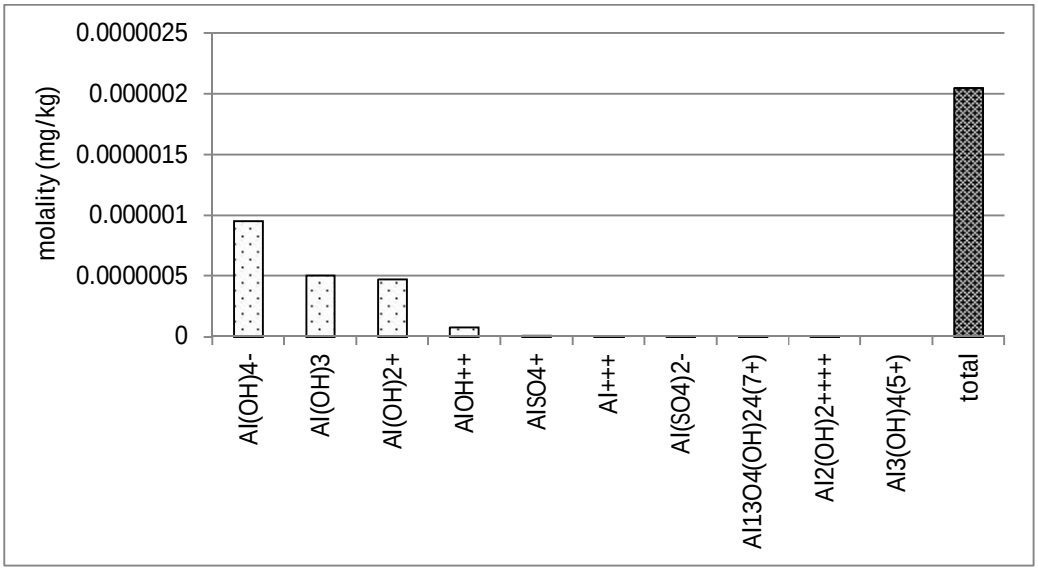

Figure 4.7.3: Aluminium aqueous species distribution in Matla mine water

The speciation of Fe in Matla mine water is shown in Figure 4.7.4. It was shown by SpecE8 program of the GWB software that Fe mainly existed in the form of hydroxyl species. The species were 64 % of $Fe(OH)_2^+$ and 35 % of $Fe(OH)_3$.

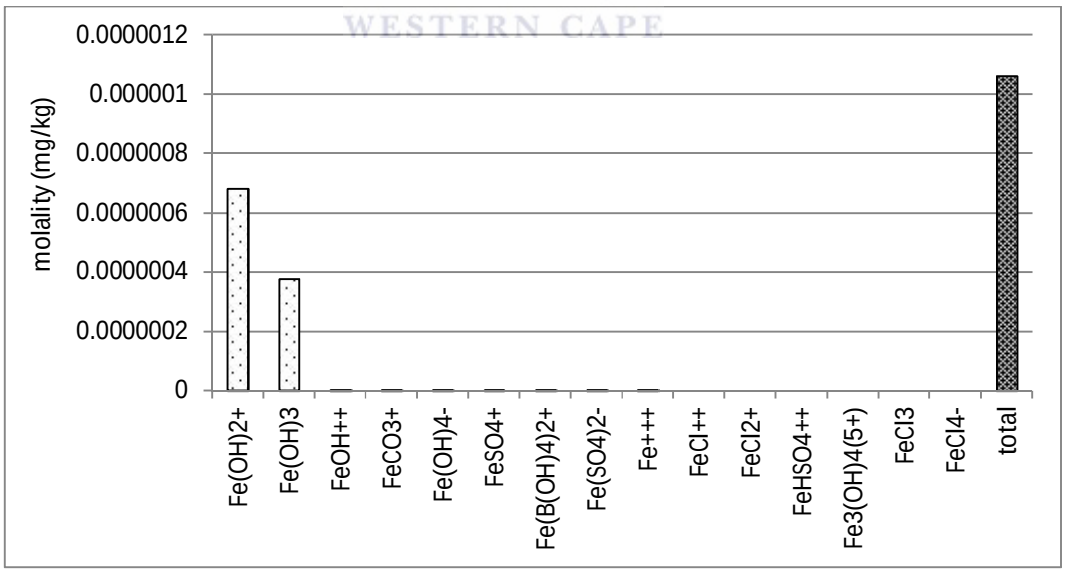

Figure 4.7.4: Iron aqueous species distribution in Matla mine water.

The other Fe species predicted by GWB software comprised of less than 1 % of the total Fe content in Matla mine water. These species were $FeOH^{2+}$, $FeCO_3^+$, $Fe(OH)_4$, $FeSO_4^+$, $Fe(B(OH)_4)_2^+$, $Fe(SO_4)_2^-$, Fe^{3+}, $FeCl^{2+}$, $FeCl_2^+$, $FeHSO_4^{2+}$, $Fe_3(OH)_4^{5+}$, $FeCl_3$ and $FeCl_4^-$.

In the case of Ca, the predicted species in Matla mine water were mainly free Ca^{2+} and $CaSO_4$ species as shown in Figure 4.7.5. These species contributed about 61 % and 34 % of the total Ca content in Matla mine water. $CaHCO_3^+$ species made up about 5 % of the total Ca content in Matla mine water.

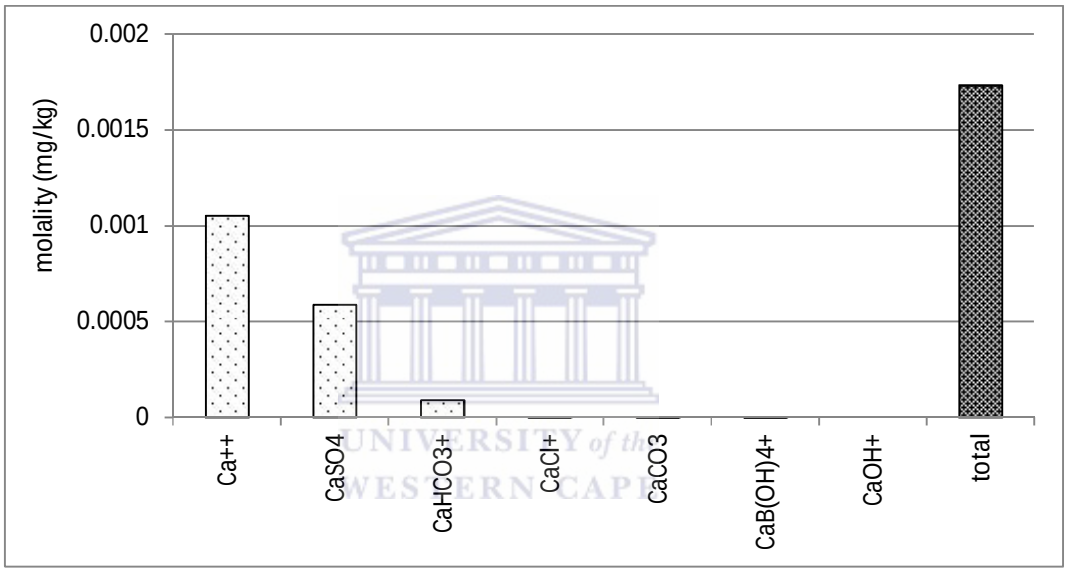

Figure 4.7.5: Calcium aqueous species distribution in Matla mine water.

The other aqueous species such as; $CaCl^+$, $CaCO_3$, $CaB(OH)_4^+$ and $CaOH^+$ were negligible in Matla mine water.

The Mn present in Matla mine water was predicted to be distributed mainly between Mn^{2+} ions and $MnSO_4$ which contributed about 62 % and 32 % respectively as shown in Figure 4.7.6. About 6 % of Mn present in Matla mine water was predicted to be in the form of $MnHCO_3^+$. The other species; $MnCO_3$, $MnOH^+$, $MnCl_2$, $Mn(OH)_2$, Mn_2OH^{3+}, $Mn_2(OH)_3^+$, $Mn(OH)_3^-$ and $Mn(OH)_4^{2-}$ constituted less than 0.07 % of the total Mn content in Matla mine water.

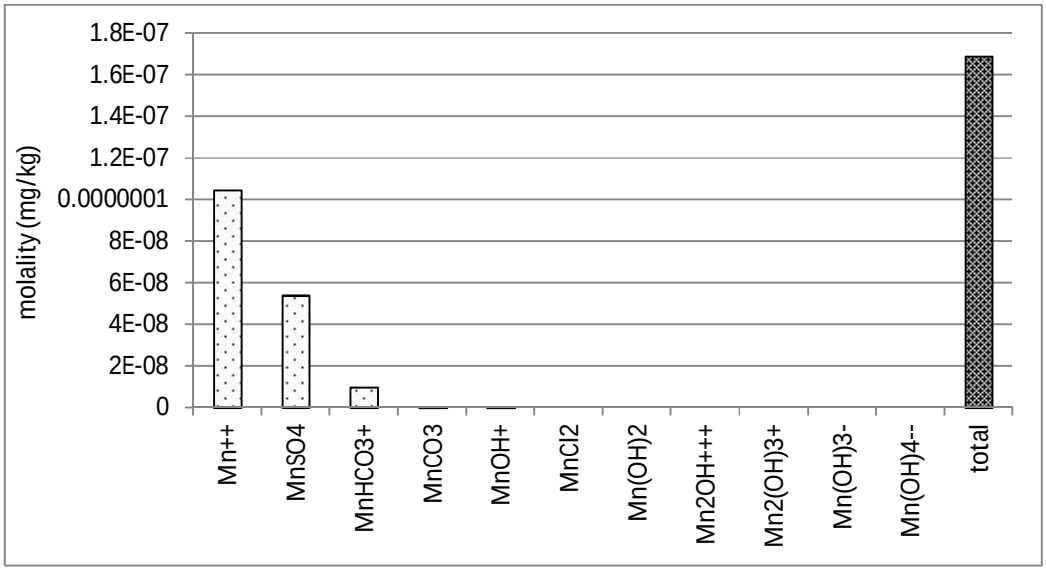

Figure 4.7.6: Manganese aqueous species distribution in Matla mine water.

Sodium species in Matla mine water were comprised of free Na^+ ions which constituted about 96.2 % of the total Na content as shown in Figure 4.7.7. The other Na species were comprised of $NaSO_4^-$ which constituted about 3 % in Matla mine water.

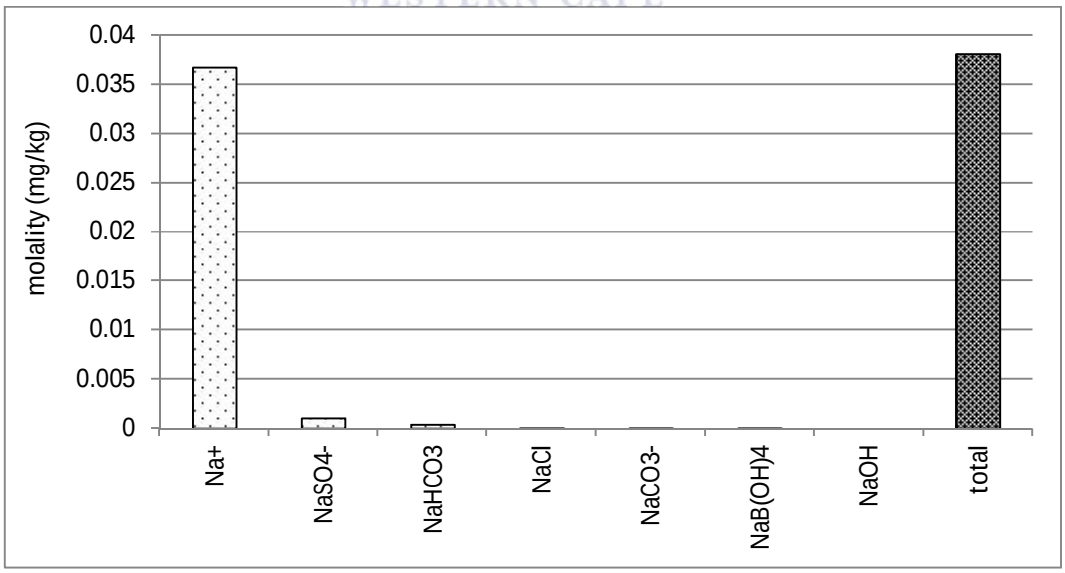

Figure 4.7.7: Sodium aqueous species distribution in Matla mine water.

Other Na species in Matla mine water predicted using the GWB software, were $NaHCO_3$, NaCl, $NaCO_3^-$, $NaB(OH)_4$ and NaOH. These species contributed an insignificant percentage to the total Na content in Matla mine water. This shows that Na is a very conservative mineral that exists mainly as free ions in the aqueous media.

In Matla mine water the K concentration was predicted to be mainly free K^+ species which constituted about 96 % as shown in Figure 4.7.8. The KSO_4^- species in Matla mine water contributed about 4 % of the total K content.

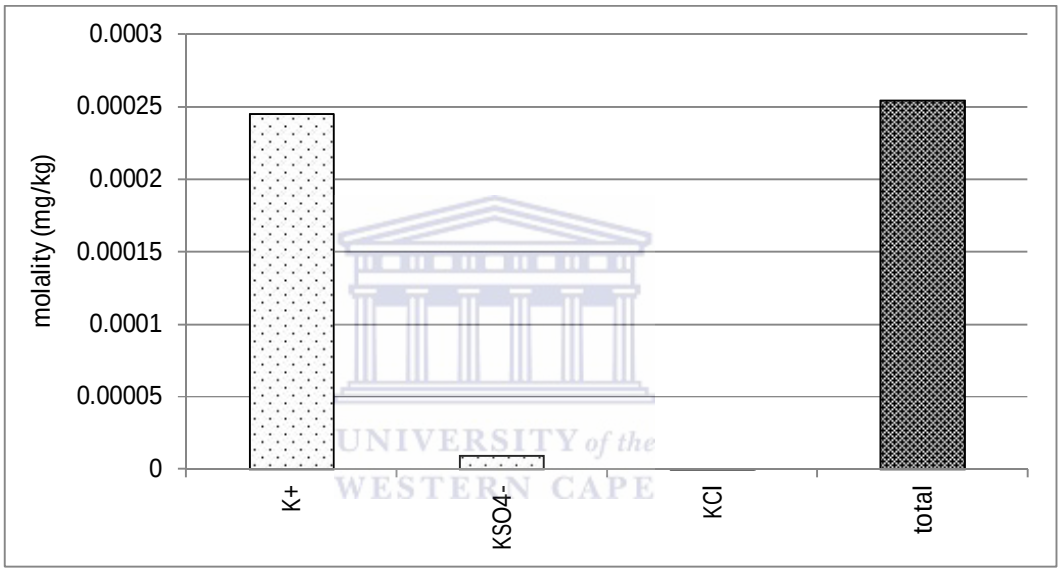

Figure 4.7.8: Potassium aqueous species distribution in Matla mine water.

The KCl species were very negligible in terms of the total K content in Matla mine water. Just like Na, K is also a conservative mineral because it mainly exists as free K^+ ions in aqueous media.

4.7.2. AQUEOUS DISTRIBUTION OF MAJOR ELEMENTS IN RAND URANIUM MINE WATER

The Rand Uranium mine water was speciated using the SpecE8 sub program of the GWB software as outlined in Chapter 3, section 3.6. Rand Uranium mine water was found to be Ca-SO_4 type of water.

The predicted distribution of the Mg species in Rand Uranium mine water is shown in Figure 4.7.9a and b below. From Figure 4.7.9a, the Mg species in RU1 mine water existed mainly as free Mg^{2+} and $MgSO_4$ species which constituted about 61 % and 39 % respectively of the total Mg species distribution. Other species; $MgCl^+$, $MgH_2PO_4^+$, $MgB(OH)_4^+$, $Mg(OH)^+$, $MgHPO_4$, Mg_2OH^{3+}, $MgPO_4^-$ and $Mg(OH)4^{4+}$ constituted less than 0.07 % of the total Mg species distribution in RU1 as shown in Figure 4.7.9a.

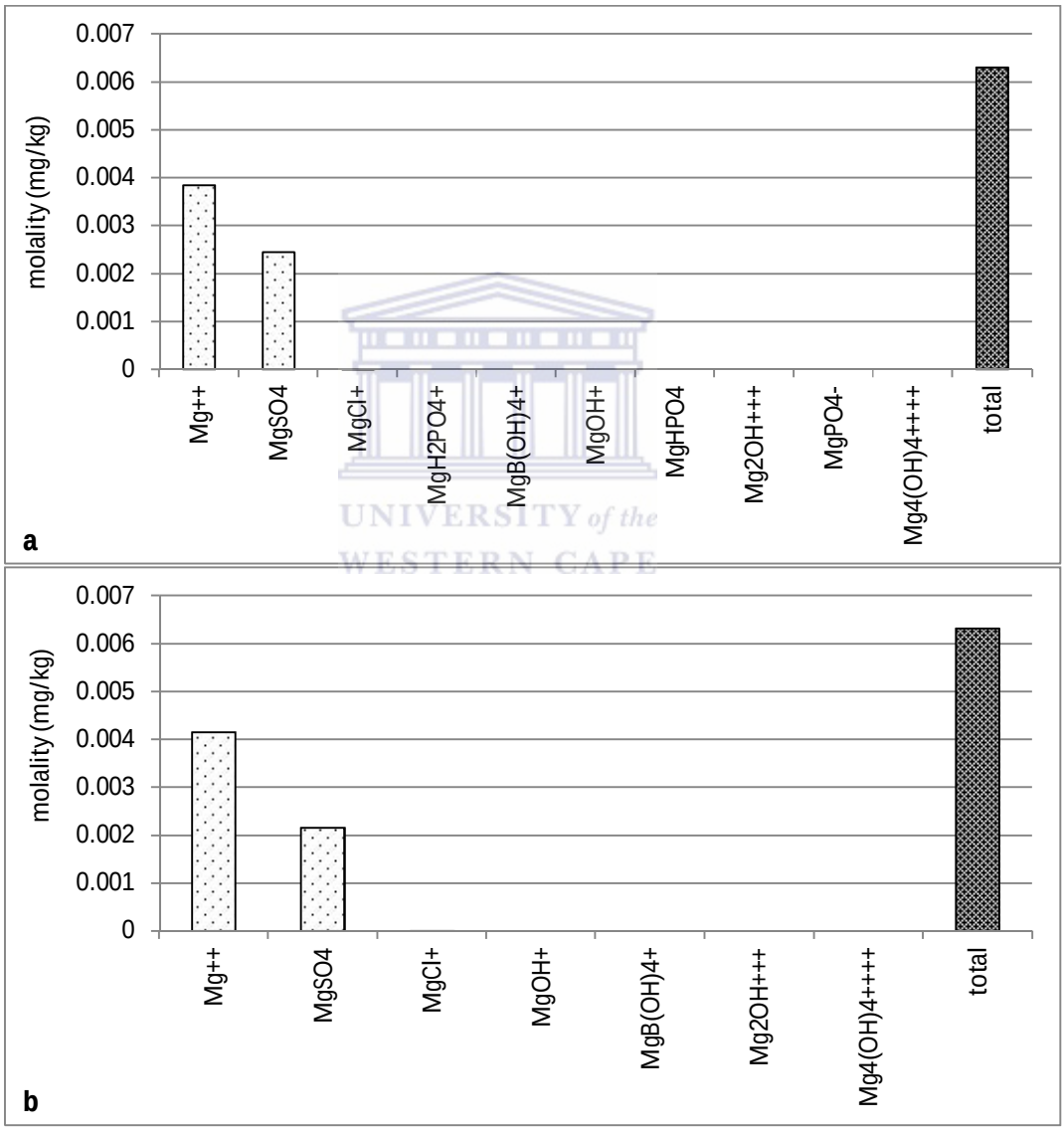

Figure 4.7.9: Magnesium aqueous species distribution in Rand Uranium mine water (RU1 (a) and RU2 (b)).

The species distribution of Mg in RU2 was similar to that in RU1 except that there was no Mg associated with PO_4^{3-} ions. This was because no PO_4^{3-} ions were detected in RU1. The major species that were in RU2 were free Mg^{2+} and $MgSO_4$ which contributed about 66 % and 34 % respectively as shown in Figure 4.7.9b. The other species such as $MgCl^+$, $MgOH^+$, $MgB(OH)_4^+$, Mg_2OH^{3+} and $Mg_4(OH)_4^{4+}$ were negligible in RU2.

Sulphate species distribution in Rand Uranium mine water is as shown in Figure 4.7.10. The distribution of sulphate species was mainly comprised of free SO_4^{2-} ions.

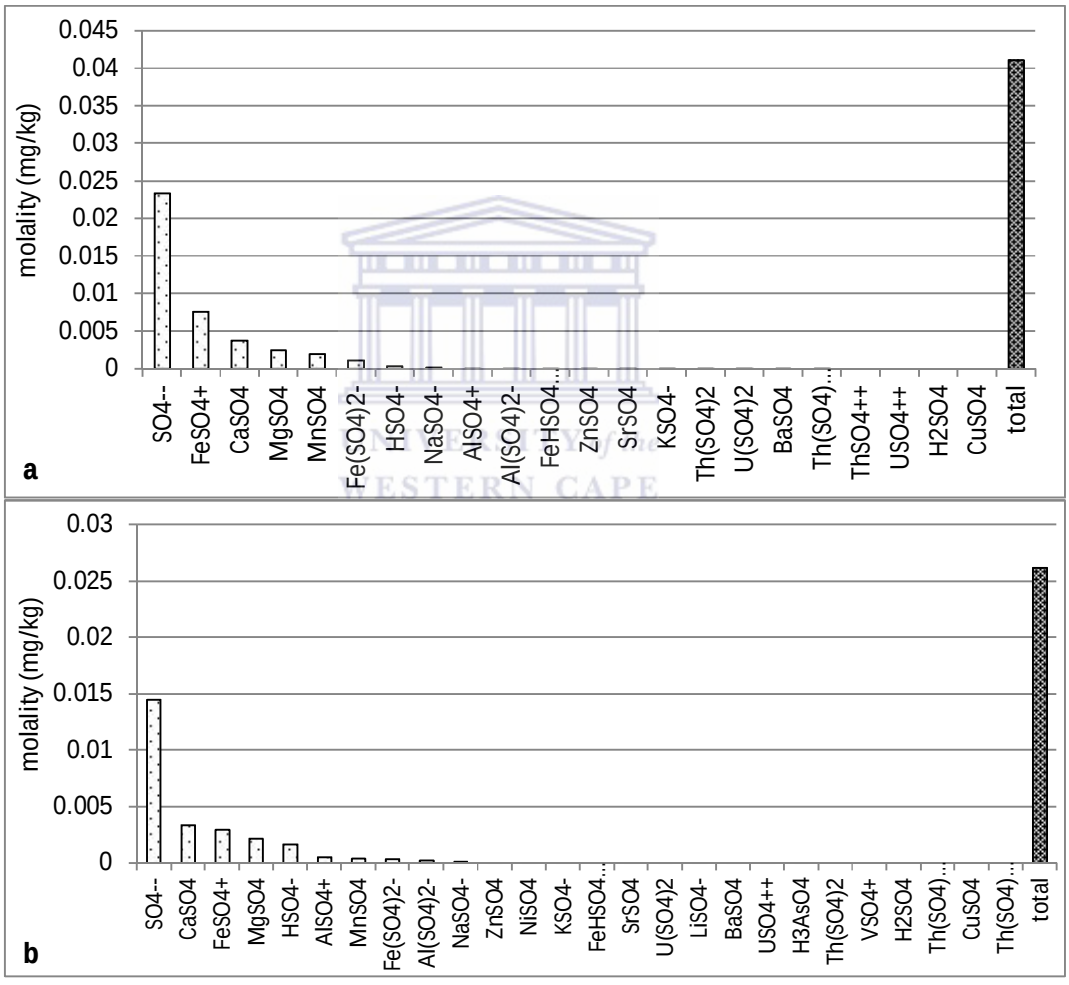

Figure 4.7.10: Sulphate aqueous species distribution in Rand Uranium mine water (RU1 (a), RU2 (b)).

Figure 4.7.10a shows that free sulphate ions in RU1 amounted to about 57 % of the total sulphate species. About 19 %, 9 %, 4 %, 4 % and 3 % of the total sulphate species in RU1 was comprised of $FeSO_4^+$, $CaSO_4$, $MgSO_4$, $MnSO_4$, $Fe(SO_4)_2^-$ respectively. Less than 0.1 % of the total sulphate species in RU1 was comprised of HSO_4^-, $NaSO_4^-$, $AlSO_4^+$, $Al(SO_4)_2^-$, $FeHSO_4^{2+}$, $ZnSO_4$, $SrSO_4$, KSO_4^-, $Th(SO_4)_2$, $U(SO_4)_2$, $BaSO_4$, $Th(SO_4)_3^{2-}$, $ThSO_4^{2+}$, USO_4^{2+}, H_2SO_4, $CuSO_4$. In RU2, the distribution of sulphate ions followed a similar trend as in RU1. The free SO_4^{2-} ions contributed about 55 % of the total sulphate species in RU2. The sulphate ions associated with Ca (12 %), Fe (11 %), Mg (8 %) were almost similar because the concentration of these elements in RU2 was very similar to each other. There were higher proportions of sulphate ions associated with H protons in RU2 compared to those in RU1, because the pH of RU2 was slightly lower than that of RU1.

Aluminium aqueous species in Rand Uranium mine water are as shown in Figure 4.7.11. Most of the Al species in RU1 (Figure 4.7.11a) were predicted to be mainly associated with sulphate, as $Al(SO_4)^-$ and free Al^{3+} species, which make up about 66 % and 33 % of the total species distribution of Al respectively. Less than 1 % of the total species predicted for Al in RU1 mine water were $AlOH^{2+}$, $Al(OH)_2^+$, $AlHPO_4^+$, $AlH_2PO_4^{2+}$, $Al_2(OH)_2^{4+}$, $Al(OH)_3$, $Al(OH)_4^-$ and $Al_3(OH)_4^{5+}$ species as shown in Figure 4.7.11a.

In RU2 the Al species mainly existed in association with sulphate ions as $AlSO_4^+$ (49 %) and $Al(SO_4)_2^-$ (23 %). Free Al^{3+} species constituted about 28 % of the total Al concentration in RU2 as shown in Figure 4.7.11b. The difference observed in the species distribution in the two mine waters could be due to the slight difference in pH and the slight difference in the composition of the water. Since the water was found to differ according to the season, the bioavailability and the toxicity or even the treatment parameters of the water from the same source could vary.

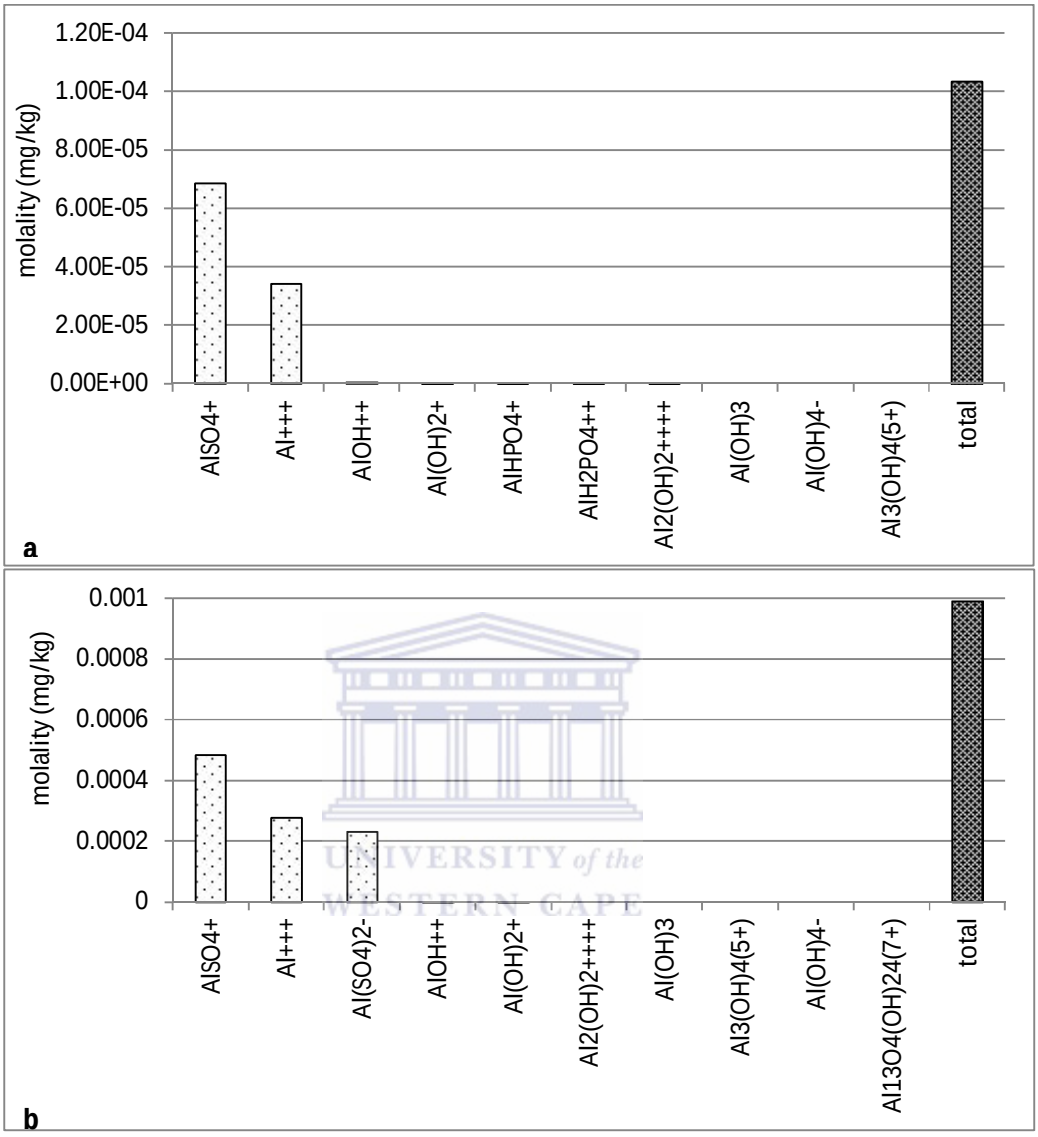

Figure 4.7.11: Aluminium aqueous species distribution in Rand Uranium mine water (RU1 (a) and RU2 (b)).

The predicted distribution of Fe species in Rand Uranium mine water is shown in Figure 4.7.12. Iron species occurred mainly in association with sulphate ions. The species in RU1 included about 53 % of $FeSO_4^+$ and about 8 % of $Fe(SO_4)^{2-}$. Other predominant species for Fe were associated with hydroxyl ions such as $FeOH^{2+}$, $Fe(OH)_2^+$, $Fe_3(OH)_4^{5+}$ and $Fe_2(OH)_2^{4+}$ which constituted about 19 %, 10 %, 3.5 % and 3.5 % respectively of the total Fe

species distribution in RU1 as shown in Figure 4.7.12a. Free Fe^{3+} ions constituted about 2 % of the total Fe species in Rand Uranium mine water. Other ions such as $FeCl^{2+}$, $FeHSO_4^{2+}$, $Fe(OH)_3$, $FeB(OH)_4^{2+}$, $FeHPO_4^{+}$, $FeH_2PO_4^{2+}$, $FeCl_2^{+}$, $Fe(B(OH)_4)_2^{+}$, $FeCl_3$, $Fe(OH)_4^{-}$ and $FeCl_4^{-}$ constituted about 3.5 % of the total Fe species.

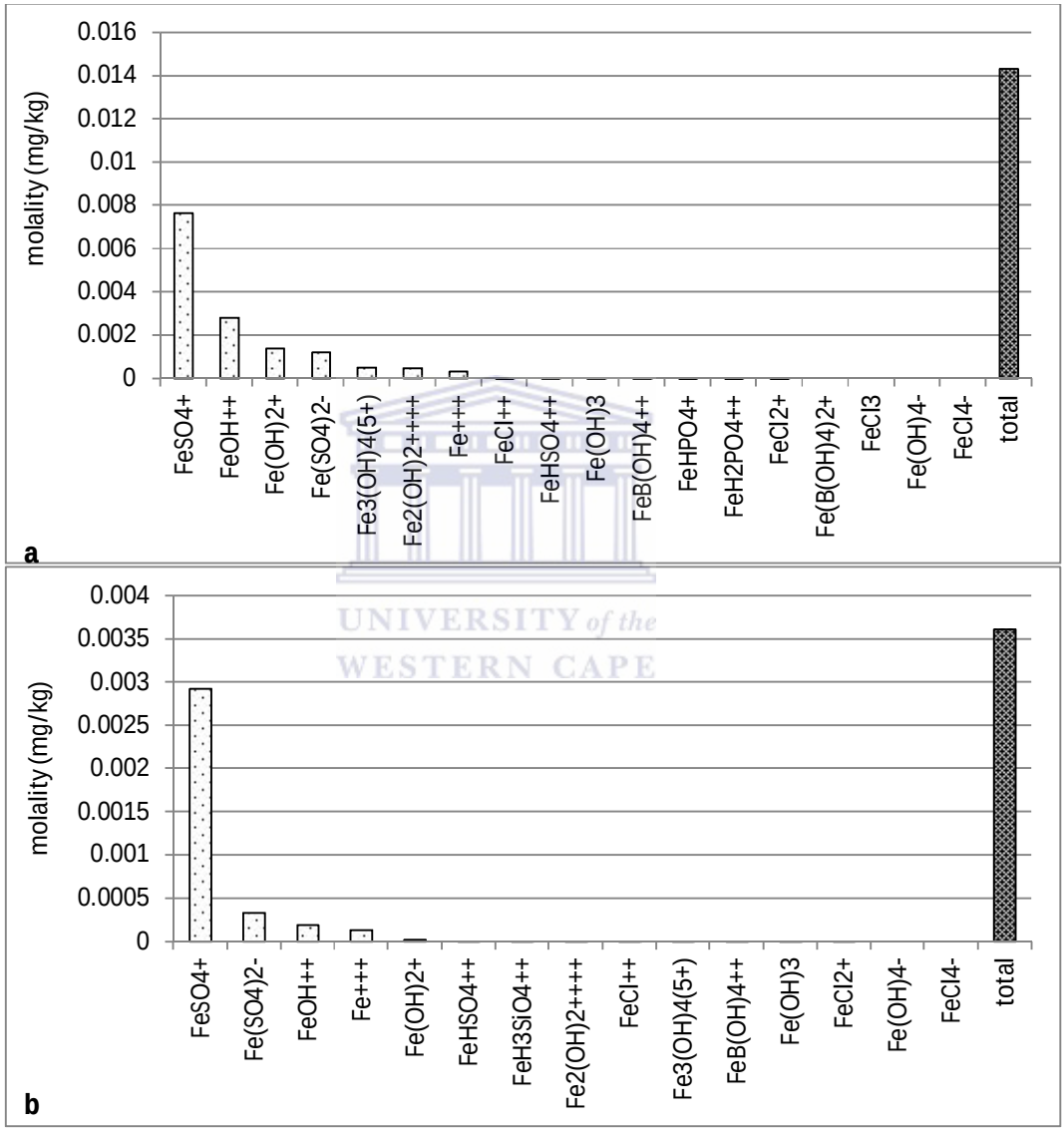

Figure 4.7.12: Iron aqueous species distribution in Rand Uranium mine water (RU1 (a) and RU2 (b)).

The predicted distribution of Fe species in RU2 differed considerably from RU1 as shown in Figure 4.7.12b. The $FeSO_4^+$ and $Fe(SO_4)^{2-}$ made up about 81 % and 9 % respectively of the total Fe concentration in RU2. Other significant Fe species in RU2 were $FeOH^{2+}$, free Fe^{3+}, and $Fe(OH)_2^+$, which made up about 5, 4 and 0.4 % respectively of the total Fe species predicted for RU2 as shown in Figure 4.7.12b

The predicted aqueous calcium distribution in Rand Uranium mine waters are depicted in Figure 4.7.13.

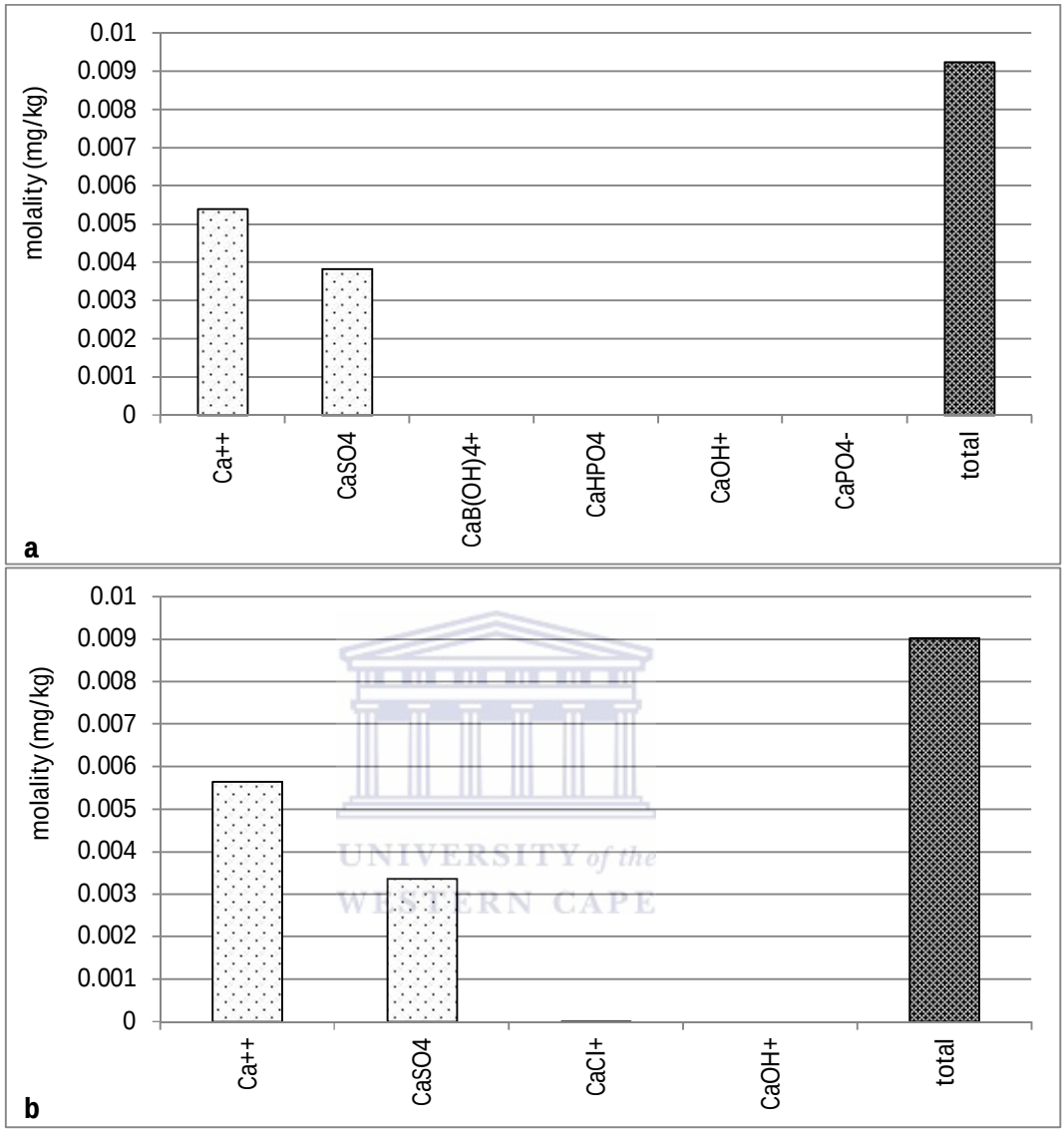

Figure 4.7.13: Calcium aqueous species distribution in Rand Uranium mine water (RU1 (a) and RU2 (b)).

Calcium species in RU1 (Figure 4.7.13a) were predicted to mainly exist as free Ca^{2+} and $CaSO_4$ species which constituted about 58 % and 42 % of the total Ca species respectively. Other Ca aqueous species in RU1; $CaB(OH)_4^+$, $CaHPO_4$, $CaOH^+$ and $CaPO_4^-$ contributed about 1 % of the total Ca species in RU1. In RU2, Ca existed almost exclusively of free Ca^{2+} and

$CaSO_4$ species as shown in Figure 4.7.13b. From Figure 4.7.13b Ca^{2+} and $CaSO_4$ contributed almost 100 % of the total Ca species in RU2.

The predicted species distribution of Mn in Rand Uranium mine water is depicted in Figure 4.7.14. The predicted Mn aqueous species distribution in RU1 and RU2 was mainly comprised of free Mn^{2+} ions and $MnSO_4$. Free Mn^{2+} and $MnSO_4$ species constituted about 60 % and 40 % respectively of the total Mn species in RU1 as shown in Figure 4.7.14a. In RU2, free Mn^{2+} and $MnSO_4$ constituted about 64 % and 36 % of the total Mn species as shown in Figure 4.7.14b. The distribution of Mn between other species such as $MnCl^+$, $MnCl_2$, $MnH_2PO_4^+$, $MnOH^+$, $MnHPO_4$, $MnCl_3^-$, Mn_2OH^{+++}, $MnPO_4^-$, $Mn(OH)_2$, $Mn_2(OH)_3^+$, $Mn(OH)_3^-$ and $Mn(OH)_4^{2-}$ was negligible in Rand Uranium mine water.

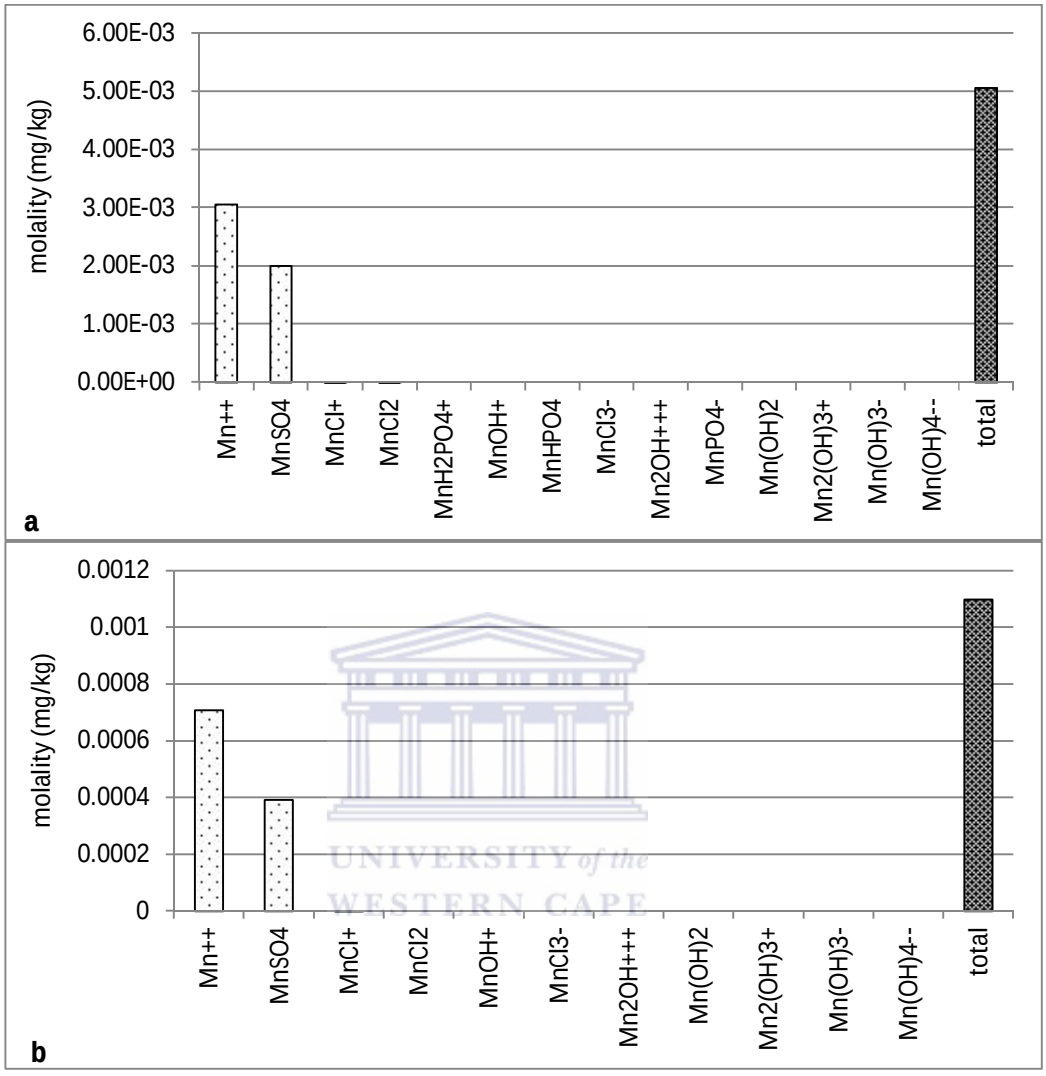

Figure 4.7.14: Manganese aqueous species distribution in Rand Uranium mine water (RU1 (a) and RU2 (b)).

The predicted Na species in Rand Uranium mine water are as shown Figure 4.7.15. Sodium species in Rand Uranium mine water were mainly free Na^+ ions which contributed about 96 %. The other Na species was comprised of $NaSO_4$ which was predicted to contribute about 4 % of the total Na in Rand Uranium mine water in both cases. This shows that Na is an element that does not form many complexes compared to other elements modelled such

as Fe, Al and Mn. The other species predicted by the model were negligible such as NaCl, $NaHPO_4^-$ and $NaOH^-$.

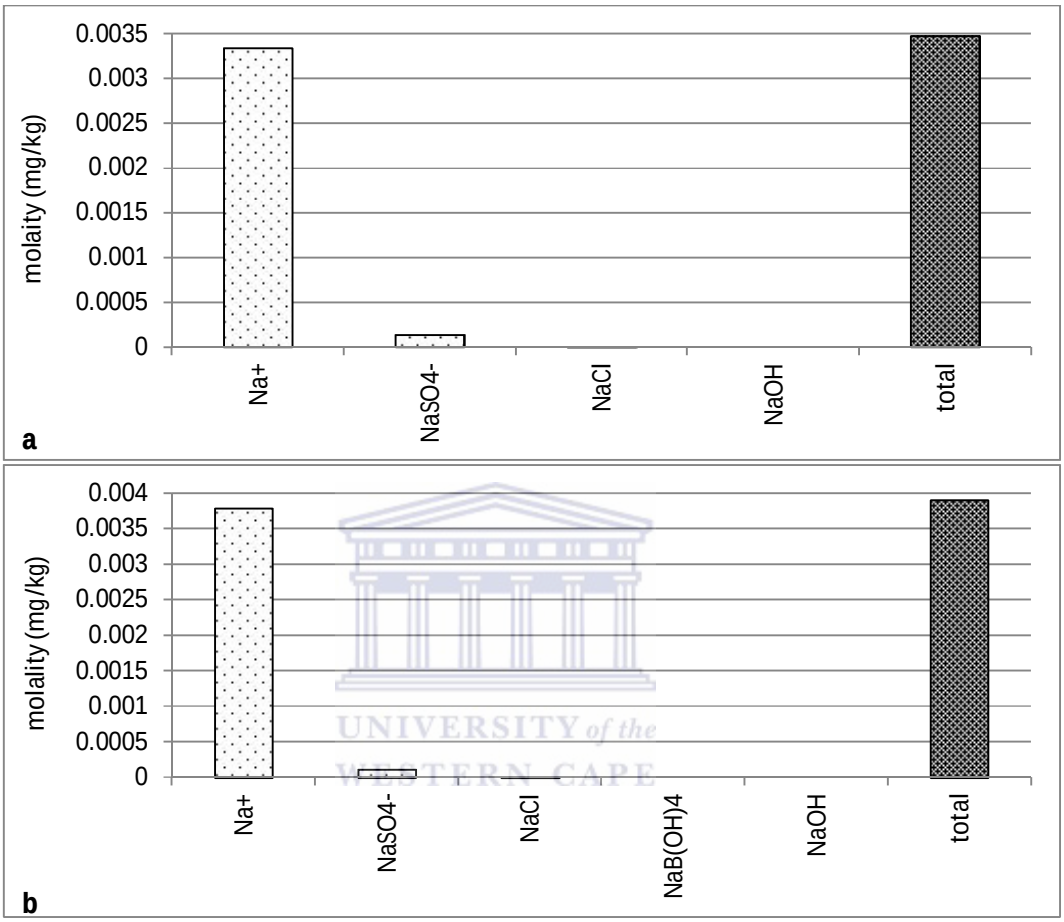

Figure 4.7.15: Sodium aqueous species distribution in Rand Uranium mine water (RU1 (a) and RU2 (b)).

Potassium in Rand Uranium mine water was found to be distributed mainly as free K^+ ions (94 %) and as KSO_4^- (6 %) in aqueous media as shown in Figure 4.6.16. The other negligible species of K predicted in Rand Uranium mine water were KCl, $KHPO_4^-$ and KOH. Potassium is also a conservative element similar to Na and does not readily form complexes with other ions in the aqueous media.

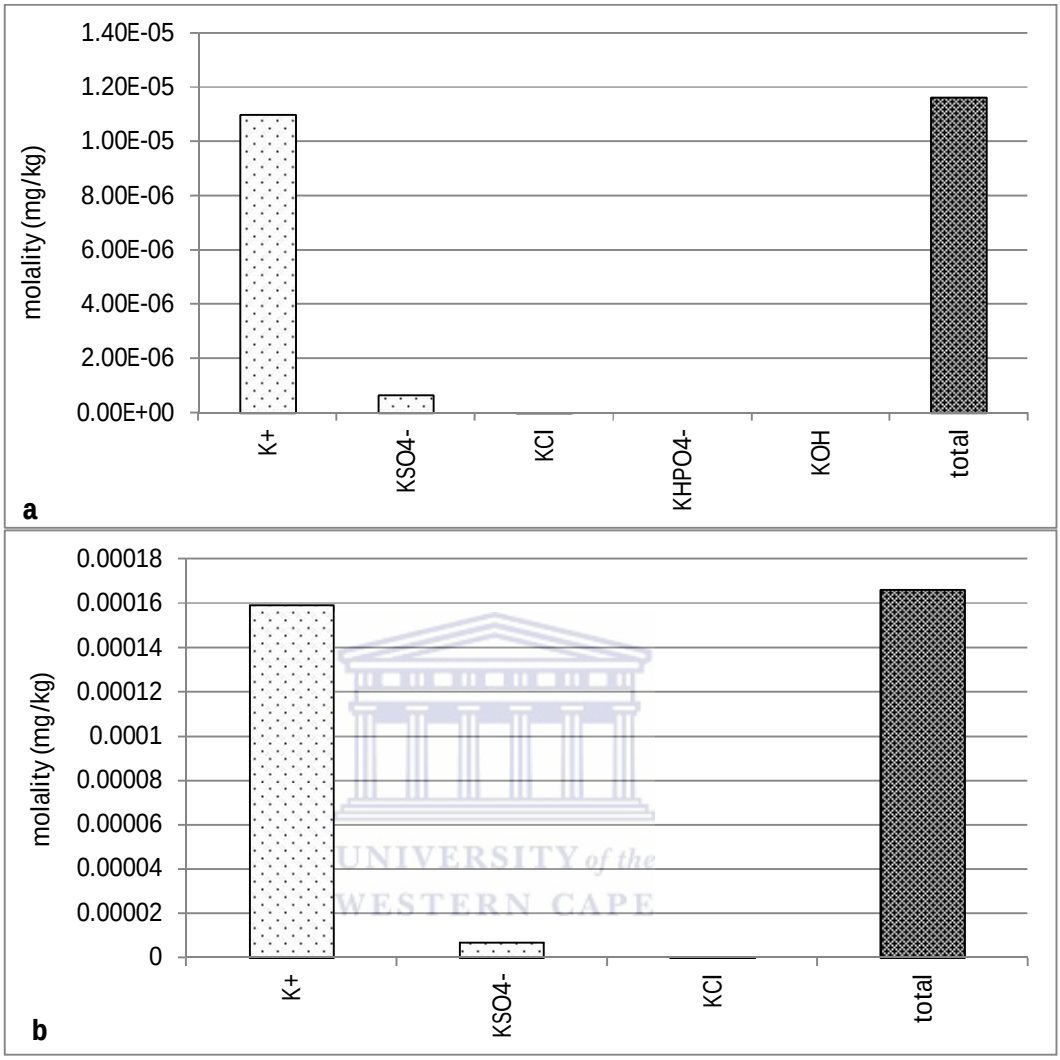

Figure 4.7.16: Potassium aqueous species distribution in Rand Uranium mine water (RU1 (a) and RU2 (b)).

4.7.3. AQUEOUS DISTRIBUTION OF NATURAL OCCURRING RADIONUCLIDE MATERIALS

Two of the natural occurring radionuclide materials (NORMs) identified in Rand Uranium mine water was U and Th. The distributions of these NORMs were modelled using SpecE8

program of the GWB as outlined in Chapter 3, section 3.6.1. The predicted distribution of U species in Rand Uranium mine water is shown in Figure 4.7.17.

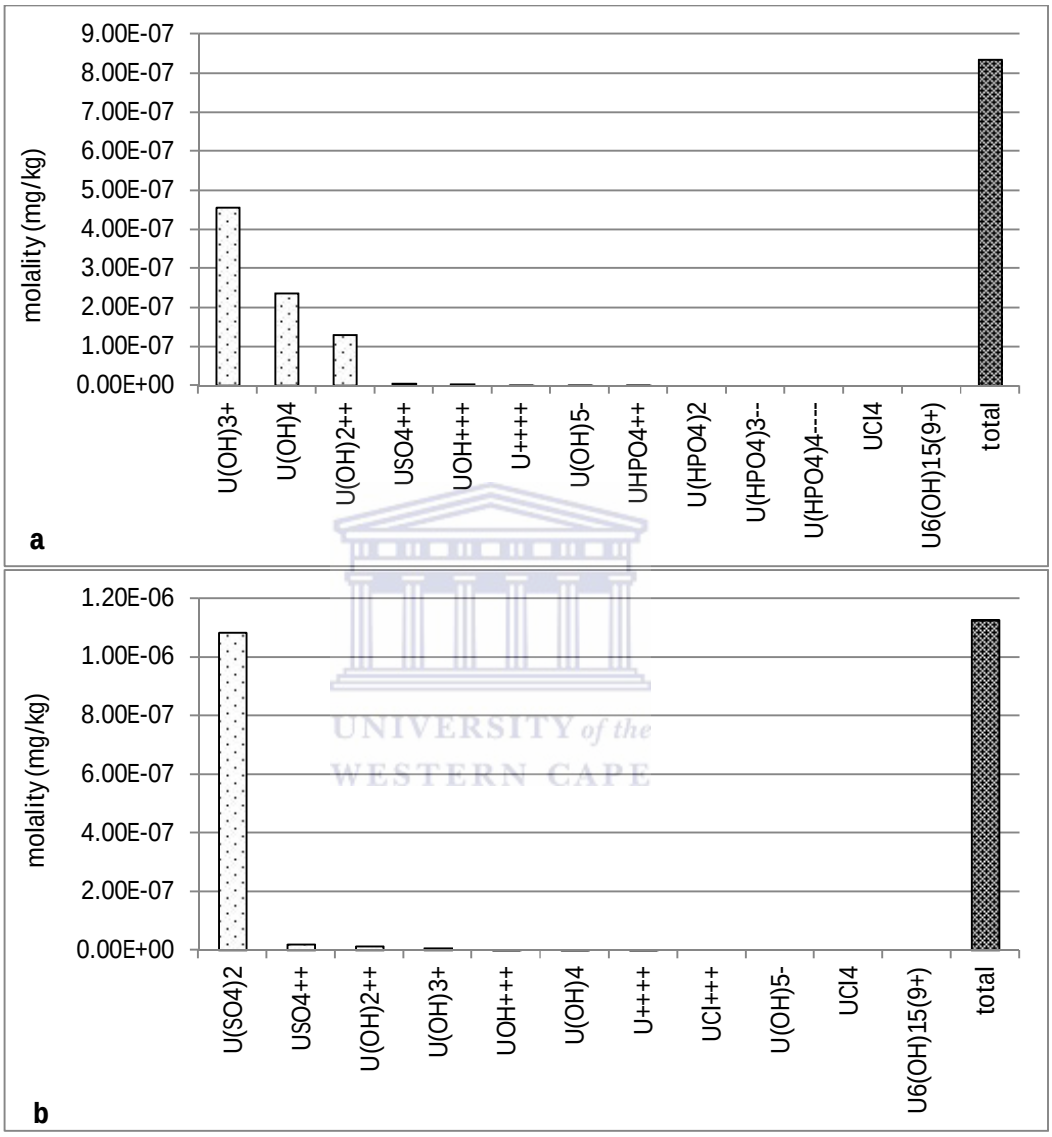

Figure 4.7.17: Uranium aqueous distribution in Rand Uranium mine water (RU1 (a) and RU2 (b)).

The modelling results show that U species in RU1 were predicted to be mainly comprised of species associated with hydroxyl ions such as $U(OH)_3^+$, $U(OH)_4$ and $U(OH)_2^{2+}$, which made up about 57, 28 and 16 % of the total U species respectively as shown in Figure 4.7.17a. On the

other hand U species in RU2 were mainly those of U associated with sulphate ions, that is 96 % of $U(SO_4)_2$ and 2 % of USO_4^{2+} as shown in Figure 4.7.147b. This showed that different samples of mine water from the same location differ significantly in their species distribution, depending on the season of sampling. This was because of seasonal variability in pH and the elemental composition of the mine water.

The modelling results produced by GWB software of Th species in Rand Uranium mine water are shown in Figure 4.7.18.

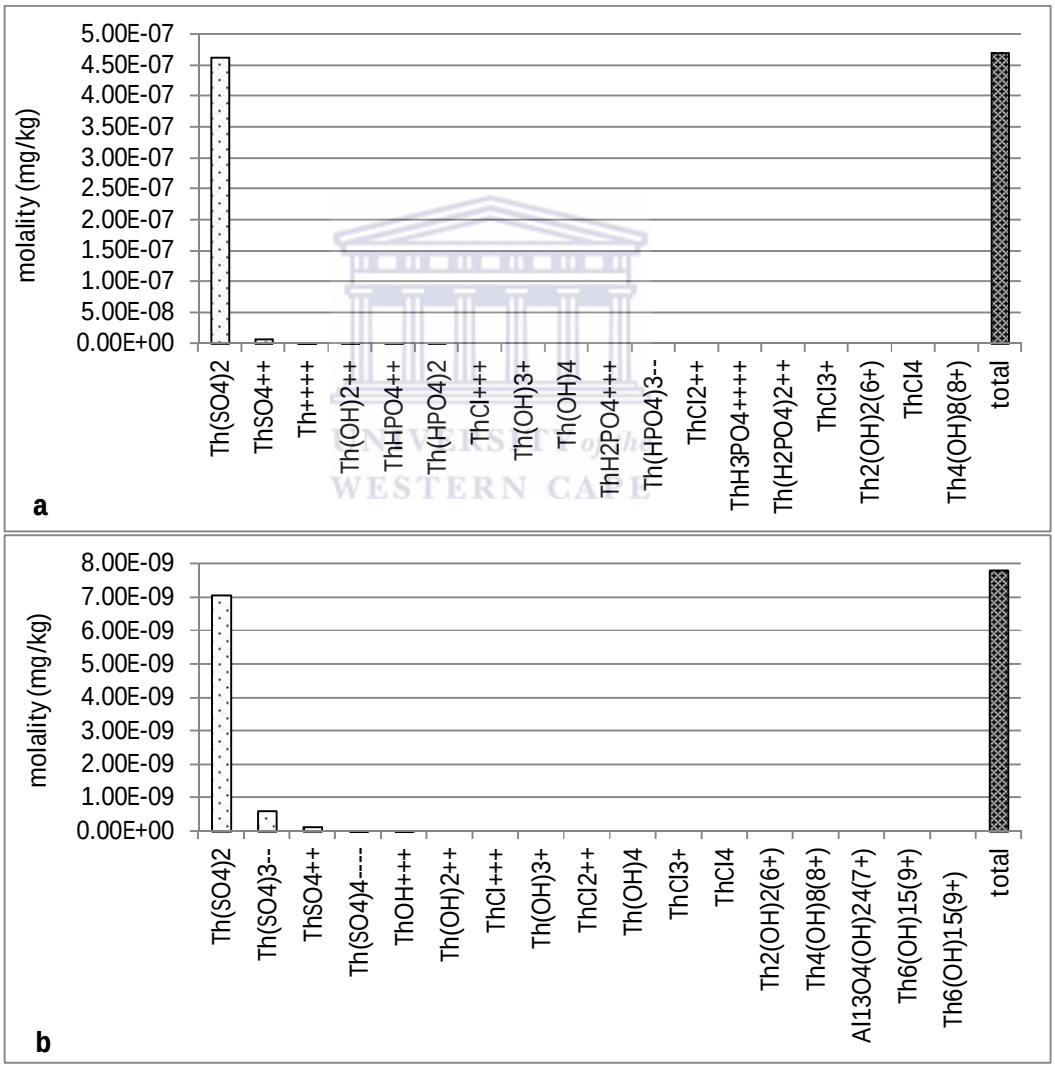

Figure 4.7.18: Thorium aqueous distribution in Rand Uranium mine water (RU1 (a) and RU2 (b)).

According to SpecE8 program the main species of Th in RU1 were $Th(SO_4)_2$ and $ThSO_4^{2+}$ which comprised about 98 % and 2 % respectively of the total Th species as shown in Figure 4.7.18a. In RU2, Th species comprised of 90 % of $Th(SO_4)$, 8 % of $Th(SO_4)_3^{2-}$ and 2 % of $ThSO_4^{2+}$ as shown in Figure 4.7.18b.

4.8. CONCLUSION

Matla coal FA could be classified as Class F coal FA. It was made up of mullite, quartz, hematite, gypsum and lime. The radioactive analysis of coal FA showed that the radioactivity was within the range of the radioactivity of some ashes in the world, but was well above the average radioactivity of soil. Since coal FA has found wide application in construction as well as in mine water remediation, it is worthwhile to pay attention to the radioactivity of the products produced from these applications. The quality of the product water that will be produced from the use of Matla coal FA to treat Rand Uranium mine water needs be investigated to find out if the radionuclides will not leach into the treated water.

Matla mine water can be classified as neutral mine drainage because the pH was 8. Rand Uranium mine water can be classified as acid mine drainage because the pH was less than 5 and contained elevated concentration of Fe, Al and Mn. The sulphate concentration of Rand Uranium was much greater than that of Matla mine water showing that in situ natural buffering by minerals such as dolomite of the acidity produced from pyrite oxidation was lower in Rand Uranium mine water compared to that of Matla mine water. Analysis of Matla mine water using ICP-OES and IC showed that the concentration of Na and sulphate were very high such that the water was unsuitable for irrigation, domestic and industrial purposes. Rand Uranium mine water was unsuitable for any purpose (drinking, irrigation or industrial) because of the lower pH and the elevated concentration of Fe, Al, Mn, Pb and sulphate ions in the water.

The radioactivity of the Rand Uranium mine water was found to be well above the required limit for potable water. The gross alpha and beta radio activities of the water were 12 and 6 times above the potable limit respectively. The radioactivity was mainly due to U, Th, K and

Ra radioisotopes. Treatment of Rand Uranium mine water therefore requires evaluation of the radioactivity of the product water.

The SpecE8 program of the GWB software have shown that major elements (or ions) in Matla mine water and Rand Uranium mine water such as Mg, sulphate, Mn, Na and K ions mainly existed in aqueous media as free ions. This means they existed mainly unassociated or not complexed with ligands or other ions. This increases their mobility in the ecosystem thereby enhancing bioavailability and toxicity. On the other hand Fe and Al were found to occur in association with hydroxyl ions. It is known that complexed species are less mobile, thereby have reduced bioavailability and toxicity. The NORMs such as Th and U were found to exist in association with sulphate ions in Rand Uranium mine water. This meant that these ions were less bioavailable as their mobility was reduced because of their nature.

The two Rand Uranium mine waters that were characterized showed that they differ depending on the season of sampling. The difference ranged from the slight change in pH, the variability in the concentration of various elements and the distribution of the species in these waters. This implies that any treatment process of the Rand Uranium mine water requires rigorous process control in order to adjust the process parameters according to the quality of the water.

CHAPTER 5: PROBABLE MINERAL PHASES DURING TREATMENT OF MINE WATER WITH COAL FLY ASH

5.1. INTRODUCTION

The Act2 program of Geochemist's workbench (GWB) software was used to predict the different mineral phases that could form if Matla mine water or Rand Uranium mine water was treated with Matla coal FA. The predicted minerals that were investigated are those of the major elements (Fe, Al, Mn, Na, K and sulphate ions) and radioactive elements (Th and U) in Matla mine water or Rand Uranium mine water. The following assumptions were made to obtain these modelling results:

1. Treatment of mine water with Matla coal FA occurs due to the dissolution of the CaO fraction in coal FA resulting in the increase in the concentration of Ca^{2+} and the pH of the mine water.
2. The % of CaO determined by XRF (Table 4.1.1) was assumed to be equivalent to the % of lime in Matla coal FA.

During treatment of mine water with Matla coal FA the pH increase will be dependent on the amount of lime that dissolves into the water. Therefore the independent variable chosen in this modelling was the concentration of Ca^{2+} added to the mixture in terms of log activity of the Ca^{2+} ($logaCa^{2+}$). The dependent variable was pH.

5.1.1. PROBABLE MINERALS DURING MATLA MINE WATER TREATMENT

Treatment of Matla mine water with Matla coal FA was modelled using Act2 program of the GWB software to predict the probable sulphate and Mg phases that could form at various log_aCa^{2+} and pH points. The predicted sulphate and Mg phases that could form when Matla mine water was to be treated with Matla coal FA at various log_aCa^{2+} and pH end values is shown in Figure 5.1.1.

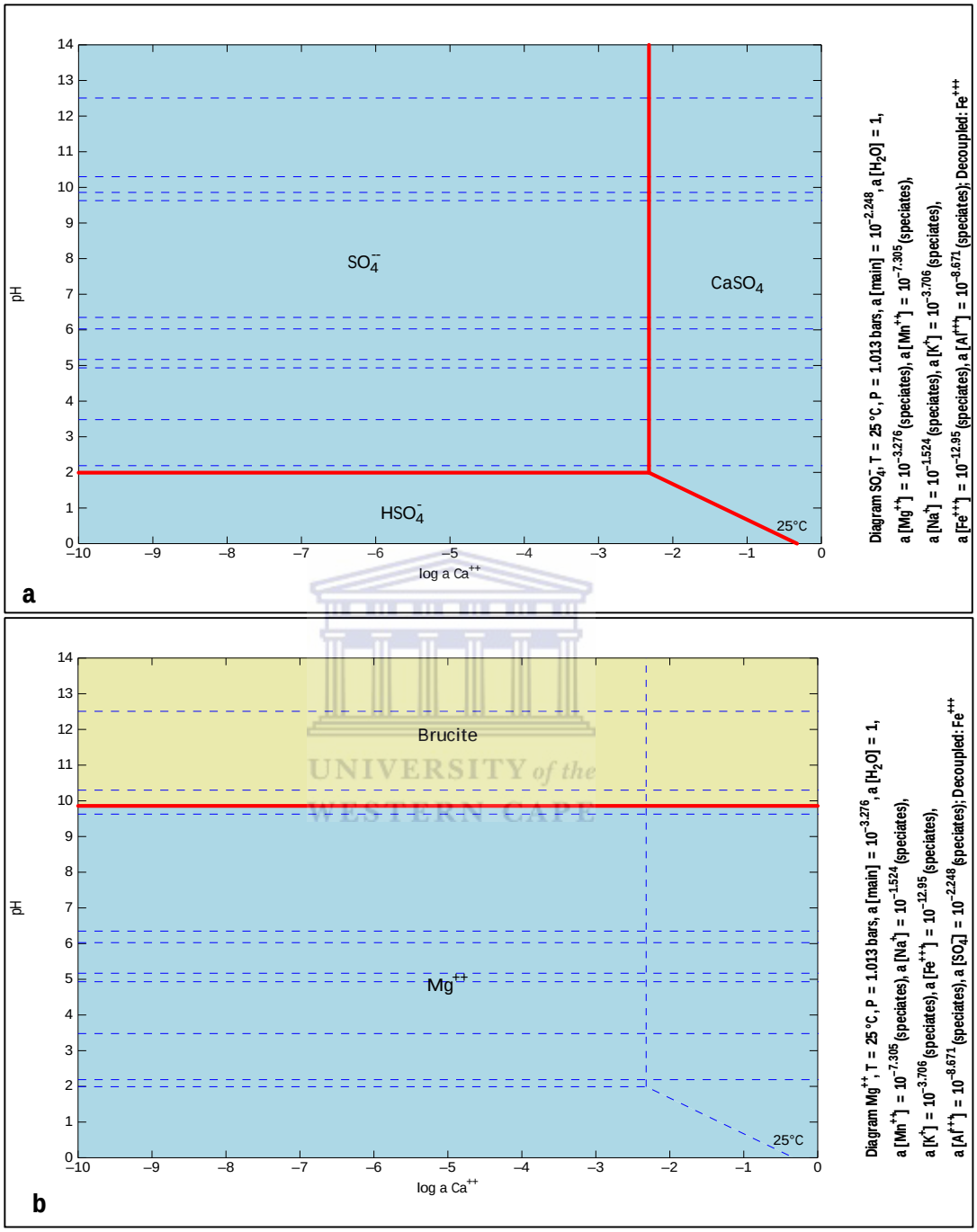

Figure 5.1.1: Sulphate (a) and magnesium (b) phases that were predicted to form by Act2 program of the GWB software when Matla mine water was treated with Matla coal FA to various $\log_a Ca^{2+}$ and pH values *(yellow colour show mineral phases and blue colour represents aqueous phases).*

From Figure 5.1.1a the sulphate ions existed mainly as free ions because the pH of Matla water was 8 (Table 4.5.1). As the $\log aCa^{2+}$ Ca ions was increased to greater than -2.4, the Act2 program showed that the sulphate ions in Matla mine water would form $CaSO_4$ aqueous species. Although the solution will be supersaturated with respect to gypsum at $\log_a Ca^{2+}$ of -2 and greater, there was no gypsum that was predicted to form by the Act2 program. This can be attributed to the fact that the high concentration of Na^+ in Matla mine water could inhibit the formation of gypsum growth by inhibiting the growth rate of gypsum crystals (Reznik et al., 2009; Zhang and Nancollas, 1992).

The Act2 program showed that Mg ions existed mainly as free ions in Matla mine water as shown in Figure 5.1.1b. If Matla mine water was to be treated with Matla coal FA, the Act2 program showed that the Mg ions in Matla mine water would start precipitating at pH greater than 10 as brucite ($Mg(OH)_2$). The formation of brucite was shown by the Act2 program to be pH dependent and independent of Ca concentration. Below pH 10, Mg was predicted to remain in Matla mine water as free Mg^{2+} ions regardless of the amount of Ca^{2+} added to the mixture.

The modelled results for K and Na phases obtained using Act2 program for the treatment of Matla mine water with Matla coal FA are shown in Figure 5.1.2. From the results K and Na would remain as free ions in aqueous solution at various pH and $\log_a Ca^{2+}$ values (Figure 5.1.2). These results were confirmed when Matla mine water was treated with Matla coal FA as will be discussed in section 7.1. This means that if Matla coal FA was to be used to treat Matla mine water, no K or Na will be removed.

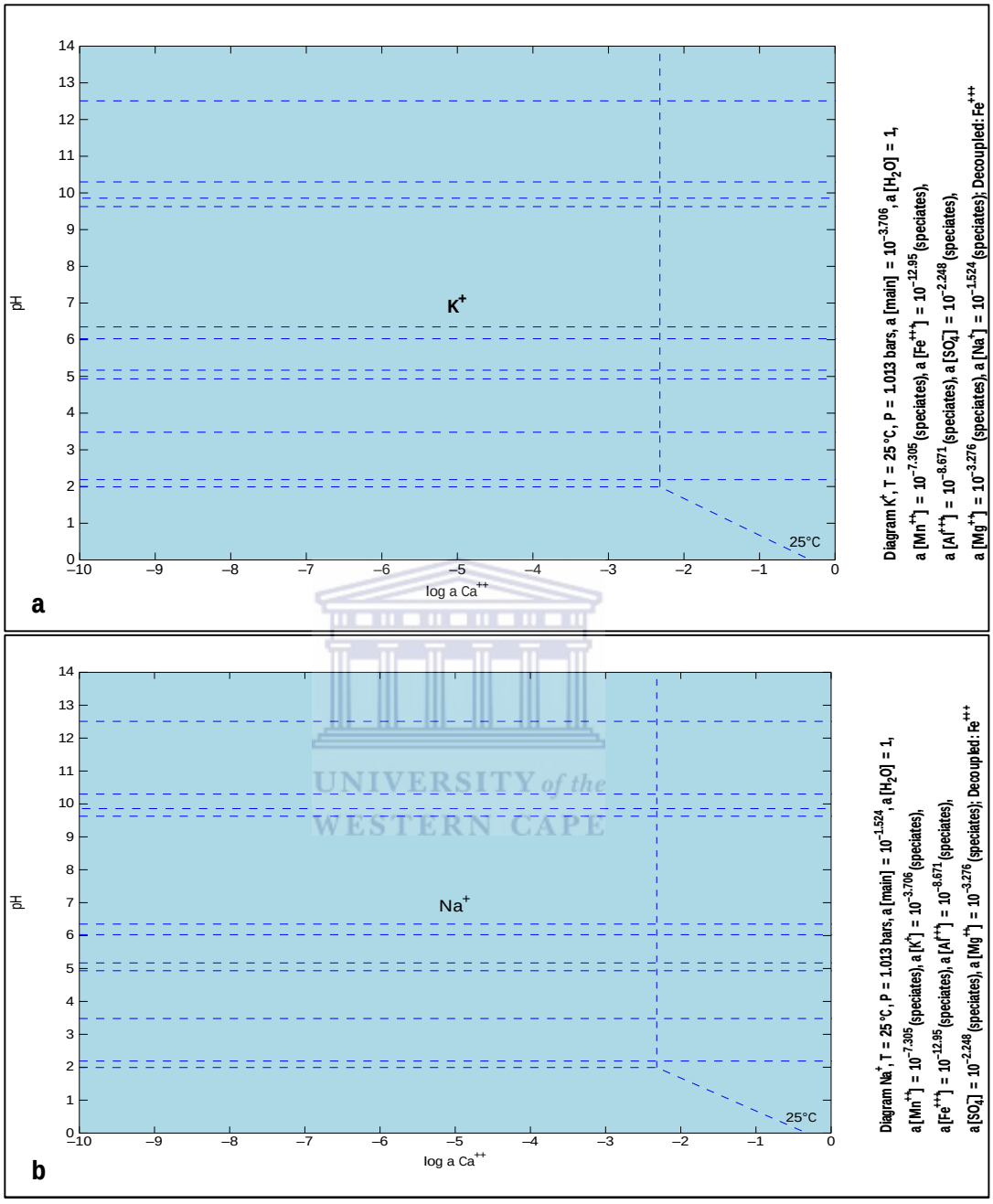

Figure 5.1.2: Potassium (a) and sodium (b) phases predicted to form by Act2 program of the GWB software when Matla mine water was treated with Matla coal FA to various $\log_a Ca^{2+}$ and pH values *(yellow colour show mineral phases and blue colour represents aqueous phases).*

The GWB has shown that if Matla mine water was to be treated with Matla coal FA only Mg ions can be removed if and only if the pH could be increased to greater than 10. No mineral phases were predicted by the Act2 program to precipitate out sulphate, Na and K from Matla mine water when treated with Matla coal FA.

5.1.2. PROBABLE MINERALS OF RAND URANIUM MINE WATER TREATMENT

The probable mineral phases that could form when Rand Uranium mine water was mixed with Matla coal FA were predicted using Act2 program of the GWB software. The two types of Rand Uranium mine waters that were modelled were RU1 and RU2 and their composition is shown in Table 4.6.1. These waters differ in composition because of the season they were sampled as explained in section 4.6.

5.1.2.1. Probable minerals for major elements

Act2 program of the GWB software was used to predict the phases of Fe, Al, Mn, Mg and sulphate ions that could form when Rand Uranium mine waters were to be treated with Matla coal FA. It was assumed that the addition of Matla coal FA will results in the dissolution of CaO causing the concentration of Ca^{2+} in the mine water to increase. The dissolution of lime was assumed to cause the pH of the mine water to increase. Therefore the increase in pH was dependent on the amount of CaO that dissolved into the mine water.

Removal of sulphate ions from the two types of Rand Uranium mine waters when treated with Matla coal FA was modelled using Act2 program of the GWB software. Rand Uranium mine waters contained elevated concentration of sulphate, Fe, Al, Mn, Mg and Ca ions as shown in Table 4.6.1. The predicted sulphate phases at various $\log_a Ca^{2+}$ and pH values are shown in Figure 5.1.3.

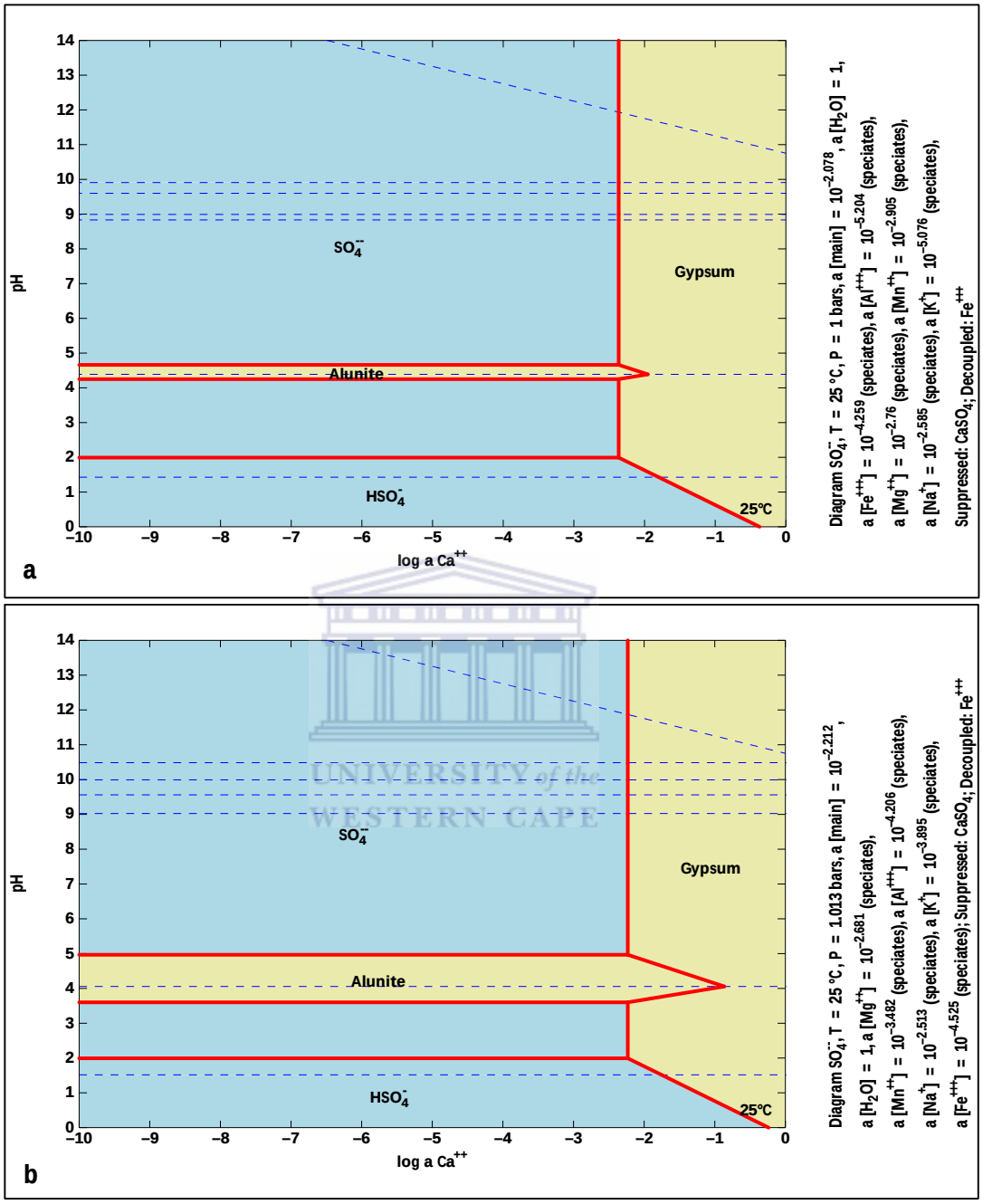

Figure 5.1.3: Sulphate phases that were predicted to form by Act2 program of the GWB software when RU1 (a) or RU2 (b) mine water was treated with Matla coal FA to various pH end points *(yellow colour show mineral phases and blue colour represents aqueous phases).*

The Act2 program of the GWB software showed that similar sulphate phases would form if Rand Uranium mine waters were treated with Matla coal FA to specific pH end points. The GWB had shown that if RU1 or RU2 was to be treated with Matla coal FA, sulphate could precipitate as alunite ($KAl_3(SO_4)_2(OH)_6$) or gypsum ($CaSO_4.2H_2O$) as shown in Figure 5.1.3.

Formation of gypsum in RU1 and RU2 was predicted by Act2 program to be mainly dependent upon the amount of Ca ions added to the mine water. Gypsum precipitation could occur when $\log_a Ca^{2+}$ was greater than -2.5. This was because at this concentration the mixture was supersaturated with respect to gypsum. Since the pH of RU1 and RU2 were greater than 2, the formation of gypsum was independent of the pH of the mixture. From Figure 5.1.3, the formation of gypsum is affected only when the pH is less than 2.

The formation of alunite in Rand Uranium mine waters was found to be mainly dependent on pH. The concentration of Ca ions added to Rand Uranium mine waters would tend to affect the pH at which alunite is stable. When $\log_a Ca^{2+}$ was greater than -2, the formation of alunite tends to decrease in favour of the formation of gypsum a more stable mineral as shown in Figure 5.1.3. These results were proved by the decrease in the sulphate concentration when Rand Uranium mine water was treated with Matla coal FA in section 7.2.1. Usually the sulphate ions are removed from mine water by gypsum precipitation to concentration between 1500 mg/L and 2000 mg/L (Madzivire, 2010; Geldenhuys et al., 2001). This amount of sulphate ions is still above the required limit for domestic purposes. Further treatment would still be required to remove the sulphate concentration to less than 500 mg/L.

According to the Act2 program of the GWB software, the probable Al mineral phases that were predicted to form when RU1 and RU2 were treated using Matla coal FA are shown in Figure 5.1.4. Aluminium could be removed as gibbsite ($Al(OH)_3$) in RU1 according to the Act2 program as shown in Figure 5.1.4a. In RU2 the Act2 program predicted that Al could be removed as alunite ($KAl_3(SO_4)_2(OH)_6$) and gibbsite as shown in Figure 5.1.4b.

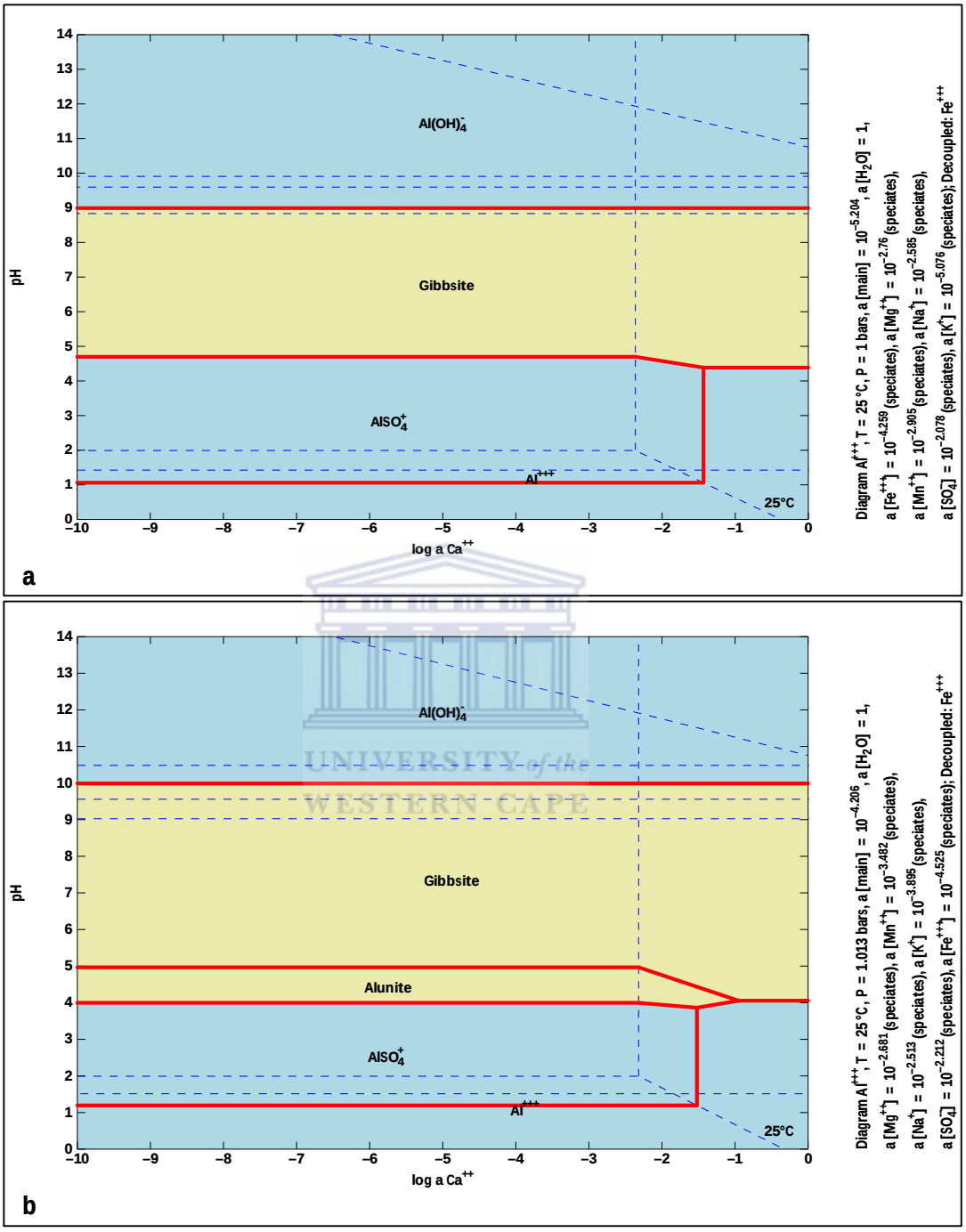

Figure 5.1.4: Aluminium phases that were predicted to form by Act2 program of the GWB software when RU1 (a) or RU2 (b) mine water was treated with Matla coal FA to various $\log_a Ca^{2+}$ and pH values *(yellow colour show mineral phases and blue colour represents aqueous phases).*

Precipitation of gibbsite was found to depend on pH and $\log_a Ca^{2+}$. Gibbsite formation occurs if the pH of the mixture was between 4.7 and 9 when $\log_a Ca^{2+}$ was less than -2.5 in RU1, as shown in Figure 5.1.4a. In the case of RU2, gibbsite was predicted to form if the pH was between 5 and 10 when $\log_a Ca^{2+}$ was less than -2.5 as shown in Figure 5.1.4b. When $\log_a Ca^{2+}$ was increased to -2.5 and greater the formation of gibbsite would start occurring at pH 4 in both RU1 and RU2 as shown in Figure 5.1.4. The Act2 program predicted that alunite would form in RU2 only. The precipitation of alunite was predicted to occur at pH 4 and 5 when $\log_a Ca^{2+}$ was less than -1. No alunite would form in RU2 when $\log_a Ca^{2+}$ was increased to greater than -1 (Figure 5.1.4b). Alunite mineral was not predicted to form in RU1 because the concentration of Al was very low.

Increasing the pH of Rand Uranium mine water to greater than 10, $Al(OH)_4^-$ phase would be formed according to the Act2 program. This phase was expected to react with Ca^{2+} and sulphate ions to form ettringite mineral phase (Madzivire, 2010). The ettringite mineral phase was not predicted by the Act2 program of the GWB software because the databases contained in the GWB software did not have the thermodynamic parameters for ettringite.

According to the Act2 program, the probable Fe mineral phases that were predicted to form when RU1 and RU2 were treated with Matla coal FA to various $\log_a Ca^{2+}$ and pH values are shown in Figure 5.1.5. The GWB software has shown that the mineral phases that could form were similar when Matla coal FA was to be added to both mine waters. The Fe minerals that were predicted using the GWB were jarosite-K ($KFe_3(SO_4)_2(OH)_6$) and $Fe(OH)_3$.

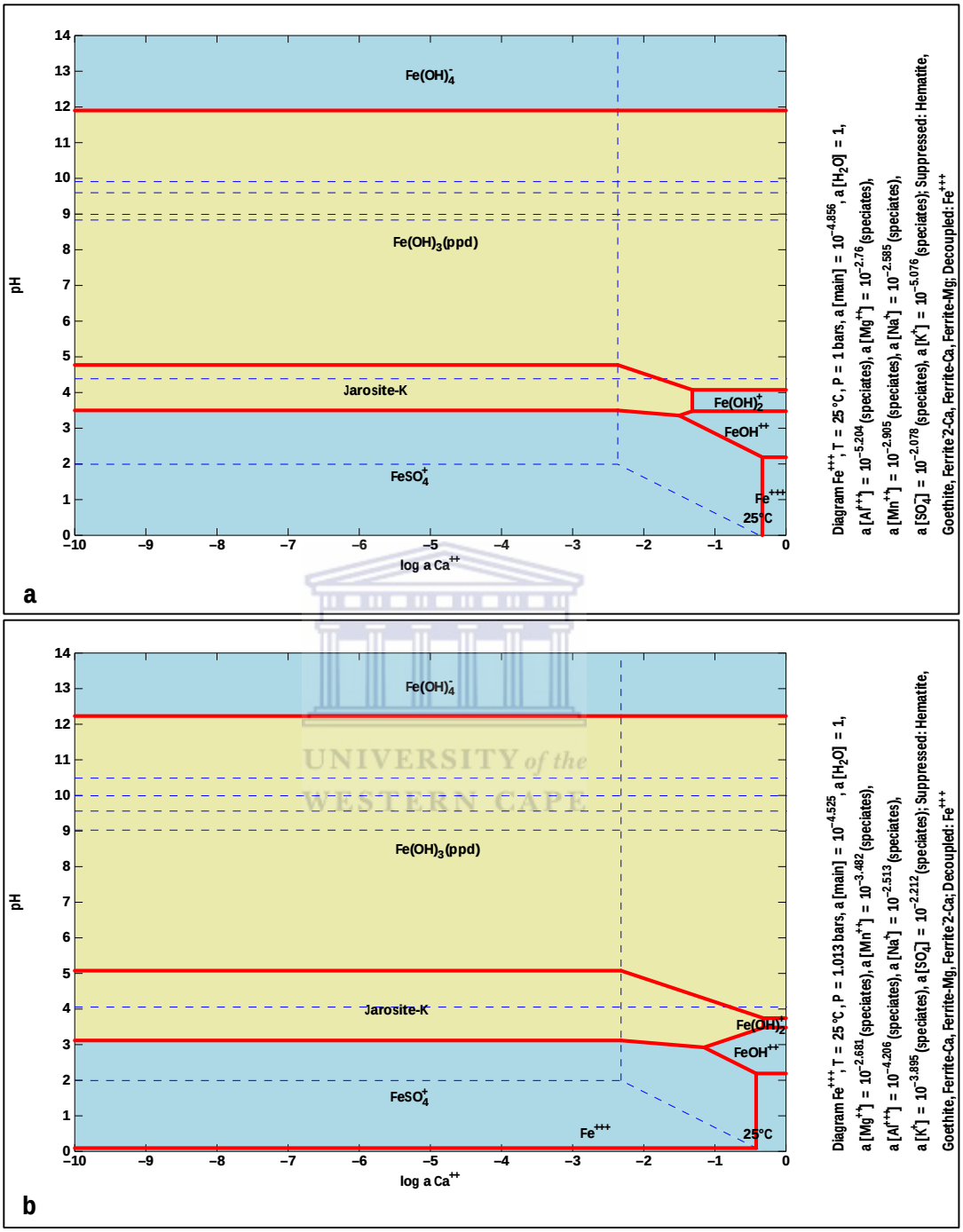

Figure 5.1.5: Iron phases that were predicted to form by Act2 program of the GWB software when RU1 (a) or RU2 (b) mine water was treated with Matla coal FA to various $\log_a Ca^{2+}$ and pH values *(yellow colour show mineral phases and blue colour represents aqueous phases).*

The formation of these minerals was dependent on both pH and $\log_a Ca^{2+}$ according to the Act2 program. The formation of jarosite-K was predicted to occur at pH 3.5 to 4.5 when $\log_a Ca^{2+}$ was between -10 and -2.5 in RU1 (Figure 5.1.5a). In RU2, jarosite-K was predicted to form between pH 3 and 5 when $\log aCa^{2+}$ was less tha -2.5 (Figure 5.1.5b). At $\log_a Ca^{2+}$ greater than -2.5, pH range at which jarosite-K narrowed gradually. In RU1, the no jarosite-K will form at $\log_a Ca^{2+}$ greater than -2 as shown in Figure 5.1.5a. In RU2, no jarosite-K formation will form if $\log_a Ca^{2+}$ is greater than -1 as shown in Figure 5.1.5b. Precipitation of $Fe(OH)_3$ when $\log_a Ca^{2+}$ was between -10 to -2.5, $Fe(OH)_3$ occurred at pH between 5 and 12 in both RU1 and RU2 when $\log_a Ca^{2+}$ was less than -2.5 as shown in Figure 5.1.5. If the $\log_a Ca^{2+}$ was to be increased to greater than -2.5, the lower limit pH for $Fe(OH)_3$ decreased gradually to 4. The upper limit of $Fe(OH)_3$ was not affected by $\log_a Ca^{2+}$ in both RU1 and RU2.

The GWB model showed that if Rand Uranium mine water was to be treated with Matla coal FA, Mn ions could be removed from mine water as amorphous $Mn(OH)_2$. The formation of $Mn(OH)_2$ was found to be pH dependent and independent of the concentration of Ca ions added to the mine water as is shown in Figure 5.1.6. Keeping the pH of the mine water less than 9 would result in the Mn existing as free Mn^{2+} and $MnSO_4$ species. If the pH of the mine water was to be increased to between 9 and 10, Mn would exist in aqueous solution as $Mn_2(OH)_3^+$.

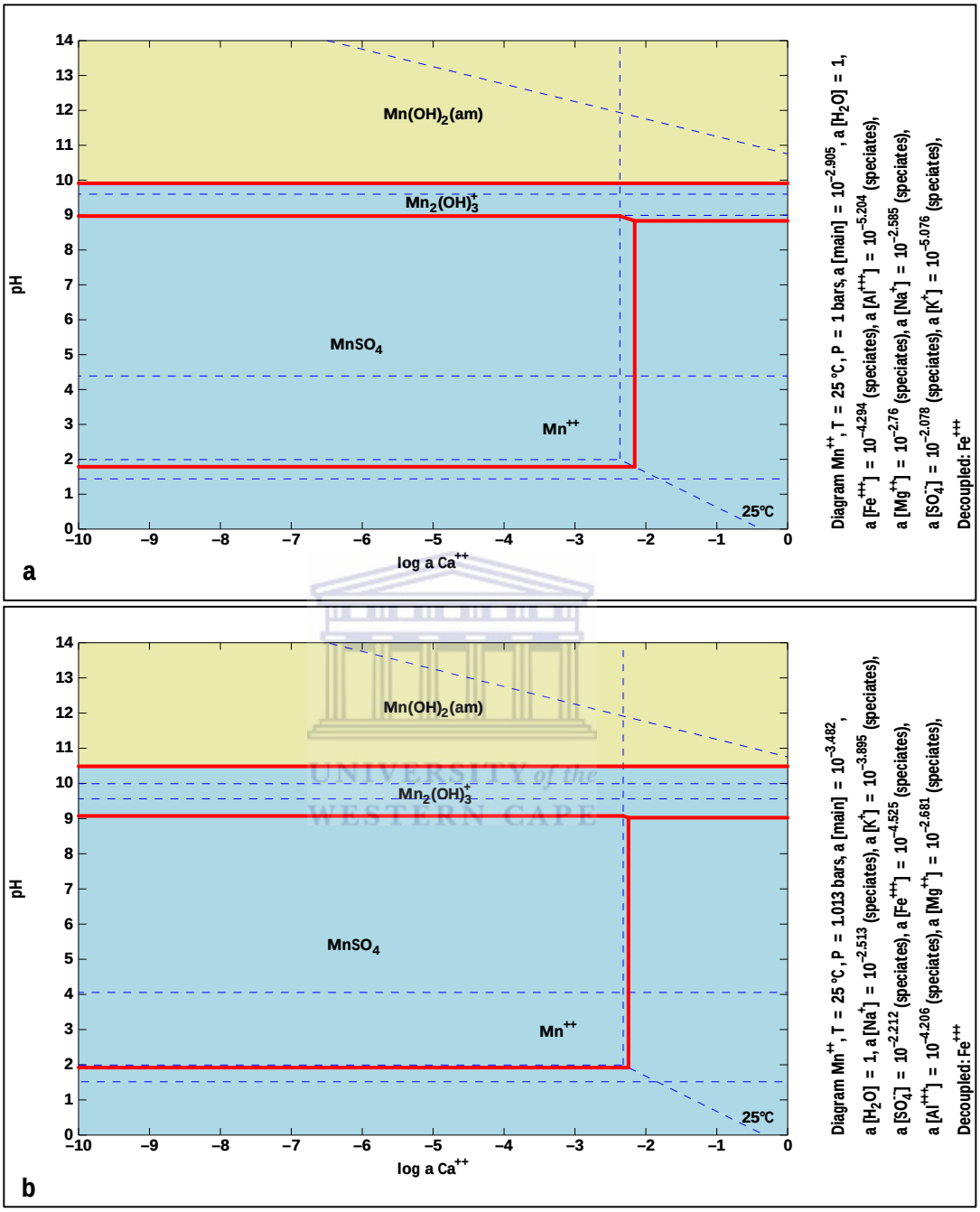

Figure 5.1.6: Manganese phases that were predicted to form by Act2 program of the GWB software when RU1 (a) or RU2 (b) mine water was treated with Matla coal FA to various $\log_a Ca^{2+}$ and pH values *(yellow colour show mineral phases and blue colour represents aqueous phases)*.

In RU1 amorphous $Mn(OH)_2$ was predicted to start precipitating at pH 10 (Figure 5.1.6a), while in RU2, it was predicted to start precipitating at pH 10.5 (Figure 5.1.6b). This was because the concentration of Mn^{2+} in RU2 was less than that of RU1. Therefore more OH^- would be required to start effecting the precipitation of $Mn(OH)_2$.

Magnesium was predicted to be removed from Rand Uranium mine as brucite ($Mg(OH)_2$) when Rand Uranium mine water was to be treated with Matla coal FA as shown in Figure 5.1.7. According to the Act2 program the formation of brucite in Rand Uranium mine water was dependent on pH but independent of the amount of Ca ions added to the mine water. The formation of brucite was predicted to occur when the pH of Rand Uranium mine water was increased to greater than 9.5 with alkalinity generated by the dissolution of lime from Matla coal FA.

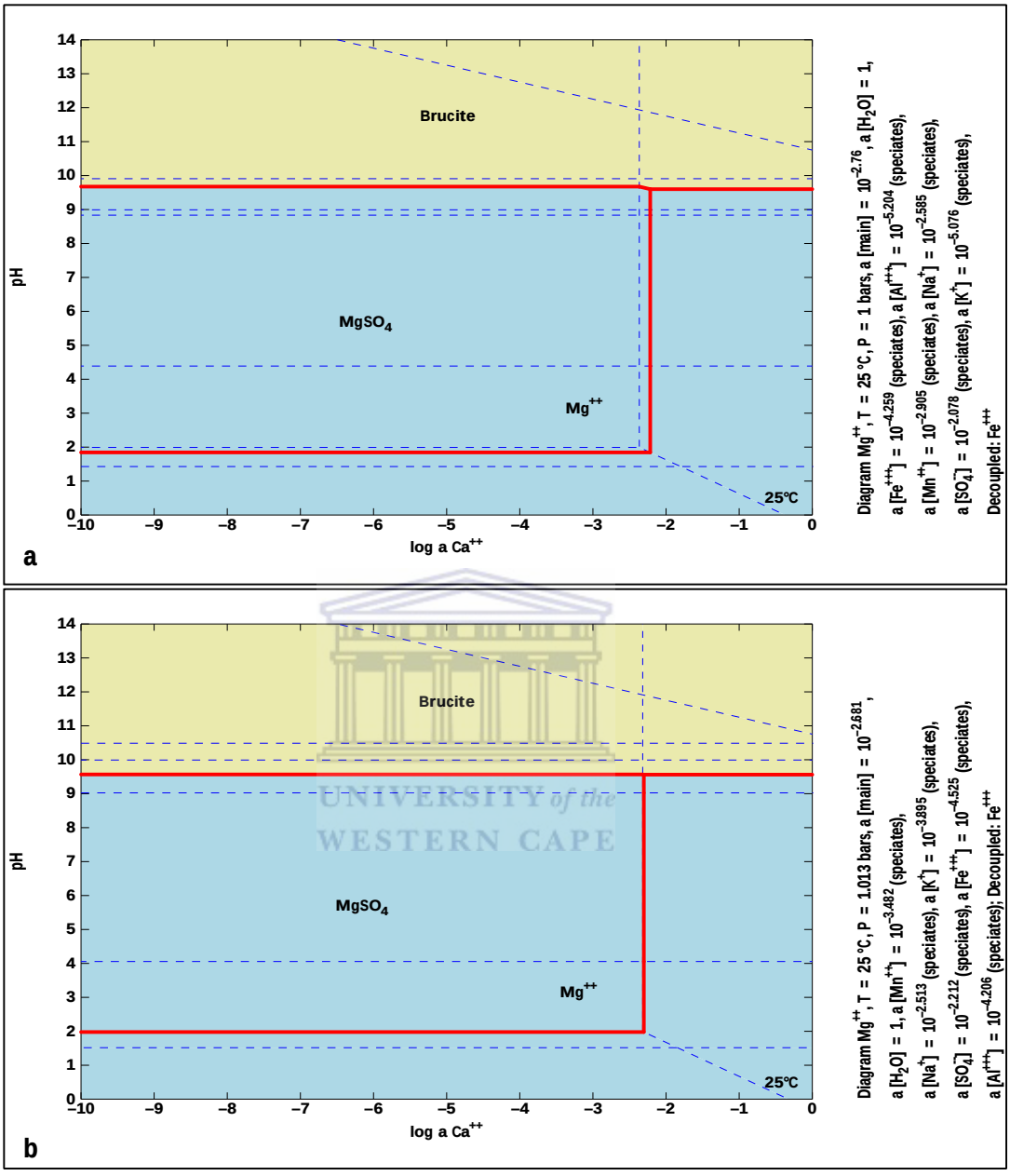

Figure 5.1.7: Magnesium phases that were predicted to form by Act2 program of the GWB software when RU1 (a) or RU2 (b) mine water was treated with Matla coal FA to various $\log_a Ca^{2+}$ and pH values *(yellow colour show mineral phases and blue colour represents aqueous phases).*

The potassium phases predicted by Act2 program of GWB software when Rand Uranium mine water was to be treated with Matla coal FA are shown in Figure 5.1.8.

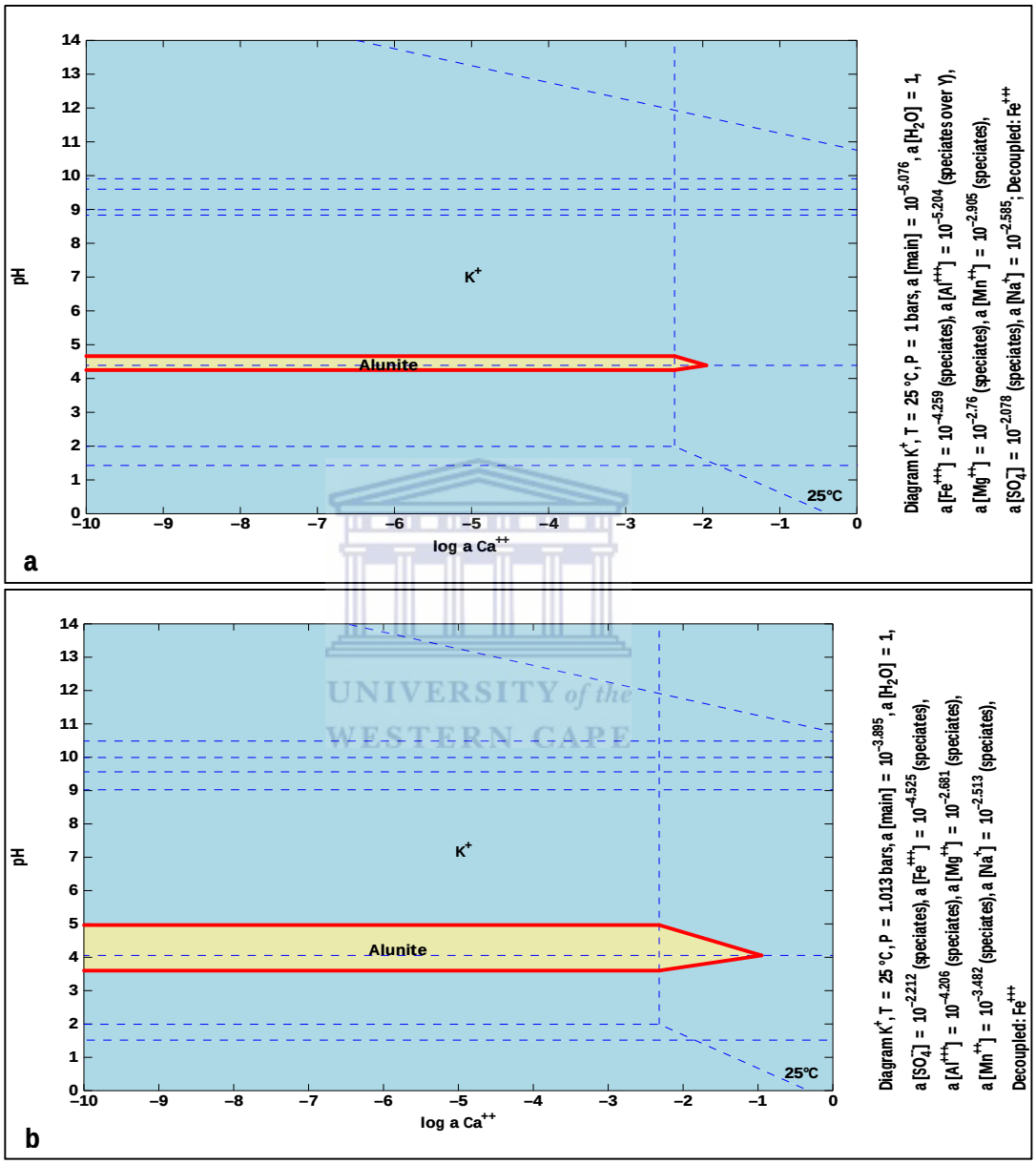

Figure 5.1.8: Potassium phases that were predicted to form by Act2 program of the GWB software when RU1 (a) and RU2 (b) mine water was treated with Matla coal FA various $\log_a Ca^{2+}$ and pH values *(yellow colour show mineral phases and blue colour represents aqueous phases).*

The Act2 program predicted that when Rand Uranium mine water was to be treated with Matla Coal FA, K can only precipitate in the form alunite ($KAl_3(SO_4)_2(OH)_6$) at a specific pH and Ca concentration. Alunite could only form at pH between 4.3 and 4.8 when $\log_a Ca^{2+}$ less than -2 in RU1 as shown in Figure 5.1.8a. At all other pH and $\log_a Ca^{2+}$ conditions K was predicted by Act2 program to exist as free K^+ ions in RU1. In RU2 alunite could form at pH 3.7 to 5 when $\log_a Ca^{2+}$ less than -1 as shown in Figure 5.1.8b. The Act2 program showed that at all other pH and $\log_a Ca^{2+}$, K would exist as free K^+ free ions. The wider range of pH predicted for the formation of alunite in RU2 was because there was a higher concentration of K in RU2 than in RU1. This meant a lower concentration of hydroxyl ions would be required to push the equilibrium reaction for the formation of alunite in RU2 than RU1.

According to the Act2 program of the GWB software, if Rand Uranium mine water was to be treated with Matla coal to various pH and $\log_a Ca^{2+}$ values, Na would remain in aqueous solution as free Na^+ ions as shown in Figure 5.1.9.

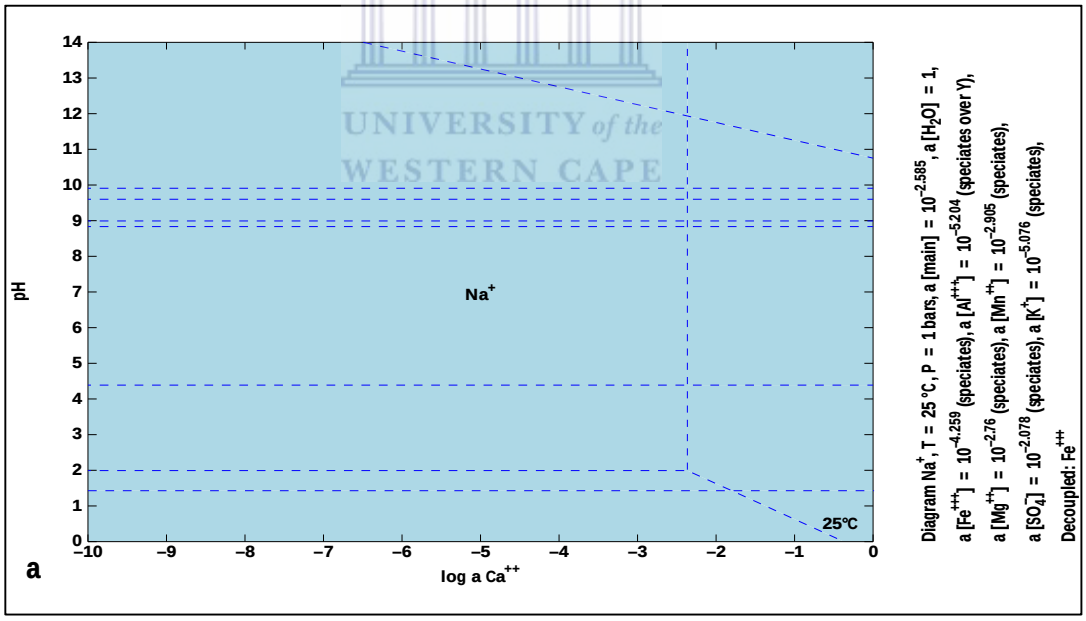

Figure 5.1.9: Sodium phases that were predicted to form by Act2 program of the GWB software when Rand Uranium mine water was treated with Matla coal FA to various $\log_a Ca^{2+}$ and pH values *(yellow colour show mineral phases and blue colour represents aqueous phases).*

So if Rand Uranium mine water was to be treated with FA it was predicted that no Na ions would be removed from mine water by precipitation in any mineral form.

5.1.2.2. Probable mineral phases for natural radioactive elements

Naturally occurring radioactive elements that were found to be above the required limit for potable water in Rand Uranium mine water were Th and U as shown in Table 4.6.2. The probable phases of Th and U that could form when Rand Uranium mine water was to be treated with Matla coal FA were modelled using Act2 program of GWB software. The probable phases of U that were predicted to form using Act2 program are shown in Figure 5.1.10.

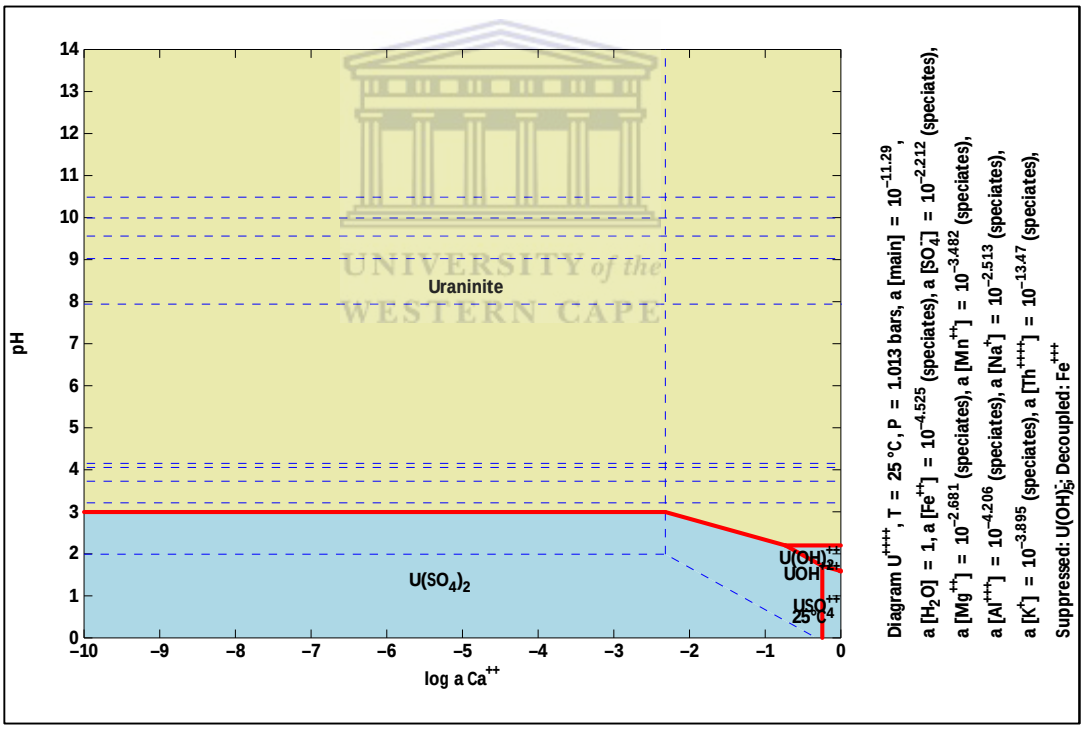

Figure 5.1.10: Uranium phases that were predicted to form by Act2 program of the GWB software when Rand Uranium mine water was treated with Matla coal FA to various $\log_a Ca^{2+}$ and pH values *(yellow colour show mineral phases and blue colour represents aqueous phases).*

From the Act2 results, if Rand Uranium mine water was to be treated with Matla coal FA, it was predicted that U could precipitate in the form of uraninite (UO_2). The formation of UO_2 was found to be pH dependent if the log_aCa^{2+} was less than -2.7. When log_aCa^{2+} was less than -2.7, precipitation of UO_2 occurs when the pH of mine water was increased to greater than 3. If log_aCa^{2+} of the mine water was to be increased from -2.7 to 0, the pH at which UO_2 could start precipitating would decrease from 3 to 2 as more Ca ions were added to the mixture. At pH less than 3 and log_aCa^{2+} less than about -0.3, U will exist as $U(SO_4)_2$ in solution. If log_aCa^{2+} was increased to greater than about -0.3 and the pH kept below 3, U will exist as USO_4^{2+}, UOH^{3+} and $U(OH)_2^{2+}$ as shown in Figure 5.1.10.

The Act2 program predicted that if Rand Uranium mine water was to be treated with Matla coal FA, Th could be removed as thorianite (ThO_2) as shown in Figure 5.1.11.

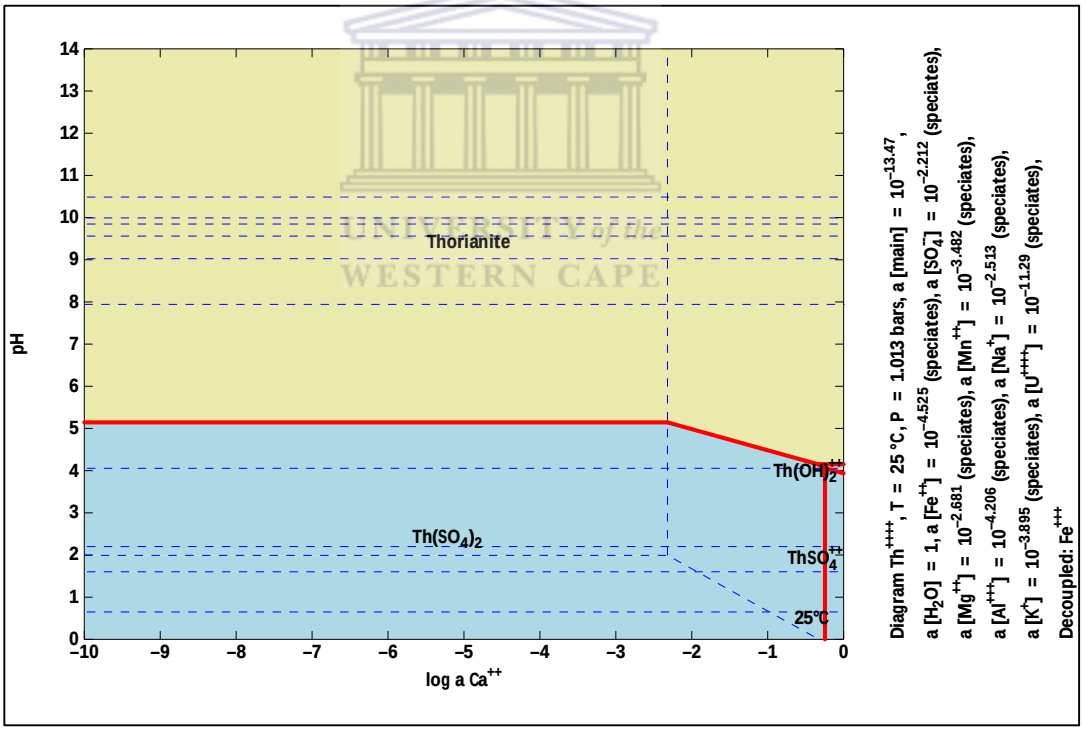

Figure 5.1.11: Thorium phases that were predicted to form by Act2 program of the GWB software when Rand Uranium mine water was treated with Matla coal FA to various log_aCa^{2+} and pH values *(yellow colour show mineral phases and blue colour represents aqueous phases).*

The formation of ThO_2 was found to be pH dependent, when log_aCa^{2+} was less than -2.3. When log_aCa^{2+} was less than -2.3, ThO_2 could form if the pH of the mine water was increased to greater than 5. Increasing log_aCa^{2+} from -2.3 to 0 would result in the decrease in the pH at which ThO_2 would precipitate from about 5 to about 4, as shown in Figure 5.1.11. At pH less than 5 and log_aCa^{2+} less than about -0.2, Th would exist as $Th(SO_4)_2$. If the log_aCa^{2+} was to be increased to greater than -0.2 and the pH kept less than 4, Th would exist as $ThSO_4^{2+}$ and $Th(OH)_2^{2+}$.

5.2. CONCLUSION

The Act2 sub program of the GWB model predicted that if Matla water mine water or Rand Uranium mine water was to be treated with coal FA, the removal of the potential toxic elements depended on pH end point of the treatment and the concentration of Ca ions added to the mine water. The results are very helpful especially to determine the amount of coal FA or alkaline chemicals that would be required to treat a particular composition of the mine water.

It was predicted by the Act2 program that the removal of Mg ions from Matla mine was found to be pH dependent. It was found that increasing the pH of Matla mine water to greater than 10 would result in the precipitation of Mg as brucite. No removal of sulphate, K and Na ions from Matla mine water was predicted if the concentration of Ca ions in mine was increased such that log_aCa^{2+} was to be increased from -10 to 0 and pH was increased to 14.

The Act2 program of the GWB predicted that treatment of Rand Uranium mine water with coal FA could remove sulphate ions as alunite or gypsum. Removal of alunite and gypsum from Rand Uranium mine water was found to be log_aCa^{2+} and/or pH dependent. If sulphate ions were to be removed in the form of alunite, the pH of the mixture would need to be maintained between 3.5 and 5 and log_aCa^{2+} less than -1. If the sulphate ions were to be removed in the form of gypsum the log_aCa^{2+} of the mixture would have to be increased to greater than -2.5. Removal of Al ions from Rand Uranium mine water was predicted to take

place through alunite or gibssite precipitation according to Act2 program. Formation of alunite and gibbsite was found to be dependent upon pH and concentration of Ca ions of the mine water. The conditions for the removal of Al as alunite are the same as the conditions for the removal of sulphate ions as alunite. Removal of Al ions as gibssite would occur when the pH of the mine water was increased to between 4.5 and 10. The probable Fe containing mineral phases that were predicted to form when Rand Uranium water was to be treated with coal FA were, jarosite-K and $Fe(OH)_3$. The formation of these minerals was found to be pH and $\log_a Ca^{2+}$ dependent. Jarosite-K was predicted to form at pH between 3.5 and 5 if $\log_a Ca^{2+}$ was between -10 and -2.5. As $\log_a Ca^{2+}$ was increased from -2.5 to -1, the range of stability of jarosite-K decreased. As $\log_a Ca^{2+}$ was increased to greater than -1, no jarosite would form in Rand Uranium mine water. Formation of $Fe(OH)_3$ could only form if the pH of the mine water was to between 5 and 12. Modelling results using the GWB model have shown that if Rand Uranium mine was to be treated with coal FA, Mn and Mg ions would be removed as $Mn(OH)_2$ and $Mg(OH)_2$ respectively. The formation of $Mn(OH)_2$ and $Mg(OH)_2$ will depend on the final pH attained during treatment and independent on the amount of Ca^{2+} ions added into the mixture. $Mn(OH)_2$ and $Mg(OH)_2$ were found to precipitate at pH 10 and 9.5 respectively.

Removal of K ions from Rand Uranium mine water was found to be through the precipitation of alunite according to the GWB. On the other hand the GWB model showed that if Rand Uranium mine water was to be treated with FA, there is no expected Na-mineral phase that would form. Therefore if Rand Uranium is to be treated with FA, Na concentration would remain the same if there is no leaching of Na from FA or adsorption or absorption of Na ions by the FA particles.

These results are very important in the planning stage of the treatment of mine water during exploration or mining. The information from the Act2 modelling results can be used for deciding the treatment technology and budgeting of the treatment process. It is advisable to try to use the software such as GWB so that scientists can reduce the amount of time and the number of experiments during research and development of the treatment technology of the remediation techniques at a particular mine.

CHAPTER 6: TREATMENT OF MINE WATER WITH FLOCCULANTS

6.1. INTRODUCTION

Flocculants such as polyaluminium chloride and $AlCl_3$ have wide application in the removal of colloidal particles in water. Recently, sulphate removal from mine water using polyaluminium chloride and $AlCl_3$ was investigated (Silva et al., 2010). The performance of these flocculants in the removal of colloids was found to be pH dependent. This chapter investigates the effect of pH and amount of aluminium chlorohydrate (ACH) or $Al(OH)_3$ added on the removal of sulphate ions from Matla mine water and Rand Uranium mine water as outlined in section 3.7.

6.2. TREATMENT OF MATLA MINE WATER WITH FLOCCULANTS

Matla mine water containing 1475 mg/L of sulphate ions as shown in Table 4.5.1 was treated with $Al(OH)_3$ or aluminium chlorohydrate (ACH) with the aim of removing sulphate ions to the allowed effluent limits as outlined in section 3.7.1. The removal of sulphate ions using these options was optimized by studying the effect of variation in pH of mine water and the effect of the amount of Al ions added to Matla mine water ($Al:SO_4^{2-}$ mol ratio). This mol ratio was chosen based on the findings obtained by previous researchers when they used polyaluminium chloride and $AlCl_3$ (Silva et al., 2010).

6.2.1. EFFECT OF PH ON THE REMOVAL OF SULPHATE IONS

The effect of pH was evaluated by mixing Matla mine water with $Al(OH)_3$ or ACH at various pH values as outlined in section 3.7.1.1. In this section the chemistry that contributed to the findings is highlighted. This will enhances the knowledge on how the flocculants interact with sulphate ions at various pH values.

Effect pH of the removal of sulphate ions using $Al(OH)_3$.

Matla mine water pH was first adjusted to various pH values using 1 M HCl. After the pH was adjusted to the required value, the mine water (500 mL) was mixed with 2.3942 g of $Al(OH)_3$ for 20 min as outlined in section 3.7.1.1a. Addition of 2.3942 g of $Al(OH)_3$ was equivalent to 0.031 mols of Al ions added in 500 mL of Matla mine water containing 1475 mg/L of sulphate ions. This meant that the mixture contained 4:1 ($Al:SO_4^{2-}$) mol ratio. The results of the analysis of the water treated at various pH values with $Al(OH)_3$ is shown in Figure 6.2.1.

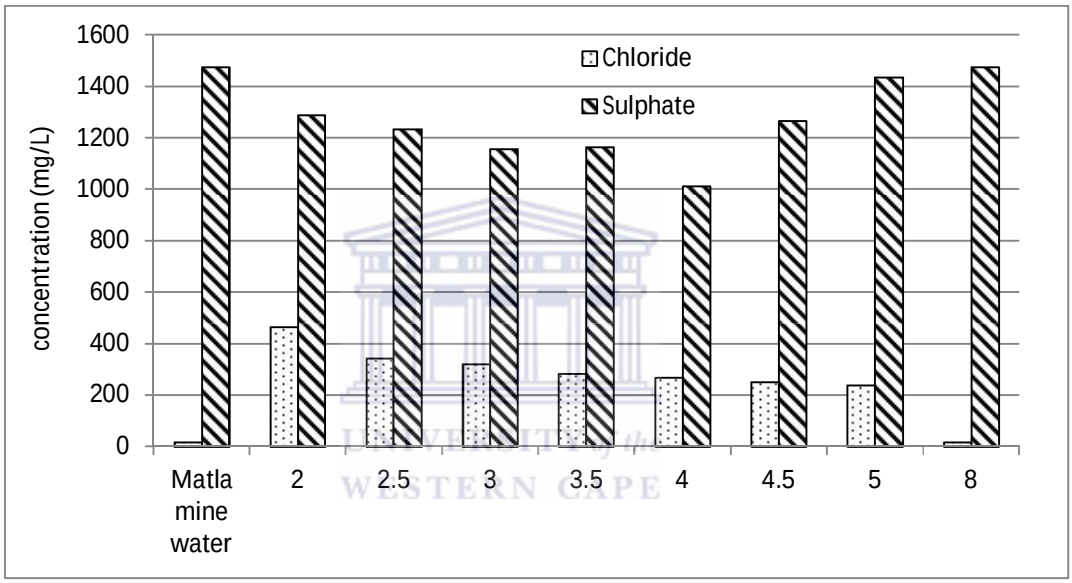

Figure 6.2.1: Effect of pH on the sulphate and chloride concentration in Matla mine water during treatment using $Al(OH)_3$ ($Al^{3+}:SO_4^{2-}$ mol ratio 4:1).

Treatment of Matla mine water with $Al(OH)_3$ at various pH values demonstrated that sulphate ions removal was pH dependent as shown in Figure 6.2.1. The optimum pH for sulphate removal during treatment of Matla mine water with $Al(OH)_3$ was 4. At pH 4 the sulphate concentration in the mine water decreased from 1475 mg/L to 1013 mg/L. Reducing the pH of Matla mine water further to less than 4, the removal of sulphate ions started to decrease as shown in Figure 6.2.1.

Effect of pH on the removal of sulphate ions using ACH

Matla mine water (50 mL) was mixed with ACH (0.61 mL) for 20 min, whilst maintaining the pH of the mixture at various set values using 0.1 M HCl and 0.1 M NaOH as outlined in section 3.7.1.1b. The amount of ACH added results in the Al:SO_4^{2-} mol ratio in the mixture of 4:1. The sulphate concentration of the water produced by treating Matla mine water with ACH at various pH end points is shown in Figure 6.2.2.

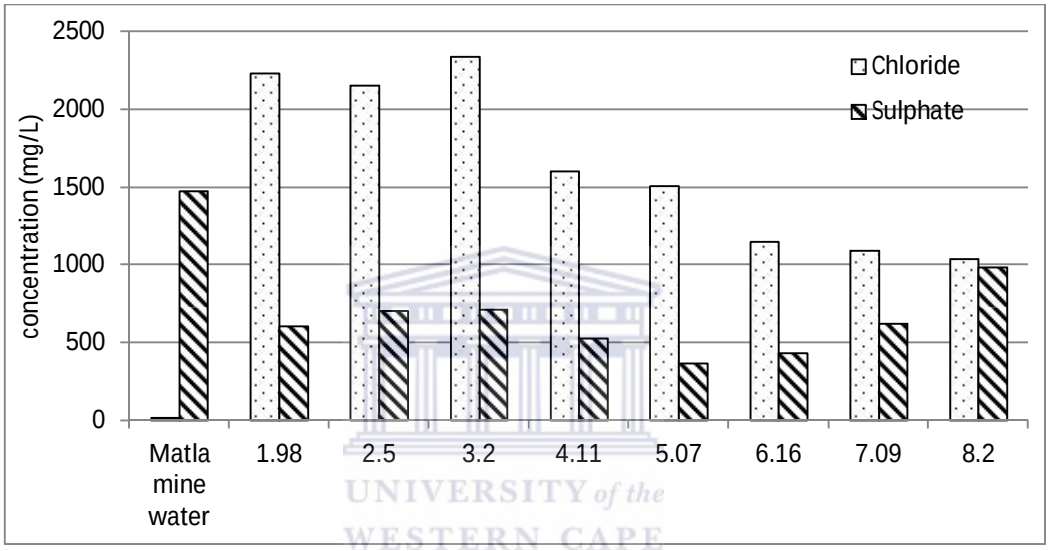

Figure 6.2.2: Effect pH on the sulphate and chloride concentration in Matla mine water during treatment using aluminium chlorohydrate (Al^{3+}:SO_4^{2-} mol ratio 4:1).

As shown in Figure 6.2.2, treatment of Matla mine water with ACH proved that sulphate removal was pH dependent. The optimum pH for sulphate removal for the treatment of Matla mine water with ACH was found to be 5.07 as shown in Figure 6.2.2. The sulphate concentration was decreased from 1475 mg/L to 367.24 mg/L when Matla mine water (50 mL) was treated with 0.16 mL of ACH at pH 5.07. This sulphate concentration was less than the required limit for potable water of 500 mg/L (WHO, 2011; DWAF, 1996). Treatment of Matla mine water (50 mL) with 0.16 mL of ACH at pH greater or less than 5.07 was not efficient for sulphate removal. The sulphate concentration that remained when Matla mine water (50 mL) was treated with 0.16 mL of ACH at pH 1.98, 2.50 and 3.2 was 603.34 mg/L,

704.24 mg/L and 711.97 mg/L respectively. Treatment of Matla mine water (50 mL) with 0.61 mL of ACH at pH 6.16, 7.09 and 8.20 resulted in the treated water containing 431.97 mg/L, 625.76 mg/L and 984.54 mg/L of sulphate ions respectively. So treatment of Matla mine water (50 mL) with 0.61 mL of ACH at pH between 5 and 6 resulted in the sulphate concentration decreasing from 1475 mg/L to less than 500 mg/L.

The pH was found to have a significant effect on the removal of sulphate ions from mine water using $Al(OH)_3$ or ACH. This is because Al compounds are amphoteric and form positive or negative ionic species depending on the pH of the solution. Georgantas and Grigoropoulou in 2007 noted that Al compounds exist in different forms depending on pH. At pH less than 3, Al species mainly exist as mononuclear Al^{3+} ions, while at pH between 3 and 5 the polynuclear positively charged species such as $Al_2(OH)_2^{4+}$, $Al_3(OH)_4^{5+}$, and $Al_{13}O_4(OH)_{24}^{7+}$ are predominant. At pH from 6 to about 10, Al mainly exists as amorphous $Al(OH)_3$. Increasing the pH to greater than 11 results in Al existing mainly as $Al(OH)_4^-$ (Georgantas and Grigoropoulou, 2007).

At pH between 4 and 6 about 31 % and 75 % sulphate ions were removed when Matla mine water was treated with $Al(OH)_3$ (Figure 6.2.1) and ACH (Figure 6.2.2) respectively. At pH 2 $Al(OH)_3$ or ACH removed about 13 % (Figure 6.2.1) or 49 % (Figure 6.2.2) sulphate ions from Matla mine water respectively. More sulphate ions were removed at pH between 4 and 6 because of the interaction of negatively charged sulphate ions with positively charged polynuclear Al species. The polynuclear species had higher positive charges (+4, +5 and +7) than +3 for mononuclear Al^{3+}. This means that polynuclear species were able to form stronger complexes with negatively charged sulphate ion compared to the mononuclear Al species. Generally ACH showed a better removal of sulphate ions than $Al(OH)_3$. This was because $Al(OH)_3$ was a solid and ACH was a liquid. Therefore the kinetics of the in situ formation of the positively polynuclear species that were responsible for the charge destabilization of sulphate ions was greater in ACH than in $Al(OH)_3$.

The major setback of using ACH or $Al(OH)_3$ was the amount of Cl ions that remained in the treated water that would need further polishing to remove. For the optimum pH, the Cl ions that remained in solution were 1012.58 mg/L and 1508.42 mg/L when Matla mine water

was treated with $Al(OH)_3$ or ACH respectively. This was above the limit for potable water of 200 mg/L (WHO, 2011 and DWA, 1996). The Cl ions came from the ACH structure since ACH contained about 171 000 mg/L of Cl ions as shown in Table 4.2.1. In the case of $Al(OH)_3$ the Cl ions came from the acidification of the water using HCl.

6.2.2. EFFECT OF THE AL:SO_4^{2-} MOLAR RATIO

The optimum pH for the treatment of Matla mine water containing 1475 mg/L of sulphate ions with $Al(OH)_3$ or ACH (Al^{3+}:SO_4^{2-} molar ratio 4:1) was found to be 4 and 5.07 respectively. This section presents the results obtained when Matla mine water was treated with different amounts of $Al(OH)_3$ or ACH at pH 4 and 5.07 respectively. The Al:SO_4^{2-} was thus varied between 1:2 and 8:1 during treatment of Matla mine water with ACH or $Al(OH)_3$ as outlined in section 3.7.1.2a.

Effect Al:SO_4^{2-} mol ratio on the removal of sulphate ions using $Al(OH)_3$.

Matla mine water was treated with different amounts of $Al(OH)_3$ as outlined in section 3.7.1.2a. The amount of $Al(OH)_3$ added to Matla mine water was such that the Al:SO_4^{2-} mol ratio was varied between 1:1 and 8:1. The pH was maintained between 4 and 6 by adding 0.1 M of HCl. Results of the treatment of Matla mine water with different amounts of $Al(OH)_3$ are shown in Figure 6.2.3.

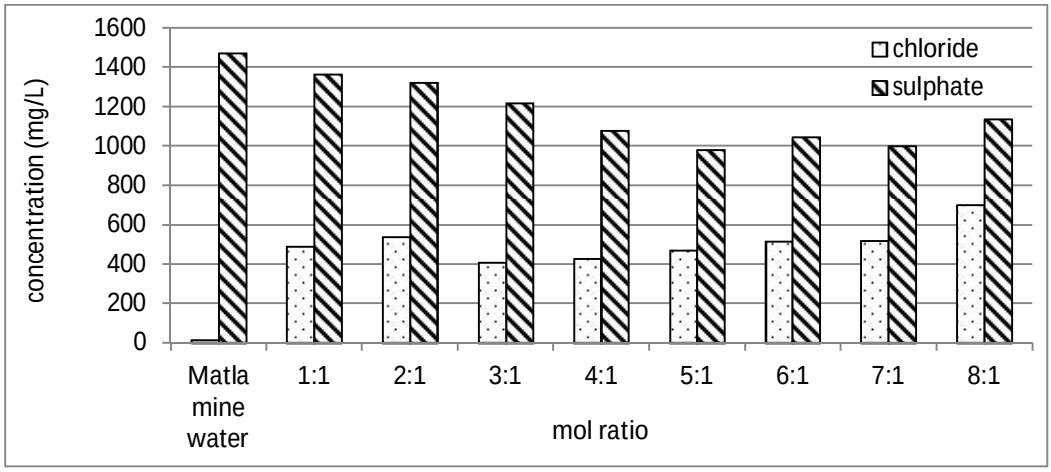

Figure 6.2.3: Effect of the Al:SO_4^{2-} molar ratio on the removal of sulphate and chloride from Matla mine water using $Al(OH)_3$ at pH between 4 and 6.

Treatment of Matla mine water with $Al(OH)_3$ at pH between 4 and 6 was dependent on the amount of $Al(OH)_3$. The sulphate ion in the treated water decreased as more $Al(OH)_3$ was added from 1:1 to 5:1. Increasing the Al:SO_4^{2-} mol ratio above 5:1 did not result in enhancement of sulphate removal from Matla mine water as shown in Figure 6.2.3. When Matla mine water was treated with $Al(OH)_3$ with Al:SO_4^{2-} molar ratio set at 1:1, 2:1, 3:1, 4:1, 5:1, 6:1, 7:1 or 8:1 and pH between 4 and 6, the sulphate concentration in the mine water decreased from 1475.02 mg/L to 1366.75 mg/L, 1324.12 mg/L, 1082.13 mg/L, 982.94 mg/L, 1044.79 mg/L, 1000.16 mg/L or 1137.24 mg/L respectively. The optimum Al:SO_4^{2-} for the treatment of Matla mine water with $Al(OH)_3$ at pH between 4 and 6 was found to be 5:1. As more $Al(OH)_3$ was added to Matla mine water, more HCl was needed to maintain the pH between 4 and 6 since $Al(OH)_3$ addition at this pH range tends to act as base, causing the pH to increase beyond the optimum range of between 4 and 6. The pH was maintained between 4 and 6 (by 0.1 M HCl) since it was the optimum pH for the removal of sulphate ions from mine water using $Al(OH)_3$ as found out in section 6.2.1. This resulted in the Cl concentration of between 490 mg/L to 699.59 mg/L in the treated water compared to untreated Matla mine water which had a concentration of 15.52 mg/L.

Effect of Al:SO_4^{2-} mol ratio on the removal of sulphate ions using ACH

Matla mine water was treated with various amounts of ACH at pH between 5 and 6. This was because the optimum pH was 5.07 when Matla mine water was treated with ACH at a Al:SO_4^{2-} mol ratio of 4:1. The amount of ACH was varied such that Al:SO_4^{2-} ratio varied from 2:1 to 8:1 as outlined in section 3.7.1.2b. The IC analysis results of the water obtained after treating Matla mine water with various amounts of ACH at pH between 4 and 6 are shown in Figure 6.2.4.

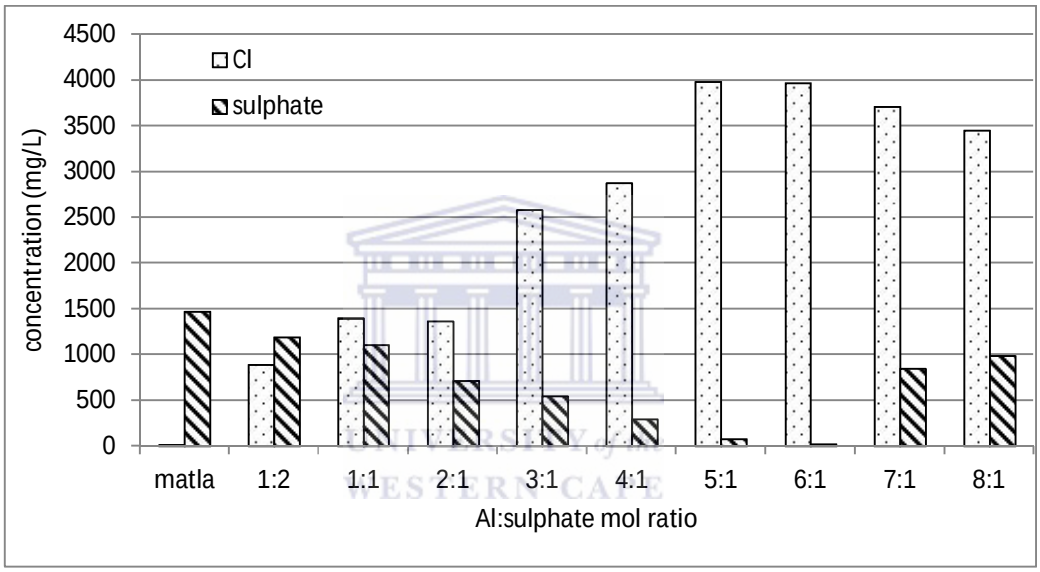

Figure 6.2.4: Effect of the Al:SO_4^{2-} molar ratio on the removal of sulphate and chloride from Matla mine water using aluminium chlorohydrate at pH between 4 and 6.

The results show that the removal of sulphate ions from Matla mine water using ACH depended on the amount of Al added to the Matla mine water at pH 5.07. More sulphate ions were removed from Matla mine water as more Al was added (from Al:SO_4^{2-} molar ratio of 2:1 to 6:1). Addition of ACH such that the Al:SO_4^{2-} molar ratio was greater than 6:1 resulted in the removal of sulphate ions from mine water decreasing. This can be attributed to the fact that when more Al was added such that the molar ratio was greater than 6:1, the ACH could not dissolve properly. The mixture was more of a viscous sludge rather than a mixture of solid material and liquid as was the case with other molar ratios of 6:1 and less.

This severely limited this treatment option because the treated water was difficult to separate from the sludge. The optimum Al:SO_4^{2-} molar ratio for the removal of sulphate ions from Matla mine water was found to be 6:1. At a 4:1 mol ratio (Al:SO_4^{2-}) the sulphate concentration in the treated water was 296 mg/L which was less than the limit set by the World Health Organization of 500 mg/L.

Addition of ACH to Matla mine water in order to remove the sulphate ions resulted in the addition of Cl ions in the treated water. At mol ratio of 4:1, where the sulphate concentration was within the TWQR for domestic use, the Cl ion concentration was almost 3000 mg/L in the treated water which was well above the TWQR for potable water of 500 mg/L (WHO, 2011). This was because of the contamination of Cl from ACH. The high Cl concentration in the treated water and high viscosity of the mixture of treated mine water and sludge were the main setbacks of using ACH for the removal of sulphate ions from mine water.

6.3. TREATMENT OF RAND URANIUM MINE WATER WITH MATLA COAL FLY ASH FOLLOWED BY FLOCCULANTS

This section details results obtained from the experiments in which Rand Uranium mine water was treated with flocculants. Before applying the flocculant treatment, Rand Uranium mine water was first treated with Matla coal FA. This was done in order to remove heavy metals from the mine water. Matla mine water was not treated first with Matla coal FA because it did not contain heavy metals such as Fe, Al and Mn. The coal FA treated Rand Uranium mine water was then recovered and further treated with different amounts of $Al(OH)_3$ or ACH to remove the remaining sulphate ions after adjusting the pH with 0.1 M of HCl to between 4 and 6.

Treatment of Rand Uranium mine water with Matla coal FA

Rand Uranium mine water (RU1) with pH of 2.23 was treated with Matla coal FA to pH 6.12 and 9.48 using liquid to solid residue of 6:1, as outlined in section 3.7.2. The pH of Rand

Uranium mine water was increased from 2.23 to 6.12 and 9.48 after 10 and 15 min respectively. Results of the analysis of the product water using ICP-OES to determine the concentration of Ca, Fe, Mg, Na, Al and Mn after the initial treatment of RU1 with Matla coal FA only to pH 6.12 and 9.48 are shown in Figure 6.3.1.

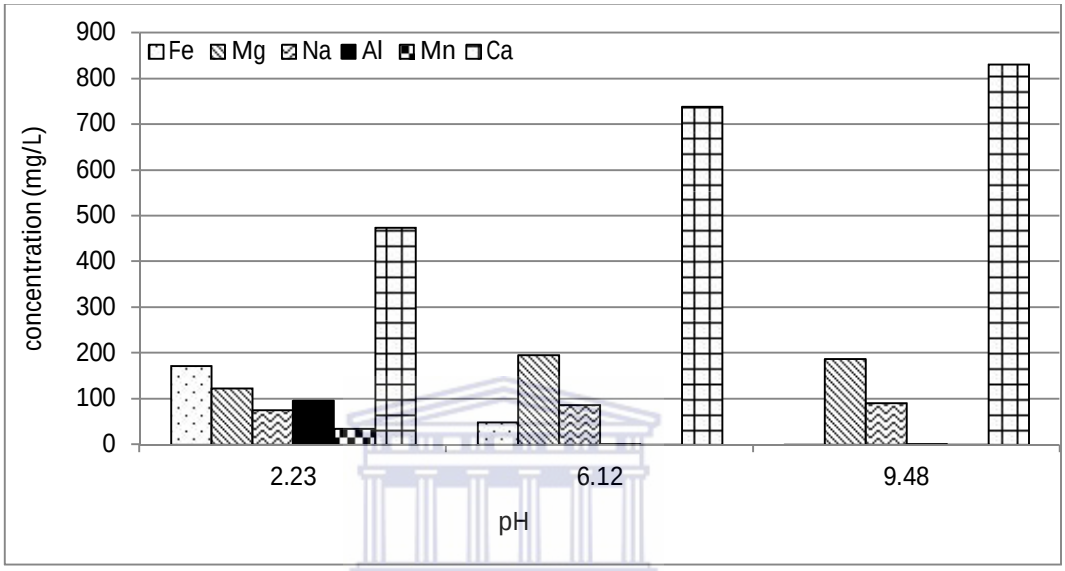

Figure 6.3.1: The concentration of Ca, Fe, Mg, Na, Al and Mn during treatment of 50 mL of Rand Uranium mine water with 8 g of Matla coal fly ash.

The results in Figure 6.3.1 show that the Fe, Al and Mn were removed from Rand Uranium mine water by almost 100 % when treated with Matla coal FA. This was due to the formation of their respective hydroxides (Gitari et al., 2008). The concentration of Ca increased in the mine water due to the dissolution of CaO from Matla coal FA thereby causing the pH of Rand Uranium mine water to increase. The concentration of Na and Mg remained almost constant. Magnesium is known to form $Mg(OH)_2$ at pH greater than 11 (Madzivire et al., 2011), while an increase in pH has no known effect on Na.

The concentrations of sulphate and chloride ions after the initial treatment of RU1 with FA to pH 6.12 and 9.48 are shown in Figure 6.3.2.

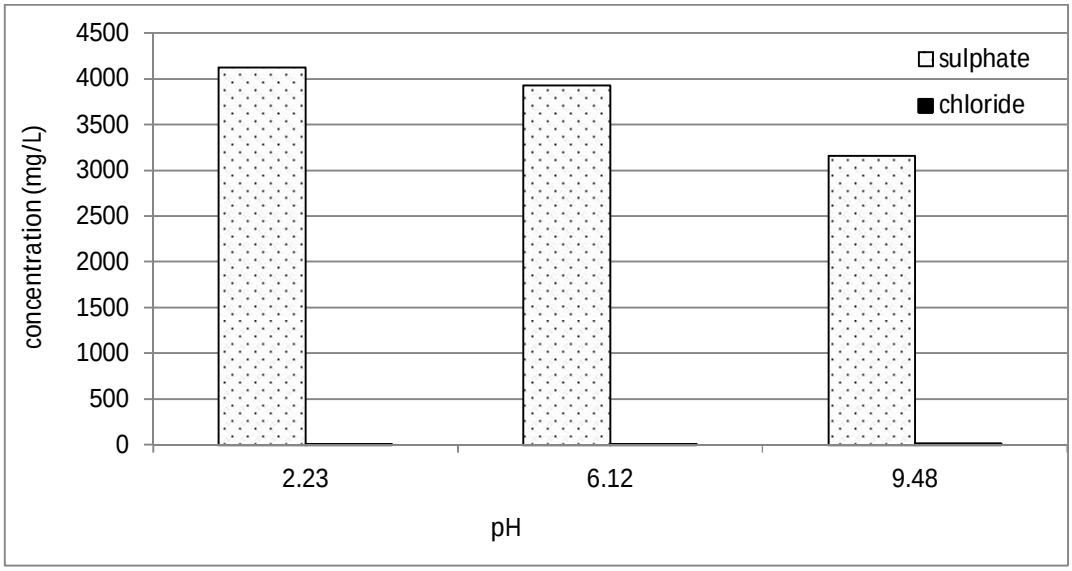

Figure 6.3.2: The concentration of sulphate and chloride ions during treatment of 50 mL of Rand Uranium mine water with 8 g of Matla fly ash.

Treatment of Rand Uranium mine water (50 mL) with 8 kg of Matla FA resulted in the sulphate concentration decreasing from 4126 mg/L to 3928.85 mg/L and 3161.00 mg/L after the pH was increased to 6.12 and 9.48 respectively. So treatment of Rand Uranium mine water (50 mL) with Matla coal FA resulted in only 4.77 % and 23.39 % removal of sulphate ion when the pH was increased to 6.12 and 9.48 respectively. This can be attributed to the formation of gypsum and Fe and Al oxyhdroxosulphate mineral phases (Madzivire et al., 2011). There was a slight increase of the chloride ions from 10.24 mg/L to 16.93 mg/L during treatment of Rand Uranium mine water (50 mL) with 8 kg of Matla coal FA to pH 9.48. This could have leached from the Matla coal FA. The concentration of Fe, Al and Mn in the treated Rand Uranium mine water was reduced by almost 100 % to TWQR for potable water. The concentration of sulphate ions was above the TWQR for potable water of 500 mg/L. The following section explains how the product water from Matla coal FA treatment of Rand Uranium mine water was treated with ACH or $Al(OH)_3$ in order to remove the remaining sulphate ions.

Effect Al:SO_4^{2-} mol ratio on the removal of sulphate ions using flocculants.

The treated Rand Uranium mine water which had a sulphate concentration of 3161 mg/L was then treated with various amounts of $Al(OH)_3$ or ACH in order to remove the high sulphate ions as explained in section 3.7.2.

i. Effect of $Al(OH)_3$

Product water from the treatment of Rand Uranium mine water with Matla coal FA was further treated with different amount of $Al(OH)_3$ as outlined in section 3.7.2. The amount of $Al(OH)_3$ was varied such that the Al:SO_4^{2-} mol ratio was from 1:1 to 8:1. During treatment the pH of the mixture was maintained between 4 and 6 using 0.1 M HCl. The product water was analysed for the concentrations of sulphate and chloride using IC and the results are shown in Figure 6.3.3.

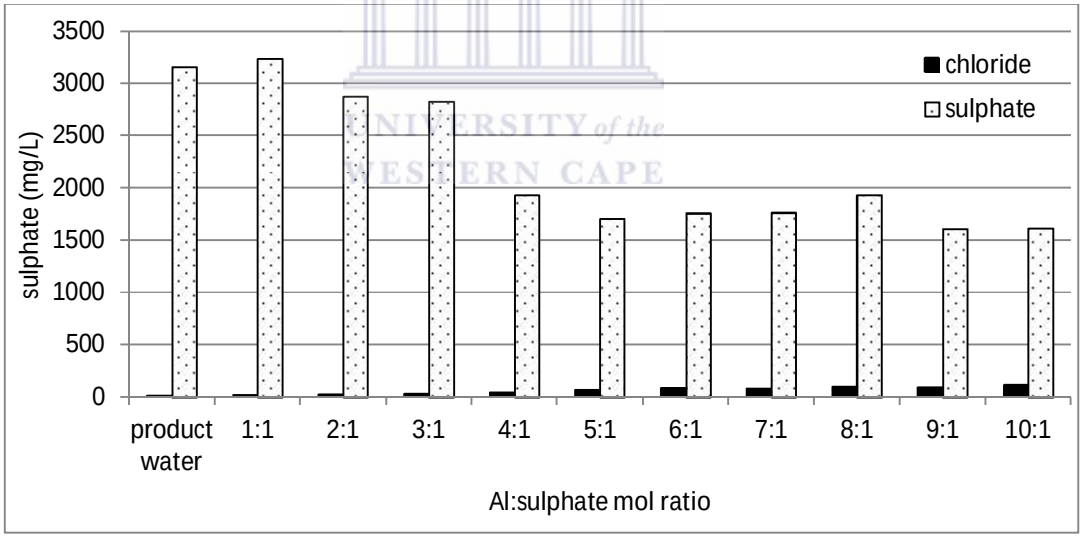

Figure 6.3.3: The concentration of sulphate and chloride ions during treatment of product water from FA treatment with $Al(OH)_3$ at pH between 4 and 6.

The results in Figure 6.3.3 show a gradual decrease in sulphate concentration when more $Al(OH)_3$ was added to the water from 1:1 to 5:1 Al:SO_4^{2-} mol ratio. Addition of more $Al(OH)_3$

(that is, Al:SO_4^{2-} mol ratio 6:1 and greater) could not remove extra sulphate ions under these conditions. The sulphate concentration was decreased from 3161 mg/L to 1626 mg/L when $Al(OH)_3$ was added to the mine water at pH between 4 and 6. The removal of sulphate ions using $Al(OH)_3$ resulted in the gradual increase in chloride ions in the mine water as more $Al(OH)_3$ was added. This was because as more $Al(OH)_3$ was added more HCl was added to the mixture to maintain the pH in the optimum range of 4 to 6 which was shown to be necessary in section 6.2.1 for the removal of sulphate ions from mine water.

ii. Effect of ACH

Product water from the treatment of Rand Uranium mine water to pH 9.48 using Matla coal FA was further treated with various amounts of ACH. The product water containing 3161 mg/L of sulphate ions was mixed with different amounts of ACH such that the Al:SO_4^{2-} mol ratios (in the mixture) varied from 1:2 to 4:1 as outlined in section 3.7.2. The product water from the treatment of mine water with different amounts of ACH was analysed for the concentration of sulphate and chloride ions and the results are shown in Figure 6.3.4.

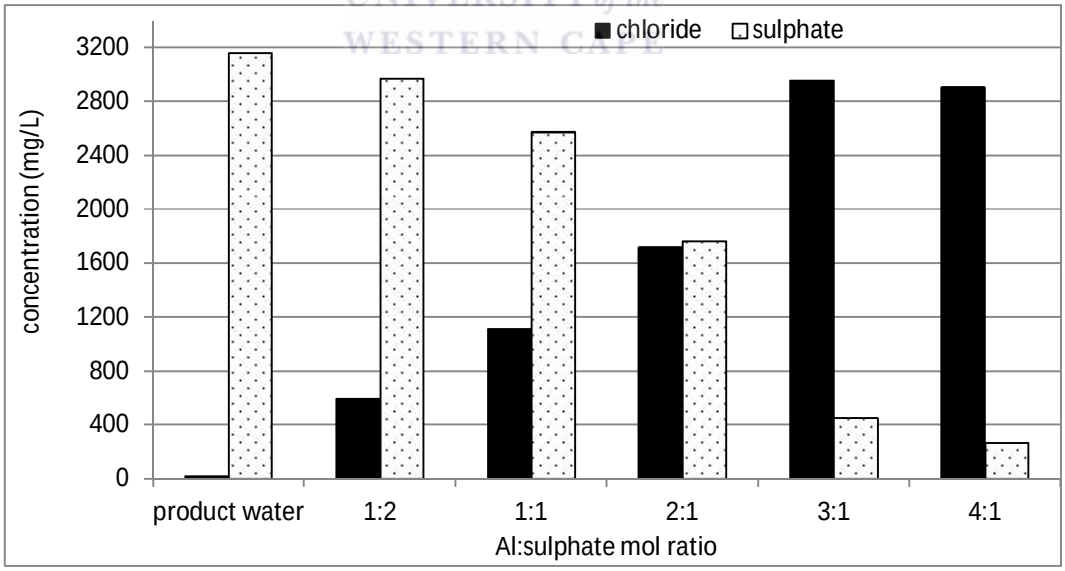

Figure 6.3.4: The concentration of sulphate and chloride ions during treatment of product water from FA treatment with ACH at pH between 4 and 6.

Results in Figure 6.3.4 show that the sulphate removed from mine water depended on the amount of ACH added. A sharp decrease in sulphate concentration was observed as more ACH was added to the water from 1:2 to 3:1 Al:SO_4^{2-} mol ratio. A further decrease in sulphate concentration was observed when more ACH was added (that is, Al:SO_4^{2-} mol ratio 3:1 to 4:1) at pH between 4 and 6. The sulphate concentration was decreased from 3161 mg/L to 450 mg/L or 268 mg/L when the water was treated with 3:1 or 4:1 Al:SO_4^{2-} mol ratios respectively. The 4:1 ratio resulted in the mixture becoming very viscous such that the recovery of the treated water through filtration was almost impossible. This prevented the use of higher amounts of ACH from being investigated.

The major obstacle of using ACH or $Al(OH)_3$ to remove sulphate ions from Rand Uranium mine water is the high concentration of chloride ions that remain. The chloride ions during treatment of Rand Uranium mine water with ACH came from the flocculants itself. It was also necessary to adjust the pH using HCl during treatment of mine water with $Al(OH)_3$ to the optimum pH of 4. This caused the concentration of Cl in the treated water to increase.

6.4. CONCLUSION

Removal of sulphate ions from either Rand Uranium mine water or Matla mine water using $Al(OH)_3$ or ACH depends on the pH of the mixture and the amount of Al ions added. The optimum pH for sulphate removal during treatment of mine water with $Al(OH)_3$ or ACH was found to be between 4 and 6. The optimum Al^{3+}:SO_4^{2-} mol ratio for the removal of sulphate ions was 5:1 and 6:1 for $Al(OH)_3$ and ACH respectively. Removal of sulphate ions using ACH resulted in better removal compared to using $Al(OH)_3$. Addition of ACH to mine water (with Al^{3+}:SO_4^{2-} mol ratio of 5:1 and 6:1) resulted in the removal of sulphate concentration to less than the potable limit.

The disadvantage of using $Al(OH)_3$ or ACH to remove sulphate ions from mine water is the amount of Cl ions that remain in the treated water. The Cl ions comes from the ACH or HCl added to the mixture in the case of $Al(OH)_3$ in order to maintain the pH at the optimum range. Since the product water contained a high concentration of Cl ions, it is not worthwhile to use flocculants to remove sulphate ions from water. The optimum pH at

which $Al(OH)_3$ and ACH performs well in removing sulphate ions is in the acidic range. This means that most of the heavy metals need to be removed by other processes. This was because at pH 4, heavy metals such as Mn^{2+} and Mg^{2+} would not precipitate out as their respective hydroxides and would remain in the treated water.

CHAPTER 7: APPLICATION OF THE JET LOOP REACTOR

This Chapter explains the chemistry and kinetics of the removal of potentially toxic and/or radioactive elements from Matla mine water and Rand Uranium mine water when treated with Matla coal FA, lime and/or $Al(OH)_3$. The kinetics of the removal of potentially toxic elements was compared when mine water was treated using either an overhead stirrer or using a jet loop reactor. The first section covers the work done on Matla mine water and the second section of this Chapter covers the work done on Rand Uranium mine water.

7.1. TREATMENT OF MATLA MINE WATER

This section covers the chemistry involved when Matla mine water was treated in a jet loop reactor using Matla coal FA, lime and $Al(OH)_3$. The parameters discussed in this chapter are; the effect of the jet size settings in the jet loop reactor and the effect of the different combination of Matla coal FA, lime and $Al(OH)_3$ in the treatment of Matla mine water. A comparison of the effect of mixing Matla mine water with Matla coal FA, lime and $Al(OH)_3$ using a jet reactor was compared to the mixing using an overhead stirrer. The comparison was done to understand if the jet loop reactor enhances the kinetics of the removal of sulphate ions from Matla mine water. The last part of this section investigated the effect of temperature on the removal of sulphate ions from Matla mine water during treatment with Matla coal FA, lime and $Al(OH)_3$.

Matla mine water, Matla coal FA, lime and $Al(OH)_3$ were characterized as outlined in Chapter 3 and the results were presented in Chapter 4. Matla mine water contained high concentration of Na and sulphate ions, with very low concentration of Fe, Al, Mn, Ca and Mg as shown in Table 4.5.1. Matla coal FA was made up of mullite ($Al_2Si_2O_{13}$), quartz (SiO_2), hematite (Fe_2O_3), lime (CaO) and gypsum ($CaSO_4.2H_2O$) as depicted in Figure 4.1.2. Lime contained calcite contaminants (Figure 4.3.2) and $Al(OH)_3$ was made up of boehmite (AlOOH) and bayerite ($Al_2O_3.3H_2O$) (Figure 4.3.1).

7.1.1. OPTIMIZATION OF THE AMOUNT FLY ASH AND LIME REQUIRED

Previous studies have shown that when Middleburg coal mine water was treated with Hendrina coal FA and $Al(OH)_3$ at pH greater than 11, sulphate ions were removed to within the target water quality range (TWQR) set by the Department of Water Affairs (DWAF) and World Health Organization (WHO) for potable water (Madzivire, 2010). This section will present the results to optimize the minimum amounts of Matla coal FA and lime that could take up the pH to greater than 11, so that addition of $Al(OH)_3$ would affect the removal of sulphate ions in the form of ettringite to within the TWQR for potable water. It was necessary to raise the pH of the mine water to greater than 11 before addition of $Al(OH)_3$ because ettringite is known to be stable within pH 11.5 to 12.5 (Mynemi et al., 1998).

Matla coal FA and Matla mine water were reacted together using a liquid to solid ratio of 6:1 (80 L of mine water and 13 kg of coal FA) and 5:1 (80 L of mine water and 16 kg of coal FA) in a jet loop reactor with jet sizes set at 8 mm as outlined in section 3.8.1.1a and 3.8.1.1b. The trends of pH, EC and temperature during treatment of Matla mine water (80 L) with Matla coal FA (13 kg or 16 kg) are shown in Figure 7.1.1.

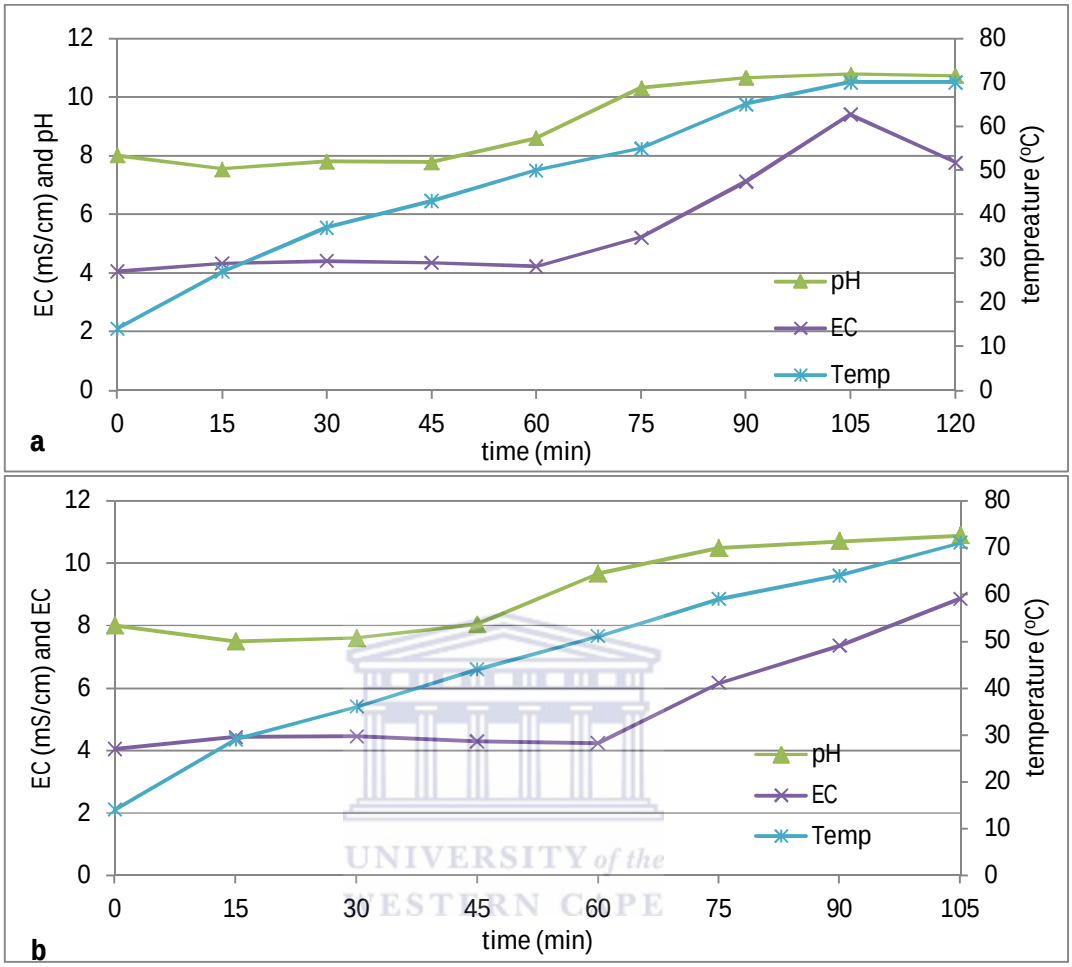

Figure 7.1.1: The pH, electrical conductivity (EC) and temperature profile during treatment of Matla mine water (80 L) with Matla coal FA in a jet loop reactor with 8 mm jet sizes (13 kg of coal FA (a) and 16 kg of coal FA (b)).

Treatment of 80 L of Matla mine water with 13 kg or 16 kg of Matla coal FA in a jet loop reactor has shown that pH and EC remained almost constant up to 45 min (Figure 7.1.1). From 45 min to 90 min the pH of the mixtures increased gradually and then remained constant up to 120 min (Figure 7.1.1). Increase in pH during mixing of Matla mine water and Matla coal FA mixture was due to the dissolution of CaO in Matla coal FA as shown in Equation 7.1. The dissolution of CaO resulted in the increase in EC. This could be attributed to the release of Ca and OH^- ions into the mine water.

$$CaO + H_2O \rightarrow Ca^{2+} + 2OH^- \quad \text{.....7.1}$$

The pH increased from 8 to about 10.77 when 13 kg of Matla coal FA was mixed with 80 L of Matla mine water in a jet loop reactor for 105 min (Figure 7.1.1a). The pH was less than when Matla mine water (80 L) was mixed with 16 kg of Matla coal FA (Figure 7.1.1b). The pH when Matla mine water (80 L) was mixed with 16 kg of Matla coal FA in a jet loop reactor for 105 min was 10.89. This was because as more coal FA was added to Matla mine water; it resulted in more CaO being available for dissolution and therefore causing the pH to increase. During treatment of Matla mine water with Matla coal FA in a jet loop reactor, there was a gradual increase in the temperature from 14 ^{o}C to 70 ^{o}C after 105 min. This was because of the hydrodynamic cavitation mixing that occurred in the jet loop reactor (Jyoti and Pandit, 2001; Mason, 2007).

During treatment of 80 L of Matla mine water with 13 kg or 16 kg of Matla coal FA in the jet loop reactor, aliquot samples were collected after every 30 min. The aliquot samples were filtered using a 0.45 µm filter paper and analysed using ICP-OES and IC. The results obtained are shown in Figure 7.1.2.

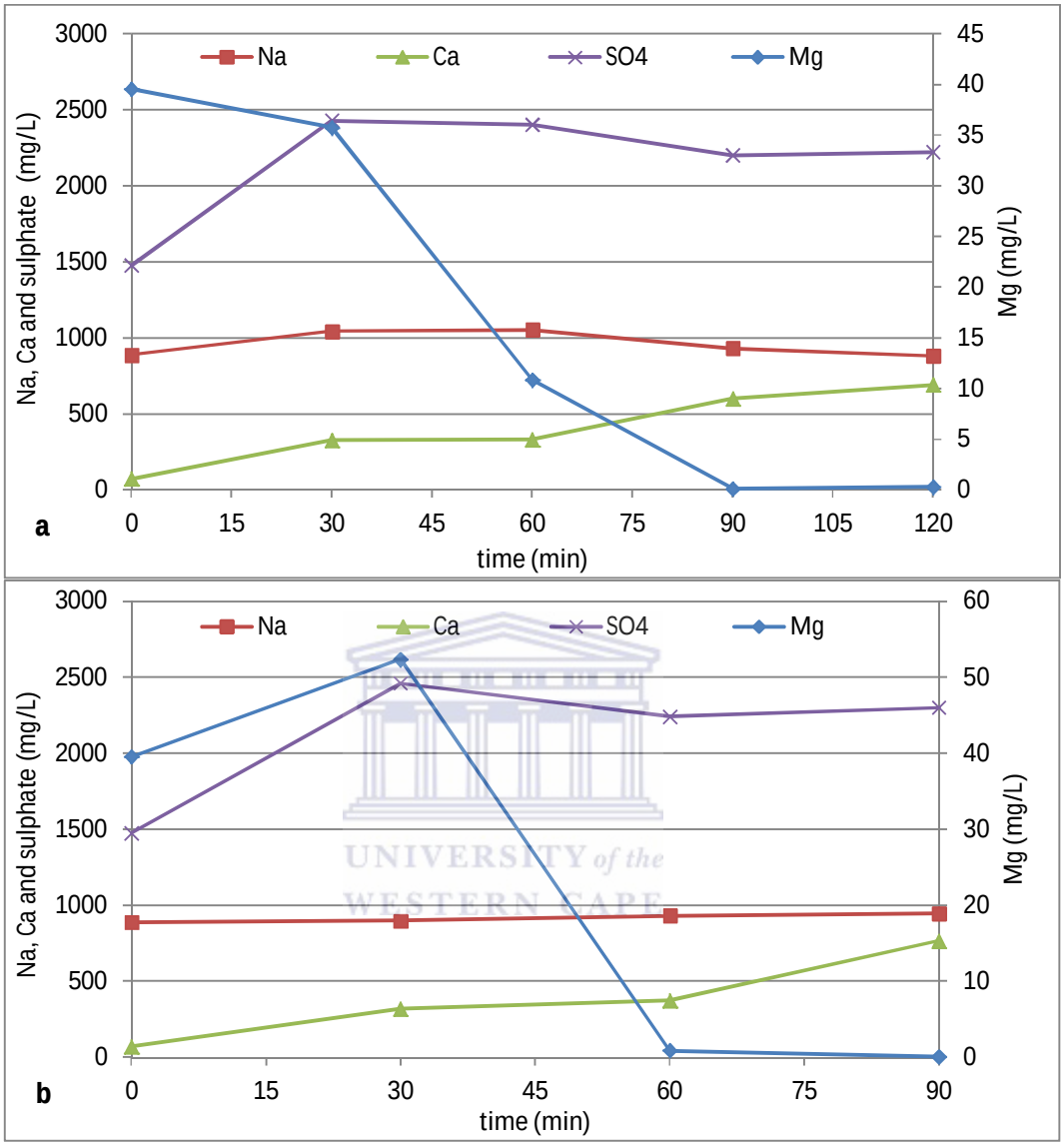

Figure 7.1.2: Na, Ca, Mg and sulphate concentration during treatment of Matla mine water (80 L) with Matla coal FA in a jet loop reactor with 8 mm jet sizes (13 kg of FA (a) and 16 kg of FA (b)).

Results in Figure 7.1.2 indicate that increasing the amount of Matla coal FA from 13 kg to 16 kg did not show any increased performance in the clean-up of the mine water. The Na concentration remained constant during treatment of Matla mine water (80 L) with 13 kg or 16 kg of Matla coal FA. The Ca concentration increased in the treated mine water due to the

dissolution of CaO from Matla coal FA into the mine water as shown in Equation 7.1. Also the concentration of sulphate ions increased from 1475 mg/L to 2430 mg/L or 2460 mg/L during the first 30 min of treating Matla mine water (80 L) with 13 kg or 16 kg of Matla coal FA respectively. The increase in the concentration of Ca and sulphate caused by the dissolution of CaO and gypsum from Matla coal FA resulted in the increase in EC (Figure 7.1.1). After 30 min, the sulphate concentration slightly decreased. This was because after 30 min the Ca and sulphate concentration in the mixture was higher, such that the ionic product (***IP*** = 2.05 x 10^{-4} $mol^2.L^{-2}$) was greater than the solubility product constant ($K_{sp} \approx 3.2 \times 10^{-5}$). This resulted in the precipitation of gypsum, because the ***IP*** was greater than the K_{sp}. Ionic product is the product of the concentration of ionic species added together, while Ksp is the product of ionic species at equilibrium.

$$IP = [Ca^{2+}][SO_4^{2-}]$$

$$K_{sp} = [Ca^{2+}]_{eq}[SO_4^{2-}]_{eq};$$

Where [] is the concentration of ionic species added into the solution in $mol.L^{-1}$ and $[]_{eq}$ is concentration of ionic species in solution at equilibrium

The modelling results given in section 5.1.1 showed that no Ca containing mineral phase would form when Matla mine water was treated with Matla coal FA, by increasing the concentration of Ca from $\log_a Ca^{2+}$ of -10 to 0 as shown in Figure 5.1.1a. This was because the sulphate concentration was assumed to remain constant during modelling. The sulphate ions removed during treatment of Matla mine water with Matla coal FA after 30 min were less than the sulphate that leached into the mine water from Matla coal FA. In fact, there was no net sulphate removal from Matla mine water during treatment with Matla coal FA. This agrees well with the modelling results obtained using Act2 program of the GWB software in section 5.1.1.

The concentration of Mg was decreased by almost 100 % when the pH of the mine water was increased to above 10 when Matla mine water (80 L) was mixed with 13 kg (after 90 min) or 16 kg of Matla coal FA (after 60 min) as shown in Figure 7.1.2a and Figure 7.1.2b respectively. Magnesium is known to precipitate out as $Mg(OH)_2$ at pH greater than 10

(Madzivire, 2010). This was also in agreement with the modelling results obtained by the Act2 program of the GWB model, which predicted that Mg will start precipitating at pH 10 as shown in Figure 5.1.1b.

Treatment of 80 L of Matla mine water with 13 kg or 16 kg of Matla coal FA added could not overcome the pH barrier to achieve a pH of 11.5 and above after mixing in a jet loop reactor for 105 min or longer, as shown in Figure 7.1.1. The pH of at least 11.5 was required so that $Al(OH)_3$ could be added to precipitate out sulphate as ettringite. Since the pH of the mixture of 80 L of Matla mine water and 13 kg or 16 kg of Matla coal FA could not be taken up to greater than 11, the jet nozzle sizes on the jet reactor were reduced from 8 mm to 6 mm. This was carried out in an attempt to increase the mixing intensity of Matla coal FA and Matla mine water through the increase in cavitation in order to increase the dissolution of CaO from coal FA to effect a pH increase to greater than 11.5. After the jet sizes were reduced to 6 mm, Matla mine water (80 L) and 16 kg of Matla coal FA were mixed in the jet loop reactor with the jet sizes set at 6 mm as outlined in section 3.8.1.1c. The pH, EC and temperature were measured after every 15 min and the results obtained are as shown in Figure 7.1.2.

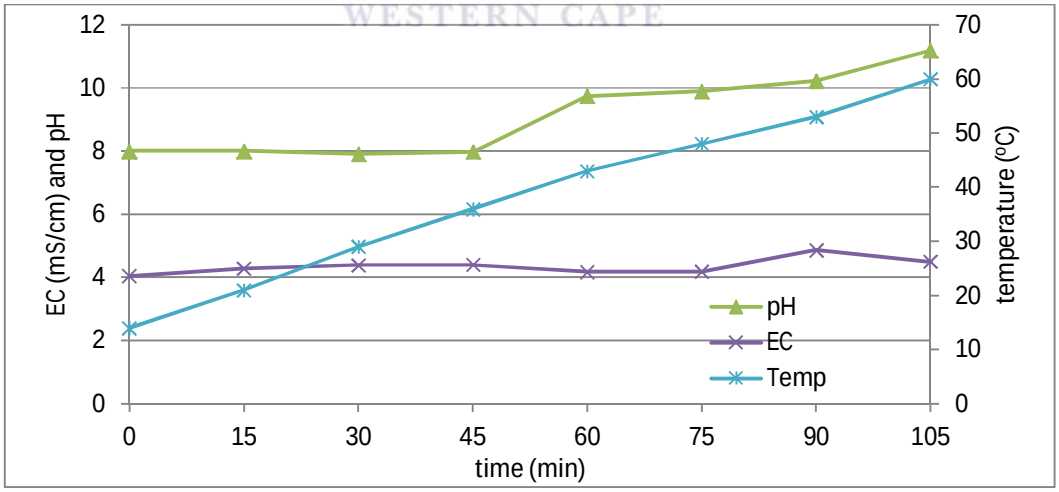

Figure 7.1.3: The pH, electrical conductivity (EC) and temperature profile during treatment of Matla mine water (80 L) with 16 kg of Matla coal FA in a jet reactor with jet sizes set at 6 mm.

Treatment of Matla mine water (80 L) with Matla coal FA (16 kg) in a jet loop rector with jet sizes set at 6 mm resulted in pH increasing from 8 to 11.19 after 105 min (Figure 7.1.3). Forcing the mixture of Matla coal FA and Matla mine water through smaller jet sizes of 6 mm could not cause any significant increase in pH compared to when jet sizes of 8 mm were used. The pH attained by mixing 80 L of Matla mine water with 13 kg of Matla coal FA was still less than the required of 11.5 for addition of $Al(OH)_3$ so that sulphate ions can precipitate as ettringite.

During treatment of Matla mine water (80 L) with 16 kg of Matla coal FA in a jet loop reactor with jet sizes set at 6 mm, aliquot samples were collected after every 30 min. The samples were filtered through a 0.45 µm filter paper and analysed using ICP-OES and IC. The results obtained are shown in Figure 7.1.4.

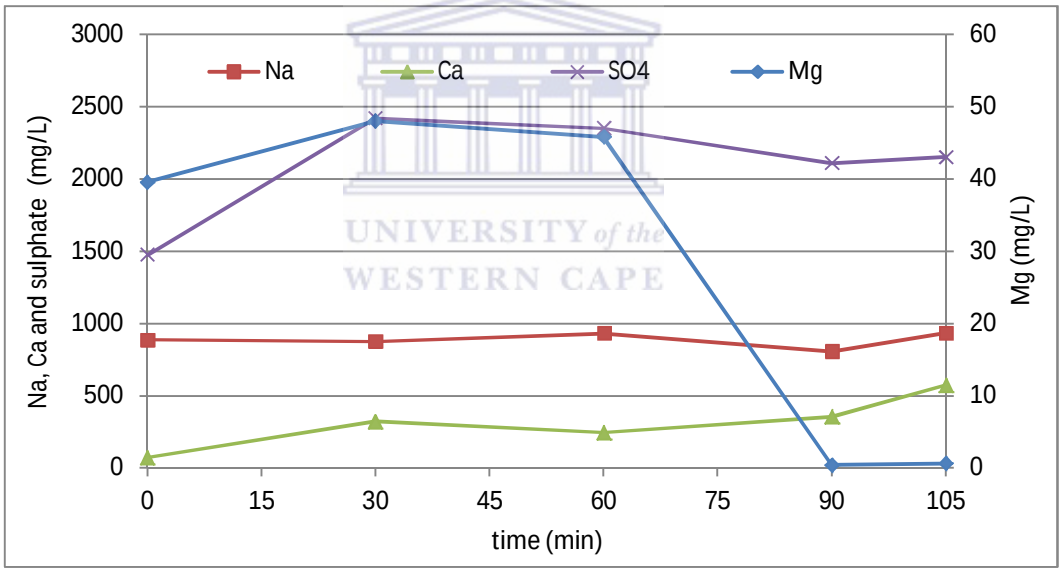

Figure 7.1.4: Na, Ca, Mg and sulphate concentration during treatment of Matla mine water (80 L) with 16 kg of Matla coal FA in a jet loop reactor with jet sizes set at 6 mm.

Reducing the jet nozzle sizes to 6 mm and maintaining the amount of coal FA at 16 kg did not result in a significant difference from the results obtained using a jet size of 8 mm (Figure 7.1.2b and 7.1.4). The Na concentration remained almost the same, while Ca increased steadily from 10 mg/L to about 570 mg/L after 105 min. The sulphate

concentration increased from 1475 mg/L to 2420 mg/L in the first 30 min. After 30 min, the sulphate concentration decreased from 2420 mg/L to 2150 mg/L as shown in Figure 7.1.4. The Mg concentration initially leached into the mine water in the first 30 min and then decreased by almost 100 % after the pH increased to above 10 after 90 min. $Al(OH)_3$ was not added to precipitate sulphate as ettringite; since the pH could not be taken up to 11.5 and above with Matla coal FA only. This prompted a series of bench scale experiments to evaluate the minimum amount of lime that could be added together with Matla coal FA to Matla mine water in order to increase the pH to greater than 11.5. Lime was added to assist Matla coal FA to increase the pH to greater than 11.5 so that $Al(OH)_3$ could be added.

Matla mine water (500 mL) was reacted with a combination of Matla coal FA (83 g) and various amounts of lime (0.125 g, 0.250 g, 0.375 g and 0.620 g). After 30 min, 0.52 g of $Al(OH)_3$ was added to the mixture and the reaction was continued up to 150 min as outlined in section 3.8.1.1d. This amount was equivalent to 6.67×10^{-3} mols of $Al(OH)_3$. This number of mols was enough to remove 1922 mg/L of sulphate ions from 500 mL of Matla mine water as ettringite according to Equation 7.2.

$$6Ca^{2+} + 3SO_4^{2-} + 2Al(OH)_3 + 32H_2O \leftrightarrow 3CaO.3CaSO_4.Al_2O_3.32H_2O + 6H^+ \quad \text{.....7.2}$$

During treatment of Matla mine water (500 mL) with Matla coal FA (83 g), different amounts of lime (0.125 g, 0.250 g, 0.375 g and 0.620 g) and 0.52 g of $Al(OH)_3$, the pH, EC and temperature were measured after every 15 min and the results are shown in Figure 7.1.5.

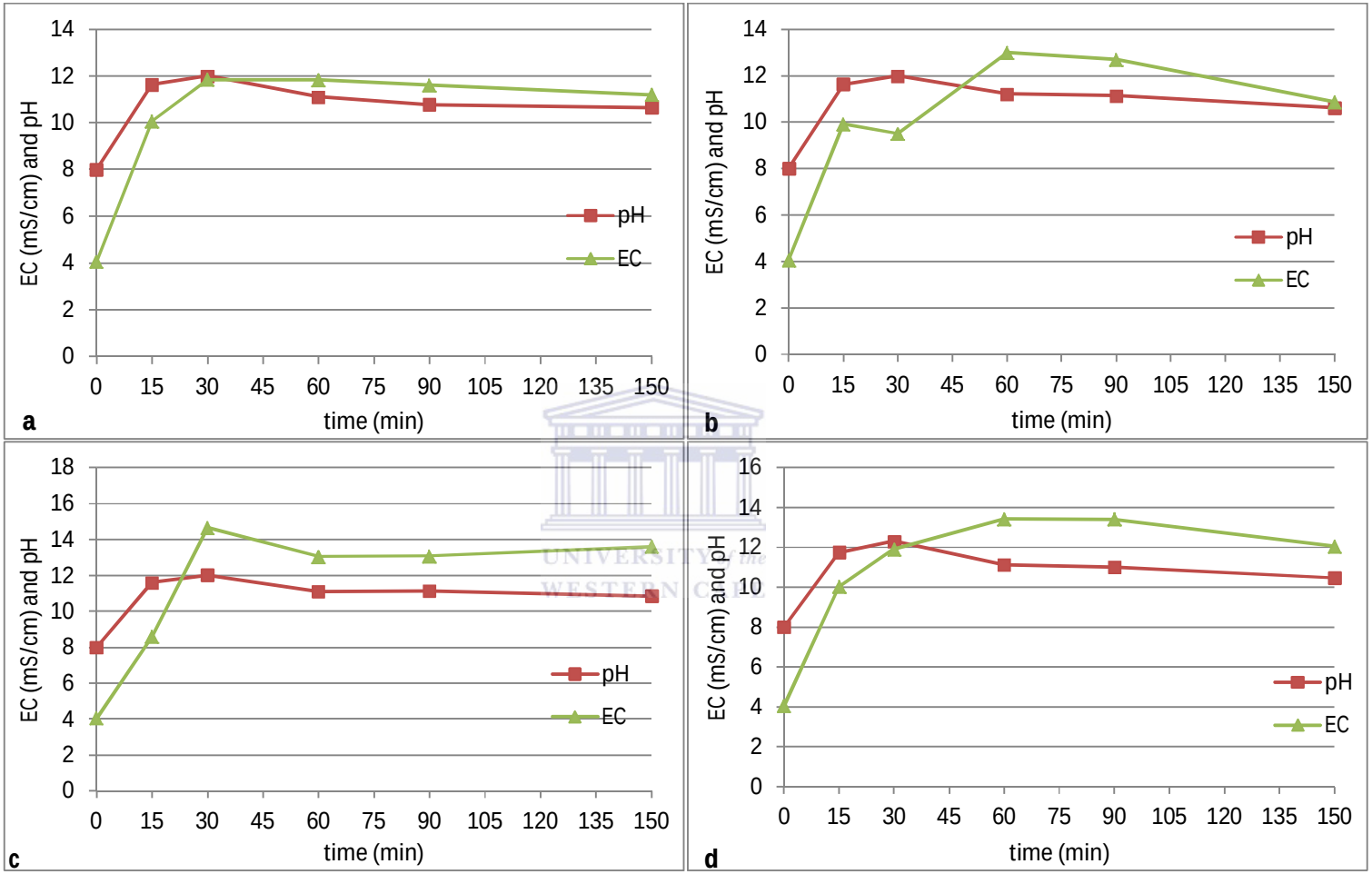

Figure 7.1.5: pH and EC profile during treatment of Matla mine water (500 mL) with 83 g of Matla coal FA, different proportions of lime (0.125 g (a), 0.250 g (b), 0.375 g (c) and 0.620 g (d) of lime) and 0.52 g of $Al(OH)_3$ using an overhead stirrer.

From the pH results shown in Figure 7.1.5, a pH greater than 11.5 for all the mixtures was attained after 15 min. After 30 min of mixing Matla mine water (500 mL) with 83 g of Matla coal FA and different amounts of lime (0.125 g, 0.250 g, 0.375 g or 0.620 g), 0.52 g of $Al(OH)_3$ was then added to the mixtures. The pH of the mixture containing 0.125 g, 0.250 g, 0.375 g or 0.620 g resulted in the pH increasing from 8 to 11.64, 11.63, 11.60 or 11.75 after 30 min respectively. After the addition of $Al(OH)_3$, the pH of all mixtures decreased to 10.66, 10.87, 10.87 or 10.48 for mixture containing 0.125 g, 0.250 g, 0.375 g or 0.620 g respectively. This could be attributed to the formation of ettringite which produced protons according to Equation 7.2. The EC of the mixtures followed the same trend as the pH.

During treatment of 500 mL of Matla mine water with Matla coal FA (83 g), different amounts of lime and 0.52 g of $Al(OH)_3$ using an overhead stirrer, aliquot samples were collected after every 30 min as outlined in section 3.8.1.1d. The samples were filtered through a 0.45 µm filter paper and analysed using ICP-OES and IC. Results obtained from the analysis of the product water are shown in Figure 7.1.6.

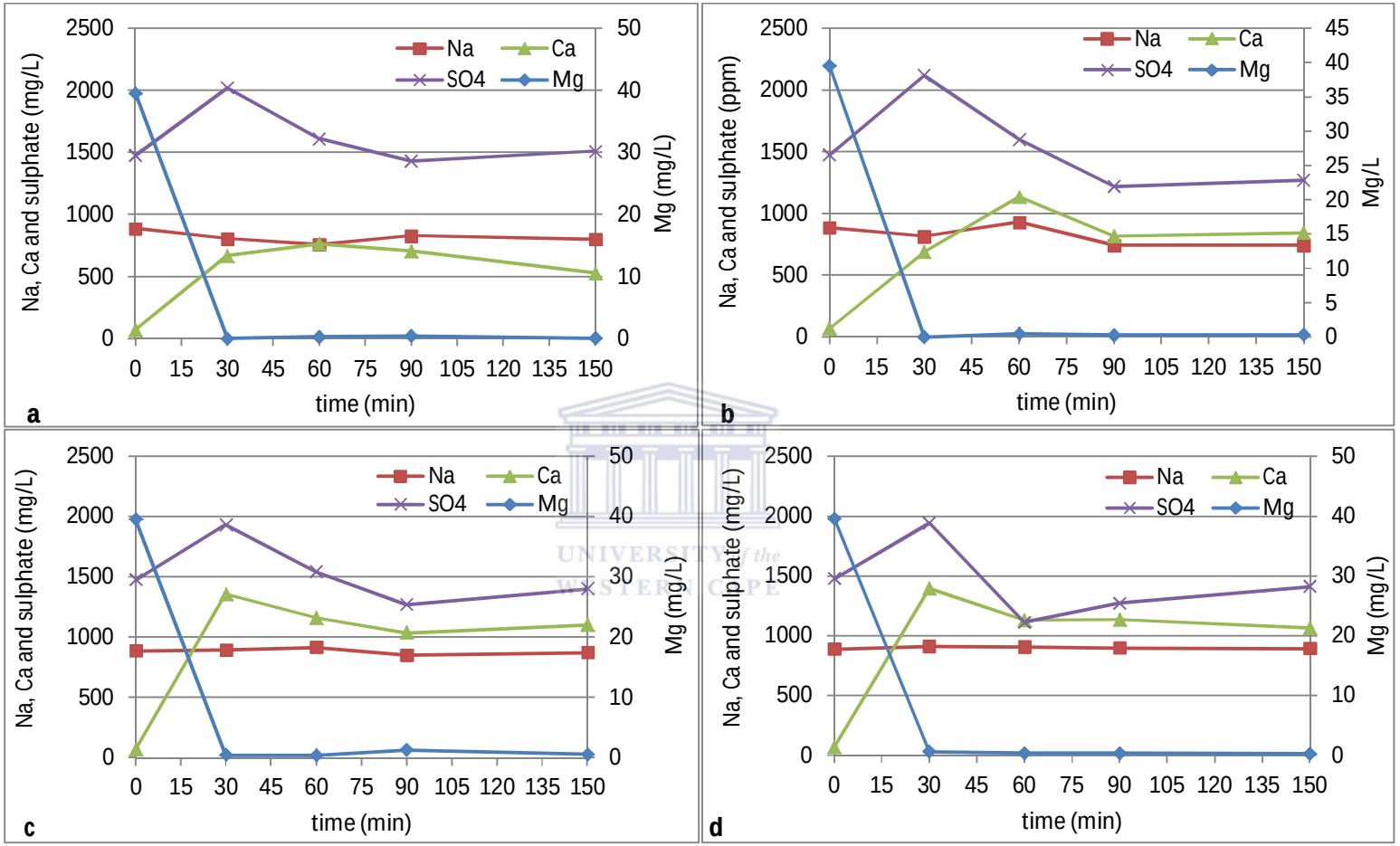

Figure 7.1.6: Na, Ca Mg and sulphate concentrations during Matla mine water (500 mL) treatment with 83 g of Matla coal FA, different amounts of lime (0.125 g (a), 0.250 g (b), 0.375 g (c) and 0.620 g of lime (d)) and 0.52 g of $Al(OH)_3$ using an overhead stirrer.

The results in Figure 7.1.6 show that the Na concentration remained constant during treatment of Matla mine water with Matla coal FA and various amounts of lime. About 100 % of Mg was removed in the first 30 min. The sulphate and Ca ions concentration initially increased in the mine water and then decreased slightly after addition of 0.52 g of $Al(OH)_3$. This correlates well with the decrease in EC when $Al(OH)_3$ was added in Figure 7.1.5. The decrease in EC, sulphate and Ca concentration could be due to the formation of ettringite according to Equation 7.2. As more lime was added to the mixture, more sulphate ions were removed from Matla mine water. Mixtures containing 0.125 g, 0.250 g, 0.375 g and 0.620 g of lime in addition to 83 g of Matla coal FA and 0.52 g of $Al(OH)_3$ resulted in the sulphate concentration decreasing to 1430 mg/L, 1220 mg/L, 1270 mg/L and 1110 mg/L respectively in the product water.

The ettringite formation reaction can reach dynamic equilibrium. The position of the equilibrium depends on the concentrations of the reactants (Ca, sulphate ions, $Al(OH)_3$ and water) and the products (ettringite and H^+ protons). All other reactants were constant and the pH was maintained around 10.80 for all the mixtures. It implied that as more Ca was added (by adding more lime), it shifted the equilibrium reaction to the right according to Le Chatelier's principle and resulted in more ettringite formation. Hence more sulphate ions were removed from Matla mine water when more lime was added.

The expected amount of sulphate to be removed when 0.52 g of $Al(OH)_3$ was added was 1922 mg/L. After addition of 0.52 g of $Al(OH)_3$, it was expected that the concentration of sulphate ions in the treated water should have been less than 100 mg/L. The sulphate concentration in the treated water was greater than expected. This can be attributed to the fact that ettringite formation reaction released protons and the final pH of all the mixtures was less than 11.5, which was below the optimum pH for sulphate removal as ettringite. Therefore the amount of ettringite that formed was not as expected after adding 0.52 g of $Al(OH)_3$.

Matla mine water was treated with 0.620 g of lime and 0.52 g of $Al(OH)_3$ (without adding Matla coal FA) using an overhead stirrer as outlined in section 3.8.1.1d. The pH, EC and temperature were measured after 15 min and the results are shown in Figure 7.1.7.

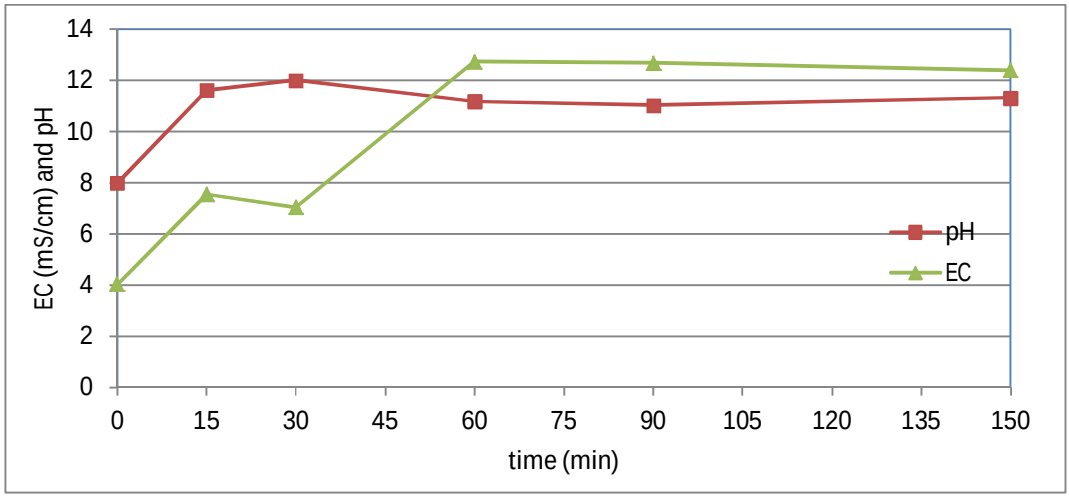

Figure 7.1.7: pH and EC profile during treatment of Matla mine water (500 mL) with 0.620 g of lime and 0.52 g of $Al(OH)_3$.

Treatment of Matla mine water with 0.620 g of lime only showed that the pH of the mixture was greater than 11.5 after 15 min as shown in Figure 7.1.7. $Al(OH)_3$ (0.52 g) was then added after 30 min. After addition of $Al(OH)_3$ there was a slight decrease in pH. The EC slightly deceased for the first 15 after and increased sharply after the addition of $Al(OH)_3$ between 30 min and 60 min. The slight decrease in pH could be attributed to the formation of ettringite (Equation 7.2).

During treatment of Matla mine water (500 mL) with 0.620 g of lime and 0.52 g of $Al(OH)_3$ only using an overhead stirrer, aliquot samples were collected, filtered and analysed using ICP-OES and IC. The results that were obtained are shown in Figure 7.1.8.

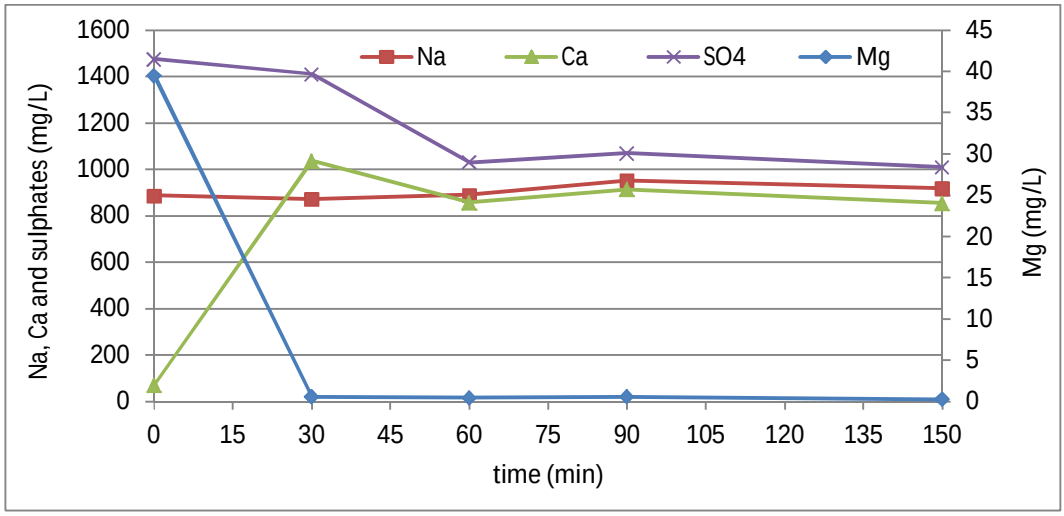

Fig 7.1.8: Na, Ca, Mg and sulphate concentrations during Matla mine water (500 mL) treatment with 0.620 g of lime and 0.52 g of lime.

The results in Figure 7.1.8 show that Ca ions initially leached into the water. This was because of the dissolution of CaO from lime causing the pH increase that was observed in Figure 7.1.7. After the addition of $Al(OH)_3$, the Ca concentration decreased slightly. This was because of the formation of ettringite (Equation 7.2). The concentration of Mg decreased by almost 100 % in first 30 min and this is attributed to the formation of $Mg(OH)_2$ at pH greater than 11. Again the concentration of Na remained unchanged. The concentration of sulphate ions decreased from 1475 mg/L to 1010 mg/L after mixing mine water with lime and $Al(OH)_3$. This concentration was still above the recommended limit for potable water.

From the results of the bench scale experiments (Figure 7.1.7 and 7.1.8) the highest sulphate removal was noted in the case where 0.620 g of lime and 0.52 g of $Al(OH)_3$ only was used to treat Matla mine water (500 mL) without Matla coal FA addition. This was because there were no sulphate ions that initially leached into the water from Matla coal FA. In experiments (Figure 7.1.6), where a combination of lime and Matla coal FA was used, sulphate ions initially leached into the water from Matla coal FA and then started precipitating after addition of $Al(OH)_3$, through ettringite formation according to Equation 7.2.

During treatment of Matla mine water (500 mL) with 83 g of Matla coal FA, 0.52 g of $Al(OH)_3$ and different amounts of lime, the amount of sulphate ions removed was not as expected. An excess number of mols (6.67×10^{-3} mols) of $Al(OH)_3$ was added to remove 1922 mg/L of sulphate ions from 500 mL of Matla mine water as ettringite according to Equation 7.2. The actual sulphate ion concentration in Matla mine water was 1475 mg/L. During treatment of 500 mL of Matla mine water with 83 g of Matla coal FA and different amounts of lime, the sulphate concentration increased to about 2000 mg/L as shown in Figure 7.1.6. After addition of 0.52 g of $Al(OH)_3$ the sulphate concentration was expected to decrease by 1922 mg/L to 78 mg/L assuming all the $Al(OH)_3$ added had reacted with sulphate ions to form ettringite according to Equation 7.2. The lower amount of sulphate ions actually removed than expected could be attributed to the fact that the overhead stirring technique could not speed up the reaction of the formation of ettringite. This could have resulted in some of the $Al(OH)_3$ remaining unreacted. This prompted a repeat of the treatment of Matla mine water (500 mL) with 0.125 g of lime and 0.52 g of $Al(OH)_3$ at 80 L pilot scale. This was done by optimizing the settings of the jet loop reactor to speed up the removal of sulphate ions as ettringite as explained in section 3.8.1.2

7.1.2. OPTIMIZING THE SETTINGS OF JET LOOP REACTOR

From the bench scale experiments it was discovered that a combination of 0.125 g of lime and 83 g of Matla coal FA could increase the pH of 500 mL of Matla mine water to greater than 11.5. The same experiments (using the same proportions of lime, coal FA and mine water) were repeated using a jet loop reactor at 80 L capacity. The mixing techniques inside the jet loop reactor were either a combination of cavitation and impingement or cavitation only as outlined in section 3.8.

7.1.2.1. Optimization of cavitation and impingement mixing

Matla mine water (80 L) was treated using 13 kg of Matla coal FA and 200 g of lime for 30 min using a jet loop reactor, varying the jet orifice sizes from 8, 10 and 12 mm as outlined in section 3.8.1.2. After 30 min, 83.2 g of $Al(OH)_3$ was added and the mixing

continued. The pH, EC and temperature were measured after every 15 min and the results obtained are shown in Figure 7.1.9.

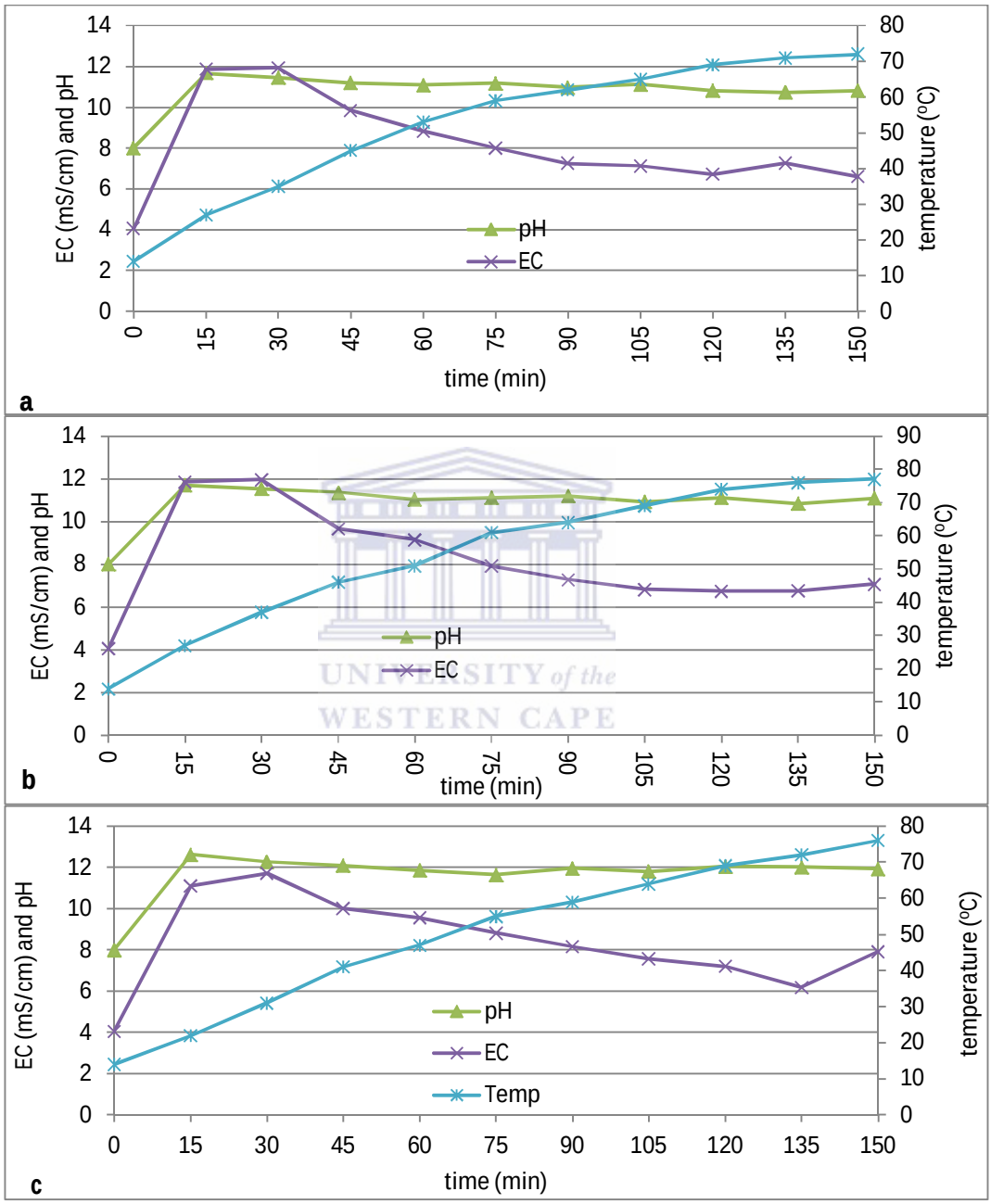

Figure 7.1.9: pH, EC and temperature profiles during treatment of 80 L of Matla mine water with 13 kg of Matla coal FA, 200 g of lime and 83.2 g of $Al(OH)_3$ in a jet loop reactor with different jet sizes (8 mm (a), 10 mm (b) and 12 mm (c)).

The results obtained after mixing Matla mine water (80 L) with 13 kg of Matla coal FA and 200 g lime for 30 min using a jet loop reactor with jet sizes 8, 10 or 12 mm showed that pH increased to 11.46, 11.53 and 12.27 respectively as shown in Figure 7.1.9. There was a slight increase in pH when the jet sizes were increased from 8 mm to 12 mm. The increase in pH was because of the dissolution of CaO in Matla coal FA and lime (Equation 7.1), so it means that the increase in jet sizes of the jet loop reactor did not result in a major increase in the amount of CaO that dissolved from Matla coal FA and lime. After addition of 83.2 g of $Al(OH)_3$ to the mixture at 30 min, the pH started to decrease. This could be because of the precipitation of ettringite (Equation 7.2). The EC followed the same trend as the pH, that is; it increased sharply in first the 30 min of mixing Matla mine water with Matla coal FA and 200 g lime and then decreased after addition of 83.2 g of $Al(OH)_3$ as shown in Figure 7.1.9. The temperature of the mixture increased gradually in the jet loop reactor during treatment of Matla mine water with Matla coal FA, lime and $Al(OH)_3$ from about 14 ^oC to about 70 ^oC as shown in Figure 7.1.9. This was due to the hydrodynamic cavitation mixing, which caused the temperature to increase (Cobley and Mason, 2010).

During treatment of Matla mine water (80 L) with 13 kg of Matla coal FA and 200 g of lime and 83.2 g of $Al(OH)_3$ using a jet reactor with various jet sizes (8, 10 and 12 mm), aliquot samples were collected, filtered and analysed using ICP-OES and IC as explained in section 3.8.1.2. The results of the composition of the water recovered are shown in Figure 7.1.10.

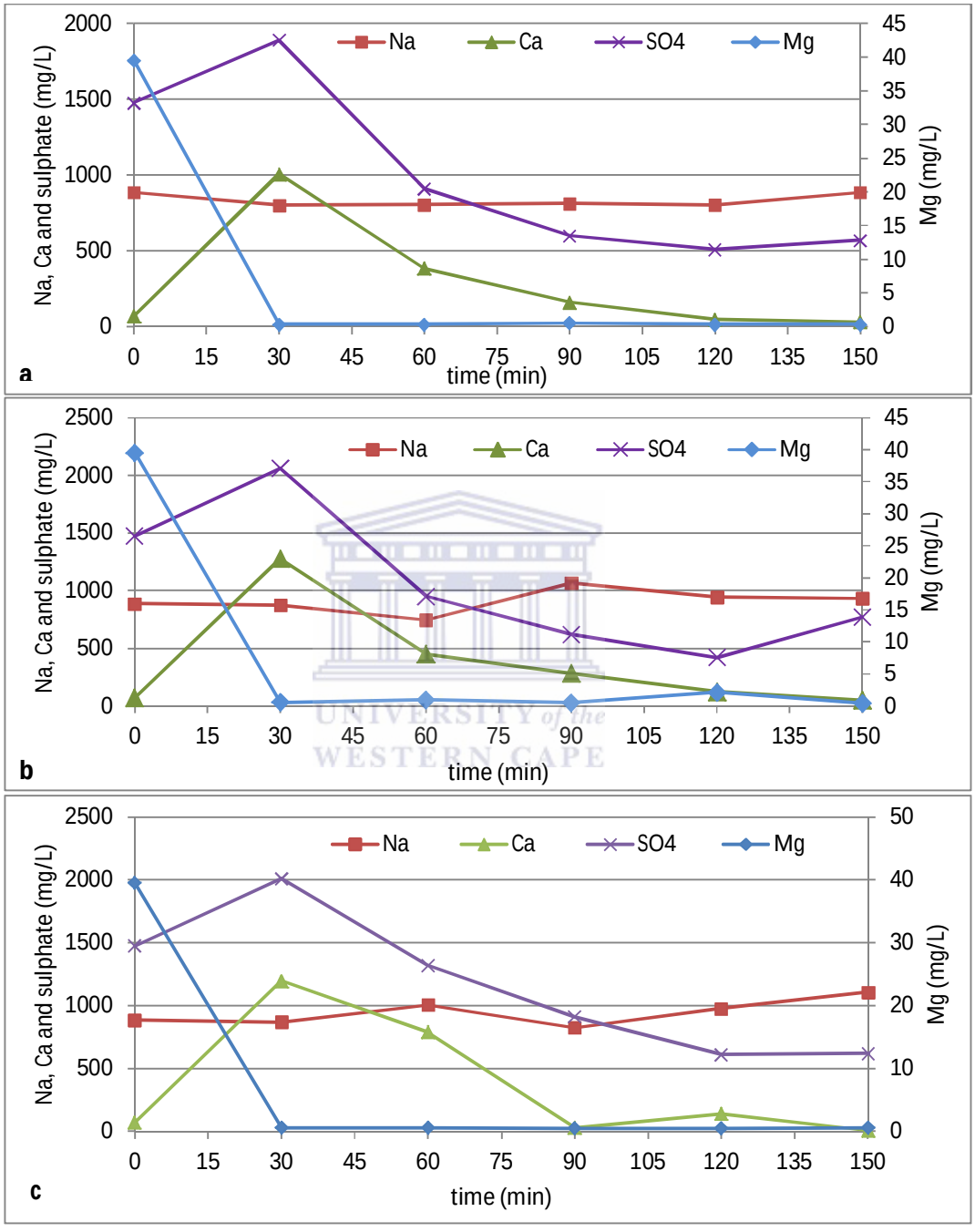

Figure 7.1.10: Na, Ca and sulphate concentrations during treatment of Matla mine water (80 L) with 13 kg of Matla coal FA, 200 g of lime and 83.2 g of $Al(OH)_3$ in a jet loop reactor with different jet sizes (8 mm (a), 10 mm (b) and 12 mm (c)).

As shown in Figure 7.1.10, there was no major difference in the jet reactor with different jet sizes. The Na concentration remained constant implying that there was no mineral phase that could precipitate and remove Na from the solution. This agreed well with modelling results obtained using Act2 program of the GWB software. The modelling results predicted that no Na containing mineral phase can form when FA was mixed with Matla mine water at any pH or Ca concentration (Figure 5.1.2a). Magnesium concentration decreased by almost 100 % after the first 15 min. Magnesium is known to be precipitated in the form of brucite, $Mg(OH)_2$ at pH greater than 10 (Madzivire, 2010). This also agreed well with modelling results obtained using Act2 program of the GWB software (Figure 5.1.1b). The model predicted that brucite would start forming at pH 10, when Matla mine water was mixed with FA.

Results obtained from the analysis of the water using ICP-OES and IC of the treated water after 30 min of treating 80 L of Matla mine water with 13 kg of Matla coal FA and 200 g of lime have shown that the Ca and sulphate concentration initially increased in the treated water as shown in Figure 7.1.10. The sulphate concentration increased from 1475 mg/L to about 2000 mg/L, while that of Ca increased from 70 mg/L to about 1100 mg/L. More Ca ions leached into the mine water compared to when overhead stirring was used to mix similar combination of Matla mine water, Matla coal FA, lime and $Al(OH)_3$ as shown in Figure 7.1.6a. This means that the Ca and sulphate ions leached from the Matla coal FA due to the dissolution of CaO and gypsum into the water. The dissolution of CaO resulted in the pH increase observed in Figure 7.1.9. The increase in the concentration of Ca and sulphate concentration resulted in the increase in EC in the first 30 min of treatment of mine water (Figure 7.1.9). After the addition of 83.2 g of $Al(OH)_3$ to the mixture the sulphate concentration and the Ca concentration decreased as shown in Figure 7.1.10. This was because of the formation of ettringite (Equation 7.2).

The sulphate concentration decreased from about 2000 mg/L to 400-500 mg/L after addition of 83.2 g of $Al(OH)_3$ to the mixture containing 13 kg of Matla coal FA and 200 g lime and mixing for 120 min in a jet loop reactor. The sulphate concentration was now within target water quality range (TWQR) set for drinking water (DWAF, 1996, WHO, 2011). The Ca

concentration decreased from about 1100 mg/L to about 120 mg/L. The decrease in the sulphate and Ca concentration correlated well with the decrease in the EC (Figure 7.1.9).

After the addition of 83.2 g of $Al(OH)_3$, the sulphate concentration decreased by about 1500 mg/L. The sulphate concentration was expected to decrease by 1922 mg/L. This was because 83.2 g of $Al(OH)_3$ was equivalent to 0.013 mol/L of Al ions added to the mixture. This amount of $Al(OH)_3$ was expected to precipitate out about 0.02 mol/L of sulphate ions according to the ettringite formation reaction (Equation 7.2), which was equivalent to 1922 mg/L of sulphate ions. After 120 min of mixing 13 kg of Matla coal FA, 200 g of lime and 83.2 g of $Al(OH)_3$, the concentration of Ca^{2+}, SO_4^{2-}, Al^{3+} and OH^- that remained in solution were such that the solution had reached equilibrium with respect to ettringite as shown in Table 7.1.1.

Table 7.1.1: Ionic product (IP) of ettringite calculated for aliquot solutions collected after 120 min of mixing 13 kg of Matla FA, 200 g of lime, 83.2 g of $Al(OH)_3$ with 80 L of Matla mine water in a jet loop reactor with different jet sizes.

	8 mm		**10 mm**		**12 mm**	
	mg/L	mol/L	mg/L	mol/L	mg/L	mol/L
Ca	50.11	1.25×10^{-3}	124	3.10×10^{-3}	137	3.43×10^{-3}
Al	2.28	8.44×10^{-5}	1.74	6.44×10^{-5}	1.38	5.11×10^{-5}
SO_4^{2-}	510	5.31×10^{-3}	420	4.37×10^{-3}	430	4.47×10^{-3}
OH^-		6.61×10^{-3}		1.29×10^{-3}		1.07×10^{-2}
IP		7.86×10^{-42}		8.52×10^{-43}		4.95×10^{-39}

The equilibrium was attained because the ionic product (IP) of ettringite was equal to the solubility product (Ksp) of ettringite. The Ksp of ettringite is between 10^{-36} and 10^{-45} (Hampson and Bailey, 1982; Warren and Reardon, 1994). Therefore, the amount of sulphate ions removed was not as expected. This can be attributed to the fact that when Matla mine water was mixed with mine water not enough CaO dissolved into the mine water.

The kinetics of the removal of sulphate ions from mine water through the formation of ettringite was enhanced by mixing using a jet reactor (Figure 7.1.10) compared to using an overhead stirrer (Figure 7.1.6a). In the jet loop reactor the reaction occurred faster due to

the efficient mixing caused by hydrodynamic cavitation inside the reactor. Cavitation enhances the rate of reaction because of the intense micro mixing of the reactants (Mason 2007). This shows that kinetics of the removal of sulphate ions as ettringite played an important role in order to achieve the required removal.

During treatment of Matla mine water with Matla coal FA, 200 g of lime and $Al(OH)_3$, the solid residues produced were collected and separated from the product water after 150 min reaction time. The solid residues were dried and then analysed using XRD as explained in section 3.8.1.2. The XRD spectrum of the solid residues was compared to the spectrum of the reactants (Matla coal FA, lime and $Al(OH)_3$) and the results are shown in Figure 7.1.11.

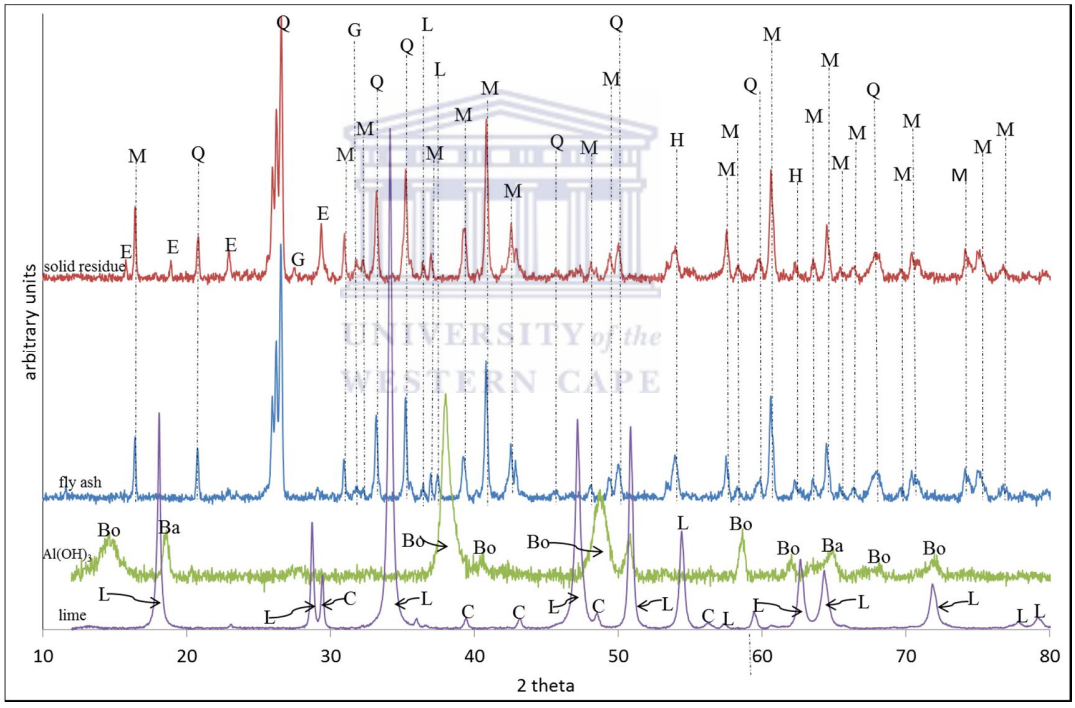

Figure 7.1.11: The XRD spectra of Matla coal FA, $Al(OH)_3$, lime and the solid residues collected after 120 min of treatment of Matla mine water (80 L) with 13 kg of Matla coal FA, 200 g of lime and 83.2 g of $Al(OH)_3$ in a jet loop rector (E-ettringite, L-CaO, M-mullite, G-gypsum, Bo-boehmite, Ba-bayarite, C-calcium carbonate, H-hematite and Q-quartz).

The spectrum of the solid residues recovered after treating Matla mine water showed the disappearance of the CaO peaks in Matla coal FA and lime spectra as well as the boehmite

(AlOOH) and bayerite ($Al_2O_3.3H_2O$) peaks in $Al(OH)_3$ spectrum. New ettringite peaks appeared in the spectrum of the solid residue collected after 150 min as shown in Figure 7.1.11. The appearance of ettringite peaks in the XRD spectrum of the solid residue collected after treatment of Matla mine water proved that indeed sulphate and Ca concentration decreased in the product water due to formation of ettringite crystals according to Equation 7.2.

During treatment of Matla mine water (80 L) with 13 kg of Matla coal FA, 200 g of lime and 83.2 g of $Al(OH)_3$ in jet reactor with jet sizes of 12 mm, the solid residues produced were collected after 150 min reaction time. The solid residues were then analysed using XRF as explained in section 3.8.1.2. The XRF results of the solid residues were compared to the XRF results of the Matla coal FA and the results are shown in Table 7.1.2.

Table 7.1.2: Comparison of the elemental composition of Matla coal FA and the solid residues produced after treatment of Matla mine water (80 L) with 13 kg of Matla coal FA, 200 g of lime and 83.2 g of $Al(OH)_3$ in a jet loop reactor for 150 min.

% oxide	Matla coal FA ± stdev	150 min solid residue ± stdev
SiO_2	48.27 ± 0.04	44.02 ± 0.04
Al_2O_3	30.89 ± 0.22	31.39 ± 0.18
CaO	6.71 ± 0.08	9.22 ± 0.06
Fe_2O_3	2.81 ± 0.03	2.80 ± 0.01
MgO	2.12 ± 0.04	2.52 ± 0.05
TiO_2	1.26 ± 0.02	1.24 ± 0.01
P_2O_5	0.89 ± 0.01	1.02 ± 0.01
K_2O	0.84 ± 0.02	0.80 ± 0.01
Na_2O	0.55 ± 0.01	0.54 ± 0.01
SO_3	0.19 ± 0.002	0.35 ± 0.003
MnO	0.02 ± 0.0004	0.02 ± 0.001
Loss on ignition	5.24 ± 0	5.38 ± 0
Sum	99.79 ± 0.07	99.23 ± 0.60

stdev stands for standard deviation for 3 replicate analysis.

From the XRF results obtained; the percentage of SiO_2 in the solid residues decreased as compared to that in Matla coal FA. The percentage of Al_2O_3, CaO, SO_3, MnO and MgO in the solid residue was more than in Matla coal FA. Percentage oxides of Fe, Ti, K and Na remained the same as in Matla coal FA as shown in Table 7.1.2. The percentage of Al_2O_3 and CaO increased because of the addition of lime and $Al(OH)_3$ to the reaction mixture. This

addition could have diluted the SiO_2 content in Matla coal FA, thereby reducing the percentage of SiO_2 detected in the solid residue. This was because there was no Si containing chemical added to the reaction mixture. Also the SiO_2 content in the solid residue could have decreased due to the leaching of Si from Matla coal FA into the mine water. The amount of Fe_2O_3 and TiO_2 remained constant because, there was little or no Fe, Ti and P detected in the mine water, while the content of Na_2O and K_2O in the solid residues remained almost constant because the K and Na concentration remained unchanged in Matla mine water during treatment with Matla coal FA, lime and $Al(OH)_3$ in the jet reactor with jet sizes of diameter 12 mm. This correlated well with results shown in Figure 7.1.10d that showed that the concentration of Na remained unchanged. The content of MgO, MnO and SO_3 increased in the solid residue because the Mg and sulphate concentration decreased in the mine water during treatment with Matla coal FA, lime and $Al(OH)_3$ as shown in Figure 7.1.10d.

All these experiments were done using cavitation and impingement mixing in a jet loop reactor. This resulted in the sulphate concentration decreasing from 1475 mg/L to less than 500 mg/L when Matla mine (80 L) was treated with 13 kg of Matla coal FA, 200 g of lime and 83.2 g of $Al(OH)_3$ using a combination of cavitation and impingement mixing inside the jet loop reactor. The following experiments were done in order to find out if cavitation or impingement mixing were responsible for the enhanced sulphate removal.

7.1.2.2. Cavitation mixing only

Matla mine water (80 L) was mixed with 13 kg of Matla coal FA, 200 g of lime and 83.2 g of $Al(OH)_3$ using a jet loop reactor. The jet sizes were set at 12 mm, but one side of the jet was blocked to stop impingement mixing as explained in section 3.8.1.2. This set of experiments was done to find if impingement was important in enhancing the treatment of Matla mine water using a jet loop reactor or whether cavitation only will suffice. The pH, EC and temperature trends, obtained when mine water was mixed using cavitation only inside the jet reactor, are shown in Figure 7.1.12.

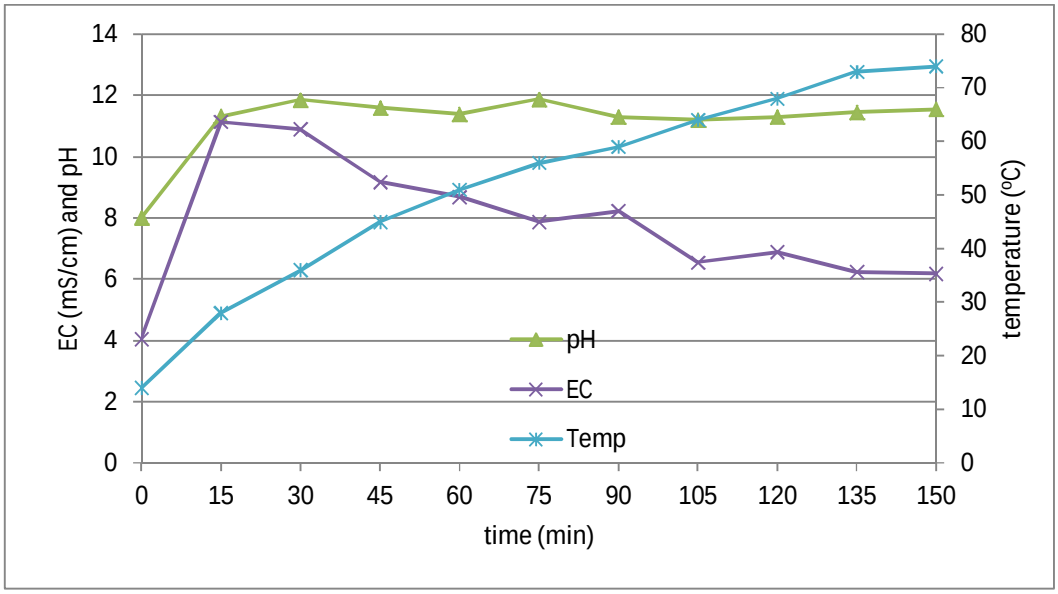

Figure 7.1.12: pH, EC and temperature profiles during treatment of 80 L of Matla mine water with 13 kg of FA, 200 g of lime and 83.2 g of $Al(OH)_3$ in a jet loop reactor with 12 mm jet size (one side of the jet was closed so that cavitation only mixing occurs inside the reactor).

The results obtained in Figure 7.1.12 show that the pH and EC increased to about 11.86 and 10.89 respectively after 30 min of cavitation mixing Matla mine water (80 L) with 13 kg of Matla coal FA and 83.2 g of lime in a jet loop rector. This was also the case when the mixing was carried out using a combination of impingement and cavitation with jet sizes set at 12 mm (Figure 7.1.9). It meant that cavitation only, without impingement can enhance the dissolution of CaO from coal FA and lime sufficiently and cause the pH to increase to the required value of about 11.5. Also from Figure 7.1.12, cavitation mixing of Matla mine water with Matla coal FA, lime and $Al(OH)_3$ using a jet reactor resulted in a gradual increase in temperature from 14 ^{o}C to 74 ^{o}C after 150 min. This temperature trend was also observed when the same mixture was mixed with cavitation and impingement (Figure 7.1.10). This meant that cavitation mixing caused the temperature increase of the mixture.

Matla mine water (80 L) was mixed with 13 kg of Matla coal FA, 200 g of lime and 83.2 g of $Al(OH)_3$ was treated in a jet loop reactor with jet sizes set at 12 mm (one side of the jet

blocked), as explained in section 3.8.1.2. Aliquot samples were collected after every 30 min, filtered and analysed suing ICP-OES and IC. The results obtained are shown in Figure 7.1.13.

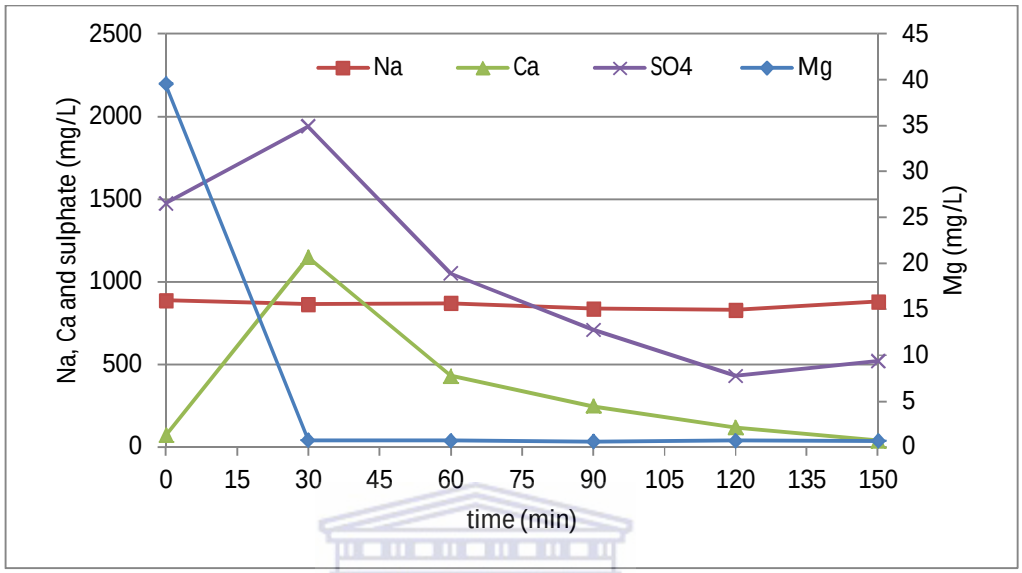

Figure 7.1.13: Na, Ca, Mg and sulphate concentrations during treatment of Matla mine water (80 L) with 13 kg of Matla coal FA, 200 g of lime and 83.2 g of $Al(OH)_3$ in a jet loop reactor with jet sizes 12 mm (one side of the jet was closed so that cavitation only mixing occurs inside the reactor).

The results shown in Figure 7.1.13, indicate that cavitation mixing resulted in the decrease of the sulphate from about 2000 mg/L to 430 mg/L at 120 min after addition of $Al(OH)_3$ at 30 min. This was within the TWQR for potable water set by WHO or DWAF (WHO, 2011; DWAF, 1996). The Mg concentration was decreased by almost 100 % after 30 min of treating Matla mine water with Matla coal FA and lime using cavitation only. No Na was removed from Matla mine water during treatment with Matla coal FA, lime and $Al(OH)_3$ using cavitation only. These trends are the same as when Matla mine water (80 L) was treated with 13 g of Matla coal FA, 200 g of lime and 83.2 g of $Al(OH)_3$ using a combination of cavitation and impingement. This means that cavitation only can achieve the same results obtained by a combination of cavitation and impingement (Figure 7.1.10c).

Treatment of Matla mine water (80 L) with 13 kg of Matla coal FA, 200 g of lime and 83.2 g of $Al(OH)_3$ in jet reactor has resulted in the sulphate concentration decreasing to less than

500 mg/L. The jet loop reactor showed better kinetics compared to an overhead stirrer. The differences with between a jet reactor and an overhead stirrer were:

i. mixing technique (impingement and/or hydrodynamic cavitation that occurred in the jet reactor) and;
ii. the increase in temperature that occurred during mixing using a jet reactor.

The following set of experiments aimed to determine if temperature enhanced or affected the kinetics of the removal of sulphate ions from Matla mine water when mixed with Matla coal, lime and $Al(OH)_3$.

7.1.2.3. Effect of temperature on the removal of sulphate ions

Matla mine water (500 mL) was mixed with Matla coal FA (83 g) and lime (0.125 g) using a magnetic stirrer at 20 ^oC. After 30 min of mixing, 0.52 g of $Al(OH)_3$ was added. These were the same proportions of Matla coal FA, lime and $Al(OH)_3$ that were used to remove the sulphate ions to less than 500 mg/L using a jet reactor (section 7.1.2). The reaction was carried on after adding $Al(OH)_3$ measuring pH and EC after every 15 min for 150 min as outlined in section 3.8.1.3. The above reaction was repeated at 30 ^oC, 40 ^oC, 50 ^oC, 60 ^oC, 70 ^oC and 80 ^oC. The samples were filtered through 0.45 µm and analysed using ICP-OES and IC. The results obtained are shown in Figure 7.1.14.

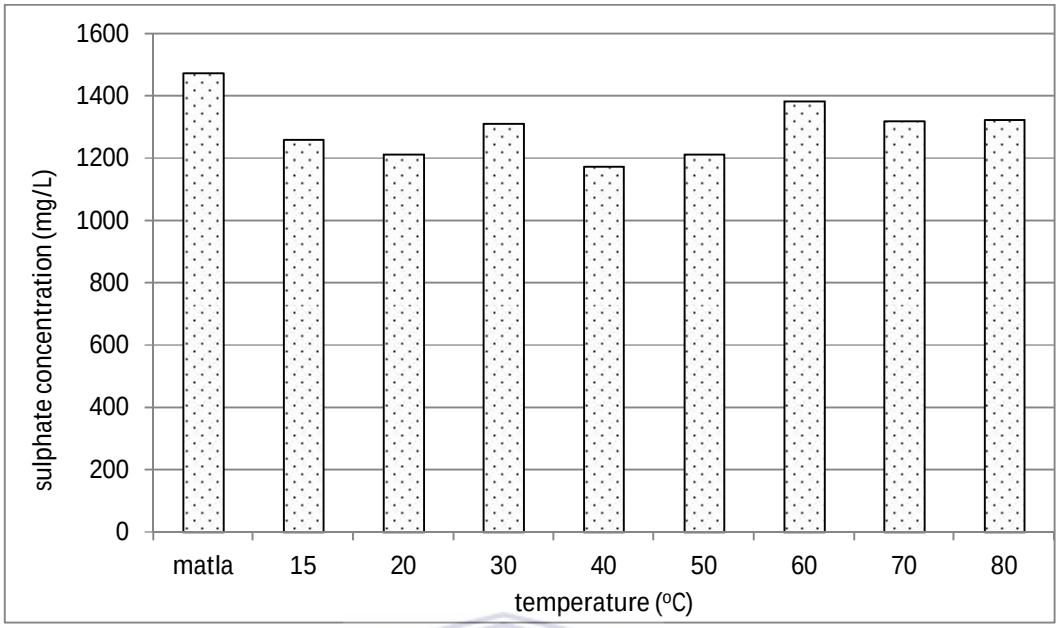

Figure 7.1.14: Effect of temperature on sulphate removal from Matla mine water.

The results in Figure 7.1.14 show that the sulphate ions were removed from 1475 mg/L to between 1100 mg/L to 1400 mg/L at various temperatures between 15 °C and 80 °C. Treatment of Matla mine water with Matla coal FA, lime and $Al(OH)_3$ at lower temperatures generally recorded lower sulphate ions in the treated water than levels observed at higher temperatures. According to Perkins and Palmer (1999), the solubility product of ettringite increases with increase in temperature according to the following relationship;

$$\log K_{sp} = \frac{-10689}{T} - 8.8673$$; where T is temperature in K.

These results showed that the removal of sulphate ions was slightly affected by temperature because the sulphate concentration slightly increased in the product water produced at higher temperatures. The results indicated that removal of sulphate ions during mixing of Matla mine water with Matla coal FA, lime and $Al(OH)_3$ in the jet reactor was mainly caused by hydrodynamic cavitation. Temperature did not enhance the sulphate removal achieved during cavitation. It is noteworthy that no significant amount of sulphate ions could be removed by overhead mixing of Matla mine water with Matla coal FA, lime

and $Al(OH)_3$. Whereas when the mixing of Matla mine water, Matla coal FA, lime and $Al(OH)_3$ was carried out using impingement and hydrodynamic cavitation or hydrodynamic cavitation only, the sulphate concentration in the treated water decreased significantly. This shows the importance of adequate mixing of mine water, coal FA, lime and $Al(OH)_3$ to achieve the desired sulphate removal as ettringite. These results indicated that it may be necessary to redesign the jet loop reactor to incorporate heat exchanger in order to absorb the temperature and use the energy produced for other purposes.

7.1.3. SUMMARY OF RESULTS

The pH and percentage removal of Mg, Na, Ca and sulphate ions during treatment of Matla mine water with different combination of chemicals is shown in Figure 7.1.15.

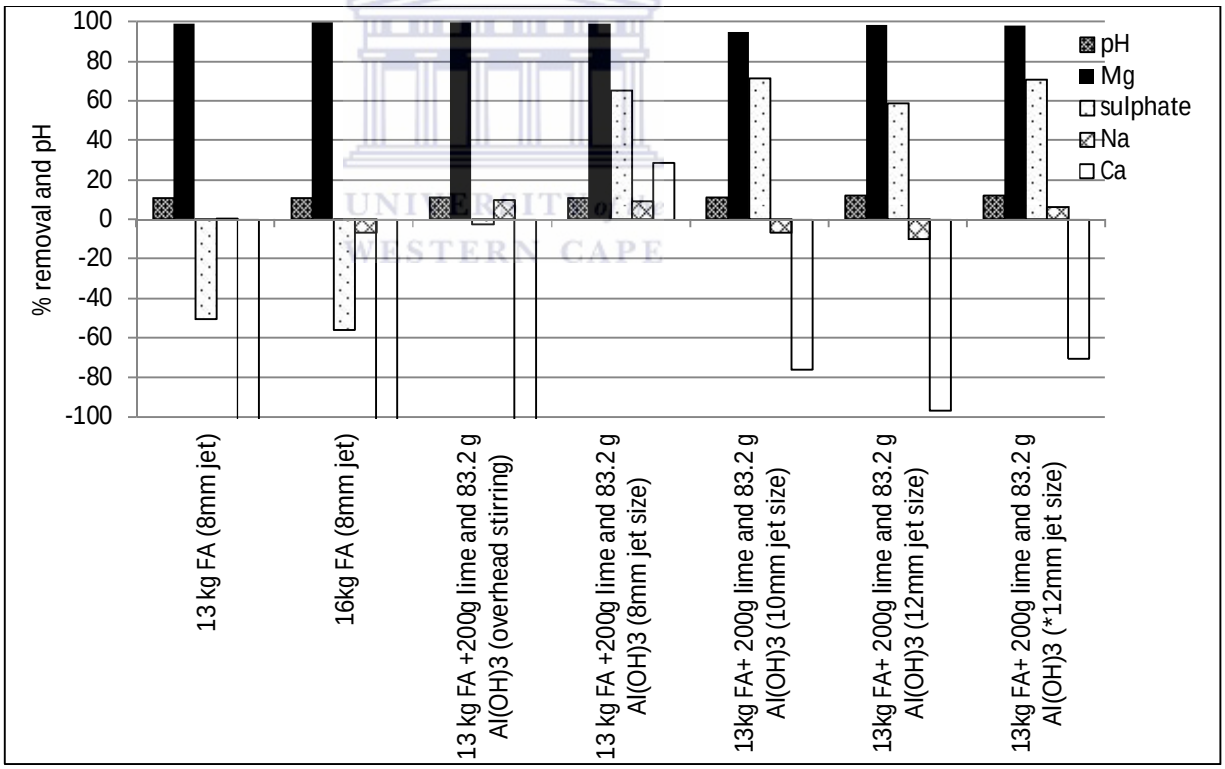

Figure 7.1.15: The pH and percentage removal of Mg, Ca, Na, sulphate ions during treatment of Matla mine water with various combinations of chemicals (* shows that cavitation mixing only occurred in the jet loop reactor).

Results in Figure 7.1.15 show that treatment of Matla mine water with coal FA (8 or 13 kg), lime (100, 150 or 200 g) and/or 83.2 g of $Al(OH)_3$ resulted in about 99 % removal of Mg ions only. The Act2 program of the GWB software (Figure 5.1.1b) showed that if the pH of Matla mine was increased to 10 and above $Mg(OH)_2$ precipitation would occur. This means that the Mg ions in Matla mine water were removed as $Mg(OH)_2$ when the pH was increased to greater than 10. Na remained almost constant during treatment of Matla mine water with Matla coal FA, lime and $Al(OH)_3$. The Act2 program showed that no Na containing mineral can form when Matla mine water was treated with Matla coal FA (Figure 5.1.2b). Ions such as Ca and sulphates remained unchanged or leached (negative % removal) into the mine water treated with Matla coal FA only as shown in Figure 7.1.15. This agreed with the modelling results obtained using Act2 program of the GWB which predicted that sulphate ions would not be removed when it was treated with coal FA.

Treatment of Matla mine water with coal FA (13 kg or 16 kg) has shown that pH of the mixture could be taken up to about 10.5 after 120 min of mixing in a jet reactor by cavitation and impingement. This was due to the dissolution of the CaO fraction in Matla coal FA. This was not in the pH range of 11.5 to 12.5 that was required for optimum sulphate precipitation as ettringite. Addition of 200 g of lime to the mixture of Matla mine water (80 L) and Matla coal FA (13 kg) was found to increase the pH to greater than 11.5. After mixing Matla mine water (80 L) with Matla coal FA (13 kg) and lime (200 g), the sulphate and Ca leached into the mine water from coal FA and lime. This was due to the dissolution of CaO (in coal FA and lime) and gypsum minerals (in coal FA). Addition of $Al(OH)_3$ to the mixture of Matla mine water, Matla coal FA and lime in a jet loop reactor resulted in the concentration of sulphate and Ca decreasing due to the precipitation of ettringite. The sulphate and Ca concentration decreased to about 450 mg/L and 40 mg/L respectively. This was about 70 % sulphate removal and 40 % Ca removal of the original concentration in Matla mine water. When the same mixtures were mixed using an overhead stirrer, the 19 % of sulphate ions were removed from mine water as shown in Figure 7.1.15. This showed that jet loop mixing enhanced the removal of sulphate ions compared to overhead stirring. The increased sulphate removal in a jet loop reactor was due to the increased rate of formation of ettringite caused by the hydrodynamic cavitation mixing

inside a jet loop reactor. Jet sizes of the jet reactor did not have a major effect on sulphate removal as shown in Figure 7.1.15. Treatment of Matla mine water with Matla coal FA, lime and $Al(OH)_3$ in a jet reactor with jet sizes 8, 10 and 12 mm resulted in 65 %, 71 % and 59 % sulphate removal respectively as shown in Figure 7.1.15.

Cavitation mixing technique on its own resulted in a slight increase in sulphate removal from Matla mine water. Treatment of Matla mine water with Matla coal FA, lime and $Al(OH)_3$ inside a jet reactor by a combination of cavitation and impingement (jet sizes set at 12 mm) resulted in about 59 % sulphate removal. The percentage sulphate removal when Matla mine water was treated with Matla coal FA and lime and $Al(OH)_3$ inside a jet reactor by cavitation only (with jet sizes set at 12 mm) was about 71 %.

Mixing Matla mine water with Matla coal FA, lime and $Al(OH)_3$ in a jet reactor by a combination of cavitation and impingement or cavitation only resulted in a gradual increase in temperature of the mixture. The temperature increase was due to hydrodynamic cavitation that occurred inside the jet reactor. Temperature increase was shown to have no effect the removal of sulphate ions during treatment of Matla mine water with Matla coal FA, lime and $Al(OH)_3$. These findings have shown that Matla mine water can be successfully cleaned up in terms of the removal of Mg and sulphate ions at 80 L capacity pilot plant. The product water still has high a pH and Na concentration that would require reduction and removal respectively. The water can be polished using ion exchange to remove Na and pH can be reduced by carbonation using CO_2.

The composition of Matla mine water before and after treatment with the best combination of chemicals in a jet loop was compared to the required target water quality range (TQWR) for individual elements for potable water. The comparison is shown in Table 7.1.3.

Table 7.1.3: Composition of Matla mine water and the product water from the treatment of Matla mine water (80 L) with 13 kg of Matla coal FA, 200 g of lime and 83.2 g of $Al(OH)_3$ in a jet loop reactor for 120 min.

Parameter	Matla mine water	Product water	TWQR for potable water
pH	8 .00 ± 1.07	**11.08 ± 1.25**	6-9
EC (µS/cm)	**3371 ± 24**	**6740 ± 17**	0-700
sulphate	**1475.25 ± 2**	420 ± 15	200-500
Na	**956.05 ± 19.26**	**945.62 ± 31.05**	0-200 (100)
Ca	**70.35 ± 3.05**	**374.00 ± 7.61**	(0-32)
Mg	**39.54 ± 1.12**	2.13 ± 0.97	(0-30)
Cl	24.00 ± 1.84	25.01 ± 2.07	0-250 (100)
B	**14.93 ± 1.07**	0.66 ± 0.22	0-2.4
K	10.08 ± 0.92	19.09 ± 3.45	(0-50)
Hg	**2.43 ± 0.13**	**1.78 ± 0.45**	0-0.006 (0.001)
Sr	2.05 ± 0.06	15.71 ± 1.46	NA
Si	1.28 ± 0.33	7.02 ± 0.81	NA
Se	**1.12 ± 0.09**	nd	0-0.04 (0.02)
Zn	0.41 ± 0.12	nd	0-0.5 (3)
Ba	0.20 ± 0.0009	0.45 ±0.09	0-0.7
Cu	0.19 ± 0.0073	0.23 ± 0.0012	0-2 (1)
Fe	0.059 ± 0.0017	nd	0-0.3 (0.1)
Al	0.056 ± 0.0013	0.04 ± 0.0013	0-0.2 (0.15)
Ni	0.023 ±0.0012	nd	0-0.07
Be	**0.017 ± 0.0035**	0.0074 ± 0.0012	0.012
Mn	0.0094 ±1.12 x 10^{-4}	0.0013 ± 0.00014	0-0.1 (0.05)
Cd	**0.005 ± 1.98 x 10^{-4}**	nd	0-0.003 (0-0.005)
As	0.0014 ± 3.01x 10^{-5}	0.0016 ± 0.00037	0-0.01
Mo	nd	0.065 ± 0.0071	0-0.07
Cr	nd	0.019 ± 0.0087	0-0.05
V	nd	0.0081 ± 0.00045	0-0.01
Co	nd	0.073 ± 0.0013	NA
Pb	nd	nd	0-0.01

Note: values in brackets obtained from Department of Water Affairs of South Africa if the values are different from those indicated by World Health Organization (WHO, 2011; DWAF, 1996). NA and nd stand for "not applicable" and "not detected" respectively. TWQR stands for target water quality target.

Results in Table 7.1.3 show that raw Matla mine water had nine parameters (EC, Na, Ca, Mg, B, Hg, Se, Cd and sulphate ions) that were not within the required TWQR range for potable water set by WHO and DWAF (DWAF, 1996; WHO, 2011). When Matla mine water was treated with 13 kg of Matla coal FA, 200 g of lime and 83.2 g of $Al(OH)_3$, the product water

had six parameters (pH, EC, Na, Ca, Hg and Mo) that were above the TWQR for potable water. The product water requires polishing to regulate pH and remove Na, Ca, Hg and Mo from the water before it can be used for domestic purposes. This can be achieved by polishing the water using strong cation and weak anion resin to remove the cation and anions and in the process regulating the pH.

7.1.4. CONCLUSION

Treatment of Matla mine water that contained high concentration of Na and sulphate ions as well as B, Hg, Se and Cd with Matla coal FA only resulted in the product water containing more sulphate ions than that was originally in the mine water. This was because of leaching of sulphate ions from Matla coal FA. Good quality water was produced when Matla mine water was treated with Matla coal FA, lime and $Al(OH)_3$. During treatment of Matla mine water with Matla coal FA, lime and $Al(OH)_3$, sulphate ions were removed as ettringite. The removal of sulphate ions was dependent on the type of mixing technique used. Hydrodynamic cavitation and/or impingement mixing of Matla mine water, Matla coal FA, lime and $Al(OH)_3$ has shown that sulphate ions were removed from 1475 mg/L to 420 mg/L, which was within the TWQR for potable water. On the other hand when Matla mine was mixed with Matla coal FA, lime and $Al(OH)_3$ using normal stirring, the sulphate ions could not be removed to within the TWQR for potable water. More sulphate ions were removed when Matla mine water, Matla coal FA, lime and $Al(OH)_3$ was treated in a jet loop reactor because hydrodynamic mixing that occurred in the jet loop reactor increased the kinetics of the removal of sulphate ions as ettringite. Although Matla coal FA contained radionuclides, they did not leach into Matla mine water during treatment of Matla mine water. Only small amount of Mo leached into the mine water from coal FA.

Treatment of Matla mine water with Matla coal FA, lime and $Al(OH)_3$ was carried out at 80 L capacity. This is a straightforward, one step process that requires only pH control. This meant that the process is capable of being up scaled to an industrial scale. If this process would be used to treat water at industrial scale, this would go a long way in achieving a cheap and sustainable solution to mine water treatment. This is because coal FA is a waste

material and usually produced close to coal mine. This reduces the costs of transporting the coal FA to the treatment facility. The cost evaluation of this treatment process fell outside the scope of the study.

7.2. TREATMENT OF RAND URANIUM MINE WATER

The optimum conditions obtained during treatment of Matla mine water with Matla coal FA, lime and $Al(OH)_3$ in a jet loop reactor were applied to treat Rand Uranium mine water. Rand Uranium mine water was acidic mine water and contained elevated concentration of Fe, Al, Mn, Mg, Ca and sulphate ions. It was also found to contain elevated concentration of radioactive elements. The full physicochemical characteristics are shown in Table 4.6.1 and Table 4.6.2. The jet orifice diameter sizes of the jet loop reactor were maintained at 12 mm. The mixing of the Rand Uranium mine water and the Matla coal FA (with or without addition of lime and $Al(OH)_3$) in a jet reactor was done using cavitation only.

Matla coal FA and lime contained about 6.71 % (Table 4.1.1) and 72.19 % (Table 4.4.1) of CaO respectively. The aluminium hydroxide used in the treatment of Rand Uranium mine water was 95 % pure and the elemental composition is shown in Table 4.3.1. During treatment of Rand Uranium mine water, various combinations of Matla coal FA, additional lime and $Al(OH)_3$ were investigated. The parameters investigated during treatment of Rand Uranium mine water in a jet loop were;

a. Effect of $Al(OH)_3$ only
b. Effect of the amount of Matla coal FA.
c. Effect of the amount of Matla coal FA and $Al(OH)_3$
d. Effect of the amount of lime and $Al(OH)_3$
e. Effect of the combination of Matla coal FA, lime and $Al(OH)_3$
f. Effect of jet reactor mixing followed by overhead stirring

It was observed that treatment of Matla mine water with Matla coal FA, lime and $Al(OH)_3$ resulted in the removal of sulphate ions to within the TWQR for potable water (WHO, 2011, DWAF, 1996). However it was not clear if $Al(OH)_3$, lime or Matla coal FA, could be effective in the removal of sulphate from the mine water on their own. If so, this could reduce the amount of substances needed to treat Rand Uranium mine water. The following two sections (7.2.1 and 7.2.2) presents the results obtained when Rand Uranium mine water was treated with $Al(OH)_3$ or Matla coal FA separately. This was done in order to find the effect of

these substances on the removal of potentially toxic and radioactive elements from Rand Uranium mine water. The composition of Rand Uranium mine water used in this study is shown in Table 4.6.1 and contained 2561 mg/L of sulphate ions.

7.2.1. EFFECT OF ALUMINIUM HYDROXIDE

Rand Uranium mine water (80 L) was treated with 86.58 g of $Al(OH)_3$ only in a jet loop reactor as outlined in section 3.8.2.1. The amount of $Al(OH)_3$ (86.58 g) was chosen based on the proportion added when Matla mine water was treated with Matla coal FA lime and $Al(OH)_3$ to precipitate sulphate ions as ettringite in section 7.1. The pH, EC and temperature were measured after every 15 min and the results are shown in Figure 7.2.1.

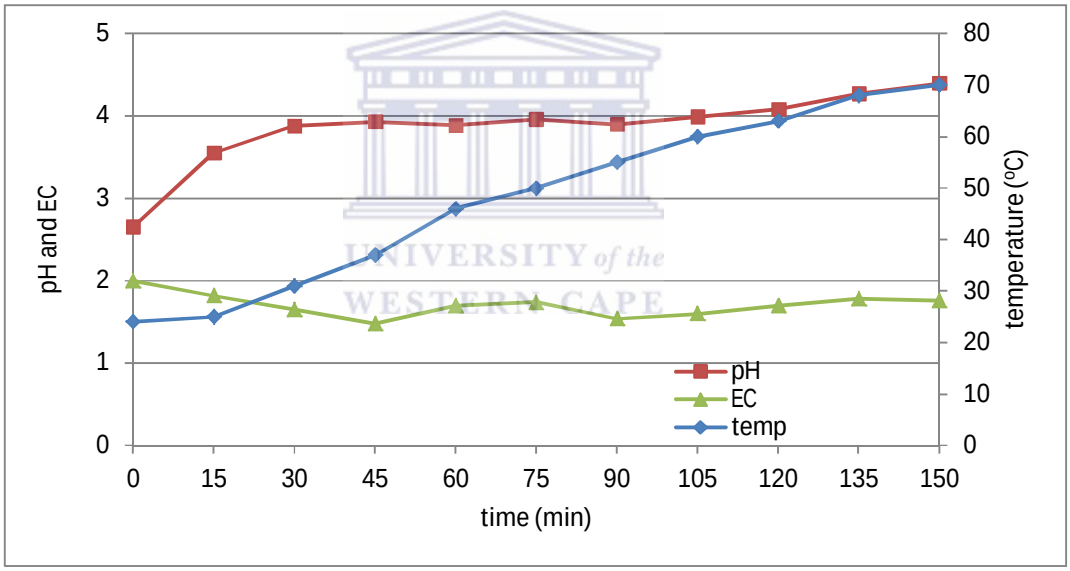

Figure 7.2.1: pH, EC (mS/cm) and temperature profile during treatment of 80 L of Rand Uranium mine water with 86.58 g of $Al(OH)_3$ using a jet loop reactor.

Results in Figure 7.2.1 showed that treatment of Rand Uranium mine water (80 L) with 86.58 g of $Al(OH)_3$ resulted in the pH increasing from 2.54 to only 3.88 after 30 min. The pH remained constant for about 75 min and then increased slightly to 4.40 at 150 min. The pH increased because $Al(OH)_3$ is amphoteric and acts as a base in acidic medium therefore

neutralizing the acidity of Rand Uranium mine water to some extent as shown in Equation 7.3-7.5.

$$Al(OH)_3 + H^+ \rightarrow Al(OH)_2^+ + H_2O \quad \text{.....7.3}$$

$$Al(OH)_2^+ + H^+ \rightarrow Al(OH)^{2+} + H_2O \quad \text{.....7.4}$$

$$Al(OH)^{2+} + H^+ \rightarrow Al^{3+} + H_2O \quad \text{.....7.5}$$

The EC decreased from 2 to 1.48 mS/cm after 45 min of treatment of Rand Uranium mine water in a jet loop reactor. From 45 min to 150 min the EC remained constant.

During treatment of Rand Uranium mine water (80 L) with 86.58 g of $Al(OH)_3$, samples were collected after every 30 min. The samples were filtered through a 0.45 µm filter paper and analysed for their elemental and ionic content using ICP-OES and IC. The results obtained for the major ions such as Fe, Al, Mg, Mn, Ca and sulphate ions are shown in Figure 7.2.2.

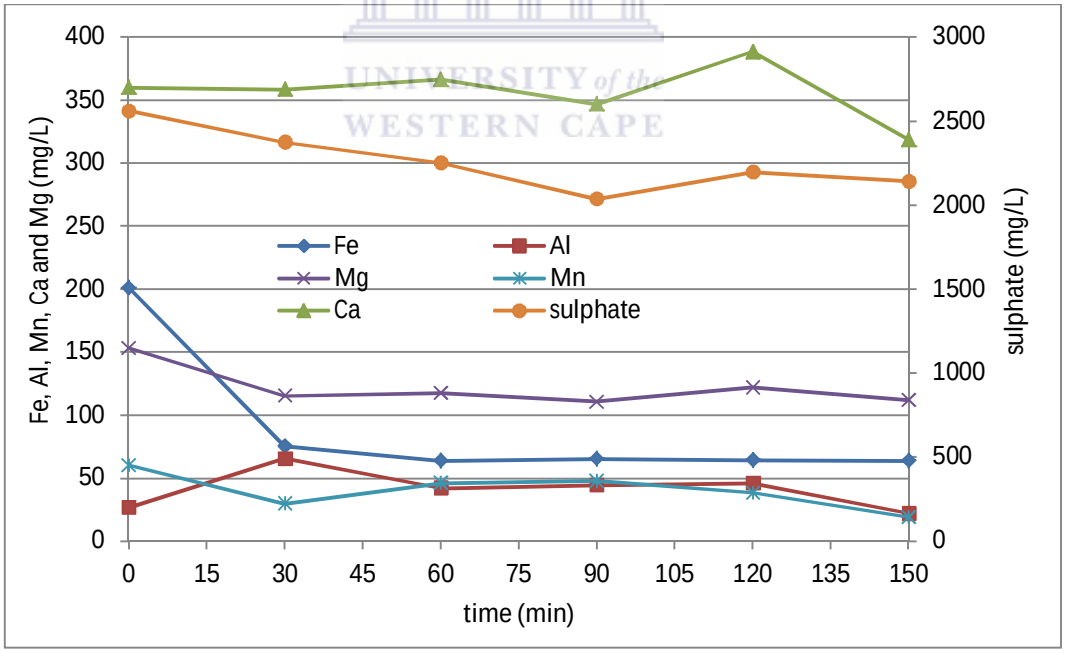

Figure 7.2.2: The Fe, Al, Mg, Mn, Ca and sulphate concentration during treatment of 80 L of Rand Uranium mine water with 86.58 g of $Al(OH)_3$ using a jet loop reactor.

From the results in Figure 7.2.2, the concentration of Fe, Mn and Mg slightly decreased in the first 30 min and then remained constant from 30 min to 150 min. The Fe concentration was decreased from 201 mg/L to 75 mg/L, that of Mn was decreased from 60 mg/L to 30 mg/L and that of Mg was decreased from 153 mg/L to 115 mg/L after 30 min of mixing of Rand Uranium mine water and $Al(OH)_3$ in jet loop reactor. Iron concentration decreased the most compared to levels of Mn and Mg removed. This was because the pH of the mixture was increased to 3.88 after 30 min of mixing Rand Uranium mine water (80 L) with 86.58 g of $Al(OH)_3$ in the jet reactor. According to the Act2 program of the GWB, Fe precipitates at pH 3.5 as jarosite-K (Figure 5.1.5) while Mn and Mg require the pH of the mixture to be increased to 10 and above to form $Mn(OH)_2$ (Figure 5.1.6) and $Mg(OH)_2$ (Figure 5.1.7) respectively. The concentration of Al slightly increased in the solution during the first 30 min and then remained the same for the duration of the treatment process. The slight increase in Al concentration was due to the added $Al(OH)_3$. The sulphate concentration decreased from 2562 mg/L to 2142 mg/L after 150 min. The decrease in sulphate concentration could be ascribed to the interaction of the sulphate ions with the positively charged Al species. The slight decrease in the concentration of Fe, Mg, Mn and sulphate ions correlates well with the decrease in EC observed in Figure 7.2.1.

The solid residue collected after 150 min of treating Rand Uranium mine water (80 L) with 86.58 g of $Al(OH)_3$ using a jet reactor was analysed using XRD. The spectrum of the solid residue was compared to that of $Al(OH)_3$ as shown in Figure 7.2.3.

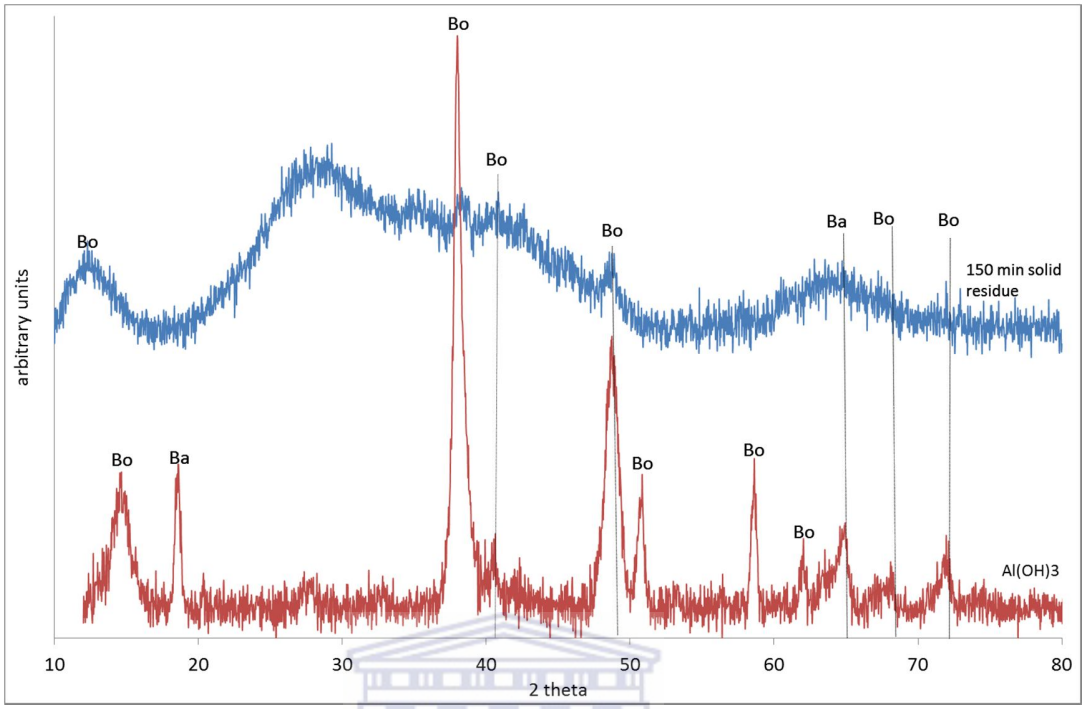

Figure 7.2.3: XRD spectra of $Al(OH)_3$ and the solid residue after treatment of 80 L of Rand Uranium mine water with 86.58 g of $Al(OH)_3$ using a jet loop reactor (Bo-boehmite; Ba-bayerite).

The XRD results obtained in Figure 7.2.3 showed that the boehmite and bayerite peaks in $Al(OH)_3$ disappeared and the 150 min solid residues were composed of mainly amorphous minerals (Figure 7.2.18). These amorphous materials could have been oligomeric Al species with adsorbed sulphate ions that were removed from Rand Uranium mine water.

The solid residues collected after 150 min of treating Rand Uranium mine water (80 L) with $Al(OH)_3$ was analysed using XRF. The results were compared to the XRF results of the aluminium hydroxide and the results are shown in Table 7.2.1.

Table 7.2.1: Composition of $Al(OH)_3$ and the solid residues produced after treatment of Rand Uranium mine water (80 L) with 86.58 g of $Al(OH)_3$ in a jet loop reactor for 150 min.

% mass oxide	$Al(OH)_3$ ± stdev	150 min solid residue ± stdev
Al_2O_3	65.13 ± 0.86	63.71 ± 0.64
Fe_2O_3	11.67 ± 0.54	13.82 ± 0.14
SO_3	4.24 ± 0.45	5.56 ± 0.11
SiO_2	1.75 ± 0.24	1.76 ± 0.01
CaO	0.48 ± 0.05	0.43 ± 0.004
Na_2O	0.38 ± 0.004	0.37 ± 0.004
K_2O	0.05 ± 0.01	0.04 ± 0.0005
P_2O_5	ND	0.10 ± 0.001
TiO_2	ND	0.04 ± 0.0005
MnO	ND	0.04 ± 0.0005
Cr_2O_3	ND	0.01 ± 0.004
MgO	ND	ND
Loss on ignition	16.25 ± 0.13	14.16 ± 0.71
Sum	99.93 ± 0.29	100.04 ± 0.018

ND means not detected and stdev means standard deviation.

The XRF results presented in Table 7.2.1 showed that the amount of Al_2O_3, SiO_2, CaO, Na_2O and K_2O in the solid residues was the same as the amount in $Al(OH)_3$. The concentration of Fe_2O_3, SO_3, P_2O_5, TiO_2, MnO and Cr_2O_3 increased in the solid residues. The increase in the amount of Fe_2O_3, SO_3 and MnO in the 150 min solid residue correlated well with the decrease in the concentration of Fe, Mn and S in Rand Uranium mine water during treatment with $Al(OH)_3$ (Figure 7.2.2).

7.2.2. EFFECT OF AMOUNT OF FLY ASH

In this second set of experiments, only Matla coal FA was used as an ameliorant. Rand Uranium mine water (80 L) was mixed with 8 kg or 13 kg of Matla FA in the jet loop reactor. The pH, EC and temperature were measured after every 15 min as explained in section 3.8.2.1. The results obtained are shown in Figure 7.2.1.

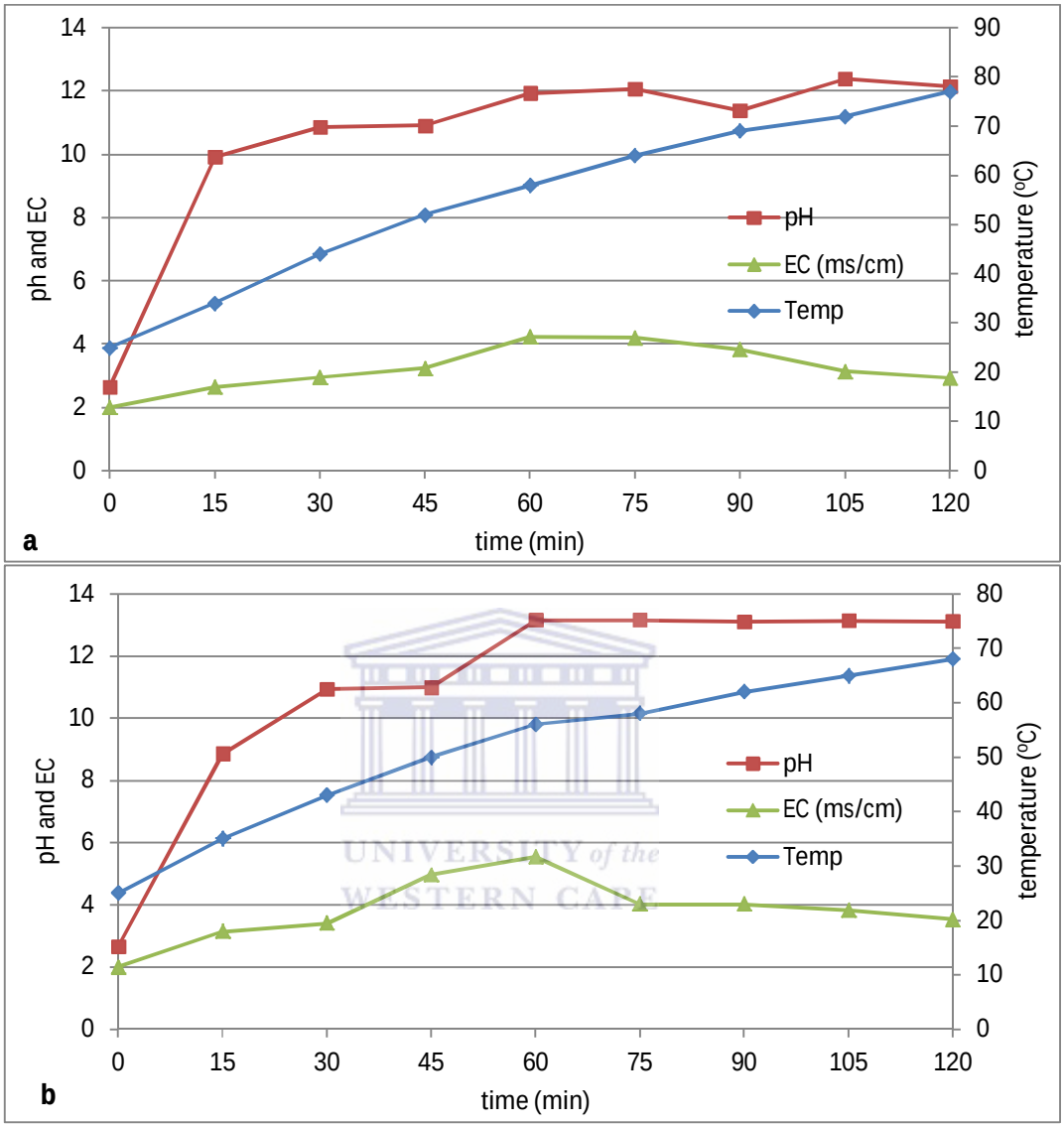

Figure 7.2.4: pH, EC and temperature profile during treatment of 80 L of Rand Uranium mine water with 8 kg (a) or 13 kg (b) of Matla coal FA for 120 min in a jet reactor.

From Figure 7.2.4, the pH of Rand Uranium mine water increased rapidly to pH greater than 10.86 in the first 30 min, after which there was a gradual increase in pH to around 11.97 after 60 min for the mixture containing 8 kg of Matla coal FA as shown in Figure 7.2.4a. Mixing of 80 L of Rand Uranium mine water and 16 kg of Matla coal resulted in the pH

increasing rapidly to 10.94 in the first 30 min; it was buffered for the next 15 min and then increased to 13.50 as shown in Figure 7.2.4b.

The increase in pH was caused by the dissolution of CaO from Matla coal FA according to Equation 7.1 in section 7.1.1. Treatment of Rand Uranium with 13 kg of Matla coal FA resulted in higher pH of the mixture than with 8 kg. This was because the addition of more Matla coal FA added meant that more CaO was available to dissolve out of Matla coal FA matrix to cause a higher pH increase.

The buffering of the pH could be attributed to the Fe, Al, Mn and Mg precipitation/hydrolysis reactions that occurred during treatment Rand Uranium mine water with Matla coal FA as shown in Equations 7.6, 7.7, 7.8 and 7.9. These reactions produce acidity or consume alkalinity.

$$Fe^{3+} + 2H_2O + OH^- \leftrightarrow Fe(OH)_3 + 2H^+ \quad \text{.....7.6}$$

$$Al^{3+} + 2H_2O + OH^- \leftrightarrow Al(OH)_3 + 2H^+ \quad \text{.....7.7}$$

$$Mn^{2+} + 2H_2O \leftrightarrow Mn(OH)_2 + 2H^+ \quad \text{.....7.8}$$

$$Mg^{2+} + 2H_2O \leftrightarrow Mg(OH)_2 + 2H^+ \quad \text{.....7.9}$$

Electrical conductivity initially increased for the first 60 min and then started decreasing. The increase in EC could be because of the dissolution of CaO from Matla coal FA that added more Ca ions in the water. There was a gradual increase in the temperature of the mixture. This was caused by the hydrodynamic cavitation that occurred inside the jet loop reactor after 120 min to about 70 ^{o}C.

During treatment of Rand Uranium mine water (80 L) with 8 kg or 13 kg of Matla coal FA, aliquot samples were collected after every 30 min. The treated mine water samples were, filtered and analysed using IC and ICP-OES. The results obtained are shown in Figure 7.2.5.

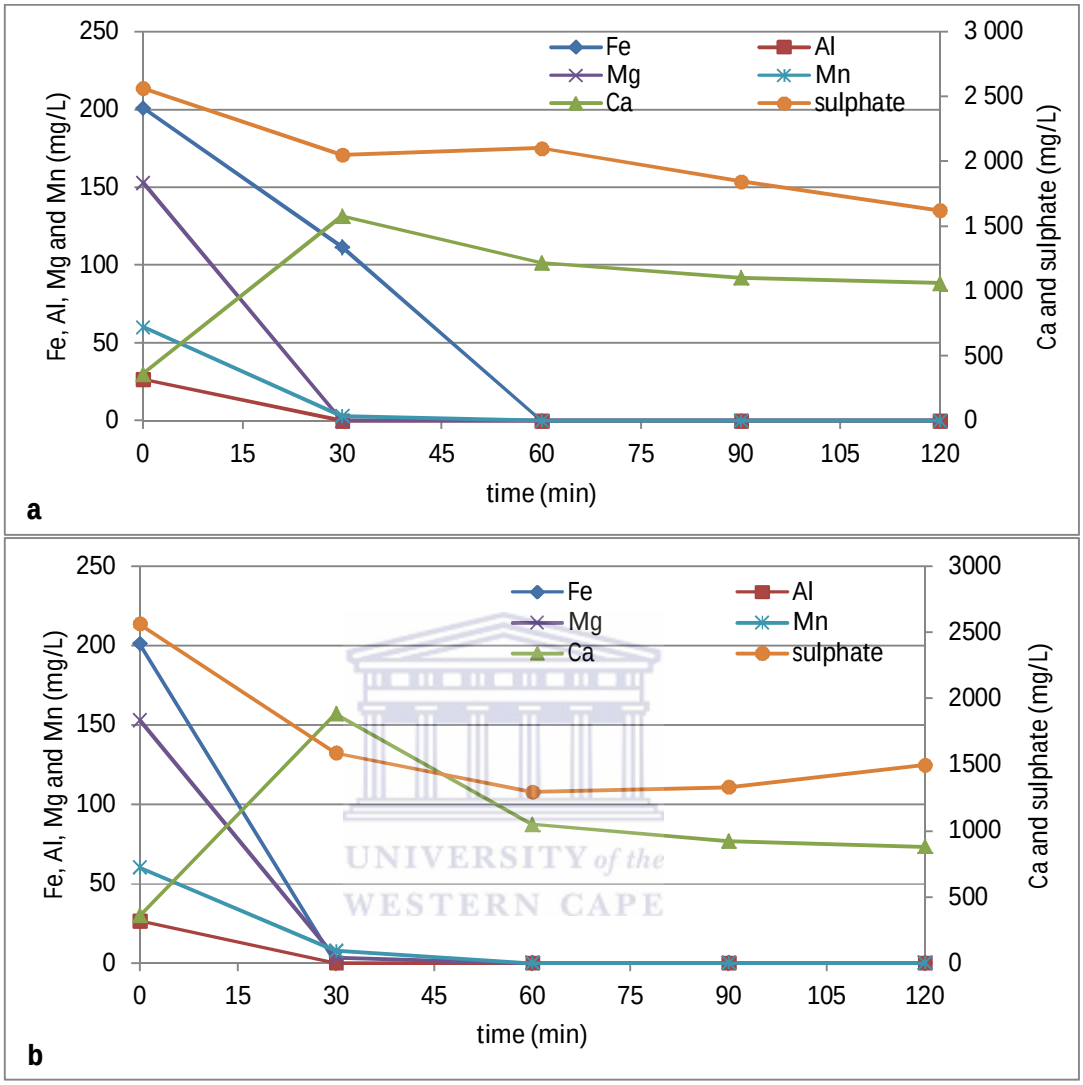

Figure 7.2.5: The Al, Ca, Fe, Mg, Mn and sulphate concentration during treatment of 80 L of Rand Uranium mine water with 8 kg (a) or 13 kg (b) of Matla coal FA for 120 min in jet loop reactor.

The results in Figure 7.2.5a show that the sulphate concentration decreased from 2500 mg/L to 1621 mg/L after 120 min of treating Rand Uranium mine water (80 L) with 8 kg of Matla coal FA in a jet reactor. The Ca concentration in the treated mine water initially increased from 360 mg/L to about 1577 mg/L in the first 30 min of treating Rand Uranium mine water with 8 kg of Matla coal FA (Figure 7.2.5a). This was because of the dissolution of

CaO from Matla coal FA which also caused the pH and EC to increase (Figure 7.2.4). After 30 min, the Ca concentration started decreasing gradually. This was attributed to the fact that the mixture was supersaturated with respect to gypsum and therefore it was assumed that precipitation of gypsum occurred at this stage, according to Act2 modelling results in section 5.1.2.1.

Treatment of Rand Uranium mine water (80 L) with 13 kg of Matla coal FA resulted in the sulphate concentration decreasing from 2500 mg/L to 1496 mg/L after 120 min (Figure 7.2.5b). The Ca concentration during treatment of Rand Uranium mine water (80 L) with 13 kg of Matla coal FA increased from 360 mg/L to 1883 mg/L in the first 30 min. This Ca concentration was more than when Rand Uranium mine water was mixed with 8 kg of Matla coal FA for 30 min. This was because as more Matla coal FA was used, it resulted in more CaO dissolution thereby increasing the Ca concentration (Figure 7.2.5b) and pH (Figure 7.2.4b). The higher amount of Ca that was made available by the addition of 13 kg would result in more sulphate ions being removed in the form gypsum compared to the case when using 8 kg of Matla coal FA (Figure 7.2.5a). The kinetics of sulphate removal was increased by the addition of more Matla coal FA. This was because the minimum sulphate concentration was achieved after 60 min of mixing Rand Uranium mine water (80 L) with 13 kg (Figure 7.2.5b). The sulphate concentration continued to decrease to 1621 mg/L after 120 min of mixing Rand Uranium mine water (80 L) with 8 kg of coal FA (Figure 7.2.5b).

Analysis of the water sampled during treatment of Rand Uranium mine water with Matla coal FA (8 kg or 13 kg) using ICP-OES has shown that the concentration of Al, Mn and Mg decreased to almost zero after 30 min, when the pH of the water had been increased to greater than 10, which corresponded to the decrease in EC observed in Figure 7.2.4. The Fe concentration decreased to almost zero after Rand Uranium mine water was mixed with 13 kg and 8 kg for 30 min and 60 min respectively. Potentially toxic elements such as Al and Fe are known to precipitate out at pH greater than 3; while Mn and Mg are known to precipitate out at pH greater than 9 and 10 respectively due to the formation of their respective hydroxides according to Equation 7.6, 7.7, 7.8 and 7.9 (Madzivire, 2010, Gitari et al., 2008).

The empirical data obtained for the removal of sulphate ions, Fe, Al, Mn and Mg from Rand Uranium mine water with Matla coal FA agreed well with the results obtained from modelling using the Act2 program of the GWB software in section 5.1.2.1. The GWB software predicted that sulphate ions removal as gypsum was dependent on the concentration of Ca ions added to the mixture (Figure 5.1.3). Removal of Al, Fe, Mn and Mg was predicted to be pH dependent by the GWB software as shown in Figures 5.1.4, 5.1.5, 5.1.6 and 5.1.7. It was predicted by Act2 program that Al and Fe would precipitate at a pH greater than 4, while Mn and Mg would precipitate out from Rand Uranium mine water at a pH greater than 10.

Solid residues that were collected after 120 min of treatment of Rand Uranium mine water (80 L) with 8 kg of Matla coal FA were analysed using XRD to determine the mineral phases that may have disappeared or new minerals that may have formed. Comparison of the XRD spectrum of the solid residues that remain after treatment of Rand Uranium mine water to that of Matla coal FA is shown in Figure 7.2.6.

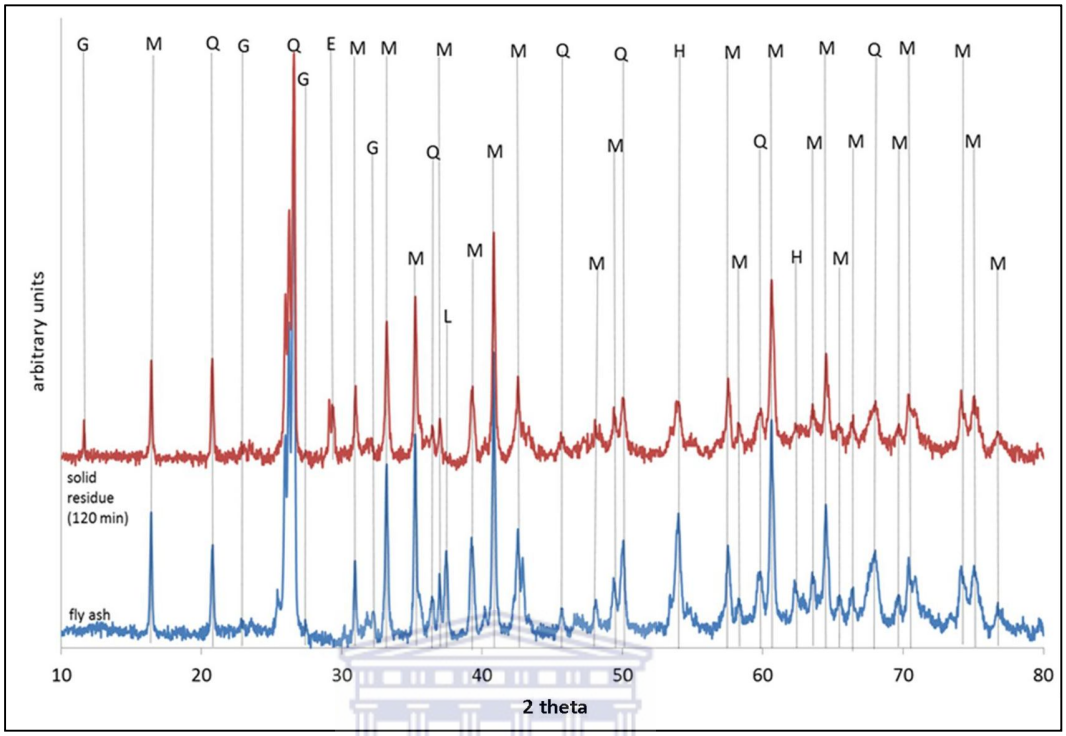

Figure 7.2.6: XRD for fly ash and solid residue after treatment of Rand Uranium mine water (80 L) with Matla coal FA (8 kg or 13 kg) for 120 min using a jet loop reactor (G-gypsum; M-mullite; Q-quartz; M-mullite; L-CaO; H-hematite; E-ettringite).

The XRD spectra (Figure 7.2.6) showed that CaO peak (at 2 θ of 37.36) became less distinct in the solid residue XRD spectrum, while gypsum (at 2 θ of 11.63) and ettringite (at θ of 29.07) peaks appeared in the solid residue XRD spectrum. This confirmed that the decrease observed in sulphate and Ca ion concentration shown in Figure 7.2.5 was due to gypsum and ettringite precipitation. No Al, Fe or Mn mineral phases could be discerned by XRD because the minerals might be present in low abundance or as amorphous hydroxide mineral phases that cannot be detected by XRD.

The XRF analysis of the solid residues that were recovered during the treatment of Rand Uranium mine water (80 L) at 60 min and 120 min with 13 kg of Matla coal FA in a jet loop reactor is shown in Table 7.2.2.

Table 7.2.2: The elemental composition of Matla coal FA and the solid residues collected after 60 min and 120 min of treatment of 80 L of Rand Uranium mine water with 13 kg of Matla coal FA.

% Oxide	Matla coal FA	60 min solid residue	120 min solid residue
SiO_2	48.27 ± 0.04	48.10 ± 0.08	48.35 ± 0.14
Al_2O_3	30.89 ± 0.22	30.98 ± 1.02	31.57 ± 0.37
CaO	6.71 ± 0.08	5.26 ± 0.12	5.72 ± 0.09
Fe_2O_3	2.81 ± 0.03	2.89 ± 0.04	2.89 ± 0.01
MgO	2.12 ± 0.04	2.91 ± 0.06	2.91 ± 0.02
TiO_2	1.26 ± 0.02	1.62 ± 0.08	1.58 ± 0.06
P_2O_5	0.89 ± 0.01	1.05 ± 0.02	1.03 ± 0.01
K_2O	0.84 ± 0.01	0.73 ± 0.01	0.71 ± 0.02
Na_2O	0.55 ± 0.01	0.59 ± 0.04	0.58 ± 0.02
SO_3	0.19 ± 0.002	0.20 ± 0.01	0.38 ± 0.04
MnO	0.02 ± 0.0004	0.10 ± 0.001	0.10 ± 0.004
Loss on ignition	5.24 ± 0	4.18 ± 0.15	4.09 ± 0.09
Sum	99.79 ± 0.07	98.61 ± 0.05	99.91 ± 0.14

The XRF results in Table 7.2.2 showed that the CaO in Matla coal FA was more than in the in the solid residues collected after 60 min. This was because of the dissolution CaO in the Matla coal FA that caused the pH of the mine water (Figure 7.2.4a) and the concentration of Ca in the mine water (Figure 7.2.5a) to increase. The subsequent slight increase in CaO in 120 min solid residue is attributed to the formation of gypsum and ettringite in the solid residues that was confirmed with XRD in Figure 7.2.6. This correlates well with the increase in the amount of SO_3 in solid residues collected at 120 min compared to that collected after 60 min. The increase in SO_3 observed in the solid residues was due to the formation of gypsum and ettringite in solid residues noted by XRF which correlated well with the decrease in the sulphate concentration in the Rand Uranium mine water during treatment with 13 kg of Matla coal FA (Figure 7.2.5a).

The XRF results in Table 7.2.2 showed that the Fe_2O_3, Al_2O_3, MgO and MnO increased in the solid residues compared to that in Matla coal FA. This was because the Fe, Mg and Mn concentration decreased in Rand Uranium mine water (Figure 7.2.5a) and formed part of the solid residue. According to Act2 program, Fe, Al, Mg and Mn precipitated as hydroxides

when Rand Uranium mine was treated with Matla coal FA. The amount of SiO_2 and Na_2O remained relatively the same, while that of P_2O_5 and K_2O slightly decreased in the solid residues when compared to that in Matla coal FA. This was because Rand Uranium mine water contained low amounts of these elements and there was no dissolution of these elements from Matla coal FA into the mine water.

Treatment of Rand Uranium mine water (80 L) with Matla coal FA (8 kg or 13 kg) has showed that the concentration of heavy metals such as Fe, Al, Mg and Mg can be removed by almost 100 %. The sulphate concentration that remained in the treated water was around 1500-1600 mg/L. This concentration was above the target water quality range (TWQR) for potable water, industrial use and livestock watering (DWAF, 1996 and WHO, 2011). The removal of sulphate ions during treatment of Rand Uranium mine water (80 L) with Matla coal FA (8 or 13 kg) was limited by the solubility of gypsum and the low concentration of Al in Rand Uranium mine water to form ettringite. Therefore the addition of $Al(OH)_3$ was applied to investigate the possibility to further precipitate out the remaining sulphate ions as ettringite since the pH of the water was above 11.5 (Smit, 1999, Smit and Sibilski, 2003 and Madzivire, 2010).

7.2.3. EFFECT OF THE AMOUNT OF FLY ASH AND ALUMINIUM HYDROXIDE

In the following experiments, the effect of adding $Al(OH)_3$ to the treatment system involving Rand Uranium mine water and Matla coal FA was investigated. Rand Uranium mine water (80 L) was mixed with 8 kg or 13 kg of Matla coal FA in a jet loop reactor for 30 min. After 30 min, 86.58 g of $Al(OH)_3$ was added to each mixture and aliquot samples were collected after every 30 min as outlined in section 3.8.2.3. The aliquot samples were filtered and analysed using ICP-OES and IC. The pH, EC and temperature were measured after every 15 min. Since treatment of Rand Uranium mine water with Matla coal FA in section 7.2.2 has resulted in the sulphate concentration decreasing to about 1600 mg/L, the $Al(OH)_3$ added (86.58 g) was calculated to be theoretically equivalent to precipitate out about 2000 mg/L of sulphate ions as ettringite ($3CaO.3CaSO_4.Al_2O_3.26H_2O$). This means excess amount of $Al(OH)_3$ was added to the reaction mixture assuming that the $Al(OH)_3$ added would react

with sulphate ions in solution only, and not with sulphate ions that was already in the solid phase before the addition of $Al(OH)_3$.

The pH, EC and temperature results obtained during treatment of Rand Uranium mine (80 L) with Matla coal FA (8 kg or 13 kg) and 86.58 g of $Al(OH)_3$ is shown in Figure 7.2.7.

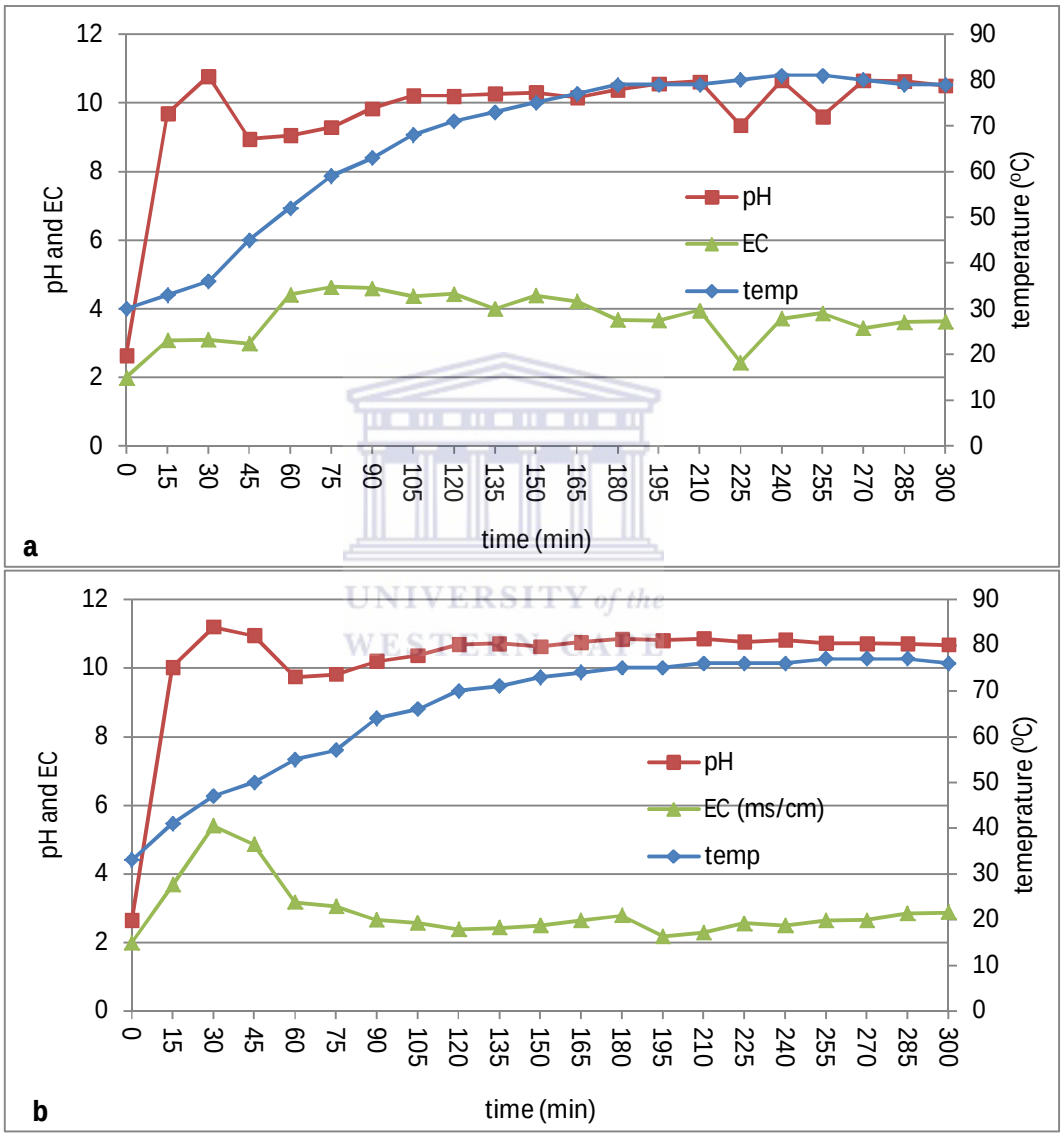

Figure 7.2.7: pH, EC and temperature profile during treatment of 80 L of Rand Uranium mine water with 8 kg (a) or 13 kg (b) of Matla FA and 86.58 g of $Al(OH)_3$.

From Figure 7.2.7, the pH of Rand Uranium mine water was increased to 10.78 and 11.19 when mixed with 8 kg and 13 kg of FA respectively in a jet loop reactor for 30 min. The EC of both mixtures followed the same trend as that of pH. The increase in pH and EC after mixing Rand Uranium mine water with Matla coal FA could be ascribed to the increase in Ca concentration caused by the dissolution of CaO in Matla coal FA.

After 30 min, 86.58 g of $Al(OH)_3$ was added to both mixtures. After the addition of $Al(OH)_3$ the pH decreased to about 9 and 10 for the mixtures containing 8 kg or 13 kg of Matla coal FA respectively. The decrease in pH was ascribed to the protons that were produced during the precipitation of ettringite (Equation 7.2). As shown in Figure 7.2.7 the pH gradually increased again to pH 10.20 and 10.70 for the mixture containing 8 kg and 13 kg respectively. The pH of the mixture containing 13 kg of Matla coal FA was higher than the mixture containing 8 kg of Matla coal FA because higher amount of coal FA added meant that more CaO was made available to increase the pH. Addition of 86.58 g of $Al(OH)_3$ to the mixture containing 13 kg of Matla coal FA after 30 min resulted in the decrease in EC to about 2 mS/cm. The EC was maintained around this value thereafter. This decrease could be ascribed to the precipitation of sulphate and Ca ions as ettringite. After addition of 86.58 g of $Al(OH)_3$, the EC remained at about 3 mS/cm up to 45 min and increased sharply to 4.41 mS/cm the mixture containing 8 kg of Matla coal FA. This was because the pH of the mixture was well below the pH of stability of ettringite of 11.5-12.5 as shown in Figure7.2.7a (Myneni et al., 1998). It was expected for ettringite to re-dissolve as the pH decreased.

Aliquot samples collected after every 30 min during treatment of Rand Uranium mine water (80 L) with Matla coal FA (13 kg or 8 kg) and 86.58 g of $Al(OH)_3$ were filtered and analysed using ICP-OES and IC. The results obtained are shown in Figure 7.2.8.

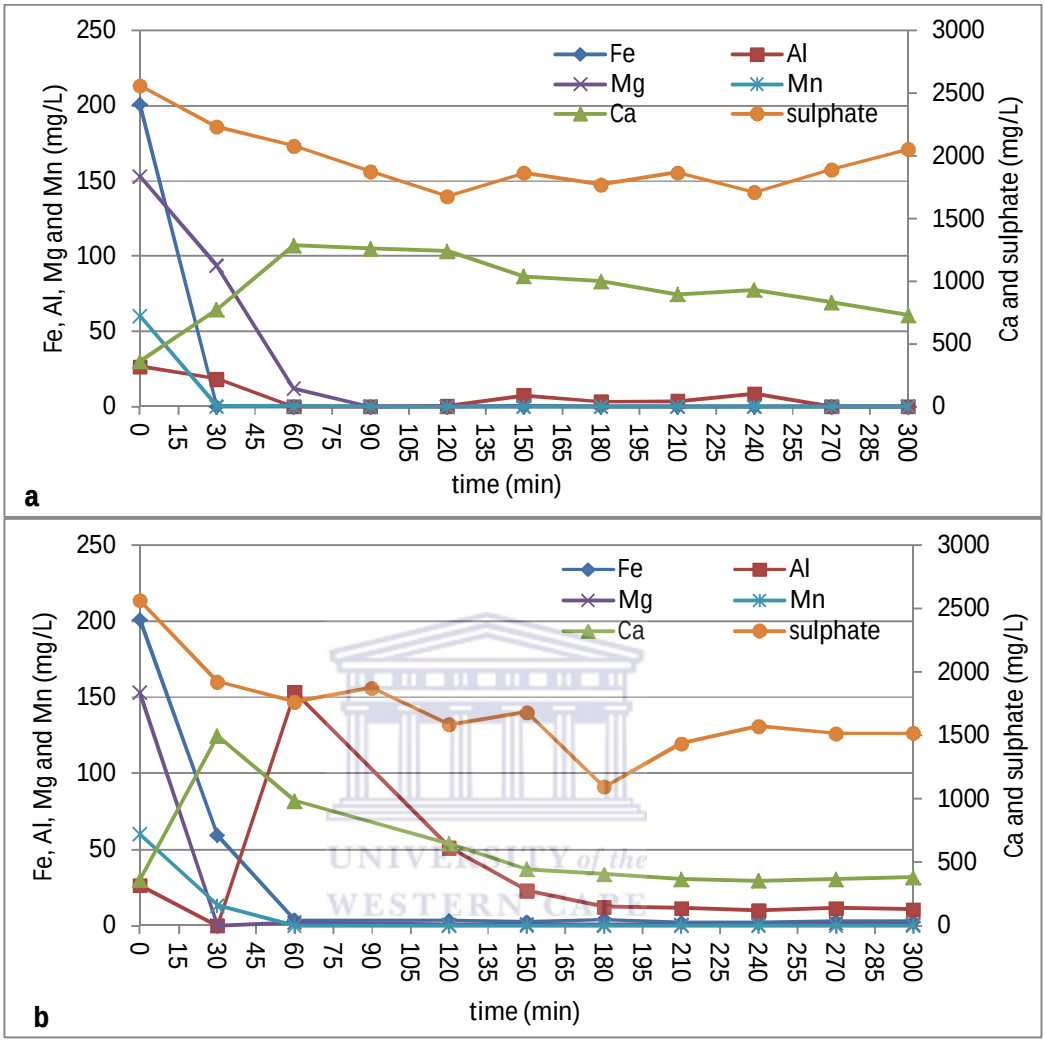

Figure 7.2.8: The Al, Ca, Fe, Mg, Mn and sulphate concentration during treatment of 80 L of Rand Uranium mine water with 8 kg (a) or 13 kg (b) of Matla FA and 86.58 $Al(OH)_3$.

Figure 7.2.8 showed that during treatment of Rand Uranium mine water (80 L) with Matla coal FA (8 kg or 13 Kg) and 86.58 g of $Al(OH)_3$, Fe, Mn and Mg were removed by almost 100 % in the first 60 min. This was because these elements formed their respective hydroxides at the applied pH. This agrees with the modelling results obtained using Act2 program of the GWB software in section 5.1.2. The Act2 program showed that removal of Fe, Mg and Mn from mine water with coal FA was pH dependent.

The results in Figure 7.2.8 showed that treatment of Rand Uranium mine water (80 L) with 8 kg or 13 kg of Matla coal FA for 30 min resulted in the decrease in sulphate concentration to 2231 mg/L (Figure 7.2.8a) and 1922 mg/L (Figure 7.2.8b) respectively. After the addition of 86.58 g of $Al(OH)_3$ to the mixture containing 8 kg of Matla coal FA, the sulphate concentration decreased further to 1678 mg/L at 120 min (Figure 7.2.8a). After 120 min the sulphate concentration in the mixture containing 8 kg started to increase again as shown in Figure 7.2.8a. This might be due to the dissolution of ettringite such that the sulphate concentration was 2052 mg/L after 300 min because the pH was well below 11.5, which is the optimum pH for ettringite stability.

After addition of 86.58 g of $Al(OH)_3$ at 30 min to the mixture containing 13 kg of Matla coal FA, the sulphate concentration continued to decrease to 1094 mg/L after 180 min due to ettringite precipitation. After 180 min, the sulphate concentration started increasing again to 1518 mg/L as shown in Figure 7.2.8b. In both cases (8 kg and 13 kg), the decrease in sulphate concentration was lagging behind the trend of pH. The sulphate concentration decreased after the pH had decreased and increased after the pH had increased. This showed that the removal of sulphate ions after addition of $Al(OH)_3$ was pH dependent. The removal of sulphate ions from Rand Uranium mine water followed the same trend as the decrease in Ca concentration as shown in Figure 7.2.8. This was because both these ions precipitated out in the form of ettringite.

During treatment of Rand Uranium mine water (80 L) with 13 kg of Matla coal FA and 86.58 g of $Al(OH)_3$, the solid residues were collected after 30 min and 300 min. The solid residues were analysed using XRD to determine the mineral phases and were compared to those of Matla coal FA and $Al(OH)_3$ as shown in Figure 7.2.9.

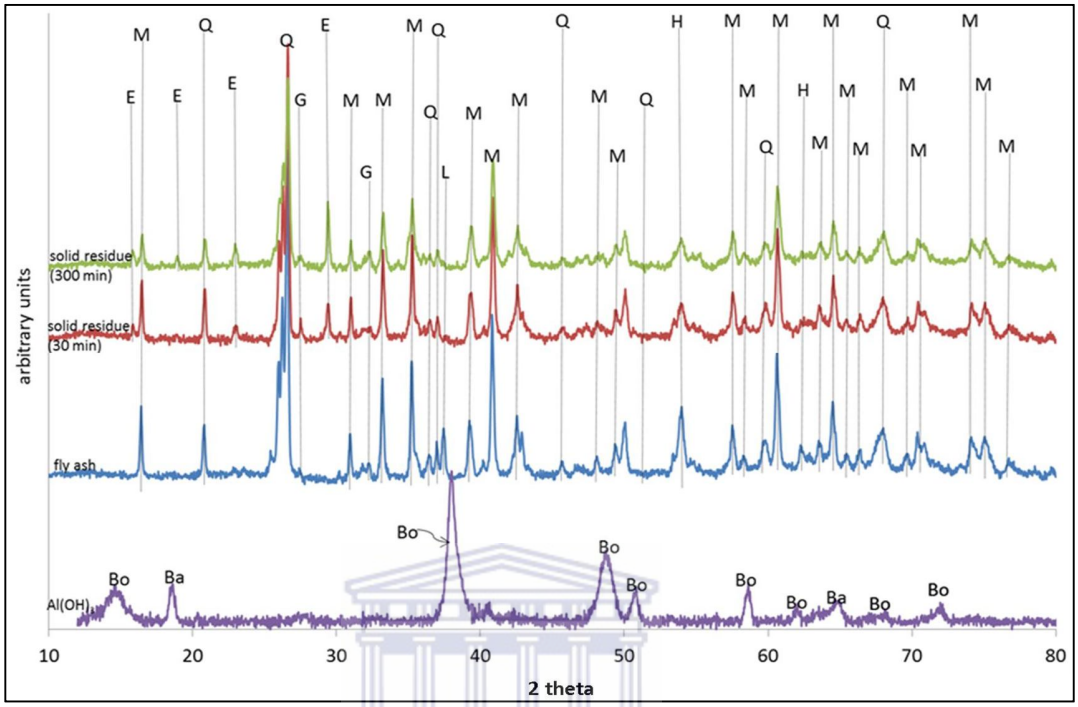

Figure 7.2.9: The spectra of Matla coal FA and $Al(OH)_3$ compared to the spectra of the solid residues collected after 30 min and 300 min of treating Rand Uranium mine water (80 L) with Matla coal FA (13 kg) and 86.58 g of $Al(OH)_3$ (Bo-boehmite; Ba-bayerite; E-ettringite; M-mullite; Q-quartz; C-CaO; L-lime; H-hematite).

The appearance of ettringite peaks in the solid residues XRD spectrum (Figure 7.2.9) confirmed that indeed sulphate and Ca concentration decreased due to the formation of ettringite. The CaO peaks in Matla FA as well as the bayerite and boehmite peaks from the $Al(OH)_3$ disappeared during treatment of Rand Uranium mine water. The disappearance of CaO in the solid residues was due to its dissolution, thereby causing the pH of the mixture to increase (Figure 7.2.7). The disappearance of bayerite and boehmite peaks was due to the reaction of these $Al(OH)_3$ mineral phases with Ca and sulphate ions to form ettringite, shown to be present in the XRD spectrum of the solid residues.

As noted, 86.58 g of $Al(OH)_3$ was added after 30 min to the mixture of 80 L of Rand Uranium mine water and Matla coal FA (8 kg or 13 kg) containing between 1900 mg/L and 2200 mg/L

of sulphate ions. The amount of $Al(OH)_3$ that was added, was theoretically supposed to precipitate out about 2000 mg/L of sulphate ions as ettringite ($3CaO.3CaSO_4.Al_2O_3.32H_2O$). In this case only 179 mg/L and 400 mg/L of the sulphate ions were removed from the mixture containing 8 kg and 13 kg of Matla coal FA respectively. This was because; when the ettringite was being formed it released protons. This caused the pH of the mixture to decrease to below 11, which was below the optimum pH for ettringite stability of 11.5-12.5. This showed the need for careful pH control during treatment of Rand Uranium mine water with Matla coal FA and lime. More sulphate ions were removed in the mixture containing 13 kg of coal FA than in the mixture with 8 kg of coal FA. This was because of a slightly higher pH in the mixture containing 13 kg of coal FA.

Treatment of Rand Uranium mine water (80 L) with Matla coal FA (8 kg or 13 kg) and 86.58 g of $Al(OH)_3$ in a jet reactor removed most of the heavy metals such as Fe, Mg and Mn to within the TQWR. The sulphate concentration was greater than 1500 mg/L. This was still above the TWQR for industrial and domestic applications. The following section investigates the effect of adding different amounts of lime and 86.58 g of $Al(OH)_3$ on the removal of sulphate ions from Rand Uranium mine water.

7.2.4. EFFECT OF THE AMOUNT LIME AND ALUMINIUM HYDROXIDE

In the next set of experiments, no fly ash was added to the system. Rand Uranium mine water was treated with lime and $Al(OH)_3$. In order to investigate the amount of lime required to achieve and maintain the correct pH to precipitate out sulphate ions as ettringite, Rand Uranium mine water (80 L) was treated with 100, 150 or 200 g of lime only for 30 min in a jet reactor with jet sizes of 12 mm diameter. After 30 min 86.58 g of $Al(OH)_3$ was added to each mixture as outlined in section 3.8.2.4. The pH, EC and temperature of each mixture were measured after every 15 min and the results are shown in Figure 7.2.10.

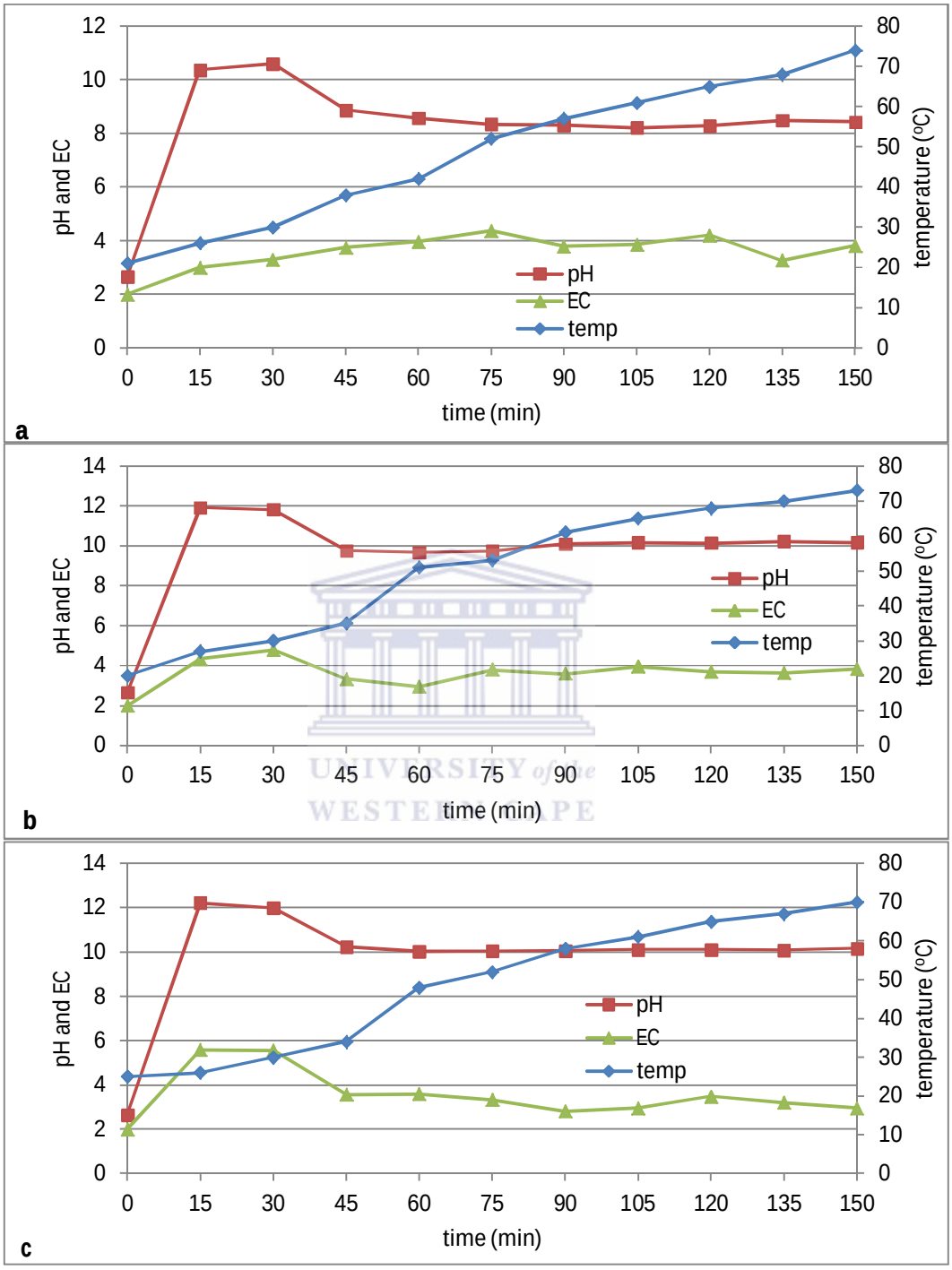

Figure 7.2.10: pH, EC and temperature profile during treatment of 80 L of Rand Uranium mine water with 100 g (a), 150 g (b) or 200 g (c) of lime and 86.58 g of $Al(OH)_3$.

Results in Figure 7.2.10 showed that the increase in pH of the mixture was dependent on the amount of lime added. Treatment of 80 L of Rand Uranium mine water with 100 g, 150 g and 200 g of lime resulted in the pH increasing to 10.60 (Figure 7.2.10a), 11.82 (Figure 7.2.10b) and 11.99 (Figure 7.2.10c) respectively. Addition of $Al(OH)_3$ after 30 min to each mixture resulted in the decrease in pH. When the $Al(OH)_3$ was added to the mixture containing 100 g, the pH of the mixture decreased to around 9, while in the case of the mixtures containing 150 g and 200 g, the pH of the mixtures were slightly greater than 10. The decrease in pH could be attributed to the formation of ettringite, which produces protons during its formation (Equation 7.2).

During treatment of Rand Uranium mine water with 100 g, 150 g or 200 g of lime and $Al(OH)_3$ in a jet loop reactor, aliquot samples were collected after every 30 min. The samples were filtered using a 0.45 µm filter and analysed using ICP-OES and IC. The results obtained are shown in Figure 7.2.11.

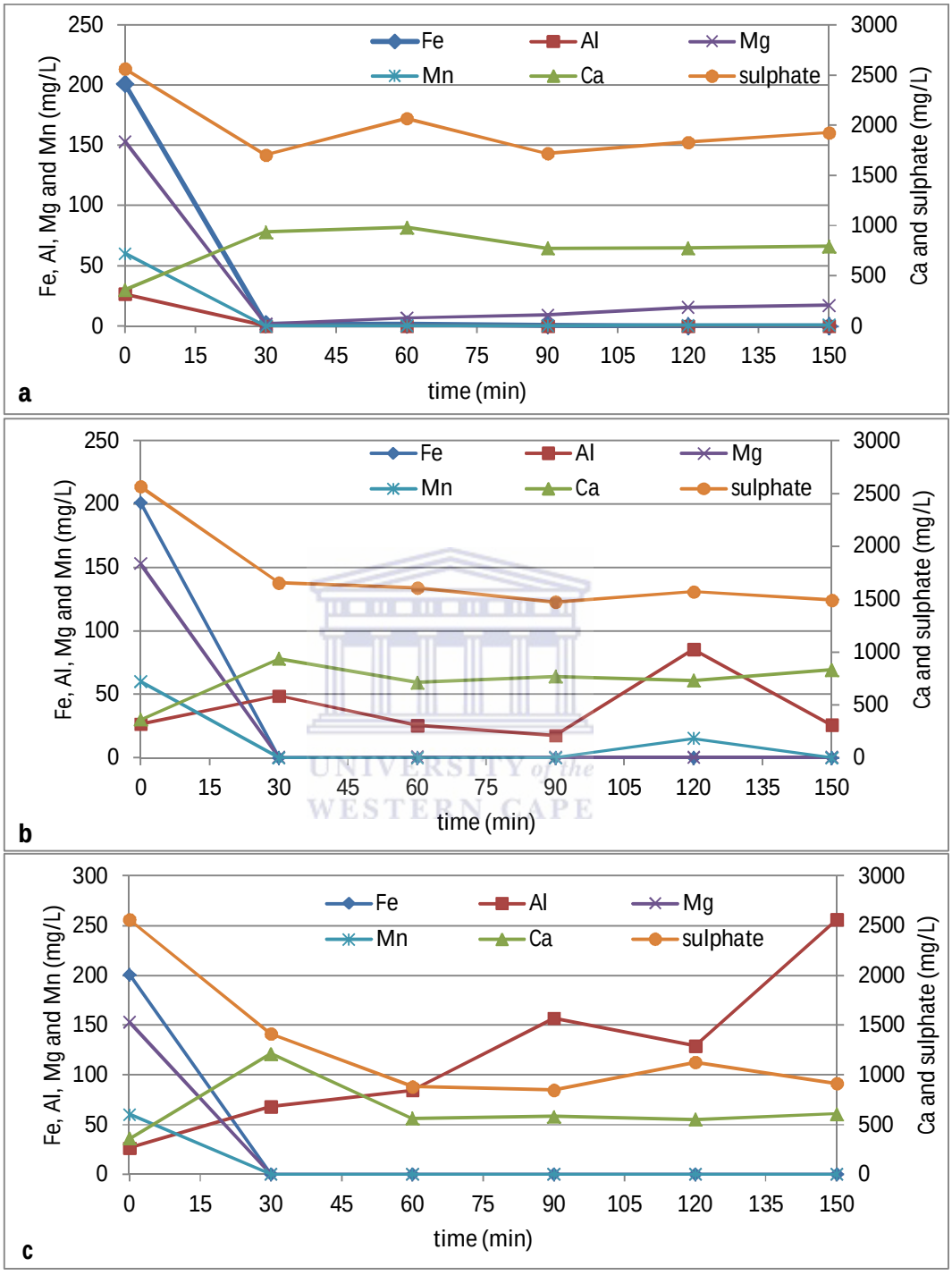

Figure 7.2.11: The Fe, Al, Mg, Mn, Ca and sulphate concentration during treatment of 80 L of Rand Uranium mine water with 100 g (a), 150 g (b) or 200 g (c) of lime and 86.58g $Al(OH)_3$ in a jet loop reactor.

Treatment of Rand Uranium mine water with lime for 30 min in a jet reactor showed that Fe, Mn and Mg were removed by almost 100 % (Figure 7.2.11). This was due to the formation of $Fe(OH)_3$, $Mn(OH)_2$ and $Mg(OH)_2$ at pH around 6, 9 and 10 respectively. In the case of treatment of Rand Uranium mine water with 100 g lime, the Mg concentration slightly increased after addition of $Al(OH)_3$ as shown in Figure 7.2.11a. This was because of the decrease in pH to less than 9, which was below the optimum pH for the formation of $Mg(OH)_2$. This agrees well with the modelling results obtained using Act2 model of the GWB software in section 5.1.2, which showed that the removal of Fe, Mn and Mg was pH dependent.

The Al concentration during the treatment of Rand Uranium mine water with 150 g or 200 g of lime remained significantly high as show in Figure 7.2.11b and Figure 7.2.11c. This was because of the formation of $Al(OH)_4^-$ at pH greater than 10 after the addition of $Al(OH)_3$. The $Al(OH)_4^-$ could not be incorporated into the ettringite structure since the pH was around 10.2, which was far less than the optimum pH of 11.5.

Treatment of Rand Uranium mine water with different amounts of lime has shown that Ca ions initially leached into the mine water during the first 30 min of treatment. As more lime was added more CaO ions dissolved into the water thereby causing the concentration of Ca ions and pH of the solution to increase. After adding $Al(OH)_3$ to the mixture at 30 min, the Ca ions concentration decreased. The sulphate concentration decreased from about 2500 mg/L to about 1700 mg/L in the first 30 min of treating Rand Uranium mine water (80 L) with 100 g of lime (Figure 7.2.11a). This could be ascribed to the formation of gypsum and/or ettringite. Addition of 86.58 g of $Al(OH)_3$ to the mixture at 30 min resulted in no further sulphate removal from Rand Uranium mine water as shown in Figure 7.2.11a. In this case ettringite could not form because the pH was around 9, which was well below the optimum pH for ettringite formation.

During treatment of Rand Uranium mine water (80 L) with 150 g of lime in jet reactor for 30 min, the Ca concentration increased from 360 mg/L to 936 mg/L, while the sulphate concentration decreased from 2500 mg/L to about 1650 mg/L as shown in Figure 7.2.11b. The decrease in the sulphate concentration could be attributed to the formation of gypsum

and or ettringite. After addition of 86.58g of $Al(OH)_3$, the concentration of Ca and sulphate slightly decreased as shown in Figure 7.2.11b. Increasing the amount of lime to 200 g has shown that sulphate concentration decreased from about 2500 mg/L to about 1500 g in the first 30 min (Figure 7.2.11c). Addition of 86.58 g of $Al(OH)_3$ at 30 min resulted in the further decrease of sulphate concentration to about 850 mg/L (Figure 7.2.11c). Although the pH of the solution was almost the same as using 150 mg/L, the more lime added by adding 200 g of lime to the mixture resulted in the addition of more Ca ions. This resulted in the shifting of the ettringite equilibrium reaction to the right thereby forming more products.

Solid residues that were collected after 30 min treating of Rand Uranium mine water (80 L) with 200 g of lime and 150 min after addition of 86.58 g of $Al(OH)_3$ were analysed using XRD. The XRD spectra of, lime and the solid residues collected after 150 min are shown in Figure 7.2.12.

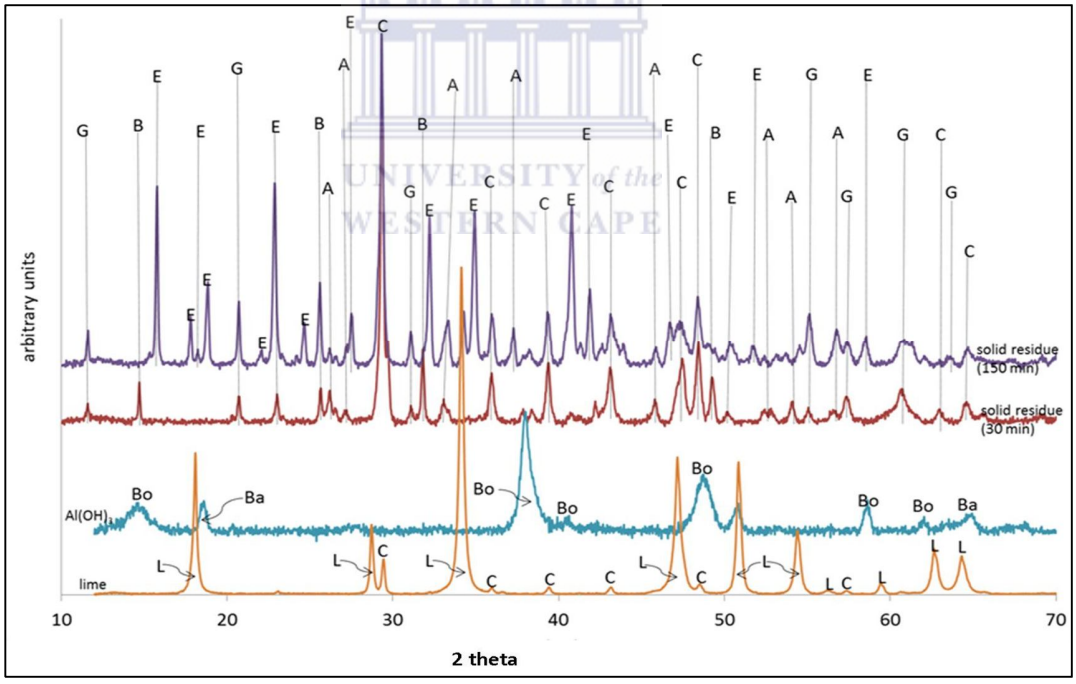

Figure 7.2.12: Comparison of the XRD spectra of lime and $Al(OH)_3$ to that of the solid residues produced after treatment of Rand Uranium mine water with lime and $Al(OH)_3$ using a jet loop reactor (L-CaO; C-calcite; Bo-boehmite; Ba-bayerite; G-gypsum; B-bassannite; E-ettringite, A-aragonite).

Comparing the XRD spectrum of the solid residues formed after 30 min of mixing lime and Rand Uranium mine water showed that the CaO peaks disappeared from lime spectrum and new peaks of gypsum ($CaSO_4.2H_2O$), bassanite ($CaSO_4.0.5H_2O$), calcite ($CaCO_3$) and aragonite ($CaCO_3$) appeared in the 30 min solid residue spectrum. This means that the decrease in the sulphate concentration (Figure 7.2.11) in the first 30 min of mixing Rand Uranium mine water and lime was due to gypsum and bassanite formation.

$$Ca^{2+} + SO_4^{2-} + 2H_2O \leftrightarrow CaSO_4.2H_2O \quad \text{.....7.10}$$

$$Ca^{2+} + SO_4^{2-} + 0.5H_2O \leftrightarrow CaSO_4.0.5H_2O \quad \text{.....7.11}$$

The characteristic peaks of CaO disappeared due to the dissolution of lime according to Equation 7.1, causing the pH of the mixture to increase (Figure 7.2.10). Calcite and aragonite were products of the carbonation of the mixture with atmospheric CO_2 during mixing in a jet loop reactor.

$$3Ca^{2+} + 3CO_2 + \tfrac{3}{2}O_2 \leftrightarrow 3CaCO_3 \quad \text{.....7.12}$$

The XRD spectrum of the solid residues that were formed after addition of $Al(OH)_3$ (that is at 150 min) as well as the spectra of $Al(OH)_3$ and lime are shown in Figure 7.2.12. The spectra showed the disappearance of the characteristic CaO and calcite peaks in the lime spectrum and the bayerite (AlOOH) and boehmite ($Al(OH)_3$) peaks in the $Al(OH)_3$ spectrum and the appearance of ettringite peaks in addition to the gypsum, bassanite, calcite and aragonite peaks in the 150 min solid residue XRD spectrum. This proved that the removal of sulphate ions from mine water after addition of $Al(OH)_3$ was due to the formation of ettringite and gypsum.

The solid residues produced after 150 min of treating Rand Uranium mine water (80 L) with 200 g of lime and 86.58 g of $Al(OH)_3$ in a jet loop reactor were analysed using XRF and the results are presented in Table 7.2.3.

Table 7.2.3: Composition of lime and the solid residues collected after 150 min of treating Rand Uranium mine water (80 L) with 200 g of lime and 86.58 g of $Al(OH)_3$ in a jet loop reactor.

% oxide	Lime (mg/kg)	150 min solid residue (mg/kg)
CaO	72.19 ± 1.54	25.88 ± 2.09
MgO	0.72 ± 0.11	4.27 ± 0.55
Na_2O	0.23 ± 0.02	0.19 ± 0.08
SiO_2	0.12 ± 0.03	3.40 ± 0.18
Al_2O_3	0.09 ± 0.01	9.83 ± 1.03
Fe_2O_3	0.06 ± 0.005	2.18 ± 0.17
SO_3	0.05 ± 0.002	16.51 ± 0.98
K_2O	0.02 ± 0.007	0.06 ± 0.006
MnO	0.02 ± 0.001	1.00 ± 0.01
P_2O_5	0.01 ± 0.006	0.08 ± 0.004
TiO_2	0.01 ± 0.004	0.10 ± 0.02
Loss on ignition	26.65 ± 0.97	35.52 ± 1.08
Sum	100.17 ± 1.67	99.02 ± 1.57

From Table 7.2.3, the Ca content in the solid residue collected after 150 min had significantly decreased. This was because the amount of Ca that went into solution during the dissolution of CaO and caused the pH to increase as shown in Figure 7.2.10c. The amount of Ca ions that precipitated as gypsum, bassanite and ettringite was not equal to the amount of Ca ions that was added to the water due to the dissolution of CaO. More Ca ions remained in solution as shown in Figure 7.2.11c.

The solid residue collected after 150 min of treatment of Rand Uranium mine water (80 L) with 200 g and 86.58 g of $Al(OH)_3$ showed an increase in MgO, SiO_2, Al_2O_3, Fe_2O_3, K_2O, MnO, SO_3 and P_2O_5. The increased content of Mg, Fe and Mn in the solid residues was because of the removal of these ions from mine water as shown in Figure 7.2.11c. The increase in Al content in the solid residue was due to the added $Al(OH)_3$. There was also a higher content of SO_3 in the solid residue compared that found in lime. This was because of the precipitation of sulphate ions in mine water as gypsum, bassannite and ettringite as shown in Figure 7.2.12.

Treatment of Rand Uranium mine water with various amount of lime and 86.58 g $Al(OH)_3$ has showed the removal of sulphate ion from mine water was dependent on the amount of lime added. Although the amount of lime was increased to 200 g per 80 L of Rand Uranium mine water, the sulphate concentration that remained in the mine was about 900 mg/L, which was above the TWQR for potable water of 500 mg/L. Treatment of mine water using lime is very expensive and not sustainable (Coetzee et al., 2000). Therefore the combination of coal FA, lime and $Al(OH)_3$ was investigated. This was done in order to reduce the amount of lime to be added and also to reduce the sulphate concentration to within TWQR for potable water.

7.2.5. EFFECT OF THE COMBINATION OF FLY ASH, LIME AND AL(OH)$_3$

In this section a combination of Matla coal FA, lime and $Al(OH)_3$ was investigated in order to reduce the sulphate levels to within the TWQR for potable water. Rand Uranium mine water (80 L) was treated with 8 kg of Matla coal FA and 100 g or 200 g of lime for 30 min in the jet loop reactor. The jet reactor had the jet sizes set at 12 mm. After 30 min, 86.58 g of $Al(OH)_3$ was added to each mixture as outlined in section 3.8.2.5. The pH, EC and temperature were measured after every 15 min. The results obtained are shown in Figure 7.2.13.

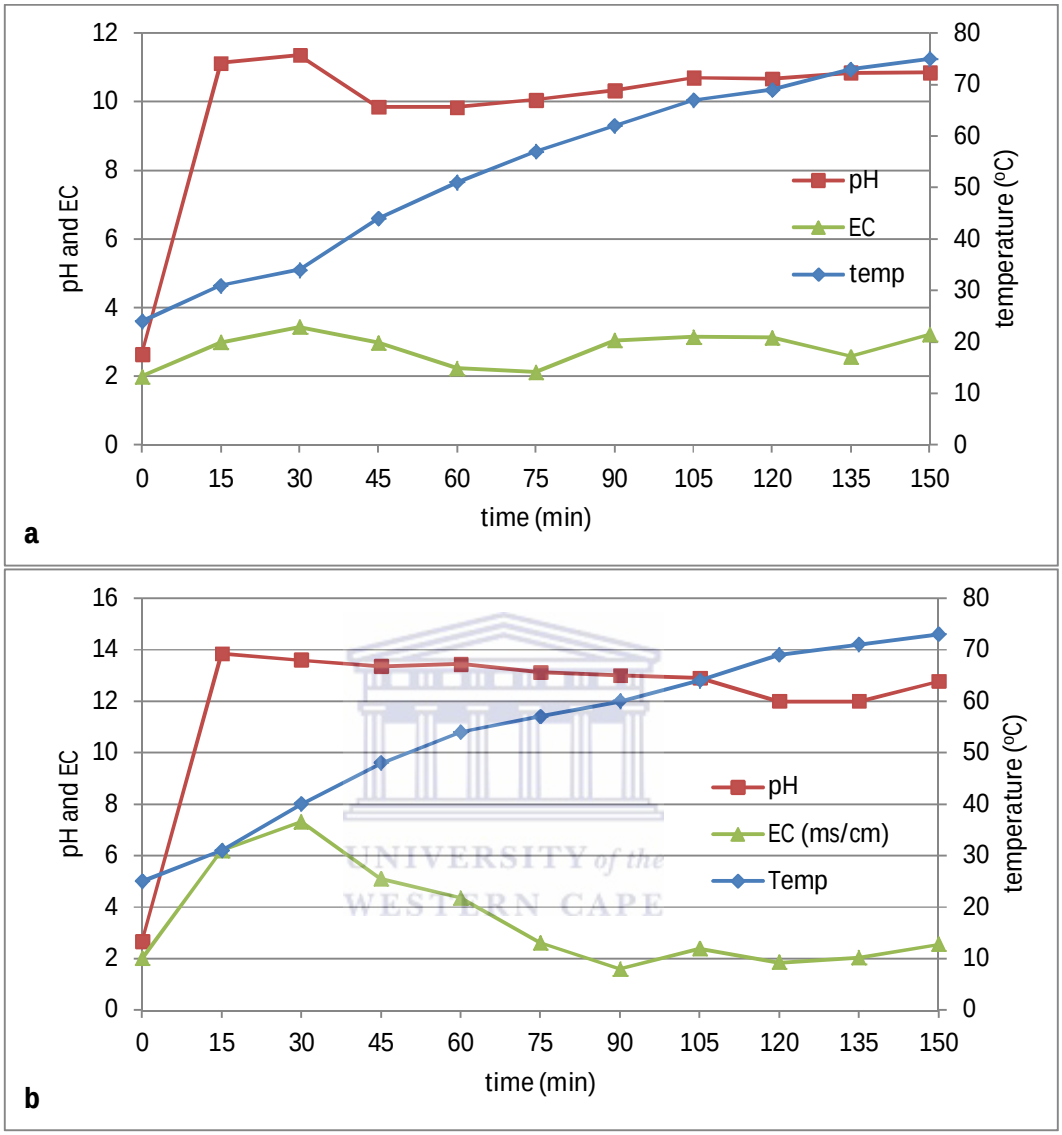

Figure 7.2.13: pH and EC profile during treatment of 80 L of Rand Uranium mine water with 8 kg of Matla coal FA, 86.58 g of $Al(OH)_3$ and 100 g (a) or 200 g (b) of lime using a jet loop reactor.

Results in Figure 7.2.13a showed that treatment of Rand Uranium mine water (80 L) with 8 kg of Matla coal FA and 100 g of lime in the jet loop reactor for 30 min resulted in the pH increasing to 11.36. After adding $Al(OH)_3$, the pH of the mixture decreased from 11.36 to

9.85 at 45 min. Then the pH started increasing gradually again as shown in Figure 7.2.13a. The EC followed the same trend as the pH.

Mixing of Rand Uranium mine water (80 L) with 8 kg of Matla coal FA and 200 g of lime in a jet loop reactor for 30 min resulted in the pH increasing to 13.59. Addition of $Al(OH)_3$ to the mixture after 30 min resulted in the pH of the mixture decreasing gradually to 12 as shown in Figure 7.2.13b. The decrease in pH after addition of $Al(OH)_3$ could be due to the formation of ettringite, which releases protons. The EC followed the same trend as the pH of the mixture in both cases. There was a gradual increase in temperature due to the hydrodynamic cavitation which was also observed previously in sections 7.2.1, 7.2.2, 7.2.3 and 7.2.4.

During treatment of Rand Uranium mine water (80 L) with 8 kg of Matla coal FA, lime (100 g or 200 g) and 86.58 g of $Al(OH)_3$ in a jet loop reactor, aliquot samples were collected after every 30 min. The samples were filtered through a 0.45 µm filter paper and analysed using ICP-OES and IC. The results obtained are shown in Figure 7.2.14.

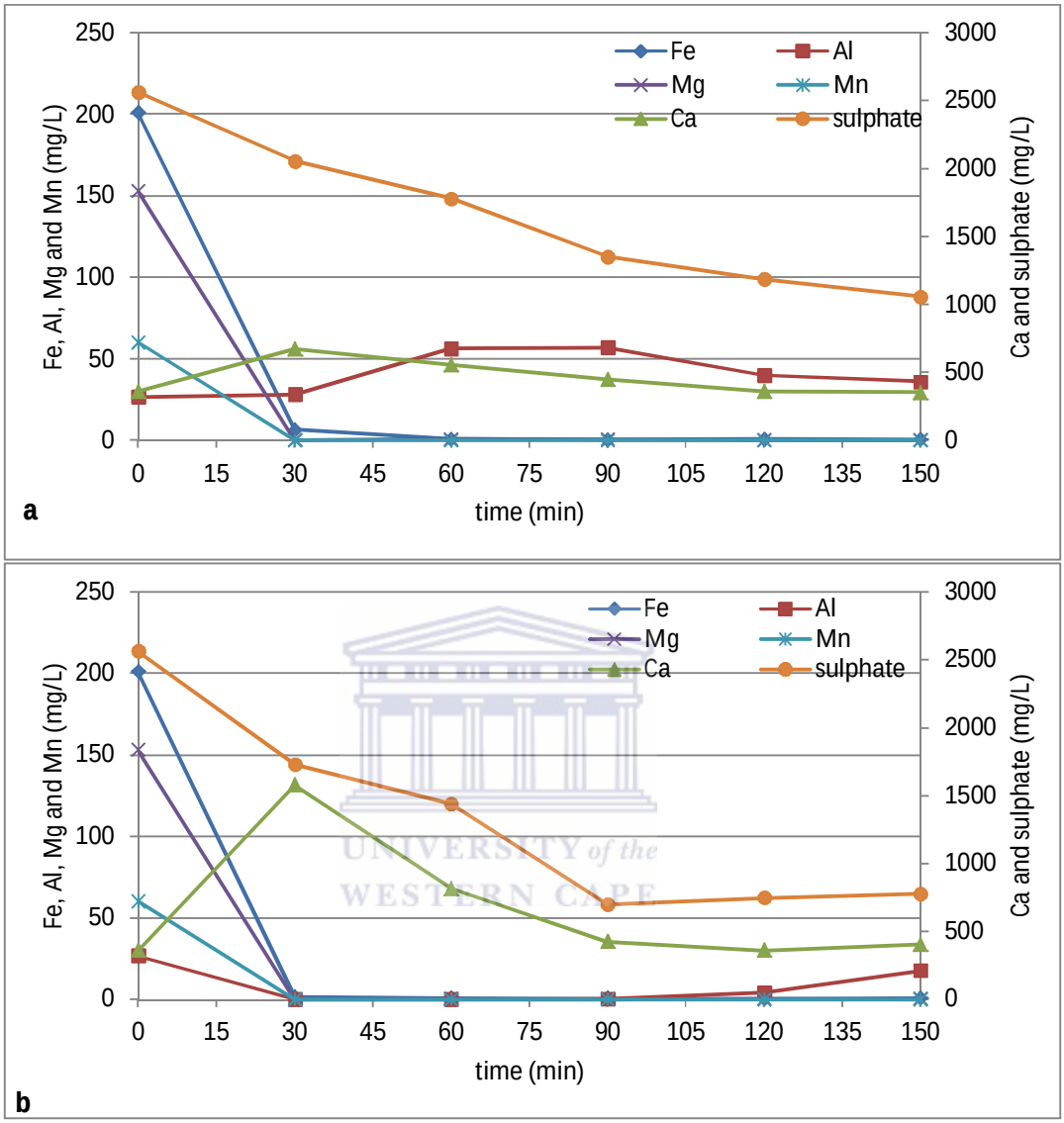

Figure 7.2.14: The Fe, Al, Mg, Mn, Ca and sulphate concentration during treatment of 80 L of Rand Uranium mine water with 8 kg of Matla FA, 86.58 g of $Al(OH)_3$ and 100 g (a) or 200 g (b) of lime using a jet loop reactor.

Treatment of Rand Uranium mine water (80 L) with 8 kg Matla coal FA and 100 g of lime in the jet loop reactor for 30 min showed that the sulphate concentration decreased from about 2500 mg/L to 2057 mg/L as shown in Figure 7.2.14a. When 200 g of lime was added to 80 L of Rand Uranium and 8 kg of Matla coal FA and mixed in a jet loop reactor for

30 min, the sulphate concentration decreased from about 2500 mg/L to 1729 mg/L as shown in Figure 7.2.14b. The sulphate concentration decreased because of gypsum precipitation. More sulphate was removed when 200 g of lime was added than when 100 g of lime was added because as more lime was added to the mixture, more Ca ions were added into the mixture resulting in the shifting of the gypsum precipitation reaction to the right according to Le Chatelier's principle. This agrees well with modelling results obtained using Act2 program of the GWB software in section 5.1.2.1. The GWB software showed that if Rand Uranium mine water was mixed with Matla coal FA sulphate ions can be removed as gypsum, if the right amount of Ca ions has been added to the solution.

After adding 86.58 g of $Al(OH)_3$ the sulphate concentration decreased to 1057 mg/L in the mixture containing 8 kg of Matla coal FA and 100 g of lime (Figure 7.2.14a). The addition of 86.58 g of $Al(OH)_3$ to the mixture containing 8 kg of Matla coal FA and 200 g of lime resulted in the decrease in sulphate concentration to 700 mg/L (Figure 7.2.14b). Adding 86.58 g of $Al(OH)_3$ to the mixture containing 8 kg of Matla coal FA and 200 g of lime showed that more sulphate ions were removed than in the mixture containing 8 kg of Matla coal FA and 100 g of lime. This was because the mixture containing 200 g of lime maintained the pH in the optimum range of ettringite stability, while the mixture containing 100 g of lime could not maintain the pH in the required range of 11.5 to 12.5 (Figure 7.2.13).

Analysis of the water during treatment of Rand Uranium mine water (80 L) with 8 kg of Matla coal FA and either 100 g or 200 g of lime showed that the Ca concentration increased in both mixtures for the first 30 min of mixing as shown in Figure 7.2.14. The Ca concentration in the mixture containing 8 kg of Matla coal FA and 100 g of lime increased from 360 mg/L to 675 mg/L after 30 min (Figure 7.2.14a). In the mixture containing 8 kg of Matla coal FA and 200 g of lime, the Ca concentration increased to 1577 mg/L after 30 min. This was due to the dissolution of CaO in both the lime and Matla coal FA added to the mine water. More Ca was added into the water when 8 kg of Matla coal FA and 200 g of lime were used than when 8 kg of Matla coal FA and 100 of lime were used because more CaO was available to dissolve. This resulted in a higher pH increase of the mixture containing 8 kg of Matla coal FA and 200 g of lime than in the mixture containing 100 g of lime and 8 kg of Matla coal FA.

After adding 86.58 g of $Al(OH)_3$, the Ca concentration decreased gradually in the mixture containing 100 g of lime and 8 kg of Matla coal to 362 mg/L after 120 min of mixing in a jet loop reactor. The Ca concentration in the mixture decreased sharply in the mixture containing 200 g of lime and 8 kg of Matla coal FA to 362 mg/L after 120 min of mixing in the jet loop reactor. The decrease in the Ca followed the same trend as the removal of sulphate ions from mine water after adding $Al(OH)_3$. This was because Ca and sulphate ions were both precipitating as ettringite.

Results depicted in Figure 7.2.14 showed that Fe, Al, Mg and Mn were removed by almost 100 % when the pH of Rand Uranium mine water was increased to greater than 10 by mixing with 8 kg of Matla coal FA and either 100 g or 200 g of lime for 30 min in a jet reactor. This agreed well with the modelling results obtained using Act2 program of the GWB software which showed that removal of Fe, Al, Mg and Mn was pH dependent. The GWB showed that Al and Fe could be removed if the pH of the mixture was above 4 (Figure 5.1.4 and 5.1.5) and Mn and Mg when the pH was above 10 (Figure 5.1.6 and 5.1.7).

During treatment of Rand Uranium mine water (80 L) with Matla FA (8 kg) and lime (200 g) in a jet reactor, a sample of the solid residues was collected after 30 min. Then after addition of 86.58 g of $Al(OH)_3$ to the mixture, another sample of the solid residues was collected after 150 min of mixing in a jet loop reactor. The two samples of the solid residues were analysed using XRD to determine the mineral composition. The spectra of the solid residues after 30 min and 150 min and the spectra of Matla coal FA, lime and $Al(OH)_3$ are shown in Figure 7.2.15.

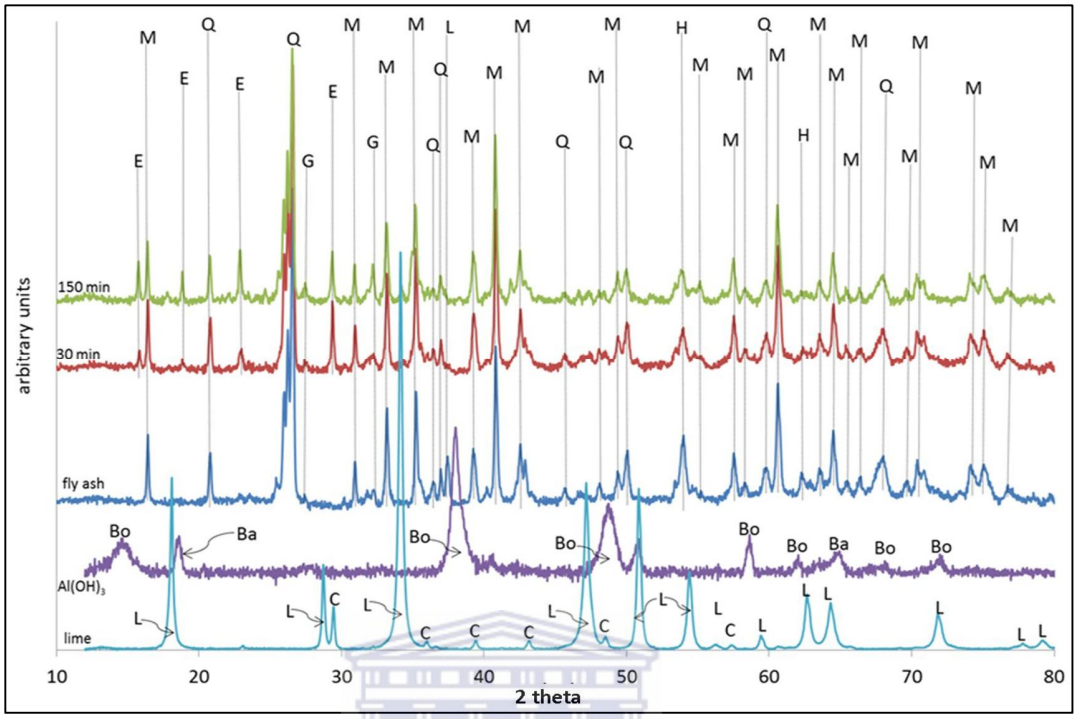

Figure 7.2.15: Comparison of the XRD spectra of lime, $Al(OH)_3$ and Matla coal FA to that of the solid residues produced during treatment of Rand Uranium mine water with 8 kg of Matla coal FA, 200 g of lime and 86.58 g $Al(OH)_3$ using a jet loop reactor (L-CaO; C-calcite; Bo-boehmite; Ba-bayerite; G-gypsum; B-bassannite; E-ettringite, A-aragonite; M-mullite; Q-quartz; H-hematite).

The XRD results showed that neither the lime nor the bayerite and boehmite peaks were present in the spectra of the solid residues. New peaks of ettringite and gypsum appeared in the spectra of both solid residues. This means that the decrease in sulphate concentration observed when Rand Uranium mine water (80 L) was treated with 8 kg of Matla coal FA and 200 g of lime before and after addition of 86.58 g of $Al(OH)_3$ was due to ettringite and gypsum precipitation. The intensity of the ettringite peaks increased in the 150 min solid residues (after addition of $Al(OH)_3$). This was because more Al was made available for formation of more ettringite by adding $Al(OH)_3$ into the reaction mixture. The disappearance of the characteristic CaO peaks in the solid residues spectra correlates well with the increase

in pH of the mixture (Figure 7.2.13). This means that the dissolution of CaO from lime and coal FA was responsible for the pH increase.

Solid residues collected at 30 min and 150 min of treatment of Rand Uranium mine water (80 L) with 8 kg of Matla coal FA, 200 g of lime and 86.58 g of $Al(OH)_3$ were analysed using XRF. The results obtained are shown in Table 7.2.4.

Table 7.2.4: Composition of Matla coal FA and the solid residues produced after treatment of Rand Uranium mine water (80 L) with 8 kg of Matla coal FA, 200 g of lime and 86.58 g of $Al(OH)_3$ in a jet loop reactor for 30 min and 150 min.

% oxide	Matla coal FA	30 min solid residue	150 min solid residue
SiO_2	48.27 ± 0.04	48.20 ± 0.05	48.24 ± 0.04
Al_2O_3	30.89 ± 0.22	31.12 ± 0.17	31.44 ± 0.25
CaO	6.71 ± 0.08	6.83 ± 0.11	7.17 ± 0.07
Fe_2O_3	2.81 ± 0.03	3.62 ± 0.01	3.49 ± 0.01
MgO	2.12 ± 0.04	2.88 ± 0.02	2.80 ± 0.07
TiO_2	1.26 ± 0.02	1.60 ± 0.04	1.53 ± 0.03
P_2O_5	0.89 ± 0.01	1.00 ± 0.2	0.95 ± 0.02
K_2O	0.84 ± 0.01	0.73 ± 0.0.3	0.70 ± 0.01
Na_2O	0.55 ± 0.01	0.58 ± 0.02	0.57 ± 0.02
SO_3	0.19 ± 0.002	0.32 ± 0.01	0.63 ±0.03
MnO	0.02 ± 0.0004	0.99 ± 0.001	0.98 ± 0.003
Loss on ignition	5.24 ± 0	1.09 ± 0.18	1.03 ± 0.05
Sum	99.79 ± 0.07	98.96 ± 0.12	99.53 ± 0.27

Results obtained on the analysis of Matla coal and solid residues collected after 30 min and 150 min showed that major elements such as Al, Ca, Fe, Mg and Mn increased in the solid residues. The amount of Al and Ca increased because of the precipitation of Al and Ca from Rand Uranium mine water as ettringite. Also the amount of Al and Ca in the solid residues increased because of the addition of $Al(OH)_3$ and lime to the mine water. The content of Fe, Mg and Mn increased in the solid residues compared to Matla coal FA because of the precipitation of these elements out of Rand Uranium mine water. This correlated well with the decrease in the concentration of Fe, Mg and Mn concentration during treatment of Rand Uranium mine water with Matla coal FA, lime and $Al(OH)_3$ (Figure 7.2.14b).

The content of SO_3 in the solid residue was higher than that of Matla coal FA. This correlated well with decrease in the sulphate concentration in the treated water during treatment of Rand Uranium mine water with Matla coal FA, lime and $Al(OH)_3$ (Figure 7.2.14b). The content of Na_2O and P_2O_5 in Matla coal FA was almost the same to that of the solid residues collected after 150 min. This was because Rand Uranium mine water contained small quantities of P and Na which did not change during treatment of Rand Uranium mine water. The SiO_2 content in solid residues was the same as that of Matla coal FA.

Treatment of mine water with 8 kg of Matla coal FA, lime (100 g or 200 g) and 86.58 g of $Al(OH)_3$ in a jet loop reactor, have shown that most major elements such as Fe, Al, Mg and Mn were removed from mine water to within the TWQR for potable water. The sulphate concentration was reduced to 700 mg/L when Rand Uranium mine water (80 L) was treated with 8 kg of Matla coal FA, 200 g of lime and 86.58 g of $Al(OH)_3$. This amount of sulphate ions was still above the TWQR for potable water.

The following set of experiments were carried out in order to reduce the sulphate concentration to less than 500 mg/L. Rand Uranium mine water was treated with 13 kg of Matla coal FA, lime (100 g or 200 g) and 86.58 g of $Al(OH)_3$ in a jet loop reactor. It was chosen to increase more coal FA and not lime in this case so as to avoid the costs associated with lime. The pH, EC and temperature profile during treatment of Rand Uranium mine water under these conditions is as shown in Figure 7.2.16.

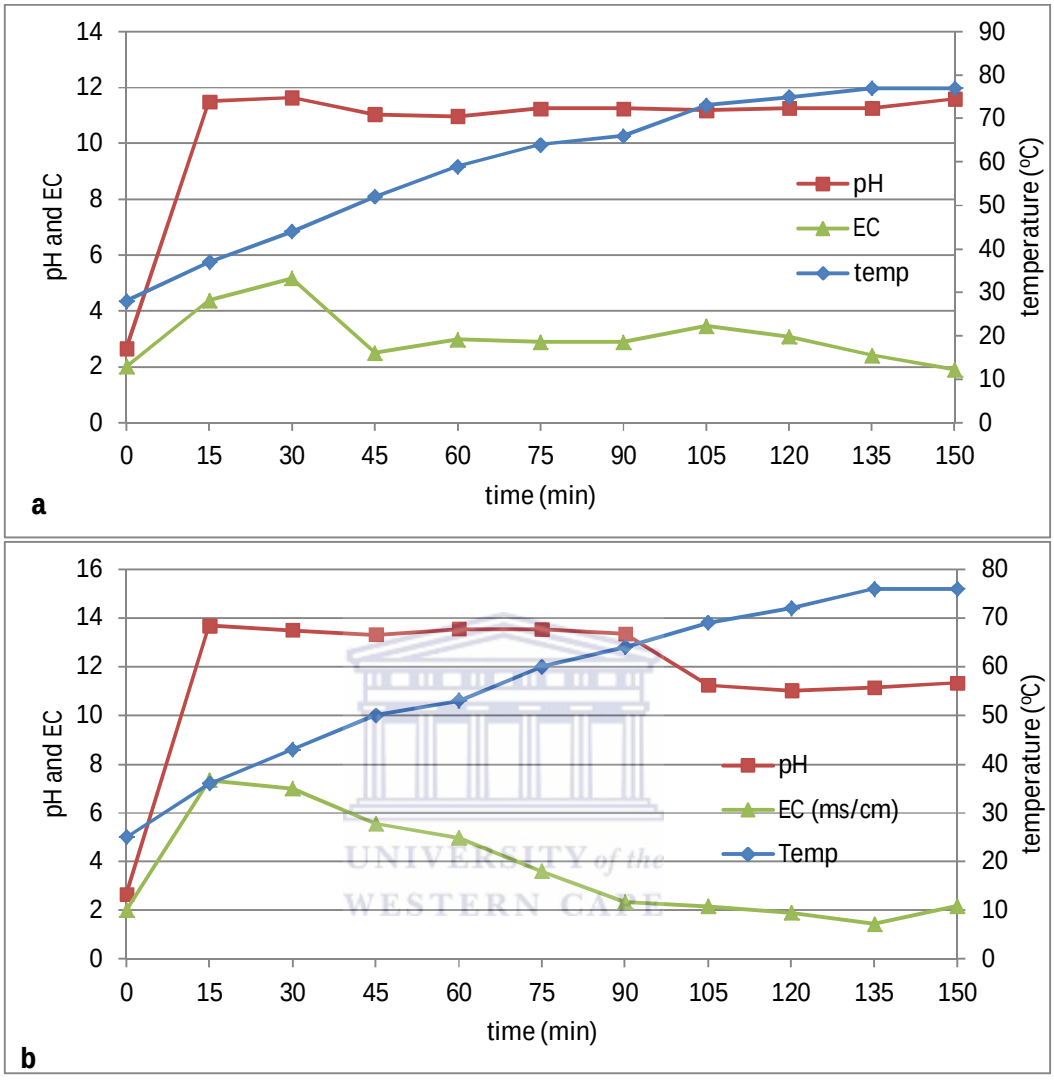

Figure 7.2.16: pH and EC profile during treatment of 80 L of Rand Uranium mine water with 13 kg of Matla coal FA, 86.58 g of $Al(OH)_3$ and 100 g (a) or 200 g (b) of lime using a jet loop reactor.

When Rand Uranium mine water (80 L) was mixed with 13 kg of Matla coal FA and 100 g or 200 g of lime for 30 min, the pH increased to 11.64. After 30 min of mixing Rand Uranium mine water with Matla coal FA and lime, 86.58 g of $Al(OH)_3$ was added to the mixture. Addition of $Al(OH)_3$ resulted in the pH of the mixture decreasing slightly to 11.04 as shown in Figure 7.2.16a. The EC also followed the same trend. The EC of the solution containing 100 g of lime decreased sharply from 5.12 mS/cm to 2.5 mS/cm after 15 min of addition of

$Al(OH)_3$ to the mixture. The EC was maintained around 2.5 mS/cm for the duration of the experiment.

Treatment of Rand Uranium mine water (80 L) with 13Kg of Matla coal FA and 200 g of lime for 30 min resulted in the pH increasing to 13.69. After addition of 86.58 g of $Al(OH)_3$ the pH decreased gradually to 11.24 as shown in Figure 7.2.16b. The EC also followed the same trend. The EC initially increased to 7.5 mS/cm after mixing Rand Uranium mine water with Matla coal FA and 200 g of lime. The EC decreased gradually from about 7.5 mS/cm to about 2 mS/cm after addition of 86.58 g of $Al(OH)_3$. The decrease in EC can be attributed to the removal of Ca and sulphate ions from the mixture due the formation of ettringite as was observed before.

The increase in pH and EC after addition of Matla coal FA and lime was due to the dissolution of lime. Addition of 200 g of lime resulted in pH increasing more compared to the mixture containing 100 g of lime. The EC increased because of the increase in the concentration of Ca ions in the water. After addition of $Al(OH)_3$ the pH and EC decreased. The pH decreased because the formation of ettringite produced acidity, while the EC decreased because of the removal of sulphate and Ca ions during the formation of ettringite. In both mixtures the temperature increased from around 25 ^oC to about 80 ^oC. This was caused by hydrodynamic cavitation that occurred inside the jet loop reactor.

During treatment of Rand Uranium mine water (80 L) with 13 kg of Matla coal FA and lime (100 g or 200 g) and 86.58 g of $Al(OH)_3$, aliquot samples were collected after every 30 min. The samples were filtered through a 0.45 µm filter paper and analysed using ICP-OES and IC. The results obtained are shown in Figure 7.2.17.

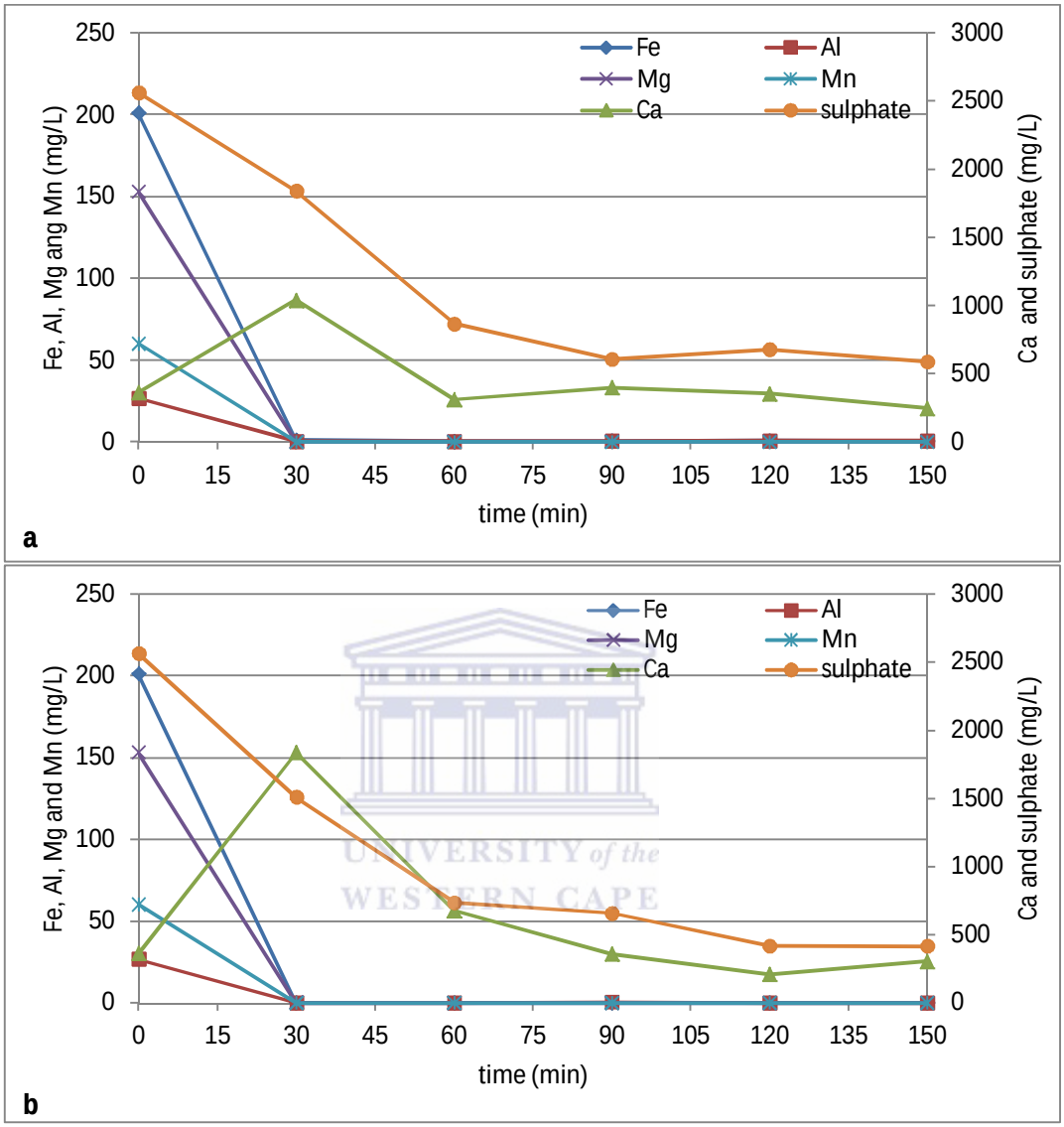

Figure 7.2.17: The Fe, Al, Mg, Mn, Ca and sulphate concentration during treatment of 80 L of Rand Uranium mine water with 13 kg of Matla FA, 86.58 g of $Al(OH)_3$ and 100 g (a) or 200 g (b) of lime.

As shown in Figure 7.2.17, treatment of Rand Uranium mine water (80 L) with 13 kg of Matla coal FA, lime (100 g or 200 g) has resulted in the removal of Fe, Al, Mn and Mg by almost 100 %. These results agreed well with the modelling results obtained using Act2 program of the GWB software. It showed that removal of Fe, Al, Mn and Mg from Rand Uranium mine

water was pH dependent. The modelling results had showed that Al could be removed as alunite and gibbsite when the pH was increased to greater than 5, while Fe could be removed as, jarosite-K and $Fe(OH)_3$ when the pH of Rand Uranium mine water was increased to greater than 4 (Figure 5.1.4 and 5.1.5). The GWB modelling results also showed that Mn and Mg could be removed if the pH of Rand Uranium mine water was increased to greater than 10 as $Mn(OH)_2$ and $Mg(OH)_2$ (Figure 5.1.6 and 5.1.7).

During treatment of Rand Uranium mine water (80 L) with 13 kg of Matla coal FA and 100 g of lime in jet reactor for 30 min the sulphate concentration decreased from about 2500 mg/L to about 1840 mg/L and the Ca concentration increased from 360 mg/L to 1038 mg/L as shown in Figure 7.2.17a. The sharp increase in Ca concentration could have caused the increase in EC (Figure 7.2.16a). After 30 min, 86.58 g of $Al(OH)_3$ was added to the mixture and the concentration of sulphate decreased further from 1038 mg/L to about 600 mg/L and the Ca concentration decreased from 1038 mg/L to 300 mg/L after 90 min. The decrease in the sulphate and Ca concentration was ascribed to the formation of ettringite and correlates well with the decrease in the EC observed after addition of $Al(OH)_3$ (Figure 7.2.16a)

Treatment of Rand Uranium mine water (80 L) with 13 kg and 200 g of lime in jet reactor for 30 min resulted in the sulphate concentration decreasing from about 2500 mg/L to about 1500 mg/L and the Ca concentration increasing from 360 mg/L to 1838 mg/L as shown in Figure 7.2.17b. Adding 86.58 g of $Al(OH)_3$ resulted in the sulphate concentration decreasing further to 418 mg/L and the Ca concentration decreasing from 1838 mg/L to 300 mg/L after 120 min. The decrease in sulphate and Ca concentration after addition of $Al(OH)_3$ was ascribed to the formation of ettringite and correlates well with the decrease in EC (Figure 7.2.16b).

There was more sulphate ions removed in the mixture containing 200 g of lime than the mixture containing 100 g of lime. This was because of the fact that as more Ca was added in the form of lime to the mixture, more Ca was available to participate in the removal of sulphate ions in the form of ettringite and/ or gypsum (Figure 7.2.17). The Ca concentration initially increased in both mixtures, due to the dissolution of CaO in Matla coal FA and the

extra lime added. After adding $Al(OH)_3$ to both mixtures the Ca concentration decreased as it participated in the formation of ettringite. The decrease in Ca concentration after adding $Al(OH)_3$ explains why the EC decreased in Figure 7.2.16.

The solid residues that were produced from treating Rand Uranium mine water (80 L) with 13 kg of Matla FA, 200 g of lime and 86.58 g of $Al(OH)_3$ were analysed using XRD. The spectra of the solid residues were compared to the XRD spectra of $Al(OH)_3$, lime and Matla FA as shown in Figure 7.2.18.

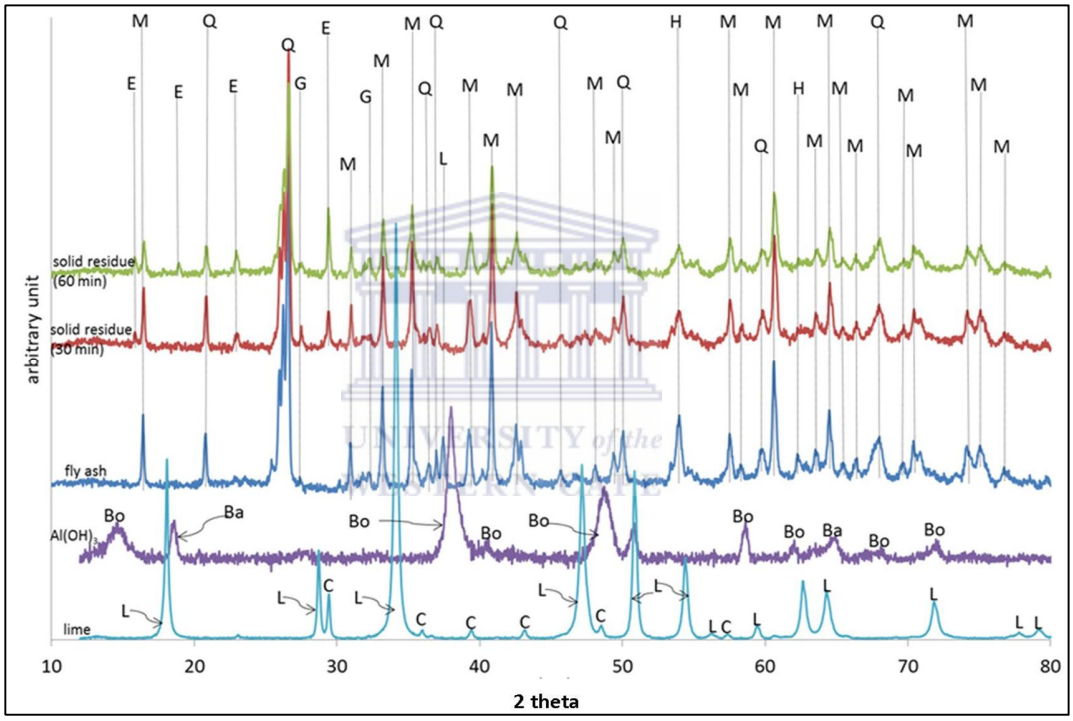

Figure 7.2.18: Comparison of the XRD spectra of lime, $Al(OH)_3$ and Matla fly ash to that of the solid residues produced during treatment of 80 L of Rand Uranium mine water with 13 kg of fly ash, 200 g of lime and 86.58 g of $Al(OH)_3$ using a jet loop reactor (L-CaO; C-calcite; Bo-boehmite; Ba-bayerite; G-gypsum; B-bassannite; E-ettringite, A-aragonite; M-mullite; Q-quartz; H-hematite).

The results showed that the characteristic peaks of CaO (in fly ash and lime spectra), as well as the boehmite and bayerite peaks (in $Al(OH)_3$ spectrum) disappeared and ettringite peaks

emerged in the solid residues spectra. The disappearance of the CaO peaks was due to its dissolution during mixing with Rand Uranium mine water in a jet loop reactor. This resulted in the observed pH increase of the mixture as shown in Figure 7.2.16b. The disappearance of the boehmite and bayerite peaks (Figure 7.2.18) and the concomitant decrease of the concentration of Ca and sulphate ions after addition of $Al(OH)_3$ into the reaction mixture (Figure 7.2.17b) resulted in the appearance of the ettringite peaks (Figure 7.2.18). The XRD confirmed that sulphate removal was due to the formation of ettringite and gypsum.

The solid residues that were sampled after 30 min and 150 min during treatment of Rand Uranium mine water (80 L) with 13 kg of Matla coal FA, 200 g of lime and 86.58 g of $Al(OH)_3$ at 30 min were analysed using XRF. The results obtained were compared to the XRF results of Matla coal FA as shown in Table 7.2.5.

Table 7.2.5: Composition of Matla coal FA and the solid residues produced after treatment of Rand Uranium mine water (80 L) with 13 kg of Matla coal FA, 200 g of lime and 86.58 g of $Al(OH)_3$ in a jet loop reactor for 30 min and 150 min.

% oxide	Matla coal FA	30 min solid residue	150 min solid residue
SiO_2	48.27 ± 0.04	48.22 ± 0.07	48.16 ± 0.14
Al_2O_3	30.89 ± 0.22	30.94 ± 0.16	31.51 ± 0.09
CaO	6.71 ± 0.08	6.14 ± 0.07	6.72 ± 0.01
Fe_2O_3	2.81 ± 0.03	3.50 ± 0.05	3.41 ± 0.05
MgO	2.12 ± 0.04	2.77 ± 0.01	2.72 ± 0.09
TiO_2	1.26 ± 0.02	1.29 ± 0.03	1.25 ± 0.04
P_2O_5	0.89 ± 0.01	0.98 ± 0.04	0.95 ± 0.01
K_2O	0.84 ± 0.01	0.76 ± 0.03	0.74 ± 0.01
Na_2O	0.55 ± 0.01	0.68 ± 0.05	0.57 ± 0.02
SO_3	0.19 ± 0.002	0.41 ± 0.01	0.71 ± 0.01
MnO	0.02 ± 0.0004	0.06 ± 0.002	0.06 ± 0.001
Loss on ignition	5.24 ± 0	3.99 ± 1.34	3.08 ± 1.02
Sum	99.79 ± 0.07	99.74 ± 0.17	99.88 ± 0.05

The results in Table 7.2.5 show that there was an increase in the content of Al, Fe, Mg, Mn and S in the solid residues. This was because of the precipitation of these elements out of the mine water and their incorporation into the solid residue. This correlated well with the observed decrease in the concentration of sulphate ions during the treatment of Rand

Uranium mine water (80 L) with 13 kg of Matla coal FA, 200 g of lime and 86.58 g of $Al(OH)_3$ (Figure 7.2.17b). The Ca content initially increased in the first 30 min. This was due to the dissolution of CaO thereby causing the sharp increase in pH (Figure 7.2.16b) and Ca concentration (Figure 7.2.17b) noticed during the first 30 min. The solid residues collected after 150 min had more Ca content than the solid residue collected after 30 min. This was because of the decrease in the Ca concentration over time after addition of $Al(OH)_3$ in the reaction mixture as shown in Figure 7.2.17b.

From all the combination of chemicals used under the applied conditions; treatment of Rand Uranium mine water (80 L) with 13 kg of Matla FA, 200 g of lime and 86.58 g of $Al(OH)_3$ resulted in the removal of most major elements to within TWQR for potable water. This also resulted in the sulphate concentration decreasing to less than 500 mg/L, which was within the TWQR for potable water (WHO, 2011; DWAF, 1996).

The effect of $Al(OH)_3$, the effect of Matla coal FA, the effect of the combination of lime and $Al(OH)_3$, the effect of the combination of Matla coal FA and $Al(OH)_3$ and the effect of the combination of Matla coal FA, lime and $Al(OH)_3$ on the removal of sulphate ions and heavy metals have been investigated systematically using a jet loop reactor. The following section explains the effect of treating mine water with a jet loop reactor first followed by overhead stirring. This was done to find out if the hydrodynamic cavitation can be initially used to dissolve the CaO in coal FA and lime, and then further reactions can take place under normal stirring. If the results prove to be positive, then the intense mixing in a jet loop reactor which caused the temperature to increase could be avoided and save energy.

7.2.6. EFFECT OF JET REACTOR MIXING FOLLOWED BY OVERHEAD STRIRRING

Treatment of Rand Uranium mine water using Matla coal FA, lime and $Al(OH)_3$ in a jet reactor enhanced the removal of sulphate ions (section 7.2.5). The following set of experiments were carried out to determine if the formation of ettringite was enhanced by hydrodynamic mixing, or whether hydrodynamic mixing was important for the initiation of the reaction by releasing the Ca ions from Matla coal FA and lime.

Rand Uranium mine water (80 L) was mixed with 13 kg of Matla coal FA and 100 g of lime. Aluminium hydroxide (86.58 g) was added after 30 min of mixing with a jet loop reactor. About 1 L of the sample was collected and mixed using an overhead stirrer after 15 min of the addition of $Al(OH)_3$ as outlined in section 3.8.2.6. Temperature, pH and EC were continuously measured after every 15 min and the results are shown in Figure 7.2.19.

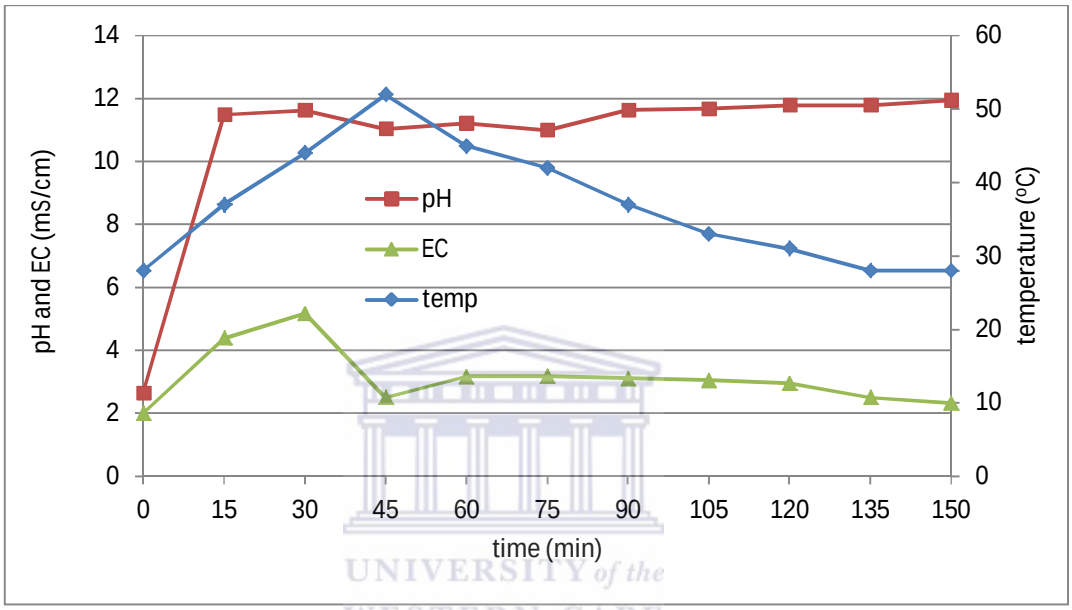

Figure 7.2.19: pH, EC and temperature profile during treatment of 80 L of Rand Uranium mine water with 13 kg of FA, 100 g of lime and 86.58 g of $Al(OH)_3$ in a jet loop rector for 45 min followed by normal mixing in an open tank.

The results in Figure 7.2.19 show that the temperature of the mixture increased in first 45 min when the mixing was done in a jet loop reactor due to hydrodynamic cavitation. Changing the mixing technique to the use of normal overhead stirrer resulted in a gradual decrease in temperature.

The pH of the mixture increased sharply from 2.65 to 11.5 in first the 15 min during mixing of Rand Uranium mine water with FA and lime using a jet loop reactor. This was because of the dissolution of CaO from Matla coal FA and lime. A slight decrease in pH to 11.04 was noticed after the addition of $Al(OH)_3$ at 30 min, which increased slightly again after 75 min due to the formation of ettringite which produces protons. The EC of the mixture followed

the trend of pH. The EC of the mixture increased rapidly in first 30 min of mixing of Rand Uranium mine water with lime and FA. After addition of $Al(OH)_3$ the EC of mixture decreased sharply and then remained constant.

During treatment of Rand Uranium mine (80 L) with 13 kg of Matla coal FA, 100 g of lime and 86.58 g of $Al(OH)_3$, aliquot samples were collected after every 30 min. The first 45 min of mixing was done in a jet loop reactor followed by overhead stirring until the end of the treatment process. The samples were filtered through a 0.45 µm filter paper and then analysed using IC. The results of the sulphate concentration obtained from the IC analysis are shown in Figure 7.2.20.

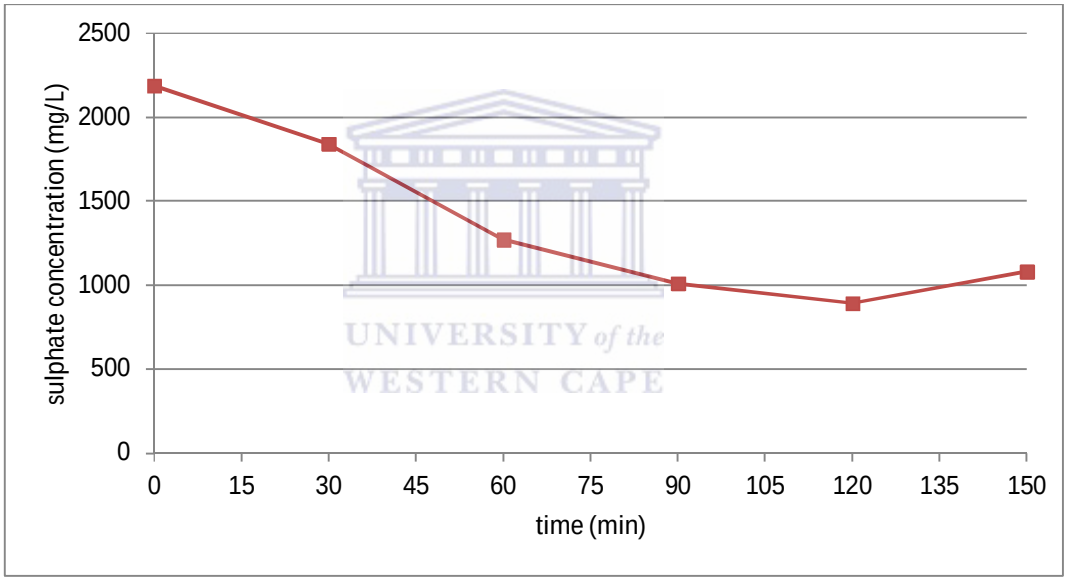

Figure 7.2.20: The sulphate concentration during treatment of 80 L of Rand Uranium mine water with 13 kg of FA, 100 g of lime and 86.58 g of $Al(OH)_3$ in a jet loop rector for 45 min followed by normal mixing in an open tank.

Results in Figure 7.2.20 showed that the sulphate concentration of the mixture decreased from 2188 mg/L to 1840 mg/L during mixing of Rand Uranium mine water with Matla coal FA and lime in the first 30 min. After addition of $Al(OH)_3$ and changing the mixing technique, the sulphate concentration continued to decrease to 1270 mg/L after 60 min. After 90 and

120 min the sulphate concentration was 1009 and 893 mg/L respectively as shown in Figure 7.2.20.

These results showed that the mixing of Rand Uranium mine water (80 L), 13 kg of Matla coal FA, 100 g of lime and 86.58 g of $Al(OH)_3$ using a jet loop reactor followed by overhead mixing decreased the rate of removal of sulphate ions compared to when the mixing was done in a jet loop reactor only (Figure 7.2.18). When the same mixture was mixed in a jet loop reactor the sulphate concentration was 606 mg/L, 678 mg/L and 587 mg/L after 90, 120 and 150 min respectively. This showed that hydrodynamic mixing that occurred in the jet loop reactor increased the rate of formation of ettringite and thus enhanced the removal of sulphate ions.

Treatment of Rand Uranium mine water (80 L) with 13 kg of Matla coal FA, 200 g of lime and 86.58 g of $Al(OH)_3$ removed the major ions such as Fe, Al, Mn, Mg and sulphate ions to within the TWQR for potable water. The following section presents the composition of the product water in terms of the potentially toxic and radioactive elements during treatment of Rand Uranium mine water (80 L) with 13 kg of Matla coal FA, 200 g of lime and 86.58 g of $Al(OH)_3$.

7.2.7. POTENTIALLY TOXIC AND RADIOACTIVE ELEMENTS

During treatment of Rand Uranium mine water (80 L) with 13 kg of Matla coal FA, 200 g lime and 86.58 g of $Al(OH)_3$ using a jet reactor as described in section 3.8.2.4, the product water met the requirements for potable water in terms of Fe, Al, Mn, Mg and sulphate concentration. Aliquot samples that were collected during treatment of Rand Uranium mine water (80 L) with 13 kg of Matla coal FA, 200 g of lime and 86.58 g of $Al(OH)_3$ after every 30 min, were filtered through a 0.45 µm filter paper and analysed using ICP-OES. This was done to establish the concentration of naturally occurring radioactive materials (NORM) such as Th and U as well as other potentially toxic trace elements. The results are presented in section 7.2.7.1 to section 7.2.7.6.

7.2.7.1. Uranium and thorium

When Rand Uranium mine water was treated with 13 kg of Matla coal FA, 200 g lime and 86.58 g of $Al(OH)_3$, the ICP-OES analysis of the product water has shown that Th and U were removed by almost 100 %, as shown in Figure 7.2.21.

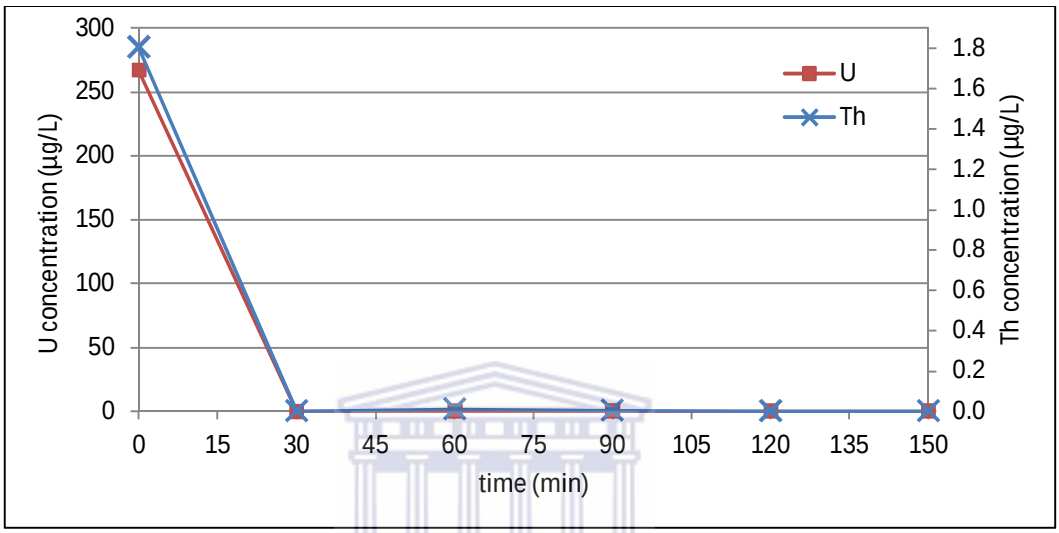

Figure 7.2.21: The Th and U concentration in the product water during treatment of Rand Uranium mine water (80 L) with 13 kg of Matla coal FA, 200 g lime and 86.58 g of $Al(OH)_3$.

Results in Figure 7.2.21, show that most of the Th and U was removed before the addition of $Al(OH)_3$ into the mixture (in the first 30 min). This means the removal of Th and U was due to the addition of Matla coal FA and lime. According to the GWB modelling results obtained using the Act2 sub program, the removal of Th and U was predicted to be pH dependent. Th and U were predicted to start precipitating at pH 5 and 3 as thorianite (ThO_3) and uraninite (UO_3) respectively (Figure 5.1.10 and 5.1.11). After 30 min of mixing Rand Uranium mine water (80 L) with 13 kg of Matla coal FA and 200 g of lime the pH was greater than 10, which means that Th and U could have been removed as ThO_3 and UO_3. The U concentration in Rand Uranium mine water was 267 µg/L. This was almost 10 times higher than the required limit for potable water. After treatment with Matla coal FA and lime for 30 min the U concentration decreased to 0.08 µg/L which was less than the limit for U in potable water of 30 µg/L (WHO, 2011). The limit of total concentration of Th for potable water is not stated

in the WHO guidelines for drinking water. Only the radioactivity limits for ^{227}Th (10 Bq/L), ^{228}Th (1 Bq/L), ^{230}Th (1 Bq/L) and ^{232}Th (1 Bq/L) are stated in WHO guidelines for drinking water.

The solid residues collected after 30 min and 150 min of treatment of Rand Uranium mine water (80 L) with Matla coal FA, 200 g of lime and 86.58 g of $Al(OH)_3$ were analysed using laser ablation-inductively coupled-mass spectrometer (LA-ICP-MS) to determine the concentration of Th and U. The results obtained are shown in Figure 7.2.22.

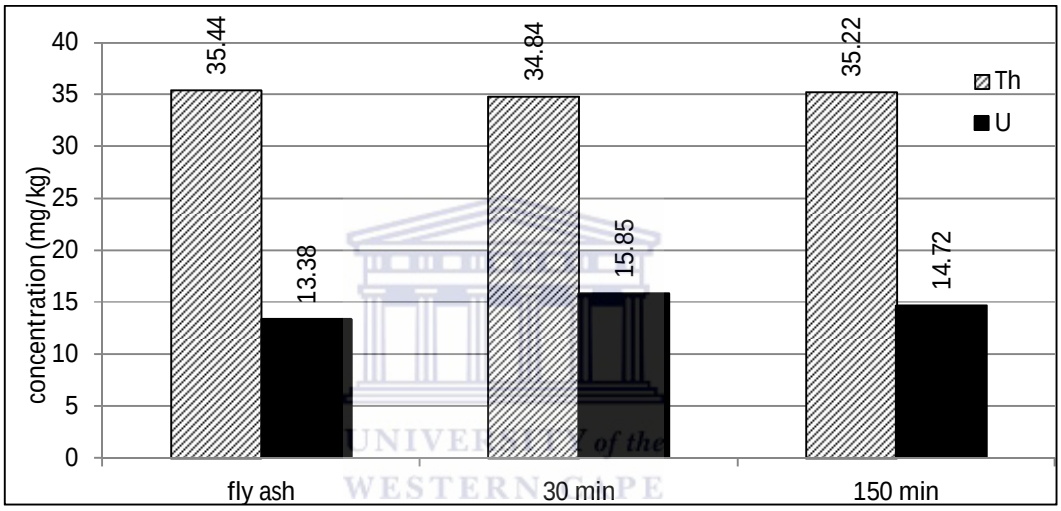

Figure 7.2.22: The concentration of Th and U in Matla coal FA compared to the solid residues collected after 30 min and 150 min of treating Rand Uranium mine water (80 L) with 13 kg of Matla coal FA, 200 g of lime and 86.58 g of $Al(OH)_3$ in jet reactor.

The results from the analysis of Matla coal FA and the solid residues using LA-ICP-MS showed that the concentration of U increased in the first 30 min of treating Rand Uranium mine water with 13 kg of Matla coal FA and 200 g of lime. The concentration of U in solid residues collected after 30 min and 150 min were almost the same. This correlates well with the results shown in Figure 7.2.21, which showed a sharp decrease of the concentration of U during the first 30 min of treatment. The concentration of Th in the solid residues collected after 30 min and 150 min was close to that in Matla coal FA. This was because the concentration of Th in Matla coal FA was orders of magnitude greater than that was in Rand Uranium mine water. So even after Th precipitated from Rand Uranium mine water as

shown in Figure 7.2.21 and form part of the solid residues, no significant change was noted in the solid residues.

7.2.7.2. Zinc, nickel and copper

Rand Uranium mine water (80 L) was treated with 13 kg of Matla coal FA, 200 g of lime and 86.58 g of $Al(OH)_3$for 150 min in a jet loop reactor. The product water was analysed using ICP-OES for Zn, Ni and Cu and the results obtained are shown in Figure 7.2.23.

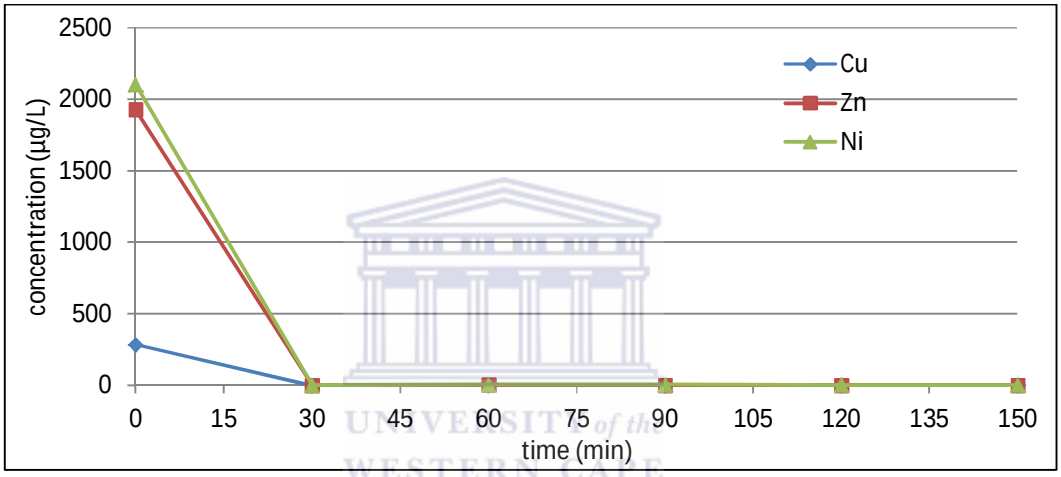

Figure 7.2.23: The Zn, Ni and Cu concentration in the product water during treatment of Rand Uranium mine water (80 L) with 13 kg of Matla coal FA, 200 g lime and 86.58 g of $Al(OH)_3$.

As Figure 7.2.23 shows, Rand Uranium mine water contained 284.86 µg/L, 2107.90 µg/L and 1931µg/L of Cu, Ni and Zn respectively. These values for Cu and Zn were less than the potable limit of 3000 µg/L and 2000 µg/L respectively. There is no value set for Ni for potable water (WHO, 2011; DWAF, 1996). The results in Figure 7.2.23 show that Zn, Ni and Cu were removed by almost 100 %. The removal occurred in the first 30 min of mixing mine water with Matla coal FA and lime. This shows that the removal of Zn, Ni and Cu from Rand Uranium mine water occurred because of the addition of Matla coal FA and lime. Removal of Zn, Ni and Cu from Rand Uranium mine water occurred due the increase in pH. It was

reported that Zn, Ni and Cu could be removed by 80-100 % when the pH was increased to between 8-9 by addition of limestone (Aziz et al., 2008).

The solid residues collected after 30 min and 150 min of treatment of Rand Uranium mine water (80 L) with Matla coal FA, 200 g of lime and 86.58 g of $Al(OH)_3$ were analysed using LA-ICP-MS to determine the concentration of Zn, Ni and Cu. The results obtained are shown in Figure 7.2.24.

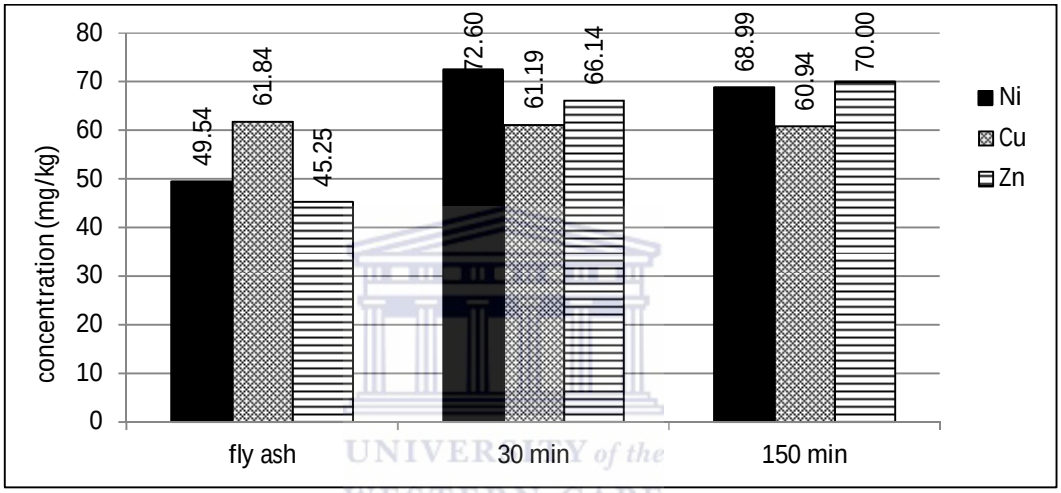

Figure 7.2.24: The concentration of Ni, Cu and Zn in Matla coal FA compared to the solid residues collected after 30 min and 150 min of treating Rand Uranium mine water (80 L) with 13 kg of Matla coal FA, 200 g of lime and 86.58 g of $Al(OH)_3$ in jet reactor.

The LA-ICP-MS analysis of the solid residues obtained after 30 min of treating Rand Uranium mine water (80 L) with 13 kg of Matla coal FA and 200 g of lime showed that the concentration of Ni and Zn was higher than that in Matla coal FA (Figure 7.2.24). The concentration of Ni and Zn in Matla coal FA was 49.54 and 45.25 mg/kg respectively. The solid residues collected after 30 min of treating Rand Uranium mine water (80 L) with 13 kg of Matla coal, 200 g of lime contained 72.60 mg/kg of Ni and 66.14 mg/kg of Zn. This correlates with the decrease in the concentration of Ni and Zn during treatment of Rand Uranium mine water (80 L) with 13 kg of Matla coal FA, 200 g of lime and 86.58 g of $Al(OH)_3$ using a jet reactor (Figure 7.2.23). The concentration of Ni and Zn in the 150 min solid

residue was 68.99 mg/kg and 70 mg/kg respectively. The increase in the concentration of Ni and Zn observed in the solid residue was due the precipitation of these elements from Rand Uranium mine water. After 30 min the concentration of Ni and Zn in the treated water was almost zero. Therefore the concentration of these elements remained the same in the solid residues collected after that point; since there was nothing further to remove from Rand Uranium mine water after 30 min.

The concentration of Cu in the solid residues collected after 30 min (61.19 mg/kg) and 150 min (60.94 mg/kg) was almost the same as the concentration in the Matla coal FA (61.84 mg/kg). This was because the amount of Cu in the Rand Uranium mine was very low as shown in Figure 7.2.25. Although the Cu present in Rand Uranium mine water precipitated out at 30 min treatment time, the amount in the mine water was not high enough to cause a significant change in the amount of Cu that was already in Matla coal FA.

7.2.7.3. Arsenic and lead

Rand Uranium mine water (80 L) was treated with 13 kg of Matla coal FA, 200 g of lime and 86.58 g of $Al(OH)_3$ in a jet loop reactor for 150 min. Aliquot samples were collected after every 30 min to determine the concentration of As and Pb in the product water using ICP-OES and the results obtained are shown in Figure 7.2.25.

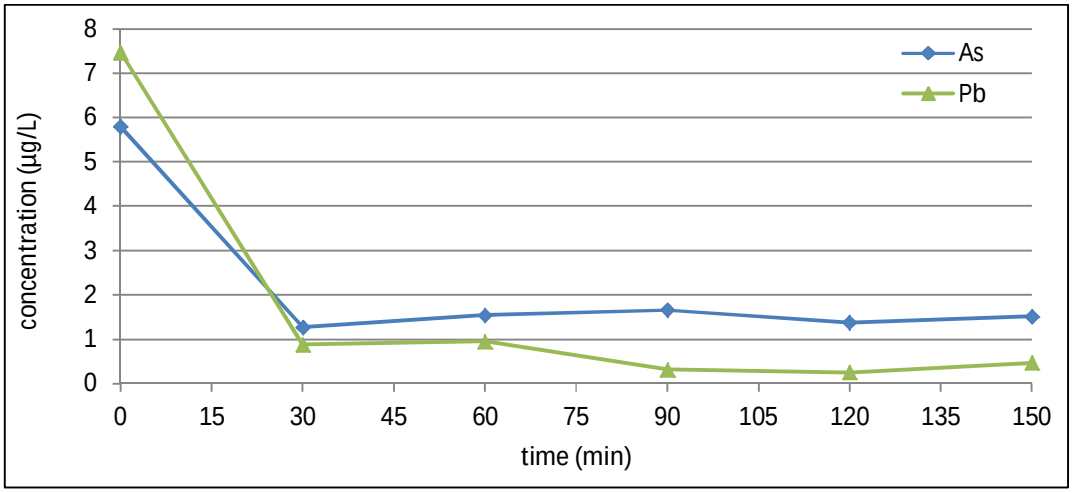

Figure 7.2.25: The As and Pb concentration in the product water during treatment of Rand Uranium mine water (80 L) with 13 kg of Matla coal FA, 200 g lime and 86.58 g of $Al(OH)_3$.

Rand Uranium mine water contained 7.48 µg/L of Pb and 5.79 µg/L of As. The concentration of As was above the TWQR for potable water of 0-1 µg/L and the concentration of Pb was within the TWQR for potable water of 0-10 µg/L (WHO, 2011; DWAF, 1996). The ICP-OES results in Figure 7.2.25 show that about 75 % of As and Pb was removed from Rand Uranium mine water. Removal of Pb from mine water is known to be due to the precipitation as $Pb(OH)_2$ which occurs when the pH of the mine water is increased to greater than 8 (Aziz et al., 2008). In this case the pH was greater than 10 after 30 min. This resulted in the decrease of the Pb concentration from 7.48 µg/L to 0.88 µg/L in 30 min.

The As concentration in mine water decreased from 5.79 µg/L to 1.27 µg/L when Rand Uranium mine water (80 L) was treated with 13 kg of Matla coal FA and 200 g of lime in a jet loop reactor. Removal of As from mine water is known to be due to adsorption on to FeOOH through octahedral bidentate-binuclear coordination mechanism (Dong et al., 2011; Guan et al., 2009). Since Rand Uranium mine water contained about 200 mg/L Fe (Table 4.6.1), the removal of As from Rand Uranium mine water could be attributed to the adsorption to FeOOH precipitates. The FeOOH forms in situ during treatment of Rand Uranium mine water with Matla coal FA and lime. The hydroxide minerals of Fe were also

predicted to form in Rand Uranium mine water by the Act2 program of the GWB software (Figure 5.1.5)

The solid residues collected after 30 min and 150 min of treatment of Rand Uranium mine water (80 L) with Matla coal FA, 200 g of lime and 86.58 g of $Al(OH)_3$ were analysed using LA-ICP-MS to determine the concentration of Pb and As. The results obtained are shown in Figure 7.2.26.

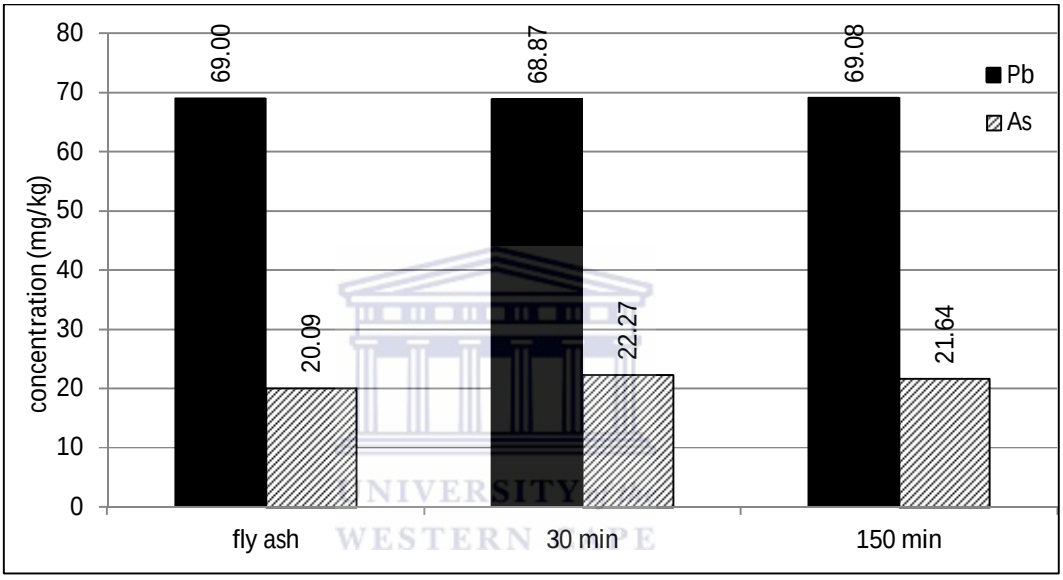

Figure 7.2.26: The concentration of Pb and As in Matla coal FA and solid residues collected after 30 min and 150 min of treating Rand Uranium mine water (80 L) with 13 kg of Matla coal FA, 200 g of lime and 86.58 g of $Al(OH)_3$ in jet reactor.

The results of the solid residue composition obtained using LA-ICP-MS showed that the concentration of As and Pb in Matla coal FA and the solid residues was almost the same. This was because the concentration of As and Pb in Rand Uranium mine water was orders of magnitude lower than in Matla coal FA. Therefore when As and Pb precipitated out or were adsorbed onto coal FA as shown in Figure 7.2.26, it was too little to cause a measurable change in the amount of these elements which were also present in Matla coal FA.

7.2.7.4. Beryllium, cadmium and selenium

When Rand Uranium mine water was treated with Matla coal FA, lime and $Al(OH)_3$ the ICP-OES analysis of the product water has shown that almost 100 % of Be and Cd and 78 % of Se was removed after 30 min as shown in Figure 7.2.27.

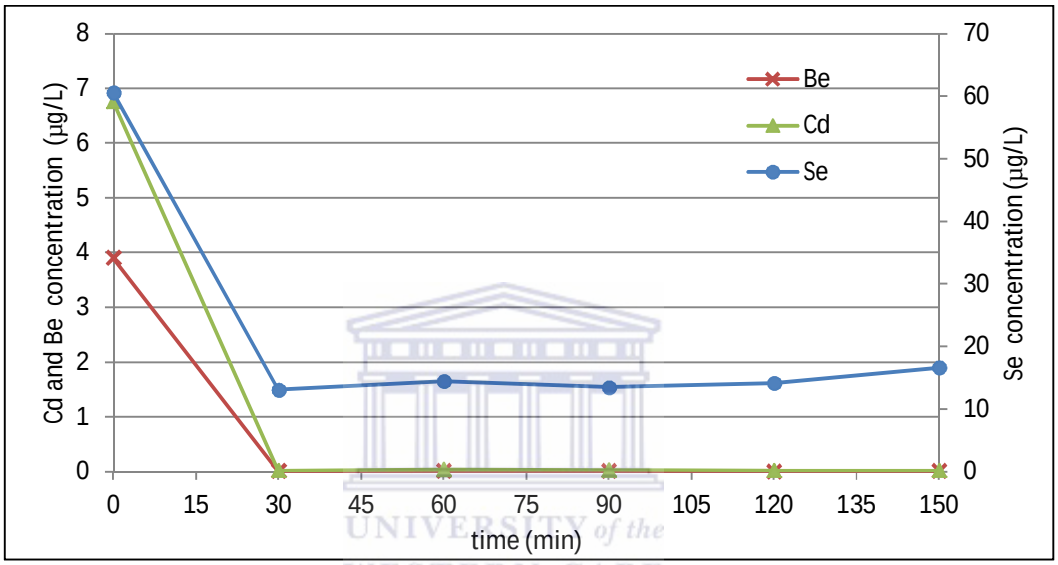

Figure 7.2.27: The Be, Cd and Se concentration in the product water during treatment of Rand Uranium mine water (80 L) with 13 kg of Matla coal FA, 200 g lime and 86.58 g of $Al(OH)_3$.

Rand Uranium mine water contained about 3.9 µg/L, 6.76 µg/L and 60.57 µg/L of Be, Cd and Se respectively. The required limit for potable water is 12 µg/L of Be, 3 µg/L of Cd and 20 µg/L of Se (WHO, 2011). This means that the concentration of Cd and Se were above the allowable limit for potable water. $Al(OH)_3$ was added after 30 min of treatment at which time all the Cd and Be had already been removed. Therefore removal of Cd and Be was due to the added Matla coal FA and lime.

Treatment of Rand Uranium mine water with Matla coal FA and lime resulted in the decrease in Be concentration in the water from 3.9 µg/L to 0.01 µg/L as the pH was

increased to above 10. Beryllium is known to form $Be(OH)_2$ when the pH is increased to above 7 (Lytle et al., 1992). The concentration of Cd in the water was decreased from 6.76 µg/L to 0.03 µg/L within 30 min, which was lower than the allowable limit for potable water of 12 µg/L. Cadmium is known to form otavite ($CdCO_3$) at pH 8.5 and $Cd(OH)_2$ at pH greater than 10 (Rotting et al., 2005; INAP, 2012). The pH of Rand Uranium mine water was increased to greater than 10 in 30 min of treatment with Matla coal FA and lime. Therefore Cd could have been removed as $CdCO_3$ and $Cd(OH)_2$.

7.2.7.5. Strontium and molybdenum

During treatment of Rand Uranium mine water (80 L) with 13 kg of Matla coal FA, 200 g of lime and 86.58 g of $Al(OH)_3$, the product water was analysed for the concentration of Sr and Mo after every 30 min using ICP-OES. The concentration of Sr and Mo during treatment of Rand Uranium mine water is shown in Figure 7.2.28.

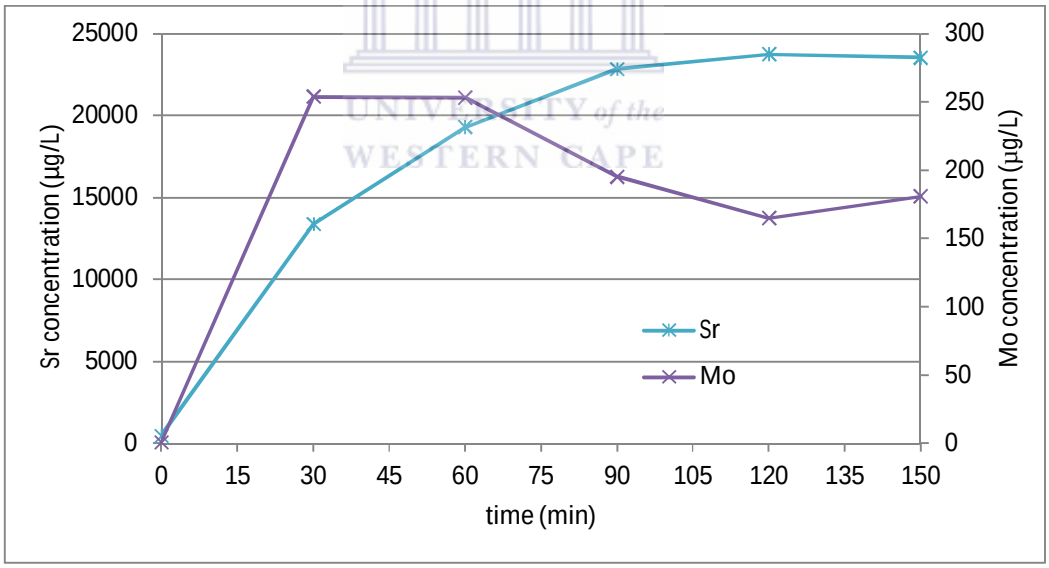

Figure 7.2.28: The Sr and Mo concentration in the product water during treatment of Rand Uranium mine water (80 L) with 13 kg of Matla coal FA, 200 g lime and 86.58 g of $Al(OH)_3$.

Rand Uranium mine water contained 448 µg/L and 0.51 µg/L of Sr and Mo respectively. During treatment of Rand Uranium mine water with Matla coal FA, lime and $Al(OH)_3$, the

concentration of Sr increased gradually from 448 µg/L to 23748 µg/L after 120 min. The WHO guideline for Sr in potable water is set for the radioactive species of Sr (10 Bq/L). There was no radioactive species of Sr detected in the Matla coal FA (Table 4.1.3) and Rand Uranium mine water (Table 4.6.2). The increase in the Sr concentration in the product water can be attributed to the leaching of Sr from Matla coal FA into the water. Matla coal FA contained 2137 mg/kg of Sr. Other researchers have found that Sr leaches into the water from coal FA (Querol et al., 2001; Madzivire, 2010; Fatoba, 2010). Querol et al (2001) found that Sr leached into normal water through the dissolution of small solid particles in coal FA or from the coatings on the surface of the coal FA.

The Mo concentration also increased in the treated water when Rand Uranium mine water was mixed with Matla coal FA and lime during the initial 30 min of mixing in a jet loop reactor from 0.51 µg/L to 254 µg/L which was above the limit for potable water of 70 µg/L set by WHO in 2011. This was due to the leaching of the Mo from Matla coal FA particles into the aqueous media (Neupane and Donahoe, 2012, Madzivire, 2010). After addition of $Al(OH)_3$ at 30 min the Mo concentration remained constant up to 60 min after which it started to decrease to about 180 µg/L. It was found that treatment of Rand Uranium mine water with Matla coal FA, lime and $Al(OH)_3$ results in the formation of ettringite (section 7.2.1 to 7.2.4). The slight decrease in the Mo concentration after 60 min could be ascribed to the incorporation of Mo into the ettringite structure during its formation. Kumarathasan et al (1990) has found that oxyanions of Mo (MoO_4^{2-}) can be incorporated into the ettringite structure. These potential toxic elements (Mo and Sr) could be removed from the product water using zeolite adsorbents synthesized from coal FA (Moreno et al., 2001).

The solid residues collected after 30 min and 150 min of treatment of Rand Uranium mine water (80 L) with Matla coal FA, 200 g of lime and 86.58 g of $Al(OH)_3$ were analysed using LA-ICP-MS to determine the concentration of Sr and Mo. The results obtained are shown in Figure 7.2.29.

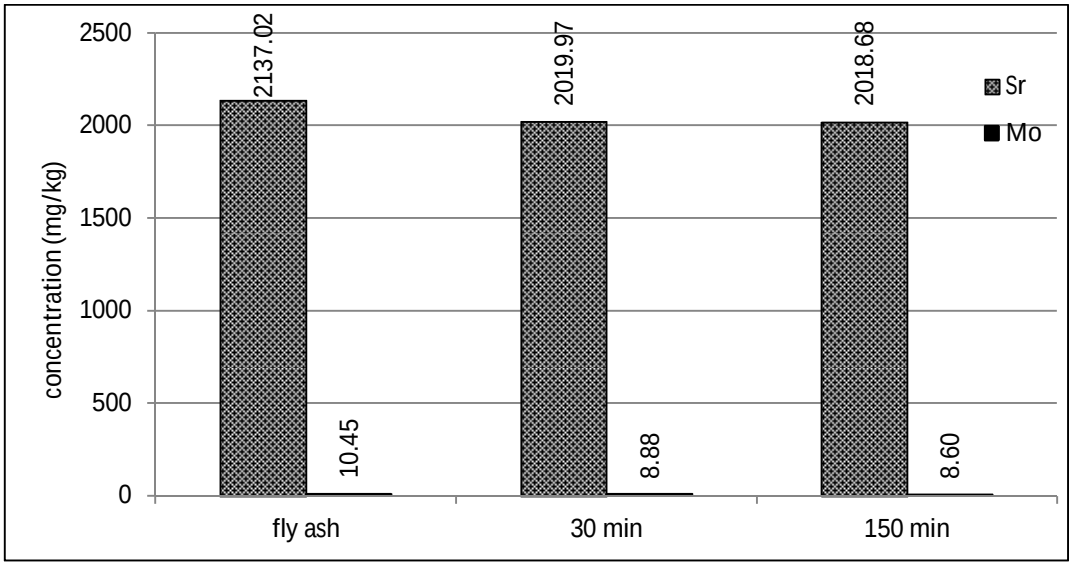

Figure 7.2.29: The composition of Sr and Mo in Matla coal FA and solid residues collected after 30 min and 150 min of treating Rand Uranium mine water (80 L) with 13 kg of Matla coal FA, 200 g of lime and 86.58 g of $Al(OH)_3$ in jet reactor.

The LA-ICP-MS results in Figure 7.2.29 show that the concentration of Sr and Mo in Matla coal FA was higher than that in 30 min solid residues. The concentration of Sr and Mo in the 150 min solid residues was almost the same as in 30 min solid residue. This showed that Sr and Mo leached into the product water during the first 30 min of treating Rand Uranium mine water with Matla coal FA and lime. This correlated with the results in Figure 7.2.28, which showed an increase in the concentration of Mo and Sr in the treated water, when Rand Uranium mine water was treated with Matla coal FA.

7.2.7.6. Chromium, vanadium and barium

When Rand Uranium mine water was treated with Matla coal FA, lime and $Al(OH)_3$, the ICP-OES analysis of the product water showed that there was an increase in the concentration of Cr, V and Ba in the product water as shown in Figure 7.2.30.

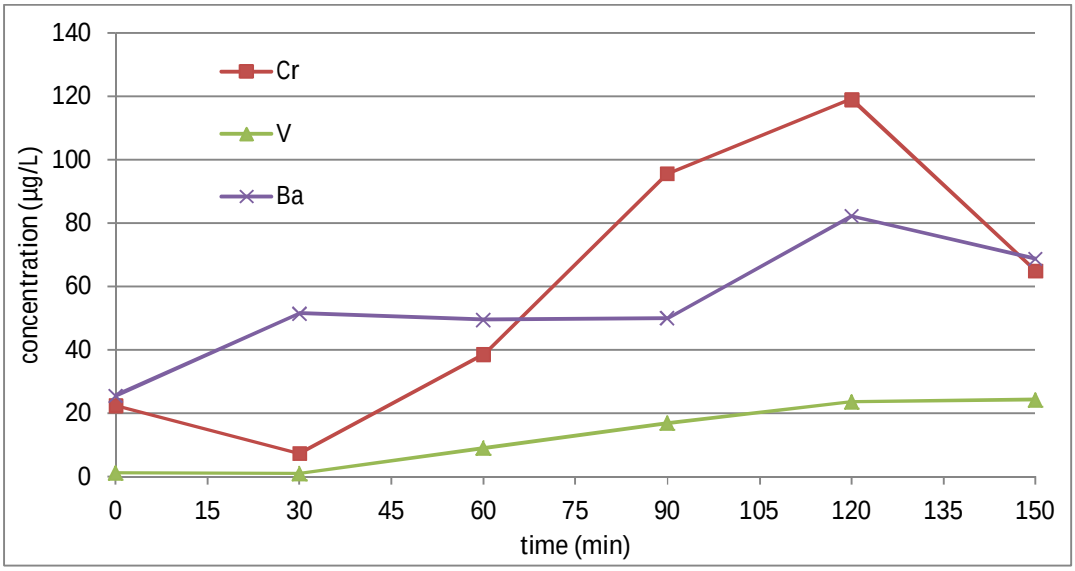

Figure 7.2.30: The Cr, V and Ba concentration in the product water during treatment of Rand Uranium mine water (80 L) with 13 kg of Matla coal FA, 200 g lime and 86.58 g of $Al(OH)_3$.

Rand Uranium mine water contained 22.53, 1.21 and 25.50 µg/L of Cr, V and Ba (Figure 7.2.30) respectively. The concentration of Cr and Ba were above the allowable limits for potable water of 50 and 70 µg/L respectively (WHO, 2011). There is no value stated for V in the WHO guidelines for potable water. The concentration of Cr decreased when mine water was reacted with Matla coal FA and lime during the initial 30 min from 22.53 µg/L to 7.36 µg/L. After adding $Al(OH)_3$ at 30 min the Cr increased to 119.3 µg/L after 120 min thereafter it decreased to 68.80 µg/L at 150 min. Vanadium concentration deceased slightly when mine water was mixed with Matla coal FA and lime from 1.21 to 1.04 µg/L. After adding $Al(OH)_3$ at 30 min the V concentration increased gradually to 24.37 µg/L. The addition of $Al(OH)_3$ to the reaction mixture resulted in the increase of the V and Cr concentration in the aqueous media. This could be due to the fact that adsorbed anion species on the Matla FA particles could have been displaced by the $Al(OH)_4^-$ ions that form at very high pH of greater than 11.

The Ba concentration increased when mine water was mixed with FA and lime for the first 30 min. After adding $Al(OH)_3$ at 30 min, the Ba concentration remained constant up to

90 min after which it increased again. Barium is known to leach out of FA into the aqueous media if mixed with mine water or normal water (Fatoba, 2010; Querol, 2001). Fatoba (2010) found that Ba salts leached into the water when FA was mixed with brine solutions.

The solid residues collected after 30 min and 150 min of treatment of Rand Uranium mine water (80 L) with Matla coal FA, 200 g of lime and 86.58 g of $Al(OH)_3$ were analysed using LA-ICP-MS to determine the concentration of V and Cr. The results obtained are shown in Figure 7.2.31.

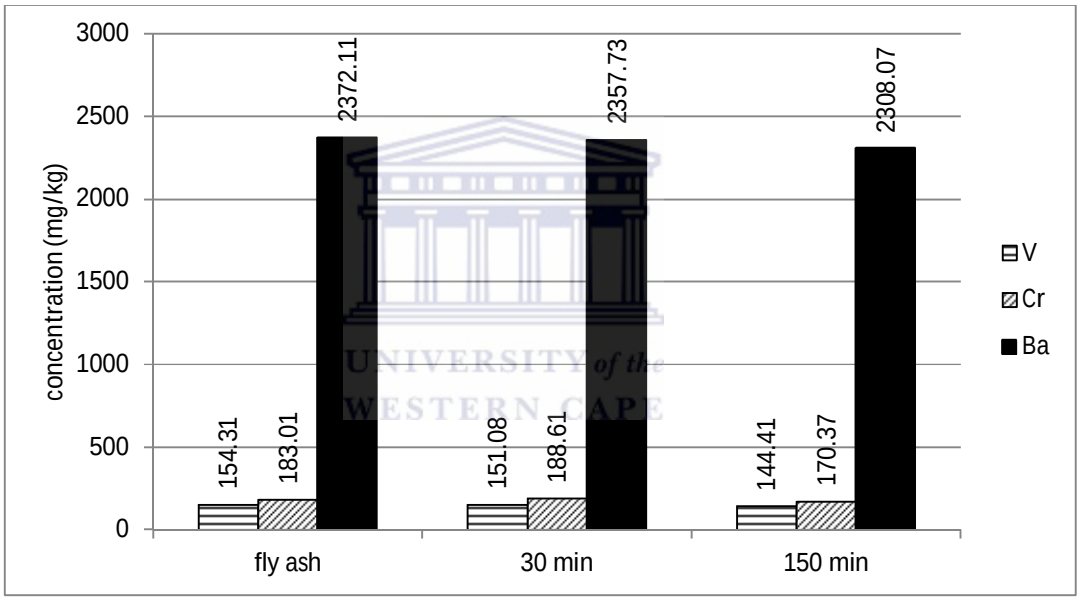

Figure 7.2.31: The concentration of Ba, V and Cr in Matla coal FA and solid residues collected after 30 min and 150 min of treating Rand Uranium mine water (80 L) with 13 kg of Matla coal FA, 200 g of lime and 86.58 g of $Al(OH)_3$ in jet reactor.

The concentration of Ba and V in Matla coal FA was 2372.11 mg/kg and 154.31 mg/kg respectively. The solid residues collected after 30 min of treating Rand Uranium mine water (80 L) with 13 kg of Matla coal FA and 200 g of lime contained lower concentration of Ba (2357.73 mg/kg) and V (151.08 mg/kg). The solid residues collected after 150 min of treating Rand Uranium mine water (80 L) with 13 kg of Matla coal FA, 200 g of lime and 86.58 g of

$Al(OH)_3$ contained lower concentration of Ba (2308.07 mg/kg) and V (144.41 mg/kg) than Matla coal FA as well as the solid residues collected after 30 min. This correlates well with the results shown in Figure 7.2.30, which shows an increase in the concentration of Ba and V in the mine water. Therefore Ba and V leached from Matla coal FA into the water when Rand Uranium mine water mixed with Matla coal FA, lime and $Al(OH)_3$. The concentration of Cr in the 30 min solid residue (188.61 mg/kg) was higher than that in Matla coal FA (183.01 mg/kg), but the concentration in the 150 min solid residue (170.37 mg/kg) was less than that in Matla coal FA. This correlates well with the results depicted in Figure 7.2.30. The flowing section summarises the finding for section 7.2 which involved the treatment of Rand Uranium mine water with different combination of Matla coal FA, lime and $Al(OH)_3$.

7.2.8. SUMMARY OF RESULTS

This section gives a summary, compares and explains the results obtained when Rand Uranium mine water was treated with various combination of substances. The different mols that were mixed together when Rand Uranium mine water (80 L) was treated with various combinations of substances are calculated and the summary is shown in Table 7.2.6.

Table 7.2.6: Number of mols of Ca, Al and sulphate ions and the mol ratios of $Ca:SO_4^{2-}$ and $Al:SO_4^{2-}$ during treatment of Rand Uranium mine water (80 L) with different combinations of substances.

substances mixed with 80 L of RU	$n(SO_4^{2-})$	n(Al)	n(Ca)	pH
86.58g $Al(OH)_3$	2.13	1.18	**0.72**	4.08
100g lime+86.58g $Al(OH)_3$	2.13	1.18	**2.01**	8.29
150g lime+86.58g $Al(OH)_3$	2.13	1.18	**2.65**	10.14
200g lime+86.58g $Al(OH)_3$	2.13	1.18	**3.30**	10.11
8kg FA	2.13	**0.079**	3.44	12.15
13kg FA	2.13	**0.079**	5.14	13.11
8kg FA +86.58g $Al(OH)_3$	2.13	1.18	3.44	10.20
13kg FA +86.58g $Al(OH)_3$	2.13	1.18	5.14	10.68
8kg FA +100g lime+86.58g $Al(OH)_3$	2.13	1.18	4.73	10.67
8kg FA +200g lime+86.58g $Al(OH)_3$	2.13	1.18	6.02	10.99
13kg FA +100g lime+86.58g $Al(OH)_3$	2.13	1.18	6.43	11.02
13kg FA +200g lime+86.58g $Al(OH)_3$	2.13	1.18	7.72	11.26

Treatment of Rand Uranium mine water with different combinations of chemicals in a jet loop reactor was compared. This was done in order to find out which combination produced best quality treated water. The pH and the percentage removal of Fe, Mg and sulphate during treatment of Rand Uranium mine water (80 L) with different combination of substances is shown in Figure 7.2.32.

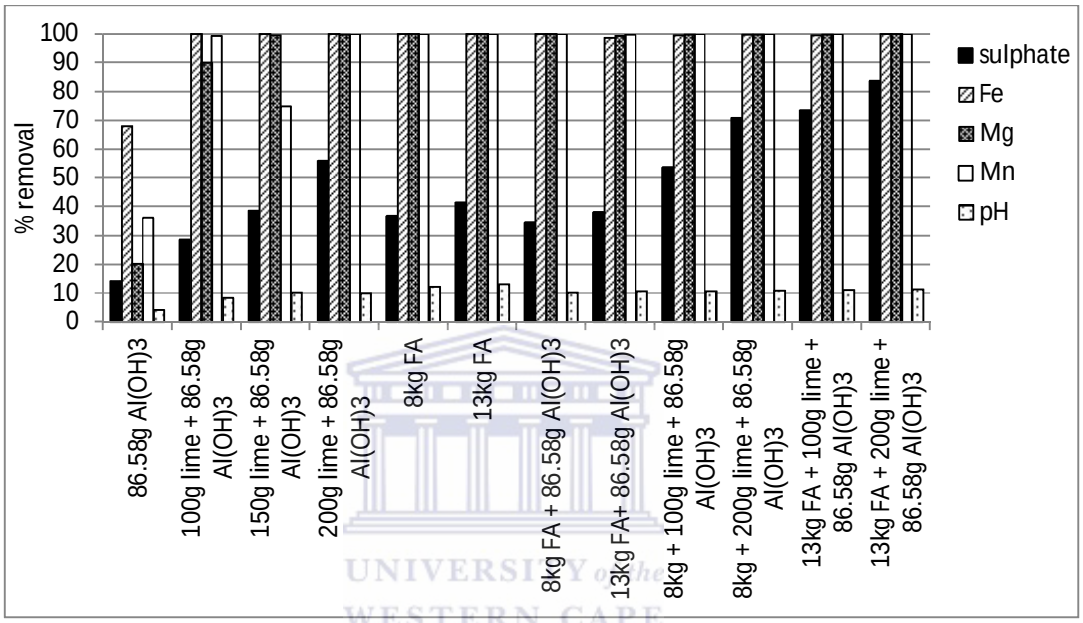

Figure 7.2.32: The pH and percentage removal of Fe, Mg, Mn, and sulphate ions from Rand Uranium mine water (80 L) during treatment with different combination of substances in a jet loop reactor for 120 min.

From Figure 7.2.32, the concentration of Fe, Mn and Mg decreased by almost 100 % during treatment of Rand Uranium mine water (80 L) with most combination of substances. Lower percentage removal of Fe, Mn and Mg was observed when Rand Uranium mine water (80 L) was treated with 86.58 g of $Al(OH)_3$ only as shown in Figure 7.2.32. This was because the pH of the mine water was increased to above 10 by most combination except when $Al(OH)_3$ only was used. It was observed by Act2 model that Fe and Al can be removed when pH of the mine water increased to greater than 4, while Mn and Mg can be removed when pH was greater than 10.

As shown in Figure 7.2.32, the most sulphate removal was removed (84 %) by mixing Rand Uranium mine water (80 L) with 13 kg of Matla coal FA, 200 g of lime and 86.58 g of $Al(OH)_3$. Removal of sulphate ion from mine water depended on the; amount of Ca and Al added to the mixture as well as the final pH. The Matla coal FA and lime were important for the addition of Ca ions and increase the pH of the mine water thorough CaO dissolution. According to the XRD spectra of Matla coal FA and solid residues collected during treatment of Rand Uranium (80 L) with various amounts of substances, the removal of sulphate ions was due to precipitation of ettringite and gypsum.

Removal of gypsum was limited by its solubility product (Ksp). The Ksp of gypsum is very high (3.2×10^{-5}). This means that a lot of Ca ions (2.22 mols per 80 L of Rand Uranium mine water) would be required to precipitate out sulphate ions to within the TWQR of 500 mg/L. This happens if the product water contains at least 0.0063 mol/L (250 mg/L), such that that ionic product of gypsum is greater or equal to the Ksp to avoid the dissolution of gypsum. Ettringite could remove the sulphate ions to within the TWQR easily because of its very low Ksp. The Ksp of ettringite is approximately 10^{-45}.

$$Ksp\ of\ ettringite = [Ca^{2+}]^6[SO_4^{2-}]^3[Al^{3+}]^2[OH^-]^6, \text{ where [] represents mol/L}$$

From the Ksp equation above the precipitation of ettringite depends on concentration of OH^- (pH), Ca^{2+}, SO_4^{2-} and Al^{3+}. All mixtures contained equal amounts of sulphate ions. The amount of Al ions added depended on the mass of $Al(OH)_3$ added to the mixture. The amount of Ca^{2+} dependent on the amount of Matla coal FA and/or lime added. According the ettringite formation reaction (Equation 7.2), to remove sulphate ions to at most 500 mg/L (that is to precipitate 1.72 mols of sulphate ions from 80 L of Rand Uranium mine water), it requires 3.43, 1.14 and 3.43 mols of Ca^{2+}, SO_4^{2-} and OH^- respectively to be added to the mixture. Addition of 3.43 mols of OH^- to 80 L is equivalent to pH of 13.09.

According to Table 7.2.6, when Rand Uranium mine water was treated with 86.58 g of $Al(OH)_3$ only, pH and the amount of Ca^{2+} was far less than the expected. This resulted in no ettringite formation as shown by the XRD spectrum of the solid residue collected after 150 min (Figure 7.2.3). The sulphate ions removal could be attributed to the adsorption mechanism. According to Figures 7.2.6, 7.2.9, 7.2.12, 7.2.15 and 7.2.18, the sulphate

removal from Rand Uranium mine (80 L) during treatment with Matla coal FA (8 or 13 kg), lime (100, 150 or 200 g) and 86.58 g of $Al(OH)_3$ was due to precipitation of ettringite and gypsum. The removal of sulphate ions from the mixture that contained Rand Uranium mine water (80 L) and Matla coal FA (8 and 13 kg) only was limited by the number of mols of Al^{3+} (to form ettringite) and the Ksp of gypsum. All other mixtures that contained Rand Uranium mine water (80 L), 86.58 g of $Al(OH)_3$, Matla coal and/or lime contained enough Al^{3+} and Ca^{2+} ions to precipitate out sulphate ions to within TWQR of less than 500 mg/L. The main variable was the final pH of the mixture which dependent of the amount of Matla coal FA and/or lime added to the mixture. As more Matla coal FA and/or lime was added to the mixture, the pH of the mixture also increased.

The mixture that had the highest pH (11.26) was the one containing; Rand Uranium mine water (80 L), Matla coal FA (13 kg), lime (200 g) and 86.56 g of $Al(OH)_3$. This mixture contained; 1.18 mols of Al^{3+} and 7.72 mols of Ca^{2+} in 80 L. So the limiting reactant in this mixture for the removal of sulphate ions as ettringite was the amount of Al^{3+} ions. Based on this limiting reactant, the expected sulphate ions to be removed as $Ca_6Al_2O_3(SO_4)_3.32H_2O$ were 1.77 mols in 80 L. This was equivalent to 2126 mg/L. The actual sulphate ions that remained in the treated water after treatment of Rand Uranium mine water with Matla coal FA (13 g), lime (200 g) and 86.58 g of $Al(OH)_3$ was 418 mg/L. This represented about 84 % of sulphate removal as shown in Figure 7.2.32. This meant that 2145 mg/L of sulphate ions were removed. This value was very close to the expected amount of sulphate ions that were supposed to be removed as ettringite. This confirmed that the sulphate ions were mainly removed as ettringite.

This study has shown that treatment of Rand Uranium mine water (80 L) with 13 kg of Matla coal FA, 200 g and 86.58 g of $Al(OH)_3$ produced the best quality water. The physicochemical parameters of Rand Uranium mine water and the product water produced were compared to the DWAF and WHO limits for potable water as shown in Table 7.2.7.

Table 7.2.7: Comparison of the physicochemical parameters of Rand Uranium mine water and the product water produced from the treatment of Rand Uranium mine water (80 L) with 13 kg of Matla coal FA, 200 g of lime and 86.58 g of $Al(OH)_3$ to the DWAF and the WHO limits for potable water.

parameter	Rand Uranium mine water	Product water	Potable limit
pH	**2.65 ± 0.81**	**11.02**	6-9
EC	**2000 ± 27**	**1900**	700
sulphate	**2562.41 ± 6.85**	417.58 ± 4.93	500
Fe	**201.05 ± 0.55**	0.015 ± 0.001	0.3 (0.1)
Al	**26.63 ± 0.29**	0.071 ± 0.0002	0.2 (0.15)
Ca	**360.15 ± 4.25**	**209.85 ± 0.75**	32
Mg	**153 ± 0.7**	0.02 ± 0.003	30
Mn	**60.16 ± 0.17**	$9.6 \times 10^{-4} \pm 1 \times 10^{-4}$	0.1(0.05)
Ni	2.11 ± 0.0043	$3.96 \times 10^{-3} \pm 2.9 \times 10^{-4}$	NV
Zn	1.93 ± 0.013	$4.99 \times 10^{-4} \pm 2.3 \times 10^{-4}$	3(0.5)
Sr	0.45 ± 0.0034	23.75 ± 0.45	NV
Cu	0.28 ± 0.0033	$6.63 \times 10^{-5} \pm 6.63 \times 10^{-5}$	2(1)
U	**0.28 ± 0.001**	$2.4 \times 10^{-4} \pm 2.98 \times 10^{-6}$	0.03(0.07)
Li	$0.069 \pm 2.9 \times 10^{-4}$	1.34 ± 0.006	NV
Se	**0.061 ± 0.0023**	0.014 ± 0.001	0.02(0.04)
Ba	$0.026 \pm 4.3 \times 10^{-4}$	0.082 ± 0.001	0.7
Cr	$0.023 \pm 2.9 \times 10^{-4}$	**0.12 ± 0.0062**	0.05
Pb	$7.5 \times 10^{-3} \pm 1.73 \times 10^{-5}$	$2.6 \times 10^{-4} \pm 2.82 \times 10^{-5}$	0.01
Cd	$\mathbf{6.76 \times 10^{-3} \pm 1.22 \times 10^{-5}}$	$2.50 \times 10^{-5} \pm 5.09 \times 10^{-6}$	0.003(0.005)
As	$\mathbf{5.6 \times 10^{-3} \pm 2.49 \times 10^{-5}}$	$\mathbf{1.4 \times 10^{-3} \pm 5.64 \times 10^{-5}}$	0.001
Be	$3.90 \times 10^{-3} \pm 4.17 \times 10^{-5}$	$8.31 \times 10^{-6} \pm 2.56 \times 10^{-6}$	0.012
Th	$1.8x\ 10^{-3} \pm 3.06 \times 10^{-5}$	$2.17 \times 10^{-6} \pm 1.86 \times 10^{-7}$	NV
V	$1.2 \times 10^{-3} \pm 7.6 \times 10^{-6}$	0.024 ± 0.0011	(0.01)
Mo	$5.3 \times 10^{-4} \pm 2.4 \times 10^{-5}$	$\mathbf{0.16 \pm 3.7 \times 10^{-4}}$	0.07
B	$2.3\ x10^{-4} \pm 4x\ 10^{-6}$	$0.0018 \pm 3 \times 10^{-6}$	2.4
Hg	$3.93 \times 10^{-6} \pm 1.18 \times 10^{-6}$	$4.65 \times 10^{-4} \pm 1.79 \times 10^{-6}$	0.006(0.001)

All units are mg/L except that of EC (µS/cm) and pH. NV means no value mentioned in the WHO and DWAF guidelines for potable water.

From Table 7.2.7, Rand Uranium mine water did not conform to drinking water requirements with respect to twelve parameters. These were pH, EC and the concentration of sulphate, Fe, Al, Ca, Mg, Mn, U, Se, Cd and As. After treatment of Rand Uranium mine water (80 L) with 13 kg of Matla coal FA, 200 g of lime and 86.58 g of $Al(OH)_3$, the product water did not conform to the requirements with respect to six parameters. These

parameters were pH, EC and the concentration of Ca, Cr, As and Mo. The concentration of As was slightly above the TWQR for potable water. The pH, EC and the concentration of Ca can be adjusted to the required limits by bubbling CO_2 into the product water (Madzivire, 2010; Bologo et al., 2012). So the product water needs polishing to remove Cr, As and Mo using ion exchange resins or zeolites (Moreno et al., 2001).

It was found that treatment of Rand Uranium mine water (80 L) with 13 kg of Matla coal FA, 200 g of lime and 86.58 g of $Al(OH)_3$ resulted in the removal of U, Th, Zn, Ni, Cu, As, Pb, Be and Cd. The concentration of U, Th, Zn, Ni, Cu, Pb, Be and Cd was within the limit for potable water set by the World Health Organization. On the hand Sr, Mo, Cr, V and Ba leached into the water when Matla coal FA was used to treat Rand Uranium mine water. The final concentration of Cr, V and Ba was less than the limit for potable water. The pH, EC and final concentration of Mo, As and Ca was above the limit for potable water. This means that the product water from Matla coal FA, lime and $Al(OH)_3$ treatment need a bit of polishing to adjust the pH and the concentration of Mo, As and Ca using ion exchange resins before it can be used for domestic purposes. Otherwise, with adjustment of pH only by bubbling CO_2, the water would be fit for agricultural and industrial uses.

Removal of sulphate ions from Rand Uranium mine water as ettringite using Matla coal FA, lime and $Al(OH)_3$ was found to be enhanced by the hydrodynamic cavitation that occurs in the jet loop reactor. This was confirmed when the mixture was first mixed in a jet loop reactor for 45 min and then the mixing technique was changed to normal stirring. This resulted in reduced sulphate removed compared to when the mixing was done in jet loop reactor throughout the duration of the mixing process. Hydrodynamic mixing of Rand Uranium mine water with Matla coal FA, lime and $Al(OH)_3$ resulted in an increase in temperature of the mixture gradually to about 80 ^{0}C.

This research has found a novel way of removing many potentially toxic elements such as Cd, Fe, Mn and sulphate ions and radioactive active elements such as U and Th from mine water using coal FA. Recycling waste mine water and FA will go a long way to attain zero effluent discharge in the mines and the coal fired power stations. Since coal FA contained

radionuclides initially, the added radionuclides from contaminated mine water did not cause a significant increase in the amount of these radioactive elements in the solid residues.

7.2.9. CONCLUSION

Treatment of Rand Uranium mine water with Matla coal FA has resulted in the removal of potentially toxic elements such as Fe, Al, Mn, Mg, U, Th, Zn, Ni, Cu, As, Pb, Be and Cd by almost 100 % to within the TWQR for potable water. The removal was achieved after mixing Rand Uranium mine water with Matla coal FA for 30 min using a jet loop reactor. During treatment of Rand Uranium mine water with Matla coal FA and/or lime, the sulphate concentration was removed by about 40-60% . The final concentration of the sulphate after treatment of Rand Uranium mine water was above the TQWR for potable water. The removal of Fe, Al, Mn, Mg, U, Th and sulphate confirmed the modelling results that were predicted by Act2 program of the GWB software.

The sulphate ions in Rand Uranium mine water were removed to within the TWQR for potable water of 0-500 mg/L by treating Rand Uranium mine water in a one step and simple process using Matla coal FA, lime and $Al(OH)_3$. Matla coal FA and lime were added such that the pH of the mixture was maintained around or above 11.5, which is the optimum pH for ettringite precipitation. $Al(OH)_3$ was added to provide more Al^{3+} for the formation of ettringite. Formation of ettringite was effective to remove sulphate ions to within the TWQR because of its low solubility product of 1×10^{-45}, if the pH was kept within 11.5 and 12.5. The kinetics of the removal of sulphate ions as ettringite was dependent on the type of mixing employed. It was found that hydrodynamic mixing of Rand Uranium mine water enhanced the kinetics of the removal of sulphate ions as ettringite.

CHAPTER 8: CONCLUSIONS AND RECOMMENDATIONS

This chapter covers the overall scientific conclusions reached based on the objectives that were set. It also highlights the recommendations and the future work that need to be undertaken.

8.1. CONCLUSION FROM FINDINGS

This research focused on the treatment of Matla mine water or Rand Uranium mine water with Matla coal FA, lime or $Al(OH)_3$. The treatment was conducted using a jet reactor or an overhead stirrer. This research investigated the effect of the jet reactor on the removal of potentially toxic contaminants and proved that the jet reactor had impact on the kinetics of the removal of sulphate ions from mine water. The chemistry of the removal of sulphate ions using $Al(OH)_3$ or aluminium chlorohydrate (ACH) was also studied. This part of research aimed to understand the effect of pH and effect of the ratio of Al:sulphate ions on the removal of sulphate ions from mine water using $Al(OH)_3$ and ACH.

Matla coal FA used in this research was Class F according to the American Standard of Testing and Measurement system. It was made up of amorphous material (59.76 %), mullite (24.84 %), quartz (18.88 %), hematite (1.57 %), lime (0.68 %) and gypsum (0.21 %). Matla coal FA contained naturally occurring radioactive materials (NORMs) such as ^{238}U, ^{234}U, ^{235}U, ^{232}Th, ^{228}Th, ^{228}Ra, ^{226}Ra, ^{210}Pb, ^{40}K. The radioactivity in Matla coal FA was within the range of most ashes all over the world. The radioactivity of Matla coal FA was significantly above the average radioactivity of soil. Matla mine water and Rand Uranium mine water were found to be neutral mine drainage and acid mine drainage respectively. This was because the pH of Matla mine was 8, which was close to the neutral pH and that of Rand Uranium mine water was acidic. Rand Uranium mine water contained elevated concentrations of sulphate, Fe, Al, Mn, Ca and Mg. Matla mine water contained high concentrations of Na and sulphate, such that the water was unsuitable for domestic and industrial purposes. Rand Uranium mine water was unsuitable for any purpose (drinking, irrigation or industrial) because the lower pH and the elevated concentration of Fe, Al, Mn, Pb, U and sulphate ions in the water.

The gross alpha and beta radioactivity of Rand Uranium mine water were 12 and 6 times above the potable limit respectively. This was caused by U, Th and Ra radioisotopes that were found in Rand Uranium mine water.

Geochemist workbench (GWB) speciation using SpecE8 program of the major elements in Matla mine water and Rand Uranium mine water have shown that major elements (or ions), Mg, sulphate, Mn, Na and K ions mainly exist in aqueous media as free ions. This means they exist mainly as unassociated or uncomplexed with ligands or other ions. Free ions are very mobile and thus have increased bioavailability and toxicity. Cations such as Fe and Al were found to occur associated with hydroxyl ions in Rand Uranium mine water. This means that Al and Fe had reduced mobility and bioavailability. Reduced mobility and bioavailability reduced the toxicity of these ions.

The Act2 sub program of the GWB model has shown that if Matla mine water or Rand Uranium mine water was to be treated with Matla coal FA, the removal of the potential toxic elements such as Fe, Al, Mn, Mg, U, Th and sulphate ions would depend on pH end point of the treatment and the concentration of Ca ions added to the mine water. The results are very helpful especially to predict the amount of FA or chemicals that would be required to treat a particular composition of the mine water. The removal of Mg ions from Matla mine was found to be mainly pH dependent. It was found that increasing the pH of Matla mine water to greater than 10 would result in the precipitation of Mg as brucite $(MgOH)_2$. No removal of sulphate, K and Na ions from Matla mine water was predicted by Spec8 program if the concentration of Ca ions in mine was increased such that $\log_a Ca^{2+}$ was to be increased from -10 to 0 and pH was increased to 14.

The Act2 program of the GWB predicted that treatment of Rand Uranium mine water with Matla coal FA could remove sulphate ions as alunite $(KAl_3(SO_4)_2(OH)_6)$ or gypsum. Removal of alunite and gypsum from Rand Uranium mine water was found to depend on pH and $\log_a Ca^{2+}$. If sulphate ions were to be removed in the form of alunite, the pH of the mixture would have to be kept between 3.5 and 5 and $\log_a Ca^{2+}$ less than -1. If the sulphate ions were to be removed in the form of gypsum, $\log_a Ca^{2+}$ of the mixture would have to be increased to greater than -2.5. Removal of Al ions from Rand Uranium mine was through alunite or

gibbsite ($Al(OH)_3$) precipitation according to the GWB model. The formation of alunite was dependent mainly on pH while the formation of gibbsite was found to be dependent upon the concentration of Ca ions added to the mine water. The conditions for the removal of Al as alunite are the same as the conditions for the removal of sulphate ions as alunite. Removal of Al ions as gibbsite would occur if the pH of the mine water was to be increased to between 4 and 10. The probable mineral phases that were predicted to form when Rand Uranium water was to be treated with FA were, jarosite-K ($KFe_3(SO_4)_2(OH)_6$) and $Fe(OH)_3$. The formation of jarosite-K was found to be pH dependent and the concentration of Ca^{2+} added to the mine water. Jarosite-K was found to form at pH between 3 and 5. As $\log_a Ca^{2+}$ was increased to greater than -0.5, no jarosite would form in Rand Uranium mine water. Formation of $Fe(OH)_3$ could only occur if the pH of the mine water was to be increased to between 4 and 12. Modelling results using the GWB model have shown that if Rand Uranium mine was to be treated with FA, Mn and Mg ions will be removed as $Mn(OH)_2$ and $Mg(OH)_2$ respectively. The formation of $Mn(OH)_2$ and $Mg(OH)_2$ would depend on the final pH attained during treatment and would be independent of the amount of Ca^{2+} ions added into the mixture. $Mn(OH)_2$ and $Mg(OH)_2$ were found to precipitate at pH 10 and 9.5 respectively. Removal of K ions from Rand Uranium mine water was found to be through the precipitation of alunite according to the GWB. On the hand the GWB model have shown that if Rand Uranium mine water was to be treated with FA, there is no expected Na-mineral phase that would form. Therefore if Rand Uranium is to be treated with FA, Na concentration would remain the same if there is no leaching of Na from FA or adsorption or absorption of Na ions by the FA particles.

Removal of sulphate ions from mine water using $Al(OH)_3$ or ACH depends on the pH of the mixture and the amount of Al ions added. The optimum pH for sulphate removal during treatment of mine water with $Al(OH)_3$ and ACH was found to be between 4 and 6. The optimum Al^{3+}:SO_4^{2-} mol ratio for the removal of sulphate ions was 5:1 and 6:1 for $Al(OH)_3$ and ACH respectively. Removal of sulphate ions using ACH resulted in better removal as compared to using $Al(OH)_3$. This was because ACH was jelly-like and $Al(OH)_3$ was in solid form. Therefore the dissolution and rearrangement to form species that interact and

remove the sulphate ions in the mine water occurs faster when ACH was added to the mixture. Addition of ACH to mine water 5:1 and 6:1 of the Al^{3+}:SO_4^{2-} mol ratio resulted in the removal of sulphate concentration to less than the potable limit. The disadvantage of using $Al(OH)_3$ or ACH to remove sulphate ions from mine water is the amount of Cl ions that remained in the treated water. The Cl ions come from the ACH or added to the mixture as HCl in the case of $Al(OH)_3$ in order to maintain the pH at the optimum range. Aluminium chlorohydrate also produced a mixture of mine water and flocculants of high viscosity that made the recovery of treated water almost impossible.

From the results obtained when coal FA only was used to treat Matla mine water, sulphate and Ca initially leached into the Matla mine water from FA. After addition of $Al(OH)_3$ to the mixture the concentration of sulphate and Ca started to decrease due to the precipitation of ettringite. Na remained almost constant during treatment of mine water with fly ash, while the concentration of Mg decreased to approximately zero when pH was increased to greater than 12. Experiments conducted using an overhead stirrer has shown low sulphate removal compared to jet loop experiments. This was due to the increased rate of formation of ettringite caused by the superior mixing in a jet loop reactor compared to an overhead stirrer. Jet sizes did not have any effect on sulphate removal. Changing of the mixing technique from a combination of impingement and cavitation to cavitation only did not result in any noticeable difference on sulphate removal. Finally, cavitation and impingement mixing of Matla mine water and coal FA resulted in a gradual increase in temperature of the mixture. It was shown that the temperature did not affect the removal of sulphate ions. This proved that the removal of sulphate ions was enhanced by hydrodynamic cavitation that occurred inside the jet loop reactor. These findings proved that treatment of mine water with FA could be up scaled very easily to 80 L pilot plant capacity using a jet loop reactor.

Treatment of Rand Uranium mine water using Matla FA, lime and $Al(OH)_3$ has shown that major elements such as Fe, Al, Mn and Mg can be removed by almost 100 % with coal FA. This was achieved by mixing mine water with FA and lime for 30 min in jet loop reactor. On the other hand only a small amount of sulphate ions were removed when Rand Uranium mine water was mixed with coal FA for 30 min. The removal of Fe, Al, Mn and Mg was due

to the precipitation of their respective hydroxides. Fe and Al were found to be removed at pH greater than 4, while Mn and Mg were removed at pH greater than 10. The slight decrease in the sulphate concentration observed was due to the formation of ettringite and gypsum when Rand Uranium mine water was mixed with FA and lime.

Addition of $Al(OH)_3$ at 30 min (when the pH of the mixture was greater than 11) resulted in a further decrease of sulphate concentration in the product water to within the TWQR of 500 mg/L. This was due to the formation of ettringite. The formation of ettringite was found to cause a pH decrease, which required more alkalinity from FA or lime in order to maintain the pH of the mixture in the range of 11.5 to 12.5. This pH range is where ettringite is stable. When there was less alkalinity that could buffer the pH drop due to the H^+ ions released during the formation of ettringite, the percentage sulphate removal from the mixture was reduced due to the dissolution of ettringite.

Removal of sulphate ions from Rand Uranium mine water as ettringite using coal FA, lime and $Al(OH)_3$ was found to be enhanced by the hydrodynamic cavitation that occurs in the jet loop reactor. This was confirmed when the mixture was first mixed in a jet loop reactor for 45 min and then the mixing technique was changed to normal stirring. This resulted in reduced sulphate removal compared to when the mixing was done in jet loop reactor throughout the duration of the mixing process. Hydrodynamic mixing of Rand Uranium mine water with FA, lime and $Al(OH)_3$ resulted in an increase in temperature of the mixture gradually to about 80 ^{0}C.

Treatment of Rand Uranium mine water with Matla coal FA, lime and $Al(OH)_3$ has resulted in the removal of U, Th, Zn, Ni, Cu, As, Pb, Be and Cd to below the limit for potable water set by the World Health Organization. On the hand Sr, Mo, Cr, V and Ba leached into the water when FA was used to treat Rand Uranium mine water. The final concentration of Cr, V and Ba was less than the limit for potable water. The final concentration of Mo and Sr was above the limit for potable water. This means that the product from coal FA, lime and $Al(OH)_3$ treatment need only a bit of polishing to adjust the pH and reduce the concentration of Mo and Sr before it can be used for domestic purposes. Otherwise if only pH of the water is adjusted the water will be fit for agricultural and industrial uses.

8.2. SIGNIFICANCE OF THE FINDINGS

Results obtained in this research are of importance to scientists and the water treatment and mining industry. The novel findings obtained by this research are as follows:

1. Matla coal FA was found to be radioactive. Since coal FA has found application in construction (brick and cement making), the products from the reuse of coal FA need assessment for precautionary purposes.

2. Geochemist's workbench (GWB) software was used to calculate the species distribution of potentially toxic elements in mine water. The results can be used to predict how species are distributed and these results can be used to predict the mobility, bioavailability and hence toxicity of the potential toxic element. According to the literature, the free ions are more mobile and therefore have high probability of uptake by the flora and fauna, thereby increasing their toxicity.

   The GWB was also used to predict the probable mineral phases that could occur during treatment of mine water with coal FA. The results obtained correlated with the experimental results. This showed that GWB can be used to predict what can happen during treatment of mine water at specific conditions. This is important for planning of the treatment protocol of a particular mine water and would result in saving time during optimization.

3. During treatment of Rand Uranium mine water with Matla coal FA, naturally occurring radioactive materials (NORM) such as Th and U were removed by almost 100 %. This means that coal FA (a radionuclide containing waste material) can be used to treat radionuclide containing mine water without adding NORMs into the treated water. Since coal FA had relatively high concentration of Th and U compared to mine water, the added radionuclides would not change the radioactivity of the solid residues. This means that the solid residues can be reused in the same way as the original coal FA without any significant enhancement of the radionuclide concentration.

4. Treatment of Matla mine water with coal FA in the jet loop reactor enhanced the kinetics of the removal of sulphate ions. During treatment of mine water with coal FA, lime and $Al(OH)_3$ it was discovered that hydrodynamic cavitation increased the rate of removal of sulphate ions as ettringite. This was because hydrodynamic mixing increased the mixing intensity of mine water with coal FA, lime and $Al(OH)_3$. The treatment of mine water in the jet loop reactor was conducted at 80 L capacity and after 120 min; the sulphate ions and many other contaminants were removed to within TWQR for potable water. This means that there is potential of up scaling the treatment of mine water with coal FA to an industrial scale.

5. Removal of sulphate ions using only flocculants resulted in the product water containing elevated concentration of chloride ions. From the results obtained in this study, it is not recommended to use Al based flocculants such as ACH to remove sulphate ions from mine water. This was because the product water after precipitating sulphate ions (to within TWQR) from mine water contained elevated concentration of Cl ions (greater than 1000 mg/L) which was well above the TWQR for potable water.

8.3. ADVANTAGES OF THE FLY ASH-LIME-AL(OH)$_3$ PROCESS

- This process does not require pre-treatment and can handle any quality of the raw water
- The sludge produced dewaters easily and according to previous researchers can be used for mine backfilling so the waste material is not difficult to handle. This would result in the prevention of further formation of mine water at abandoned mines.
- The process is a one step and simple process. The process control requires pH monitoring.

8.4. RECOMMENDATIONS AND FUTURE WORK

Although the total concentration of U and Th was found be very low after treatment of Rand Uranium mine water with Matla coal FA, the gross alpha and beta radioactivity still need to be assessed. This is because Matla coal fly ash and Rand Uranium mine water have shown radioactivity values greater than the normal values. After the radioactivity of the product water has been confirmed to be low, the process would be up scaled to 1000 L pilot plant at one of the Eskom coal mines. It is suggested to study the effect of ACH on the removal of sulphate ions from mine water at pH greater than 11 at 1000 L pilot scale.

REFERENCES

Adlem, C.J.L., 1997. *Treatment of sulfate-rich effluents with the barium sulfide process*, University of Pretoria, South Africa.

Adriano, D.C., Page, A.L., Elseewi, A.A., Chang, A.C. and Straughan, I., 1980. Utilization and disposal of fly ash and other coal residues in terrestrial ecosystems: A review. *Journal of Environmental Quality,* **9**, pp. 333-344.

Allen, H.E., Hall, R.H. and Brisbin, T.D., 1980. Metal Speciation: Effects on Aquatic Toxicity. *American Chemical Society,* **14**(4), pp. 441-443.

ASTM, 1994. *Standard specification for fly ash and raw or calcined natural pozzolan for use as mineral admixture in Portland cement concrete.* Pennsylvania: American Society for Testing and Materials.

Aziz, H.A., Adlan, M.N. and Ariffin, K.S., 2008. Heavy metals (Cd, Pb, Zn, Ni, Cu and Cr(III)) removal from water in Malaysia: Post treatment by high quality limestone. *Bioresource Technology,* **99**(6), pp. 1578-1583.

Baykal, G. and Saygili, A., 2011. A new technique to reduce the radioactivity of fly ash utilized in the construction industry. *Fuel,* **90**(4), pp. 1612-1617.

Beer, M., Maree, J., Wilsenach, J., Motaung, S., Bologo, L., Radebe, V., 2010. Acid Mine Water Reclamation using the ABC Process (Alkali Barium Calcium Process), Wolkersdorfer & Freund, *Mine Water & Innovative Thinking*, September 5-9 2010, Cape Brenton University, pp. 115.

Bethke, C.M. and Yeakel, S., 2010. *The Geochemist's Workbench® Release 8.0: GWB Essentials Guide.* Colorado, USA: Hydrogeology Program University of Illinois.

Blowes, D.W. and Ptacek, C.J., 1994. Acid-neutralization mechanisms in inactive mine tailings. *Short Course Handbook on Environmental Geochemistry of Sulfide Mine Waste.* 22 edn. Canada: Mineralogical Association of Canada, Nepean, pp. 271-291.

Bologo, V., Maree, J. and Carlsson, F., 2012. Application of magnesium hydroxide and barium hydroxide for the removal of metals and sulphate from mine water. *Water SA,* **38**(1), pp. 23-28.

Bonotto, D.M., Bueno, T.O., Tessari, B.W. and Silva, A., 2009. The natural radioactivity in water by gross alpha and beta measurements. *Radiation Measurements,* **44**(1), pp. 92-101.

Bosman, D.J., 1983. Lime treatment of acid mine water and associated solids/liquid separation. *Wat. Sci. Tech.,* **15**, pp. 71-84.

Bosman, D.J., Clayton, J.A., Maree, J.P. and Adlem, C.J.L., 1990. Removal of sulphates from mine water with sulphide, *Proceedings of the Lisbon 90 International Symposium: Acidic Mine Water in Pyritic Environments* 1990, pp. 16.

Bratby, J., 2006. *Coagulation and flocculation in water and wastewater treatment.* 2nd edn. London, UK: IWA Publishing.

Chen, Z., Luan, Z., Jia, Z. and Li, X., 2009. Study on the hydrolysis/precipitation behaviour of Keggin Al13 and Al30 polymers in polyaluminium solutions. *Journal of Environmental Management,* **90**(8), pp. 2831-2840.

Chung, Y.M. and Luo, K.H., 2002. Unsteady Heat Transfer Analysis of an Impinging Jet. *Journal of Heat Transfer,* **124**, pp. 1039-1048.

Cobley, A.J. and Mason, T.J., 2010. Ultrasound is Not Just for Cleaning! http://www.pcbdesign007.com [10/11, 2012].

Coetzee, H., Hobbs, P.J., Burgess, J.E., Thomas, A. and Keet, M., 2010. *Report to the Inter-ministerial committee on acid mine drainage: Mine water management in the*

Witwatersrand gold fields with special emphasis on acid mine drainage. South Africa: Council for Geoscience.

Cole, D.I., 1998. Handbook, Council for Geoscience. In: M.G.C. WILSON and C.R. ANHAUSSER, eds, *Uranium In: The mineral resources of South Africa.* 16 edn. South Africa: Council of Geosciences of South Africa, pp. 642-652.

Cravotta, C.A., Brady, K.B.C., Smith, M.W. and Beam, R.L., 1990. Effectiveness of the addition of alkaline materials at surface coal mines in preventing or abating acid mine drainage- Part 1, Geochemical considerations, Charleston, W.V., ed. In: *Proceedings of the 1990 Mining and Reclamation Conference* 1990, West Virginia University, pp. 221-223.

Cravotta, C.A. and Trahan, M.K., 1999. Limestone drains to increase pH and remove dissolved metals from acidic mine drainage. *Applied Geochemistry,* **14**, pp. 581-606.

Debertin, K., 1996. The art of realizing the Becquerel. *Applied Radiation and Isotopes,* **47**(4), pp. 423-431.

Del Pino, M.P. and Durham, B.D., 1999. Wastewater reuse through dual-membrane processes: opportunities for sustainable water resources. *Desalination,* **124**(1-3), pp. 271-277.

Department of Water Affairs and Forestry, 1996. *South African Water Quality Guidelines (second edition), Volume 3: Industrial Use.* Pretoria, South Africa: CSIR Environmental Services.

Department of Water Affairs and Forestry, 1996. *South African Water Quality, Guidelines (second edition). Volume 1: Domestic Use.* Pretoria, South Africa: CSIR Environmental Services.

Department of Water Affairs and Forestry, 1996. *South African Water Quality, Guidelines (second edition). Volume 4: Agricultural Use: Irrigation.* PRETORIA, Republic of South Africa: CSIR.

Depoi, F.S., Pozebon, D. and Kalkreuth, W.D., 2008. Chemical characterization of feed coals and combustion by products from Brazilian power plants. *International Journal of Coal Geology,* **76**(3), pp. 227-236.

Dong, H., Guan, X., Wang, D., Li, C., Yang, X. and Dou, X., 2011. A novel application of H_2O_2-Fe(II) process for arsenate removal from synthetic acid mine drainage (AMD) water. *Chemosphere,* **85**(7), pp. 1115-1121.

Duan, J. and Gregory, J., 2003. Coagulation by hydrolysing metal salts. *Advances in Colloid and Interface Science,* **100-102**, pp. 475-502.

Durand, J.F., 2012. The impact of gold mining on the Witwatersrand on the rivers and karst system of Gauteng and North West Province, South Africa. *Journal of African Earth Sciences,* **68**(0), pp. 24-43.

Eaton, A.D., Lenore, S.C. and Arnold, E.G., 1995. *Standard methods for the examination of water and wastewater.* Washington D.C.: American Public Health Association,.

Entezari, M.H., Mostafai, M. and Sarafraz-Yazdi, A., 2006. A combination of ultrasound and a bio-catalyst: removal of 2-chlorophenol from aqueous solution. *Ultrasonics Sonochemistry,* **13**(1), pp. 37-41.

Fatoba, O.O., 2010. *Chemical interactions and mobility of species in fly ash-brine co-disposal systems*, University of the Western Cape, Cape Town, South Africa.

Florence, T.M., Morrison, G.M. and Stauber, J.L., 1992. Determination of trace element speciation and the role of speciation in aquatic toxicity. *Science of the Total Environment,* **125**(0), pp. 1-13.

Gavaskar, A.R., 1999. Design and construction techniques for permeable reactive barriers. *Journal of Hazardous Materials,* **68**(1–2), pp. 41-71.

Gavi, E., Marchiso, D.L. and Barresi, A.L., 2007. CFD modelling and scale-up of Confined Impinging Jet Reactors. *Chemical Engineering Science 62 (2007) 2228 – 2241,* **62**, pp. 2228-2241.

Gazea, B., Adam, K. and Kontopoulos, A., 1996. A review of passive systems for the treatment of acid mine drainage *Journal of Minerals Engineering,* **9**(1), pp. 23-42.

Geldenhuys, A.J., Maree, J.P., De Berr, M. and Hlabela, P., 2001. An Integrated limestone/lime process for partial sulphate removal, 2001, CSIR.

Georgantas, D.A. and Grigoropoulou, H.P., 2007. Orthophosphate and metaphosphate ion removal from aqueous solution using alum and aluminium hydroxide. *Journal of colloid and interface science,* **315**(1), pp. 70-79.

Gitari, M.W., Petrik, L.F., Etchebers, O., Key, D.L., Iwuoha, E. and Okujeni, C., 2006. Treatment of acid mine drainage with fly ash: removal of major contaminants and trace elements. *Journal of Environmental Science Health A: Toxicological, Hazardous. Substances,* **41**, pp. 1729-1747.

Gitari, W.M., Petrik, L.F., Etchebers, O., Key, D.L., Iwuoha, E. and Okujeni, C., 2008. Utilization of Fly Ash for Treatment of coal mines waste water: Solubility controls on major inorganic contaminants. *Fuel,* **87**, pp. 2450-2462.

Guan, X., Ma, J., Dong, H. and Jiang, L., 2009. Removal of arsenic from water: Effect of calcium ions on As(III) removal in the $KMnO_4$–Fe(II) process. *Water research,* **43**(20), pp. 5119-5128.

Gunter, P., Naidu, T., 2008. Mine water reclamation-towards zero disposal. WISA Biennial Conference, Johannesburg http://www.ewisa.co.za/misc/WISAConf/default2008.htm

Hammack, R.W., Dvorak, D.H. and Edenborn, H.M., 1993. The Use of Biogenic Hydrogen Sulfide to Selectively Recover Metals from a Severely Contaminated Mine Drainage, *Proceedings of the International Biohydrometallurgy Symposium*.

Hampson, C.J. and Bailey, J.E., 1982. On the structure of some precipitated calcium alumino–sulphate hydrates. *Journal of Material Science,* **17**, pp. 3341-3346.

Hedin, R.S., Nairn, R.W. and Kleinmann, R.L.P., 1994. *Passive Treatment of Coal Mine Drainage.* Information Circular No. 9389. US Bureau of Mines.

Hlabela, P., Maree, J. and Bruinsma, D., 2007. Barium Carbonate Process for Sulphate and Metal Removal from Mine Water. *Mine Water and the Environment,* **26**, pp. 14-22.

INAP (International network for acid prevention), The Global Acid Rock Drainage Guide, http://64.130.26.41/index.php/History_of_Passive_Treatment [07/2012, 2012].

Jagea, C.R., Zipper, C.E. and Noble, R., 2001. Factors Affecting Alkalinity Generation by Successive Alkalinity-Producing Systems: Regression Analysis. *Journal of Environmental Quality,* **30**(3), pp. 1015-1022.

Jain, C.K. and Ali, I., 2000. Arsenic: occurrence, toxicity and speciation techniques. *Water Research,* **34**(17), pp. 4304-4312.

Johnson, B.D. and Hallberg, K.B., 2005. Acid mine drainage remediation options: a review. *Science of the Total Environment,* **338**, pp. 3-14.

Johnson, D.B., 2000. Biological removal of sulfurous compounds from inorganic wastewaters In: Lens P, Hulshoff Pol L, Environmental Technologies to treat sulfur pollution: Principles and Engineering, ed. In: *International Association on Water Quality* 2000, pp. 175–-206.

Johnson, D.B. and Hallberg, K.B., 2003. The microbiology of acidic mine waters. *Res Microbiol,* **154**, pp. 466-473.

Johnson, D.B. and Hallberg, K.B., 2004. Biogeochemistry of the compost bioreactor components of a composite acid mine drainage passive remediation system. *Science Total Environmental,* **338**, pp. 81-93.

Juby, G.J.G., Shutte, C.F., Van Leeuwen, J.W., 1996. Desalination of calcium sulphate scaling: design and operation of the SPARRO process. *Water SA,* **22**(2), pp. 166-172.

Jyoti, K.K. and Pandit, A.B., 2001. Water disinfection by acoustic and hydrodynamic cavitation. *Biochemical Engineering Journal,* **7**(3), pp. 201-212.

Kaksonen, A., Sulfate-reduction based bioprocesses in mining biotechnology: Remediation of surface waters [Homepage of Tampere University of Technology, Environmental Engineering and Biotechnology, Finland], [Online]. Available: http://wiki.biomine.skelleftea.se/biomine/srb/index_19.htm [June 2012, 2012].

Kentish,S.E. and Stevens, G.W., 2001. Innovations in separations technology for the recycling and re-use of liquid waste streams. *Chemical Engineering Journal,* **84**(2), pp. 149-159.

Keplar, D.A. and McCleary, E.C., 1994. Successive Alkalinity Producing Systems (SAPS) for the treatment of acidic mine drainage, *Proceedings of the International Land Reclamation and Mine Drainage Conference and 3rd International Conference on the Abatement of Acidic Drainage* 1994, pp. 195.

Kitchener, J.A., 1957. *Ion-exchange Resins.* Great Brittan: Butler and Tanner Ltd.

Kovler, K., 2012. Does the utilization of coal fly ash in concrete construction present a radiation hazard? *Construction and Building Materials,* **29**(0), pp. 158-166.

Kumarathasan, P., McCarthy, G.J., Hassett, D.J. and Pflughoeft-Hassett, D.F., 1990. Oxyanion substituted ettringites: synthesis and characterization, and their potential role in immobilization of As, B, Cr, Se, and V, *Materials Research Society Symposia* 1990, pp. 83.

Lapakko, K.A., 1994. Determinations for Metal Mine Waste and a Proposed Alternative. *Proc. International Land Reclamation and Mine Drainage Conference and 3rd International Conference on the Abatement of Acidic Drainage, Pittsburgh,* **1**, pp. 129-137.

Lawrence, R.W. and Wang, Y., 1997. Determination of Neutralization Potential in the Prediction of Acid Rock Drainage, *Proc. 4th International Conference on Acid Rock Drainage* 1997, pp. 449.

Liu, T. and Chin, C.M., 2009. Improved coagulation performance using preformed polymeric iron chloride (PICl). *Colloids and Surfaces A: Physicochemical and Engineering Aspects,* **339**(1-3), pp. 192-198.

Long, K.R., Van Gosen, B.S., Foley, N.K. and Cordier, D., 2010-last update, The Geology of Rare Earth Elements: Rare Earth Elements Are Not "Rare" [Homepage of geology.com], [Online]. Available: http://geology.com/usgs/ree-geology/ [June, 6, 2012].

Lottermoser, B.G., 2007. *Mine Wastes: Characterization, Treatment and Environmental Impacts.* 2nd edn. Springer.

Lytle, D.A., Summers, R.S. and Sorg, T.J., 1992. Removal of beryllium from drinking water by chemical coagulation and lime softening, *Journal of Water Supply Research and Technology-AQUA, 41*(5), pp. 330-339.

Madzivire, G., 2010. *Removal of sulphates from South African mine water using coal fly ash*, MSc Thesis, University of the Western Cape.

Madzivire, G., Petrik, L.F., Gitari, W.M., Ojumu, T.V. and Balfour, G., 2010. Application of coal fly ash to circumneutral mine waters for the removal of sulphates as gypsum and ettringite. *Mineral Engineering,* **23**, pp. 252-257.

Madzivire, G., Gitari, W.M., Vadapalli, V.R.K., Ojumu, T.V. and Petrik, L.F., 2011. Fate of sulphate removed during the treatment of circumneutral mine water and acid mine drainage with coal fly ash: Modelling and experimental approach. *Mineral Engineering,* **24**(13), pp. 1467-1477.

Maree, J.P., Bosman, D.J. and Jenkins, G.R., 1989. Chemical removal of sulphate and calcium and heavy metals from mining and power station effluents. *Water Sewage and Effluents,* **9**, pp. 10-25.

Mason, T.J., 2007. Developments in ultrasound—Non-medical. *Progress in biophysics and molecular biology,* **93**(1–3), pp. 166-175.

Matsuura, T., 2001. Progress in membrane science and technology for seawater desalination-a review. *Desalination,* **134**(1-3), pp. 47-54.

Mattigod, S.V., Dhanpat, R., Eary, L.E. and Ainsworth, C.C., 1990. Geochemical factors controlling the mobilization of inorganic constituents from fossil fuel combustion residues: Review of the major elements. *Journal of Environmental Quality,* **19**, pp. 188-201.

Mayes, W.M., Batty, L.C., Younger, P.L., Jarvis, A.P., Koiv, M., Vohla, C. and Mander, U., 2009. Wetland treatment at extremes of pH: A review. *Science of the Total Environment,* **407**(13), pp. 3944-3957.

McCarthy, G.J., 1988. X-ray powder diffraction for studying the mineralogy of fly ash, in Fly Ash and Coal Conversion By-Products: Characterization, Utilization and Disposal IV. *Material Research Society Symposium Proceeding*, pp. 75.

Moreno, N., Querol, X., Ayora, C., Pereira, C.F. and Janssen-Jurkovicava, M., 2001. Utilization of zeolites synthesized from coal fly ash for the purification of acid mine waters. *Environmental Science and Technology,* **35**, pp. 3526-3534.

Morin, K.A. and Hutt, N.M., 1997. *Environmental Geochemistry of Minesite Drainage: Practical, Theory and Case Studies.* Vancouver, Canada: MDAG.

Mukhopadhyay, B., Bastias, L. and Mukhopadhyay, A., 2007. Limestone drain design parameters for acid rock drainage mitigation. *Mine Water and the Environment,* **26**, pp. 29-45.

Myneni, S.C.B., Samuel J. Traina, S.J. and Logan, T.J., 1998. Ettringite solubility and geochemistry of the $Ca(OH)_2$-$Al_2(SO_4)_3$-H_2O system at 1 atm pressure and 298 K. *Chemical Geology,* **148**, pp. 1-19.

Nairn, R.W., Hedin, R.S. and Watzlaf, G.R., 1991. A Preliminary Review of the Use of Anoxic Limestone Drains in the Passive Treatment of Acid Mine Drainage, *Proceedings of the 12th Annual West Virginia Surface Mine Drainage Task Force Symposium* 1991.

Nairn, R.W. and Mercer, M.N., 2000. Alkaline generation and metals retention in a successive alkalinity producing system. *Mine Water and the Environment,* **19**, pp. 124-133.

Neculita, C.M., Zagury, G.J. and Brussie, B., 2007. Passive treatment of acid mine drainage in bioreactors using sulfate-reducing bacteria: critical review and research needs. *Journal of Environmental Quality,* **36**, pp. 1-36.

Neupane, G. and Donahoe, R.J., Leachability of elements in alkaline and acidic coal fly ash samples during batch and column leaching tests. *Fuel,* (http://dx.doi.org/10.1016/j.fuel.2012.06.013).

Newman, R.T., Lindsay, R., Maphoto, K.P., Mlwilo, N.A., Mohanty, A.K., Roux, D.G., De Meijer, R.J. and Hlatshwayo, I.N., 2008. Determination of soil, sand and ore primordial radionuclide concentrations by full-spectrum analyses of high-purity germanium detector spectra. *Applied Radiation and Isotopes,* **66**(6–7), pp. 855-859.

Papastefanou, C., 2010. Escaping radioactivity from coal-fired power plants (CPPs) due to coal burning and the associated hazards: A review. *Journal of Environmental Radioactivity,* **101**(3), pp. 191-200.

Paschoa, A.S. and Steinhausler, F., (2010). CHAPTER 3: Terrestrial, Atmospheric, and Aquatic Natural Radioactivity. *Radioactivity in the Environment.* Elsevier, pp. 29-85.

Peppas, T.K., Karfopoulos, K.L., Karangelos, D.J., Rouni, P.K., Anagnostakis, M.J. and Simopoulos, S.E., 2010. Radiological and instrumental neutron activation analysis

determined characteristics of size-fractionated fly ash. *Journal of Hazardous Materials,* **181**(1–3), pp. 255-262.

Perkins, R.B. and Palmer, C.D., 1999. Solubility of ettringite ($Ca_6[Al(OH)_6]_2(SO_4)_3.26H_2O$) at 5-75°C. *Geochimica et Cosmochimica Acta,* **63**(13/14), pp. 1969-1980.

Pinetown, K.L., Ward, C.R. and Van Der Westhuizen, W.A., 2007. Quantitative evaluation of minerals in coal deposits in the Witbank and Highveld Coalfields, and the potential impact on acid mine drainage. *International Journal of Coal Geology,* **70**(1-3), pp. 166-183.

Postgate, J.R., 1984. *The Sulphate-Reducing Bacteria.* 2 edn. New York: Cambridge University Press.

Pulles, W., Juby, G.J.B., Busby, R.W., 1992. Development of the Slurry Precipitation and Recycle Reverse Osmosis (SPARRO) technology for the scaling mine waters. *Water Science Technology,* **25**(10), pp. 177-192.

Querol, X., Umana, J.C., Alastuey, A., Ayora, C., Lopez-Soler, A. and Plana, F., 2001. Extraction of soluble major and trace elements from fly ash in open and closed leaching systems. *Fuel,* **80**(6), pp. 801-813.

Reznik, I.J., Gavrieli, I. and Ganor, J., 2009. Kinetics of gypsum nucleation and crystal growth from Dead Sea brine. *Geochimica et Cosmochimica Acta,* **73**(20), pp. 6218-6230.

Robb, G. A., Robinson, J. D. F., 1995. Acid drainage from mines. *The Geographical Journal,* **161**(1), pp. 47-55.

Rotting, T., Cama, J., Ayora, C., Cortina, J.L. and De Pablo, J., 2005. The use of caustic magnesia to remove cadmium from Water, *9th International mine water congress, Oviedo, Spain, 5-7 September 2005*, pp. 641-647.

Rowley, M., Warkentin, D.D. and Sicotte, V., 1997. Site demonstration of the biosulfide processes at the former Britannia mine. *Proceedings of the Fourth International Conference on Acid Rock Drainage* 1997, pp. 1531.

Roy. D.M., Luke. K., Diamond. S., 1985. Characterization of fly ash and its reactions in concrete. *Mater. Res.Soc. Symp. Proc.,* **43**, pp. 3-20.

Russeva, E., 1995. Speciation analysis-peculiarities and requirements.. *Anal. Lab.,* **4**(3), pp. 143-148.

Scheid, N., Becker, S., Ducking, M., Hampel, G., Volker Kratz, J., Watzke, P., Weis, P. and Zauner, S., 2009. Forensic investigation of brick stones using instrumental neutron activation analysis (INAA), laser ablation–inductively coupled plasma–mass spectrometry (LA–ICP–MS) and X-ray fluorescence analysis (XRF). *Applied Radiation and Isotopes,* **67**(12), pp. 2128-2132.

Schoeman, J.J and Steyn, A, 2001. Investigation into alternative Water Treatment Technologies for the treatment of underground mine water discharged by Grootvlei Proprietary Ltd Into the Blesbokspruit in South Africa. *Desalination,* **133**, pp. 13-30.

Scott, R., 1995. *Flooding of Central and East Rand gold mines – an investigation into controls over the inflow rate, water quality and the predicted impacts of flooded mines.* Report No. 486/1/95. Pretoria, South Africa: Water Research Commission.

Senior, C.L., Zeng, T., Che, J., Ames, M.R., Sarofim, A.F., Olmez, I., Huggins, F.E., Shah, N., Huffman, G.P., Kolker, A., Mroczkowski, S., Palmer, C. and Finkelman., 2000. Distribution of trace elements in selected pulverized coals as a function of particle size and density. *Fuel Processing Technology,* **63**(2–3), pp. 215-241.

Senthil, K. P., Siva Kumar, M. and Pandit, A.B., 2000. Experimental quantification of chemical effects of hydrodynamic cavitation. *Chemical Engineering Science,* **55**(9), pp. 1633-1639.

Silva, R., Cadorin, L. and Rubio, J., 2010. Sulphate ions removal from an aqueous solution: I. Co-precipitation with hydrolysed aluminium-bearing salts. *Mineral Engineering,* **23**(15), pp. 1220-1226.

Skousen, J., Renton, J., Brown, H., Evans, P., Leavitt, B., Brady, K., Cohen, L. and Ziemkiewicz, P., 1997. Neutralization Potential of Overburden Samples Containing Siderite. *Journal of Environmental Quality,* **6**(3), pp. 673-681.

Skousen, J.G., Smith, R.M., Sencindiver, J.C., 1990. The development of the acid base account. Green Lands. *West Virginia Mining and Reclamation Association,* **20**(1), pp. 32-37.

Smit, J. and Sibilski, U.E., 2003. Pilot Plant Study to Treat Typical Gold Mine Minewater Using the SAVMIN Process, *Water in Mining Conference*.

Smit, J.P., 1999. The purification of polluted mine water. *International symposium of Mine Water & Environment for the 21st Century*.

Sobek, A.A., Schuller, W.A., Freeman, J.R. and Smith, R.M., 1978. *Field and laboratory methods applicable to overburden and minesoils.* EPA 600/2-78-054.

Steed, V.S., Suidan, M.T., Gupta, M., Miyahara, T., Acheson, C.M. and Sayles, G.D, 2000. Development of a sulfate-reducing biological process to remove heavy metals from acid mine drainage. *Water Environment Research,* **72**, pp. 530-535.

Strathmann, H., 2010. Chapter 6 Ion-Exchange Membrane Processes in Water Treatment. *Sustainability Science and Engineering.* Elsevier, pp. 141-199.

Stumm, W. and Morgan, J., 1996. *Aquatic Chemistry.* New York: Wiley & Sons.

Surender, D., 2009. *Active neutralization and amerioration of acid mine drainage with fly ash*, MSc thesis, University of the Western Cape.

Tongwen, X., 2002. Electrodialysis processes with bipolar membranes (EDBM) in environmental protection—a review. *Resources, Conservation and Recycling,* **37**(1), pp. 1-22.

Tran, A.T.K., Zhang, Y., Jullok, N., Meesschaert, B., Pinoy, L. and Van Der Bruggen, B., 2012. Reverse osmosis concentrate treatment by a hybrid system consisting of a pellet reactor and electrodialysis. *Chemical Engineering Science,* **79**(0), pp. 228-238.

Turhan, Ş., Parmaksiz, A., Kose, A., Yuksel, A., Arikan, I.H. and Yucel, B., 2010. Radiological characteristics of pulverized fly ashes produced in Turkish coal-burning thermal power plants. *Fuel,* **89**(12), pp. 3892-3900.

TUTORVISTA.COM, 2010. Radioactivity. Available: http://chemistry.tutorvista.com/nuclear-chemistry/radioactivity.html [October 9, 2012].

United States Geological Survey, October 1997, 1997-last update, Radioactive Elements in Coal and Fly Ash: Abundance, Forms, and Environmental Significance [Homepage of USGS], [Online]. Available:http://pubs.usgs.gov/fs/1997/fs163-97/FS-163-97.pdf [November, 2011].

Vadapalli, V.R.K., Klink, M.J., Etchebers, O., Petrik, L.F., Gitari, W., White, R.A., Key, D. and Iwuoha, E., 2008. Neutralization of acid mine drainage using fly ash, and strength development of the resulting solid residues. *South African Journal of Science,* **104**(7/8), pp. 317-322.

Valerdi-Pérez, R., Lopez-Rodriguez, M. and Ibanez-Mengual, J.A., 2001. Characterizing an electrodialysis reversal pilot plant. *Desalination,* **137**(1-3), pp. 199-206.

Vassilev, S.V. and Vassileva, C.G., 2007. A new approach for the classification of coal fly ashes based on their origin, composition, properties, and behaviour. *Fuel,* **86**(10–11), pp. 1490-1512.

Warren, C.J. and Reardon, E.J., 1994. The solubility of ettringite at 25°C. *Cement and Concrete Research,* **24**(8), pp. 1515-1524.

Wei, C., Wang, W., Deng, Z. and Wu, C., 2007. Characteristics of high-sulfate wastewater treatment by two-phase anaerobic digestion process with Jet-loop anaerobic fluidized bed. *Journal of Environmental Sciences,* **19**(3), pp. 264-270.

Wieder, R.K. and Lang, G.E., 1982. Modification of acid mine drainage in a freshwater wetland, B.R. MCDONALD, ed. In: *Proceedings of the Symposium on Wetlands of the Unglaciated Appalachian Region* 1982, West Virginia University, pp. 43.

Winde, F., 2010. Uranium pollution of the Wonderfonteinspruit, 1997-2008 Part 1: uranium toxicity, regional background and mining-related sources of uranium pollution. *Water SA,* **36**(3), pp. 239-256.

WNA, August, 2011, 2011-last update, Naturally-Occurring Radioactive Materials (NORM) [Homepage of World Nuclear Association], [Online]. Available: http://www.world-nuclear.org/info/inf30.html[June, 2012, 2012].

World Health Organization, 2011. *Guidelines for drinking-water quality, third edition, incorporating first and second addenda Volume 1 - Recommendations.* Geneva: WHO Press.

World Health Organization, 2011. Radiological aspects: *Guidelines for Drinking water Quality.* Third edn. Geneva: World Health Organization, pp. 197-209.

Yang, Z., Gao, B. and Yue, Q., 2010. Coagulation performance and residual aluminium speciation of $Al_2(SO_4)_3$ and polyaluminium chloride (PAC) in Yellow River water treatment. *Chemical Engineering Journal,* **165**(1), pp. 122-132.

Younger, P.L., Banwart, S.A. and Hedin, R.S., 2002. *Mine Water: Hydrology, Pollution, Remediation.* Dordrecht Kluwer Academic Publishers.

Zhang, J. and Nancollas, G.H., 1992. Influence of calcium/sulfate molar ratio on the growth rate of calcium sulfate dihydrate at constant supersaturation. *Journal of Crystal Growth,* **118**(3–4), pp. 287-294.

Zhou, W., Gao, B., Yue, Q., Liu, L. and Wang, Y., 2006. Al-Ferron kinetics and quantitative calculation of Al(III) species in polyaluminium chloride coagulants. *Colloids and Surfaces A: Physicochemical and Engineering Aspects,* **278**(1–3), pp. 235-240.

Zielinski, R.A. and Budahn, J.R., 1998. Radionuclides in fly ash and bottom ash: improved characterization based on radiography and low energy gamma-ray spectrometry. *Fuel,* **77**(4), pp. 259-267.

Ziemkiewicz, P.F., Skousen, J.G., Brandt, D.L., Sterner, P.L. and Lovett, R.J., 1997. Acid mine drainage treatment with armoured limestone in open limestone channels. *Journal of Environmental Quality,* **26**, pp. 1017-1024.

APPENDIX

Appendix A1: This shows the raw spectra obtained by the XRD machine. It also shows the process that was used to identify the mineral phases that were in the different spectra obtained.

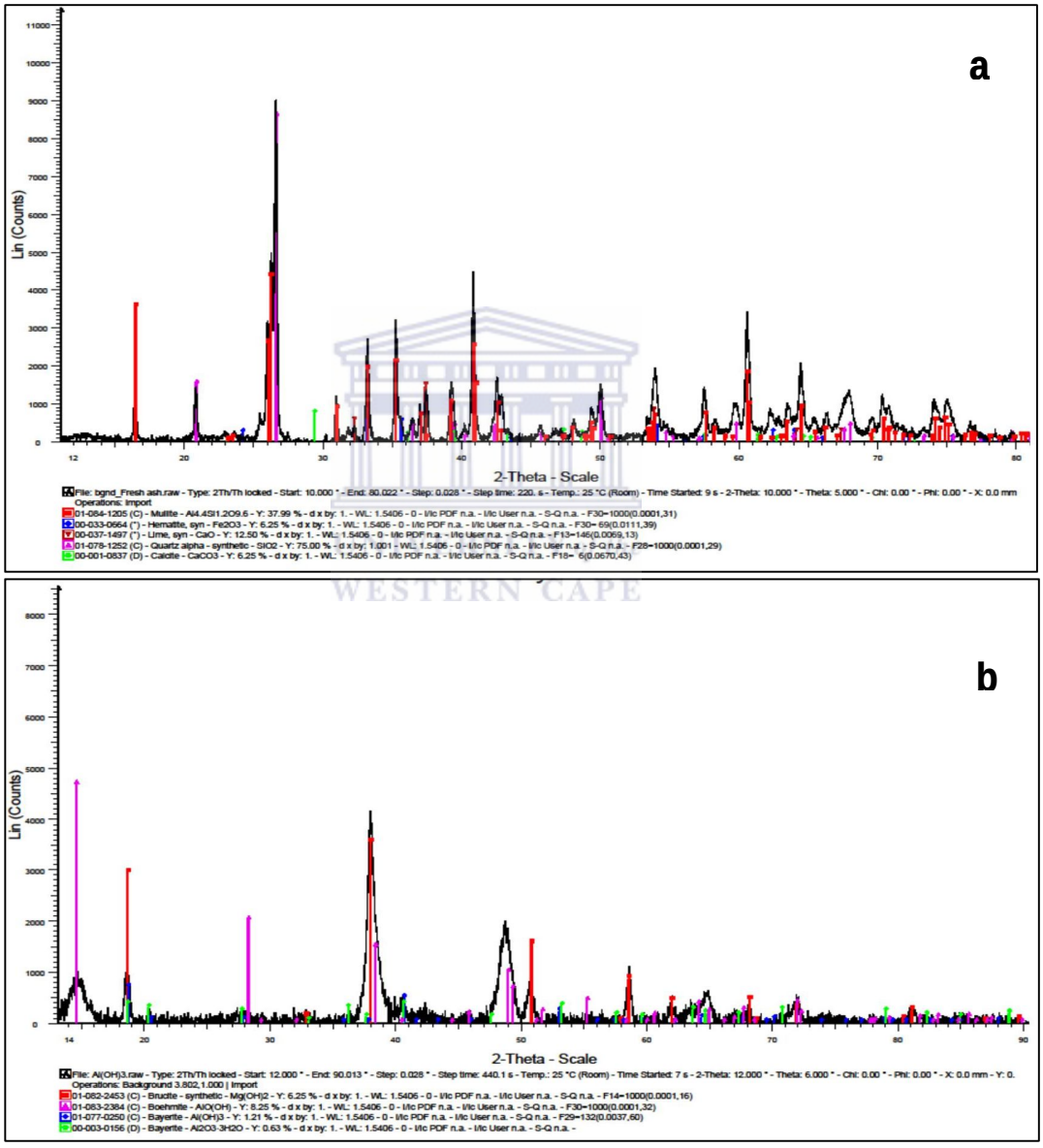

Figure A1.1: Identification of minerals responsible for the peaks in Matla coal FA (a) and aluminium hydroxide spectra (b)

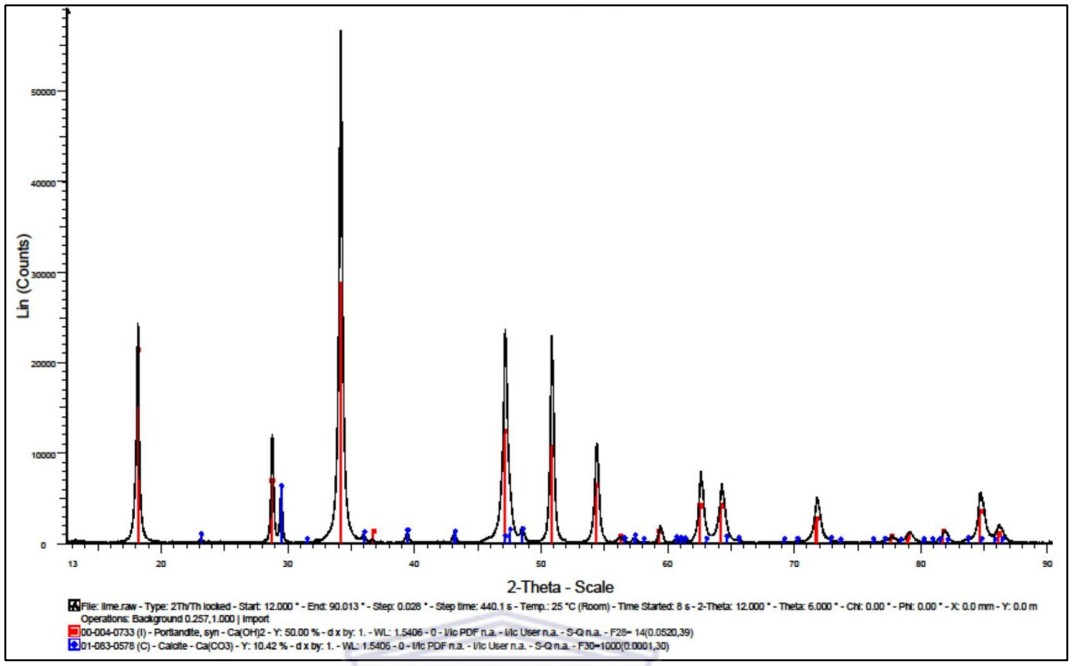

Figure A1.2: Identification of minerals responsible for the peaks on lime spectrum.

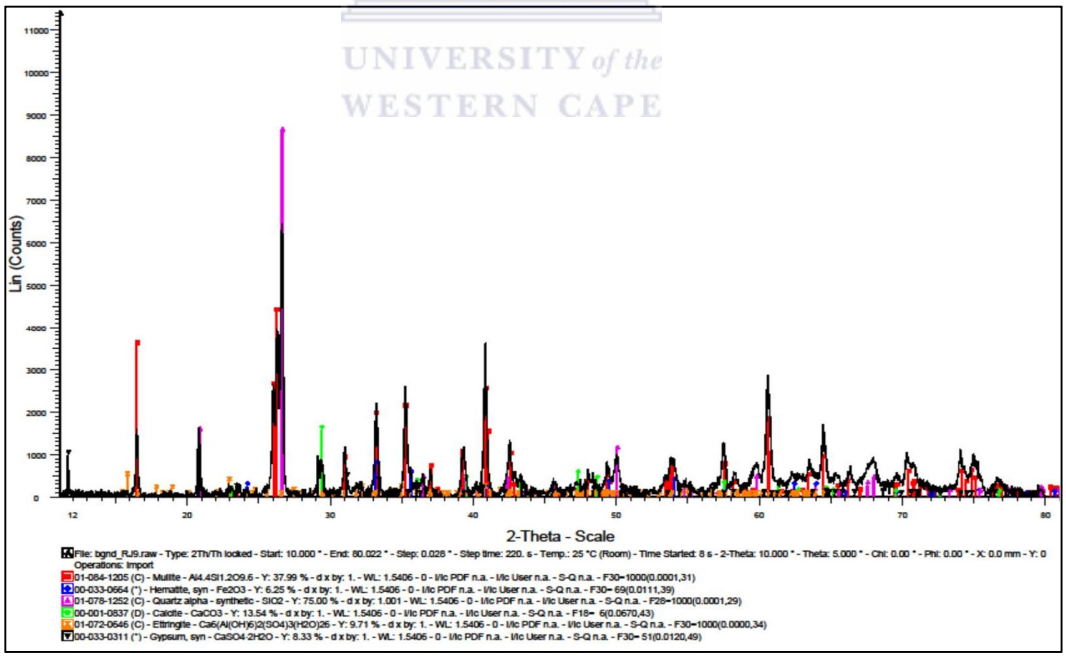

Figure A1.3: Identification of minerals responsible for the peaks on solid residues produced when Rand Uranium mine water was treated with Matla coal FA for 120 min using a jet loop reactor

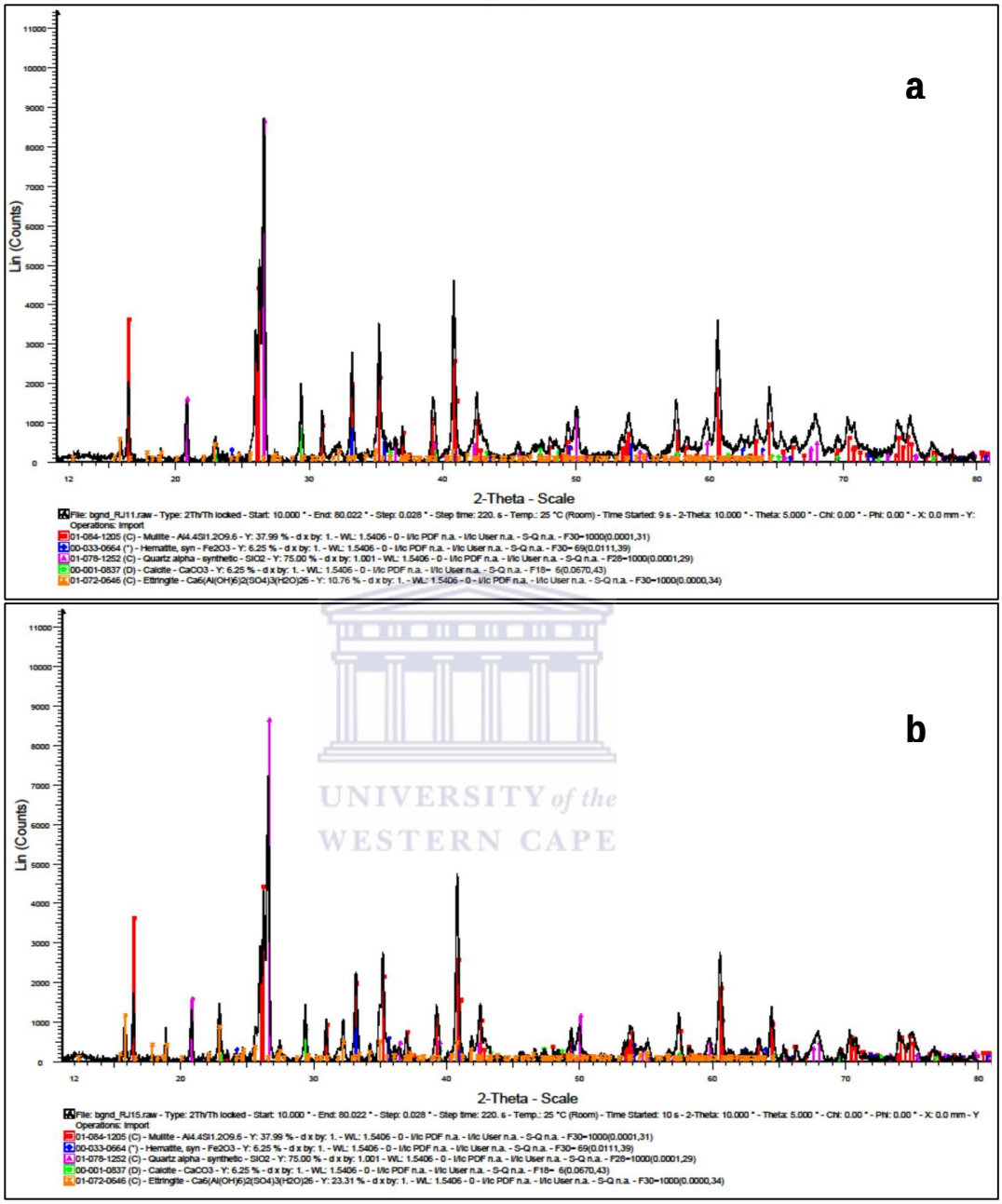

Figure A1.4: Identification of minerals responsible for the peaks on the spectra of the solid residues produced when Rand Uranium mine water was treated with Matla coal FA and lime for 30 min (a) and Matla coal, lime and aluminium hydroxide spectra 120 min (b) using a jet loop reactor.

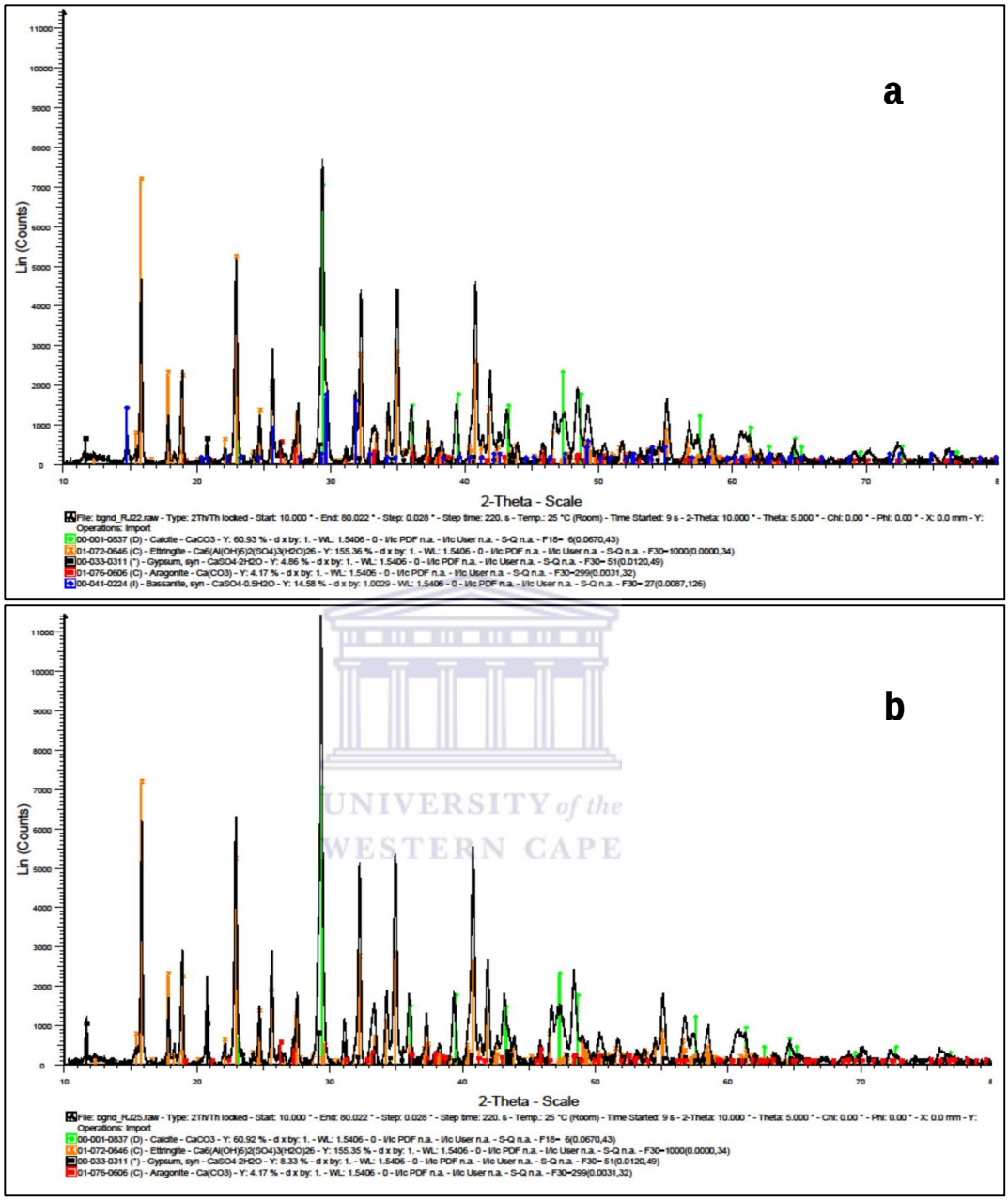

Figure A1.5: Identification of minerals responsible for the peaks on the spectrum of the solid residues produced when Rand Uranium mine water was treated with lime for 30 min (a) and lime and aluminium hydroxide spectra for 120 min (b) suing a jet loop reactor.

Appendix A2: This shows the speciation raw data from the Geochemist's workbench using the Spec8 program.

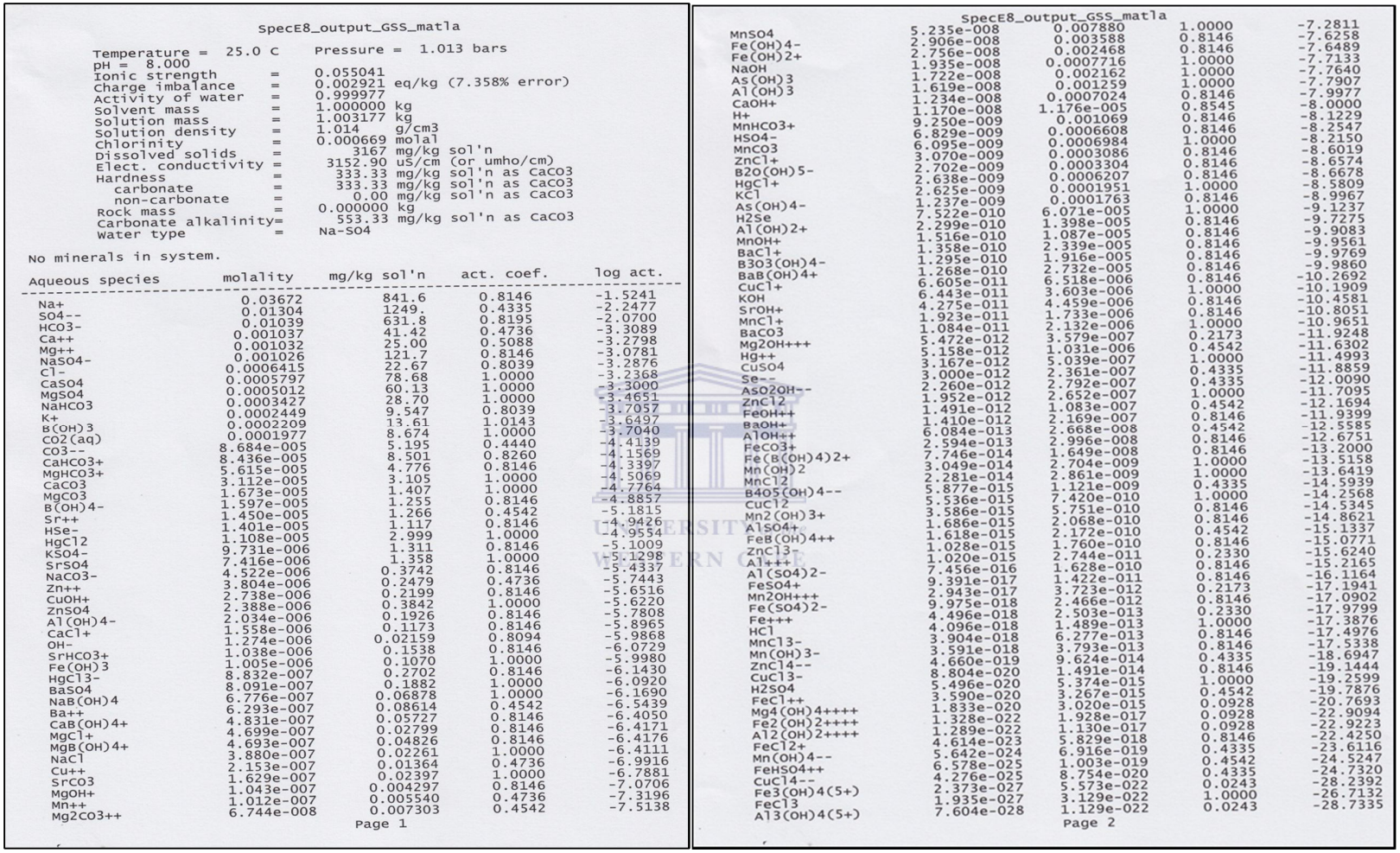

SpecE8_output_GSS_matla

Temperature = 25.0 C Pressure = 1.013 bars
pH = 8.000
Ionic strength = 0.055041
Charge imbalance = 0.002921 eq/kg (7.358% error)
Activity of water = 0.999977
Solvent mass = 1.000000 kg
Solution mass = 1.003177 kg
Solution density = 1.014 g/cm3
Chlorinity = 0.000669 molal
Dissolved solids = 3167 mg/kg sol'n
Elect. conductivity = 3152.90 uS/cm (or umho/cm)
Hardness = 333.33 mg/kg sol'n as CaCO3
carbonate = 333.33 mg/kg sol'n as CaCO3
non-carbonate = 0.00 mg/kg sol'n as CaCO3
Rock mass = 0.000000 kg
Carbonate alkalinity = 553.33 mg/kg sol'n as CaCO3
Water type = Na-SO4

No minerals in system.

Aqueous species	molality	mg/kg sol'n	act. coef.	log act.
Na+	0.03672	841.6	0.8146	-1.5241
SO4--	0.01304	1249.	0.4335	-2.2477
HCO3-	0.01039	631.8	0.8195	-2.0700
Ca++	0.001037	41.42	0.4736	-3.3089
Mg++	0.001032	25.00	0.5088	-3.2798
NaSO4-	0.001026	121.7	0.8146	-3.0781
Cl-	0.0006415	22.67	0.8039	-3.2876
CaSO4	0.0005797	78.68	1.0000	-3.2368
MgSO4	0.0005012	60.13	1.0000	-3.3000
NaHCO3	0.0003427	28.70	1.0000	-3.4651
K+	0.0002449	9.547	0.8039	-3.7057
B(OH)3	0.0002209	13.61	1.0143	-3.6497
CO2(aq)	0.0001977	8.674	1.0000	-3.7040
CO3--	8.684e-005	5.195	0.4440	-4.4139
CaHCO3+	8.436e-005	8.501	0.8260	-4.1569
MgHCO3+	5.615e-005	4.776	0.8146	-4.3397
CaCO3	3.112e-005	3.105	1.0000	-4.5069
MgCO3	1.673e-005	1.407	1.0000	-4.7764
B(OH)4-	1.597e-005	1.255	0.8146	-4.8857
Sr++	1.450e-005	1.266	0.4542	-5.1815
HSe-	1.401e-005	1.117	0.8146	-4.9426
HgCl2	1.108e-005	2.999	1.0000	-4.9554
KSO4-	9.731e-006	1.311	0.8146	-5.1009
SrSO4	7.416e-006	1.358	1.0000	-5.1298
NaCO3-	4.522e-006	0.3742	0.8146	-5.4337
Zn++	3.804e-006	0.2479	0.4736	-5.7443
CuOH+	2.738e-006	0.2199	0.8146	-5.6516
ZnSO4	2.388e-006	0.3842	1.0000	-5.6220
Al(OH)4-	2.034e-006	0.1926	0.8146	-5.7808
CaCl+	1.558e-006	0.1173	0.8146	-5.8965
OH-	1.274e-006	0.02159	0.8094	-5.9868
SrHCO3+	1.038e-006	0.1538	0.8146	-6.0729
Fe(OH)3	1.005e-006	0.1070	1.0000	-5.9980
HgCl3-	8.832e-007	0.2702	0.8146	-6.1430
BaSO4	8.091e-007	0.1882	1.0000	-6.0920
NaB(OH)4	6.776e-007	0.06878	1.0000	-6.1690
Ba++	6.293e-007	0.08614	0.4542	-6.5439
CaB(OH)4+	4.831e-007	0.05727	0.8146	-6.4050
MgCl+	4.699e-007	0.02799	0.8146	-6.4171
MgB(OH)4+	4.693e-007	0.04826	0.8146	-6.4176
NaCl	3.880e-007	0.02261	1.0000	-6.4111
Cu++	2.153e-007	0.01364	0.4736	-6.9916
SrCO3	1.629e-007	0.02397	1.0000	-6.7881
MgOH+	1.043e-007	0.004297	0.8146	-7.0706
Mn++	1.012e-007	0.005540	0.4736	-7.3196
Mg2CO3++	6.744e-008	0.007303	0.4542	-7.5138

Page 1

SpecE8_output_GSS_matla

MnSO4	5.235e-008	0.007880	1.0000	-7.2811
Fe(OH)4-	2.906e-008	0.003588	0.8146	-7.6258
Fe(OH)2+	2.756e-008	0.002468	0.8146	-7.6489
NaOH	1.935e-008	0.0007716	1.0000	-7.7133
As(OH)3	1.722e-008	0.002162	1.0000	-7.7640
Al(OH)3	1.619e-008	0.001259	1.0000	-7.7907
CaOH+	1.234e-008	0.0007024	0.8146	-7.9977
H+	1.170e-008	1.176e-005	0.8545	-8.0000
MnHCO3+	9.250e-009	0.001069	0.8146	-8.1229
HSO4-	6.829e-009	0.0006608	0.8146	-8.2547
MnCO3	6.095e-009	0.0006984	1.0000	-8.2150
ZnCl+	3.070e-009	0.0003086	0.8146	-8.6019
B2O(OH)5-	2.702e-009	0.0003304	0.8146	-8.6574
HgCl+	2.638e-009	0.0006207	0.8146	-8.6678
KCl	2.625e-009	0.0001951	1.0000	-8.5809
As(OH)4-	1.237e-009	0.0001763	0.8146	-8.9967
H2Se	7.522e-010	6.071e-005	1.0000	-9.1237
Al(OH)2+	2.299e-010	1.398e-005	0.8146	-9.7275
MnOH+	1.516e-010	1.087e-005	0.8146	-9.9083
BaCl+	1.358e-010	2.339e-005	0.8146	-9.9561
B3O3(OH)4-	1.295e-010	1.916e-005	0.8146	-9.9769
BaB(OH)4+	1.268e-010	2.732e-005	0.8146	-9.9860
CuCl+	6.605e-011	6.518e-006	0.8146	-10.2692
KOH	6.443e-011	3.603e-006	1.0000	-10.1909
SrOH+	4.275e-011	4.459e-006	0.8146	-10.4581
MnCl+	1.923e-011	1.733e-006	0.8146	-10.8051
BaCO3	1.084e-011	2.132e-006	1.0000	-10.9651
Mg2OH+++	5.472e-012	3.579e-007	0.2173	-11.9248
Hg++	5.158e-012	1.031e-006	0.4542	-11.6302
CuSO4	3.167e-012	5.039e-007	1.0000	-11.4993
Se--	3.000e-012	2.361e-007	0.4335	-11.8859
AsO2OH--	2.260e-012	2.792e-007	0.4335	-12.0090
ZnCl2	1.952e-012	2.652e-007	1.0000	-11.7095
FeOH++	1.491e-012	1.083e-007	0.4542	-12.1694
BaOH+	1.410e-012	2.169e-007	0.8146	-11.9399
AlOH++	6.084e-013	2.668e-008	0.4542	-12.5585
FeCO3+	2.594e-013	2.996e-008	0.8146	-12.6751
Fe(B(OH)4)2+	7.746e-014	1.649e-008	0.8146	-13.2000
Mn(OH)2	3.049e-014	2.704e-009	1.0000	-13.5158
MnCl2	2.281e-014	2.861e-009	1.0000	-13.6419
B4O5(OH)4--	5.877e-015	1.121e-009	0.4335	-14.5939
CuCl2	5.536e-015	7.420e-010	1.0000	-14.2568
Mn2(OH)3+	3.586e-015	5.751e-010	0.8146	-14.5345
AlSO4+	1.686e-015	2.068e-010	0.8146	-14.8621
FeB(OH)4++	1.618e-015	2.172e-010	0.4542	-15.1337
ZnCl3-	1.028e-015	1.760e-010	0.8146	-15.0771
Al+++	1.020e-015	2.744e-011	0.2330	-15.6240
Al(SO4)2-	7.456e-016	1.628e-010	0.8146	-15.2165
FeSO4+	9.391e-017	1.422e-011	0.8146	-16.1164
Mn2OH+++	2.943e-017	3.723e-012	0.2173	-17.1941
Fe(SO4)2-	9.975e-018	2.466e-012	0.8146	-17.0902
Fe+++	4.496e-018	2.503e-013	0.2330	-17.7999
HCl	4.096e-018	1.489e-013	1.0000	-17.3876
MnCl3-	3.904e-018	6.277e-013	0.8146	-17.4976
Mn(OH)3-	3.591e-018	3.793e-013	0.8146	-17.5338
ZnCl4--	4.660e-019	9.624e-014	0.4335	-18.6947
CuCl3-	8.804e-020	1.491e-014	0.8146	-19.1444
H2SO4	5.496e-020	5.374e-015	1.0000	-19.2599
FeCl++	3.590e-020	3.267e-015	0.4542	-19.7876
Mg4(OH)4++++	1.833e-020	3.020e-015	0.0928	-20.7693
Fe2(OH)2++++	1.328e-022	1.928e-017	0.0928	-22.9094
Al2(OH)2++++	1.289e-022	1.130e-017	0.0928	-22.9223
FeCl2+	4.614e-023	5.829e-018	0.8146	-22.4250
Mn(OH)4--	5.642e-024	6.916e-019	0.4335	-23.6116
FeHSO4++	6.578e-025	1.003e-019	0.4542	-24.5247
CuCl4--	4.276e-025	8.754e-020	0.4335	-24.7320
Fe3(OH)4(5+)	2.373e-027	5.573e-022	0.0243	-28.2392
FeCl3	1.935e-027	3.129e-022	1.0000	-26.7132
Al3(OH)4(5+)	7.604e-028	1.129e-022	0.0243	-28.7335

Page 2

Figure A2.1: The speciation results of Matla mine water obtained using the Spec8 program of the Geochemist's workbench software.

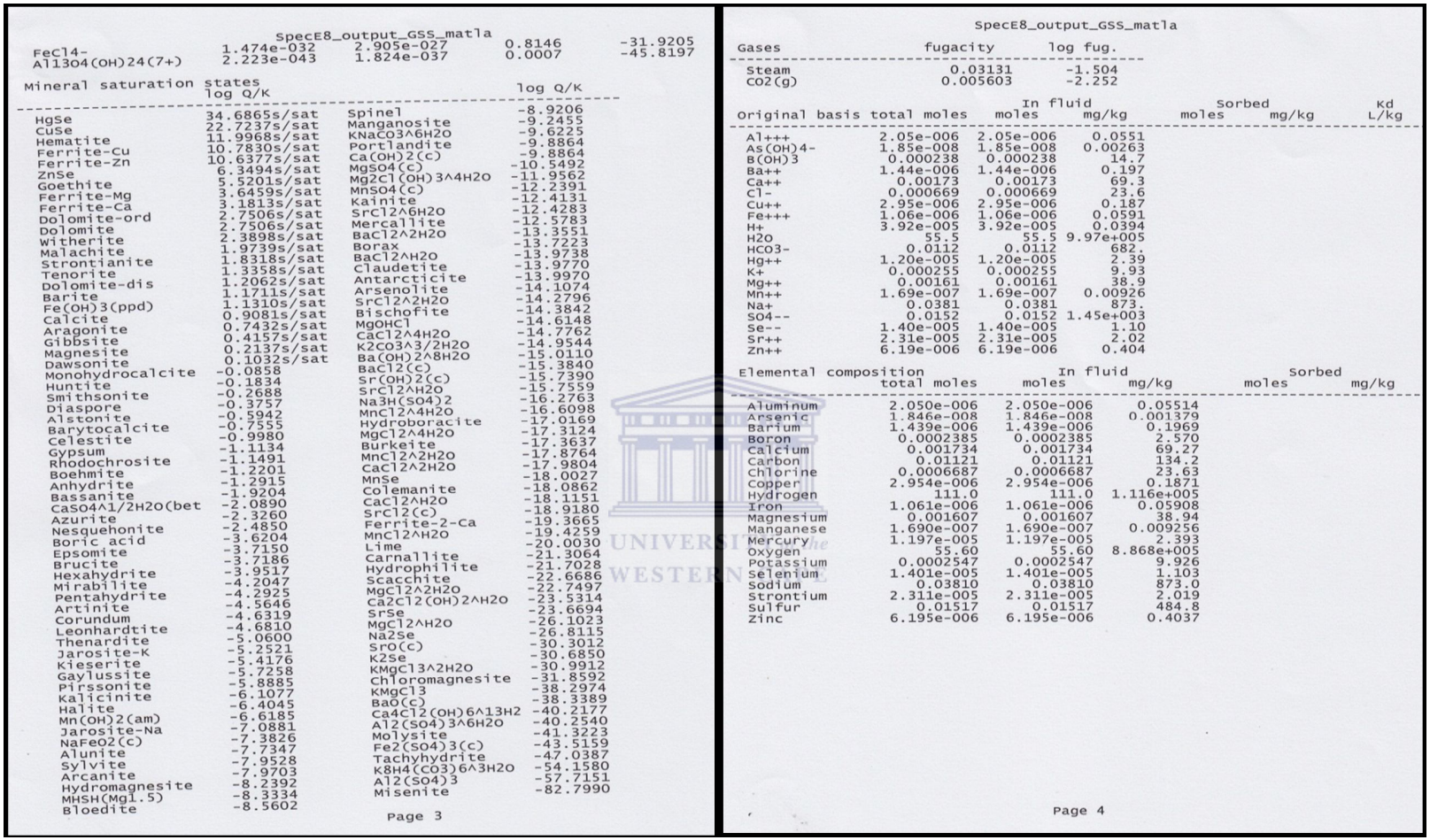

SpecE8_output_GSS_matla

FeCl4-	1.474e-032	2.905e-027	0.8146	-31.9205
Al13O4(OH)24(7+)	2.223e-043	1.824e-037	0.0007	-45.8197

Mineral saturation states

	log Q/K		log Q/K
HgSe	34.6865s/sat	Spinel	-8.9206
CuSe	22.7237s/sat	Manganosite	-9.2455
Hematite	11.9968s/sat	KNaCO3^6H2O	-9.6225
Ferrite-Cu	10.7830s/sat	Portlandite	-9.8864
Ferrite-Zn	10.6377s/sat	Ca(OH)2(c)	-9.8864
ZnSe	6.3494s/sat	MgSO4(c)	-10.5492
Goethite	5.5201s/sat	Mg2Cl(OH)3^4H2O	-11.9562
Ferrite-Mg	3.6459s/sat	MnSO4(c)	-12.2391
Ferrite-Ca	3.1813s/sat	Kainite	-12.4131
Dolomite-ord	2.7506s/sat	SrCl2^6H2O	-12.4283
Dolomite	2.7506s/sat	Mercallite	-12.5783
Witherite	2.3898s/sat	BaCl2^2H2O	-13.3551
Malachite	1.9739s/sat	Borax	-13.7223
Strontianite	1.8318s/sat	BaCl2^H2O	-13.9738
Tenorite	1.3358s/sat	Claudetite	-13.9770
Dolomite-dis	1.2062s/sat	Antarcticite	-13.9970
Barite	1.1711s/sat	Arsenolite	-14.1074
Fe(OH)3(ppd)	1.1310s/sat	SrCl2^2H2O	-14.2796
Calcite	0.9081s/sat	Bischofite	-14.3842
Aragonite	0.7432s/sat	MgOHCl	-14.6148
Gibbsite	0.4157s/sat	CaCl2^4H2O	-14.7762
Magnesite	0.2137s/sat	K2CO3^3/2H2O	-14.9544
Dawsonite	0.1032s/sat	Ba(OH)2^8H2O	-15.0110
Monohydrocalcite	-0.0858	BaCl2(c)	-15.3840
Huntite	-0.1834	Sr(OH)2(c)	-15.7390
Smithsonite	-0.2688	SrCl2^H2O	-15.7559
Diaspore	-0.3757	Na3H(SO4)2	-16.2763
Alstonite	-0.5942	MnCl2^4H2O	-16.6098
Barytocalcite	-0.7555	Hydroboracite	-17.0169
Celestite	-0.9980	MgCl2^4H2O	-17.3124
Gypsum	-1.1134	Burkeite	-17.3637
Rhodochrosite	-1.1491	MnCl2^2H2O	-17.8764
Boehmite	-1.2201	CaCl2^2H2O	-17.9804
Anhydrite	-1.2915	MnSe	-18.0027
Bassanite	-1.9204	Colemanite	-18.0862
CaSO4^1/2H2O(bet	-2.0890	CaCl2^H2O	-18.1151
Azurite	-2.3260	SrCl2(c)	-18.9180
Nesquehonite	-2.4850	Ferrite-2-Ca	-19.3665
Boric acid	-3.6204	MnCl2^H2O	-19.4259
Epsomite	-3.7150	Lime	-20.0030
Brucite	-3.7186	Carnallite	-21.3064
Hexahydrite	-3.9517	Hydrophilite	-21.7028
Mirabilite	-4.2047	Scacchite	-22.6686
Pentahydrite	-4.2925	MgCl2^2H2O	-22.7497
Artinite	-4.5646	Ca2Cl2(OH)2^H2O	-23.5314
Corundum	-4.6319	SrSe	-23.6694
Leonhardtite	-4.6810	MgCl2^H2O	-26.1023
Thenardite	-5.0600	Na2Se	-26.8115
Jarosite-K	-5.2521	SrO(c)	-30.3012
Kieserite	-5.4176	K2Se	-30.6850
Gaylussite	-5.7258	KMgCl3^2H2O	-30.9912
Pirssonite	-5.8885	Chloromagnesite	-31.8592
Kalicinite	-6.1077	KMgCl3	-38.2974
Halite	-6.4045	BaO(c)	-38.3389
Mn(OH)2(am)	-6.6185	Ca4Cl2(OH)6^13H2	-40.2177
Jarosite-Na	-7.0881	Al2(SO4)3^6H2O	-40.2540
NaFeO2(c)	-7.3826	Molysite	-41.3223
Alunite	-7.7347	Fe2(SO4)3(c)	-43.5159
Sylvite	-7.9528	Tachyhydrite	-47.0387
Arcanite	-7.9703	K8H4(CO3)6^3H2O	-54.1580
Hydromagnesite	-8.2392	Al2(SO4)3	-57.7151
MHSH(Mg1.5)	-8.3334	Misenite	-82.7990
Bloedite	-8.5602		

Page 3

SpecE8_output_GSS_matla

Gases

	fugacity	log fug.
Steam	0.03131	-1.504
CO2(g)	0.005603	-2.252

Original basis	total moles	In fluid moles	In fluid mg/kg	Sorbed moles	Sorbed mg/kg	Kd L/kg
Al+++	2.05e-006	2.05e-006	0.0551			
As(OH)4-	1.85e-008	1.85e-008	0.00263			
B(OH)3	0.000238	0.000238	14.7			
Ba++	1.44e-006	1.44e-006	0.197			
Ca++	0.00173	0.00173	69.3			
Cl-	0.000669	0.000669	23.6			
Cu++	2.95e-006	2.95e-006	0.187			
Fe+++	1.06e-006	1.06e-006	0.0591			
H+	3.92e-005	3.92e-005	0.0394			
H2O	55.5	55.5	9.97e+005			
HCO3-	0.0112	0.0112	682.			
Hg++	1.20e-005	1.20e-005	2.39			
K+	0.000255	0.000255	9.93			
Mg++	0.00161	0.00161	38.9			
Mn++	1.69e-007	1.69e-007	0.00926			
Na+	0.0381	0.0381	873.			
SO4--	0.0152	0.0152	1.45e+003			
Se--	1.40e-005	1.40e-005	1.10			
Sr++	2.31e-005	2.31e-005	2.02			
Zn++	6.19e-006	6.19e-006	0.404			

Elemental composition	total moles	In fluid moles	In fluid mg/kg	Sorbed moles	Sorbed mg/kg
Aluminum	2.050e-006	2.050e-006	0.05514		
Arsenic	1.846e-008	1.846e-008	0.001379		
Barium	1.439e-006	1.439e-006	0.1969		
Boron	0.0002385	0.0002385	2.570		
Calcium	0.001734	0.001734	69.27		
Carbon	0.01121	0.01121	134.2		
Chlorine	0.0006687	0.0006687	23.63		
Copper	2.954e-006	2.954e-006	0.1871		
Hydrogen	111.0	111.0	1.116e+005		
Iron	1.061e-006	1.061e-006	0.05908		
Magnesium	0.001607	0.001607	38.94		
Manganese	1.690e-007	1.690e-007	0.009256		
Mercury	1.197e-005	1.197e-005	2.393		
Oxygen	55.60	55.60	8.868e+005		
Potassium	0.0002547	0.0002547	9.926		
Selenium	1.401e-005	1.401e-005	1.103		
Sodium	0.03810	0.03810	873.0		
Strontium	2.311e-005	2.311e-005	2.019		
Sulfur	0.01517	0.01517	484.8		
Zinc	6.195e-006	6.195e-006	0.4037		

Page 4

Figure A2.2: The speciation results continued of Matla mine water obtained using the Spec8 program of the Geochemist's workbench software.

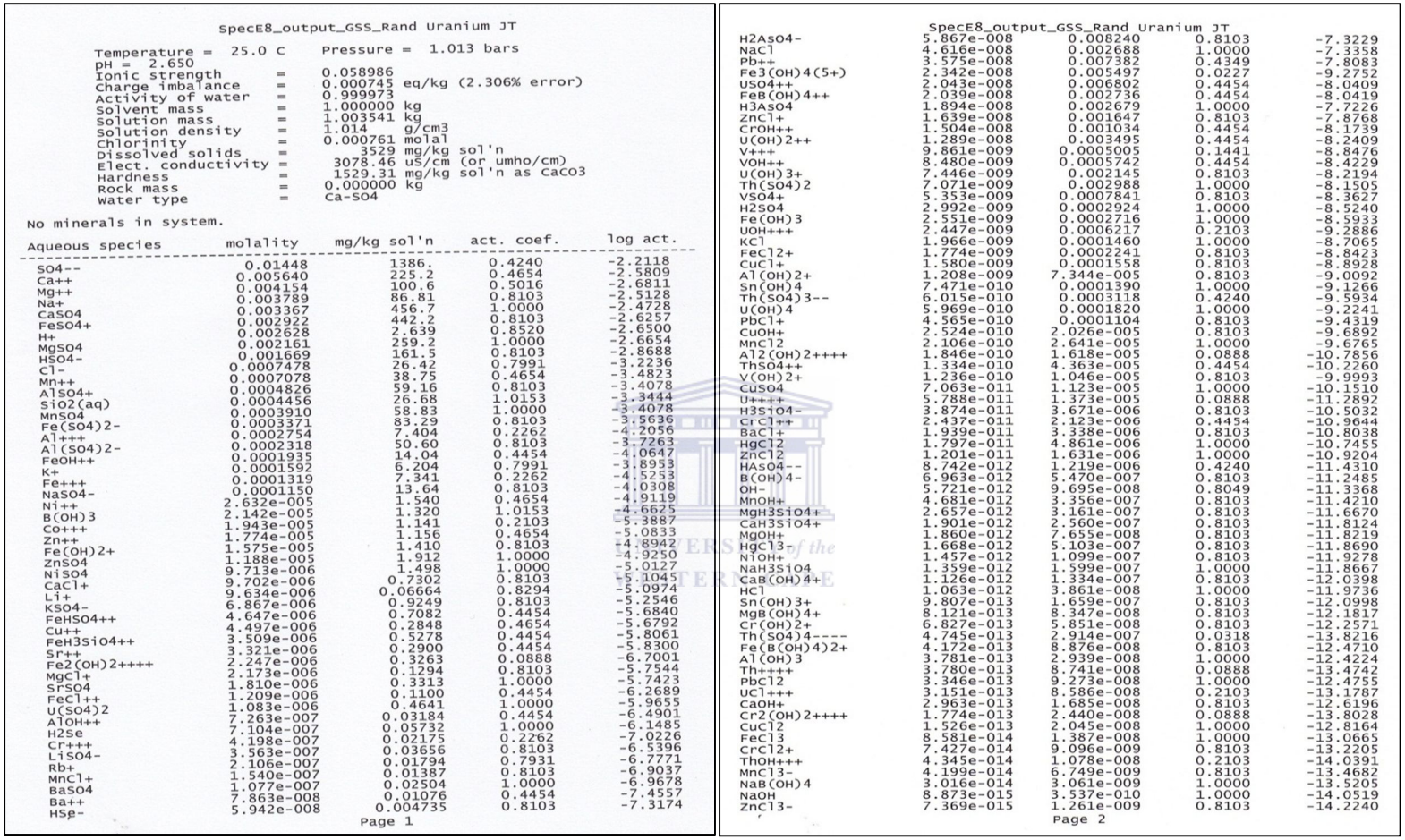

SpecE8_output_GSS_Rand Uranium JT

Temperature = 25.0 C Pressure = 1.013 bars
pH = 2.650
Ionic strength = 0.058986
Charge imbalance = 0.000745 eq/kg (2.306% error)
Activity of water = 0.999973
Solvent mass = 1.000000 kg
Solution mass = 1.003541 kg
Solution density = 1.014 g/cm3
Chlorinity = 0.000761 molal
Dissolved solids = 3529 mg/kg sol'n
Elect. conductivity = 3078.46 uS/cm (or umho/cm)
Hardness = 1529.31 mg/kg sol'n as CaCO3
Rock mass = 0.000000 kg
Water type = Ca-SO4

No minerals in system.

Aqueous species	molality	mg/kg sol'n	act. coef.	log act.
SO4--	0.01448	1386.	0.4240	-2.2118
Ca++	0.005640	225.2	0.4654	-2.5809
Mg++	0.004154	100.6	0.5016	-2.6811
Na+	0.003789	86.81	0.8103	-2.5128
CaSO4	0.003367	456.7	1.0000	-2.4728
FeSO4+	0.002922	442.2	0.8103	-2.6257
H+	0.002628	2.639	0.8520	-2.6500
MgSO4	0.002161	259.2	1.0000	-2.6654
HSO4-	0.001669	161.5	0.8103	-2.8688
Cl-	0.0007478	26.42	0.7991	-3.2236
Mn++	0.0007078	38.75	0.4654	-3.4823
AlSO4+	0.0004826	59.16	0.8103	-3.4078
SiO2(aq)	0.0004456	26.68	1.0153	-3.3444
MnSO4	0.0003910	58.83	1.0000	-3.4078
Fe(SO4)2-	0.0003371	83.29	0.8103	-3.5636
Al+++	0.0002754	7.404	0.2262	-4.2056
Al(SO4)2-	0.0002318	50.60	0.8103	-3.7263
FeOH++	0.0001935	14.04	0.4454	-4.0647
K+	0.0001592	6.204	0.7991	-3.8953
Fe+++	0.0001319	7.341	0.2262	-4.5253
NaSO4-	0.0001150	13.64	0.8103	-4.0308
Ni++	2.632e-005	1.540	0.4654	-4.9119
B(OH)3	2.142e-005	1.320	1.0153	-4.6625
Co+++	1.943e-005	1.141	0.2103	-5.3887
Zn++	1.774e-005	1.156	0.4654	-5.0833
Fe(OH)2+	1.575e-005	1.410	0.8103	-4.8942
ZnSO4	1.188e-005	1.912	1.0000	-4.9250
NiSO4	9.713e-006	1.498	1.0000	-5.0127
CaCl+	9.702e-006	0.7302	0.8103	-5.1045
Li+	9.634e-006	0.06664	0.8294	-5.0974
KSO4-	6.867e-006	0.9249	0.8103	-5.2546
FeHSO4++	4.647e-006	0.7082	0.4454	-5.6840
Cu++	4.497e-006	0.2848	0.4654	-5.6792
FeH3SiO4++	3.509e-006	0.5278	0.4454	-5.8061
Sr++	3.321e-006	0.2900	0.4454	-5.8300
Fe2(OH)2++++	2.247e-006	0.3263	0.0888	-6.7001
MgCl+	2.173e-006	0.1294	0.8103	-5.7544
SrSO4	1.810e-006	0.3313	1.0000	-5.7423
FeCl++	1.209e-006	0.1100	0.4454	-6.2689
U(SO4)2	1.083e-006	0.4641	1.0000	-5.9655
AlOH++	7.263e-007	0.03184	0.4454	-6.4901
H2Se	7.104e-007	0.05732	1.0000	-6.1485
Cr+++	4.198e-007	0.02175	0.2262	-7.0226
LiSO4-	3.563e-007	0.03656	0.8103	-6.5396
Rb+	2.106e-007	0.01794	0.7931	-6.7771
MnCl+	1.540e-007	0.01387	0.8103	-6.9037
BaSO4	1.077e-007	0.02504	1.0000	-6.9678
Ba++	7.863e-008	0.01076	0.4454	-7.4557
HSe-	5.942e-008	0.004735	0.8103	-7.3174

Page 1

SpecE8_output_GSS_Rand Uranium JT

H2AsO4-	5.867e-008	0.008240	0.8103	-7.3229
NaCl	4.616e-008	0.002688	1.0000	-7.3358
Pb++	3.575e-008	0.007382	0.4349	-7.8083
Fe3(OH)4(5+)	2.342e-008	0.005497	0.0227	-9.2752
UO2++	2.043e-008	0.006802	0.4454	-8.0409
FeB(OH)4++	2.039e-008	0.002736	0.4454	-8.0419
H3AsO4	1.894e-008	0.002679	1.0000	-7.7226
ZnCl+	1.639e-008	0.001647	0.8103	-7.8768
CrOH++	1.504e-008	0.001034	0.4454	-8.1739
U(OH)2++	1.289e-008	0.003495	0.4454	-8.2409
V+++	9.861e-009	0.0005005	0.1441	-8.8476
VOH++	8.480e-009	0.0005742	0.4454	-8.4229
U(OH)3+	7.446e-009	0.002145	0.8103	-8.2194
Th(SO4)2	7.071e-009	0.002988	1.0000	-8.1505
VSO4+	5.353e-009	0.0007841	0.8103	-8.3627
H2SO4	2.992e-009	0.0002924	1.0000	-8.5240
Fe(OH)3	2.551e-009	0.0002716	1.0000	-8.5933
UOH+++	2.447e-009	0.0006217	0.2103	-9.2886
KCl	1.966e-009	0.0001460	1.0000	-8.7065
FeCl2+	1.774e-009	0.0002241	0.8103	-8.8423
CuCl+	1.580e-009	0.0001558	0.8103	-8.8928
Al(OH)2+	1.208e-009	7.344e-005	0.8103	-9.0092
Sn(OH)4	7.471e-010	0.0001390	1.0000	-9.1266
Th(SO4)3--	6.015e-010	0.0003118	0.4240	-9.5934
U(OH)4	5.969e-010	0.0001820	1.0000	-9.2241
PbCl+	4.565e-010	0.0001104	0.8103	-9.4319
CuOH+	2.524e-010	2.026e-005	0.8103	-9.6892
MnCl2	2.106e-010	2.641e-005	1.0000	-9.6765
Al2(OH)2++++	1.846e-010	1.618e-005	0.0888	-10.7856
ThSO4++	1.334e-010	4.363e-005	0.4454	-10.2260
V(OH)2+	1.236e-010	1.046e-005	0.8103	-9.9993
CuSO4	7.063e-011	1.123e-005	1.0000	-10.1510
U++++	5.788e-011	1.373e-005	0.0888	-11.2892
H3SiO4-	3.874e-011	3.671e-006	0.8103	-10.5032
CrCl++	2.437e-011	2.123e-006	0.4454	-10.9644
BaCl+	1.939e-011	3.338e-006	0.8103	-10.8038
HgCl2	1.797e-011	4.861e-006	1.0000	-10.7455
ZnCl2	1.201e-011	1.631e-006	1.0000	-10.9204
HAsO4--	8.742e-012	1.219e-006	0.4240	-11.4310
B(OH)4-	6.963e-012	5.470e-007	0.8103	-11.2485
OH-	5.721e-012	9.695e-008	0.8049	-11.3368
MnOH+	4.681e-012	3.356e-007	0.8103	-11.4210
MgH3SiO4+	2.657e-012	3.161e-007	0.8103	-11.6670
CaH3SiO4+	1.901e-012	2.560e-007	0.8103	-11.8124
MgOH+	1.860e-012	7.655e-008	0.8103	-11.8219
HgCl3-	1.668e-012	5.103e-007	0.8103	-11.8690
NiOH+	1.457e-012	1.099e-007	0.8103	-11.9278
NaH3SiO4	1.359e-012	1.599e-007	1.0000	-11.8667
CaB(OH)4+	1.126e-012	1.334e-007	0.8103	-12.0398
HCl	1.063e-012	3.861e-008	1.0000	-11.9736
Sn(OH)3+	9.807e-013	1.659e-007	0.8103	-12.0998
MgB(OH)4+	8.121e-013	8.347e-008	0.8103	-12.1817
Cr(OH)2+	6.827e-013	5.851e-008	0.8103	-12.2571
Th(SO4)4----	4.745e-013	2.914e-007	0.0318	-13.8216
Fe(B(OH)4)2+	4.172e-013	8.876e-008	0.8103	-12.4710
Al(OH)3	3.781e-013	2.939e-008	1.0000	-12.4224
Th++++	3.780e-013	8.741e-008	0.0888	-13.4742
PbCl2	3.346e-013	9.273e-008	1.0000	-12.4755
UCl+++	3.151e-013	8.586e-008	0.2103	-13.1787
CaOH+	2.963e-013	1.685e-008	0.8103	-12.6196
Cr2(OH)2++++	1.774e-013	2.440e-008	0.0888	-13.8028
CuCl2	1.526e-013	2.045e-008	1.0000	-12.8164
FeCl3	8.581e-014	1.387e-008	1.0000	-13.0665
CrCl2+	7.427e-014	9.096e-009	0.8103	-13.2205
ThOH+++	4.345e-014	1.078e-008	0.2103	-14.0391
MnCl3-	4.199e-014	6.749e-009	0.8103	-13.4682
NaB(OH)4	3.016e-014	3.061e-009	1.0000	-13.5205
NaOH	8.873e-015	3.537e-010	1.0000	-14.0519
ZnCl3-	7.369e-015	1.261e-009	0.8103	-14.2240

Page 2

Figure A2.3: The speciation results of Rand Uranium mine water obtained using the Spec8 program of the Geochemist's workbench software.

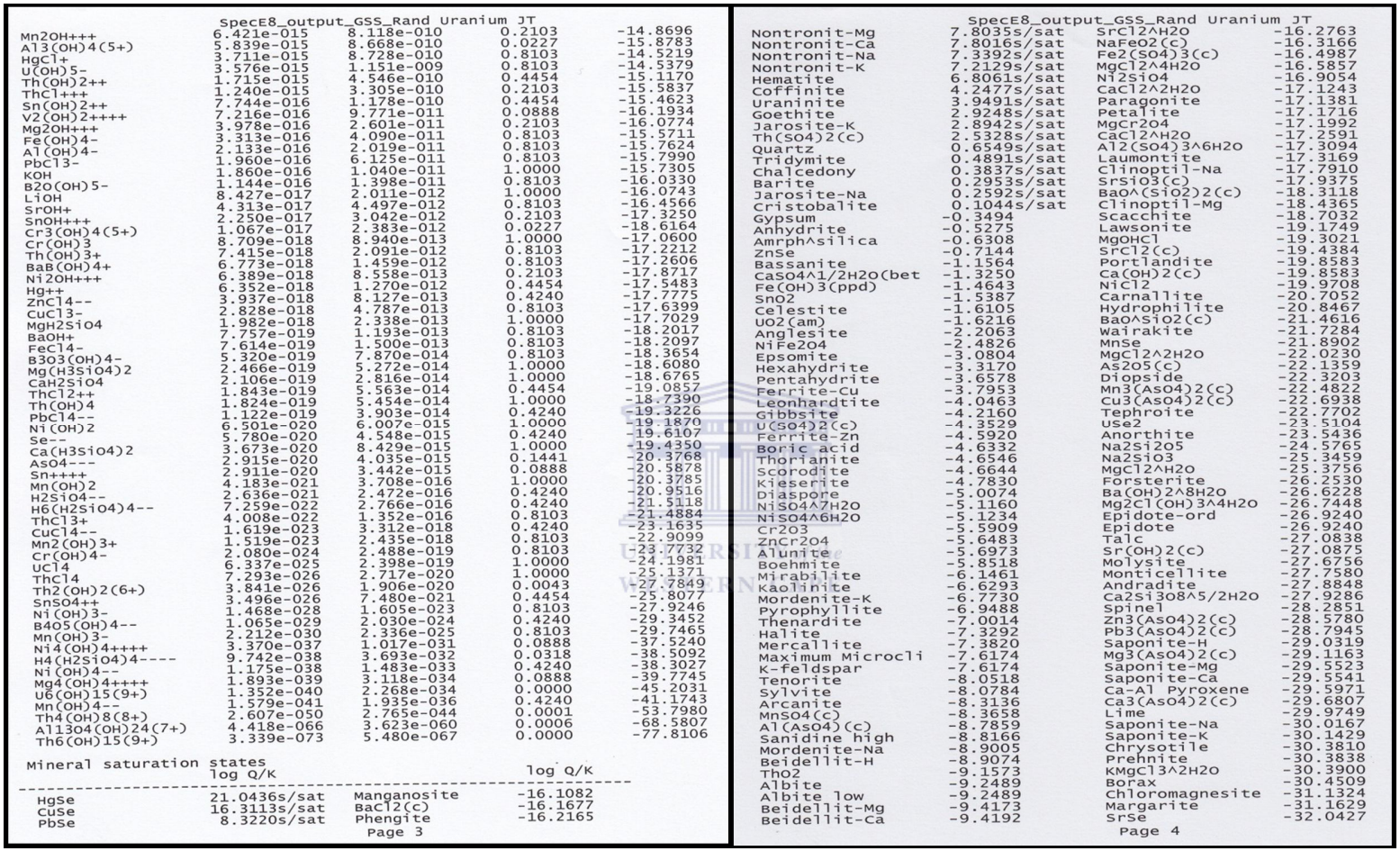

SpecE8_output_GSS_Rand Uranium JT

Mn2OH+++	6.421e-015	8.118e-010	0.2103	-14.8696
Al3(OH)4(5+)	5.839e-015	8.668e-010	0.0227	-15.8783
HgCl+	3.711e-015	8.728e-010	0.8103	-14.5219
U(OH)5-	3.576e-015	1.151e-009	0.8103	-14.5379
Th(OH)2++	1.715e-015	4.546e-010	0.4454	-15.1170
ThCl+++	1.240e-015	3.305e-010	0.2103	-15.5837
Sn(OH)2++	7.744e-016	1.178e-010	0.4454	-15.4623
V2(OH)2++++	7.216e-016	9.771e-011	0.0888	-16.1934
Mg2OH+++	3.978e-016	2.601e-011	0.2103	-16.0774
Fe(OH)4-	3.313e-016	4.090e-011	0.8103	-15.5711
Al(OH)4-	2.133e-016	2.019e-011	0.8103	-15.7624
PbCl3-	1.960e-016	6.125e-011	0.8103	-15.7990
KOH	1.860e-016	1.040e-011	1.0000	-15.7305
B2O(OH)5-	1.144e-016	1.398e-011	0.8103	-16.0330
LiOH	8.427e-017	2.011e-012	1.0000	-16.0743
SrOH+	4.313e-017	4.497e-012	0.8103	-16.4566
SnOH+++	2.250e-017	3.042e-012	0.2103	-17.3250
Cr3(OH)4(5+)	1.067e-017	2.383e-012	0.0227	-18.6164
Cr(OH)3	8.709e-018	8.940e-013	1.0000	-17.0600
Th(OH)3+	7.415e-018	2.091e-012	0.8103	-17.2212
BaB(OH)4+	6.773e-018	1.459e-012	0.8103	-17.2606
Ni2OH+++	6.389e-018	8.558e-013	0.2103	-17.8717
Hg++	6.352e-018	1.270e-012	0.4454	-17.5483
ZnCl4--	3.937e-018	8.127e-013	0.4240	-17.7775
CuCl3-	2.828e-018	4.787e-013	0.8103	-17.6399
MgH2SiO4	1.982e-018	2.338e-013	1.0000	-17.7029
BaOH+	7.757e-019	1.193e-013	0.8103	-18.2017
FeCl4-	7.614e-019	1.500e-013	0.8103	-18.2097
B3O3(OH)4-	5.320e-019	7.870e-014	0.8103	-18.3654
Mg(H3SiO4)2	2.466e-019	5.272e-014	1.0000	-18.6080
CaH2SiO4	2.106e-019	2.816e-014	1.0000	-18.6765
ThCl2++	1.843e-019	5.563e-014	0.4454	-19.0857
Th(OH)4	1.824e-019	5.454e-014	1.0000	-18.7390
PbCl4--	1.122e-019	3.903e-014	0.4240	-19.3226
Ni(OH)2	6.501e-020	6.007e-015	1.0000	-19.1870
Se--	5.780e-020	4.548e-015	0.4240	-19.6107
Ca(H3SiO4)2	3.673e-020	8.429e-015	1.0000	-19.4350
AsO4---	2.915e-020	4.035e-015	0.1441	-20.3768
Sn++++	2.911e-020	3.442e-015	0.0888	-20.5878
Mn(OH)2	4.183e-021	3.708e-016	1.0000	-20.3785
H2SiO4--	2.636e-021	2.472e-016	0.4240	-20.9516
H6(H2SiO4)4--	7.259e-022	2.766e-016	0.4240	-21.5118
ThCl3+	4.008e-022	1.352e-016	0.8103	-21.4884
CuCl4--	1.619e-023	3.312e-018	0.4240	-23.1635
Mn2(OH)3+	1.519e-023	2.435e-018	0.8103	-22.9099
Cr(OH)4-	2.080e-024	2.488e-019	0.8103	-23.7732
UCl4	6.337e-025	2.398e-019	1.0000	-24.1981
ThCl4	7.293e-026	2.717e-020	1.0000	-25.1371
Th2(OH)2(6+)	3.841e-026	1.906e-020	0.0043	-27.7849
SnSO4++	3.496e-026	7.480e-021	0.4454	-25.8077
Ni(OH)3-	1.468e-028	1.605e-023	0.8103	-27.9246
B4O5(OH)4--	1.065e-029	2.030e-024	0.4240	-29.3452
Mn(OH)3-	2.212e-030	2.336e-025	0.8103	-29.7465
Ni4(OH)4++++	3.370e-037	1.017e-031	0.0888	-37.5240
H4(H2SiO4)4----	9.742e-038	3.693e-032	0.0318	-38.5092
Ni(OH)4--	1.175e-038	1.483e-033	0.4240	-38.3027
Mg4(OH)4++++	1.893e-039	3.118e-034	0.0888	-39.7745
U6(OH)15(9+)	1.352e-040	2.268e-034	0.0000	-45.2031
Mn(OH)4--	1.579e-041	1.935e-036	0.4240	-41.1743
Th4(OH)8(8+)	2.607e-050	2.765e-044	0.0001	-53.7980
Al13O4(OH)24(7+)	4.418e-066	3.623e-060	0.0006	-68.5807
Th6(OH)15(9+)	3.339e-073	5.480e-067	0.0000	-77.8106

Mineral saturation states

	log Q/K		log Q/K
HgSe	21.0436s/sat	Manganosite	-16.1082
CuSe	16.3113s/sat	BaCl2(c)	-16.1677
PbSe	8.3220s/sat	Phengite	-16.2165

Page 3

SpecE8_output_GSS_Rand Uranium JT

Nontronit-Mg	7.8035s/sat	SrCl2^H2O	-16.2763
Nontronit-Ca	7.8016s/sat	NaFeO2(c)	-16.3166
Nontronit-Na	7.3392s/sat	Fe2(SO4)3(c)	-16.4987
Nontronit-K	7.2129s/sat	MgCl2^4H2O	-16.5857
Hematite	6.8061s/sat	Ni2SiO4	-16.9054
Coffinite	4.2477s/sat	CaCl2^2H2O	-17.1243
Uraninite	3.9491s/sat	Paragonite	-17.1381
Goethite	2.9248s/sat	Petalite	-17.1716
Jarosite-K	2.8942s/sat	MgCr2O4	-17.1992
Th(SO4)2(c)	2.5328s/sat	CaCl2^H2O	-17.2591
Quartz	0.6549s/sat	Al2(SO4)3^6H2O	-17.3094
Tridymite	0.4891s/sat	Laumontite	-17.3169
Chalcedony	0.3837s/sat	Clinoptil-Na	-17.7910
Barite	0.2953s/sat	SrSiO3(c)	-17.9375
Jarosite-Na	0.2592s/sat	BaO^(SiO2)2(c)	-18.3118
Cristobalite	0.1044s/sat	Clinoptil-Mg	-18.4365
Gypsum	-0.3494	Scacchite	-18.7032
Anhydrite	-0.5275	Lawsonite	-19.1749
Amrph^silica	-0.6308	MgOHCl	-19.3021
ZnSe	-0.7144	SrCl2(c)	-19.4384
Bassanite	-1.1564	Portlandite	-19.8583
CaSO4^1/2H2O(bet	-1.3250	Ca(OH)2(c)	-19.8583
Fe(OH)3(ppd)	-1.4643	NiCl2	-19.9708
SnO2	-1.5387	Carnallite	-20.7052
Celestite	-1.6105	Hydrophilite	-20.8467
UO2(am)	-1.6216	BaO^SiO2(c)	-21.4616
Anglesite	-2.2063	Wairakite	-21.7284
NiFe2O4	-2.4826	MnSe	-21.8902
Epsomite	-3.0804	MgCl2^2H2O	-22.0230
Hexahydrite	-3.3170	As2O5(c)	-22.1359
Pentahydrite	-3.6578	Diopside	-22.3203
Ferrite-Cu	-3.7953	Mn3(AsO4)2(c)	-22.4822
Leonhardtite	-4.0463	Cu3(AsO4)2(c)	-22.6938
Gibbsite	-4.2160	Tephroite	-22.7702
U(SO4)2(c)	-4.3529	Use2	-23.5104
Ferrite-Zn	-4.5920	Anorthite	-23.5436
Boric acid	-4.6332	Na2Si2O5	-24.5765
Thorianite	-4.6546	Na2SiO3	-25.3459
Scorodite	-4.6644	MgCl2^H2O	-25.3756
Kieserite	-4.7830	Forsterite	-26.2530
Diaspore	-5.0074	Ba(OH)2^8H2O	-26.6228
NiSO4^7H2O	-5.1160	Mg2Cl(OH)3^4H2O	-26.7448
NiSO4^6H2O	-5.1234	Epidote-ord	-26.9240
Cr2O3	-5.5909	Epidote	-26.9240
ZnCr2O4	-5.6483	Talc	-27.0838
Alunite	-5.6973	Sr(OH)2(c)	-27.0875
Boehmite	-5.8518	Molysite	-27.6756
Mirabilite	-6.1461	Monticellite	-27.7580
Kaolinite	-6.6293	Andradite	-27.8848
Mordenite-K	-6.7730	Ca2Si3O8^5/2H2O	-27.9286
Pyrophyllite	-6.9488	Spinel	-28.2851
Thenardite	-7.0014	Zn3(AsO4)2(c)	-28.5780
Halite	-7.3292	Pb3(AsO4)2(c)	-28.7945
Mercallite	-7.3820	Saponite-H	-29.0319
Maximum Microcli	-7.6174	Mg3(AsO4)2(c)	-29.1163
K-feldspar	-7.6174	Saponite-Mg	-29.5523
Tenorite	-8.0518	Saponite-Ca	-29.5541
Sylvite	-8.0784	Ca-Al Pyroxene	-29.5971
Arcanite	-8.3136	Ca3(AsO4)2(c)	-29.6807
MnSO4(c)	-8.3658	Lime	-29.9749
Al(AsO4)(c)	-8.7859	Saponite-Na	-30.0167
Sanidine high	-8.8166	Saponite-K	-30.1429
Mordenite-Na	-8.9005	Chrysotile	-30.3810
Beidellit-H	-8.9074	Prehnite	-30.3838
ThO2	-9.1573	KMgCl3^2H2O	-30.3900
Albite	-9.2489	Borax	-30.4509
Albite low	-9.2489	Chloromagnesite	-31.1324
Beidellit-Mg	-9.4173	Margarite	-31.1629
Beidellit-Ca	-9.4192	SrSe	-32.0427

Page 4

Figure A2.4: The speciation results of Rand Uranium mine water obtained using the Spec8 program of the Geochemist's workbench software.

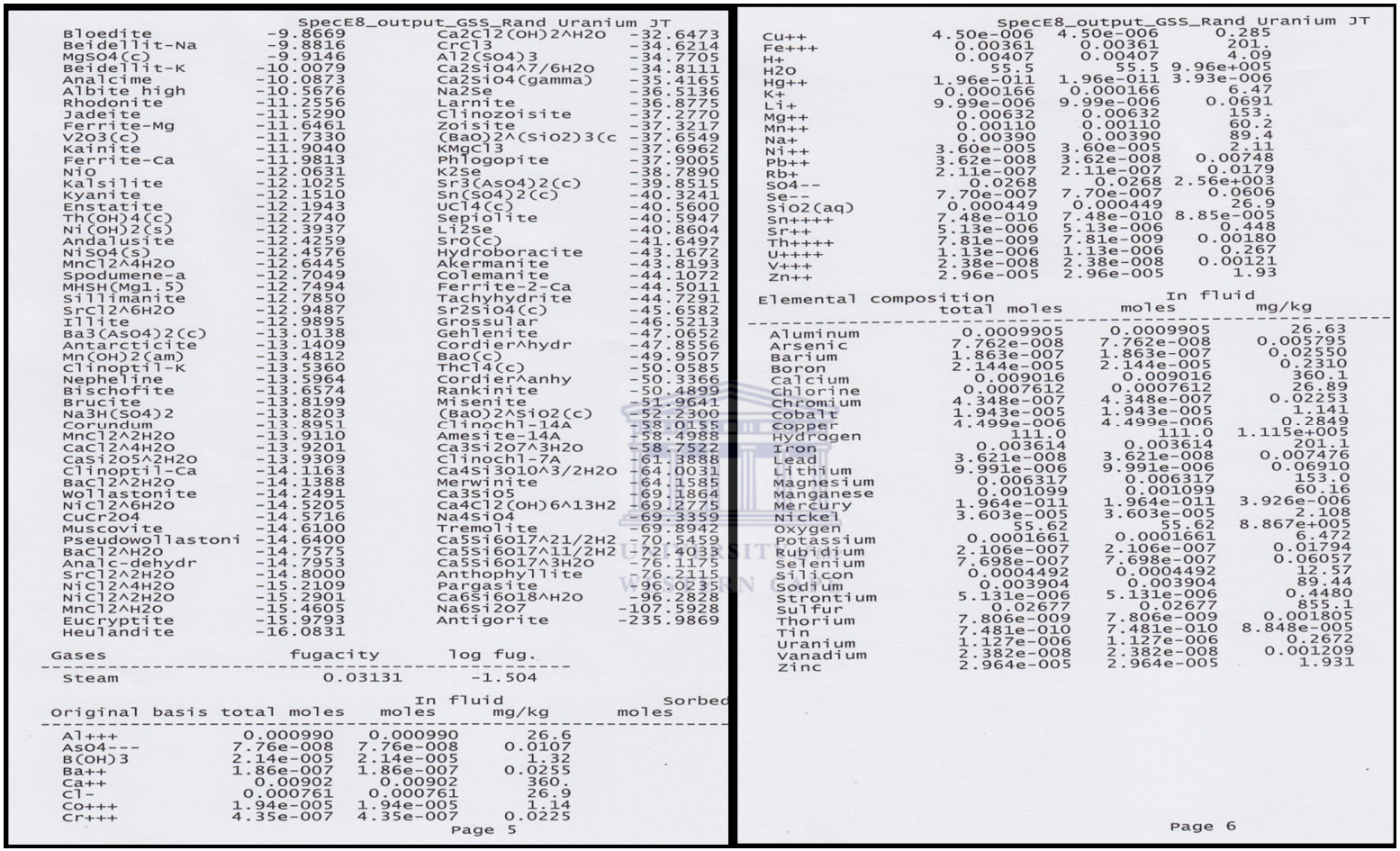

SpecE8_output_GSS_Rand Uranium JT

Bloedite	-9.8669	Ca2Cl2(OH)2^H2O	-32.6473
Beidellit-Na	-9.8816	CrCl3	-34.6214
MgSO4(c)	-9.9146	Al2(SO4)3	-34.7705
Beidellit-K	-10.0079	Ca2Si04^7/6H2O	-34.8111
Analcime	-10.0873	Ca2SiO4(gamma)	-35.4165
Albite high	-10.5676	Na2Se	-36.5136
Rhodonite	-11.2556	Larnite	-36.8775
Jadeite	-11.5290	Clinozoisite	-37.2770
Ferrite-Mg	-11.6461	Zoisite	-37.3217
V2O3(c)	-11.7330	(BaO)2^(SiO2)3(c	-37.6549
Kainite	-11.9040	KMgCl3	-37.6962
Ferrite-Ca	-11.9813	Phlogopite	-37.9005
NiO	-12.0631	K2Se	-38.7890
Kalsilite	-12.1025	Sr3(AsO4)2(c)	-39.8515
Kyanite	-12.1510	Sn(SO4)2(c)	-40.3241
Enstatite	-12.1943	UCl4(c)	-40.5600
Th(OH)4(c)	-12.2740	Sepiolite	-40.5947
Ni(OH)2(s)	-12.3937	Li2Se	-40.8604
Andalusite	-12.4259	SrO(c)	-41.6497
NiSO4(s)	-12.4576	Hydroboracite	-43.1672
MnCl2^4H2O	-12.6445	Akermanite	-43.8193
Spodumene-a	-12.7049	Colemanite	-44.1072
MHSH(Mg1.5)	-12.7494	Ferrite-2-Ca	-44.5011
Sillimanite	-12.7850	Tachyhydrite	-44.7291
SrCl2^6H2O	-12.9487	Sr2SiO4(c)	-45.6582
Illite	-12.9895	Grossular	-46.5213
Ba3(AsO4)2(c)	-13.0138	Gehlenite	-47.0652
Antarcticite	-13.1409	Cordier^hydr	-47.8556
Mn(OH)2(am)	-13.4812	BaO(c)	-49.9507
Clinoptil-K	-13.5360	ThCl4(c)	-50.0585
Nepheline	-13.5964	Cordier^anhy	-50.3366
Bischofite	-13.6574	Rankinite	-50.4899
Brucite	-13.8199	Misenite	-51.9641
Na3H(SO4)2	-13.8203	(BaO)2^SiO2(c)	-52.2300
Corundum	-13.8951	Clinochl-14A	-58.0155
MnCl2^2H2O	-13.9110	Amesite-14A	-58.4988
CaCl2^4H2O	-13.9201	Ca3Si2O7^3H2O	-58.7522
Ca3Si2O5^2H2O	-13.9309	Clinochl-7A	-61.3888
Clinoptil-Ca	-14.1163	Ca4Si3O10^3/2H2O	-64.0031
BaCl2^2H2O	-14.1388	Merwinite	-64.1585
Wollastonite	-14.2491	Ca3SiO5	-69.1864
NiCl2^6H2O	-14.5205	Ca4Cl2(OH)6^13H2	-69.2775
CuCr2O4	-14.5716	Na4SiO4	-69.3359
Muscovite	-14.6100	Tremolite	-69.8942
Pseudowollastoni	-14.6400	Ca5Si6O17^21/2H2	-70.5459
BaCl2^H2O	-14.7575	Ca5Si6O17^11/2H2	-72.4033
Analc-dehydr	-14.7953	Ca5Si6O17^3H2O	-76.1175
SrCl2^2H2O	-14.8000	Anthophyllite	-76.2115
NiCl2^4H2O	-15.2109	Pargasite	-96.0235
NiCl2^2H2O	-15.2901	Ca6Si6O18^H2O	-96.2828
MnCl2^H2O	-15.4605	Na6Si2O7	-107.5928
Eucryptite	-15.9793	Antigorite	-235.9869
Heulandite	-16.0831		

Gases	fugacity	log fug.
Steam	0.03131	-1.504

Original basis	total moles	In fluid moles	In fluid mg/kg	Sorbed moles
Al+++	0.000990	0.000990	26.6	
AsO4---	7.76e-008	7.76e-008	0.0107	
B(OH)3	2.14e-005	2.14e-005	1.32	
Ba++	1.86e-007	1.86e-007	0.0255	
Ca++	0.00902	0.00902	360.	
Cl-	0.000761	0.000761	26.9	
Co+++	1.94e-005	1.94e-005	1.14	
Cr+++	4.35e-007	4.35e-007	0.0225	

Page 5

SpecE8_output_GSS_Rand Uranium JT

Cu++	4.50e-006	4.50e-006	0.285
Fe+++	0.00361	0.00361	201.
H+	0.00407	0.00407	4.09
H2O	55.5	55.5	9.96e+005
Hg++	1.96e-011	1.96e-011	3.93e-006
K+	0.000166	0.000166	6.47
Li+	9.99e-006	9.99e-006	0.0691
Mg++	0.00632	0.00632	153.
Mn++	0.00110	0.00110	60.2
Na+	0.00390	0.00390	89.4
Ni++	3.60e-005	3.60e-005	2.11
Pb++	3.62e-008	3.62e-008	0.00748
Rb+	2.11e-007	2.11e-007	0.0179
SO4--	0.0268	0.0268	2.56e+003
Se--	7.70e-007	7.70e-007	0.0606
SiO2(aq)	0.000449	0.000449	26.9
Sn++++	7.48e-010	7.48e-010	8.85e-005
Sr++	5.13e-006	5.13e-006	0.448
Th++++	7.81e-009	7.81e-009	0.00180
U++++	1.13e-006	1.13e-006	0.267
V+++	2.38e-008	2.38e-008	0.00121
Zn++	2.96e-005	2.96e-005	1.93

Elemental composition	total moles	In fluid moles	In fluid mg/kg
Aluminum	0.0009905	0.0009905	26.63
Arsenic	7.762e-008	7.762e-008	0.005795
Barium	1.863e-007	1.863e-007	0.02550
Boron	2.144e-005	2.144e-005	0.2310
Calcium	0.009016	0.009016	360.1
Chlorine	0.0007612	0.0007612	26.89
Chromium	4.348e-007	4.348e-007	0.02253
Cobalt	1.943e-005	1.943e-005	1.141
Copper	4.499e-006	4.499e-006	0.2849
Hydrogen	111.0	111.0	1.115e+005
Iron	0.003614	0.003614	201.1
Lead	3.621e-008	3.621e-008	0.007476
Lithium	9.991e-006	9.991e-006	0.06910
Magnesium	0.006317	0.006317	153.0
Manganese	0.001099	0.001099	60.16
Mercury	1.964e-011	1.964e-011	3.926e-006
Nickel	3.603e-005	3.603e-005	2.108
Oxygen	55.62	55.62	8.867e+005
Potassium	0.0001661	0.0001661	6.472
Rubidium	2.106e-007	2.106e-007	0.01794
Selenium	7.698e-007	7.698e-007	0.06057
Silicon	0.0004492	0.0004492	12.57
Sodium	0.003904	0.003904	89.44
Strontium	5.131e-006	5.131e-006	0.4480
Sulfur	0.02677	0.02677	855.1
Thorium	7.806e-009	7.806e-009	0.001805
Tin	7.481e-010	7.481e-010	8.848e-005
Uranium	1.127e-006	1.127e-006	0.2672
Vanadium	2.382e-008	2.382e-008	0.001209
Zinc	2.964e-005	2.964e-005	1.931

Page 6

Figure A2.5: The speciation results of Rand Uranium mine water obtained using the Spec8 program of the Geochemist's workbench software.

APPENDIX A3: This show the analysis results of Matla mine water or Rand Uranium mine water during treatment with Matla coal FA, lime or $Al(OH)_3$ using either a jet loop reactor or an overhead stirrer.

Table A3.1: The composition of Matla mine water (80 L) before and after treatment with different amounts of Matla coal FA using a jet loop reactor with either jet sizes set at 8 mm or 6 mm by cavitation and impingement mixing.

13 kg of coal FA, 8mm jet sizes impinging and cavitation						16 kg of coal FA, 8mm jet sizes impinging and cavitation					13 kg of coal FA 6mm jet sizes impinging and caviatation					
min	0	30	60	90	120	min	0	30	60	90	min	0	30	60	90	105
Si	1.27911	4.1133	3.7789	0.5635	0.5074	**Si**	1.27911	12.5380	2.2663	0.2354	**Si**	1.27911	12.6390	2.9313	2.2956	4.3872
Mg	39.5356	35.7318	10.8427	0.1061	0.2915	**Mg**	39.5356	52.3373	0.8957	0.1040	**Mg**	39.5356	47.9971	45.7920	0.3830	0.5631
Na	886.584	1043.09	1053.1	930.785	882.057	**Na**	886.584	898.300	932.858	945.795	**Na**	886.584	874.668	930.64	805.953	933.786
Hg	2.43167	0	0	0	0	**Hg**	2.43167	0	0	0	**Hg**	2.43167	0	0.7154		0
Ca	70.345	325.666	330.247	599.722	689.220	**Ca**	70.345	319.525	372.547	766.064	**Ca**	70.3450	320.119	240.082	352.706	570.634
K	9.93963	8.3726	9.3487	9.4397	14.0696	**K**	9.93963	14.7989	8.0835	9.3463	**K**	9.93963	10.0466	14.2976	9.1888	14.1322
Li	0.17954	0.0817	0.1351	0.0402	0.3137	**Li**	0.17954	0.2767	0.0638	0.0584	**Li**	0.17954	0.2302	1.0036	0.3406	0.6536
Mn	0.00943	0	0	0	0	**Mn**	0.00948	0	0	0	**Mn**	0.00943	0	0.0201	0	0.0159
Co	0	0	0	0	0	**Co**	0	0	0	0	**Co**	0	0	0.0728	0.1435	0.1410
Cr	0	0.0548	0.0644	0.0897	0.3255	**Cr**	0	0.0837	0.0770	0.0595	**Cr**	0	0.4822	0	0.0943	0
Cu	0.19393	0.1687	0.0981	0.2528	0	**Cu**	0.19393	0	0.1280	0.1937	**Cu**	0.19393	0	0.0113	0	0
Mo	0	0	0.0822	0.0025	0.9180	**Mo**	0	0.4361	0	0.0222	**Mo**	0	1.5099	1.2609	0.6448	0
Se	1.115	0	0	0	4.2932	**Se**	1.11569	2.9315	0	0.7024	**Se**	1.11569	3.8349	0	5.8163	0
V	0	0.8457	0.4121	0	0.1256	**V**	0	1.4215	0.2972	0	**V**	0	0.7943	0.9188	0.2797	0
Zn	0.408	0.0219	0.1155	0.0138	0.2840	**Zn**	0.40826	0.8314	0.1097	0	**Zn**	0.40826	0.1793	0.3826	0.2046	0.1090
Pb	0	0	0	0	0	**Pb**	0	0.8879	0	0	**Pb**	0	0	0	0	0
Ni	0.023	0	0.0074	0	0	**Ni**	0.02319	0.0407	0	0	**Ni**	0.02319	0.0784	0	0	0
P	1.027	1.9156	0.8052	0.5939	9.8090	**P**	1.02689	5.6355	1.6456	0.8894	**P**	1.02689	6.4621	10.2319	3.0954	0
As	0.0014	1.2762	1.6223	1.1258	1.2130	**As**	0.00141	0	1.3887	1.1693	**As**	0.00141	0	7.0585	0	3.2874
B	2.606	0	0	0	5.1808	**B**	2.60608	7.0244	0	0	**B**	2.60608	3.7113	4.0558	2.0059	2.7530
Be	0.017	0.0895	0.0913	0.0944	0	**Be**	0.01659	0.0109	0.0922	0.1027	**Be**	0.01659	0	0.0111	0.034	0.0086
Cd	0.005	0.0226	0.0141	0	0	**Cd**	0.00498	0	0	0.0138	**Cd**	0.00498	0	0.0249	0	0
Ba	0.201	0.2707	0.5687	0.1779	0.2080	**Ba**	0.20103	0.3478	0.3456	0.1031	**Ba**	0.20103	0.5946	0.6877	0.5356	0.2310
Fe	0.059	0.1295	0.2780	0.2979	0.0163	**Fe**	0.05935	0.2062	0.1354	0.1183	**Fe**	0.05935	0.0739	0.2337	0.2924	0.2283
Al	0.552	0.1804	3.3175	0	0.6290	**Al**	0.5522	0.7765	2.1155	0	**Al**	0.5522	1.0220	3.3431	1.5014	
Ti	0.017	0	0	0	0.1438	**Ti**	0.01686	0.0414	0.0083	0	**Ti**	0.01686	0.2498	0.1298	0.2075	0.1686
Sr	2.048	4.3177	4.7088	6.7643	15.4623	**Sr**	2.04824	8.3297	4.6757	6.7102	**Sr**	2.04824	8.4157	7.1515	10.0079	14.1257
SO4	1475	2430	2400	2200	2220	**SO4**	1475	2460	2240	2300	**SO4**	1475	2420	2350	2110	2150

Table A3.2: The composition of Matla mine water (80 L) before and after treatment with 13 kg of Matla coal FA, 200 g of lime and 83.2 g of $Al(OH)_3$ using a jet loop reactor with jet sizes set at 8 mm, 10 mm or 12 mm by cavitation and impingement mixing.

		Jet loop reactor with jet sizes set at 8mm						Jet loop reactor with jet sizes set at 10 mm					Jet loop reactor with jet sizes set at 12 mm				
min	0	30	60	90	120	150	120	30	60	90	120	150	30	60	90	120	150
Si	1.28	0	1.78	5.29	1.80	3.61	12.0	0	1.03	7.29	7.02	1.79	17.1	8.83	17.2	7.86	13.9
Mg	39.5	0.33	0.36	0.55	0.34	0.37	0.64	0.58	0.97	0.54	2.13	0.45	0.69	0.70	0.59	0.58	0.68
Na	887	801	805	812	405	887	835	875	747	1065	956	933	808	833	824	796	902
Hg	2.43	0	0	0	0	0	0	0	0	5.64	1.78	0.30	0	0	0	0	1.20
Ca	70.3	1008	385	160	50.1	32.3	138	1279	451	284	124	50.4	1198	790	28.9	139	7.17
K	9.94	9.95	10.4	11.8	9.41	13.8	13.0	17.6	11.7	15.4	19.1	28.0	22.1	11.6	19.9	11.1	15.9
Li	0.18	0.47	0.21	0.47	0.03	0	0.41	0.22	0.37	1.31	0.48	0.14	0.84	0.25	0.51	0.41	0.50
Mn	0.01	0	0	0	0	0.01	0.01	0	0.01	0.03	0	0	0.01	0.01	0.01	0.01	0.03
Co	0	0.05	0	0	0	0	0	0	0	0	0.07	0.04	0	0	0	0.03	0
Cr	0.28	0	0.1398	0.3445	0.0931	0	0.0651	0	0.0465	0	0.1887	0	0.1483	0.0205	0.4032	0.0280	0.1554
Cu	0.19	0	0	0	0.0902	0	0.0809	0.2638	0.1800	0	0.2308	0	0.0632	0	0	0.0540	0.1064
Mo	0.33	0.4400	0.7696	1.2889	0	0.6823	0.3216	2.8461	0.8819	0.5861	1.6501	2.6124	0.2141	0.1149	0	0.0744	0.2785
Se	1.12	3.1501	3.9118	0	0	2.6191	0	0	3.8453	0.0462	0	0	1.2520	0.4357	0	0	1.5917
V	0.14	0.1066	0	0.0132	0.0037	0	0.0512	0	0.2092	0.2026	0.0081	0	0.5181	0.1327	0.5829	0.3061	0.2609
Zn	0.41	0.0140	0.2882	0.0802	0	0.2107	0.0141	0.4457	0.6958	0	0	0.0938	0.0037	0.0432	0.0350	0.1275	0
Pb	0	0	0	0.09	0	0	0	3.57	0	0.56	0	0	0	0	0	0	0
Ni	0.023	0.2648	0	0.1777	0	0	0.2623	0	0	0	00	0	0.5261	0.2982	0.2561	0.3142	0.1802
P	1.03	3.2966	3.9586	3.1572	2.0256	0.9837	1.8427	21.196	5.6308	0	18.348	11.132	2.4352	2.7817	4.4746	3.1455	3.1324
As	0.0014	0.0700	0	3.2084	2.7952	1.6187	1.3387	0	0	0	2.1606	0	0.8652	0.0297	0.2368	1.1002	0.0443
B	2.6	0.3163	0.1608	0.5104	0	1.4129	0	0.2411	0.6284	5.0075	0.6646	6.4528	0	0	0	0	1.1748
Be	0.0166	0	0	0	0.0976	0	0.0040	0	0	0.0091	0.0074	0	0.0090	0.0100	0.0073	0	0.0121
Cd	0.0049	0	0	0	0	0	0	0	0	0	0	0.0609	0	0	0	0	0
Ba	0.2010	0.2352	0.8434	0.9119	0.6885	0.3067	1.5273	2.3451	1.0951	1.2549	1.2531	0.7703	0.9252	1.2390	1.2716	0.9996	0.9761
Fe	0.0593	0.3315	0.1237	0.0610	0.2134	0.0882	0.1186	0	0.4997	0	0	0	0.1254	0.1628	0.0121	0.2034	0.1552
Al	0.5522	0.3122	0.4955	0	2.2826	0.8374	0.4082	0	0.8021	0.9516	1.7442	0.0212	0.1063	0.5486	0.1418	0.3647	0.4600
Ti	0.0169	0.0271	0.2873	0.1753	0.0697	0.2018	0.0271	0	0.3278	0.0569	0.1072	0	0.0060	0.0112	0	0	0.0418
Sr	2.0482	11.238	13.748	13.867	6.4295	13.499	14.514	26.569	13.102	21.398	15.715	28.542	5.5419	14.348	5.6893	12.702	13.112
SO4	1475	1890	910	600	510	570	380	2060	950	620	420	770	2010	1320	910	610	620

Table A3.3: The composition of Matla mine water (80 L) before and after treatment with 13 kg of Matla coal FA, 200 g of lime and 83.2 g of $Al(OH)_3$ using a jet loop reactor with jet sizes set at 12 mm by cavitation mixing only.

Time (min)	0	30	60	90	120	150
Si	1.28	8.77	0.29	10.98	12.61	15.66
Mg	39.54	0.74	0.62	0.59	0.68	0.66
Na	886.58	864.12	1004.87	837.62	829.86	879.64
Hg	2.43	0.92	0	0	0	0
Ca	70.35	1149.35	789.53	247.85	120.05	37.43
K	9.94	12.06	11.98	12.60	13.05	14.99
Li	0.18	0.32	0.29	0.34	0.42	0.60
Mn	0.0094	0.031	0.0017	0.0075	00.52	0.0087
Co	0	0	0	0	0	0
Cr	0	0.04	0.087	0.58	0.1425	0.12
Cu	0.19	0.14	0.46	0.13	0.09	0.06
Mo	0	0	0.06	0.21	0.39	0.17
Se	1.12	3.53	0.75	0.55	2.53	0
V	0	0.016	0.059	0.21	0.13	0.16
Zn	0.41	0.095	0.078	0.071	0.055	0
Pb	0	0	0	0	0	0
Ni	0.023	0.30	0.027	0.27	0.28	0.37
P	1.027	1.91	2.40	1.00	2.83	2.52
As	0.0014	0.91	1.62	0.72	2.34	0
B	2.61	0	0	0	0	0
Be	0.017	0	0.0097	0.0092	0.0079	0.0045
Cd	0.005	0.013	0.018	0.025	0	0
Ba	0.20	1.02	0	1.41	1.55	1.33
Fe	0.059	0.58	0.092	0.14	0.09	0.24
Al	0.55	1.43	1.55	1.53	1.58	21.49
Ti	0.017	0.0086	0.0057	0	0.0015	0
Sr	2.05	13.55	14.24	16.50	14.18	11.18
SO4	1475	1940	1 320	710	430	520

Table A3.4: The composition of Rand Uranium mine water (80 L) before and after treatment with 13 kg of Matla coal FA using a jet loop reactor with jet sizes set at 12 mm by cavitation mixing only.

Time (min)	0			30			60			90			120		
mg/L	1	2	ave	1	2	ave	1	2	ave	1	2	ave	1	2	ave
Cl	26.75	27.03	26.89	25.31	28.15	26.73	28.14	29.57	28.85	23.39	27.69	25.54	29.52	27.51	28.52
SO42-	2567.26	2557.56	2562.40	1199.08	1974.11	1586.60	1389.72	1195.73	1292.72	1340.83	1317.56	1329.20	1561.83	1431.12	1496.47
Fe	200.50	201.60	201.05	0.0051	0.0049	0.0050	0.0032	0.0040	0.0036	0.0021	0.0033	0.0027	0.0032	0.0052	0.0042
Al	26.34	26.91	26.63	0.015	0.0040	0.0097	0.015	0.0040	0.0097	0.015	0.0040	0.0097	0.015	0.0040	0.0097
Ca	355.90	364.40	360.15	1885.11	1881.89	1883.50	1019.67	1079.10	1049.39	926.83	917.30	922.06	912.43	851.55	881.99
Mg	152.30	153.70	153.00	1.88	4.96	3.42	0	0	0	0	0	0	0	0	0
Mn	59.99	60.32	60.16	0	15.40	7.70	0.0012	0.0016	0.0014	0.0036	0.0028	0.0032	0.0064	0.0079	0.0072
Na	89.36	89.53	89.45	85.70	84.97	85.33	95.23	108.75	101.99	89.88	88.08	88.98	97.28	99.64	98.46
K	6.49	6.46	6.47	8.76	9.65	9.20	7.17	8.96	8.07	10.56	9.74	10.15	10.77	10.10	10.43
As	0.0058	0.0058	0.0058	0.60	0	0.30	0.42	0.59	0.51	0.65	0.36	0.51	0.13	0.27	0.20
B	0.24	0.23	0.23	7.61	7.25	7.43	6.96	7.27	7.12	5.79	5.71	5.75	5.89	6.49	6.19
Ba	0.025	0.026	0.026	0.20	0.20	0.20	0.44	0.41	0.43	0.44	0.39	0.41	0.54	0.49	0.5
Be	0.0039	0.0039	0.0039	0	0	0	0	0	0	0	0	0	0	0	0
Cd	0.0068	0.0068	0.0068	0	0	0	0	0	0	0	0	0	0	0	0
Ce	0	0.0013	0.00067	0.91	0.088	0.50	0.70	0.73	0.72	0	0.53	0.26	0.84	1.61	1.22
Co	1.15	1.13	1.14	0	0	0	0	0	0	0.10	0	0.051	0	0	0
Cr	0.023	0.022	0.023	0	0.24	0.12	0.089	0	0.044	0	0	0	0	0.043	0.021
Cu	0.29	0.28	0.28	0	0	0	0.058	0.14	0.098	0.26	0.038	0.15	0	0.24	0.12
Hg	2.7E-06	5.1E-06	3.9E-06	0	0.016	0.0082	0.029	0	0.014	0.015	0.032	0.023	0.091	0.11	0.098
Mo	0.00056	0.00051	0.00053	0	0	0	0	0.11	0.057	0.035	0	0.018	0.36	0	0.18
Nb	0	0	0	0.1297	0	0.065	0.057	0.172	0.11	0.095	0.093	0.094	0.083	0	0.041
Ni	2.11	2.10	2.11	0.25	0.15	0.20	0.12	0.23	0.17	0.29	0.39	0.34	0.24	0.21	0.22
P	1.2E-05	3.5E-05	2.4E-05	0.56	0.14	0.35	0	0.60	0.30	0.15	0.34	0.25	0	0	0
Pb	0.0075	0.0075	0.0075	0.48	0.85	0.66	0.44	0.88	0.66	1.12	1.16	1.14	0.79	0.40	0.59
Rb	0.018	0.018	0.018	0.0059	0	0.003	0	0.019	0.0094	0.093	0.062	0.078	0.024	0.062	0.043
Se	0.058	0.063	0.061	0	0	0	0	0	0	0	0.69	0.35	0.20	0	0.10
Sr	0.44	0.45	0.45	9.10	9.40	9.25	10.87	10.81	10.84	13.51	13.80	13.65	16.54	17.76	17.15
Th	0.0018	0.0018	0.0018	0	1.27	0.63	2.63	1.14	1.88	0.28	3.44	1.86	0.98	3.02	2.00
Ti	0.0014	0.0019	0.0016	0.0084	0.070	0.039	0	0	0	0.054	0	0.027	0	0.037	0.018
U	0.27	0.27	0.27	0	0	0	0	0	0	0	0	0	0	0	0
V	0.0012	0.0012	0.0012	0	0.048	0.024	0	0	0	0	0	0	0	0	0
Y	9.7E-05	0.00014	0.00012	0.0056	0	0.0028	0	0.045	0.023	0	0.0049	0.0025	0.015	0	0.0013
Zn	1.92	1.94	1.93	0	0.0066	0.0033	0.019	0.12	0.068	0.0038	0	0.0019	0	0.049	0.025
Zr	8.5E-05	9.1E-05	8.9E-05	0.0074	0	0.0037	0	0.12	0.062	0	0.016	0.0082	0	0	0

Table A3.5: The composition of Rand Uranium mine water (80 L) before and after treatment with 8 kg of Matla coal FA, 200 g of lime and 86.58 g of $Al(OH)_3$ using a jet loop reactor with jet sizes set at 12 mm by cavitation mixing only.

Time (min)	0			30			60			90			120			150		
mg/L	1	2	ave	1	2	ave	1	2	ave	1	2	ave	1	2	ave	1	2	ave
Cl	26.75	27.03	26.89	31.34	17.81	24.58	48.15	44.01	46.08	49.18	32.26	40.72	54.68	32.96	43.82	49.33	43.71	46.52
SO_4^{2-}	2567	2558	2562	1811	1647	1729	1518	1358	1438	805.3	594.6	699.9	856.3	636.5	746.4	815.0	737	776
Fe	200.5	201.6	201.1	1.08	2.14	1.61	0.78	0.72	0.75	0.21	1.00	0.60	0.22	0.65	0.44	0.59	0.89	0.74
Al	26.34	26.91	26.63	0.015	0.004	0.01	0.051	0.035	0.04	0.41	0.42	0.41	4.15	4.10	4.121	17.17	18.05	17.61
Ca	355.9	364.4	360.1	1634	1521	1577	824.1	809.1	816.6	411.3	439.1	425.2	351.1	372.3	361.7	395.6	413.3	404.4
Mg	152.3	153.7	153	0.069	0.098	0.08	0.16	0.23	0.20	0.17	0.13	0.15	0.23	0.45	0.34	0.18	0.32	0.25
Mn	59.99	60.32	60.16	4.0E-5	3.0E-4	2.0E-4	0.02	2.0E-4	0.01	3.0E-4	1.5E-3	9.0E-4	2.0E-4	4.0E-5	1.0E-5	2.0E-4	1.0E-4	1.0E-4
Na	89.36	89.53	60.16	95.93	98.65	97.29	110.6	101.4	105.9	98.95	105.2	102.1	102.4	89.24	95.83	94.03	105.3	99.65
K	6.49	6.46	60.16	6.02	8.93	7.48	10.39	10.83	10.61	10.24	10.07	10.15	10.92	9.60	10.26	9.38	11.45	10.41
As	0.006	0.006	0.006	0.79	0.36	0.57	0.052	0.66	0.35	0.89	0	0.44	0.57	0.35	0.46	0.36	0.44	0.40
B	0.24	0.23	0.23	0.38	0.14	0.26	0.43	0.53	0.48	0.71	0.66	0.68	1.10	1.04	1.07	1.60	1.75	1.68
Ba	0.025	0.026	0.026	0.36	0.25	0.30	2.88	0.91	1.90	1.28	0.61	0.95	0.25	0.23	0.24	0.20	0.19	0.20
Be	0.004	0.004	0.004	0	0	0	0	0	0	0	0	0	0	0	0	0	0	0
Cd	0.007	0.007	0.007	0.016	0	0.002	0.006	0	0.003	0	0	0	0.005	0	0.002	0	0	0
Ce	0	0.001	0.001	1.49	1.20	1.34	0.54	0.33	0.43	0.46	0	0.23	0.34	0.51	0.43	1.38	1.03	1.21
Co	1.15	1.13	1.14	0	0	0	0	0	0	0	0	0	0.032	0	0.016	0	0	0
Cr	0.023	0.022	0.023	0.21	0	0.10	0.15	0.08	0.12	0.21	0.097	0.15	0	0	0	0.09	0	0.045
Cu	0.29	0.28	0.28	0	0.22	0.11	0	0.10	0.052	0	0	0	0.48	0.19	0.33	0.052	0.032	0.042
Hg	2.4E-6	5.1E-6	3.9E-6	0.23	0.17	0.20	0.015	0.20	0.10	0.084	0.42	0.25	0.27	0.34	0.31	1.11	0.64	0.87
Mo	0.001	0.001	0.001	0.11	0	0.055	0	0	0	0	0	0	0	0	0	0	0.071	0.035
Nb	0	0	0	0.15	0.12	0.13	0.025	0.015	0.020	0.11	0.033	0.072	0	0	0	0	0	0
Ni	2.11	2.10	2.11	0.029	0.27	0.15	0.19	0.28	0.24	0.55	0.33	0.44	0.20	0.088	0.14	0.34	0.36	0.35
P	1.2E-5	3.5E-5	2.3E-5	0	0	0	0	0.21	0.10	0	0	0	0	0	0	0	0	0
Pb	0.007	0.007	0.008	0.86	0.47	0.66	0.42	0.74	0.58	0	0.63	0.31	1.02	0.83	0.93	0.52	0.16	0.34
Rb	0.018	0.018	0.018	0	0.040	0.020	0.023	0	0.012	0.056	0	0.028	0.15	0.001	0.077	0	0.050	0.025
Se	0.058	0.063	0.061	0.412	0	0.21	0	0.57	0.28	0.58	0	0.29	0.77	0	0.39	1.06	0	0.531
Sr	0.44	0.45	0.45	8.90	8.89	8.90	10.61	9.69	10.15	12.26	12.67	12.46	12.80	12.10	12.44	12.82	12.91	12.87
Th	0.002	0.002	0.002	0	2.22	1.11	0.60	1.29	0.94	2.13	1.62	1.88	0.71	2.59	1.65	1.27	2.46	1.87
Ti	0.001	0.002	0.002	0.036	0.004	0.02	0	0.05	0.025	0.012	0	0.006	0.071	0.043	0.057	0.039	0	0.019
U	0.27	0.27	0.27	0	0	0	0	0	0	0	0	0	0	0	0	0	0	0
V	0.001	0.001	0.001	0	0	0	0	0	0	0	0	0	0	0	0	0	0	0
Y	9.7E-5	1E-4	1E-4	0.005	0	0.002	0.002	0	0.001	0	0	0	0	0	0	0.009	0	0.004
Zn	1.92	1.94	1.93	0	0.051	0.026	0	0	0	0	0.011	0.005	0	0.015	0.008	0.004	0	0.002
Zr	8.5E-5	9.1E-5	8.8E-5	0	0.072	0.036	0.042	0	0.021	0.083	0	0.041	0	0	0	0.096	0	0.048

Table A3.6: The composition of Rand Uranium mine water (80 L) before and after treatment with 13 kg of Matla coal FA, 200 g of lime and 86.58 g of $Al(OH)_3$ using a jet loop reactor with jet sizes set at 12 mm by cavitation mixing only.

Time (min)	0			30			60			90			120			150		
mg/L	1	2	ave	1	2	ave	1	2	ave	1	2	ave	1	2	ave	1	2	ave
Cl	26.75	27.03	26.89	35.60	49.64	42.62	30.85	22.95	26.90	23.77	37.42	30.59	45.66	40.03	42.84	46.70	35.60	41.15
SO_4^{2-}	2567	2557	2562	1514	1505	1509	847	623	735	689	625	657	414	421	418	443	388	416
Fe	200.5	201.6	201.1	0.008	0.00	0.004	0.01	0.005	0.008	0.004	0.006	0.005	0.014	0.016	0.015	0.008	0.007	0.007
Al	26.34	26.91	26.62	0.015	0.004	0.01	0.051	0.036	0.043	0.51	0.52	0.52	0.071	0.071	0.071	0.028	0.028	0.028
Ca	355.9	364.4	360.1	1862	1811	1837	671.5	680.5	676	355.3	364	359.7	210.6	209.1	209.9	312.7	296.4	304.6
Mg	152.3	153.7	153	0.062	0.42	0.24	0.045	0.042	0.044	0.029	0.024	0.027	0.016	0.022	0.019	0.057	0.139	0.098
Mn	59.99	60.32	60.16	0.002	2.0E-4	0.001	0.001	0.001	0.001	0.001	0.001	0.001	0.001	0.001	0.001	0.002	0.002	0.002
Na	89.36	89.53	89.45	100.9	93.72	97.31	113.8	113.4	113.6	108.9	115.2	112.1	113.1	111.9	112.5	155.7	148	151.9
K	6.49	6.46	6.472	7.37	6.86	7.11	10.20	10.10	10.15	9.53	9.99	9.76	11.42	11.27	11.35	18.27	17.51	17.89
As	0.006	0.006	0.006	0.001	0.001	0.001	0.002	0.002	0.002	0.002	0.002	0.002	0.001	0.001	0.001	0.001	0.001	0.002
B	0.235	0.227	0.231	6.9E-4	7.4E-4	7.1E-4	6.7E-4	4.7E-4	0.001	0.001	0.001	0.001	0.002	0.002	0.002	0.003	0.003	0.003
Ba	0.025	0.026	0.026	0.051	0.052	0.051	0.049	0.050	0.050	0.048	0.052	0.050	0.084	0.081	0.082	0.067	0.071	0.069
Be	3.9E-3	3.9E-3	3.9E-3	1.5E-5	1.2E-5	1.4E-5	1.5E-5	8.6E-6	1.2E-5	1.4E-5	1.2E-5	1.3E-5	1.1E-5	5.8E-6	8.3E-6	1.2E-5	1.2E-5	1.2E-5
Cd	6.8E-3	7.5E-3	6.7E-3	3.2E-5	1.8E-5	2.5E-5	5.1E-5	3.7E-5	4.4E-5	3.4E-5	2.9E-5	3.1E-5	2.0E-5	3E-05	2.5E-5	1.7E-5	2.7E-5	2.2E-5
Ce	0	1.3E-3	6.7E-4	0	8.5E-4	4.2E-4	2.8E-4	0	1.4E-4	0	0	0	0	2.2E-4	1.1E-4	0	1.6E-4	8.1E-5
Co	1.15	1.13	1.14	0.002	0.002	0.002	0.001	0.001	0.001	0.001	0.001	0.001	3.7E-4	5.1E-4	4.4E4	6.6E-4	6.2E-4	6.4E-4
Cr	0.023	0.022	0.023	0.007	0.007	0.007	0.038	0.039	0.039	0.089	0.103	0.096	0.113	0.125	0.12	0.067	0.063	0.065
Cu	0.29	0.28	0.28	0	0	0	2.7E-3	4.8E-4	1.5E-4	0	1.3E-4	1.3E-4	0	1.3E-4	1.3E-4	6.1E-4	4.5E-4	5.3E-4
Hg	2.7E-6	5.1E-6	3.9E-6	6.0E-4	4.3E-4	5.2E-4	3.0E-4	2.1E-4	2.6E-4	3.8E-4	3.8E-4	3.8E-4	4.6E-4	4.7E-4	4.7E-4	6.0E-4	5.6E-4	5.8E-4
Mo	5.4E-4	5.1E-4	5.4E-4	0.244	0.254	0.249	0.252	0.253	0.253	0.189	0.195	0.192	0.164	0.165	0.165	0.177	0.181	0.17
Nb	0	0	0	1.7E-4	2.2E-5	9.5E-5	1.5E-4	1.0E-4	1.3E-4	6.1E-5	2.4E-4	1.5E-4	1.2E-4	1.2E-4	1.2E-4	5.9E-5	1.3E-4	9.4E-5
Ni	2.11	2.10	2.11	3.0E-4	2.3E-4	2.8E-4	5.6E-3	4.6E-3	5.1E-3	4.1E-3	4.8E-3	4.5E-3	3.7E-3	4.3E-3	4.0E-3	3.8E-3	3.6E-3	3.7E-3
P	1.2E-5	3.5E-5	2.4E-5	7.4E-5	9.9E-5	8.7E-5	2.2E-5	1.8E-5	1.9E-5	7.7E-6	1.3E-5	1.1E-5	1.8E-5	3.9E-5	2.9E-5	2.8E-5	6.8E-5	4.8E-5
Pb	7.5E-3	7.4E-3	7.5E-3	7.5E-4	1.0E-3	8.8E-4	1.2E-3	7.0E-4	9.5E-4	3.2E-4	3.1E-4	3.2E-4	2.3E-4	2.8E-4	2.6E-4	4.7E-4	4.7E-4	4.7E-4
Rb	0.018	0.018	0.018	0.040	0.041	0.041	0.056	0.056	0.056	0.065	0.068	0.066	0.084	0.085	0.084	0.101	0.107	0.104
Se	0.058	0.063	0.061	0.013	0.014	0.013	0.016	0.013	0.014	0.014	0.013	0.013	0.015	0.013	0.014	0.016	0.017	0.017
Sr	0.445	0.451	0.448	13.24	13.53	13.38	19.40	19.19	19.29	22.41	23.30	22.86	23.30	24.19	23.75	22.96	24.12	23.54
Th	1.8E-3	1.8E-3	1.8E-3	2.3E-6	1.3E-6	1.8E-6	1.2E-5	9.9E-6	1.1E-5	4.3E-6	3.9E-6	4.1E-6	2.4E-6	1.9E-6	2.2E-6	2E-06	1.8E-6	1.9E-6
Ti	1.3E-3	1.9E-3	1.6E-3	0	1.3E-4	6.4E-5	9.5E-4	9.6E-4	9.5E-4	2.6E-4	3.4E-4	3.0E-4	2.4E-4	5.2E-4	3.8E-4	1.3E-4	3.8E-4	2.5E-4
U	0.27	0.27	0.27	1.6e-4	9.9E-6	8.2E-5	3.3E-4	3.3E-4	3.3E-4	2.2E-4	2.3E-4	2.2E-4	2.3E-4	2.4E-4	2.4E-4	3.4E-4	3.5E-4	3.0E-4
V	0.001	0.001	0.001	0.001	0.001	0.001	0.009	0.009	0.009	0.016	0.018	0.017	0.023	0.023	0.024	0.025	0.024	0.024
Y	9.7E-5	1.0E-4	1.0E-4	8.6E-5	4.7E-5	6.6E-5	5.0E-4	4.0E-4	4.4E-4	7.9E-4	8.3E-4	8.1E-4	2.8E-3	2.8E-3	2.8E-3	3.5E-3	3.6E-3	3.6E-3
Zn	1.918	1.944	1.931	1.9E-3	1.8E-3	1.8E-3	3.8E-3	1.3E-3	2.5E-3	5.9E-4	1.2E-3	8.9E-4	2.7E-4	7.3E-4	5.0E-4	9.4E-4	5.0E-4	7.2E-4
Zr	8.5E-5	9.1E-5	8.8E-5	2.6E-5	3.0E-5	2.8E-5	6.5E-5	3.7E-5	5.1E-5	2.6E-5	2.9E-5	2.7E-5	1.5E-5	3.2E-5	2.4E-5	9.7E-6	1.9E-5	1.4E-5

Table A3.7: The composition of Rand Uranium mine water (80 L) before and after treatment with 200 g of lime and 86.58 g of $Al(OH)_3$ using a jet loop reactor with jet sizes set at 12 mm by cavitation mixing only.

Time (min)	0			30			60			90			120			150		
mg/L	1	2	ave	1	2	ave	1	2	ave	1	2	ave	1	2	ave	1	2	ave
Cl	18.33	19.66	18.99	20.97	25.07	23.02	23.92	31.09	27.51	36.35	21.64	29.00	34.77	31.31	33.04	30.37	27.39	28.88
SO_4^{2-}	2567	2558	2562	1271	1557	1414	831	935	883	879	818	848	1200	1051	1125	943.6	882.9	913.2
Fe	200.5	201.6	201.1	0.08	0.062	0.072	0.016	0.051	0.033	0.042	0.066	0.054	0.012	0.009	0.01	0.007	0.006	0.006
Al	26.34	26.91	26.63	0.044	2.0E-4	0.022	0.064	0.002	0.033	0.002	0.008	0.005	0.001	0.001	0.001	0.003	0.002	0.003
Ca	355.9	364.4	360.1	1161	1267	1214	542.6	579.6	561.1	562.2	597.3	579.8	545.6	550.7	548.2	639.2	576.0	607.6
Mg	152.3	153.7	153	0.12	0.11	0.11	0.66	0.71	0.69	0.327	0.29	0.31	0.37	0.37	0.37	0.21	0.124	0.166
Mn	59.99	60.32	60.16	0.001	1.9E-4	4.9E-4	1.1E-3	5.7E-3	3.4E-3	6.4E-3	1.2E-4	3.3E-3	1.6E-3	1.0E-3	1.3E-3	3.4E-3	4.5E-3	3.9E-3
Na	89.36	89.53	89.45	86.72	83.89	85.30	91.19	90.50	90.84	86.14	95.76	90.95	92.41	89.53	90.97	96.34	95.11	95.73
K	6.49	6.46	6.47	7.54	7.03	7.29	8.88	7.96	8.42	8.68	7.96	8.32	8.80	8.33	8.57	7.99	7.74	7.87
As	5.8E-3	5.8E-3	5.8E-3	0.50	0.28	0.39	0.94	0.26	0.60	0.98	0	0.49	0.27	0.085	0.18	0	0.44	0.221
B	0.235	0.23	0.231	0	0	0	0.017	0	0.009	0	0	0	0	0	0	0.13	0	0.064
Ba	0.025	0.026	0.026	0.11	0.093	0.10	0.1	0.115	0.11	0.13	0.11	0.12	0.12	0.13	0.13	0.16	0.13	0.14
Be	3.9E-3	3.9E-3	3.9E-3	7.6E-3	8.0E-4	4.2E-3	8.0E-4	0	4.0E-4	0	0	0	0	0	0	0	0.002	0.001
Cd	0.007	0.007	0.007	0.031	0.025	0.028	0.019	0.025	0.022	0.039	0.088	0.064	0.039	0.048	0.044	0.053	0.049	0.05
Ce	0	0.001	6.7E-4	0	0.70	0.35	0.11	0	0.056	0	1.73	0.86	0	0.27	0.13	0.44	0	0.22
Co	1.15	1.13	1.14	0	0.12	0.06	0.061	0	0.031	0	0	0	0	0	0	0	0.052	0.026
Cr	0.023	0.022	0.023	0.063	0	0.031	0	0.019	0.009	0.25	0.022	0.14	0	0.25	0.13	0.11	0.068	0.091
Cu	0.29	0.29	0.29	0.27	0.35	0.31	0.043	0	0.021	0	0	0	0	0.093	0.047	0	0.51	0.255
Hg	2.7E-6	5.1E-6	3.9E-6	0.11	0.11	0.11	0.23	0.17	0.20	0	0	0	0.063	0.28	0.17	0.19	0.16	0.18
Mo	5.6E-4	5.1E-4	5.4E-4	0	0	0	0	0	0	0	0	0	0	0	0	0	0	0
Nb	0	0	0	0.23	0	0.11	0.28	0.25	0.27	0.11	0.18	0.14	0.17	0.24	0.21	0.077	0.001	0.039
Ni	2.11	2.10	2.11	0	0	0	0	0	0	0	0	0	0.042	0.043	0.042	0	0	0
P	1.2E-5	3.5E-5	2.4E-5	0	0.78	0.39	0.16	0	0.077	0	0	0	0	0	0	0	0.12	0.058
Pb	7.5E-3	7.5E-3	7.0E-3	0.007	0.54	0.27	0.32	0.26	0.29	0.69	0.94	0.81	0.38	0	0.19	0.71	0	0.356
Rb	0.018	0.018	0.018	0	0	0	0.047	0.15	0.099	0.046	0.017	0.031	0	0	0	0	0.042	0.021
Se	0.058	0.063	0.061	1.10	0	0.55	0	1.26	0.63	0	0.11	0.054	0	0.65	0.32	0.47	1.25	0.86
Sr	0.445	0.45	0.448	1.48	1.50	1.491	1.25	1.34	1.30	1.20	1.25	1.23	1.32	1.29	1.30	1.35	1.25	1.30
Th	1.7E-3	1.8E-3	1.8E-3	0.88	0.061	0.47	0	0	0	0.87	1.75	1.31	0	0.84	0.42	0.88	2.007	1.44
Ti	1.4E-3	1.9E-3	1.6E-3	0	0.087	0.043	0.086	0.033	0.059	0.055	0	0.027	0.098	0.049	0.074	0.069	0.054	0.062
U	0.266	0.27	0.267	0	0	0	0	0	0	0	2.06	1.03	2.67	0	1.34	1.25	0	0.62
V	1.2E-3	1.2E-3	1.2E-3	0	0.11	0.054	0	0	0	0	0	0	0.039	0.09	0.066	0.10	0.30	0.20
Y	9.8E-5	1.4E-4	1.2E-4	0	0	0	0	0	0	0	0	0	0	0	0	0	0	0
Zn	1.92	1.94	1.93	0.033	0.11	0.069	0	0.045	0.022	0.011	0.021	0.016	0.019	0	0.010	0.23	0	0.11
Zr	8.6E-5	9.1E-5	8.8E-5	0.023	0	0.011	0	0	0	0	0	0	0	0.054	0.027	0	0.062	0.03

Table A3.8: The composition of Rand Uranium mine water (80 L) before and after treatment with 100 g of lime and 86.58 g of $Al(OH)_3$ using a jet loop reactor with jet sizes set at 12 mm by cavitation mixing only.

Time (min)	0			30			60			90			120			150		
mg/L	1	2	ave	1	2	ave	1	2	ave	1	2	ave	1	2	ave	1	2	ave
Cl	18.33	19.66	18.99	21.43	19.00	20.22	30.05	30.05	30.05	24.86	25.74	25.30	21.25	34.91	28.08	33.31	25.43	29.37
SO4	2567	2558	2562	1689	1720	1704	2067	2067	2067	1706	1727	1717	1605	2059	1832	2220	1633	1926
Fe	200.5	201.6	201.1	2.052	1.218	1.635	1.294	1.199	1.246	1.256	0.066	0.669	0.002	0.002	0.002	0.008	0.009	0.008
Al	26.34	26.91	26.62	0.003	0.005	0.004	0.004	0.004	0.004	0.001	0.001	0.001	0.008	0.003	0.006	0.008	0.001	0.005
Ca	355.9	364.4	360.2	955.9	921.1	938.5	1060	905.0	983.0	792.4	755.9	774.2	775.2	776.6	775.9	807.5	778.9	793.2
Mg	152.3	153.7	153	1.587	1.692	1.639	6.715	6.455	6.585	8.943	9.417	9.179	15.20	15.57	15.38	17.12	16.81	16.97
Mn	59.99	60.32	60.16	0.002	0.007	0.004	0.051	0.040	0.046	0.160	0.132	0.146	0.433	0.436	0.434	0.529	0.501	0.515
Na	89.36	89.53	89.45	81.78	88.55	85.16	128.6	95.80	112.2	97.21	97.55	97.38	98.36	97.83	98.10	97.20	98.67	97.93
K	6.485	6.459	6.472	8.353	7.243	7.798	9.360	6.441	7.901	10.67	8.342	9.505	10.88	10.87	10.87	9.245	9.001	9.123
As	0.006	0.006	0.006	0.436	0.475	0.455	0.233	0.283	0.258	0	0.630	0.315	0.409	0.735	0.572	0.616	0.708	0.662
B	0.235	0.227	0.231	0.127	0.064	0.096	0.613	0.494	0.554	0	0	0	0	0	0	0	0	0
Ba	0.025	0.026	0.026	0.034	0.043	0.039	0.060	0.043	0.052	0.049	0.063	0.056	0.079	0.077	0.074	0.087	0.092	0.089
Be	0.004	0.004	0.004	0.002	0.001	0.001	0	0	0	0.001	0.006	0.003	0.003	0	0.001	0	0	0
Cd	0.007	0.007	0.007	0.083	0.055	0.069	0.055	0.032	0.044	0.030	0.05	0.040	0.046	0	0.023	0.068	0.034	0.051
Ce	0	0.001	0.001	0	0.676	0.338	0.743	0.871	0.807	0	0.169	0.085	0.396	0	0.198	0	0.934	0.467
Co	1.150	1.131	1.140	0.148	0.074	0.111	0	0	0	0	0.070	0.035	0.047	0.069	0.058	0.189	0.147	0.168
Cr	0.023	0.022	0.023	0	0.205	0.102	0.222	0.039	0.131	0	0	0	0	0	0	0	0	0
Cu	0.288	0.282	0.285	0	0.182	0.091	0	0	0	0	0	0	0	0	0	0.173	0.134	0.154
Hg	2.7E-6	5.1E-6	3.9E-6	0.350	0.234	0.292	0.899	0.599	0.750	0	0	0	0	0.010	0.005	0.146	0.149	0.148
Mo	0.001	0.001	0.001	0.069	0	0.034	0	0	0	0	0	0	0	0	0	0	0	0
Nb	0	0	0	0.146	0.223	0.184	0.087	0.159	0.123	0.243	0.128	0.186	0.098	0.186	0.142	0.213	0.042	0.128
Ni	2.112	2.104	2.108	0	0	0	0	0	0	0	0	0	0	0	0	0	0	0
P	1.2E-5	3.5E-5	2.4E-5	1.268	0.623	0.946	0	0.114	0.057	0	0.241	0.121	1.709	1.130	1.419	0.874	0.206	0.540
Pb	0.007	0.007	0.007	0	0	0	0	0	0	0.399	0.484	0.442	0.955	0.179	0.567	0	0.133	0.066
Rb	0.018	0.018	0.018	0.056	0.007	0.032	0.021	0.001	0.011	0.045	0.034	0.040	0	0.002	0.001	0	0.026	0.013
Se	0.058	0.063	0.061	1.225	0.647	0.936	0.909	1.401	1.155	0.007	1.389	0.698	0	0.387	0.193	0.149	0	0.074
Sr	0.445	0.451	0.448	0.960	0.890	0.925	0.991	0.973	0.982	0.996	1.058	1.027	0.980	1.061	1.020	1.131	1.078	1.104
Th	0.002	0.002	0.002	0.163	0.876	0.519	0	0.941	0.470	0	1.202	0.601	0	0.882	0.441	0	2.687	1.344
Ti	0.001	0.002	0.002	0.071	0.080	0.076	0.059	0.058	0.058	0	0	0	0	0	0	0.048	0	0.024
U	0.266	0.268	0.267	0	0	0	0	0	0	0.123	0	0.062	0	0	0	0	0	0
V	0.00	0.001	0.001	0.040	0.141	0.090	0.245	0	0.122	0.094	0.056	0.075	0.131	0	0.065	0.312	0.170	0.241
Y	9.8E-5	1.4E-4	1.2E-4	0	0	0	0	0	0	0	0	0	0.014	0.024	0.019	0.009	0.057	0.033
Zn	1.918	1.944	1.931	0	0.059	0.030	0.055	0.089	0.072	0	0	0	0	0	0	0.075	0	0.037
Zr	8.6E-5	9.1E-5	8.9E-5	0	0	0	0	0	0	0.113	0.084	0.098	0.011	0	0.005	0.055	0.061	0.058

Table A3.9: The composition of Rand Uranium mine water (80 L) before and after treatment with 150 g of lime and 86.58 g of $Al(OH)_3$ using a jet loop reactor with jet sizes set at 12 mm by cavitation mixing only.

Time (min)	0			30			60			90			120			150		
mg/L	1	2	ave	1	2	ave	1	2	ave	1	2	ave	1	2	ave	1	2	ave
Cl	18.33	19.66	18.99	30.46	15.23	22.85	24.74	23.12	23.93	29.32	81.53	55.42	48.54	42.77	45.65	43.28	30.71	36.99
SO_4^{2-}	2567	2558	2562	1787	1521	1654	1880	1333	1606	1478	1470	1474	1849	1295	1572	1114	1869	1492
Fe	200.5	201.6	201.1	5.9E-4	7.1E-4	6.5E-4	4.6E-4	4.1E-4	4.3E-4	7.4E-	4.5E-4	5.9E-4	3.4E-4	6.5E-4	4.9E-4	5.0E-4	5.1E-4	5.0E-4
Al	26.34	26.91	26.63	36.44	61.22	48.83	28.95	21.89	25.42	12.02	23.15	17.59	84.27	86.49	85.38	31.10	20.72	25.91
Ca	355.9	364.4	360.2	975.1	897.7	936.4	720.1	704.2	712.1	763.6	772.3	767.9	728.3	732.7	730.5	839.2	826.0	832.6
Mg	152.3	153.7	153	0.18	0.16	0.17	0.696	0.701	0.699	0.535	0.48	0.51	0.526	0.469	0.49	0.43	0.37	0.40
Mn	59.99	60.32	60.16	0.024	0.022	0.023	1.1E-4	9.2E-3	4.7E-3	7.4E-4	2.1E-4	4.7E-4	1.7E-4	1.3E-4	1.5E-4	5.1E-3	1.4E-4	2.6E-3
Na	89.36	89.53	89.45	90.97	97.93	94.45	93.16	96.64	94.90	94.53	90.91	92.72	98.00	95.43	96.72	97.46	97.61	97.53
K	6.49	6.459	6.472	9.67	9.84	9.75	10.31	10.65	10.48	10.61	9.51	10.06	10.32	10.68	10.50	10.03	10.84	10.44
As	0.006	0.006	0.006	0.55	0.07	0.31	0	0.61	0.31	0.93	0	0.47	0	0.30	0.15	0.29	0	0.15
B	0.24	0.23	0.231	0	0	0	0	0	0	0	0	0	0	0	0	0.021	0	0.01
Ba	0.025	0.026	0.026	0.037	0.019	0.028	0.053	0.041	0.047	0.035	0.04	0.038	0.065	0.04	0.052	0.044	0.085	0.065
Be	0.004	0.004	0.003	0	0	0	0.002	0.009	0.005	0.007	0	0.003	0	0	0	0.005	0	0.002
Cd	6.8E-3	6.8E-3	6.8E-3	0.048	0.059	0.053	0.039	0.029	0.034	0.025	0.018	0.022	0	0.038	0.019	0.024	0.029	0.027
Ce	0	0.001	0.001	0.11	0	0.053	0.32	0	0.16	0	0	0	0	0.42	0.21	0.082	0.88	0.48
Co	1.15	1.13	1.14	0.077	0	0.038	0.094	0.27	0.18	0.055	0	0.027	0	0.14	0.069	0.261	0.27	0.27
Cr	0.023	0.022	0.023	0	0	0	0	0.04	0.02	0.022	0	0.011	0	0	0	0	0	0
Cu	0.29	0.281	0.29	0.037	0.13	0.082	0.062	0.17	0.12	0	0	0	0	0.068	0.034	0.021	0.078	0.049
Hg	2.7E-6	5.1E-6	3.9E-6	0.016	0	0.008	0	0.032	0.016	0.063	0	0.031	0.21	0.20	0.20	0.12	0.24	0.18
Mo	5.6E-4	5.1E-4	5.4E-4	0.46	0	0.23	0	0	0	0	0.15	0.078	0	0	0	0	0	0
Nb	0	0	0	0.13	0.17	0.15	0.13	0.26	0.19	0.23	0	0.12	0.097	0.6	0.23	0.12	0.20	0.16
Ni	2.11	2.104	2.11	0	0	0	0	0	0	0	0	0	0	0.19	0.097	0	0	0
P	1.2E-5	3.5E-5	2.4E-5	0.71	0.32	0.51	1.40	0.22	0.81	0.42	0.46	0.44	0.46	0.39	0.43	0.64	0.13	0.38
Pb	7.5E-3	7.5E-3	7.4E-3	0.32	0.12	0.22	0	0	0	0	0.85	0.43	0.75	0	0.38	0	0	0
Rb	0.018	0.018	0.018	0.039	0.10	0.071	0.13	0.066	0.097	0.081	0.065	0.073	0.044	0.052	0.048	0	0	0
Se	0.058	0.063	0.060	0.77	0.29	0.53	0.59	0	0.30	1.24	0.37	0.81	1.11	1.65	1.38	0.21	2.42	1.31
Sr	0.45	0.45	0.45	0.78	0.75	0.76	0.77	0.78	0.78	0.82	0.84	0.83	0.89	0.81	0.85	0.99	1.01	0.99
Th	1.8E-3	1.8E-3	1.8E-3	0	0.71	0.35	0	0	0	0.40	1.52	0.96	0.11	0	0.054	0.92	0.021	0.47
Ti	1.4E-3	1.9E-3	1.6E-3	2.6E-3	0	1.3E-3	0.056	0.069	0.062	0.031	0	0.016	0	4.3E-3	2.2E-3	0.068	0.053	0.06
U	0.27	0.27	0.27	0	0.74	0.37	0	0	0	0	0	0	0.12	0.76	0.44	0	0	0
V	1.2E-3	1.2E-3	1.2E-3	0.066	0.053	0.06	0	0.16	0.079	0.013	0	0.006	0.035	0.083	0.059	0.061	0.18	0.12
Y	9.8E-5	1.4E-4	1.2E-4	0.013	0	6.7E-3	0	0.025	0.012	0	0	0	0.034	0	0.017	0.01	2.5E-3	6.3E-3
Zn	1.92	1.94	1.931	0	0	0	0.063	0	0.032	0	0.006	0.003	0.005	0.031	0.018	0.024	0.002	0.013
Zr	8.5E-5	9.1E-5	8.9E-5	0.043	0.062	0.052	0.047	0.04	0.043	0.071	0	0.036	0.029	0.01	0.019	0.16	0	0.079

Table A3.10: The composition of Rand Uranium mine water (80 L) before and after treatment with 86.58 g of $Al(OH)_3$ using a jet loop reactor with jet sizes set at 12 mm by cavitation mixing only.

Time (min)	0			30			60			90			120			150		
mg/L	1	2	ave	1	2	ave	1	2	ave	1	2	ave	1	2	ave	1	2	ave
Cl	18.32	19.66	18.99	22.9 1	28.75	25.83	29.25	22.10	25.68	23.63	25.09	24.36	21.76	33.91	27.84	20.47	23.74	22.11
SO_4^{2-}	2567	2557	2562	2425	2321	2375	2362	2143	2252	2290	2101	2196	2106	2179	2143	2047	2026	2037
Fe	200.5	201.6	201.1	66.67	83.74	75.20	56.10	71.63	63.87	60.76	69.93	65.35	65.35	63.09	64.22	66.78	60.69	63.74
Al	26.34	26.91	26.62	63.12	68.12	65.62	42.54	41.28	41.91	43.25	45.69	44.47	48.79	43.29	46.04	26.95	17.17	22.06
Ca	355.9	364.4	360.2	368.5	348.7	358.6	368.6	364.2	366.4	341.1	352.6	346.8	389.3	387.8	388.5	324.3	313.3	318.8
Mg	152.3	153.7	153	118.1	112.4	115.2	113.6	121.1	117.4	111.4	109.8	110.6	122.1	121.9	122.0	114.1	109.5	111.8
Mn	59.99	60.32	60.16	34.47	24.65	29.56	46.56	45.27	45.91	48.53	46.82	47.67	42.68	34.08	38.38	22.28	15.95	19.12
Na	86.36	89.53	89.44	94.51	90.67	92.59	90.68	89.71	90.19	90.73	86.86	88.80	82.62	79.73	81.18	77.40	82.28	79.84
K	6.49	6.46	6.47	8.34	8.41	8.88	8.71	11.60	9.65	9.99	8.629	10.81	10.09	10.43	10.76	10.93	8.19	9.561
As	5.7E-3	5.8E-3	5.8E-3	0.35	0	0.18	0.62	0	0.31	0.32	0	0.16	0.83	0.27	0.55	0.08	0	0.04
B	0.24	0.23	0.23	1.10	1.08	1.09	1.65	1.21	1.43	1.50	1.52	1.51	2.16	1.94	2.05	0	0	0
Ba	0.025	0.026	0.026	0.06	0.041	0.05	0.052	0.054	0.053	0.053	0.049	0.051	0.063	0.074	0.068	0.078	0.059	0.068
Be	3.9E-3	3.9E-3	3.9E-3	6.E-3	1E-2	9.0E-3	7E-3	9E-3	8E-3	1E-3	8E-3	4.6E-3	4E-3	2E-2	9E-3	9E-3	4E-3	7E-3
Cd	6.8E-3	6.8E-3	6.8E-3	0.016	0.096	0.056	0.023	0.044	0.034	0.068	0.03	0.049	0.054	0.047	0.05	0.042	0.034	0.038
Ce	0	1.3E-3	6.7E-4	0	0	0	0.32	0	0.16	0.39	0	0.19	0	0	0	0	0	0
Co	1.15	1.13	1.14	1.45	1.58	1.51	1.52	1.63	1.57	1.36	1.12	1.24	1.59	1.53	1.56	1.23	1.25	1.24
Cr	0.023	0.022	0.023	0	0	0	1E-3	0.12	0.059	0	0	0	0	0.13	0.062	0.13	0.22	0.17
Cu	0.29	0.28	0.29	0.022	0.012	0.016	0	0	0	0.071	0	0.035	0	0.21	0.11	0.28	0	0.14
Hg	2.7E-6	5.1E-6	3.9E-6	0.26	0.012	0.13	0.29	0.22	0.25	0.29	0.31	0.30	0.94	0.64	0.79	0.14	0.13	0.14
Mo	5.5E-4	5.1E-4	5.4E-4	0.20	0	0.10	0	0	0	0	0	0	0	0	0	0	0.02	0.01
Nb	0	0	0	0.17	0.26	0.22	0.10	0	0.052	0.17	0.15	0.16	0.05	0.12	0.083	0	0	0
Ni	2.11	2.10	2.11	3.98	4.21	4.10	3.73	3.86	3.79	3.27	2.87	3.07	3.88	4.08	3.98	3.40	3.31	3.36
P	1.2E-5	3.5E-5	2.4E-5	1.17	0.50	0.84	0.81	0.56	0.68	0.34	0.74	0.54	1.01	0.67	0.84	0	0	0
Pb	7.4E-3	7.5E-3	7.5E-3	0	0	0	0	0	0	0	0.327	0.16	0	0	0	0.103	0.13	0.12
Rb	0.018	0.018	0.018	0.051	0.057	0.054	0.087	0	0.044	0.063	0.036	0.049	0.12	0.12	0.12	0.067	0.11	0.09
Se	0.058	0.063	0.061	0.76	0.89	0.82	0	0.51	0.25	1.16	2.29	1.73	1.34	0	0.67	0	0	0
Sr	0.45	0.45	0.45	0.58	0.53	0.55	0.56	0.58	0.57	0.51	0.49	0.50	0.61	0.56	0.59	0.63	0.62	0.62
Th	1.7E-3	1.8E-3	1.8E-3	1.37	1.69	1.53	1.93	2.262	2.094	1.72	1.74	1.73	2.06	2.93	2.49	2.30	1.84	2.07
Ti	1.4E-3	1.9E-3	1.6E-3	0.059	0.014	0.037	0.026	0.069	0.048	0.03	0	0.015	0.06	0	0.03	0	0	0
U	0.27	0.27	0.27	1.97	2.33	2.15	3.63	2.91	3.27	2.79	2.71	2.75	0	3.34	1.67	3.70	3.15	3.43
V	1.2E-3	1.2E-3	1.2E-3	0.14	0.18	0.158	0	0.18	0.089	0	0	0	0	0.24	0.12	0	0	0
Y	9.7E-5	1.4E-4	1.2E-4	0.29	0.30	0.29	0.35	0.29	0.33	0.28	0.24	0.26	0.29	0.31	0.30	0.073	0.12	0.097
Zn	1.92	1.94	1.93	2.98	2.94	2.96	3.03	2.70	2.87	2.46	2.69	2.58	3.06	2.90	2.98	2.50	2.40	2.45
Zr	8.6E-5	9.1E-5	8.9E-5	0.089	0	0.045	0	0	0	0.040	0.035	0.037	0	0.014	0.007	0	0	0

Table A3.11: The composition of Rand Uranium mine water (80 L) before and after treatment with 8 kg of Matla coal FA, 100 g of lime and 86.58 g of $Al(OH)_3$ using a jet loop reactor with jet sizes set at 12 mm by cavitation mixing only.

Time (min)	0			30			60			90			120			150		
mg/L	1	2	ave	1	2	ave	1	2	ave	1	2	ave	1	2	ave	1	2	ave
Cl	18.32	19.66	18.99	30.16	25.47	27.81	34.37	29.7	32.03	25.89	31.08	28.49	36.00	34.73	35.36	37.16	46.63	41.89
SO_4^{2-}	2567	2558	2562	2392	1721	2057	1962	1594	1778	1340	1355	1352	1093	1279	1186	1045	1069	1057
Fe	200.5	201.6	201.0	4.183	8.63	6.41	0.80	0.86	0.83	0.66	0.14	0.40	0.98	0.72	0.85	0.38	0.67	0.52
Al	26.34	26.91	26.63	25.97	30.21	28.09	37.29	75.46	56.37	85.18	28.73	56.96	46.58	33.15	39.86	57.38	14.45	35.92
Ca	355.9	364.4	360.1	690.2	659.6	674.9	542.2	567.9	555.1	475.6	419.6	447.6	367.5	355.9	361.7	373.2	337.1	355.2
Mg	152.3	153.7	153	0.21	0.26	0.24	0.652	0.752	0.70	0.323	0.84	0.58	0.19	0.29	0.24	0.15	0.26	0.21
Mn	59.99	60.32	60.16	0.006	0.023	0.014	0.005	0.04	0.023	0.007	0.049	0.028	0.002	0.045	0.023	0.024	0.044	0.034
Na	89.36	89.53	89.45	90.34	93.97	92.16	94.77	97.15	95.96	92.67	91.90	92.28	95.32	97.35	96.34	94.18	90.39	92.29
K	6.49	6.46	6.47	8.62	8.36	8.49	11.48	8.965	10.22	9.92	10.11	10.02	11.21	10.54	10.87	11.91	11.02	11.47
As	0.006	0.006	0.006	0	0	0	0	0	0	0	0	0	1.516	0	0.76	0	0	0
B	0.24	0.23	0.23	0	0	0	0.032	0	0.016	0.89	0.19	0.54	1.81	1.53	1.67	2.79	2.13	2.46
Ba	0.025	0.026	0.026	0.044	0.059	0.051	0.093	0.068	0.08	0.084	0.12	0.01	0.098	0.12	0.11	0.14	0.13	0.13
Be	3.9E-3	3.9E-3	3.9E-3	2.2E-3	8.4E-3	5.3E-3	4.9E-3	0	2.4E-3	0.005	1.2E-3	3.2E-3	2.8E-3	5.1E-3	4.0E3	2.4E-3	8.9E-3	5.7E-3
Cd	6.8E-3	6.8E-3	6.8E-3	0.039	0.045	0.042	9.6E-3	8.0E-4	5.2E-3	0	0.043	0.023	0.007	0	3.5E-3	0.039	0.011	0.025
Ce	0	0.001	0.001	0.069	0.47	0.27	0.33	0.71	0.52	0.49	0.32	0.41	0	0.022	0.011	0.61	0	0.31
Co	1.15	1.13	1.14	0.001	0.25	0.13	0	0	0	0.12	0.13	0.12	0.40	0.16	0.28	0.18	0.28	0.23
Cr	0.023	0.022	0.022	0	0.25	0.13	0.086	0.055	0.07	0.089	0.47	0.28	0	0.37	0.19	0	0.08	0.04
Cu	0.29	0.28	0.29	0	0.34	0.17	0.16	0.14	0.15	0.37	0.20	0.28	0.16	0.25	0.20	0.11	0.24	0.18
Hg	2.7E-6	5.1E-6	3.9E-6	0	0	0	0.033	0	0.017	0	0.041	0.02	0.04	3.0E-4	0.02	0.037	0	0.019
Mo	0.001	0.001	0.001	0.45	0.094	0.27	0.46	1.20	0.83	0	0	0	0.031	0.094	0.062	0.36	0.69	0.52
Nb	0	0	0	0	0.075	0.038	0	0	0	0	0	0	0	0	0	0	0	0
Ni	2.11	2.10	2.11	0.005	0.19	0.01	0.09	0.093	0.092	0.19	0.11	0.15	0.087	0.007	0.047	0	0.29	0.14
P	1.2E-5	3.5E-5	2.3E-5	0	0.26	0.13	0	0	0	0	0.12	0.06	0.376	0.35	0.36	0	0.29	0.15
Pb	0.007	0.007	0.007	0.34	0.38	0.36	0	0	0	0.97	0.33	0.65	0	0	0	0.44	0.75	0.60
Rb	0.018	0.018	0.018	0.088	0.011	0.049	0.055	0	0.027	0	0.14	0.069	0.023	0	0.011	0	0.042	0.021
Se	0.058	0.063	0.061	0	0	0	0	0	0	0	0.79	0.40	1.17	0.14	0.66	0.18	0	0.089
Sr	0.44	0.45	0.45	6.69	6.536	6.62	7.90	7.94	7.92	8.49	9.41	8.95	8.88	9.24	9.06	9.50	8.93	9.21
Th	1.8E-3	1.8E-3	1.8E-3	0.30	0	0.15	0.20	0	0.099	0.10	0	0.051	0.80	1.40	1.10	1.33	0	0.664
Ti	1.4E-3	1.9E-3	1.6E-3	0	7.0E-4	3.5E-4	0.12	0.022	0.069	0.009	0.039	0.024	6.5E-3	0	2.5E-3	0	0.021	0.01
U	0.27	0.27	0.27	0	0.25	0.13	0	0.58	0.29	0	0	0	0.024	0	0.012	0	0.23	0.11
V	1.2E-3	1.2E-3	1.2E-3	0	0	0	0.035	0.076	0.055	0	0.14	0.067	0	0.088	0.044	0	0	0
Y	9.7E-5	1.4E-4	1.2E-4	0.033	0.058	0.045	3.6E-3	0	1.8E-3	0.042	0	0.021	0	0.026	0.013	0	0	0
Zn	1.918	1.94	1.93	0.072	0.077	0.074	0.10	0.056	0.078	0.085	0.054	0.07	0.058	0.10	0.08	0.064	0.031	0.047
Zr	8.6E-5	9.1E-5	8.9E-5	0	0.12	0.058	0	0	0	0.096	0.076	0.086	0	0.055	0.027	0.081	0.012	0.046

Table A3.12: The composition of Rand Uranium mine water (80 L) before and after treatment with 13 kg of Matla coal FA, 200 g of lime and 86.58 g of $Al(OH)_3$ using a jet loop reactor with jet sizes set at 12 mm by cavitation mixing only.

Time(min)	0			30			60			90			120			150		
mg/L	1	2	ave	1	2	ave	1	2	ave	1	2	ave	1	2	ave	1	2	ave
Cl	18.32	19.6	18.9	31.99	24.22	28.11	35.91	27.2	31.56	27.48	21.00	24.24	23.39	32.40	27.90	27.29	30.46	28.88
SO_4^{2-}	2567	2558	2562	1878	1801	1840	875	860	868	641.1	570.7	605.9	591.7	764.4	678.1	487.7	686.6	587.2
Fe	200	201	201	1.11	1.32	1.21	0.50	0.28	0.39	0.45	0.80	0.63	0.62	0.92	0.77	0.44	0.62	0.53
Al	26.34	26.9	26.6	0.453	0.43	0.44	0.28	0.52	0.40	0.61	0.57	0.59	0.70	0.71	0.77	0.81	0.53	0.67
Ca	356	364	360	1040	1036	1038	385.9	237	311.8	404.7	390.0	397.3	358.1	351.8	355.0	208.1	280.7	244.4
Mg	152	154	153	0.16	0.17	0.17	0.14	0.11	0.13	0.15	0.10	0.13	0.27	0.18	0.22	0.15	0.28	0.22
Mn	59.99	60.3	60.1	0.011	1E-5	0.006	0.023	0.01	0.019	1.8E-4	3.4E-3	1.7E-3	0.017	1.3E-	9.1E-3	0.012	1.1E-4	5.8E-3
Na	89.36	89.5	89.4	89.32	87.56	88.44	86.21	87.4	86.83	8.41	89.68	49.05	82.21	89.66	85.93	88.21	86.49	87.35
K	6.485	6.45	6.47	6.77	9.86	8.32	10.27	10.4	10.35	9.35	8.31	8.83	8.09	7.32	7.71	8.87	9.03	8.95
As	0.006	0.00	0.00	0.012	0	0.006	0	0	0	0	0	0	0	0	0	0	0	0
B	0.235	0.22	0.23	1.16	1.03	1.10	2.11	1.77	1.94	2.70	2.36	2.53	3.32	3.39	3.36	3.584	3.32	3.45
Ba	0.025	0.02	0.02	0.072	0.085	0.078	0.079	0.08	0.08	0.13	0.14	0.13	0.12	0.13	0.13	0.095	0.11	0.10
Be	4E-3	4E-3	4E-3	0.002	0.002	0.002	0.001	0.00	0.002	0.005	5.3E-3	5.2E-3	0	0	0	0	5.0E-4	2.5E-4
Cd	7E-3	7E-3	7E-3	0	0.031	0.016	0.045	0.02	0.035	0.024	0.013	0.019	0.026	0.031	0.028	0	0.045	0.023
Ce	0	0.00	0.00	0.088	0	0.044	0	0	0	0	0	0	0	0	0	0.088	0.22	0.15
Co	1.150	1.13	1.14	0.33	0.053	0.19	0.14	0.13	0.14	0.20	0.21	0.20	0.15	0	0.076	0	0.29	0.14
Cr	0.023	0.02	0.02	0	0.37	0.183	0.14	0.34	0.24	0.17	0.23	0.20	0	0	0	0	0.074	0.037
Cu	0.288	0.28	0.28	0.26	0.049	0.16	0.064	0.20	0.13	0.21	0.053	0.13	0.14	0.26	0.20	0.26	0.11	0.18
Hg	3E-6	5E-6	4E-6	0.044	0	0.022	0.76	0.30	0.53	0.32	0.34	0.33	0.09	0.098	0.094	0.10	0.130	0.12
Mo	0.001	0.00	0.00	0.40	0.31	0.35	0	0	0	0.54	0.33	0.43	0	0.17	0.082	0	0.558	0.28
Nb	0	0	0	0	0	0	0	0.04	0.025	0	0	0	0	0	0	0	0	0
Ni	2.112	2.10	2.10	0	0	0	0.071	0.15	0.11	0.19	0.014	0.10	0.23	0.038	0.14	0.11	0.32	0.21
P	1E-5	4E-5	2E-5	0.018	0	0.0091	0.23	0.24	0.23	0	0	0	0	0.58	0.29	0	0.062	0.031
Pb	0.007	0.00	0.00	0.47	0.18	0.33	0.56	0.48	0.52	0.25	0.17	0.21	0.46	0.32	0.39	0.73	0.98	0.85
Rb	0.018	0.01	0.01	0.05	0	0.026	0.075	0.05	0.063	0.048	0.019	0.033	0.006	0.057	0.0317	0.007	0	0.003
Se	0.058	0.06	0.06	1.03	0.53	0.78	0.39	0	0.19	0	0	0	0	0	0	0	0.043	0.021
Sr	0.444	0.45	0.44	10.49	10.56	10.52	13.58	13.8	13.71	16.34	17.09	16.72	18.45	18.54	18.50	15.18	16.14	15.66
Th	2E-3	2E-3	2E-3	0	0	0	0	0	0	0	0.814	0.41	0.19	0.11	0.15	0.20	0	0.099
Ti	1E-3	3E-3	2E-3	0.003	0.005	0.0041	0.053	0.05	0.053	0.051	0	0.024	0	0.036	0.018	0.015	0.082	0.049
U	0.266	0.26	0.26	0	0	0	0	0	0	0	0.301	0.15	0	0	0	0.028	0	0.014
V	1E-3	1E-3	1E-3	0	0.063	0.032	0	0	0	0	0	0	0	0.059	0.03	0	0	0
Y	1E-4	1E-4	1E-4	0	0	0	0.021	0.01	0.018	0.008	0	0.004	0	0	0	0.029	0.044	0.037
Zn	1.918	1.94	1.93	0.044	0.098	0.071	0.017	0.06	0.041	0.015	0.067	0.042	0.11	0.11	0.11	0.084	0.15	0.12
Zr	8.6E-	9E-5	9E-5	0	0	0	0.034	0.04	0.041	0	0	0	0.043	0	0.022	0	0	0

Table A3.13: The composition of Rand Uranium mine water (80 L) before and after treatment with 8 kg of Matla coal FA and 86.58 g of $Al(OH)_3$ using a jet loop reactor with jet sizes set at 12 mm by cavitation mixing only.

Time (min)	0			30			60			90			120			150		
mg/L	1	2	ave	1	2	ave	1	2	ave	1	2	ave	1	2	ave	1	2	ave
Cl	18.32	19.66	18.99	85.63	82.29	83.96	23.63	25.63	24.63	18.18	26.93	22.55	28.11	19.73	23.92	36.78	52.37	44.57
SO_4^{2-}	2567	2558	2562	2284	2178	2231	2084	2078	2081	1856	1896	1876	1939	1417	1678	1620	2106	1863
Fe	200.5	201.6	201.1	0.096	0.042	0.069	0.026	0.075	0.05	0.062	0.020	0.041	0.060	0.078	0.069	0.097	0.085	0.091
Al	26.34	26.91	26.63	19.08	17.92	18.50	0.008	0.004	0.006	0.025	0.091	0.058	0.046	0.89	0.47	8.50	6.53	7.51
Ca	355.9	364.4	360.2	797.9	754.7	776.3	1276	1291	1284	1279	1240	1259	1231	1248	1240	1035	1045	1040
Mg	152.3	153.7	153	96.99	90.37	93.68	11.25	12.60	11.92	0.009	9.7E-3	9.3E-3	8.8E-3	6.4E-3	7.6E-3	4.6E-3	9.8E-3	7.2E-3
Mn	59.99	60.32	60.16	0.23	0.20	0.21	0.14	0.19	0.16	0.019	0.07	0.044	0.031	0.072	0.052	0.06	0.023	0.041
Na	89.36	89.53	89.45	94.18	96.53	95.35	98.81	111.0	104.9	108.8	109.9	109.4	129.6	119.6	124.6	128.8	123.7	126.3
K	6.49	6.46	6.47	8.96	7.41	8.18	9.20	6.85	8.02	8.32	6.62	7.47	7.18	7.39	7.28	9.51	7.99	8.75
As	5.8E-3	5.8E-3	5.8E-3	0.55	0	0.27	0	0	0	0	0	0	0	0	0	0.14	0	0.068
B	0.24	0.23	0.23	5.71	5.06	5.39	7.24	7.40	7.32	7.91	6.60	7.25	6.84	7.26	7.05	8.42	8.40	8.41
Ba	0.025	0.026	0.026	0.089	0.07	0.079	0.06	0.063	0.061	0.05	0.062	0.056	0.044	0.049	0.047	0.047	0.040	0.044
Be	3.9E-3	3.0E-3	3.9E-3	0	2.8E-3	1.4E-3	1.6E-3	0	8.0E-4	1.8E-3	9.0E-4	1.4E-3	0.011	4.0E-4	58E-3	0	3.2E-3	1.6E-3
Cd	6.8E-3	6.8E-3	6.8E-3	0.032	0.017	0.024	0.032	0.051	0.041	9.3E-3	0.054	0.032	0.034	0	0.017	0.018	0.027	0.022
Ce	0	1.3E-3	6.7E-4	0	0	0	0.53	0.33	0.43	1.74	0	0.87	0.15	0	0.073	0.65	0	0.33
Co	1.15	1.13	1.14	0.083	0.66	0.37	0.24	0	0.12	0	0	0	0	0	0	0.021	0	0.011
Cr	0.023	0.022	0.023	0.36	0.09	0.23	0	0	0	0	0	0	0	0	0	0	0	0
Cu	0.29	0.28	0.29	0.40	0.24	0.32	0	0	0	0	0.28	0.14	0	0.11	0.053	0	0.094	0.047
Hg	2.7E-6	5.1E-6	3.9E-6	0.12	0	0.058	0.065	0.047	0.056	0	0	0	0	0	0	0	0	0
Mo	5.6E-4	5.1E-4	5.4E-4	0.14	0.70	0.42	0.83	0.012	0.42	0.08	0.37	0.22	0	0.006	0.003	0	0	0
Nb	0	0	0	0	0	0	6.5E-3	0	3.2E-3	0.15	0.25	0.20	0.078	0.20	0.14	0	0.081	0.04
Ni	2.11	2.10	2.11	0	0	0	0.23	0.14	0.19	0.25	0.35	0.30	0.31	0.35	0.33	0.19	0.48	0.33
P	1.2E-5	3.5E-5	2.4E-5	0.25	0	0.13	0	0.17	0.086	1.09	1.25	1.17	0.58	0.80	0.69	0.076	0.20	0.14
Pb	7.5E-3	7.5E-3	7.5E-3	0.17	0.40	0.29	0.16	0.33	0.24	0	0	0	0	0.29	0.15	0.58	0	0.29
Rb	0.018	0.018	0.018	0	0.022	0.011	0	0.021	0.01	0	0	0	0	0	0	0	0	0
Se	0.058	0.063	0.061	0.36	0	0.18	0	0	0	0.60	0.10	0.35	0	0	0	0	0	0
Sr	0.45	0.45	0.45	7.29	7.05	7.17	8.69	8.08	8.38	8.77	9.29	9.03	8.99	9.60	9.29	10.16	9.68	9.92
Th	1.8E-3	1.8E-3	1.8E-3	0.84	0	0.42	1.53	0.79	1.16	0.94	3.00	1.97	0.49	0	0.24	1.54	0	0.77
Ti	1.4E-3	1.9E-3	1.6E-3	0.076	0	0.038	0	0.023	0.012	0	0	0	0	0	0	0	0	0
U	0.27	0.27	0.27	0	0	0	0	0	0	0	0	0	0	0	0	0	0	0
V	1.2E-3	1.2E-3	1.3E-3	0.037	0.024	0.031	0.23	0.21	0.22	0.38	0.35	0.36	0.47	0.26	0.37	0.294	0.25	0.27
Y	9.8E-5	1.4E-4	1.2E-4	0	0	0	0	0	0	0	0	0	0.011	0	5.3E-3	0	0	0
Zn	1.92	1.94	1.93	0.073	0	0.036	0	0	0	0	0.011	5.3E-3	0	0.028	0.014	0	0.012	6.2E-3
Zr	8.6E-5	9.1E-5	8.9E-5	8.6E-3	0	3.4E3	0.025	0	0.012	0	0	0	0	0	0	0.033	0	0.016

Table A3.14: The composition of Rand Uranium mine water (80 L) before and after treatment with 13 kg of Matla coal FA and 86.58 g of $Al(OH)_3$ using a jet loop reactor with jet sizes set at 12 mm by cavitation mixing only.

Time (min)	0			30			60			90			120			150		
mg/L	1	2	ave	1	2	ave	1	2	ave	1	2	ave	1	2	ave	1	2	ave
Cl	18.33	19.66	18.99	38.70	35.54	37.12	36.82	51.49	44.16	33.59	42.06	37.82	38.32	35.55	36.93	53.60	45.18	49.39
SO_4^{2-}	2567	2558	2562	1851	1994	1923	1628	1905	1766	1751	1994	1873	1640	1533	1587	1741	1622	1681
Fe	200.5	201.6	201.1	30.26	88.38	59.32	3.95	3.66	3.81	3.17	3.88	3.52	2.37	2.72	2.54	5.70	2.70	4.20
Al	26.34	26.91	26.63	0.052	0.055	0.054	146.1	160.7	153.4	53.20	49.54	51.37	23.11	23.24	23.17	13.12	11.77	12.45
Ca	355.9	364.4	360.2	1498	1492	1495	1014	954.8	984.4	650.4	645.8	648.1	448.9	445.1	447.0	420.4	389.1	404.8
Mg	152.3	153.7	153	4.6E-3	8.7E-3	6.7E-3	1.98	2.068	2.03	0.69	0.85	0.77	0.78	0.91	0.84	0.81	0.51	0.66
Mn	59.99	60.32	60.16	25.13	1.64	13.39	0.051	0.057	0.054	0.003	0.004	0.004	0.13	0.12	0.12	0.001	0.021	0.011
Na	9.36	89.53	89.45	105.9	96.43	101.2	108.5	109.1	108.8	93.48	94.24	93.87	92.46	95.01	93.74	100.3	100.8	100.6
K	6.49	6.46	6.47	13.67	9.24	11.45	9.46	8.72	9.09	9.98	8.85	9.41	9.30	9.73	9.51	3.18	8.10	5.64
As	5.8E-3	5.8E-3	5.8E-3	0	0	0	0	0	0	0.051	0.20	0.13	0.034	0.16	0.097	0	0	0
B	0.24	0.23	0.23	8.15	8.03	8.09	7.17	7.06	7.11	7.49	7.05	7.27	7.50	6.16	6.83	8.81	8.88	8.84
Ba	0.025	0.026	0.026	0.076	0.058	0.067	0.063	0.074	0.068	0.095	0.083	0.089	0.064	0.053	0.058	0.10	0.097	0.099
Be	3.9E-3	3.9E-3	3.9E-3	0.01	5.4E-3	7.9E-3	0	2.9E-3	1.5E-3	4.0E-4	6.0E-4	5.0E-4	0	0	0	4.0E-4	0	2.0E-4
Cd	6.8E-3	6.8E-3	6.8E-3	0	0.019	9.3E-3	5.9E-3	0.031	0.018	0	0	0	0.038	0	0.019	0	0.001	3.5E-4
Ce	0	1.3E-3	6.7E-4	0	1.22	0.61	0.47	0.42	0.44	0	0	0	0.85	0.72	0.79	0.41	0.42	0.42
Co	1.15	1.13	1.14	0.023	0	0.011	0	0	0	0.13	3.7E-3	0.068	0	0	0	0	3.1E-3	1.6E-3
Cr	0.023	0.022	0.023	0	0.18	0.09	0	0.091	0.046	0.21	0.051	0.13	0.24	0.11	0.17	0.62	0.015	0.32
Cu	0.29	0.28	0.29	0	0	0	1.3E-3	0.13	0.067	0.60	0.23	0.41	0.44	0.19	0.32	0.26	0.41	0.34
Hg	2.7E-6	5.1E-6	3.9E-6	0	0	0	0	0	0	0.54	0.21	0.38	0.30	0.21	0.25	0.13	0	0.064
Mo	5.4E-4	5.1E-4	5.4E-4	0	0.37	0.19	0.015	0	7.5E-3	0.67	0.86	0.76	0.49	0.79	0.64	0	0.95	0.47
Nb	0	0	0	0.084	0.067	0.076	0.041	0.091	0.066	0	0	0	0.11	0.18	0.15	8.7E-3	7.1E-3	7.9E-3
Ni	2.11	2.10	2.11	0.49	0.34	0.41	0.31	0.28	0.29	0	0	0	0	0.11	0.056	0	0.062	0.031
P	1.2E-5	3.5E-5	2.4E-5	0.55	0.94	0.75	0.27	0.84	0.56	0.30	0	0.15	0	0	0	0	0	0
Pb	7.5E-3	7.5E-3	7.3E-3	0.32	0	0.16	0	0.21	0.10	0	0	0	0.023	0	0.012	0	0	0
Rb	0.018	0.018	0.018	0	0	0	1.9E-3	0	9.5E-4	0	0	0	0	0	0	0	0	0
Se	0.059	0.063	0.061	1.02	0	0.51	0	0	0	0	0	0	0.76	0	0.38	0.32	0.61	0.47
Sr	0.45	0.45	0.45	10.70	10.12	10.41	11.08	10.58	10.83	11.65	12.44	12.04	13.50	13.45	13.48	15.72	16.45	16.09
Th	1.8E-3	1.8E-3	1.8E-3	0	0.70	0.35	1.95	2.75	2.35	0	0	0	1.46	0	0.73	2.66	2.48	2.57
Ti	1.4E-3	1.9E-3	1.6E-3	0	0	0	0	0	0	0.021	0	0.010	0.048	0.044	0.046	0.12	0.13	0.13
U	0.27	0.27	0.27	0	0	0	0	0	0	0	0	0	0	0	0	0	0	0
V	1.2E-3	1.2E-3	1.2E-3	0.28	0.35	0.31	0.33	0.24	0.29	0.16	0.073	0.12	0.021	0.18	0.01	0.091	0.10	0.096
Y	9.8E-5	1.4E-4	1.2E-4	0	0	0	0	0	0	0	2.2E-3	1.1E-3	0.018	0.04	0.029	0	6.2E-3	3.1E-3
Zn	1.92	1.94	1.93	0.031	0.047	0.039	0.003	0	0.001	0	0	0	0	0	0	0	0	0
Zr	8.6E-5	9.1E-5	8.9E-5	0	0.064	0.032	0.066	0	0.033	0.033	0.041	0.037	0	0.05	0.025	0.036	0.057	0.046

UNIVERSITY of the
WESTERN CAPE